Coupling of the 4f Electrons in Lanthanide Molecules

by

Daniel Kazhdan

B.A. (Yeshiva University) 2005

A dissertation submitted in partial satisfaction of the

requirements for the degree of

Doctor of Philosophy

in

Chemistry

in the

Graduate Division

of the University of California, Berkeley

Committee in charge:

Richard A. Andersen, Chair

T. Don Tilley

Clayton Radke

Fall 2008

Abstract

Coupling Between the Spins on $(C_5Me_5)_2M(III)$, (f^x),

and Substituted Bipyridine Radical Anions in

$(C_5Me_5)_2M$(2,2'-bipyridine) Compounds

by

Daniel Kazhdan

Doctor of Philosophy in Chemistry

University of California, Berkeley

Professor Richard A. Andersen, Chair

$(C_5Me_5)_2LnOTf$ where Ln = La, Ce, Sm, Gd, and Yb have been synthesized and these derivatives are good starting materials for the synthesis of $(C_5Me_5)_2LnX$ derivatives. $(C_5Me_5)_2Ln$(2,2'-bipyridine), where Ln = La, Ce, Sm, and Gd, along with several methylated bipyridine analogues have been synthesized and their magnetic moments have been measured as a function of temperature. In lanthanum, cerium, and gadolinium complexes the bipyridine ligand ligand is unequivocally the radical anion, and the observed magnetic moment is the result of intramolecular coupling of the unpaired electron on the lanthanide fragment with the unpaired electron on the bipyridine along with the intermolecular coupling between radicals. Comparison with the magnetic moments of the known compounds $(C_5Me_5)_2Sm$(2,2'-bipyridine) and $(C_5Me_5)_2Yb$(2,2'-bipyridine) leads to an understanding of the role of the Sm^{II}/Sm^{III} and Yb^{II}/Yb^{III} couple in the magnetic properties of $(C_5Me_5)_2Sm$(2,2'-bipyridine) and $(C_5Me_5)_2Yb$(2,2'-bipyridine). In addition, crystal structures of $(C_5Me_5)_2Ln$(2,2'-bipyridine) and

$[(C_5Me_5)_2Ln(2,2'\text{-bipyridine})][BPh_4]$ (Ln= Ce and Gd), where the lanthanide is unequivocally in the +3 oxidation state, give the crystallographic characteristics of bipyridine as an anion and as a neutral ligand in the same coordination environment, respectively.

Substituted bipyridine ligands coordinated to $(C_5Me_5)_2Yb$ are studied to further understand how the magnetic coupling in $(C_5Me_5)_2Yb(2,2'\text{-bipyridine})$ changes with substitutions. In the cases of $(C_5Me_5)_2Yb(5,5'\text{-dimethyl-2,2'-bipyridine})$ and $(C_5Me_5)_2Yb(6\text{-methyl-2,2'-bipyridine})$, the valence, as measured by XANES, changes as a function of temperature. In general, the magnetism in complexes of the type $(C_5Me_5)_2Yb(bipy')$, where bipy' represents 2,2'-bipyridine and substituted 2,2'-bipyridine ligands, is described by a multiconfiguration model, in which the ground state is an open-shell singlet composed of two configurations: Yb(III, f^{13})(bipy$^{\cdot-}$) and Yb(II, f^{14})(bipy°). The relative contributions of the two configurations depends on the substituents on the bipyridine ligand.

$[(C_5H_4Me)_3Ln]_2(L)$ (Ln = Ce, Tb; L = 4,4'-bipyridine, 1,4-benzoquinone) are synthesized in order to study the effect of these ligands on the oxidation states of the metal as well as to study intramolecular coupling between two lanthanides fragments.

Acknowledgements

I would like to thank my research advisor, Richard Andersen, for teaching me most of what I know about inorganic chemistry. I would like to thank Evan Werkema for teaching me most of what I know about running experiments in inorganic chemistry. Thanks also to coworkers Guofu Zi and Sylvio Levy for helpful discussions. Thanks to Fred Hollander and Allen Oliver in the CHEXray facility for their help with crystal structures. I would also like to thank Corwin Booth and Wayne Lukens for helping me run experiments up the hill. Marc Walter pioneered much of the work which I have done, and I thank him for that. I would like to thank Phil Wolgin for taking care of me while I was hectically trying to finish my Ph.D. and I would like to thank Bea for everything.

This work was supported by the Director, Office of Science, Office of Basic Energy Sciences, of the U.S. Department of Energy under Contract No. DE-AC02-05CH11231.

Table of Contents

Introduction

Complexes of the lanthanide elements, La-Lu in the periodic table, are unique in that the valence orbitals (the 4f orbitals) do not extend beyond those of the core outermost core orbitals (the filled 5s and 5p orbitals).[1] The result is that the 4f orbitals have poor overlap with ligand orbitals and the 4f orbitals remain core-like, with the bonding in lanthanide complexes remaining largely electrostatic, i.e., determined by Coulomb's law. However, in cases where there are unpaired electrons near the lanthanide center, coupling between the unpaired electron and the lanthanide have been observed,[2,3,4,5] implying that the "core" 4f electrons can interact with the ligands.

In 2002, Andersen and coworkers showed that $(C_5Me_5)_2Yb$(2,2'-bipyridine), and related complexes with substitutions on the Cp ring or on the bipy ligand exhibit magnetic moments higher than those predicted for the diamagnetic configuration $(C_5Me_5)_2Yb(II)$(2,2'-bipyridine), but lower than those predicted for the configuration $(C_5Me_5)_2Yb(III)$(2,2'-bipyridine$^{\cdot-}$). [6] Further work in the Andersen lab has shown that this is a result of two phenomena. [7] Firstly, the complex exhibits a mixed valence (Yb(II)/2,2'-bipyridine,Yb(III)/2,2'-bipyridine^{-}) ground state. This is demonstrated by analyzing the XANES L_{III}-edge. In $(C_5Me_5)_2Yb$(2,2'-bipyridine), the estimated contribution of the configuration $(C_5Me_5)_2Yb(III)$(2,2'-bipyridine$^{\cdot-}$), based on XANES is 80%. This contribution is temperature independent. Secondly, the plot of χT vs. T curve indicates that the amount of coupling between the Yb^{III} center and the 2,2'-bipyridine^{-} is changing as a function of temperature, indicating that the 4f "core" electrons are coupling with unpaired electron on the bipyridine ligand. This coupling serves as another means of

lowering the magnetic moment. The Andersen laboratory observed similar results with 4,4'-disubstituted bipy ligands[8] and with the closely related diazadienes.[9]

The goal of the present study is to extend these results in three different ways. The first is to study molecules similar to $(C_5Me_5)_2Yb$(2,2'-bipyridine), but without the complication of the Yb(II)/Yb(III) couple. This can be accomplished by studying lanthanides in which the Ln(II) state is energetically unfavorable. Chapters 1-3 discuss the synthesis and charecterization of Cp^*_2Ln(III)(bipy) and $[Cp^*_2Ln(III)(bipy)]^+$ with Ln = La, Ce, Sm, Gd, and Lu. The metal center in these complexes is in the +3 oxidation state, and therefore, the magnetism should only reflect the coupling between the unpaired electrons on the Ln center and the unpaired electron on the 2,2'-bipyridine$^{\cdot-}$ ligand. Chapter 1 discusses the synthesis and properties of a new series of convenient starting materials for metallocene lanthanide complexes, specifically molecules of the type $(C_5Me_5)_2LnX$ (Ln = La, Ce, Sm, Gd, Yb, and Lu) (X = Cl, I, OTf). Chapter 2 outlines the synthesis and properties of $[(C_5Me_5)_2Ln$(2,2'-bipyridine)$]^+$ and 2,2'-bipyridine analogues. Chapter 3 discusses the synthesis of $(C_5Me_5)_2Ln$(2,2'-bipyridine) and 2,2'-bipyridine, where the 2,2'-bipyridine and its analogues are radical anions. The magnetism of these molecules, especially upon comparison with the magnetism of the corresponding cations of Chapter 2, allows for a useful methodology for studying the coupling of the lanthanide center with its surrounding ligands. Coupling between the lanthanide center and the ligands implies that the "core" electrons are communicating magnetically with their environment.

Chapter 4 extends the studies on $(C_5Me_5)_2Yb$(2,2'-bipyridine), with new substituents in the 4, 5, and 6-positions. The magnetism of these molecules is still

intermediate between that predicted for $(C_5Me_5)_2Yb(II)$(2,2'-bipyridine) where the 2,2'-bipyridine ligand is neutral and $(C_5Me_5)_2Yb(III)$(2,2'-bipyridine$^{\cdot-}$), where the 2,2'-bipyridine is a radical anion. However, the shape of the effective magnetic moment as a function of temperature is markedly different from that seen in the previously published molecules. Moreover, XANES studies on several of these molecules show that the relative contribution of Yb(II) and Yb(III) to the ground state of the molecule changes as a function of temperature. This is in contrast with $(C_5Me_5)_2Yb$(2,2'-bipyridine) and $(C_5Me_5)_2Yb$(4,4'-dimethyl-2,2'-bipyridine) where the relative Yb(II) and Yb(III) contributions are independent of temperature.

Chapter 5 discusses mixed valent ground state studies in cerium molecules of the type $[X_3Ce]_2(L)$ (X = Cp, MeC_5H_4, $N(SiMe_3)_2$), L = (4,4'-bipyridine and 1,4-benzoquinone), where the reduction potential of the ligands change the contribution of Ce(IV) to the ground state. This is an extension of Walter's work, in which he shows that the magnetism of $[(N(SiMe)_2)_3Ce]_2$(1,4-benzoquinone), is lower than that predicted for the configurations $[(N(SiMe)_2)_3Ce(III)]_2$(1,4-benzoquinone) and $[N(SiMe)_2)_3Ce(IV)]^+$[1,4'-benzoquinone]$^-$(Ce(III)$(N(SiMe)_2)_3$, but higher than predicted for the diamagnetic configuration $[(N(SiMe)_2)_3Ce(IV)]^+_2$[1,4-benzoquinone]$^{2-}$.[10]

References:

[1]. Freeman, A.J., Watson, R.E. *Phys. Rev.*, **1962**, *127*, 2058
[2]. Matthias, B.T.; Bozorth, R.M.; van Vleck, J.H. *Acta Cryst*, **1956**, *9*, 452
[3]. Zanowick, R.L.; Wallace, W. E. *Phys. Rev.*, **1962**, *126*, 537
[4]. Andruh, M.; Ramade, I; Codjovi, E.; Guillou, O.; Kahn, O.; Trombe, J.C. *JACS*, **1993**, *115*, 1822
[5]. Sutter, J.P.; Kahn, M.L.; Golhen, S.; Ouahab L.; Kahn, O. *Chemistry-A. European Journal*, **1998**, *4*, 571
[6]. Schultz, M.; Boncella, J. M.; Berg, D. J.; Tilley, T. D.; Andersen, R. A. *Organometallics*, **2002**, *21*, 460
[7]. Booth, C. H.; Walter, M. D.; Daniel, M.; Lukens, W. W.; Andersen, R. A. *Phys. Rev. Lett.*, **2005**, *95*, 267202
[8]. Walter, M. D.; Berg, D. J.; Andersen, R. A. *Organometallics*, **2006**, *25*, 3228
[9]. Walter, M. D.; Berg, D. J.; Andersen, R. A. *Organometallics*, **2007**, *26*, 2296
[10]. Walter, M.D., Ph.D. Thesis, Technische Universität Kaiserlautern Fachbereich Chemie, **2005.**

Chapter 1: Synthesis and Properties of Cp^*_2LnX (X = Cl, I, OTf, $N(SiMe_3)_2$)

1.1 Introduction

Compounds of the type $Cp^*_2Ln(L)(X)$ ($Cp^* = C_5Me_5$) have generally been prepared from Cp^*_2LnCl complexes, usually isolated as anionic complexes, $Cp^*_2LnCl_2Na$, or complexes with Lewis bases, $Cp^*_2LnCl(L)$, which in turn were synthesized from NaCp* and $LnCl_3$, (equation 1).[1,2]

$$2NaCp^* + LnCl_3 \rightarrow Cp^*_2LnCl_2Na + NaCl \qquad (1)$$

There are several difficulties associated with this method. Sodium pentamethylcyclopentadienide is pyrophoric and difficult to purify since it is insoluble in solvents such as hydrocarbons or diethyl ether, although it is soluble in tetrahydrofuran. Also, the initial product is the anionic complex, $Cp^*_2LnCl_2Na$, not Cp^*_2LnCl, and therefore NaCl has to be removed at some later stage. In addition, all of these reactions are air and moisture sensitive, and the $LnCl_3$ must be thoroughly dried by heating at reflux in thionyl chloride for several days. Finally, complexes such as $Cp^*_2Ce(L)(Cl)$ are often poorly soluble in hydrocarbons and ethers.

An alternative synthetic route for preparation of useful starting materials for the synthesis of metallocene derivatives was desirable. In this chapter, alternative synthetic routes are described that gave useful amounts of starting materials that were used for the preparation of the complexes outlined in the successive chapters.

Results and Discussion

1.2 Synthesis and properties of Cp^*_2CeCl ($Cp^* = C_5Me_5$) and Cp^*_2CeI

Decamethylmagnesocene, Cp^*_2Mg, is a useful alternative for the commonly used alkalimetal derivatives Cp*M. The magnesocene is obtained as white crystals either by sublimation or by crystallization from hydrocarbon solvents.[3] Although it is air and moisture sensitive, it is not pyrophoric.

The use of Cp^*_2Mg as a Cp* transfer reagent is described in Scheme 1.3.1. Stirring Cp^*_2Mg and dry $CeCl_3$ in THF affords an orange powder. It is difficult to separate the $MgCl_2$ from the Cp^*_2CeCl. However, addition of MeCN forms the yellow coordination compound $Cp^*_2CeCl(NCCH_3)_2$, which can be crystallized from the MeCN at -20°C. The room-temperature ^1H NMR spectrum of $Cp^*_2CeCl(NCCH_3)_2$ in C_6D_6 (400 MHz) contains two paramagnetic signals, one attributable to the methyl groups of the Cp* rings and the other to the coordinated CH_3CN groups in a 30:6 area ratio. Addition of MeCN to the NMR tube results in the peak of area 6 shifting to the diamagnetic region confirming that the resonance is due to CH_3CN. The CH_3CN-free compound, which had been previously prepared from LiCp*,[4] can be obtained by sublimation under dynamic vacuum (10^{-3} – 10^{-4} Torr) at 125 °C for several days. This method requires $CeCl_3$ as the starting material. The base-free compound is only sparingly soluble in ether solvents, and the overall yields are low, about 10 %.

An alternative cerium starting material is $CeI_3(THF)_3$ which reacts with Cp^*_2Mg in toluene to give Cp^*_2CeI. Crystallization from MeCN is required to separate the metallocene from MgI_2. $Cp^*_2CeI(NCCH_3)$ was previously synthesized accidentally, and

the crystal structure has been reported.[5] Like $Cp^*_2CeCl(NCCH_3)_2$, the room-temperature ^1H NMR spectrum of $Cp^*_2CeI(NCCH_3)_2$ in C_6D_6 contains two paramagnetic signals in a 30:6 ration, one attributable to the methyl groups of the Cp* rings and the other to the coordinated CH_3CN. Addition of MeCN causes the peak of area 6 to shift to the diamagnetic region confirming that the resonance is due to CH_3CN. The CH_3CN-free compound, Cp^*_2CeI, can be obtained by sublimation under dynamic vacuum (10^{-3} – 10^{-4} Torr) at 140 °C for several days. The Electron Impact (EI) mass spectrum gives a molecular ion with m/z of 537 showing that it is a monomer in the gas phase.

1.3 Synthesis and properties of $Cp^*_2Ce(OTf)$ (OTf = OSO_2CF_3) and $Cp^*_2CeN(SiMe_3)_2$

An even simpler synthetic alternative to CeI_3 for the preparation of Cp^*_2CeX complexes is based on $Ce(OTf)_3$. Addition of dilute aqueous triflic acid to $Ce_2(CO_3)_3$ gives $Ce(OTf)_3(H_2O)_x$, which is dried by heating under dynamic vacuum at 150 °C for a week.[6] $Ce(OTf)_3$ reacts with Cp^*_2Mg in THF to give a yellow solution of $Cp^*_2Ce(OTf)$. Crystallization from toluene results in orange crystals which disintegrate when subjected to vacuum, giving an orange solvent-free powder of $Cp^*_2Ce(OTf)$. The ^1H and ^{19}F NMR spectra each show a single peak. Scheme 1.3.1 summarizes the synthetic routes for making Cp^*_2CeX compounds from Cp^*_2Mg.

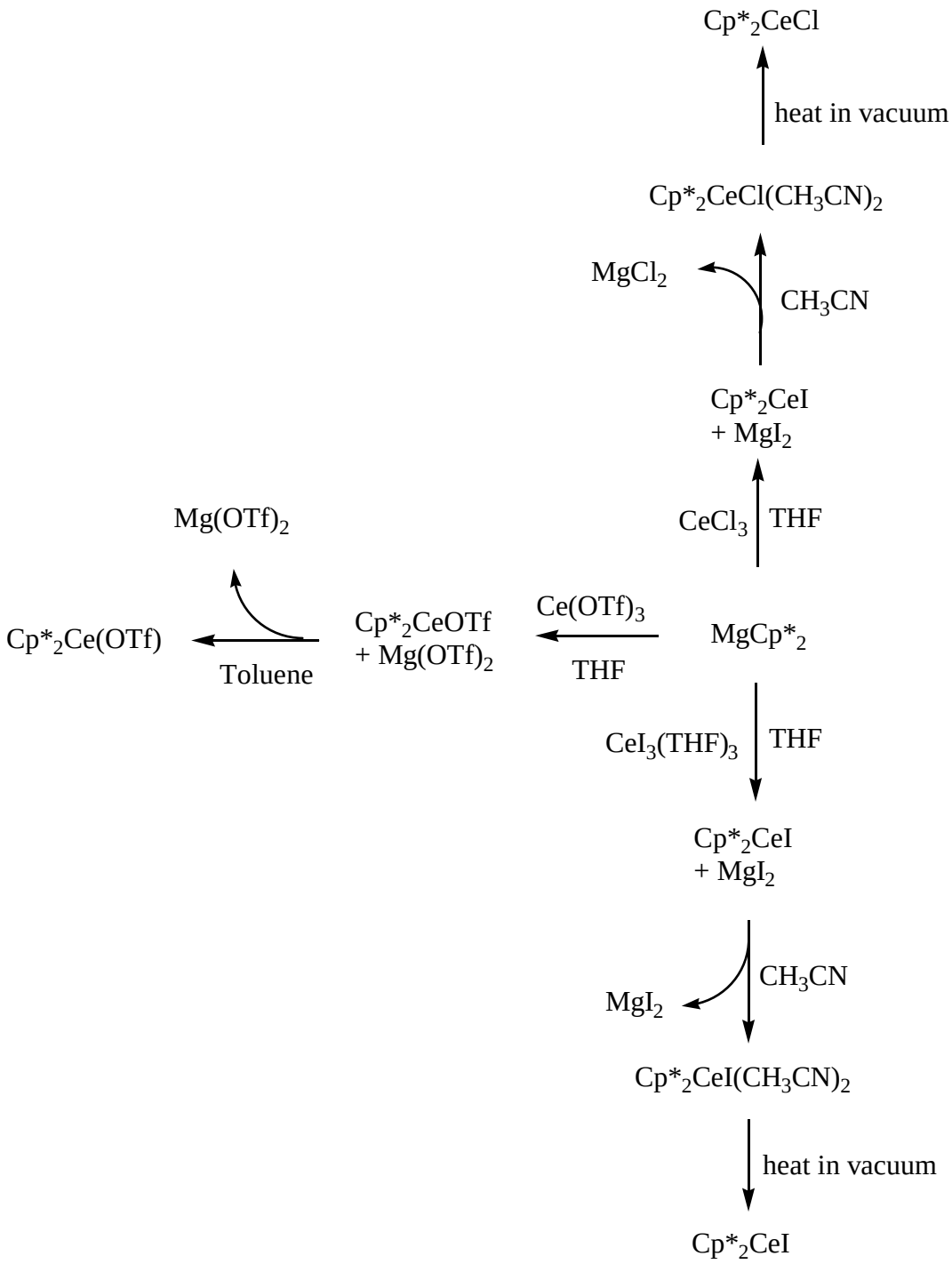

Scheme 1.3.1: Synthesis of Cp^*_2CeX starting from Cp^*_2Mg

$Cp^*_2Ce(OTf)$ is a good starting material for many of the compounds described in this thesis. For instance, it can be converted into $Cp^*_2CeN(SiMe_3)_2$ with the addition of

$NaN(SiMe_3)_2$ in pentane. $Cp^*_2CeN(SiMe_3)_2$ has been previously synthesized from $Ce(N(SiMe_3)_2)_3$.[4] In the room-temperature ^1H NMR spectrum there is only one resonance for the $N(SiMe_3)_2$ group. However, as the temperature is lowered the $N(SiMe_3)_2$ splits into two peaks, one of area 6 and one of area 12 (Figure 1.3.1).

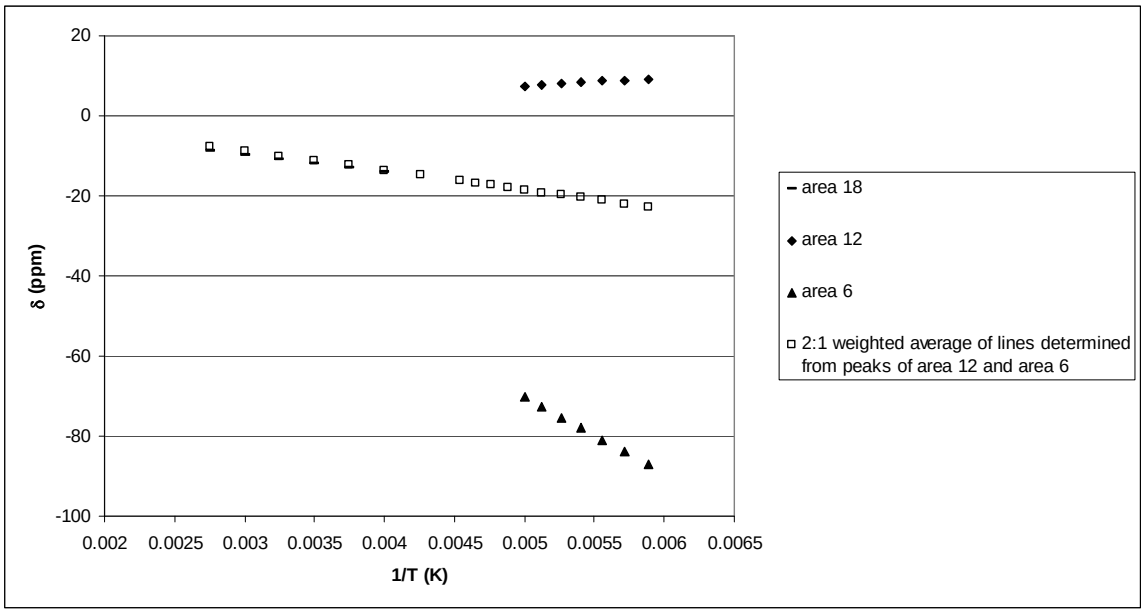

Figure 1.3.1: Variable-temperature ^1H NMR spectra represented as a δ vs. 1/T plot of $Cp^*_2CeN(SiMe_3)_2$ in methylcyclohexane-d_{14}. The numerical 2:1 weighted average of the least-squares lines determined by the δ vs. 1/T plots of the peaks of area 12 and of area 6 is shown as well.

The observed chemical shift for the coalesced peak of area 18 is in good agreement with the 2:1 weighted average of the least-squares lines determined by the δ vs. 1/T plots of the peaks of area 12 and of area 6. The crystal structure (Figure 1.3.2) shows that one carbon atom from each $SiMe_3$ group, C(21) and C(24), is oriented towards the cerium, and the space-filling diagram (Figure 1.3.3) shows that rotation about the N-Si bond is sterically hindered by the methyl groups (C15, C20, C12, and C17) of the Cp* rings. The

activation energy presumably reflects the barrier to free rotation about the N-Si bond, the physical process that exchanges the methyl group closest to the cerium atom.

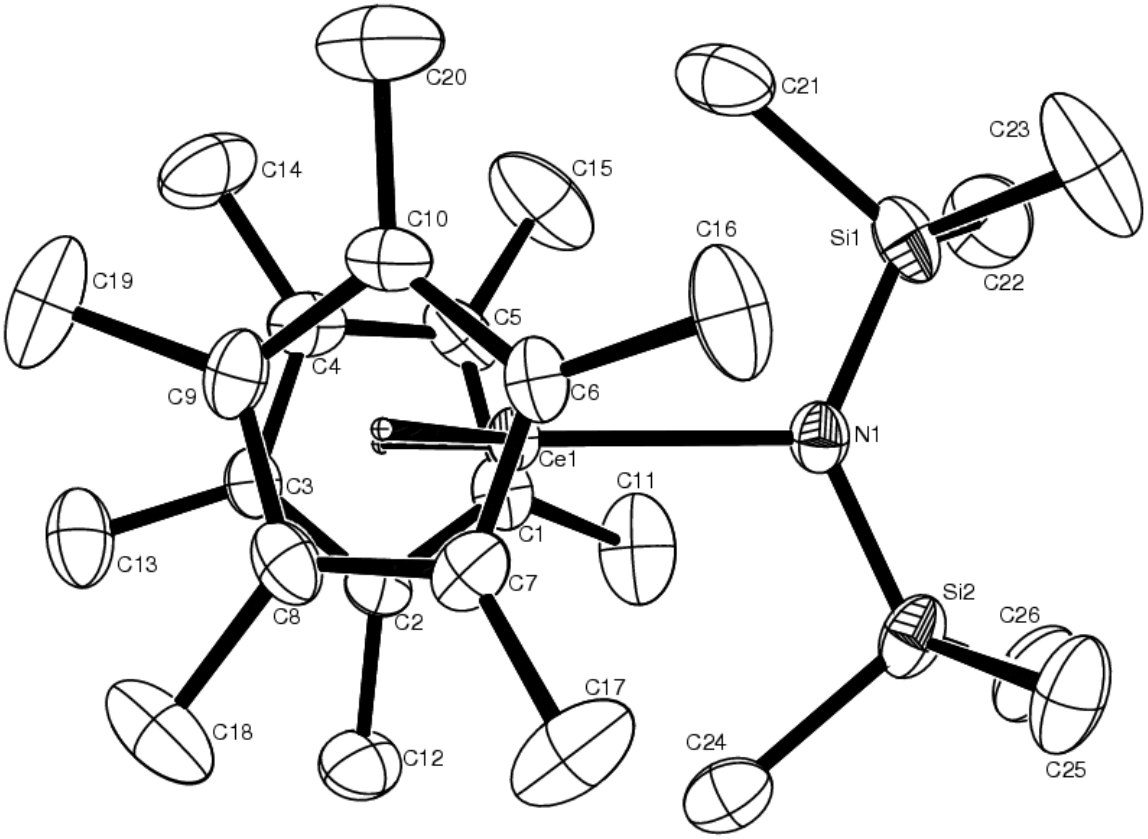

Figure 1.3.2: ORTEP diagram of $Cp^*_2CeN(SiMe_3)_2$ (50% probability ellipsoids). All non-hydrogen atoms are refined anisotropically. Hydrogen atoms are placed and not refined and are not shown. Selected bond distances and angles are given in Tables 1.3.1 and 1.3.2, respectively.

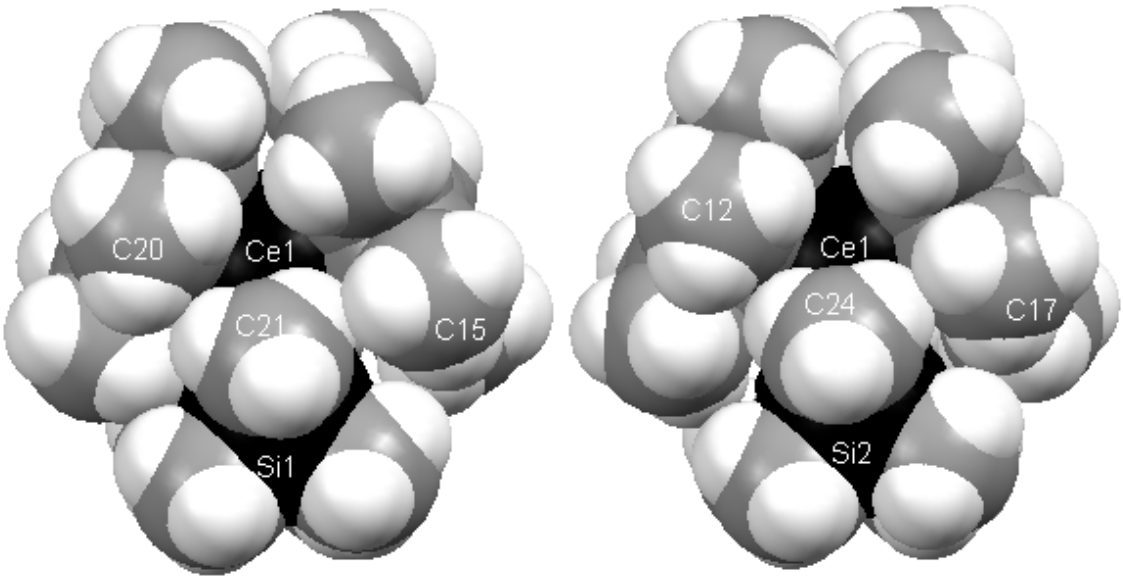

Figure 1.3.3: Space filling diagram of $Cp^*_2CeN(SiMe_3)_2$ along the C21-Ce axis and along the C24-Ce axis.

Table 1.3.1: Selected bond distances (Å) in $Cp^*_2CeN(SiMe_3)_2$

Atom	Atom	Distance		Atom	Atom	Distance
Ce(1)	N(1)	2.366(3)		Ce(1)	C(1)	2.841(4)
Ce(1)	C(2)	2.804(4)		Ce(1)	C(3)	2.809(4)
Ce(1)	C(4)	2.813(4)		Ce(1)	C(5)	2.830(4)
Ce(1)	C(6)	2.818(4)		Ce(1)	C(7)	2.833(4)
Ce(1)	C(8)	2.836(4)		Ce(1)	C(9)	2.842(4)
Ce(1)	C(10)	2.807(4)		Ce(1)	C(101)	2.55
Ce(1)	C(102)	2.56		Ce(1)	C(21)	3.233(5)
Ce(1)	C(24)	3.222(4)		Si(1)	N(1)	1.701(3)
Si(2)	N(1)	1.697(3)				

Table 1.3.2: Selected bond angles (°) in $Cp^*_2CeN(SiMe_3)_2$

Atom	Atom	Atom	Angle		Atom	Atom	Atom	Angle
C(101)	Ce(1)	C(102)	133.0		Ce(1)	N(1)	Si(1)	114.5(2)
Ce(1)	N(1)	Si(2)	114.5(2)		N(1)	Si(1)	C(21)	106.1(2)
N(1)	Si(2)	C(24)	106.0(2)					

From the coalescence temperature, 215K $\pm$ 5, and using Shanan-Atidi and Bar-Eli's method for calculating barriers in non-equal population site exchange[7,8,9] the barrier is found to be 7.8 kcal/mol $\pm$ 0.2. The variable temperature ^{1}H NMR spectra of $Cp^*_2YbN(SiMe_3)_2$ prepared as described elsewhere,[10] is shown in Figure 1.3.2, and the barrier is calculated to be 9.7 kcal/mol $\pm$ 0.5. Since Yb(III) has a smaller ionic radius than Ce(III),[11] the steric interactions between the $N(SiMe_3)_2$ and the Cp* in $Cp^*_2YbN(SiMe_3)_2$ should be larger than in $Cp^*_2CeN(SiMe_3)_2$ leading to a larger barrier. Crystals suitable for X-ray diffraction studies were grown by C.F. Choi from toluene, and the crystal structure shows two molecules in the asymmetric unit as shown in Figure 1.3.4, and they are shown separately in Figures 1.3.5 and 1.3.6.

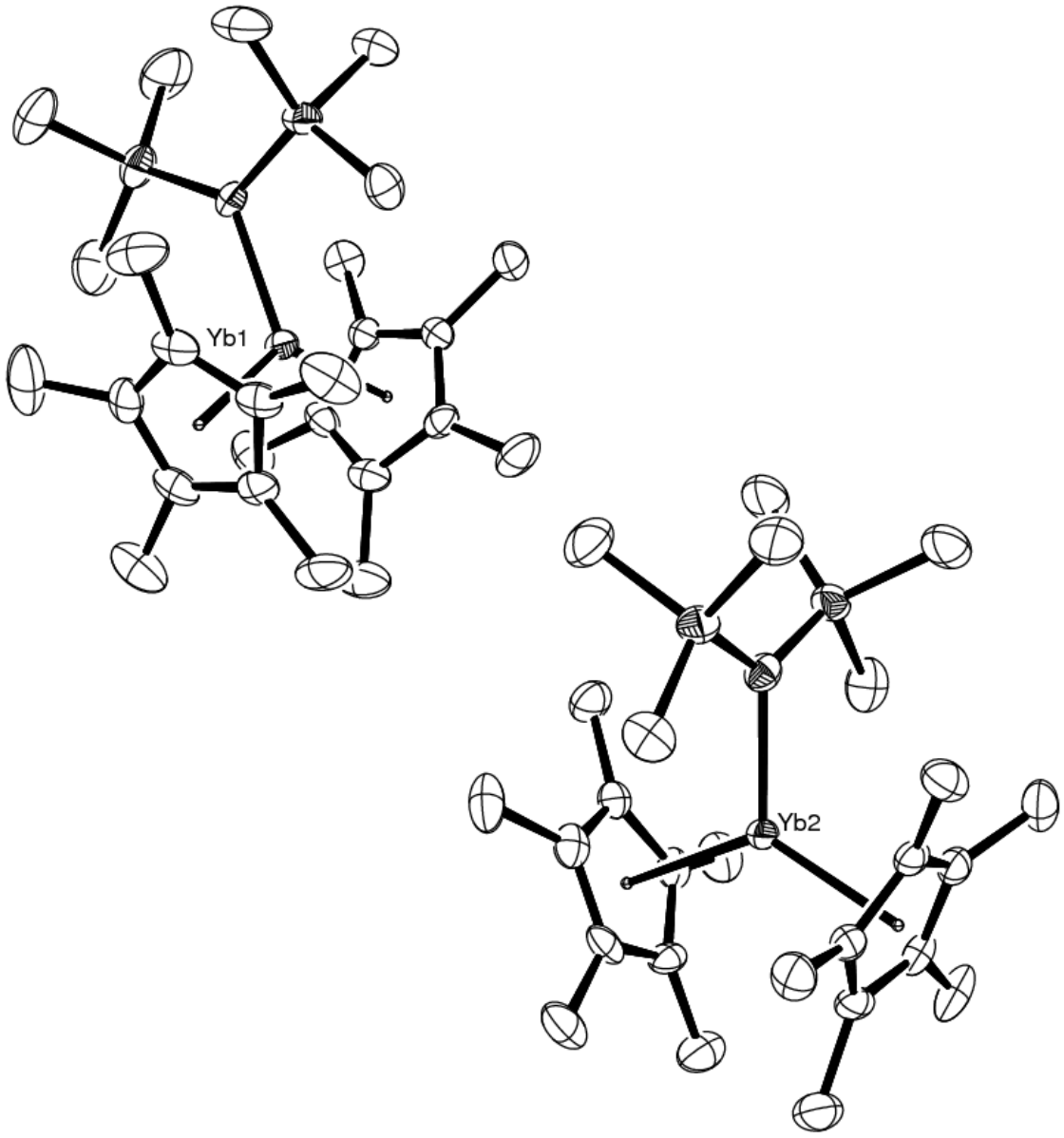

Figure 1.3.4: ORTEP diagram of $Cp^*_2YbN(SiMe_3)_2$ (50% probability ellipsoids). All non-hydrogen atoms are refined anisotropically. Hydrogen atoms are placed and not refined and are not shown. The two molecules are looked at separately in Figures 1.3.4 and 1.3.5. Selected bond distances and angles are given in Tables 1.3.3 and 1.3.4, respectively.

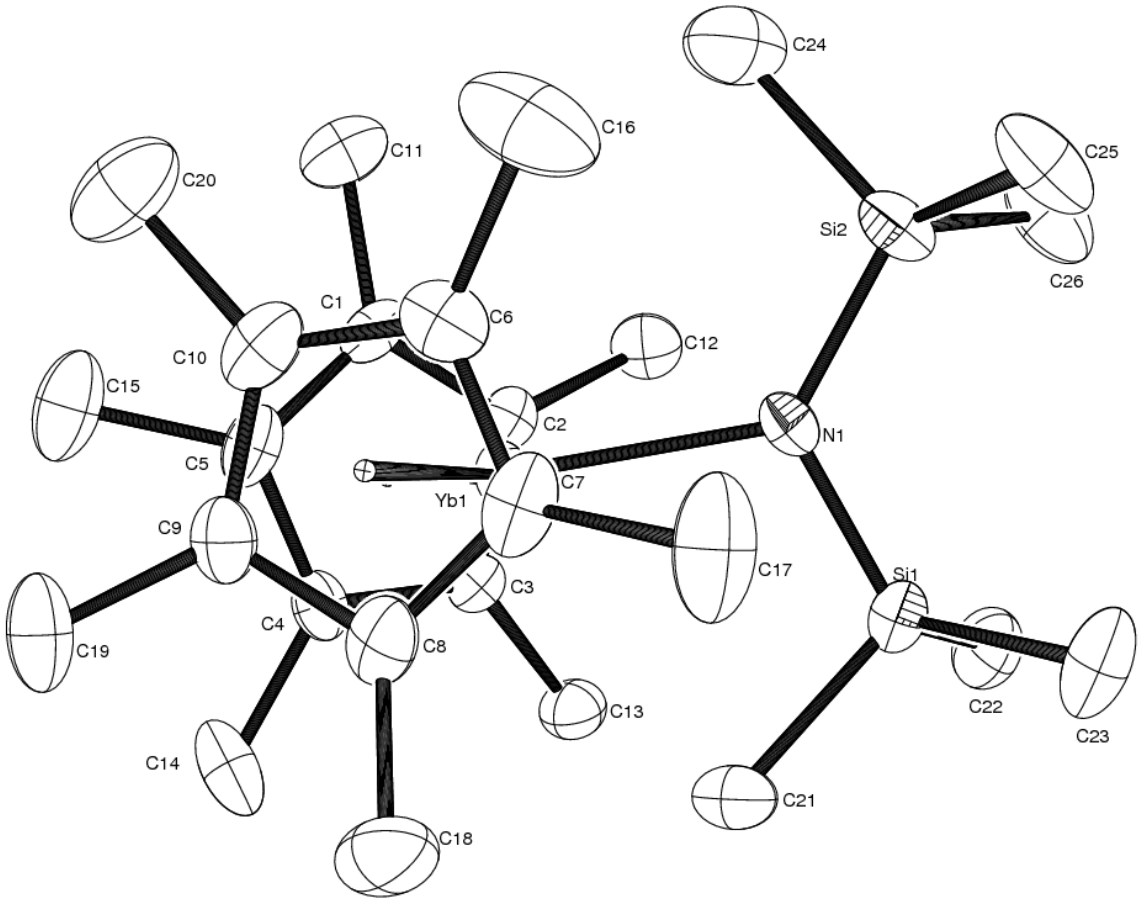

Figure 1.3.5: ORTEP diagram of one molecule of $Cp^*_2YbN(SiMe_3)_2$ of the two in the asymmetric unit (50% probability ellipsoids). All non-hydrogen atoms are refined anisotropically. Hydrogen atoms are placed and not refined and are not shown.

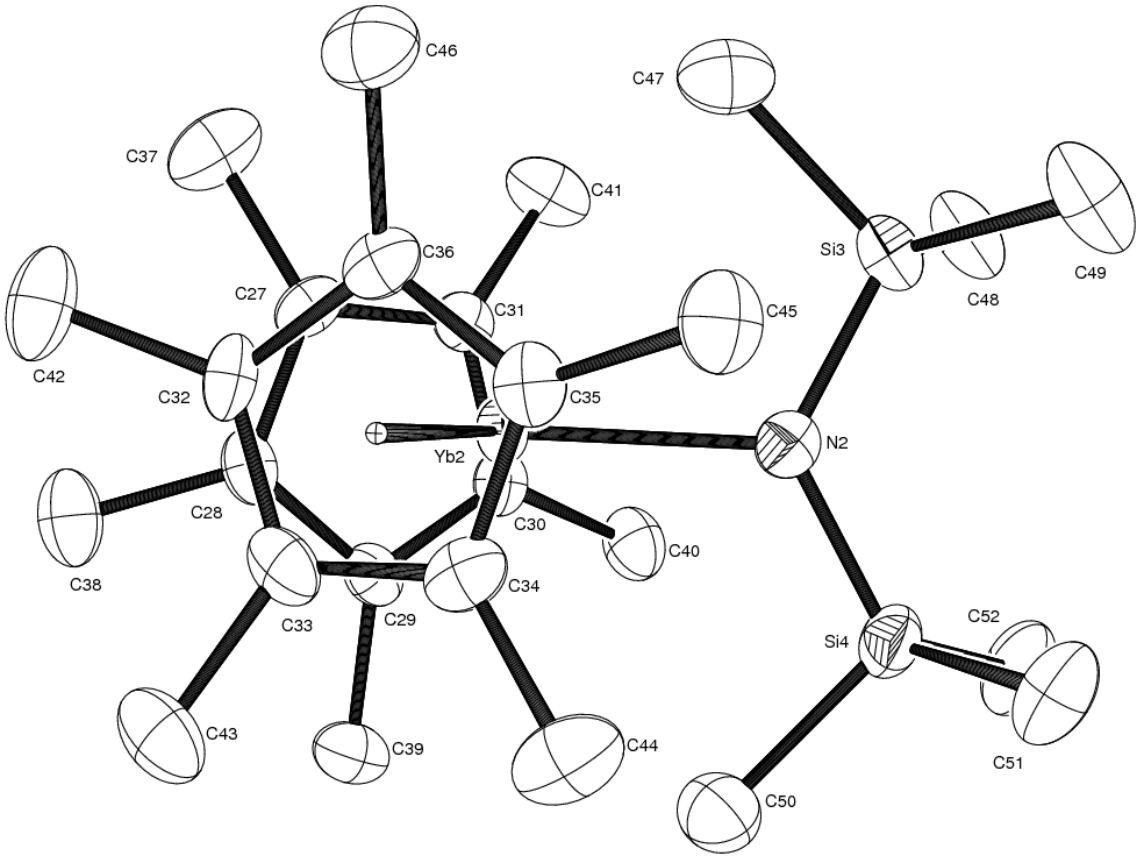

Figure 1.3.6: ORTEP diagram of the other molecule of $Cp^*_2YbN(SiMe_3)_2$ of the two in the asymmetric unit (50% probability ellipsoids). All non-hydrogen atoms are refined anisotropically. Hydrogen atoms are placed and not refined and are not shown.

Table 1.3.3: Selected bond distances (Å) in $Cp^*_2YbN(SiMe_3)_2$

atom	atom	distance		atom	atom	distance
Yb(1)	N(1)	2.228(4)		Yb(1)	C(1)	2.617(5)
Yb(1)	C(2)	2.638(4)		Yb(1)	C(3)	2.654(4)
Yb(1)	C(4)	2.652(5)		Yb(1)	C(5)	2.650(5)
Yb(1)	C(6)	2.602(5)		Yb(1)	C(7)	2.603(4)
Yb(1)	C(8)	2.639(5)		Yb(1)	C(9)	2.690(5)
Yb(1)	C(10)	2.659(5)		Yb(1)	C(101)	2.3536(2)
Yb(1)	C(102)	2.35		Yb(2)	N(2)	2.21
Yb(2)	C(27)	2.644(5)		Yb(2)	C(28)	2.659(5)
Yb(2)	C(29)	2.621(5)		Yb(2)	C(30)	2.616(5)
Yb(2)	C(31)	2.633(5)		Yb(2)	C(32)	2.671(5)
Yb(2)	C(33)	2.644(5)		Yb(2)	C(34)	2.643(5)
Yb(2)	C(35)	2.647(5)		Yb(2)	C(36)	2.635(5)

Yb(2)	C(103)	2.35		Yb(2)	C(104)	2.36
Yb(1)	C(21)	3.022(6)		Yb(1)	C(24)	3.759(6)
Yb(2)	C(47)	3.233(6)		Yb(2)	C(50)	3.405(6)

Table 1.3.4: Selected bond angles (°) in $Cp^*_2YbN(SiMe_3)_2$

atom	atom	atom	angle		Atom	atom	atom	angle
C(101)	Yb(1)	C(102)	132.4		C(103)	Yb(2)	C(104)	132.6
Yb(1)	N(1)	Si(1)	109.7(2)		Yb(1)	N(1)	Si(2)	128.3(2)
Yb(2)	N(2)	Si(3)	115.9(2)		Yb(2)	N(2)	Si(4)	120.0(2)
N(1)	Si(1)	C(21)	106.8(2)		N(1)	Si(2)	C(25)	114.3(3)
N(2)	Si(3)	C(47)	106.7(2)		N(2)	Si(4)	C(50)	107.8(2)

The basicity of the $N(SiMe_3)_2$ group is such that $Cp^*_2CeN(SiMe_3)_2$ abstracts a proton from many amines to form $HN(SiMe_3)_2$, pKa ≈ 26, and the corresponding cerium compound. For instance, addition of 1,2-diaminobenzene to $Cp^*_2CeN(SiMe_3)_2$ forms Cp^*_2Ce(1-amido-2-aminobenzene) (Figure 1.3.7). (1,3-di-tert-butylcyclopentadienyl)$_2$Ce(1-amido-2-aminobenzene) is synthesized from (1,3-di-tert-butylcyclopentadienyl)$_2$CeN$(SiMe_3)_2$ in an analogous manner.

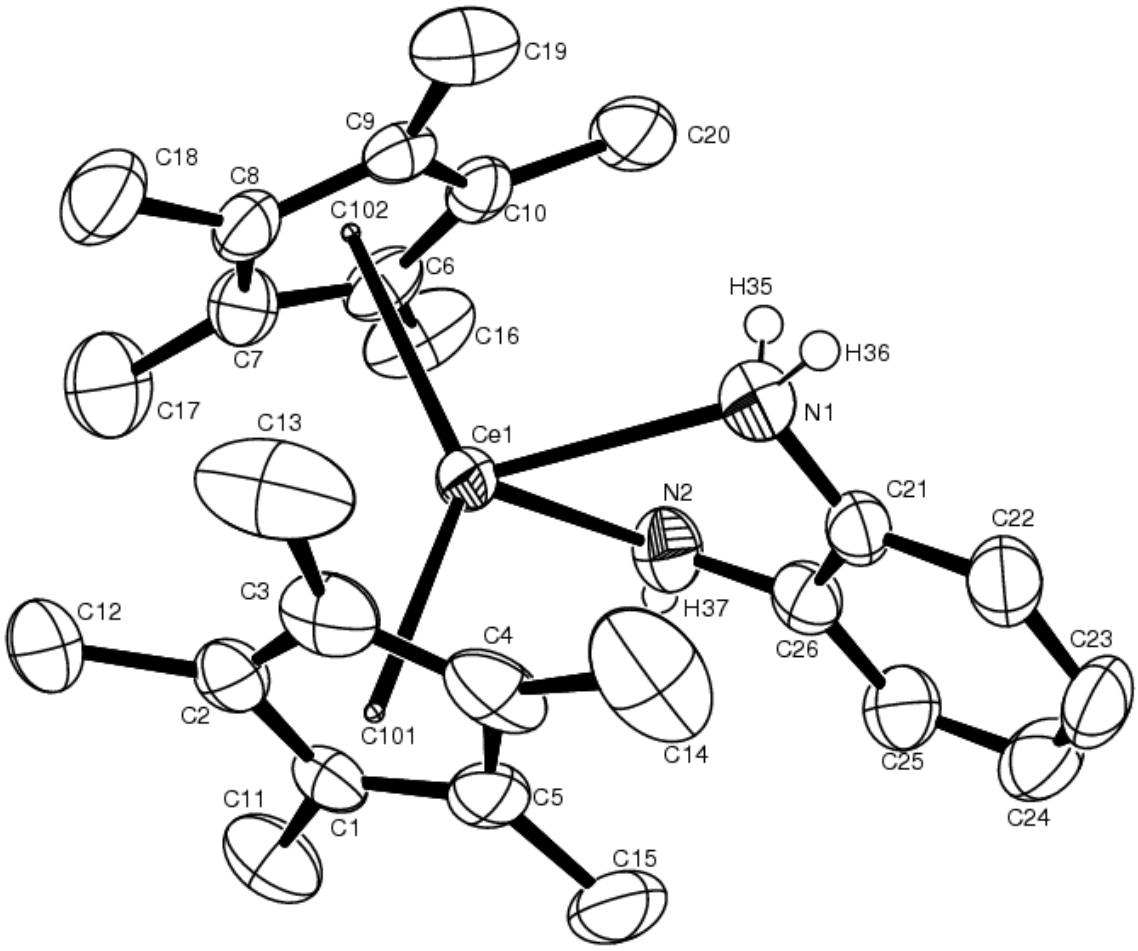

Figure 1.3.7: ORTEP diagram of Cp^*_2Ce(1-amido-2-aminobenzene) (50% probability ellipsoids). All non-hydrogen atoms are refined anisotropically. Hydrogen atoms other than the N-H hydrogens, which are found in the Fourier difference map and refined isotropically, are not shown. Selected bond distances and angles are given in Tables 1.3.5 and 1.3.6 respectively.

Table 1.3.5: Selected bond distances (Å) in Cp^*_2Ce(1-amido-2-aminiobenzene)

Atom	Atom	Distance		Atom	Atom	Distance
Ce(1)	N(1)	2.55(1)		Ce(1)	N(2)	2.43(1)
Ce(1)	C(1)	2.76(1)		Ce(1)	C(2)	2.79(1)
Ce(1)	C(3)	2.80(1)		Ce(1)	C(4)	2.80(1)
Ce(1)	C(5)	2.80(1)		Ce(1)	C(6)	2.81(1)
Ce(1)	C(7)	2.80(1)		Ce(1)	C(8)	2.79(1)
Ce(1)	C(9)	2.774(10)		Ce(1)	C(10)	2.79(1)
Ce(1)	C(101)	2.513		Ce(1)	C(102)	2.513
N(1)	C(21)	1.44(2)		N(2)	C(26)	1.38(2)
N(1)	H(35)	0.9(1)		N(1)	H(36)	0.8(1)
N(2)	H(37)	0.8(1)				

Table 1.3.6: Selected bond angles (°) in Cp^*_2Ce(1-amido-2-aminobenzene)

Atom	Atom	Atom	Angle		Atom	Atom	Atom	Angle
N(1)	Ce(1)	N(2)	66.0(4)		C(101)	Ce(1)	C(102)	136.7
Ce(1)	N(1)	C(21)	107.1(7)		Ce(1)	N(2)	C(26)	113.0(8)
Ce(1)	N(1)	H(35)	110(7)		Ce(1)	N(1)	H(36)	132(8)
C(21)	N(1)	H(35)	102(7)		C(21)	N(1)	H(36)	93(9)
H(35)	N(1)	H(36)	106(11)		Ce(1)	N(2)	H(37)	127(8)
C(26)	N(2)	H(37)	109(8)					

The variable-temperature ^{1}H NMR plot (Figure 1.3.8) shows only one Cp* resonance in temperature range 180-373 °C, whereas there are six individual protons visible on the 1-amido-2-aminobenzene fragment, implying that the amine proton is not shifting from one nitrogen to the other on the ^{1}H NMR time scale. The compound has averaged C_s symmetry. The resonances corresponding to the NH and NH_2 have slight curvature when plotted against 1/T. One physical process that could account for this is the inversion of the geometry around the two nitrogen atoms leading to a reversal in the direction of the ring.

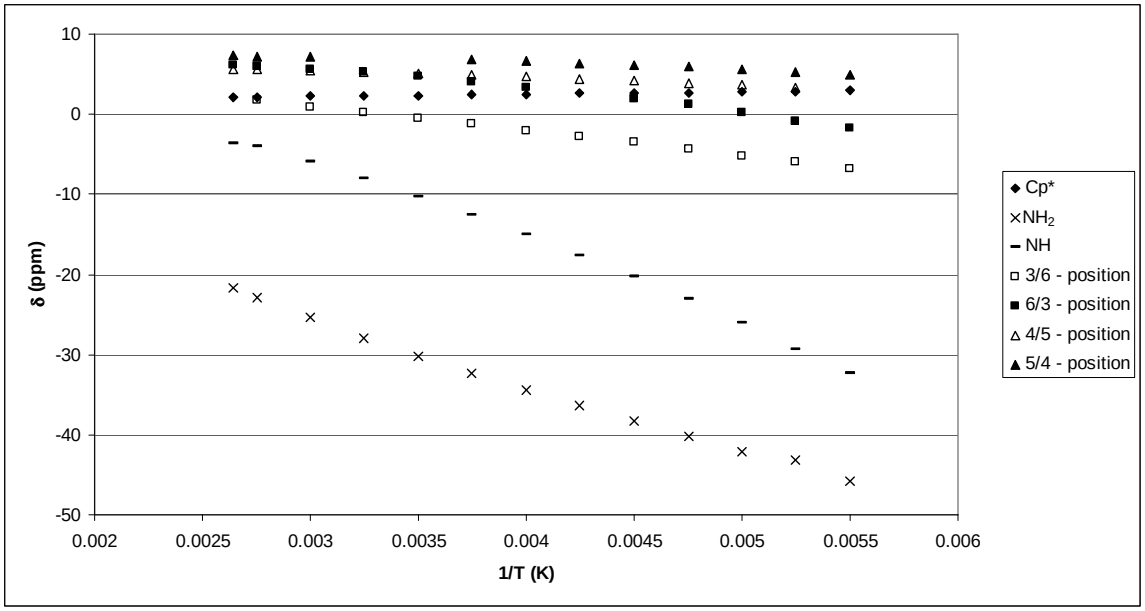

Figure 1.3.8: Variable-temperature ^{1}H NMR spectra represented as a δ vs. 1/T plot of Cp*$_2$Ce(1-amido-2-aminobenzene) in toluene-d_8. The peak labeled 5/4 is hidden by the solvent peak between 280 and 310 K.

Cp*$_2$Ce(1-amido-2-amino-benzene) decomposes at 150 °C as a solid, and at 60 °C in toluene. Even at room temperature, Cp*$_2$Ce(1-amido-2-amino-benzene) decomposes slowly ($t_{1/2}$ = 21 days in C_6D_6). (1,3-ditbutyl-cyclopentadiene) $_2$Ce(1-amido-2-amino-benzene) is formed from (1,3-ditbutyl-cyclopentadiene) $_2$CeN(SiMe$_3$)$_2$ and 1,2-diaminobenzene in good yield. The ^{1}H NMR spectrum shows that the amine proton is not shifting from one nitrogen to the other. The pure solid decomposes at 107 °C.

1.4 Synthesis and Properties of Cp^*_2LnOTf (Ln = La, Sm, Gd, Yb)

The utility of $Cp^*_2Ce(OTf)$ as a starting material led us to attempt to synthesize other metallocene derivatives of this type. Decamethylmagnesocene does not react with $Sm(OTf)_3$ in THF at room temperature or at reflux, but it does react in refluxing di-n-butylether to form $Cp^*_2Sm(OTf)$(n-butyl ether), when heated at reflux for two weeks. Recrystallization from diethyl ether gives the base-free $Cp^*_2Sm(OTf)$. The ^1H and ^{19}F NMR spectra each show a single peak. Cp^*_2SmOTf in toluene does not react with sodium amalgam in mercury and it does not even react when potassium is added to the mixture. $Cp^*_2Gd(OTf)$ is synthesized in a similar manner. Unfortunately, $La(OTf)_3$ and $Yb(OTf)_3$ do not react with Cp^*_2Mg or with NaCp* in THF or n-butyl ether at room temperature or at reflux. However, they react with Cp^*_2Mg in a 1:10 pyridine/toluene mixture to give Cp^*_2LnOTf(pyridine). In the case of Yb, the yield is good (90%), but in the case of La, it is poor (about 20%). This synthetic method also works with dry $Sm(OTf)_3$ to produce $Cp^*_2Sm(OTf)$(pyridine) in good yield (75 %).

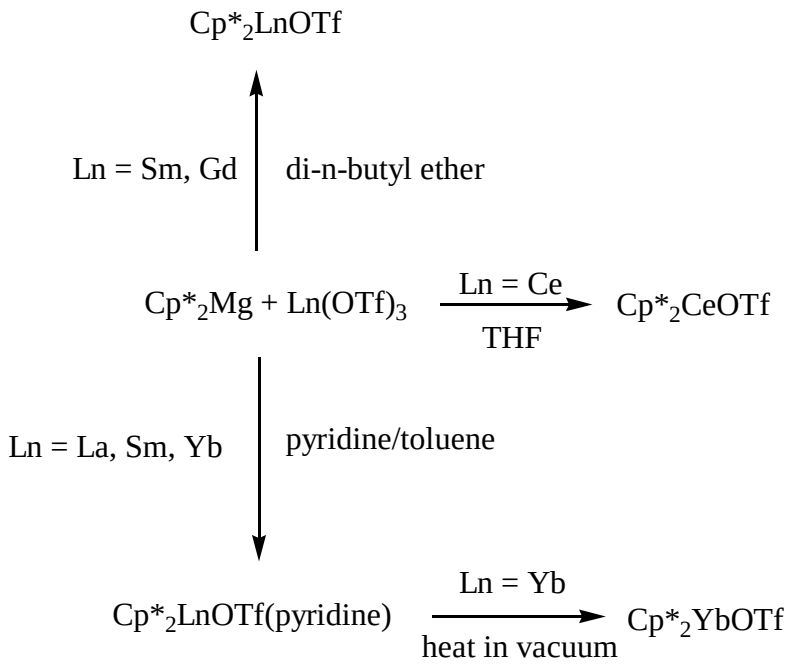

Scheme 1.4.1: Synthesis of $Cp^*_2Ln(OTf)$ starting from Cp^*_2Mg and $Ln(OTf)_3$

The room-temperature ^1H NMR spectrum of $Cp^*_2Yb(OTf)(pyridine)$ only shows the resonances due to the Cp* ligand and the para-H position of pyridine, since these resonances appear in a 30:1 area ratio, respectively. The resonances due to the ortho-H's are not observed in the temperature range 190-363 K. At lower temperature (T < 286K), two new peaks of area one appear, presumably due to the meta-H resonances. The temperature dependence of the resonances is shown in Figure 1.4.1.

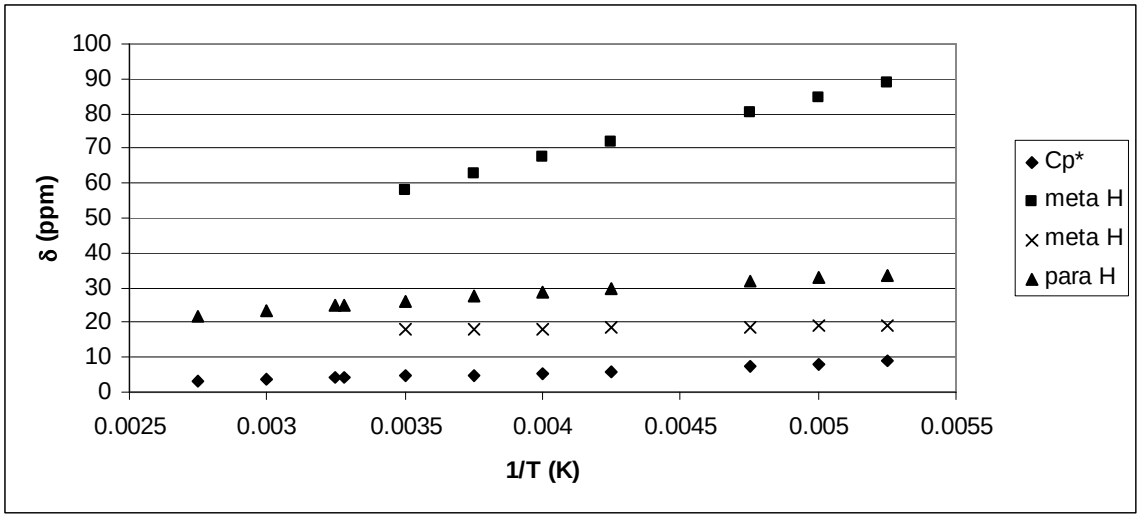

Figure 1.4.1: Variable-temperature ^{1}H NMR spectra represented as a δ vs. 1/T plot of $Cp^*_2Yb(OTf)(pyridine)$ in toluene-d_8.

The implication of the variable-temperature NMR plot is that at temperatures below 286 K the pyridine is not free to rotate and, therefore, the two protons in the meta position are not equivalent. At room temperature, the pyridine must be rotating on the NMR time scale and, therefore, the peaks are broadened to the extent that they are not visible. If the temperature is raised, pyridine should rotate faster, and the ^{1}H NMR spectrum will contain two averaged peaks, each of area two. However, this does not happen below the boiling point of toluene and, therefore, this explanation could not be experimentally verified. This explanation also requires that on the NMR time scale the equilibrium illustrated in equation 2 is completely to the left-hand side,

$$Cp^*_2Yb(OTf)(pyridine) \rightleftharpoons Cp^*_2Yb(OTf) + pyridine \qquad (2)$$

otherwise, the two meta-H's would be indistinguishable. Addition of deuterated pyridine does not affect the chemical shift of the para-H, although over a period of time the peak

begins to lose intensity, implying that there is chemical exchange, but not on the NMR time scale, equation 3.

$$Cp^*_2Yb(OTf)(C_5H_5N) + C_5D_5N \rightleftharpoons Cp^*_2Yb(OTf)(C_5D_5N) + C_5H_5N \qquad (3)$$

To verify this hypothesis, dmap (dmap = 4-dimethylaminopyridine) was added to $Cp^*_2Yb(OTf)$(pyridine) to form $Cp^*_2Yb(OTf)$(dmap) and pyridine. In the ^1H NMR spectrum (Figure 1.4.2), the two peaks of area 3, due to the dmap methyl groups, disappear at T>250 K, and reappear as a single peak of area 6 at 305K. Two of the dmap resonances, presumably the ortho-H's, are not be located, although a broad peak is observed around -5 ppm.

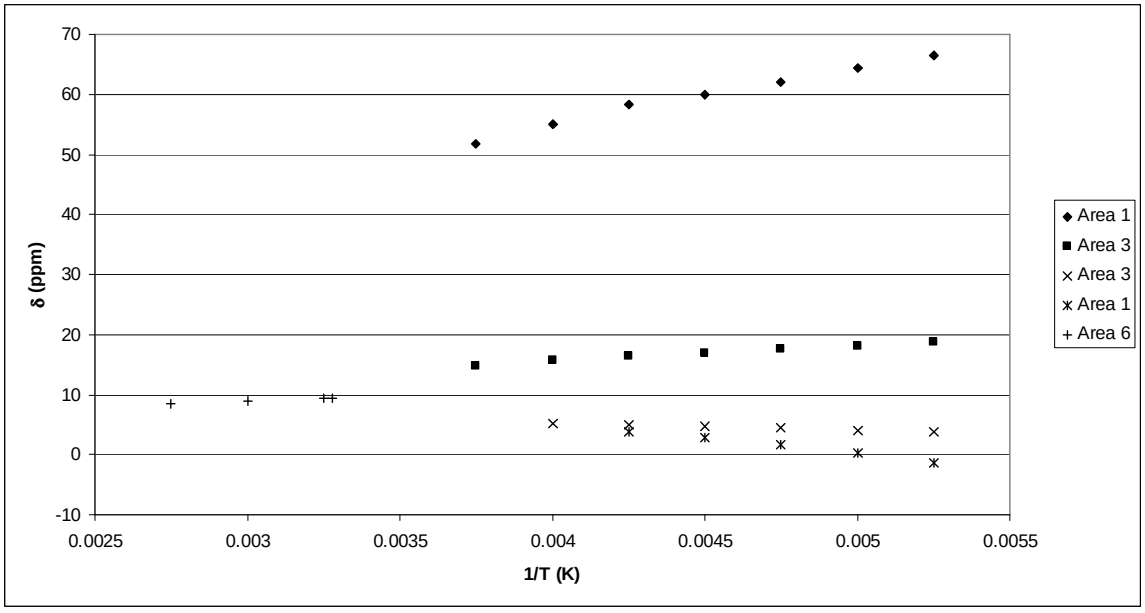

Figure 1.4.2: Variable-temperature ^1H NMR δ vs. 1/T plot of $Cp^*_2Yb(OTf)$(4-dimethylaminopyridine) in toluene-d_8. The Cp* resonance, which is essentially independent of temperature, has been omitted for clarity.

From the coalescence temperature, the free energy of rotation is calculated to be $\Delta G^{\ddagger} = 11.8 \pm 0.2$ kcal mol^{-1} using formula I

$$\Delta G^{\ddagger} = -RT_c [\ln(K/T_c) + \ln(h/k)] \qquad (I)$$

in kcal mol^{-1} where $K = \pi * \delta\nu/\sqrt{2}$, $\delta\nu$ is the separation of the resonances in Hz at the coalescence, T_C is the coalescence temperature in K (286 K), h is Planck's constant, and k is Boltzmann's constant.[12,13] The error in $\Delta G^{\ddagger}$ was estimated to be $\pm$ 0.2 kcal mol^{-1} assuming an error of $\pm$ 5 K in estimation of T_C.

Base-free Cp*$_2$Yb(OTf) is obtained by heating Cp*$_2$Yb(OTf)(pyridine) at 150° C for a week under dynamic vacuum (10^{-3} – 10^{-4} Torr). In THF-d_8, the ^{1}H NMR spectrum consists of a single peak at all temperatures. In CD_2Cl_2 and toluene-d_8, at room temperature there is also only one Cp* peak in the ^{1}H NMR spetrum. However, at low temperatures, there are two Cp* peaks (Figure 1.4.3 and Figure 1.4.4). From the coalescence temperature, the free energy of activation is calculated to be $\Delta G^{\ddagger}(T_c = 293$ K) = 12.4 $\pm$ 0.1 kcal mol^{-1} in CD_2Cl_2 and $\Delta G^{\ddagger}(T_c = 288$ K) 12.3 $\pm$ 0.1 kcal mol^{-1} in toluene-d_8 (assuming an error of $\pm$ 2 K in T_c).

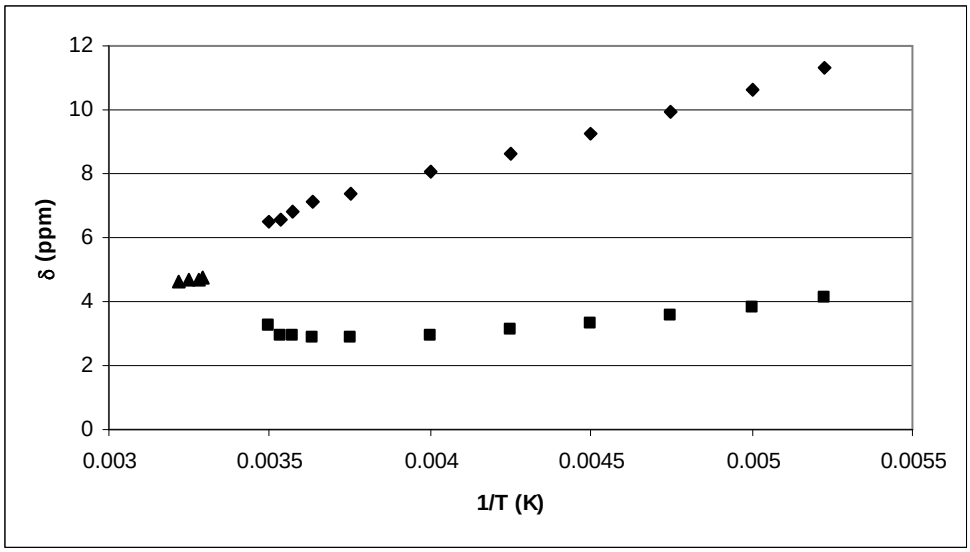

Figure 1.4.3: Variable-temperature ^{1}H NMR data shown as a plot of δ vs. 1/T for $Cp^*_2Yb(OTf)$ in CD_2Cl_2.

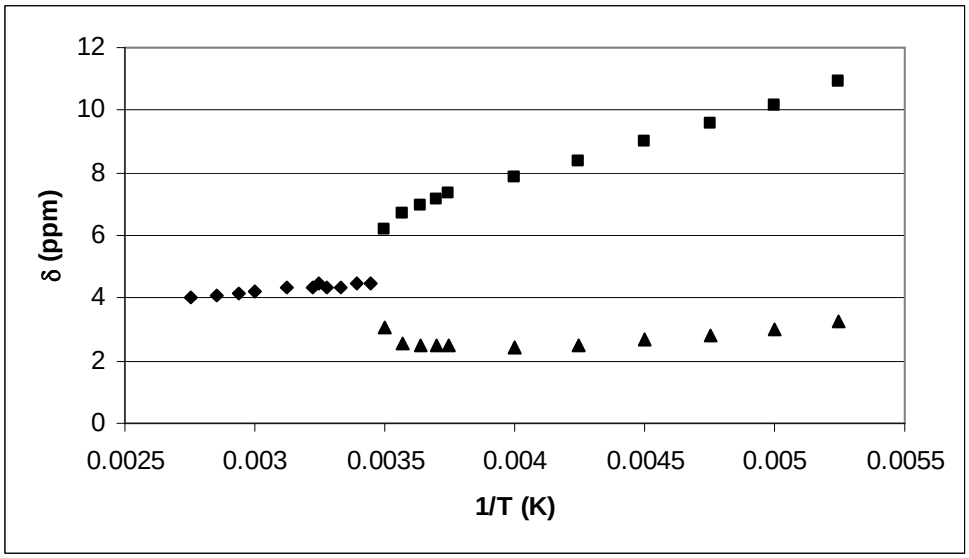

Figure 1.4.4: Variable-temperature ^{1}H NMR data shown as a plot of δ vs. 1/T for $Cp^*_2Yb(OTf)$ in toluene-d_8.

The process giving rise to the inequivalent Cp* resonances is unclear. At temperatures above about 285 K, the C_5Me_5 resonances are equivalent, consistent with a molecule with averaged C_{2v} symmetry. At lower temperatures, the Cp* resonances are inequivalent, implying that the mirror plane and the C_2-axis containing the triflate group are removed and the molecule has C_s or even C_1 symmetry. The physical processes could be due to an equilibrium between inner-sphere and outer-sphere triflate, but changing the dielectric constant of the solvent should have a larger effect on the activation energy than observed; the two activation energies are within experimental error of each other. In addition, nonlinearity is expected in the triflate peak in the ^{19}F NMR δ vs. 1/T plot, which is not observed (Figure 1.4.5). Another physical process could be bidentate and monodentate triflate coordination, but again the ^{19}F NMR δ vs. 1/T plot will be nonlinear. However, it is possible that the chemical shift difference in the ^{19}F NMR spectra between monodentate and bidentate triflate is small relative to the natural linewidth in the paramagnetic complex resulting in the appearance of a single resonance that is linear in 1/T, i.e., it follows the Curie law.

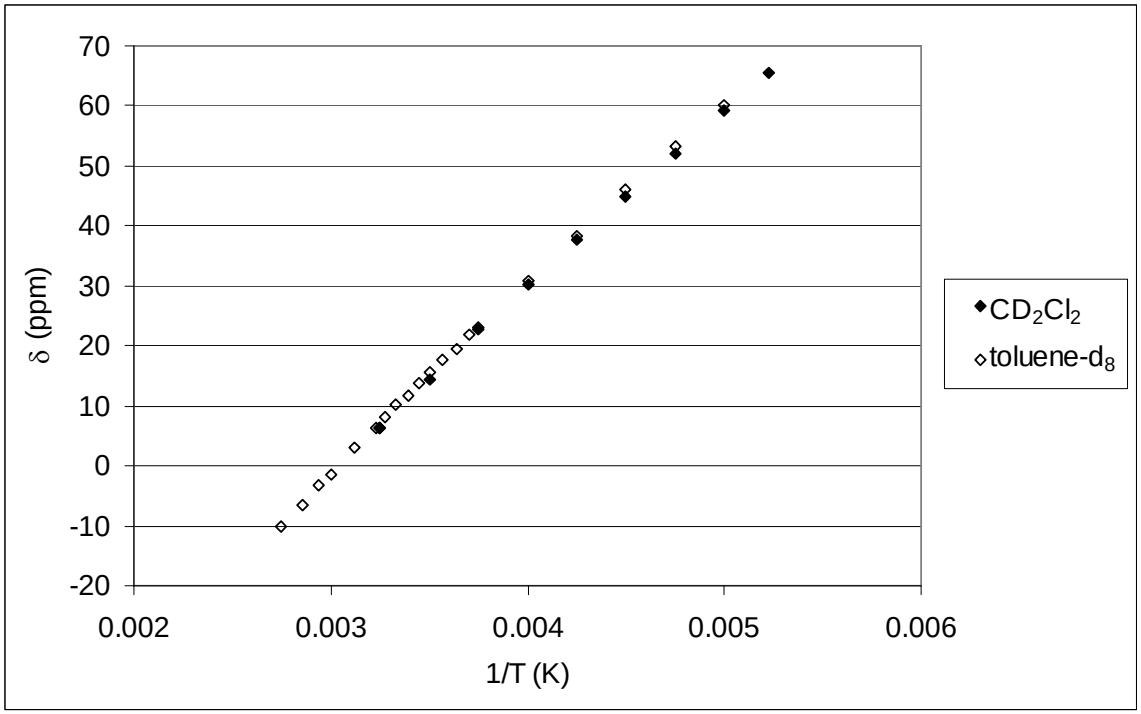

Figure 1.4.5: Variable-temperature ^{19}F NMR δ vs. 1/T plot of $Cp^*_2Yb(OTf)$ in CD_2Cl_2 and toluene-d_8.

1.5 Synthesis and Properties of $[NR_4][Cp^*_2LnOTf_2]$

In order to determine if bound triflate exchanges with free triflate in $Cp^*_2Ce(OTf)$, NMe_4OTf was added to a solution of $Cp^*_2Ce(OTf)$ in C_6D_6. Interestingly, a yellow compound formed, and therefore this reaction was repeated on a synthetic scale in toluene. The toluene was removed, and the yellow powder was dissolved in CH_2Cl_2 and crystallized by layering with pentane. The ^1H NMR spectrum shows two resonances in a 12:30 ratio due to NMe_4 and Cp*, indicating a 1:1 coordination compound. A single crystal X-ray diffraction study gives the ORTEP diagram shown in Figure 1.5.1.

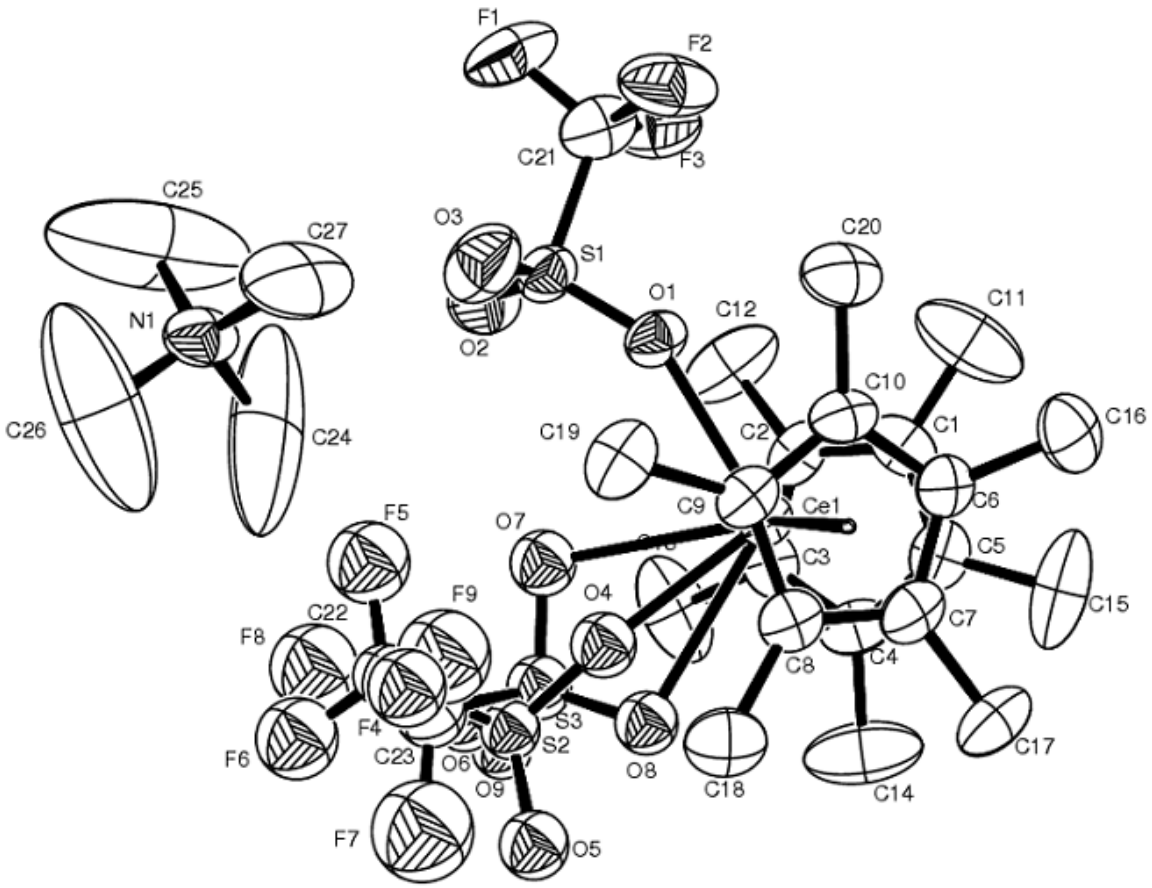

Figure 1.5.1: ORTEP diagram of $[NMe_4][Cp^*_2Ce(OTf)_2]$ (50% probability ellipsoids). All non-hydrogen atoms except for those belonging to the disordered triflate are refined anisotropically. Hydrogen atoms are placed and not refined. Hydrogen atoms and toluene of crystallization are not shown. One of the OTf groups is monodentate, while the other OTf is disordered between monodentate and bidentate binding modes; the disordered OTf is modeled with a 60% occupancy for the monodentate OTf and a 40% occupancy for the bidentate OTf, and the disordered triflate was refined isotropically. The closest cation-anion contact of 3.09(1) Å is between O(6) and C(25). Selected bond distances and angles are given in Tables 1.5.1 and 1.5.2, respectively.

Table 1.5.1: Selected bond distances (Å) in $[NMe_4][Cp^*_2Ce(OTf)_2]$.

Atom	Atom	Distance (Å)		Atom	Atom	Distance (Å)
Ce(1)	O(1)	2.440(4)		Ce(1)	O(4)	2.351(8)
Ce(1)	O(7)	2.74(1)		Ce(1)	O(8)	2.70(1)
Ce(1)	C(1)	2.761(6)		Ce(1)	C(2)	2.803(6)
Ce(1)	C(3)	2.804(6)		Ce(1)	C(4)	2.779(6)
Ce(1)	C(5)	2.764(6)		Ce(1)	C(6)	2.794(5)
Ce(1)	C(7)	2.794(5)		Ce(1)	C(8)	2.792(5)
Ce(1)	C(9)	2.769(5)		Ce(1)	C(10)	2.757(6)
Ce(1)	C(100)	2.51		Ce(1)	C(101)	2.51

Table 1.5.2: Selected bond angles (^{o}) in $[NMe_4][Cp^*_2Ce(OTf)_2]$

atom	atom	Atom	angle(^{o})		atom	atom	Atom	angle(^{o})
O(1)	Ce(1)	O(4)	96.3(2)		O(1)	Ce(1)	O(7)	70.3(3)
O(1)	Ce(1)	O(8)	118.3(2)		O(7)	Ce(1)	O(8)	50.0(3)
C(101)	Ce(1)	C(102)	134.4					

The crystal structure of $[NMe_4][Cp^*_2Ce(OTf)_2]$ has one triflate group in a monodentate binding mode and one that is disordered between a monodentate and a bidentate binding mode. The implication of this is that the free-energy change between the two modes of triflate binding in $[Cp^*_2Ce(OTf)_2]^-$, when the other triflate is bound in a monodentate manner, is small.

In order to examine the effects that the alkyl groups have on the ion-pair formation, two larger tetraalkylammonium salts are also prepared by addition of NEt_4OTf and NBu_4OTf to Cp^*_2CeOTf. The tetraethylammonium salt, $[NEt_4][Cp^*_2Ce(OTf)_2]$, is prepared in a manner similar to that for $[NMe_4][Cp^*_2Ce(OTf)_2]$ (Figure 1.5.2). However, $[NBu_4][Cp^*_2Ce(OTf)_2]$ forms an oil when it is dissolved in CH_2Cl_2 and layered with pentane. Analytically pure $[NBu_4][Cp^*_2Ce(OTf)_2]$ is prepared by stirring $Cp^*_2Ce(OTf)$ with a stoichiometric amount of NBu_4OTf in toluene, removing the toluene under dynamic vacuum, and then washing the resulting solid with pentane.

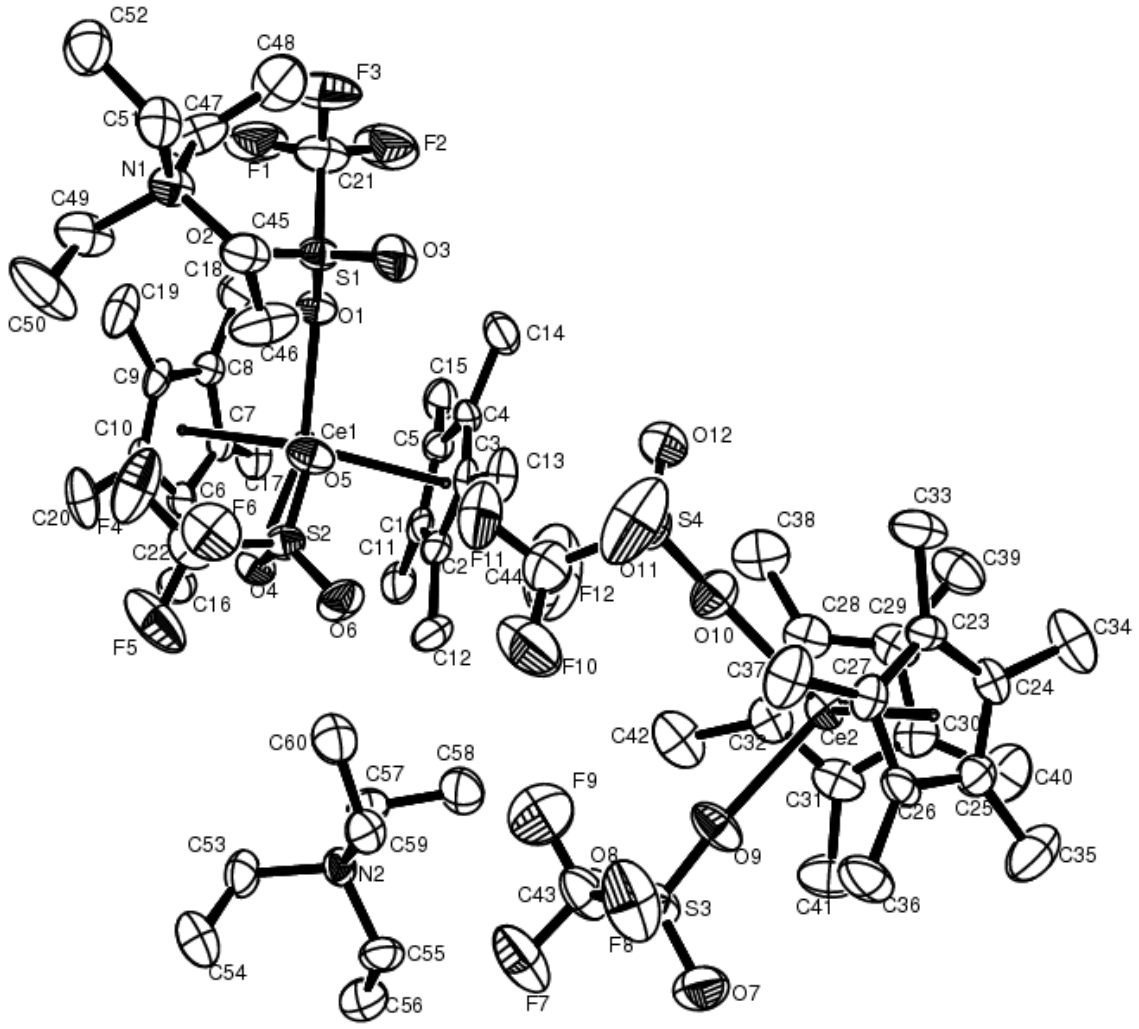

Figure 1.5.2: ORTEP diagram of $[NEt_4][Cp^*_2Ce(OTf)_2]$ showing two independent molecules in the unit cell (50% probability ellipsoids). All non-hydrogen atoms are refined anisotropically. Hydrogen atoms are placed and not refined. Hydrogen atoms and toluene of crystallization are not shown. The closest cation-anion contact of 3.292(7) Å is between O(6) and C(57). Selected bond distances and angles are given in Tables 1.5.3 and 1.5.4, respectively.

Table 1.5.3: Selected bond distances (Å) in $[NEt_4][Cp^*_2Ce(OTf)_2]$

Atom	Atom	Distance (Å)		Atom	Atom	Distance (Å)
Ce(1)	O(1)	2.431(4)		Ce(1)	O(4)	2.599(4)
Ce(1)	O(5)	2.727(4)		Ce(1)	C(1)	2.773(6)
Ce(1)	C(2)	2.780(6)		Ce(1)	C(3)	2.798(6)
Ce(1)	C(4)	2.797(5)		Ce(1)	C(5)	2.768(6)
Ce(1)	C(6)	2.789(6)		Ce(1)	C(7)	2.804(6)
Ce(1)	C(8)	2.763(6)		Ce(1)	C(9)	2.786(6)
Ce(1)	C(10)	2.788(6)		Ce(1)	C(101)	2.51
Ce(1)	C(102)	2.52		Ce(2)	O(9)	2.416(4)
Ce(2)	O(10)	2.426(4)		Ce(2)	C(23)	2.758(6)
Ce(2)	C(24)	2.801(6)		Ce(2)	C(25)	2.824(6)
Ce(2)	C(26)	2.804(6)		Ce(2)	C(27)	2.764(6)
Ce(2)	C(28)	2.795(6)		Ce(2)	C(29)	2.783(7)
Ce(2)	C(30)	2.783(6)		Ce(2)	C(31)	2.752(6)
Ce(2)	C(32)	2.755(6)		Ce(2)	C(103)	2.52
Ce(2)	C(104)	2.50				

Table 1.5.4: Selected bond angles (^{o}) in $[NMe_4][Cp^*_2Ce(OTf)_2]$

atom	atom	Atom	Angle (^{o})		atom	atom	atom	Angle (^{o})
O(1)	Ce(1)	O(4)	122.0(1)		O(1)	Ce(1)	O(5)	72.6(1)
O(4)	Ce(1)	O(5)	52.5(1)		C(101)	Ce(1)	C(102)	132.5
O(9)	Ce(2)	O(10)	91.7(2)		C(103)	Ce(2)	C(104)	133.9
O(4)	S(2)	O(5)	109.0(3)					

The tetraethylammonium salt, $[NEt_4][Cp^*_2Ce(OTf)_2]$, crystallizes with two molecules in the asymmetric unit; one molecule has both triflates bound as monodentate ligands and the other molecule has one bidentate and one monodentate triflate ligand. This, again, implies that the free-energy difference between the two modes of triflate binding in $[Cp^*_2Ce(OTf)_2]^-$, when the first is bound monodentate, is small. In contrast to what is found in the crystal of $[NMe_4][Cp^*_2Ce(OTf)_2]$, where the small free-energy difference is expressed in a disorder in the binding mode of one of the triflates, in the tetraethylammonium salt it is expressed in their being two molecules in the asymmetric unit, each of which has different binding modes of the triflate ligand.

The ytterbium salt, $[NEt_4][Cp^*_2Yb(OTf)_2]$, is synthesized in a manner analogous to that used to prepare the cerium analog. Variable-temperature NMR studies on $[NEt_4][Cp^*_2Ce(OTf)_2]$, $[NBu_4][Cp^*_2Ce(OTf)_2]$, and $[NEt_4][Cp^*_2Yb(OTf)_2]$ are examined in order to determine whether the triflate exchanges in solution (Figures 1.5.3, 1.5.4, and 1.55).

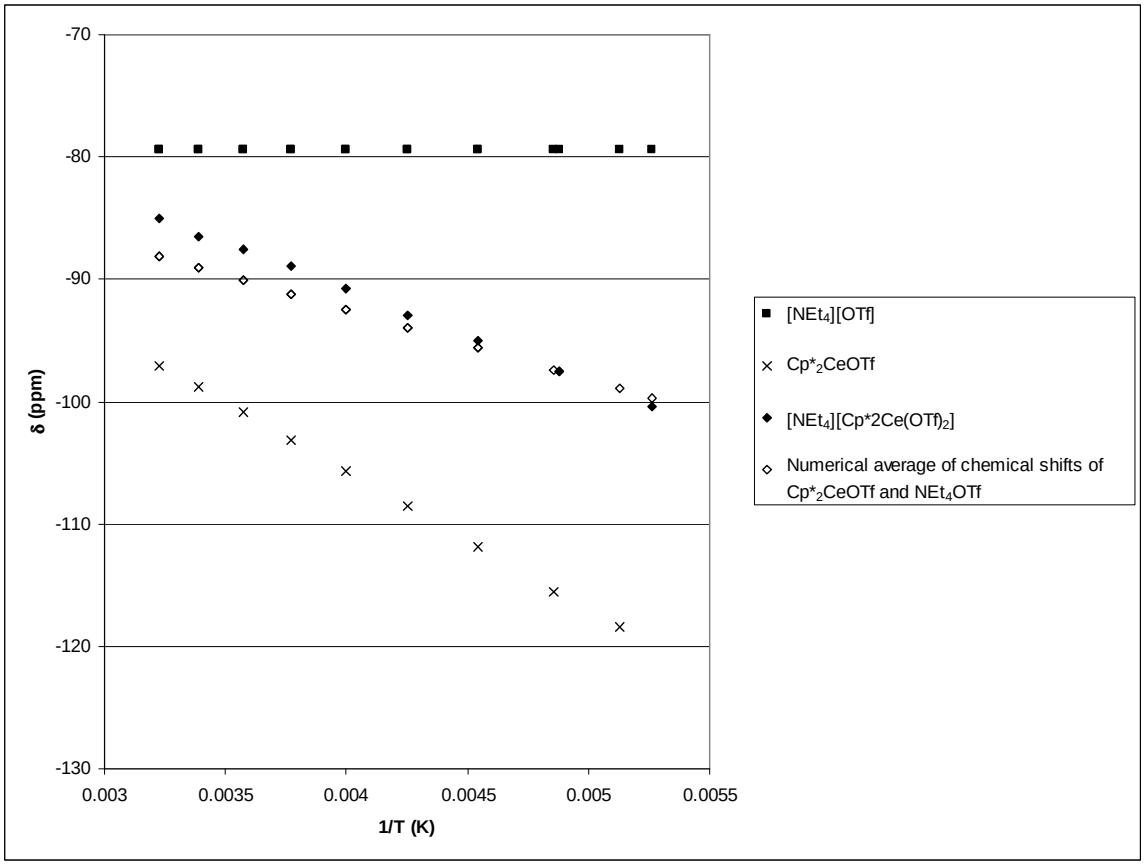

Figure 1.5.3: Variable-temperature ^{19}F NMR chemical shifts as a δ vs. 1/T plot of NEt_4OTf, $Cp^*_2Ce(OTf)$, and $[NEt_4][Cp^*_2Ce(OTf)_2]$ in CD_2Cl_2. The chemical shift of diamagnetic $[NEt_4][OTf]$ is presumed to be temperature independent. The numerical average of the chemical shifts of $Cp^*_2Ce(OTf)$ and $[NEt_4][OTf]$ is also shown.

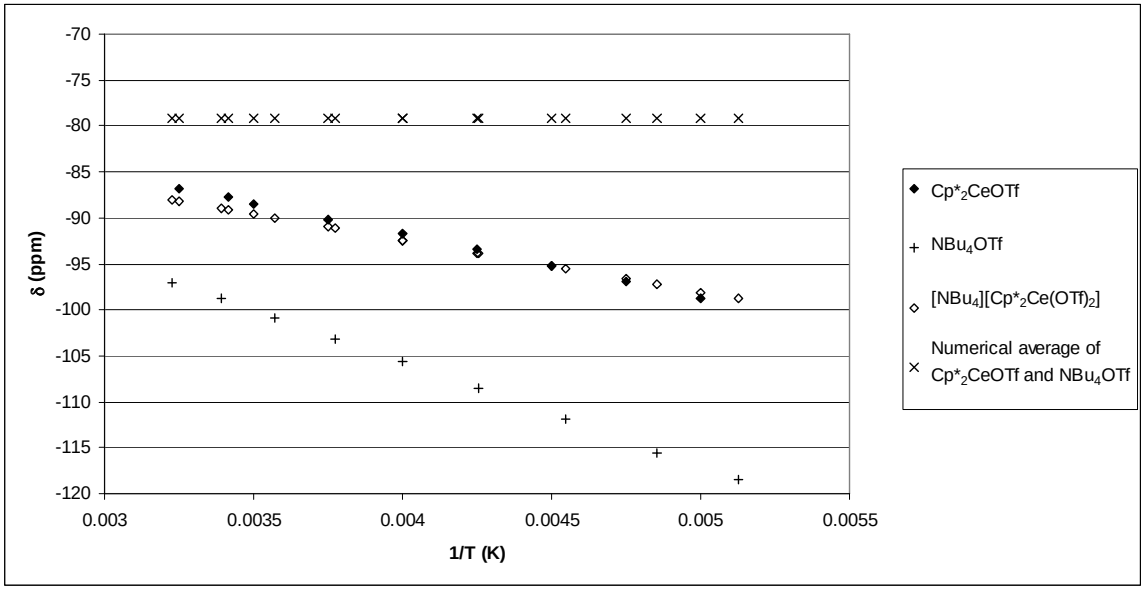

Figure 1.5.4: Variable-temperature ^{19}F NMR chemical shifts as a δ vs. 1/T plot of NBu_4OTf, $Cp^*_2Ce(OTf)$, and $[NBu_4][Cp^*_2Ce(OTf)_2]$ in CD_2Cl_2. The chemical shift of diamagnetic $[NBu_4][OTf]$ is presumed to be temperature independent. The numerical average of the chemical shifts of $Cp^*_2Ce(OTf)$ and $[NBu_4][OTf]$ is also shown.

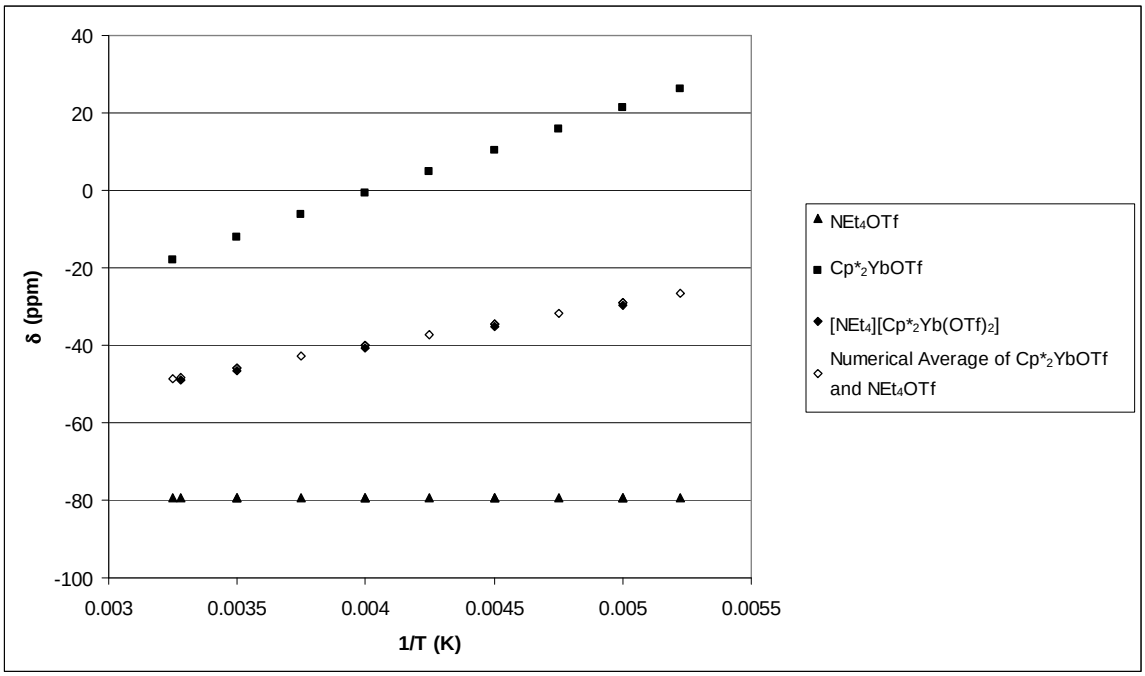

Figure 1.5.5: Variable-temperature ^{19}F NMR chemical shifts as a δ vs. 1/T plot of NEt_4OTf, $Cp^*_2Yb(OTf)$, and $[NEt_4][Cp^*_2Yb(OTf)_2]$ in CD_2Cl_2. The chemical shift of diamagnetic $[NEt_4][OTf]$ is presumed to be temperature independent. The numerical average of the chemical shifts of $Cp^*_2Yb(OTf)$ and $[NEt_4][OTf]$ is also shown.

The fact that the ^{19}F NMR chemical shifts in $[NEt_4][Cp^*_2Ce(OTf)_2]$ and $[NEt_4][Cp^*_2Ce(OTf)_2]$ are almost exactly the average of the chemical shifts of $Cp^*_2Ce(OTf)$ and $Cp^*_2Yb(OTf)$ with $[NEt_4][OTf]$ clearly shows that in solution the triflate is freely exchanging over the temperature range studied. Further addition of excess NR_4OTf shifts the ^1H and ^{19}F NMR resonances towards the values of NR_4OTf, which is also consistent with the postulate that triflate exchange is rapid.

One curious observation, however, is that the ^1H NMR peaks of all four tetraalkylammonium cations are shifted (Table 1.5.5), and they follow Curie behavior, i.e. δ vs. 1/T is linear over the temperature range 190-300 K. The variable-temperature ^1H

NMR spectra of $[NEt_4][Cp^*_2Ce(OTf)_2]$, $[NBu_4][Cp^*_2Ce(OTf)_2]$ and $[NEt_4][Cp^*_2Yb(OTf)_2]$ are shown as a δ^{iso} vs. 1/T plot in Figures 1.5.6 and 1.5.7.

R	M	H	NR_4OTf (ppm)	$[NR_4][Cp^*_2MOTf_2]$ (ppm)	Δ (ppm)
Me	Ce	α	3.279	1.605	1.674
Et	Ce	α	3.259	2.300	0.959
Et	Ce	β	1.318	0.687	0.631
Bu	Ce	α	3.156	1.843	1.313
Bu	Ce	β	1.613	0.662[1]	0.951
Bu	Ce	γ	1.412	0.829	0.583
Bu	Ce	δ	1.001	0.683	0.318
Et	Yb	α	3.259	1.766	1.494
Et	Yb	β	1.318	-0.091	1.409

Table 1.5.5: Room temperature ^{1}H NMR chemical shifts of $[NR_4][Cp^*_2Ce(OTf)_2]$ are given relative to those of $[NR_4][OTf]$. $\Delta = \delta(NR_4OTf) - \delta([NR4][Cp^*_2M(OTf)_2])$. The assignments of the NBu_4OTf peaks is made based on a 2D COSY experiment.

[1] The β-H peak is obscured at room temperature by the δ-H peak. The value shown is that obtained by extrapolation from the δ vs. 1/T plot.

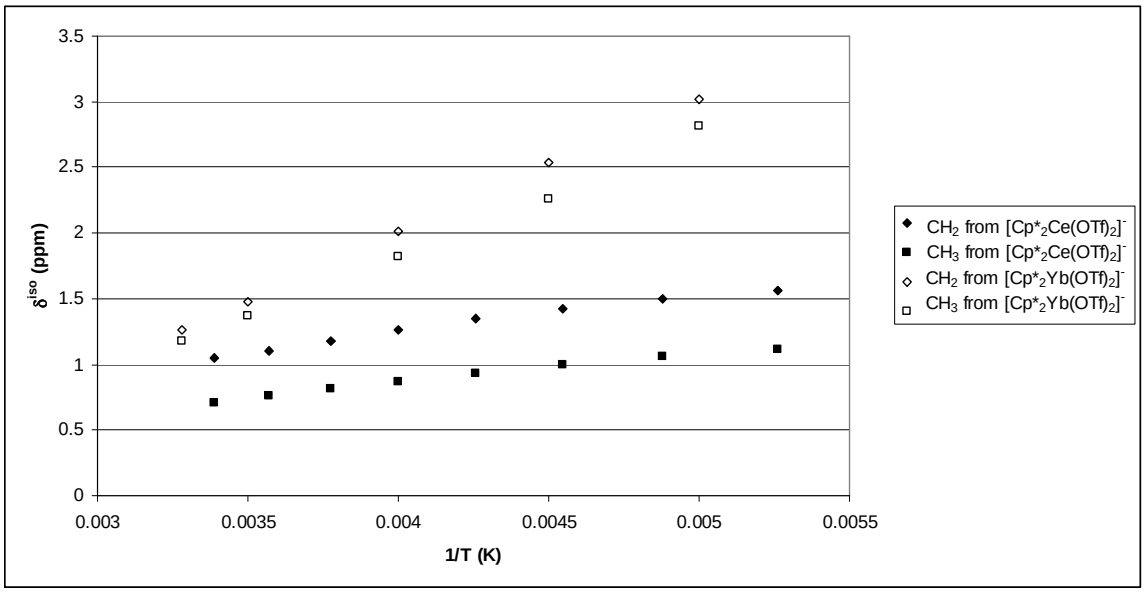

Figure 1.5.6: Variable-temperature ^{1}H NMR data shown as a plot of δ_H^{iso} ($\delta_H^{iso} = \delta_H^{dia} - \delta_H^{para}$) vs. 1/T for $[NEt_4][Cp^*_2Ce(OTf)_2]$ and $[NEt_4][Cp^*_2Yb(OTf)_2]$ in CD_2Cl_2.

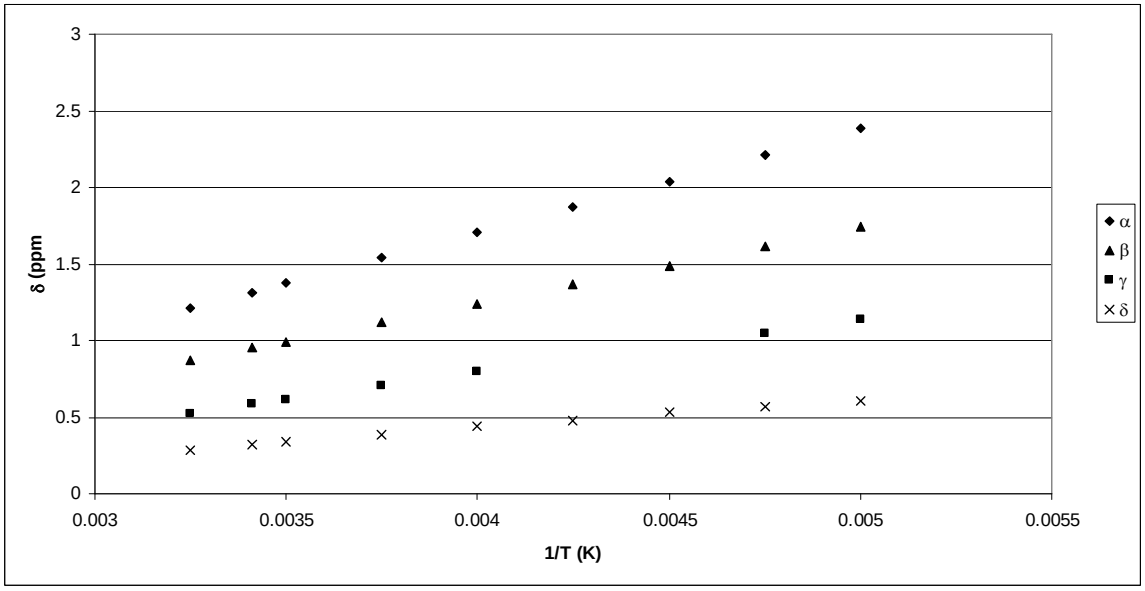

Figure 1.5.7: Variable-temperature ^{1}H NMR data shown as a plot of δ_H^{iso} ($\delta_H^{iso} = \delta_H^{dia} - \delta_H^{para}$) vs. 1/T for $[Nbu_4][Cp^*_2Ce(OTf)_2]$ in CD_2Cl_2.

The paramagnetic shift is surprising, since in the crystal structures of $[NMe_4][Cp^*_2Ce(OTf)_2]$ and $[NEt_4][Cp^*_2Ce(OTf)_2]$ show that the cations and anions are separated by greater than 3Å. To a first approximation, the ion-pairs are separated and randomly distributed in solution, which implies that the ^{1}H NMR resonances for the diamagnetic cation, in the presence of the paramagnetic anion, should not experience a shift. That this explanation is not true suggests that the anion is a lanathanide shift reagent.[14] The ^{1}H NMR resonances of tetrabutylammonium cations can experience a paramagnetic shift in the presence of some d-transition metal anions, such as $[M(PPh_3)(I_3)]^-$ and $[MX_4]^-$ where M is Co(II) or Ni(II). [15,16,17,18] Indeed, the ^{1}H NMR shifts of the tetrabutylammonium cation in the lanthanide cyclopentadienyl complex, $[NBu_4][Cp_3PrNCBH_3]$, also experience a paramagnetic shift that follows Curie law.[19]

The physical process responsible for these shifts is unclear. There are two ways a paramagnetic center can shift the NMR resonances of atoms in its vicinity. The first is through Fermi contact, which arises from the delocalization of unpaired electrons from the paramagnetic center through covalent interactions with the ligand orbitals.[20] The second is through a pseudocontact shift, which is due to direct dipolar coupling between the magnetic moment of the unpaired electrons on the paramagnetic center and the magnetic moment of the nucleus of interest.[21] Since $[R_4N]^+$ does not possesses orbitals with which to covalently bond to the paramagnetic center, a Fermi contact shift is unlikely, although some instances of Fermi contacts with $[NBu_4]$ have been reported.[17, 19]

A useful way to determine experimentally if isotropic shifts are predominantly contact or dipolar is to replace a hydrogen nucleus by a methyl group, since if the contact shift dominates the dipolar shift, the sign of δ_H^{iso} will change, since a_H and a_{Me} have

opposite signs, where a_H and a_{Me} are the electron spin-nuclear spin coupling constants.[22] If, however, the dipolar, or through space, contribution dominates, the sign of δ_H^{iso} $[N(C\underline{H}_2CH_3)_4]^+$ and $[N(CH_2C\underline{H}_3)_4]^+$ will have the same sign. Moreover, the magnitude of δ_H^{iso} for $[N(C\underline{H}_2CH_3)_4]^+$ will be larger than δ_H^{iso} of $[N(CH_2C\underline{H}_3)_4]^+$.[16] Comparing the δ_H^{iso} for $[NMe_4][Cp^*_2Ce(OTf)_2]$, $[NEt_4][Cp^*_2Ce(OTf)_2]$, $[NBu_4][Cp^*_2Ce(OTf)_2]$, and $[NEt_4][Cp^*_2Ce(OTf)_2]$ shows that all the δ_H^{iso} have the same sign, and that δ_H^{iso} for the α-Hs is larger than δ_H^{iso} for the β-Hs, which is larger than δ_H^{iso} for the γ-H, which is larger than δ_H^{iso} for the δ-H, consistent with the notion that the dipolar contribution dominates the contact contribution, as is deduced for some of the d-transition metal complexes mentioned above.

If the cation and anion are completely free to tumble independently, the dipolar shift will be zero.[23] The presence of a dipolar shift thus proves that there is a preferred orientation in solution. $[Cp^*_2Yb(OTf)_2]^-$ has two sterically bulky Cp* rings on one side of the molecule, while the other side has two negatively charged triflate groups. It seems reasonable that $[NR_4]^+$ will be able to approach the molecule from the triflate side more easily than the from the Cp* side, and therefore there should be a preferred orientation in solution, allowing for the presence of dipolar shifts.

In conclusion, several examples of Cp^*_2LnOTf have been synthesized, which are useful new precursors for other Cp^*_2LnX molecules.

References:

1. Schumann, H.; Albrecht, I.; Loebel, J.; Hahn, E.; Hossain, M. B.; van der Helm, D. *Organometallics*, **1986**, *5*, 1296
2. Schumann, H.; Meese-MarktScheffel, J.A.; Esser, L. *Chem. Rev.*, **1995**, *95*, 865
3. Andersen, R. A.; Blom, R.; Boncella, J. M.; Burns, C. J.; Volden, H. V. *Acta Chemica Scandinavica Series A-Physical and Inorganic Chemistry*, **1987**, *41*, 24
4. Heeres, H.J.; Renkema, J.; Booij, M.; Meetsma, A.; Teuben, J.H. *Organometallics*, **1988**, *7*, 2495
5. Hazin, P.N.; Lakshminarayan, C.; Brinen, L.S.; Knee, J.L.; Bruno, J.W.; Streib, W.E.; Folting, K. *Inorg. Chem.*, **1988**, *27*, 1393
6. Forsberg, J.H.; Spaziano, V. T.; Balasubramanian, T. M.; Liu, G. K.; Kinsley, S. A.; Duckworth, C. A.; Poteruca, J. J.; Brown, P. S.; Miller, J. L. *J. Org. Chem.*, **1987**, *52*, 1017
7. Shanan-Atidi, H.; Bar-Eli, K.H. *J. Chem. Phys.*, **1970**, *74*, 961. For $\Delta P = 1/3$, X = 2.086935.
8. Köhler, R.; Weiss, A.; Polzer, H.; Bischler, E. *J. Am. Chem. Soc.*, **1975**, *97*, 644.
9. Walter, M.D.; Berg, D.J.; Andersen, R.A. *Organometallics*, **2007**, *26*, 2296.
10.
11.
12. Gutowsky, H.S.; Holm, C.H. *J. Chem. Phys.*, **1956**, *25*, 1228.
13. Sandstrom, J. *Dynamic NMR Spectroscopy*; Academic Press: New York, 1982.
14. Sievers, R. *Nuclear Magnetic Resonance Shift Reagents*; Academic Press: New York, 1983.
15. La Mar, G.N. *J. Chem. Phys.*, **1964**, *41*, 2992.
16. La Mar, G.N. *J. Chem. Phys.*, **1965**, *43*, 235.
17. Walker, I. M.; Drago, R.S. *J. Am. Chem. Soc.*, **1968**, *90*, 6951.
18. Brown, D.G.; Drago, R.S. *J. Am. Chem. Soc.*, **1970**, *92*, 1871.
19. Jahn, W.; Yünlü, K.; Oroschin, W.; Amberger, H.-D.; Fischer, R.D. *Inorganica Chimica Acta*, **1984**, *95*, 85.
20. Proctor, W.G.; Yu, F.C. *Phys. Rev.*, **1950**, *77*, 717
21. Bloembergen, N.; Dickinson, W.C. *Phys. Rev.*, **1950**, *79*, 179
22. Karplus, M. *J. Am. Chem. Soc.*, **1963**, *85*, 2870.
23. McConell, H.M.; Robertson, R.E. *J. Chem. Phys.* **1958**, *29*, 1361.

Chapter 2: Synthesis of $[Cp^*_2Ln(2,2'\text{-bipyridine})]^+$ where Ln = La, Ce, Sm, Gd, Yb, and Lu, and related substituted 2,2'-Bipyridine Complexes

2.1 Introduction

The magnetic moments of molecules of the type $Cp^*_2Ln(bipy)$ are determined by three factors. The first is the relative contribution of the wave function of $Cp^*_2Ln(II)bipy$ to the wave function of $Cp^*_2Ln(III)(bipy^{\cdot-})$. For example, the magnetic moment of $Cp^*_2Eu(bipy)$ is that of a Eu(II) center because the molecule is well described as $Cp^*_2Eu(II)bipy$, where the bipy is a neutral ligand.[1] On the other hand, the magnetic moment of $Cp^*_2Yb(bipy)$ is higher than expected for diamagnetic $Cp^*_2Yb(II)(bipy)$ but lower than expected for $Cp^*_2Yb(III)(bipy^{\cdot-})$. This is at least partially a result of the fact that the total wavefunction is a mixture of the individual wavefunctions for Yb(II) and Yb(III) species, as has been shown by XANES (X-ray Absorption Near Edge Spectroscopy).[2] The second factor is how the magnetic moments of the metallocene fragment and bipy interact, since the spins can couple ferromagnetically, antiferromagnetically, or not at all. The third factor is how the paramagnetic lanthanide center interacts with the ligand field environment in an otherwise identical compound in which the ligands are neutral.

In many lanthanides, the importance of the wave function of $Cp^*_2Ln(II)bipy$ is negligible. With only a few exceptions (most notably Eu, Yb, and Sm), the +2 oxidation state in lanthanides is unstable. In cases where the oxidation state is ambiguous, XANES

(X-ray Absorption Near Edge Structure) can be used to determine the relative amount of Ln(III) and Ln(II) in the sample.

To determine how the paramagnetic lanthnide center would interact with the ligand environment in absence of the radical anion, Kahn et al. have developed an experimental way to model coupling between the magnetic moment of the lanthanide center and the unpaired spin on one ligand. Kahn et al.'s model is to compare the magnetic susceptibility, expressed in a χT versus T plot. χT is used since it is directly proportional to the magnetic moment in the following way: (a) The χT versus T plot is determined for a molecule in which the spin is localized on the metal fragment. (b) The χT versus T plot is determined for a molecule in which the spins are located on the metal fragment and on the ligand fragment. Subtraction of these curves will give these possible outcomes: (a) The spin carriers are isolated and not interacting, which will be shown by both curves being parallel. (b) The spin carriers will be ferromagnetically coupled or antiferromagnetically coupled and the subtraction will show that the slope of the difference curves will increase or decrease, respectively. This method has been applied to the question of how the paramgnetic Ln(III) center interacts with the ligand environment in $Cp^*_2Ln(III)(bipy^{\cdot -})$, and for this purpose, the magnetic moment of $[Cp^*_2Ln(III)bipy]^+$ was measured. In this chapter, the synthesis and properties of $[Cp^*_2Ln(bipy)]^+$ and of related molecules are described.

Results and Discussion

2.2 Synthesis and properties of $Cp^*_2Ce(2,2'\text{-bipyridine})(X)$ (X = OTf and halide) and substituted 2,2'-bipyridine analogues

The bipy adduct, $Cp^*_2Ce(bipy)(OTf)$, is readily synthesized by adding bipy to Cp^*_2CeOTf. The ^1H NMR spectrum at room temperature shows five resonancecs in a 30:2:2:2:2 ratio as expected for $[Cp^*_2Ce(bipy)]^+$, with C_{2v} symmetry. However, at low temperatures (T < 222 K) the ^1H NMR spectrum shows 8 peaks attributable to bipy (Figure 2.2.1), that is, each of the bipy resonancecs split into two resonances , consistent with a molecule of C_s symmetry. From the coalescence temperature of the peaks between -30 and -40 ppm, the activation energy for this process is calculated to be $\Delta G^{\ddagger}(T_c = 219$ K) = 9.2 $\pm$ 0.1 kcal mol^{-1} using formula I

I $$\Delta G^{\ddagger} = -RT_c [\ln(K/T_c) + \ln(h/k)]^{3,4}$$

Only one set of proton resonances is used to determine $\Delta G^{\ddagger}$, because one set of resonances are clearly separated from the other three sets, as is easily observed by inspection of the δ vs. 1/T plot in Figure 2.2.1.

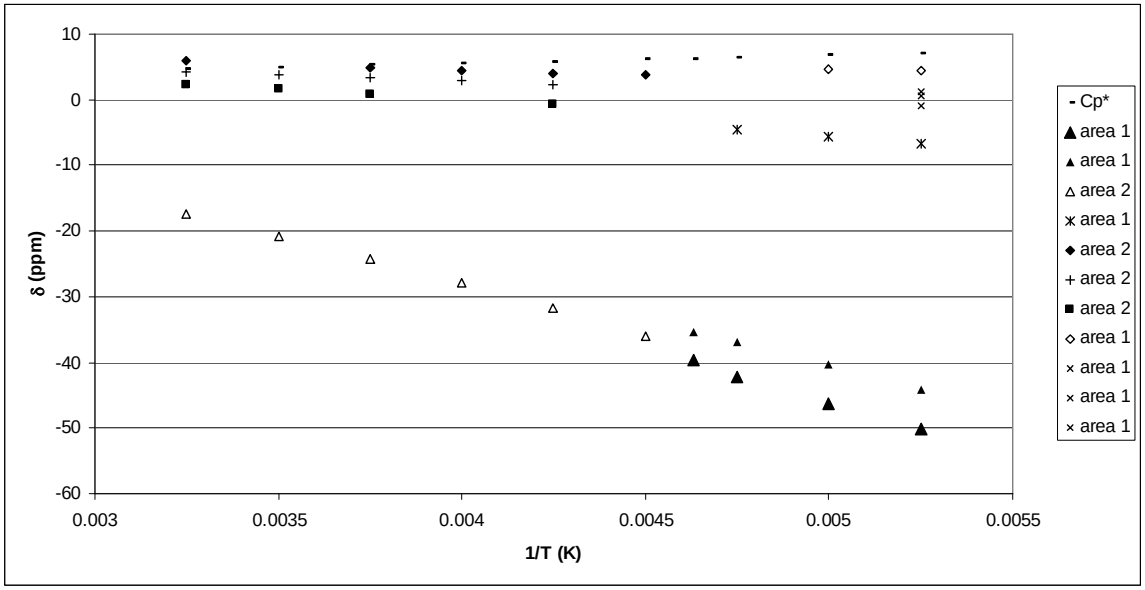

Figure 2.2.1: Variable Temperature ^{1}H NMR spectra represented as a δ vs. 1/T plot of $Cp^*_2Ce(bipy)(OTf)$ in CD_2Cl_2. Only seven of the eight possible area 1 peaks were found. Many of the area 1 peaks (those denoted by 'x') are only be found at 191 K.

The adduct, $Cp^*_2Ce(4,4'\text{-dmb})(OTf)$ (dmb is dimethyl-2,2'-bipyridine), also shows four peaks in the ^{1}H NMR spectrum attributable to 4,4'-dmb. At 270 K these 4 peaks split into 8 (Figure 2.2.2). This implies that at high temperatures the molecules has averaged C_{2v} symmetry, but at low temperatures this symmetry is lowered to C_s. From the coalescence temperature, the activation energy for this process is calculated to be $\Delta G^{\ddagger}(T_c = 271K) = 12.0 \pm 0.2$ kcal mol^{-1} based on the methyl peaks. The change in the free energy of activation calculated using the two sets of resonances due to the bipyridine-H resonances between -10 and -30 ppm (Figure 2.2.3) and the peaks which are between 2 and 3 ppm, gives $\Delta G^{\ddagger}(T_c = 287K) = \Delta G^{\ddagger}(T_c = 257K) = 12.0 \pm 0.2$ kcal mol^{-1}, respectively. The coalesence temperatures of the other set of protons is not clear.

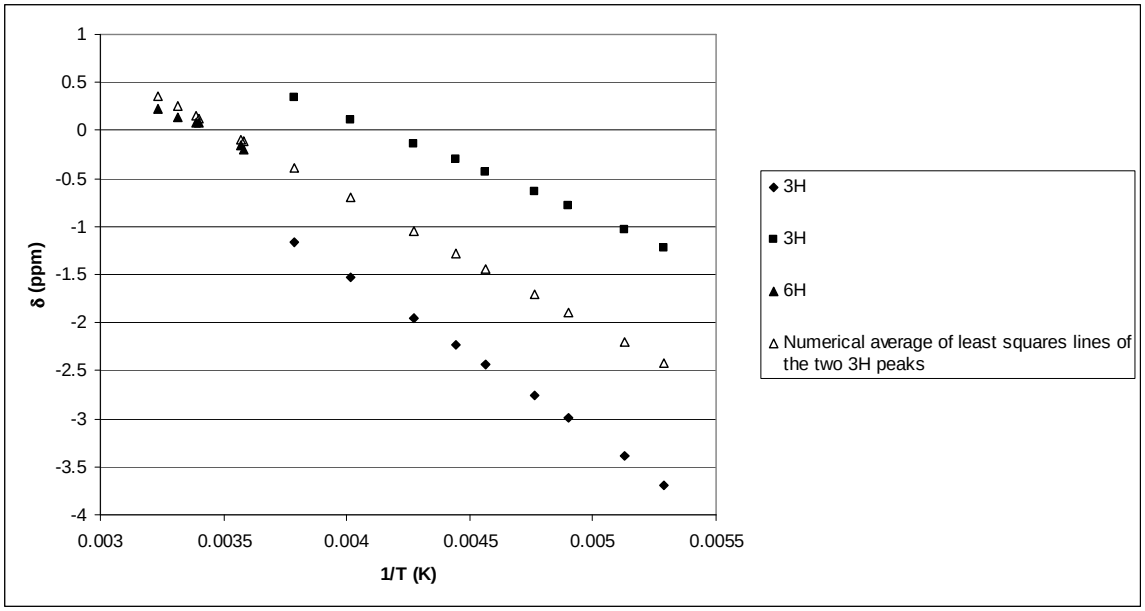

Figure 2.2.2: Variable Temperature ^{1}H NMR spectra represented as a δ vs. 1/T plot of $Cp^*_2Ce(4,4'\text{-dmb})(OTf)$ in CD_2Cl_2. For the sake of clarity only the 4,4'-methyl resonances are shown in this figure. The numerical average of the least-squares lines determined by the δ vs. 1/T plots of the peaks of area 3 is shown as well. The other resonances are shown in Figure 2.2.4.

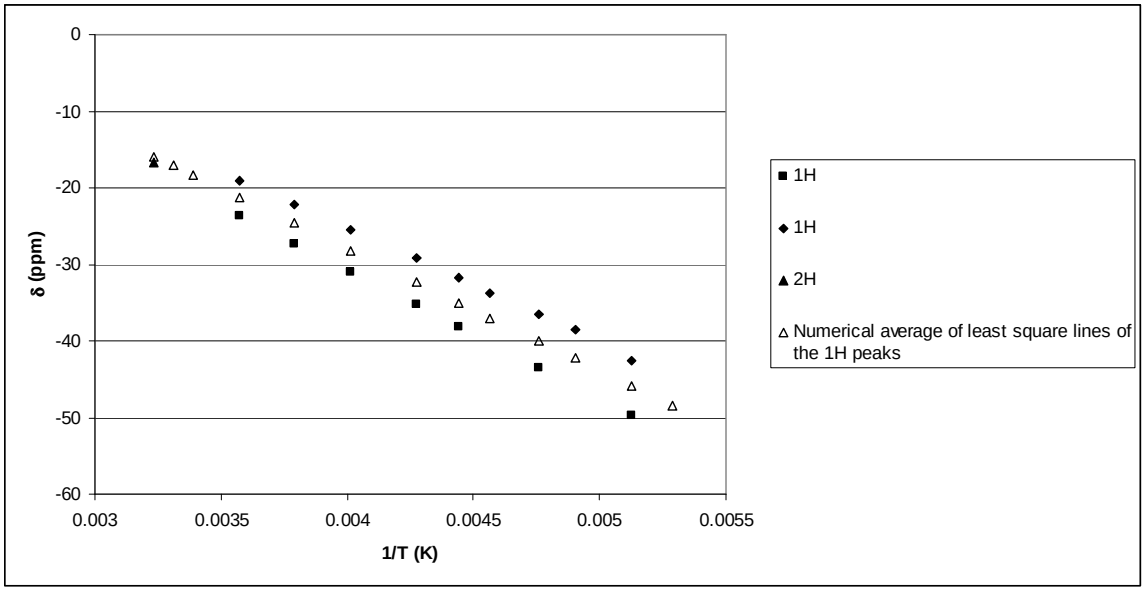

Figure 2.2.3: Variable Temperature ^{1}H NMR spectra represented as a δ vs. 1/T plot of $Cp^*_2Ce(4,4'\text{-dmb})(OTf)$ in CD_2Cl_2. For the sake of clarity only the ^{1}H resonances between -10 and -60 ppm are shown in this figure. The numerical average of the least-squares lines determined by the δ vs. 1/T plots of the peaks of area 1 is shown as well. The other resonances are shown in Figure 2.2.4.

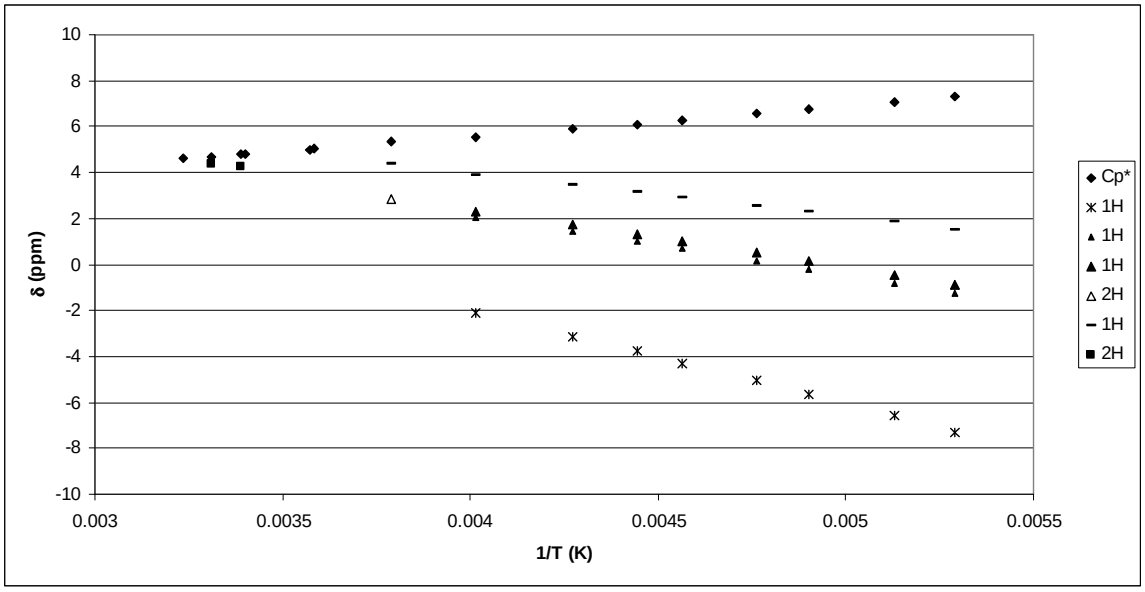

Figure 2.2.4: Variable Temperature ^{1}H NMR spectra represented as a δ vs. 1/T plot of $Cp^*_2Ce(4,4'\text{-dmb})(OTf)$ in CD_2Cl_2. The 4,4'-methyl resonances and the resonances between -10 and -60 ppm are not shown in this figure.

The activation energy for the averaging of the bipy resonances in $Cp^*_2Ce(4,4'\text{-dmb})(OTf)$ is almost 3 kcal/mol higher than in $Cp^*_2Ce(bipy)(OTf)$. To determine whether this is a result of the electron donating ability of the methyl groups, $Cp^*_2Ce(4,4'\text{-dicarbomethoxy-2,2'-bipyridine})(OTf)$, where the carbomethoxy groups are strong electron withdrawers, was synthesized and the ^{1}H NMR spectra were plotted as a

function of 1/T (Figures 2.2.5 and 2.2.6). From the coalescence temperature, the activation energy for this process is calculated to be $\Delta G^{\ddagger}(T_c = 276K) = 12.6 \pm 0.2$ kcal mol^{-1} based on the methyl peaks. The change in the free energy of activation calculated using the two sets of resonances due to the bipyridine-H resonances between -10 and -30 ppm and the peaks which are between 0 and 3 ppm, gives $\Delta G^{\ddagger}(T_c = 291K) = \Delta G^{\ddagger}(T_c = 267K) = 12.4 \pm 0.2$ kcal mol^{-1}, respectively. The coalesence temperatures of the other set of protons is not clear. The similarity in the activation energies for the averaging of the bipy ring between Cp^*_2Ce(4,4'-dmb)(OTf) and Cp^*_2Ce(4,4'-dicarbomethoxy-bipy)(OTf) implies that it is not the electronic effect of the electron donating methyl groups which cause a higher barrier to bipy averagine than in the case of Cp^*_2Ce(bipy)(OTf). It seems that Iit is the steric effects of the 4,4'-dimethyl substitution which affect the barrier.

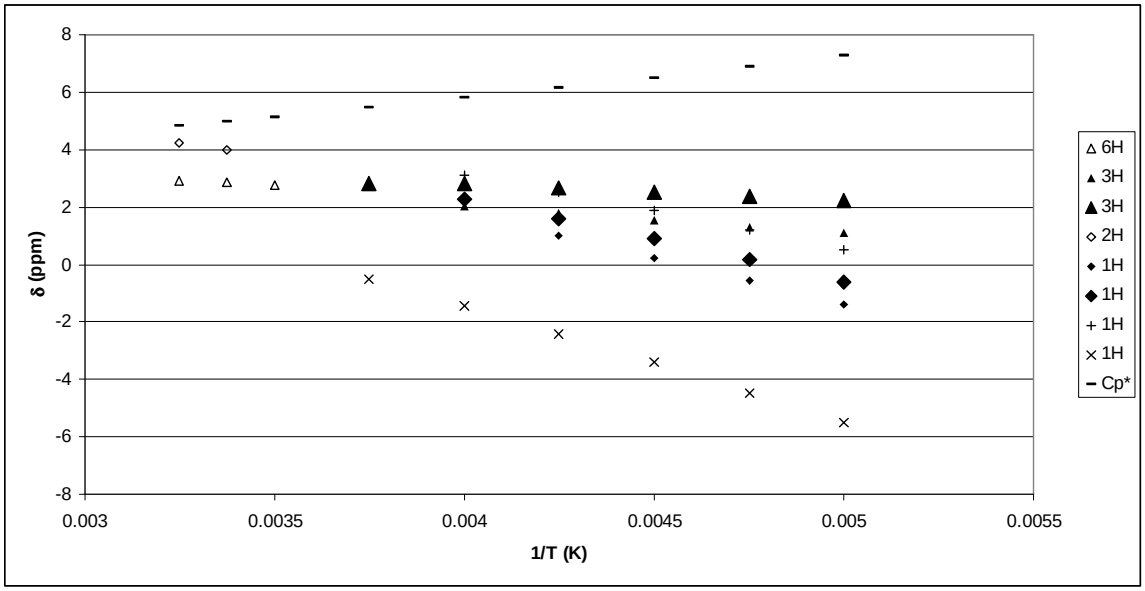

Figure 2.2.5: Variable Temperature ^1H NMR spectra represented as a δ vs. 1/T plot of Cp^*_2Ce(4,4'-dicarbomethyoxy-bipy)(OTf) in CD_2Cl_2. The resonances between -10 and -50 ppm are shown in the next figure.

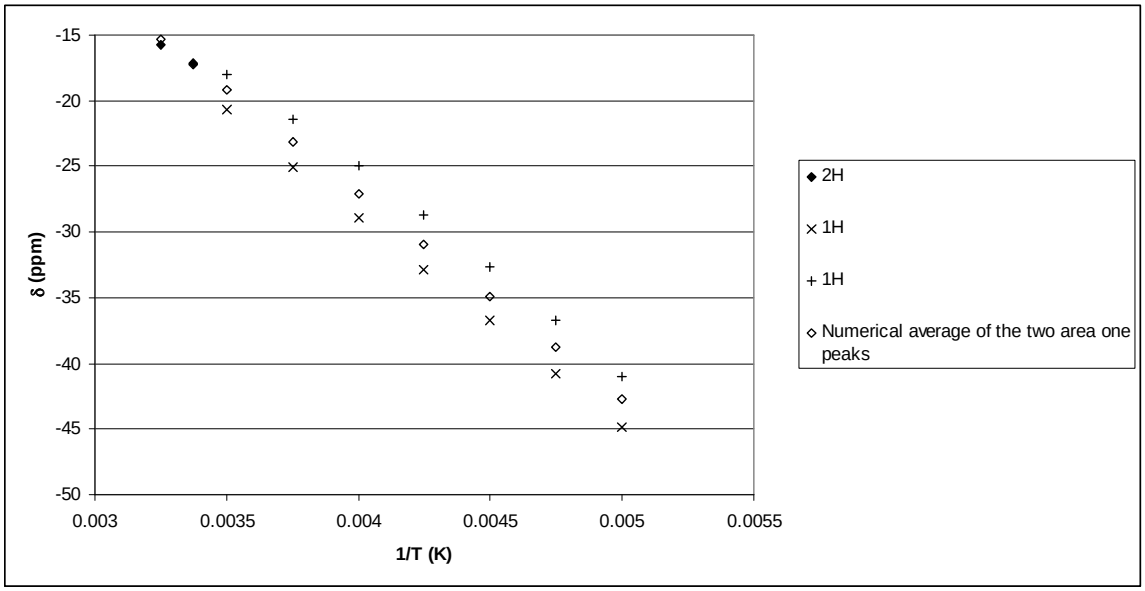

Figure 2.2.6: Variable Temperature ^{1}H NMR spectra represented as a δ vs. 1/T plot of Cp*$_2$Ce(4,4'-dicarbomethoxy-bipy)(OTf) in CD_2Cl_2. For the sake of clarity only the ^{1}H resonances between -10 and -50 ppm are shown in this figure. The numerical average of the least-squares lines determined by the δ vs. 1/T plots of the peaks of area 1 is shown as well.

The ^{1}H NMR spectrum of Cp*$_2$Ce(phenanthroline)(OTf) also shows eight different resonances at low temperature that coalesce into four peaks at 310 K. Based on the peaks that are between -10 and -20 ppm and the coalescence temperature the activation energy for this process is calculated to be $\Delta G^{\ddagger}(T_c = 303K) = 12.8 \pm 0.2$ kcal mol^{-1} (Figure 2.2.7). The coalesence temperatures of the other protons is unclear, because although the peaks of area one all broaden into the baseline, the peaks of area two do not reemerge by 310 K; it is not possible to raise the temperature further as CD_2Cl_2 boils at 313 K.

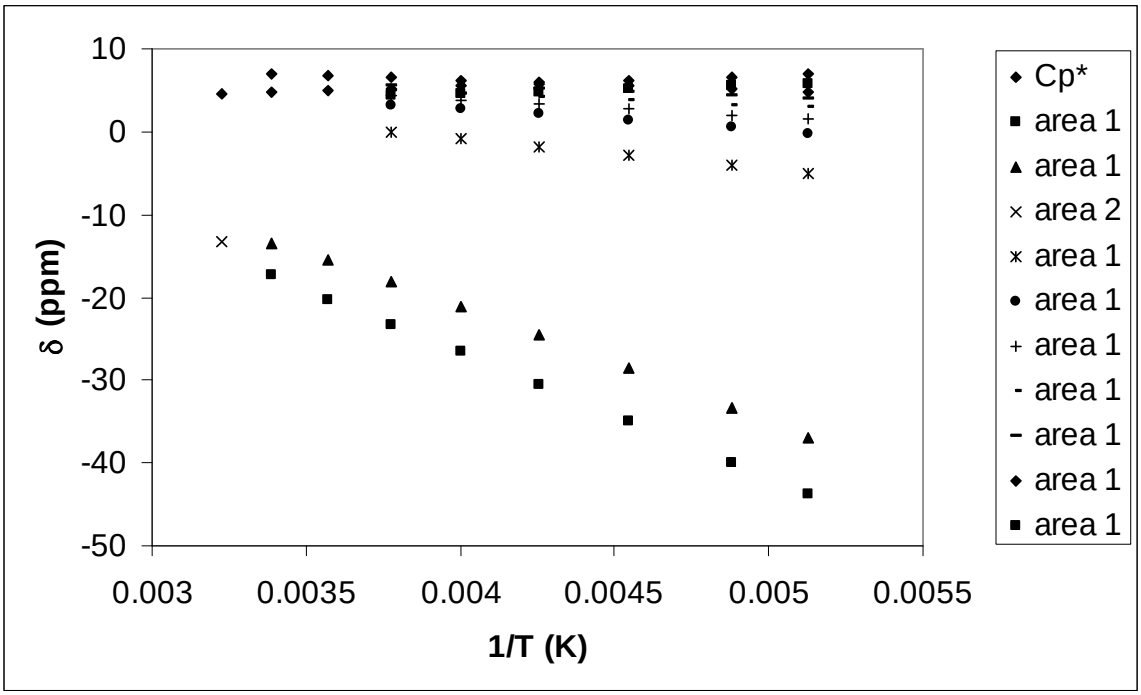

Figure 2.2.7: Variable Temperature ^{1}H NMR spectra represented as a δ vs. 1/T plot of Cp^*_2Ce(phenanthroline)(OTf) in CD_2Cl_2.

It is not possible that at high temperatures Cp^*_2Ce(x,x'-bipy)(X) has true C_{2v} symmetry, because then the molecule will be an ion-pair in which the halide or triflate is outer-sphere, $[Cp^*_2Ce(bipy)][X]$. The ^{1}H NMR spectrum does not coincide with that of $[Cp^*_2Ce(bipy)][BPh_4]$, which is an ion-pair in which the $[BPh_4]$ is outer-sphere, presented later. Therefore, the C_{2v} symmetry of the cationic fragment must be averaged C_{2v} symmetry. A reasonable rationalization for the temperature dependance of the ^{1}H NMR spectrum is that the triflate is bound inner-sphere, but at high temperatures, in a CD_2Cl_2 solution, the triflate exchanges rapidly on the NMR time scale. Therefore, this molecule has averaged C_{2v} symmetry. As the temperature is lowered, the four bipyridine resonances decoalesce into eight, consistent with the triflate not exchanging on the NMR time scale and the molecule having C_s symmetry. In order to get support for the inner-

sphere stereochemistry derived from the NMR spectra, crystals of $Cp^*_2Ce(bipy)(OTf)$ were grown by layering pentane on CH_2Cl_2 and a crystal structure was obtained (Figure 2.2.8).[5] The crystals structure shows that the triflate is bound to the cerium. The solid state structures of $Cp^*_2Ce(bipy)(I)$[6] and $Cp^*_2Ce(bipy)(Cl)$ (Figure 2.2.9) also show that the anions are inner-sphere.

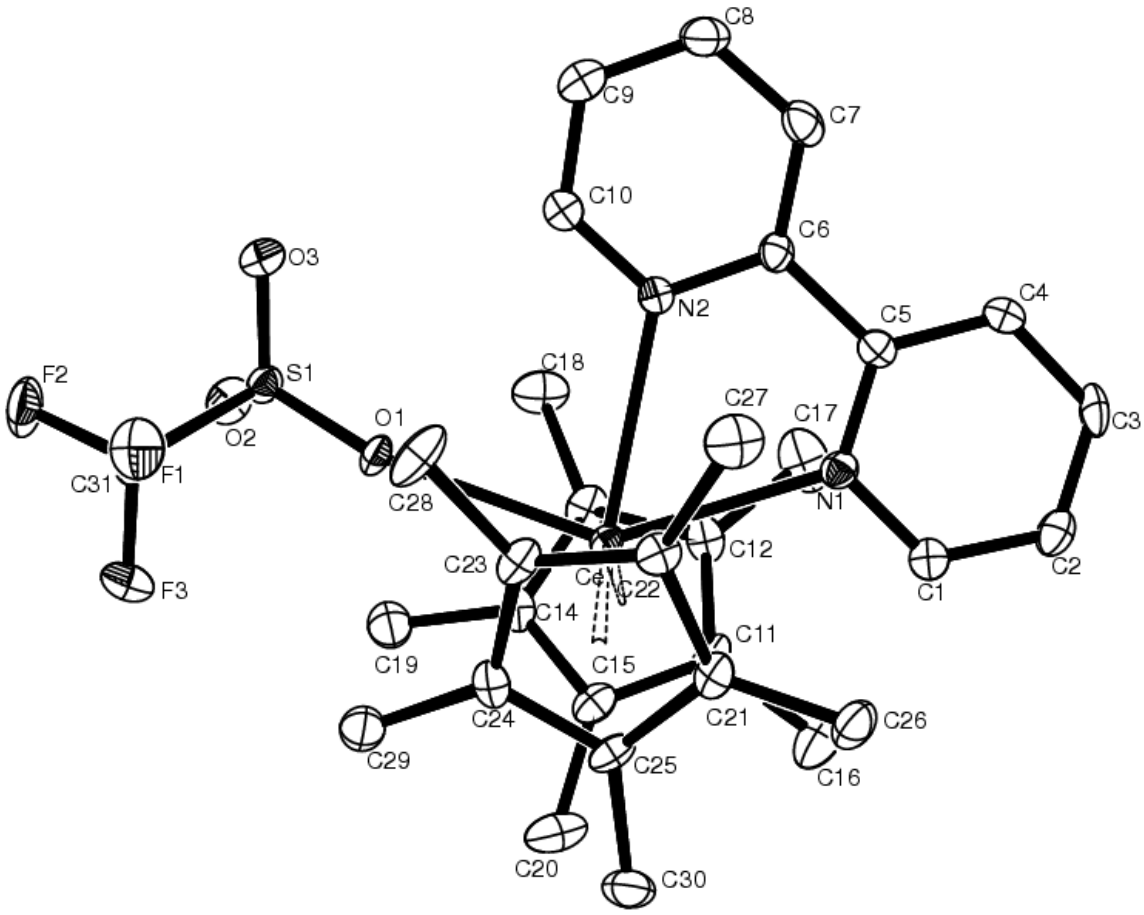

Figure 2.2.8: ORTEP diagram of $Cp^*_2Ce(bipy)(OTf)$ (50% probability ellipsoids). All non-hydrogen atoms are refined anisotropically. Hydrogen atoms are placed and not refined and are not shown. Selected Bond Distances and Angles are given in Tables 2.2.1 and 2.2.2, respectively. The N1-C25-C26-N2 torsion angle is 7.9(7)°. O1 is 0.28 Å out of the least-squares plane defined by the atoms in the bipyridine ring.

Table 2.2.1: Selected bond distances (Å) in $Cp^*_2Ce(bipy)(OTf)$

Atom	Atom	distance		atom	Atom	distance
Ce(1)	O(1)	2.649(4)		Ce(1)	N(1)	2.606(4)
Ce(1)	N(2)	2.675(5)		Ce(1)	C(1)	2.824(6)
Ce(1)	C(2)	2.845(5)		Ce(1)	C(3)	2.820(6)
Ce(1)	C(4)	2.769(5)		Ce(1)	C(5)	2.786(6)
Ce(1)	C(6)	2.825(5)		Ce(1)	C(7)	2.720(5)
Ce(1)	C(8)	2.744(5)		Ce(1)	C(9)	2.859(6)
Ce(1)	C(10)	2.923(6)		Ce(1)	C(101)	2.54
Ce(1)	C(102)	2.54		C(21)	C(22)	1.382(8)
C(22)	C(23)	1.364(8)		C(23)	C(24)	1.397(8)
C(24)	C(25)	1.399(8)		C(25)	C(26)	1.492(7)
C(26)	C(27)	1.388(8)		C(27)	C(28)	1.386(8)
C(28)	C(29)	1.370(9)		C(29)	C(30)	1.383(9)

Table 2.2.2: Selected bond angles in $Cp^*_2Ce(bipy)(OTf)$

atom	atom	atom	angle		atom	atom	atom	angle
O(1)	Ce(1)	N(1)	142.7(1)		O(1)	Ce(1)	N(2)	81.4(1)
N(1)	Ce(1)	N(2)	61.3(1)		C(101)	Ce(1)	C(102)	138.9

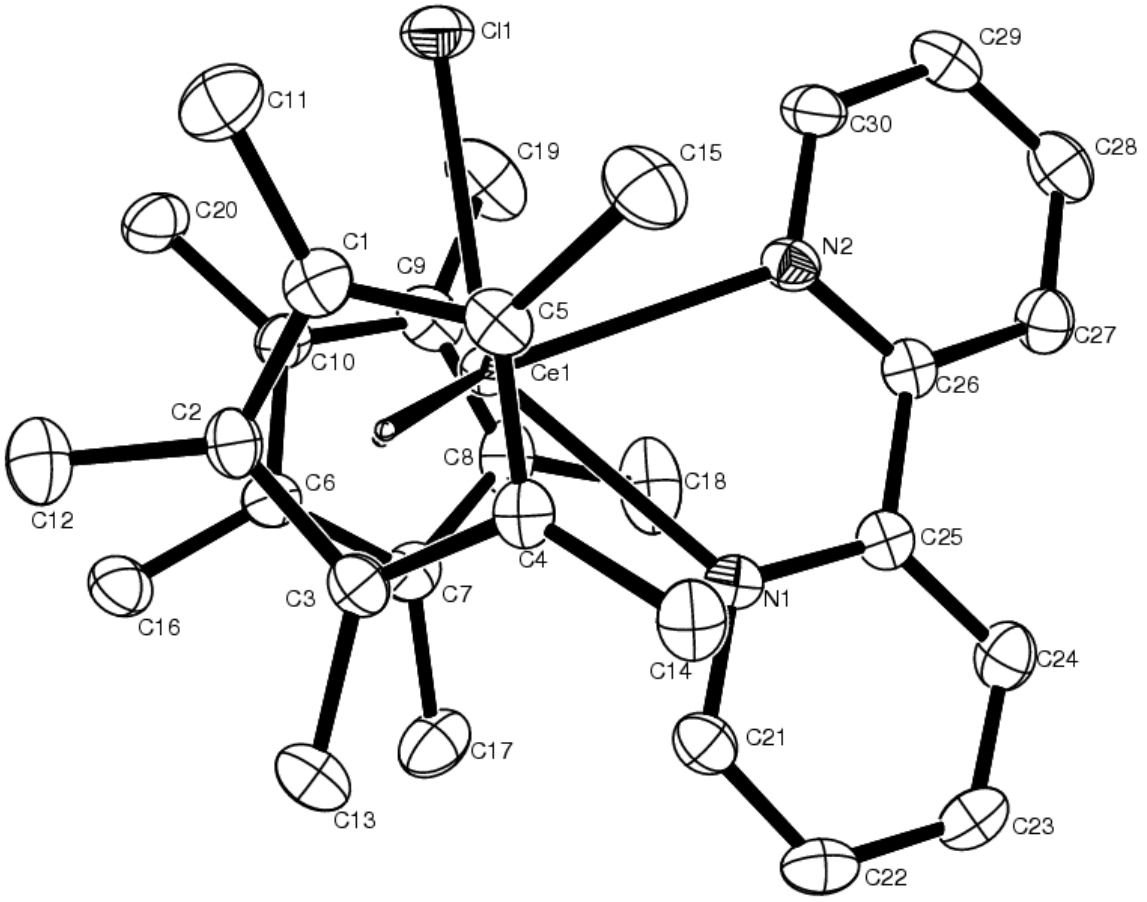

Figure 2.2.9: ORTEP diagram of $Cp^*_2Ce(bipy)(Cl)$ (50% probability ellipsoids). All non-hydrogen atoms are refined anisotropically. Hydrogen atoms are placed and not refined and are not shown. Selected Bond Distances and Angles are given in Tables 2.2.3 and 2.2.4, respectively. The N1-C25-C26-N2 torsion angle is 8.6(4)°. Cl1 is 0.15 Å out of the least-squares plane defined by the atoms in the bipyridine ring.

Table 2.2.3: Selected bond distances (Å) in $Cp^*_2Ce(bipy)(Cl)$

Atom	atom	Distance		atom	Atom	Distance
Ce(1)	Cl(1)	2.7654(7)		Ce(1)	N(1)	2.662(2)
Ce(1)	N(2)	2.741(2)		Ce(1)	C(1)	2.850(3)
Ce(1)	C(2)	2.890(3)		Ce(1)	C(3)	2.892(3)
Ce(1)	C(4)	2.854(3)		Ce(1)	C(5)	2.802(3)
Ce(1)	C(6)	2.795(3)		Ce(1)	C(7)	2.846(3)
Ce(1)	C(8)	2.841(3)		Ce(1)	C(9)	2.795(3)
Ce(1)	C(10)	2.766(3)		Ce(1)	C(101)	2.59
Ce(1)	C(102)	2.54		C(25)	C(26)	1.481(4)

Table 2.2.4: Selected bond angles (°) in $Cp^*_2Ce(bipy)(Cl)$

Atom	atom	atom	Angle		atom	atom	Atom	Angle
Cl(1)	Ce(1)	N(1)	138.82(5)		Cl(1)	Ce(1)	N(2)	79.39(5)
N(1)	Ce(1)	N(2)	59.92(7)		C(101)	Ce(1)	C(102)	134.8
Ce(1)	N(1)	C(21)	118.0(2)					

The solid-state crystal structures of the triflate, iodide, and chloride clearly show that these ligands are inner-sphere. These data suggest another physical process that can result in averaged C_{2v} symmetry in solution. This process is one in which the bipyridine ligand undergoes site exchange with the triflate or halide ligands attached to the cerium fragment as inner-sphere ligands. The bipyridine site exchange could be either inter- or intra-molecular. In order to test these postulates, $Cp^*_2Ce(bipy)(Cl)$ and $Cp^*_2Ce(bipy)(I)$ were synthesized. The variable temperature ^1H NMR spectrum of $Cp^*_2Ce(bipy)(Cl)$ is shown in Figure 2.2.10.

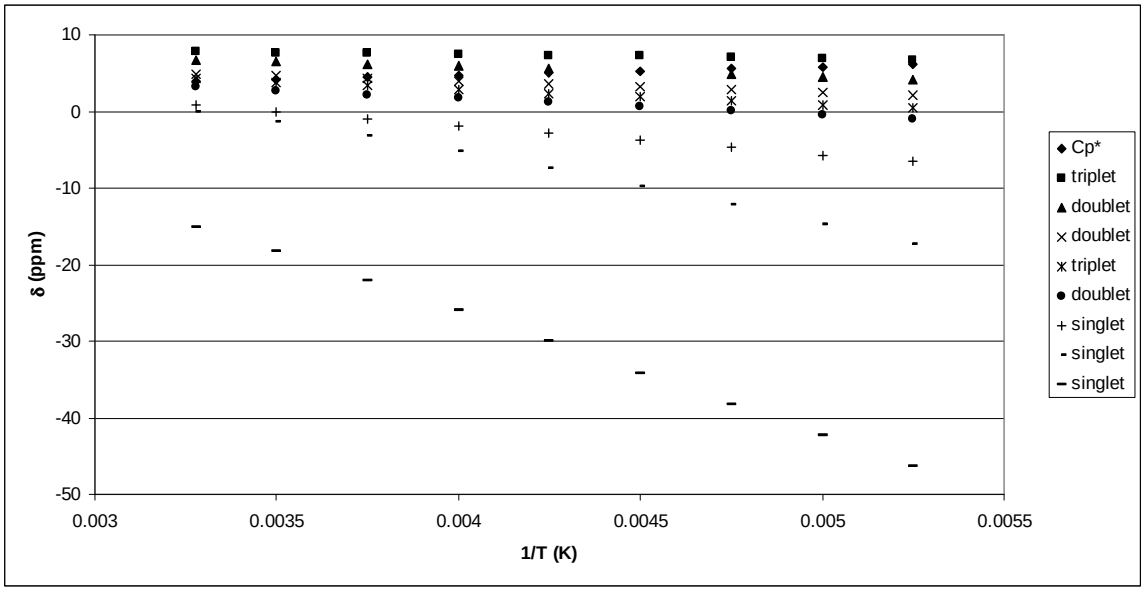

Figure 2.2.10: Variable Temperature ^1H NMR spectra represented as a δ vs. 1/T plot of $Cp^*_2Ce(bipy)(Cl)$ in CD_2Cl_2. All peaks except for the Cp* peak are of area 1.

Serendipitously, the ethyliodide used to make the $CeI_3(THF)_3$ contained a chloride impurity, as determined by the mass-spectrum peak (m/z = 64/65). Therefore the $Cp^*_2Ce(bipy)(I)$ was contaminated with $Cp^*_2Ce(bipy)(Cl)$. The presence of $Cp^*_2Ce(bipy)(Cl)$ is confirmed by the presence of chloride in the crystal structure of $Cp^*_2Ce(bipy)(I)$ prepared from the contaminated EtI (Figure 2.2.13). Attempts to recrystallize the $Cp^*_2Ce(bipy)(I)$ only increased the Cl impurity (Figure 2.2.14). The variable temperature ^1H NMR spectrum (Figure 2.2.11) also shows the presence of $Cp^*_2Ce(bipy)(Cl)$. The $Cp^*_2Ce(bipy)(Cl)$ does not appear in the ^1H NMR spectrum at room temperature. The percentage of $Cp^*_2Ce(bipy)(Cl)$ in the mixture based on the ^1H NMR spectra is shown in Figure 2.2.12. It seems reasonable to suggest that the reason the $Cp^*_2Ce(bipy)(Cl)$ peak is not seen at room temperature, but is seen at temperatures below 265K, which is also the temperature at which the C_{2v} symmetry of $Cp^*_2Ce(bipy)(I)$ is lost, is that at T > 265K the iodide is exchanging, both with other iodides in $Cp^*_2Ce(bipy)(I)$ and with chlorides in $Cp^*_2Ce(bipy)(Cl)$. The exchange of iodides in $Cp^*_2Ce(bipy)(I)$ causes averaged C_{2v} symmetry in $Cp^*_2Ce(bipy)(I)$; therefore, there are only four peaks of area two, and not eight of area one. The exchange of iodide for chloride on the NMR time scale causes broadening of the peaks in $Cp^*_2Ce(bipy)(Cl)$ such that they are not visible. As the temperature is lowered, the iodide does not exchange on the NMR time scale; therefore, the resonances due to $Cp^*_2Ce(bipy)(Cl)$ become visible. The fact that the iodide and chloride exchange on the NMR time scale at 265K is demonstrated by the decrease in the total Cp* integral in the ^1H NMR spectrum at that temperature (Figure 2.2.12). Further proof that it is not bipyridine exchange that

causes the averaged C_{2v} symmetry is the fact that in the presence of excess bipy, the ^1H NMR spectrum does not indicate exchange of the bipyridine ligand (although addition of 4,4'-dmb shows that there is exchange on the chemical time scale). Based on the peaks between -30 and -40 ppm, and on the coalescence temperature, the activation energy for this process in $Cp^*_2Ce(bipy)(I)$ is calculated to be $\Delta G^{\ddagger}(T_c = 243K) = 10.1 \pm 0.2$ kcal mol^{-1}, and based on the coalescence temperature and chemical shift difference of the peaks of between -2 and 0 ppm $\Delta G^{\ddagger}(T_c = 243K) = 10.5 \pm 0.5$ kcal mol^{-1}. The coalesence temperatures of the other protons is not as clear. Hence, the calculated $\Delta G^{\ddagger}$ based on those protons is unreliable. The activation energies of all the $Cp^*_2Ce(a,a'\text{-bipy})(X)$ are tabulated in Table 2.2.9.

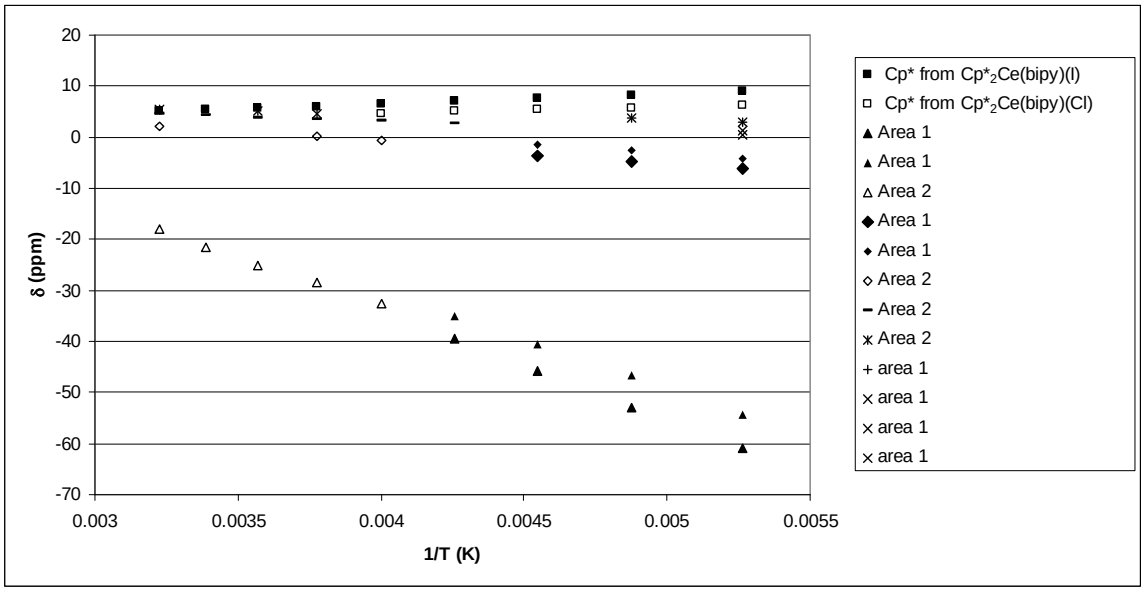

Figure 2.2.11: Variable Temperature ^1H NMR spectra represented as a δ vs. 1/T plot of $Cp^*_2Ce(bipy)(I)$ that contains 16% $Cp^*_2Ce(bipy)(Cl)$ in CD_2Cl_2. The percentage of $Cp^*_2Ce(bipy)(Cl)$ is derived from the relative areas of the peaks of the Cp* resonances at 190 K. 3 of the area 1 resonances (those denoted by 'x') are only be found at 190 K.

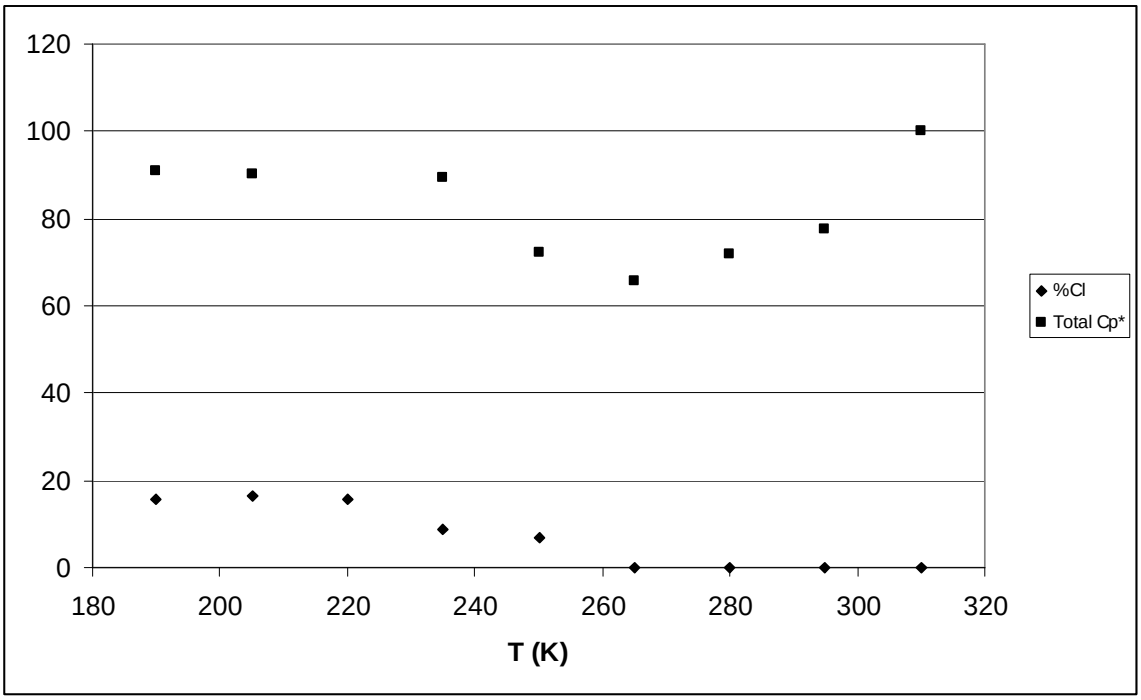

Figure 2.2.12: The % of $Cp^*_2Ce(bipy)(Cl)$ in $Cp^*_2Ce(bipy)(X)$ is based on the relative integrals of the Cp* resonances in $Cp^*_2Ce(bipy)(Cl)$ and $Cp^*_2Ce(bipy)(I)$. The total Cp* is determined by summing the integrals of the Cp* resonances in $Cp^*_2Ce(bipy)(Cl)$ and $Cp^*_2Ce(bipy)(I)$ and dividing by the intensity of the dead rings in solution (the solvent and grease peaks have other peaks moving through them, and therefore can not be used for calibration). At 220K there are peaks interfering with the integration of solvent, grease and dead rings, and therefore no value is reported for the total Cp*.

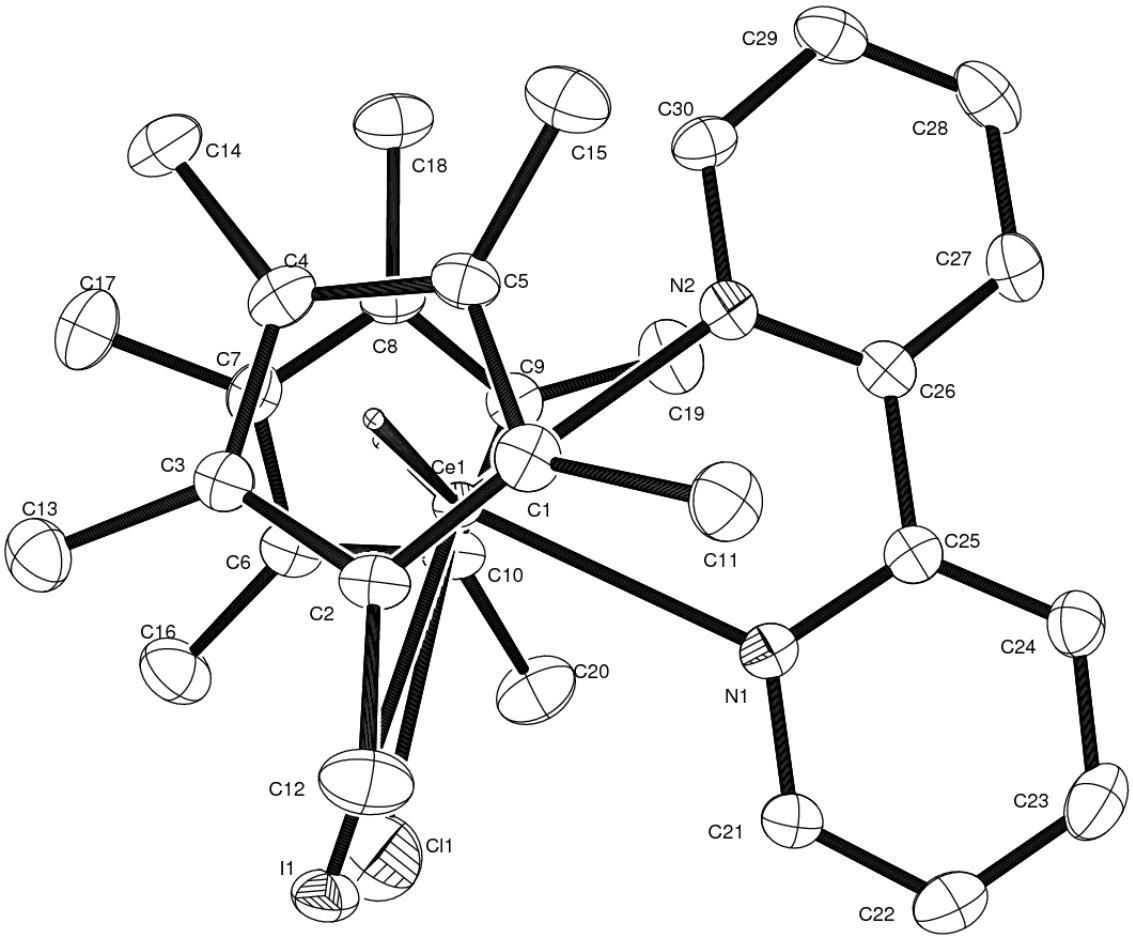

Figure 2.2.13: ORTEP diagram of $Cp^*_2Ce(bipy)(X)$ (where X is partially occupied by I/Cl where the site is modeled with a 93% occupancy of I and 7% occupancy of Cl (50% probability ellipsoids). All non-hydrogen atoms except for Cl are refined anisotropically; Cl is refined isotropically. Hydrogen atoms are placed and not refined and are not shown. Selected Bond Distances and Angles are given in Tables 2.2.5 and 2.2.6, respectively. The N1-C25-C26-N2 torsion angle is 13.8(5)°. I1 is 0.52 Å out of the least-squares plane defined by the atoms in the bipyridine ring.[7]

Table 2.2.5: Selected bond distances (Å) in $Cp^*_2Ce(bipy)(I)$ (I = 93%)

atom	atom	distance		Atom	atom	Distance
Ce1	I1	3.2457(6)		Ce1	N1	2.707(3)
Ce1	N2	2.633(3)		Ce1	C1	2.867(4)
Ce1	C2	2.838(4)		Ce1	C3	2.786(4)
Ce1	C4	2.830(4)		Ce1	C5	2.889(4)
Ce1	C6	2.868(4)		Ce1	C7	2.838(4)
Ce1	C8	2.847(4)		Ce1	C9	2.835(4)
Ce1	C10	2.820(4)		Ce1	C101	2.57
Ce1	C102	2.57		C25	C26	1.490(6)
Ce1	Cl1	2.86(3)		I1	Cl1	0.53(4)

Table 2.2.6: Selected bond angles (°) in $Cp^*_2Ce(bipy)(I)$ (I = 93%)

atom	atom	atom	angle		atom	atom	atom	Angle
I1	Ce1	N1	83.59(7)		I1	Ce1	N2	144.50(7)
C101	Ce1	C102	141.0		N1	Ce1	N2	60.9(1)
I1	Ce1	Cl1	6.8(7)					

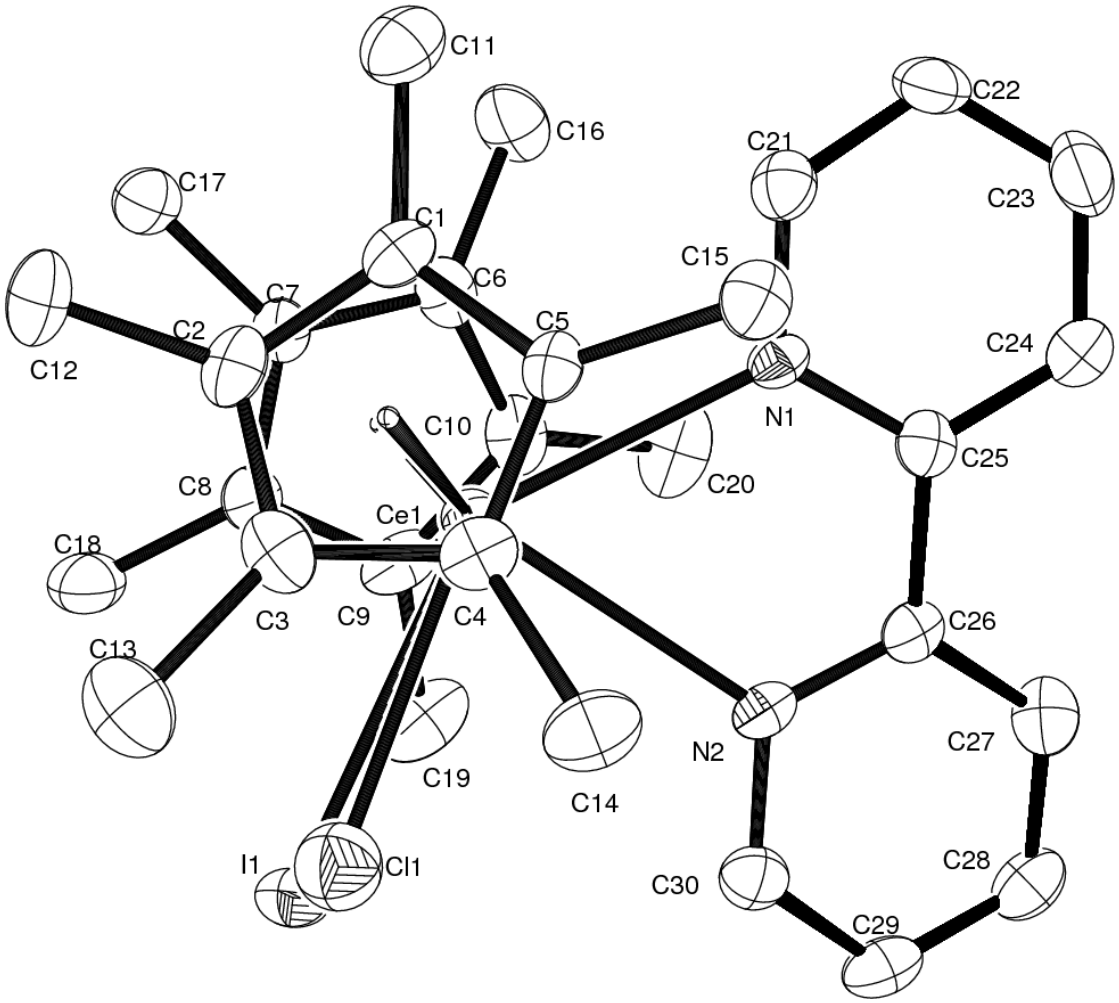

Figure 2.2.14: ORTEP diagram of $Cp^*_2Ce(bipy)(X)$ (where X is partially occupied by I/Cl where the site is modeled with a 73% occupancy of I and 27% occupancy of Cl (50% probability ellipsoids). All non-hydrogen atoms except for Cl are refined anisotropically; Cl is refined isotropically. Hydrogen atoms are placed and not refined and are not shown. Selected Bond Distances and Angles are given in Tables 2.2.7 and 2.2.8, respectively. The N1-C25-C26-N2 torsion angle is 8.5(7)°. I1 is 0.031 Å out of the least-squares plane defined by the atoms in the bipyridine ring.[7]

Table 2.2.7: Selected bond distances (Å) in $Cp^*_2Ce(bipy)(I)$ (I = 73%)

atom	atom	distance		Atom	atom	Distance
Ce1	I1	3.185(1)		Ce1	N1	2.641(4)
Ce1	N2	2.766(4)		Ce1	C1	2.862(5)
Ce1	C2	2.869(5)		Ce1	C3	2.860(5)
Ce1	C4	2.818(5)		Ce1	C5	2.851(5)
Ce1	C6	2.851(5)		Ce1	C7	2.805(5)
Ce1	C8	2.766(5)		Ce1	C9	2.792(5)
Ce1	C10	2.831(5)		Ce1	C101	2.59
Ce1	C102	2.55		C25	C26	1.483(7)
Ce1	Cl1	2.82(1)		I1	Cl1	0.489(9)

Table 2.2.8: Selected bond angles (°) in $Cp^*_2Ce(bipy)(I)$ (I = 73%)

atom	atom	atom	angle		Atom	atom	atom	Angle
I1	Ce1	N1	141.46(9)		I1	Ce1	N2	81.64(9)
C101	Ce1	C102	135.4		N1	Ce1	N2	59.9(1)
I1	Ce1	Cl1	6.3(2)					

Table 2.2.9: Activation energies for averaging of the bipy rings in $Cp^*_2Ce(a,a'\text{-bipy})(X)$

Compound	Activation Energy (kcal/mol)
$Cp^*_2Ce(bipy)(OTf)$	9.2
$Cp^*_2Ce(4,4'\text{-dmb})(OTf)$	12.0
$Cp^*_2Ce(4,4'\text{-dicarbomethoxy-bipy})(OTf)$	12.5
$Cp^*_2Ce(phen)(OTf)$	12.8
$Cp^*_2Ce(bipy)(I)$	10.3

2.3 Synthesis and properties of $[Cp^*_2Ce(bipy)]^+$ and substituted bipyridine analogues

The crystal structures of the complexes just described all contain inner-sphere anion. Their behavior in CD_2Cl_2 solution is thought to result from equilibria between contact and seperated ion-pairs. In order to examine these equilibria in more detail, complexes with a non-coordinating anion, such as BPh_4 are required. Alternatively,

diplacing the 2,2'-bipyridine with the tridentate terpy (terpy is 2,2',6',2''-terpyridine) is explored. Addition of terpy to Cp^*_2CeOTf forms $[Cp^*_2Ce(terpy)][OTf]$. The ^1H NMR shows a 30:2:2:2:2:2:1 ratio of protons at all accesible termperatures in CD_2Cl_2 (190K-310K) (Figure 2.3.1).

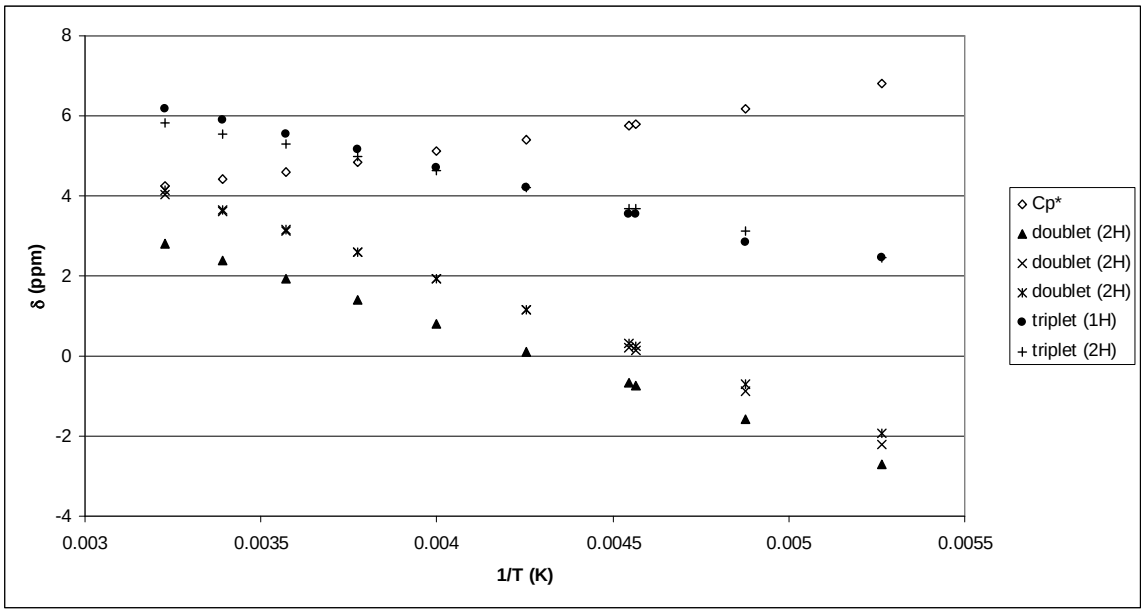

Figure 2.3.1: Variable temperature ^1H NMR spectra, represented as a δ vs. 1/T plot, of $[Cp^*_2Ce(terpy)][OTf]$ in CD_2Cl_2. For clarity's sake the area 2 singlet, which goes from -42.51 ppm at 190K to -16.02 ppm at 310K is not shown; it also obeys Curie law.

Additionally, the ^{19}F NMR spectra show a single OTf peak whose chemical shift is similar to that of diamagnetic $[NR_4][OTf]$ (δ = -79.36). The triflate resonance in the terpy complex has only a slight temperature dependance, in contrast with the variable temperature ^{19}F NMR spectrum of $Cp^*_2Ce(bipy)(OTf)$, shown in Figure 2.3.2.

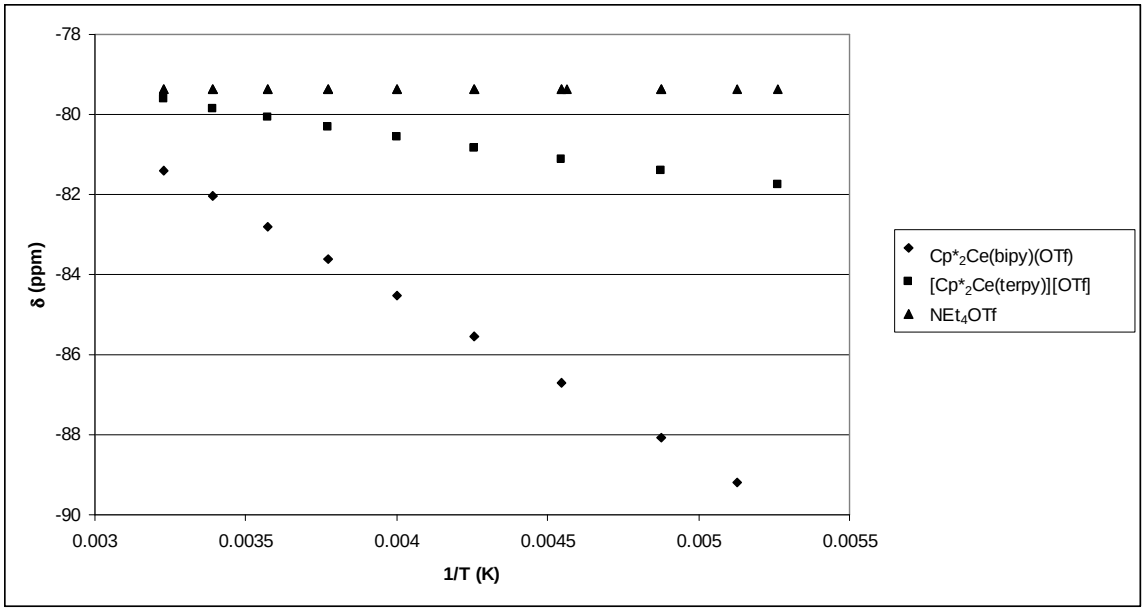

Figure 2.3.2: Variable Temperature ^{19}F NMR spectra represented as a δ vs. 1/T plot of $Cp^*_2Ce(bipy)(OTf)$ and $[Cp^*_2Ce(terpy)][OTf]$ in CD_2Cl_2.

These data are consistent with the postulate that the triflate anion is largely or completely outer-sphere in the terpy complex. The chemical shift of the triflate resonance in the bipy complex has a strong dependence on temperature, implying that the OTf spends more time in the vicinity of the paramagnetic fragment. The crystal structure shows that the triflate anion is outer-sphere (Figure 2.3.3). The crystal strutcture of $[Cp^*_2Ce(terpy)][I]$,[6] published in 2005, also shows that the iodine is outer-sphere. Thus, these two complexes contain terpy as a tridentate ligand in the solid state, and the ^{19}F NMR data, in particular, are consistent with the view that this is the only, or at least the major, species present in CD_2Cl_2 solution.

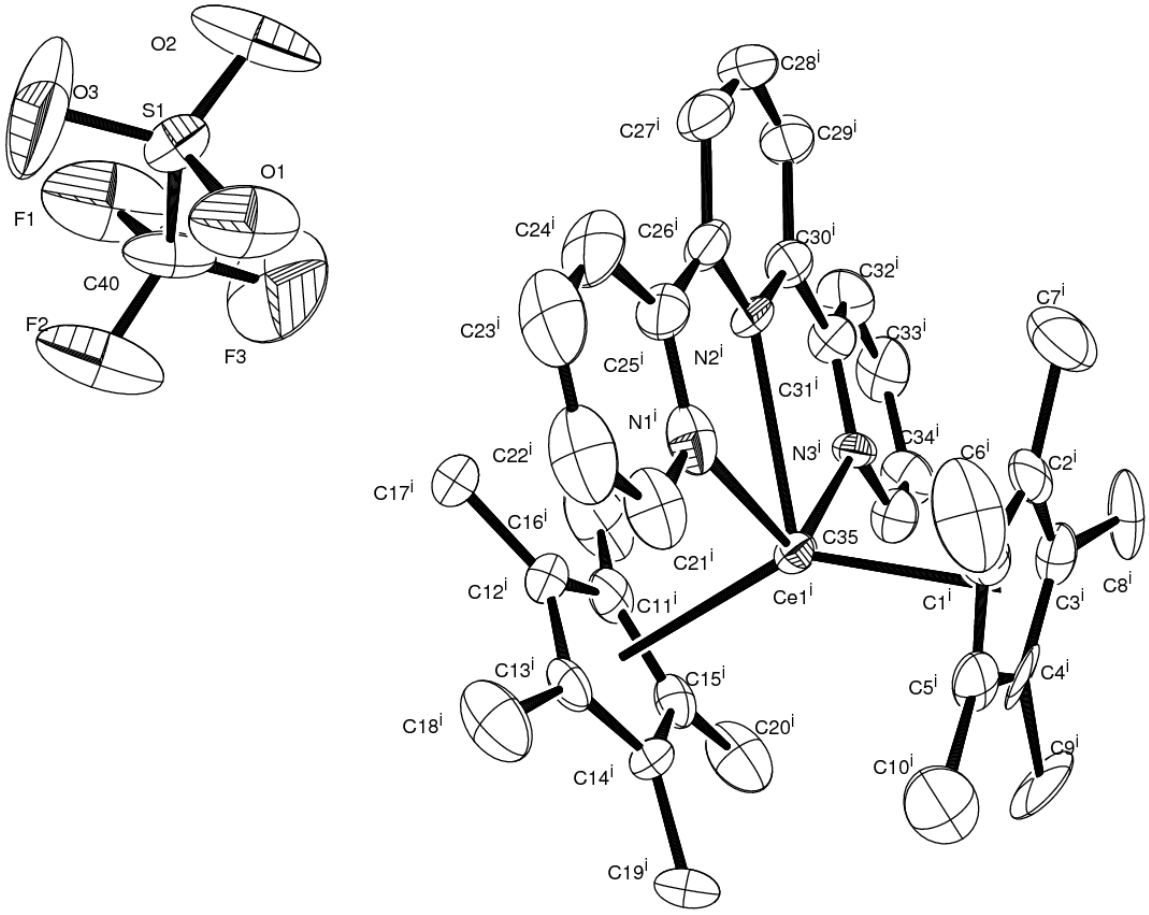

Figure 2.3.3 ORTEP diagram of $[Cp^*_2Ce(terpy)][OTf]$ (50% probability ellipsoids), with a x→-x; y→½+y; z→½ -z symmetry operation performed on the $[Cp^*_2Ce(terpy)]^+$ fragment to show the C17-F3 contact. All non-hydrogen atoms are refined anisotropically. Hydrogen atoms are placed and not refined and are not shown. Selected Bond Distances and Angles are given in Tables 2.3.1 and 2.3.2, respectively. The N1-C25-C26-N2 torsion angle is 9.7(1)° and the N2-C30-C31-N3 torsion angle is 12.5(1)°. The closest distance between anion and cation is the F(3)-C(17) distance of 3.266 (1) Å.

Table 2.3.1: Selected bond distances (Å) in [Cp*$_2$Ce(terpy)][OTf]

atom	Atom	distance		atom	atom	distance
Ce1	N1	2.600(8)		Ce1	N2	2.638(7)
Ce1	N3	2.569(7)		Ce1	C1	2.822(9)
Ce1	C2	2.821(8)		Ce1	C3	2.847(9)
Ce1	C4	2.804(9)		Ce1	C5	2.775(9)
Ce1	C11	2.818(8)		Ce1	C12	2.828(9)
Ce1	C13	2.849(9)		Ce1	C14	2.819(9)
Ce1	C15	2.815(8)		Ce1	C101	2.54
Ce1	C102	2.56				

Table 2.3.2: Selected bond angles (°) in [Cp*$_2$Ce(terpy)][OTf]

atom	atom	atom	Angle		atom	atom	atom	angle
N1	Ce1	N2	62.5(3)		N3	Ce1	N1	125.0(2)
N3	Ce1	N2	62.5(2)		Ct1	Ce1	Ct2	143.5

The other way to make [Cp*$_2$Ce(L)]$^+$ is to replace the triflate anion with a larger anion. [Cp*$_2$Ce][BPh$_4$] is unstable in most solvents,[8] so instead [Cp*$_2$Ce(bipy)][BPh$_4$] was prepared by addition of NaBPh$_4$ to Cp*$_2$Ce(bipy)(OTf). The ^{1}H NMR resonances appear in a 30:8:8:4:2:2:2:2 ratio and the relative intensities do not change as a function of temperature. Furthermore, the ^{1}H NMR shifts corresponding to [BPh$_4$]$^-$ do not change as a function of temperature (Figure 2.3.4), implying that the [BPh$_4$] is outer-sphere. In addition, free bipy exchanges with bound bipy on the ^{1}H NMR time scale. Crystals of [Cp*$_2$Ce(bipy)][BPh$_4$] were obtained by layering pentane on CH_2Cl_2. The crystal structure shows that [BPh$_4$]$^-$ is outer-sphere (Figure 2.3.5).

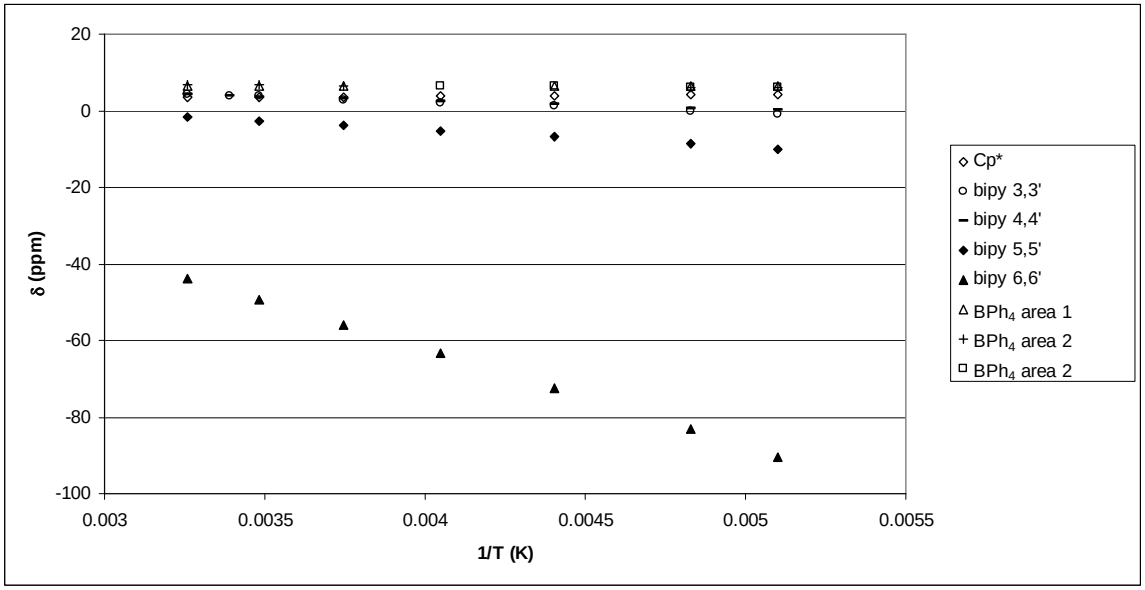

Figure 2.3.4: Variable Temperature ^{1}H NMR spectra represented as a δ vs. 1/T plot of $[Cp^*_2Ce(bipy)][BPh_4]$ in CD_2Cl_2.

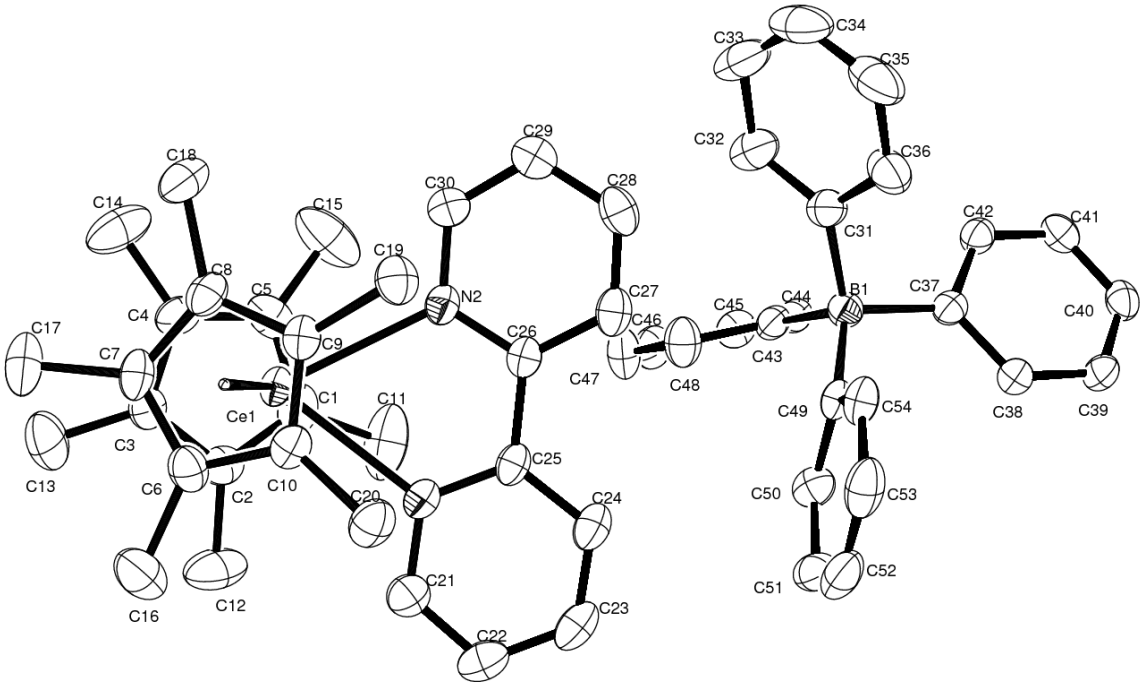

Figure 2.3.5: ORTEP diagram of $[Cp^*_2Ce(bipy)][BPh_4]$ (50% probability ellipsoids). All non-hydrogen atoms are refined anisotropically. Hydrogen atoms are placed and not refined and are not shown. Selected Bond Distances and Angles are given in Tables 2.3.3

and 2.3.4, respectively. The N1-C25-C26-N2 torsion angle is 6.0(3)°. The closest cation-anion contact is between C(28) and C(31) and is 3.248(4) Å.

Table 2.3.3: Selected bond distances (Å) in [Cp*$_2$Ce(bipy)][BPh$_4$]

Atom	atom	Distance		Atom	atom	distance
Ce(1)	N(1)	2.537(2)		Ce(1)	N(2)	2.555(2)
Ce(1)	C(1)	2.780(3)		Ce(1)	C(2)	2.763(3)
Ce(1)	C(3)	2.748(3)		Ce(1)	C(4)	2.744(3)
Ce(1)	C(5)	2.764(3)		Ce(1)	C(6)	2.760(3)
Ce(1)	C(7)	2.744(3)		Ce(1)	C(8)	2.738(3)
Ce(1)	C(9)	2.780(3)		Ce(1)	C(10)	2.788(2)
Ce(1)	C(101)	2.49		Ce(1)	C(102)	2.49
N(1)	C(21)	1.342(4)		N(1)	C(25)	1.350(3)
N(2)	C(26)	1.351(3)		N(2)	C(30)	1.346(3)
C(21)	C(22)	1.371(4)		C(22)	C(23)	1.371(4)
C(23)	C(24)	1.380(4)		C(24)	C(25)	1.392(4)
C(25)	C(26)	1.488(4)		C(26)	C(27)	1.391(4)
C(27)	C(28)	1.383(4)		C(28)	C(29)	1.384(4)
C(29)	C(30)	1.373(4)				

Table 2.3.4: Selected bond angles (°) in [Cp*$_2$Ce(bipy)][BPh$_4$]

atom	atom	atom	angle		atom	atom	atom	Angle
N(1)	Ce(1)	N(2)	64.00(7)		C(101)	Ce(1)	C(102)	146.6

Addition of [Na][BPh$_4$] to Cp*$_2$Ce(4,4'-dimethyl-2,2'-bipyridine)(OTf) and Cp*$_2$Ce(5,5'-dimethyl-2,2'-bipyridine)(OTf) allows facile synthesis of [Cp*$_2$Ce(4,4'-dmb)][BPh$_4$] and [Cp*$_2$Ce(5,5'-dmb)][BPh$_4$], respectively. When 6,6'-dimethyl-2,2'-bipyridine is added to Cp*$_2$CeOTf, it does not react. However, if Cp*$_2$CeOTf, NaBPh$_4$, and 6,6'-dmb are stirred in one pot, [Cp*$_2$Ce(6,6'-dmb)][BPh$_4$] forms. Comparing the ^{1}H NMR chemical shifts of [Cp*$_2$Ce(bipy)][BPh$_4$], [Cp*$_2$Ce(4,4'-dmb)][BPh$_4$], [Cp*$_2$Ce(5,5'-dmb)][BPh$_4$], and [Cp*$_2$Ce(6,6'-dmb)][BPh$_4$] along with the fact that the 3

and 6 positions are doublets and the 4 and 5 positions are triplets allows for unambiguous assignment of the proton peaks as shown in Table 2.3.4.

	bipy	4,4'-dmb	5,5'-dmb	6,6'-dmb
3H	3.97	3.96	3.84	5.94
4H	3.82	-0.75	3.71	4.91
5H	-2.04	-2.78	-5.07	-1.74
6H	-46	-50	-48	-49

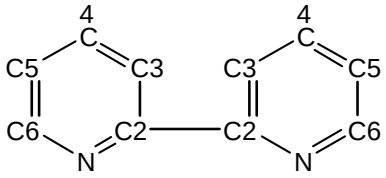

Table 2.3.4: The ^{1}H NMR chemical shifts of bipy and substituted bipyridines ligands in $[Cp^*_2Ce(x,x'\text{-bipy})][BPh_4]$ in CD_2Cl_2 at 20 °C.

2.4 Synthesis and properties of $Cp^*_2Ln(bipy)(X)$ and $[Cp^*_2Ln(bipy)]^+$ (Ln = La, Sm, Gd, Yb, and Lu; X = OTf and halide)

Adding bipy to Cp^*_2SmOTf also forms the inner-sphere adduct, $Cp^*_2Sm(bipy)(OTf)$, as shown by the ORTEP diagram in Figure 2.4.1. The ^{1}H NMR spectrum only shows the four bipy resonances of area two splitting into eight resonances of area one at 185 K (Figure 2.4.2). There are not enough data points of the split resonances to estimate the activation energy for this process. $Cp^*_2Sm(4,4'\text{-dmb})(OTf)$

does not show the peaks of area 2 splitting into two peaks of area one at all (Figure 2.4.3). This is in marked contrast with the cerium case, where $Cp^*_2Ce(4,4'\text{-dmb})(OTf)$ has a much higher activation energy for the averaging of the bipy resonances than does $Cp^*_2Ce(bipy)(OTf)$.

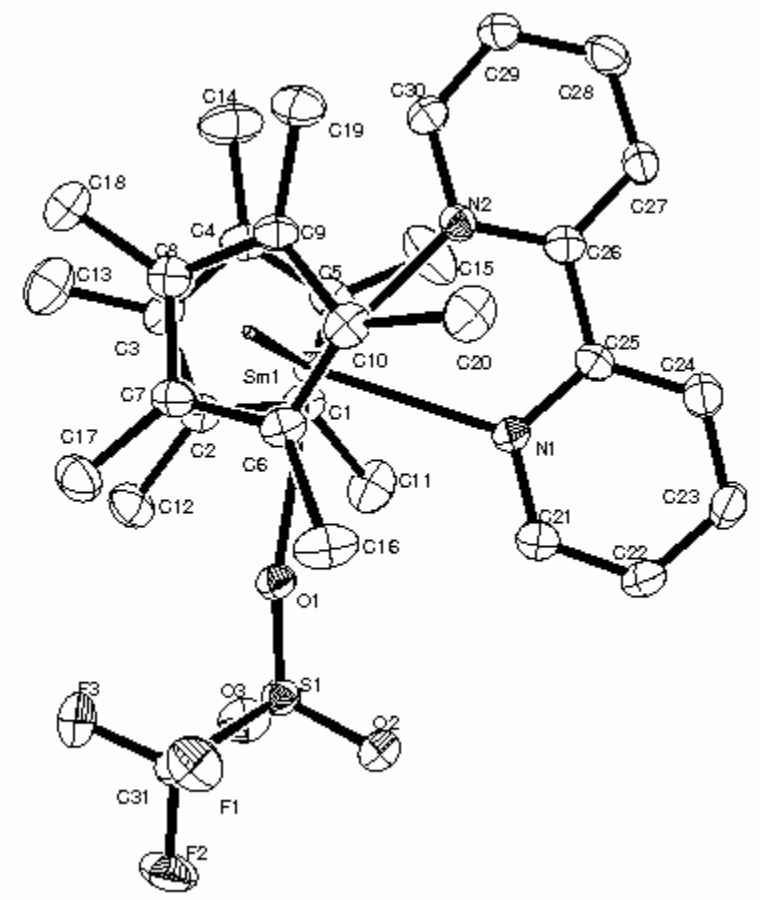

Figure 2.4.1 ORTEP diagram of $Cp^*_2Sm(bipy)(OTf)$ (50% probability ellipsoids). All non-hydrogen atoms are refined anisotropically. Hydrogen atoms are placed and not refined and are not shown. Selected Bond Distances and Angles are given in Tables 2.4.1 and 2.4.2, respectively. The N1-C25-C26-N2 torsion angle is 7.2(5)°.

Table 2.4.1: Selected bond distances (Å) in $Cp^*_2Sm(bipy)(OTf)$

atom	Atom	distance		Atom	atom	distance
Sm(1)	O(1)	2.668(3)		Sm(1)	N(1)	2.600(3)
Sm(1)	N(2)	2.542(3)		Sm(1)	C(1)	2.706(4)

Sm(1)	C(2)	2.731(4)		Sm(1)	C(3)	2.760(4)
Sm(1)	C(4)	2.783(4)		Sm(1)	C(5)	2.749(4)
Sm(1)	C(6)	2.687(4)		Sm(1)	C(7)	2.664(4)
Sm(1)	C(8)	2.772(4)		Sm(1)	C(9)	2.851(4)
Sm(1)	C(10)	2.786(4)		Sm(1)	C(101)	2.470
Sm(1)	C(102)	2.476		C(21)	C(22)	1.377(6)
C(22)	C(23)	1.369(7)		C(23)	C(24)	1.384(6)
C(24)	C(25)	1.385(6)		C(25)	C(26)	1.489(5)
C(26)	C(27)	1.394(6)		C(27)	C(28)	1.388(6)
C(28)	C(29)	1.363(6)		C(29)	C(30)	1.371(5)

Table 2.4.2: Selected bond angles (°) in $Cp^*_2Sm(bipy)(OTf)$

atom	atom	atom	angle		atom	atom	atom	angle
O(1)	Sm(1)	N(1)	80.93(9)		O(1)	Sm(1)	N(2)	143.73(9)
N(1)	Sm(1)	N(2)	62.8(1)		C(101)	Sm(1)	C(102)	139.1

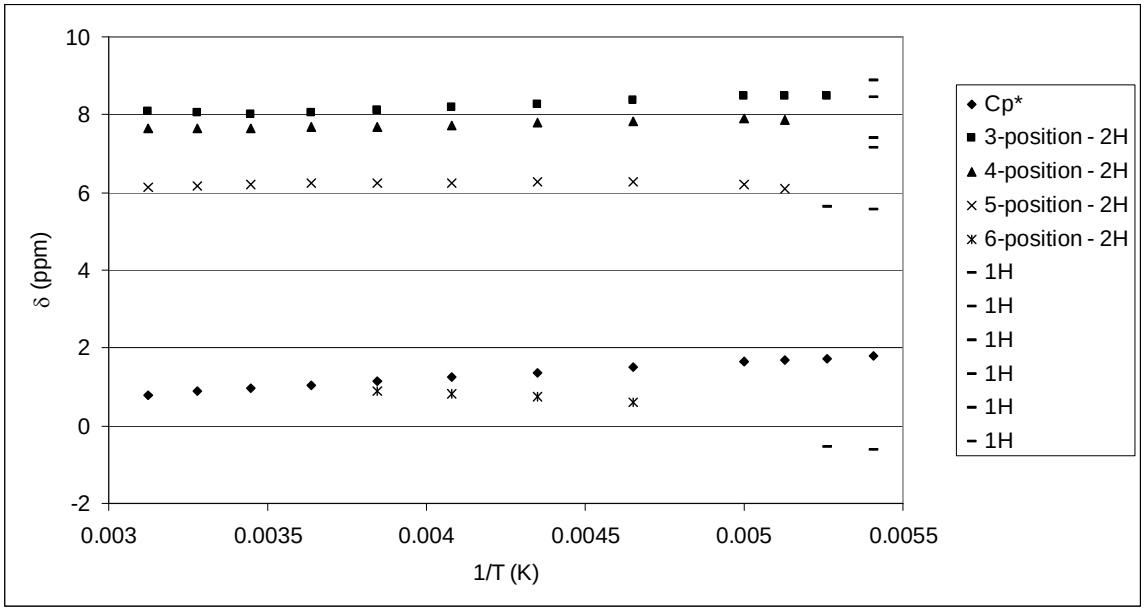

Figure 2.4.2: Variable Temperature ^1H NMR spectra represented as a δ vs. 1/T plot of $Cp^*_2Sm(bipy)(OTf)$ in CD_2Cl_2. Two of the area one resonances are not found.

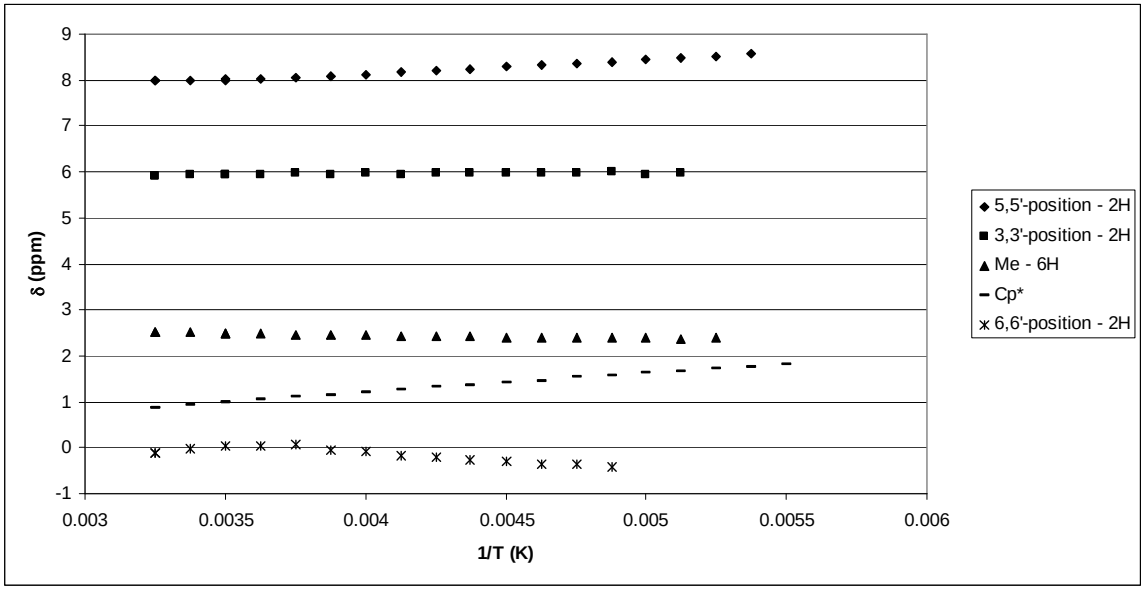

Figure 2.4.3: Variable Temperature ^{1}H NMR spectra represented as a δ vs. 1/T plot of $Cp^*_2Sm(4,4'\text{-dmb})(OTf)$ in CD_2Cl_2.

Substitution of the triflate with tetraphenylborate forms the separated-ion complex, $[Cp^*_2Sm(bipy)][BPh_4]$. The ^{1}H NMR spectra show a 30:2:2:2:2 ratio at all temperatures (Figure 2.4.4). $[Cp^*_2Sm(4,4'\text{-dmb})][BPh_4]$ is made in an analogous fashion.

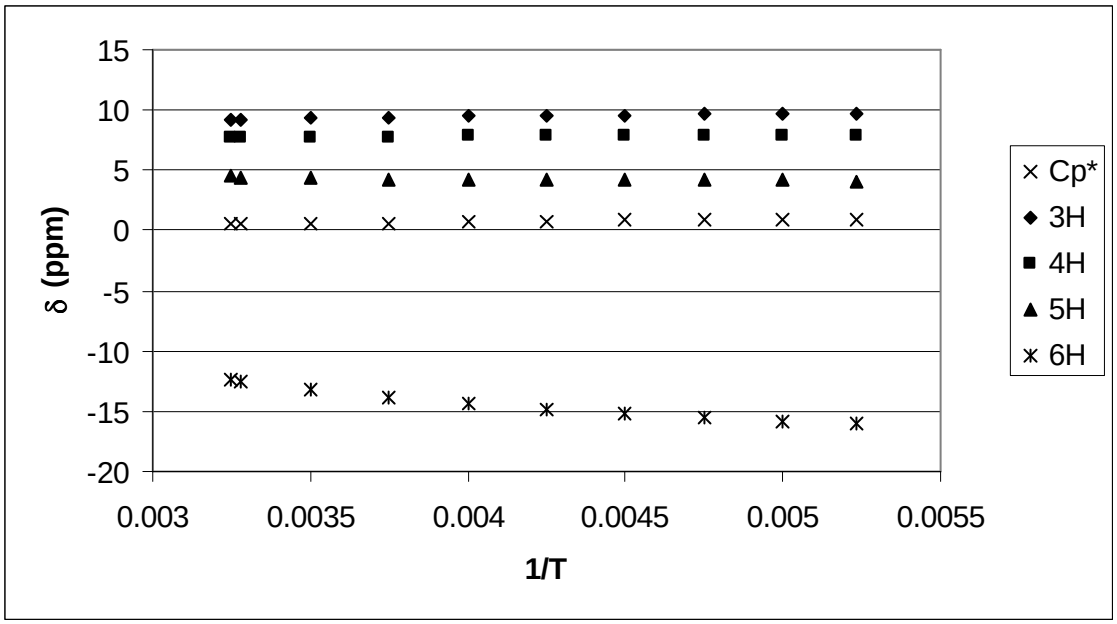

Figure 2.4.4: Variable Temperature ^{1}H NMR spectra represented as a δ vs. 1/T plot of $[Cp^*_2Sm(bipy)][BPh_4]$ in CD_2Cl_2.

Gd is NMR silent which makes the solution properties impossible to study by this physical method. However, addition of bipy to $Cp^*_2GdCl_2Na$[9] forms the inner-sphere $Cp^*_2Gd(bipy)(Cl)$ (Figure 2.4.5). Addition of $[Na][BPh_4]$ to $Cp^*_2Gd(bipy)(Cl)$ or to a mixture of Cp^*_2GdOTf and bipy forms the cation-anion pair $[Cp^*_2Gd(bipy)][BPh_4]$ (Figure 2.4.6).

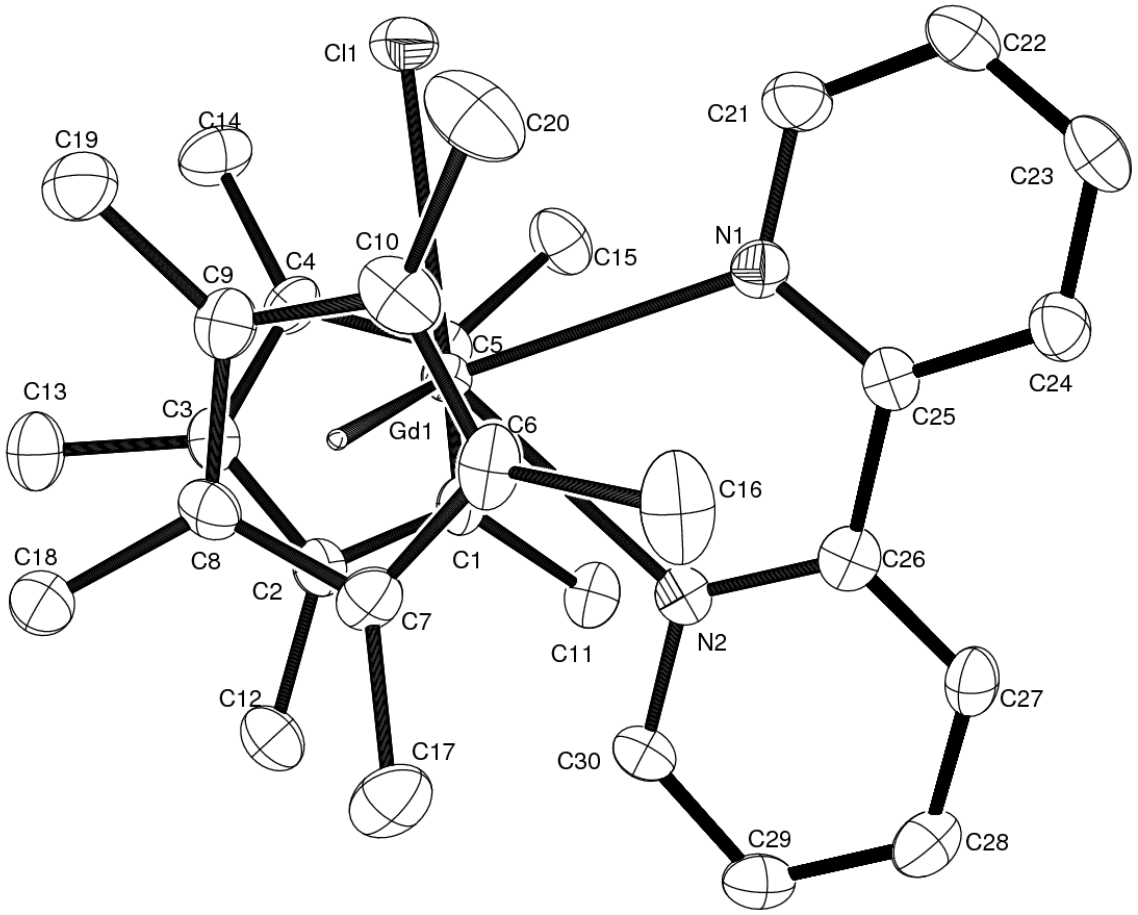

Figure 2.4.5. ORTEP diagram of $Cp^*_2Gd(bipy)(Cl)$ (50% probability ellipsoids). All non-hydrogen atoms are refined anisotropically. Hydrogen atoms are placed and not refined and are not shown. Selected Bond Distances and Angles are given in Tables 2.4.3 and 2.4.4, respectively. The N1-C25-C26-N2 torsion angle is 7.7(5)°.

Table 2.4.3: Selected bond distances (Å) in $Cp^*_2Gd(bipy)(Cl)$

atom	atom	distance		atom	atom	distance
Gd1	Cl1	2.692(1)		Gd1	N1	2.648(3)
Gd1	N2	2.578(3)		Gd1	C1	2.773(4)
Gd1	C2	2.800(4)		Gd1	C3	2.797(4)
Gd1	C4	2.773(4)		Gd1	C5	2.714(4)
Gd1	C6	2.748(4)		Gd1	C7	2.769(4)
Gd1	C8	2.723(4)		Gd1	C9	2.680(4)
Gd1	C10	2.710(4)		Gd1	C101	2.50
Gd1	C102	2.45		N1	C21	1.350(5)
N1	C25	1.349(5)		N2	C26	1.362(5)

N2	C30	1.335(5)		C21	C22	1.391(6)
C22	C23	1.368(7)		C23	C24	1.369(6)
C24	C25	1.396(5)		C25	C26	1.479(6)
C26	C27	1.383(6)		C27	C28	1.371(6)
C28	C29	1.382(6)		C29	C30	1.381(6)

Table 2.4.4: Selected bond angles (°) in $Cp^*_2Gd(bipy)(Cl)$

atom	atom	atom	angle		atom	atom	atom	angle
Cl1	Gd1	N1	78.54(8)		Cl1	Gd1	N2	139.96(8)
Cl1	Gd1	C1	112.27(9)		Cl1	Gd1	C2	120.43(9)
Cl1	Gd1	C3	94.51(9)		Cl1	Gd1	C4	72.02(9)
Cl1	Gd1	C5	82.49(9)		Cl1	Gd1	C6	106.07(10)
Cl1	Gd1	C7	125.69(9)		Cl1	Gd1	C8	107.28(9)
Cl1	Gd1	C9	78.36(10)		Cl1	Gd1	C10	78.04(10)
Cl1	Gd1	C101	96.82(3)		Cl1	Gd1	C102	99.81(2)
N1	Gd1	N2	61.9(1)		C101	Gd1	C102	134.6

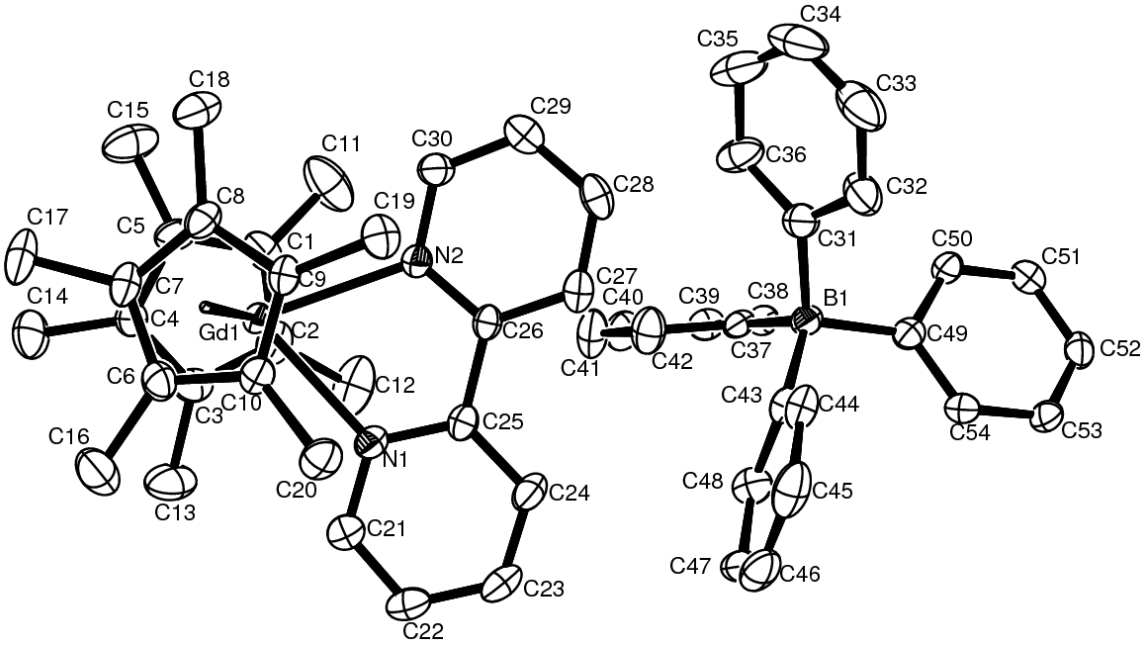

Figure 2.4.6: ORTEP diagram of $[Cp^*_2Gd(bipy)][BPh_4]$ (50% probability ellipsoids). All non-hydrogen atoms are refined anisotropically. Hydrogen atoms are placed and not refined and are not shown. Selected Bond Distances and Angles are given in Tables 2.4.5 and 2.4.6, respectively. The N1-C25-C26-N2 torsion angle is 5.7(4)°. The closest contact in the ion-pair is between C(28) and C(36); it is 3.243 (4) Å.

Table 2.4.5: Selected bond distances (Å) in [$Cp^*_2Gd(bipy)][BPh_4$]

atom	atom	Distance		Atom	atom	Distance
Gd(1)	N(1)	2.433(2)		Gd(1)	N(2)	2.445(2)
Gd(1)	C(1)	2.678(3)		Gd(1)	C(2)	2.682(3)
Gd(1)	C(3)	2.677(3)		Gd(1)	C(4)	2.667(3)
Gd(1)	C(5)	2.663(3)		Gd(1)	C(6)	2.679(3)
Gd(1)	C(7)	2.670(3)		Gd(1)	C(8)	2.661(3)
Gd(1)	C(9)	2.683(3)		Gd(1)	C(10)	2.699(3)
Gd(1)	C(101)	2.39		Gd(1)	C(102)	2.39
N(1)	C(21)	1.348(4)		N(1)	C(25)	1.354(4)
N(2)	C(26)	1.356(4)		N(2)	C(30)	1.350(4)
C(21)	C(22)	1.373(4)		C(22)	C(23)	1.373(5)
C(23)	C(24)	1.375(4)		C(24)	C(25)	1.392(4)
C(25)	C(26)	1.485(4)		C(26)	C(27)	1.396(4)
C(27)	C(28)	1.378(4)		C(28)	C(29)	1.382(4)
C(29)	C(30)	1.379(4)				

Table 2.4.6: Selected bond angles (°) in [$Cp^*_2Gd(bipy)][BPh_4$]

atom	atom	atom	Angle		Atom	atom	atom	angle
N(1)	Gd(1)	N(2)	67.12(8)		C(101)	Gd(1)	C(102)	144.0

Addition of bipy to Cp^*_2YbOTf gives a compound with ^1H NMR signals at 337.8, 57.7, 9.1, 7.7, 3.4, and -16.2 ppm in a ratio of 2:2:2:1.6:30:2, respectively. The chemical shifts of the peaks with the ratio 30:2:2:2:2 are identical to the ^1H NMR signal found for [$Cp^*_2Yb(bipy)][I]$,[10] implying that cationic partners in these two complexes are solvent separated ion-pairs $[Cp^*_2Yb(bipy)]^+$. The peak at 7.7 ppm is unexpected, and repeated recrystallizations do not remove this peak. In the ^{19}F NMR spectrum, there are two peaks: at -76.5 ppm and at -50.3 ppm in an area ratio of 7:1, respectively. In [$Cp^*_2Yb(4,4'$-dmb)][OTf], the ^1H NMR spectrum contains resonances at 336.3, 57.2, 8.0, 7.5, 3.5, and -16.9 ppm, in a ratio of 2:2:24:6:30:2, respectively. Again the peak at 8.0 ppm is unexpected, although in this sample the area ratio of the resonancecs at 3.5 and 8.0 ppm are similar, implying that these resonances are due to Cp^*_2Yb fragments. The ^{19}F NMR

spectrum shows one peak at -51.1 ppm. It seems likely that in the case of $[Cp^*_2Yb(4,4'\text{-dmb})]^+$ the counter-ion is $[Cp^*_2Yb(OTf)_2]^-$ in analogy with the isolated complex, $[Cp^*_2Yb(4,4'dmb)][Cp^*_2YbI_2]$. Extension of this reasoning to the case of $[Cp^*_2Yb(bipy)]^+$ implies that the two counter-ions are $[Cp^*_2Yb(OTf)_2]^-$ and $[OTf]^-$.[10] This inference is strengthened by comparing the variable-temperature ^1H NMR and ^{19}F NMR spectra of what we assume to be $[Cp^*_2Yb(bipy)][OTf]/[Cp^*_2Yb(OTf)_2]$, $[Cp^*_2Yb(4,4'\text{-dmb})][Cp^*_2Yb(OTf)_2]$ and the isolated complex $[NEt_4][Cp^*_2Yb(OTf)_2]$ (described in chapter 1) (Figure 2.4.7). Thus, a solution of $[Cp^*_2Yb(bipy)][OTf]$ contains two species, $[Cp^*_2Yb(bipy)][OTf]$ and $[Cp^*_2Yb(bipy)][Cp^*_2Yb(OTf)_2]$, where the C_5Me_5 resonances are at 3.4 ppm for the $[Cp^*_2Yb(bipy)]^+$ portion and at 7.7 ppm for the $[Cp^*_2Yb(OTf)_2]$ portion. If this supposition is true, then the components of the mixture can be changed by adding bipy to the mixture. Since the ratio of molecules of $[Cp^*_2Yb(4,4'\text{-dmb})][Cp^*_2Yb(OTf)_2]$ to molecules of $[Cp^*_2Yb(4,4'\text{-dmb})][OTf]$ is greater than in the unsubstituted bipy example, the shift in population is more easily demonstrated in the former case. Accordingly, addition of 4,4'-dmb to a solution of $[Cp^*_2Yb(4,4'\text{-dmb})][Cp^*_2Yb(OTf)_2]$ results in the ratio of the C_5Me_5 groups in the ^1H NMR spectrum to change from 24:30 to 2.7:30, and in the ^{19}F NMR spectrum the peak at -51.1 ppm shifts to -77.0 ppm, which is closer to -79.4 ppm, the value found in diamagnetic $[NEt_4][OTf]$. Thus, the equilibrium in equation (1)

$$[Cp^*_2Yb(4,4'\text{-dmb})][Cp^*_2Yb(OTf)_2] + 4,4'\text{-dmb} \rightarrow 2[Cp^*_2Yb(4,4'\text{-dmb})][OTf] \quad (1)$$

is implied. However, attempts to isolate [Cp*$_2$Yb(4,4'-dmb)][OTf] as a solid only results in crystallization of [Cp*$_2$Yb(4,4'-dmb)][Cp*$_2$Yb(OTf)$_2$].

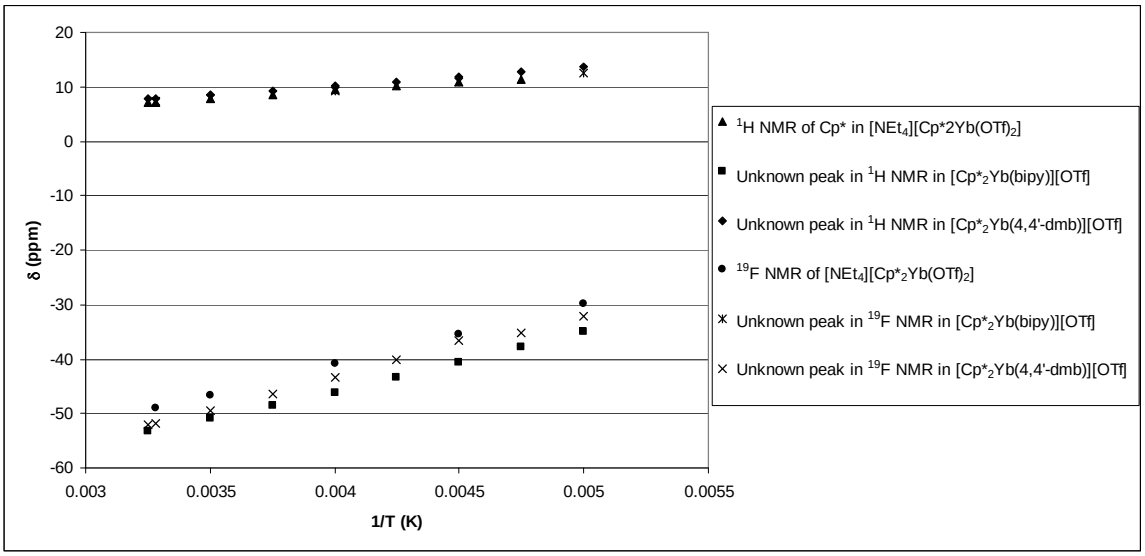

Figure 2.4.7: Variable Temperature ^{1}H and ^{19}F NMR spectra represented as a δ vs. 1/T plot of [NEt$_4$][Cp*$_2$YbOTf$_2$] compared with the unidentified peaks in [Cp*$_2$Yb(bipy)][OTf] and [Cp*$_2$Yb(4,4'-dmb)][OTf] in CD_2Cl_2.

As observed in the metallocenes derived from Ce, Sm, and Gd, addition of $NaBPh_4$ to the ytterbium bipy triflate complex gives pure [Cp*$_2$Yb(bipy)][BPh$_4$]. Addition of $NaBPh_4$ in the presence of the substituted bipy also results in formation of [Cp*$_2$Yb(4,4'-dmb)][BPh$_4$], [Cp*$_2$Yb(4,4'-CO_2Me-bipy)][BPh$_4$] and [Cp*$_2$Yb(4,4'-CO_2Et-bipy)][BPh$_4$]. 1,4-Diazabutadiene ligands do not form complexes with Cp*$_2$YbOTf. However, as in the case of [Cp*$_2$Ce(6,6'-dmb)][BPh$_4$], addition of $NaBPh_4$ to Cp*$_2$YbOTf(pyridine) in the presence of p-tolyl-dad (p-tolyl-dad = N,N'-bis(p-tolyl)-1,4-diazadiene)) gives [Cp*$_2$Yb(p-tolyl-dad)][BPh$_4$] (Figure 2.4.8), (Equation 2).

$$Cp^*_2Yb(OTf) + N,N'\text{-bis(p-tolyl)-1,4-diazadiene} + NaBPh_4 \rightarrow [Cp^*_2Yb(N,N'\text{-bis(p-tolyl)-1,4-diazadienyl})][BPh_4] + NaOTf \quad (2)$$

The same method works to give $[Cp^*_2Yb(N,N'\text{-bis(p-anisyl)-1,4-diazadienyl})][BPh_4]$ and $[Cp^*_2Yb(N,N'\text{-bis(p-anisyl)-2,3-dimethyl-1,4-diazadienyl})][BPh_4]$, but it does not work to synthesize $[Cp^*_2Yb(6,6'\text{-dmb})][BPh_4]$.

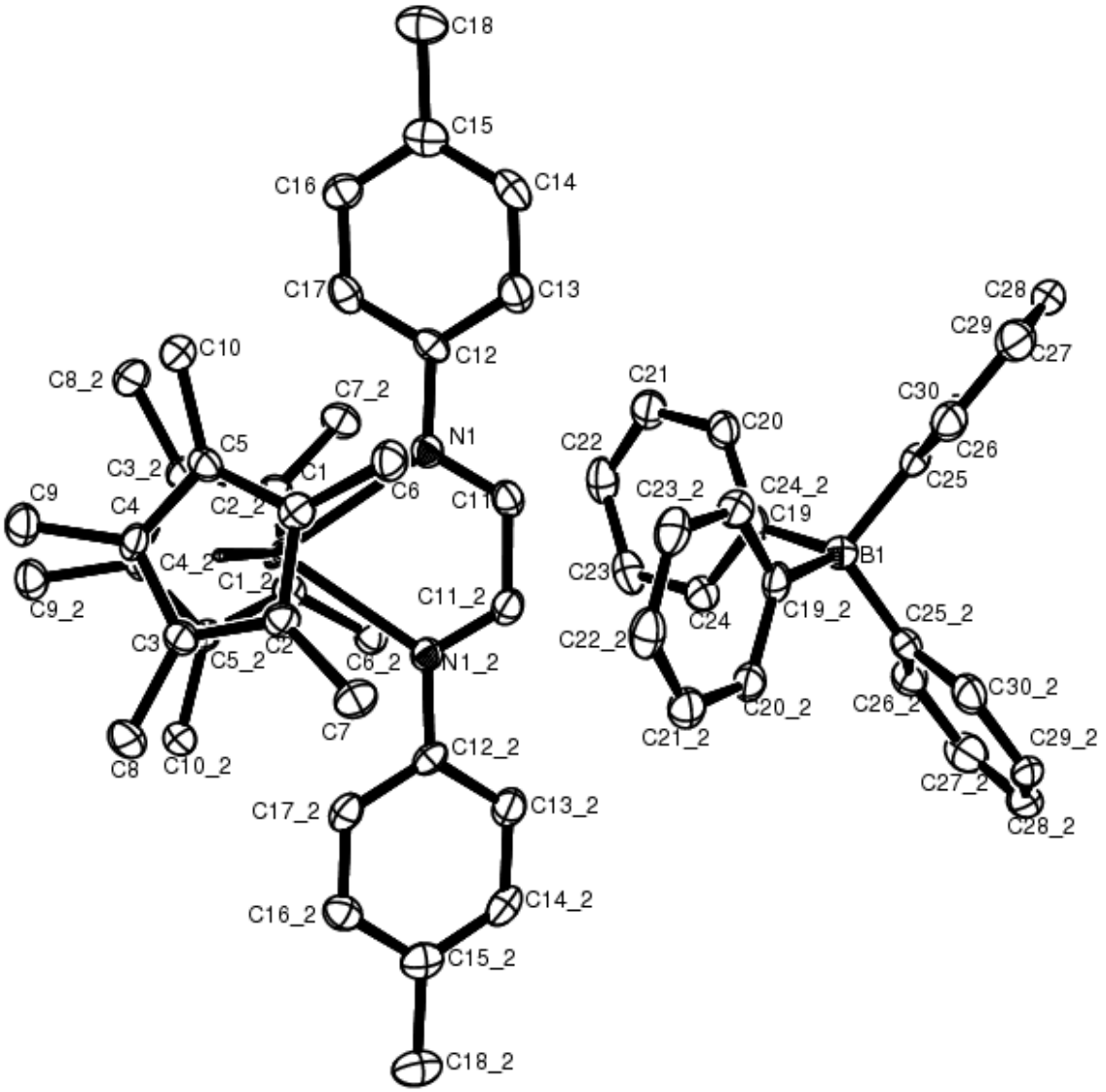

Figure 2.4.8: ORTEP diagram of [Cp*$_2$Yb(p-tolyl-dad)][BPh$_4$] (50% probability ellipsoids). All non-hydrogen atoms are refined anisotropically. Hydrogen atoms are placed and not refined and are not shown. The molecule has a crystallographic C_2 axis. Selected Bond Distances and Angles are given in Tables 2.4.7 and 2.4.8, respectively. The closest contact distance in the ion-pair is 3.507(7) Å between C(11) and C(24). The N1-C11-C11-N1 torsion angle is 1.3(1)°.

Table 2.4.7: Selected bond distances (Å) in [Cp*$_2$Yb(p-tolyl-dad)][BPh$_4$]

atom	atom	distance		Atom	Atom	Distance
Yb(1)	N(1)	2.449(4)		Yb(1)	C(1)	2.601(4)
Yb(1)	C(2)	2.631(4)		Yb(1)	C(3)	2.638(4)
Yb(1)	C(4)	2.620(4)		Yb(1)	C(5)	2.588(4)
Yb(1)	C(101)	2.32		N(1)	C(11)	1.281(6)
N(1)	C(12)	1.435(6)		C(11)	C(11)	1.478(9)
C(12)	C(13)	1.398(7)		C(12)	C(17)	1.392(7)
C(13)	C(14)	1.385(7)		C(14)	C(15)	1.396(7)
C(15)	C(16)	1.393(7)		C(15)	C(18)	1.512(7)
C(16)	C(17)	1.388(7)				

Table 2.4.8: Selected bond angles (°) in [Cp*$_2$Yb(p-tolyl-dad)][BPh$_4$]

atom	atom	atom	angle		Atom	atom	atom	angle
N(1)	Yb(1)	N(1)	69.3(2)		C(101)	Yb(1)	C(101)	138.3

It is interesting that in the cases of [Cp*$_2$Yb(p-tolyl-dad)][BPh$_4$], the ^{1}H resonances for the tetraphenylborate are shifted to 2.24 (8H), 1.19 (8H), and -0.65 (4H) ppm and show a relatively strong temperature dependence, as does the ^{11}B NMR chemical shift (Figure 2.4.9). The same is true for [Cp*$_2$Yb(N,N'-bis(p-anisyl)-1,4-diazadienyl)][BPh$_4$] (Figure 2.4.10). [Cp*$_2$Yb(N,N'-bis(p-anisyl)-2,3-dimethyl-1,4-

diazadienyl)][BPh_4] shows a smaller temperature dependance to the chemical shifts (Figure 2.4.11).

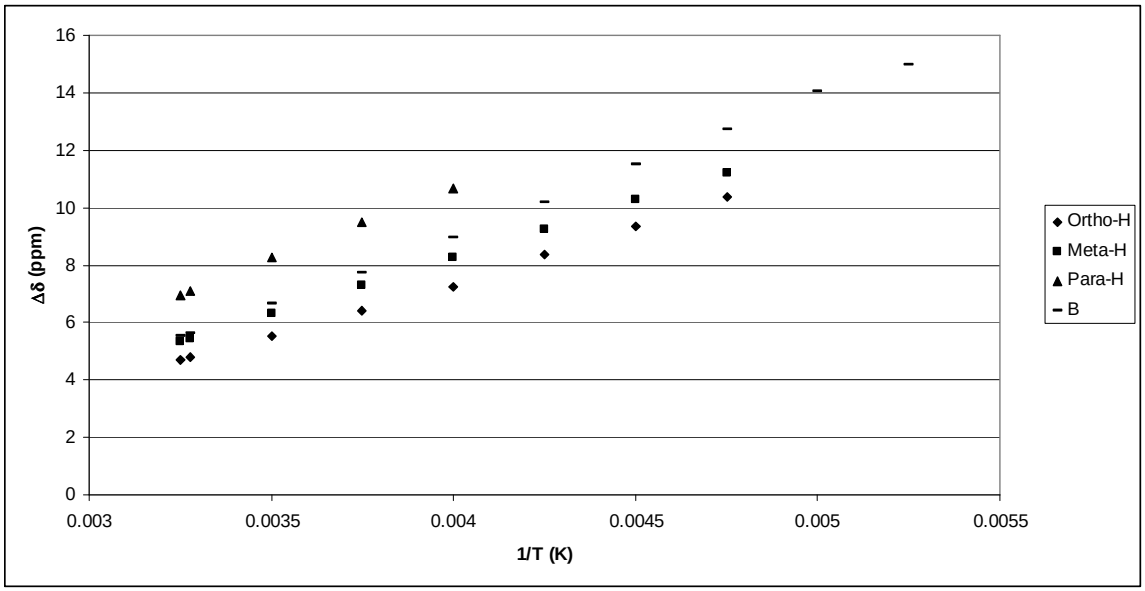

Figure 2.4.9: Variable Temperature of the isotropic values of the ^{1}H and ^{11}B NMR shifts represented as a δ vs. 1/T plot of [BPh_4] in [Cp^*_2Yb(p-tolyl-dad)][BPh_4] in CD_2Cl_2. The isotropic shift, $\Delta\delta = \delta^{dia} - \delta^{para}$, where δ^{dia} is taken from the ^{1}H and ^{11}B NMR spectra of [Cp^*_2Lu(bipy)][BPh_4] in CD_2Cl_2. In the ^{1}H NMR spectrum of [Cp^*_2Lu(bipy)][BPh_4] the ortho-H is at 7.43 ppm and the meta-H is at 7.05 ppm, and they are easily distinguishable by their coupling pattern. In [Cp^*_2Yb(p-tolyl-dad)][BPh_4] there is no coupling on the [BPh_4] resonances, and therefore it is difficult to assign which peak is which. We assume that the peak that is further downfield is the ortho-H just as in the case of [Cp^*_2Lu(bipy)][BPh_4]. The para-H is easily identified by its relative integral.

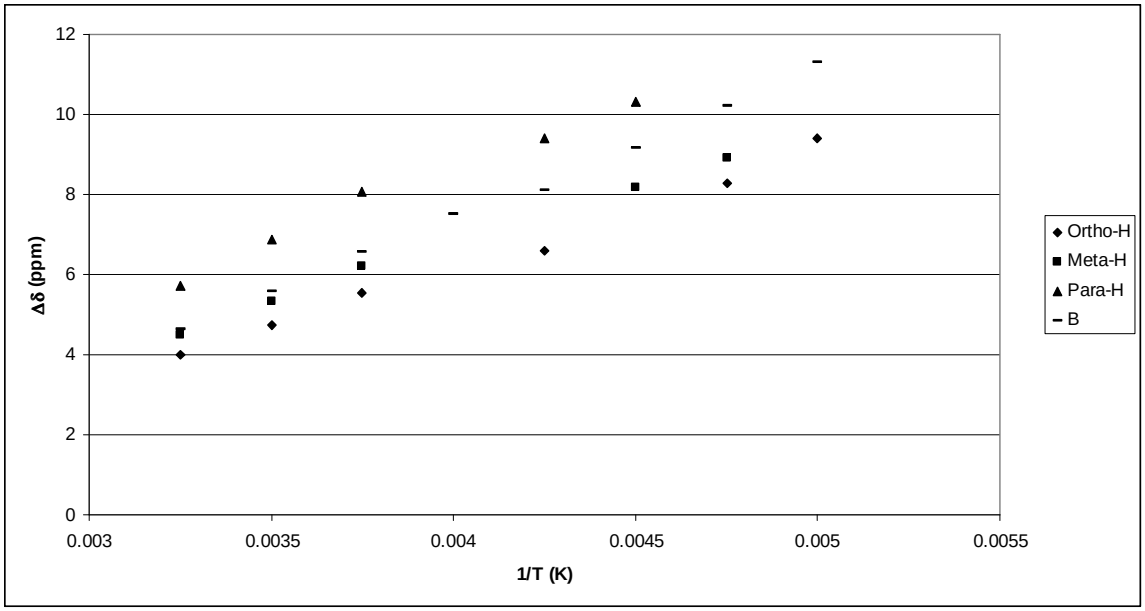

Figure 2.4.10: Variable Temperature of the isotropic values of the ^{1}H and ^{11}B NMR shifts represented as a δ vs. 1/T plot of $[BPh_4]$ in $[Cp^*_2Yb(N,N'\text{-bis(p-anisyl)-1,4-diazadienyl})][BPh_4]$ in CD_2Cl_2. The isotropic shift, $\Delta\delta = \delta^{dia} - \delta^{para}$, where δ^{dia} is taken from the ^{1}H and ^{11}B NMR spectra of $[Cp^*_2Lu(bipy)][BPh_4]$ in CD_2Cl_2. In the ^{1}H NMR spectrum of $[Cp^*_2Lu(bipy)][BPh_4]$ the ortho-H is at 7.43 ppm and the meta-H is at 7.05 ppm, and they are easily distinguishable by their coupling pattern. In $[Cp^*_2Yb(p\text{-tolyl-dad})][BPh_4]$ there is no coupling on the $[BPh_4]$ resonances, and therefore it is difficult to assign which peak is which. We assume that the peak that is further downfield is the ortho-H just as in the case of $[Cp^*_2Lu(bipy)][BPh_4]$. The para-H is easily identified by its relative integral.

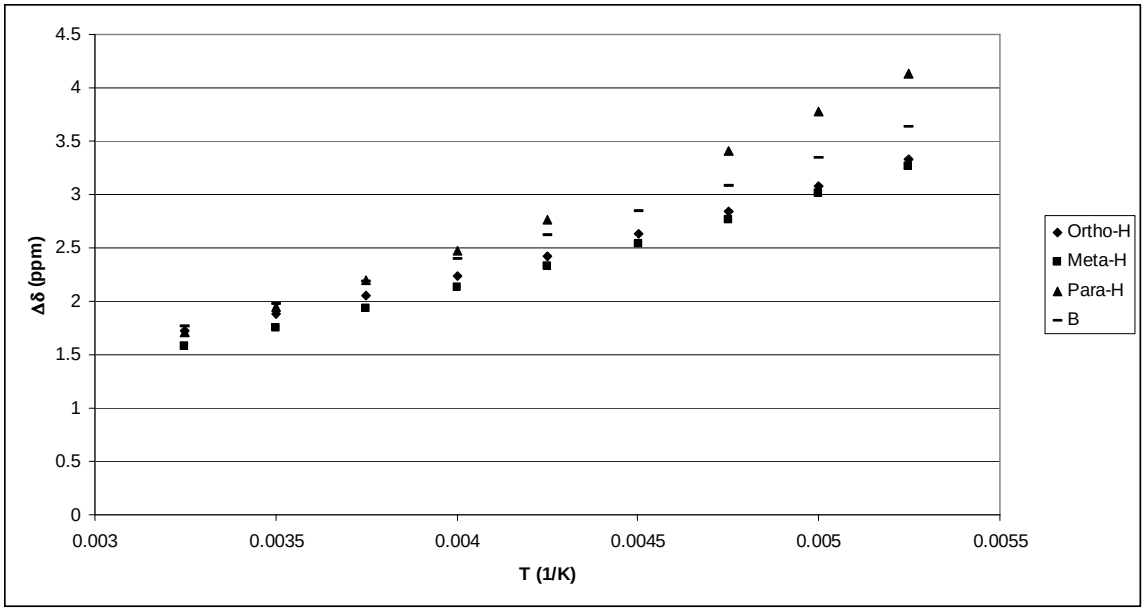

Figure 2.4.11: Variable Temperature of the isotropic values of the ^{1}H and ^{11}B NMR shifts represented as a δ vs. 1/T plot of $[BPh_4]$ in $[Cp^*_2Yb(N,N'\text{-bis(p-anisyl)-2,3-dimethyl-1,4-diazadienyl})][BPh_4]$ in CD_2Cl_2. The isotropic shift, $\Delta\delta = \delta^{dia} - \delta^{para}$, where δ^{dia} is taken from the ^{1}H and ^{11}B NMR spectra of $[Cp^*_2Lu(bipy)][BPh_4]$ in CD_2Cl_2. In the ^{1}H NMR spectrum of $[Cp^*_2Lu(bipy)][BPh_4]$ the ortho-H is at 7.43 ppm and the meta-H is at 7.05 ppm, and they are easily distinguishable by their coupling pattern. In $[Cp^*_2Yb(p\text{-tolyl-dad})][BPh_4]$ there is no coupling on the $[BPh_4]$ resonances, and therefore it is difficult to assign which peak is which. We assume that the peak that is further downfield is the ortho-H just as in the case of $[Cp^*_2Lu(bipy)][BPh_4]$. The para-H is easily identified by its relative integral.

The tetraphenylborate resonances in $[Cp^*_2Yb(4,4'\text{-}CO_2Me\text{-bipy})][BPh_4]$ also show a temperature dependence but to a much smaller degree (Figure 2.4.12), and with the reverse sign.

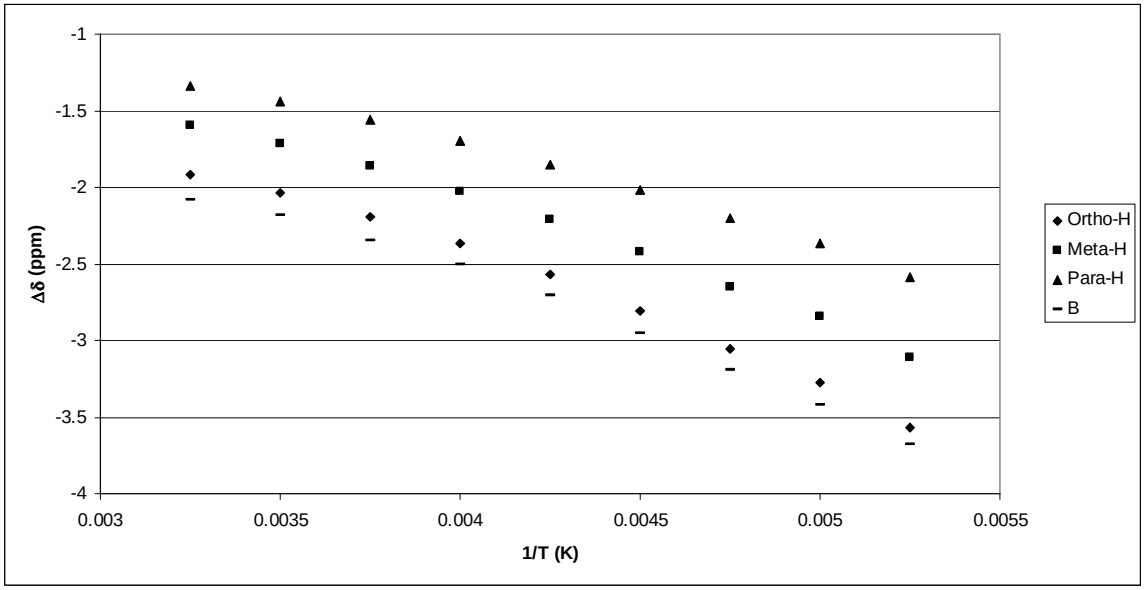

Figure 2.4.12: Variable Temperature of the isotropic values of the ^{1}H and ^{11}B NMR shifts represented as a δ vs. 1/T plot of $[BPh_4]$ in $[Cp^*_2Yb(CO_2Me\text{-}bipy)][BPh_4]$ in CD_2Cl_2. The isotropic shift, $\Delta\delta = \delta^{dia} - \delta^{para}$, where δ^{dia} is taken from the ^{1}H and ^{11}B NMR spectra of $[Cp^*_2Lu(bipy)][BPh_4]$ in CD_2Cl_2. In the ^{1}H NMR spectra of $[Cp^*_2Yb(CO_2Me\text{-}bipy)][BPh_4]$ and $[Cp^*_2Lu(bipy)][BPh_4]$ the $[BPh_4]$ resonances are easily distinguishable by their coupling pattern.

The tetraphenylborate resonances in the ^{1}H NMR spectra of $[Cp^*_2Sm(bipy)][BPh_4]$ show almost no temperature dependence (no peak shifts more than 0.03 ppm between 191 K and 308 K). In the case of $[Cp^*_2Ce(x\text{-}x'\text{-}bipy)][BPh_4]$, the largest temperature dependence is found in $[Cp^*_2Ce(6,6'\text{-}dmb)][BPh_4]$; it is only 0.82 ppm between 190 K and 305 K (Figure 2.4.13). Thus, the "isotropic shift" of the outer-sphere $[BPh_4]$ and its dependence on temperature in the p-tolyl-dad complex is unique among all of the ion-pair tetraphenylborate complexes described in this thesis.

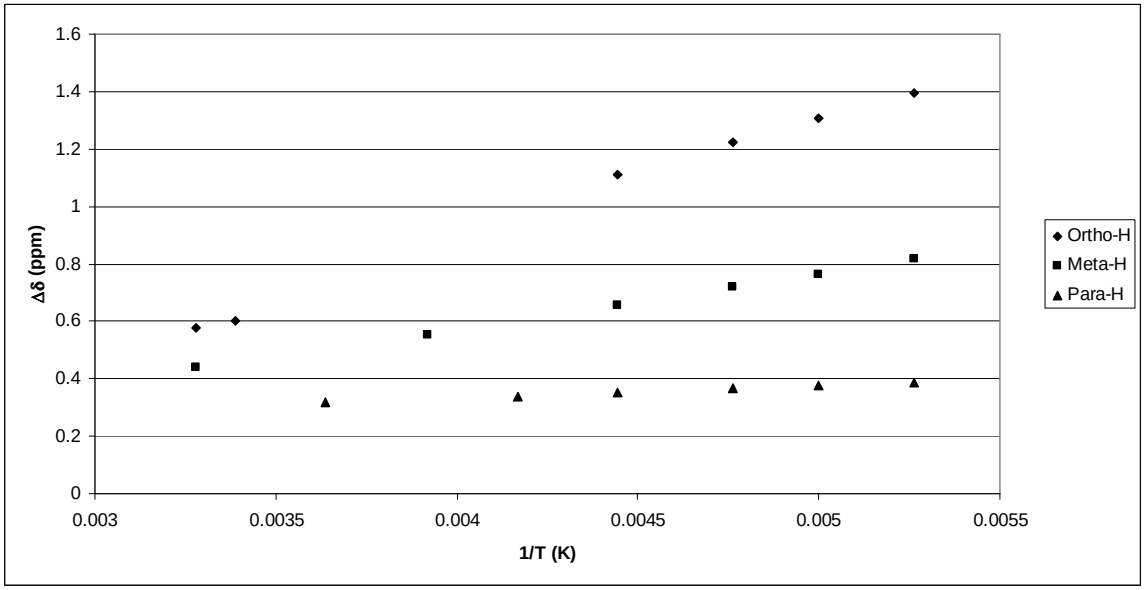

Figure 2.4.13: Variable Temperature of the isotropic values of the ^{1}H shifts represented as a δ vs. 1/T plot of [BPh_4] in [$Cp^*_2Ce(6,6'\text{-dmb})$][$BPh_4$] in CD_2Cl_2. The isotropic shift, $\Delta\delta = \delta^{dia} - \delta^{para}$, where δ^{dia} is taken from the ^{1}H NMR spectra of [$Cp^*_2Lu(bipy)$][BPh_4] in CD_2Cl_2. In the ^{1}H NMR spectra of [$Cp^*_2Ce(6,6'\text{-dmb})$][$BPh_4$] and [$Cp^*_2Lu(bipy)$][$BPh_4$] the [$BPh_4$] resonances are distinguishable by their coupling pattern.

Addition of bipy to $Cp^*_2LaOTf(pyridine)$ forms $Cp^*_2La(bipy)(OTf)$. However, addition of $NaBPh_4$ does not generate the tetraphenylborate complex. In the case of $Cp^*_2LuCl_2Na$, addition of bipy forms [$Cp^*_2Lu(bipy)$][$Cp^*_2LuCl_2$], just as in the case of [$Cp^*_2Yb(bipy)$][$Cp^*_2YbCl_2$].[1] Crystals of [$Cp^*_2Lu(bipy)$][$Cp^*_2LuCl_2$] were mounted on a diffractometer and a unit cell was obtained. The unit cell of [$Cp^*_2Lu(bipy)$][$Cp^*_2LuCl_2$] is a = 10.7758, b = 13.1584, c = 16.3876, α = 90.622, β = 93.970, and γ = 95.296 which is isomorphous with ytterbium analogue. Interestingly, whereas in the case of [$Cp^*_2Yb(4,4'\text{-dmb})$][$Cp^*_2Yb(OTf)_2$], addition of 4,4'-dmb gives [$Cp^*_2Yb(4,4'$-dmb)][OTf] in solution, in the case of [$Cp^*_2Lu(bipy)$][$Cp^*_2LuCl_2$] addition of bipy does

not give $[Cp^*_2Lu(bipy)][BPh_4]$. However, addition of $NaBPh_4$ and a stoichiometric amount of bipy to $[Cp^*_2Lu(bipy)][Cp^*_2LuCl_2]$ does indeed give $[Cp^*_2Lu(bipy)][BPh_4]$, as shown in equation 3.

$$[Cp^*_2Lu(bipy)][Cp^*_2LuCl_2] + bipy + 2NaBPh_4 \rightarrow 2[Cp^*_2Lu(bipy)][BPh_4] + 2NaCl \quad (3)$$

In conclusion, addition of bipy to Cp^*_2LnX (X = halide or OTf) typically does not give $[Cp^*_2Ln(bipy)][X]$: it either gives inner-sphere $Cp^*_2Ln(bipy)(X)$ or it gives $[Cp^*_2Ln(bipy)][Cp^*_2LnX_2]$. However, addition of bipy and $NaBPh_4$ generally gives $[Cp^*_2Ln(bipy)][BPh_4]$. The magnetic properties of these molecules will be discussed in the next chapter.

References:

1. Schultz, M.; Boncella, J. M.; Berg, D. J.; Tilley, T. D.; Andersen, R. A. *Organometallics*, **2002**, *21*, 460
2. Booth, C.H.; Walter, M.D.; Daniel, M.; Luken, W.W.; Andersen, R.A. *Phys. Rev. Lett.*, **2005**, *95*, 267202
3. Gutowsky, H.S.; Holm, C.H. *J. Chem. Phys.*, **1956**, *25*, 1228.
4. Sandstrom, J. *Dynamic NMR Spectroscopy*; Academic Press: New York, 1982.
5. Kazhdan, Daniel; Chomitz, W. A.; Harman, W. H.; Hoette, T. M.; Park, C.-H. *Acta Cryst.*, **2007**, E**63**, m1656
6. Mehdoui, T.; Berthet, J.C.; Thuéry, P.; Salmon, L.; Rivière, E.; Ephritikhine, M. *Chem. Eur. J.*, **2005**, *11*, 6994
7. In the crystal structure reported in the previous footnote the distance from the plane defined by the bipyridine ring to the I is 0.029 Å.
8. Heeres, H. J.; Meetsma, A.; Teuben, J. H. *J. Organomet. Chem.*, **1991**, *414*, 351
9. Schumann, H.; Albrecht, I.; Loebel, J.; Hahn, E.; Hossain, M. B.; van der Helm, D. *Organometallics*, **1986**, *5*, 1296
10. Walter, M. D.; Berg, D. J.; Andersen, R. A. *Organometallics*, **2006**, *25*, 3228

Chapter 3: Synthesis, Properties, and Magnetism of Cp^*_2Ln(2,2'-bipyridine) and 2,2'-Bipyridine Analogues.

3.1 Introduction

In lanthanide ions, the valence 4f orbitals do not penetrate radially the electron density of the 5s and 5p orbitals.[1] As a result, the 4f electrons are relatively unaffected by the ion's external environment, and therefore the magnetic moment of lanthanide ions is nearly independent of its ligands. Van Vleck and Frank derived an equation that predicts the value of the ground state effective magnetic moment of a free metal ion with quantum number *J*,

$$\mu_{eff} = g[J(J+1)]^{1/2} \text{ (B.M.) (B.M. = Bohr Magnetons),}^{2,3} \qquad (1)$$

where

$$g = 1 + [S(S+1) - L(L+1) + J(J+1)]/[2J(J+1)].$$

The accuracy of the assumption that lanthanide ions are well approximated by the free ion is born out by good agreement of this equation with studies of the magnetic moments of various lanthanide salts.[4] In those studies, all of the electrons on the ligands are paired, that is they are closed shell singlets. It is interesting to see if the f-electrons will interact with the ligand when the ligand has unpaired electrons. The case of Cp^*_2Yb(bipy) along with various Cp and bipy derivatives and the case of Cp^*_2Yb(N,N'-bis(x)-1,4-diazadiene) where is x = alkyl or aryl derivatives have been studied previously[5,6,7] In the case of ytterbium, the magnetism is complicated by the presence of a Yb(II)/Yb(III) couple, along with the coupling of the electron with the lanthanide center. It is, therefore,

interesting to study compounds of the general formula $Cp^*_2Ln(bipy)$, where the lanthanide is clearly in the +3 oxidation state, and the magnetism is solely determined by the coupling, or lack thereof, of the unpaired electron on the ligand with the unpaired electron(s) on the metal center. This chapter discusses these complexes when Ln = La, Ce, Sm, and Gd.

Results and Discussion

3.2 Synthesis of $Cp^*_2Ln(2,2'\text{-bipyridine})$ (Ln = La, Ce, Sm, Gd, and Yb) and substituted 2,2'-bipyridine analogues

Addition of Na(bipy) in THF to Cp^*_2CeOTf does not give an isolable product. Addition of THF to $Cp^*_2Ce(bipy)(OTf)$, prepared as discussed in the previous chapter, results in decomposition, therefore conducting the reaction in absence of THF is, perhaps, a useful synthetic strategy. Accordingly, stirring a suspension of $Cp^*_2Ce(bipy)(OTf)$ in a toluene solution over sodium amalgam gives $Cp^*_2Ce(bipy)$ in moderate yield. Crystallization from pentane results in dark red crystals. An alternate synthetic route is to prepare Na(bipy) in THF, remove the THF under dynamic vacuum, and add Cp^*_2CeOTf in toluene to the suspension of Na(bipy). The toluene is removed under dynamic vacuum and crystals are grown from pentane in good yield (71%). The ^{1}H NMR spectrum shows a 30:2:2:2:2 spectrum as expected; the bipy resonances are strongly shifted. The ^{1}H NMR spectrum will be discussed in Section 3.4.

$Cp^*_2Ce(x,x'\text{-dmb})$ (x,x' = 4,5,6) (dmb = dimethyl-2,2'-bipyridine) are prepared in a manner analogous to the second route described above. Thus, Na(x,x'-dmb) (x = 4,5,6)

is made in THF, the THF is removed under dynamic vacuum, Cp^*_2CeOTf in toluene is added to the Na(dmb), the toluene is removed under dynamic vacuum, and crystals of Cp^*_2Ce(x,x'-dmb) are grown from pentane. They all show a ^1H NMR spectra with a 30:6:2:2:2 area ratio of the protons, as expected. Cp^*_2Ce(terpy) (terpy = 2,2',6',2''-terpyridine) is prepared by stirring Cp^*_2Ce(terpy)(OTf) in toluene over a sodium amalgam.

Cp^*_2La(bipy) is prepared by stirring a suspension of Cp^*_2La(bipy)(OTf) in toluene over sodium amalgam. Cp^*_2Sm(bipy), which has been previously synthesized by the addition of bipy to Cp^*_2Sm,[8] is prepared by stirring Cp^*_2Sm(bipy)(OTf) over sodium amalgam. Cp^*_2Sm(4,4'-dmb), Cp^*_2Gd(bipy), and Cp^*_2Gd(4,4'-dmb) are all prepared by adding Cp^*_2Ln(OTf) to Na(bipy) or Na(4,4'-dmb) followed by crystallization from pentane. Cp^*_2Yb(bipy), previously made by adding bipy to $Cp^*_2Yb(OEt_2)$,[5] is made in an analogous fashion. Cp^*_2Ca(bipy), Cp^*_2Sr(bipy), and Cp^*_2Ba(bipy) are made according to the procedure described previously.[9]

Interestingly, addition of Na(N,N'-bis(iso-propyl)-1,4-diazadienyl) to Cp^*_2CeOTf gives Cp^*_2Ce(iso-propyl-N-CH=CH-N=CMe_2) (Figure 3.2.1), with loss of a hydrogen. Crystals can be grown from pentane. The mechanism for this reaction has not been studied, but a proposed mechanism is given in Figure 3.2.1. This dehydrogenation does not occur until it is mixing with Cp^*_2CeOTf; the epr spectrum of the sodium adduct, Na(N,N'-bis(iso-propyl)-1,4-diazadienyl), unambiguously identifies the sodium adduct as a radical.[10]

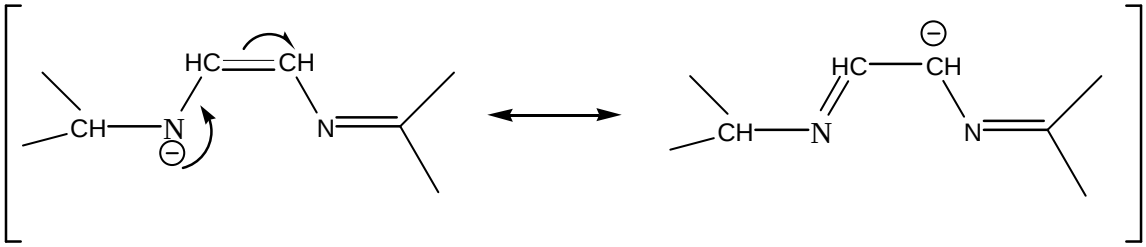

Figure 3.2.1: Resonance structures of [iso-propyl-N-CH=CH-N=CMe_2]$^-$

3.3 Solid State Measurements: X-ray Crystallography

The X-ray structures of bipyridine complexes have been used as evidence for the oxidation state of the bipyridine ligand, because donation of electron density into the LUMO of bipyridine causes systematic changes to the bond lengths.[5,11,12] Therefore the crystal structures of $Cp^*_2Ce(bipy^{\cdot-})$, $Cp^*_2Gd(bipy^{\cdot-})$, $Cp^*_2Sr(bipy)$,[13] and $Cp^*_2Ba(bipy)$ are studied, since these complexes will provide the basis set for comparing the bond lengths and angles in bipy and $bipy^{\cdot-}$ complexes. ORTEP diagrams for $Cp^*_2Ce(bipy)$, $Cp^*_2Gd(bipy)$, $Cp^*_2Sr(bipy)$, and $Cp^*_2Ba(bipy)$ are shown in Figures 3.3.1-3.3.4, respectively. The crystal structures of $Cp^*_2Ce(bipy)$, $Cp^*_2Sm(bipy)$,[8] and $Cp^*_2Gd(bipy)$ are isostructural. The crystal structures of $Cp^*_2Sr(bipy)$ and $Cp^*_2Ba(bipy)$ are isostructural. Several important crystallographic distances and angles are compared in Table 3.3.9.

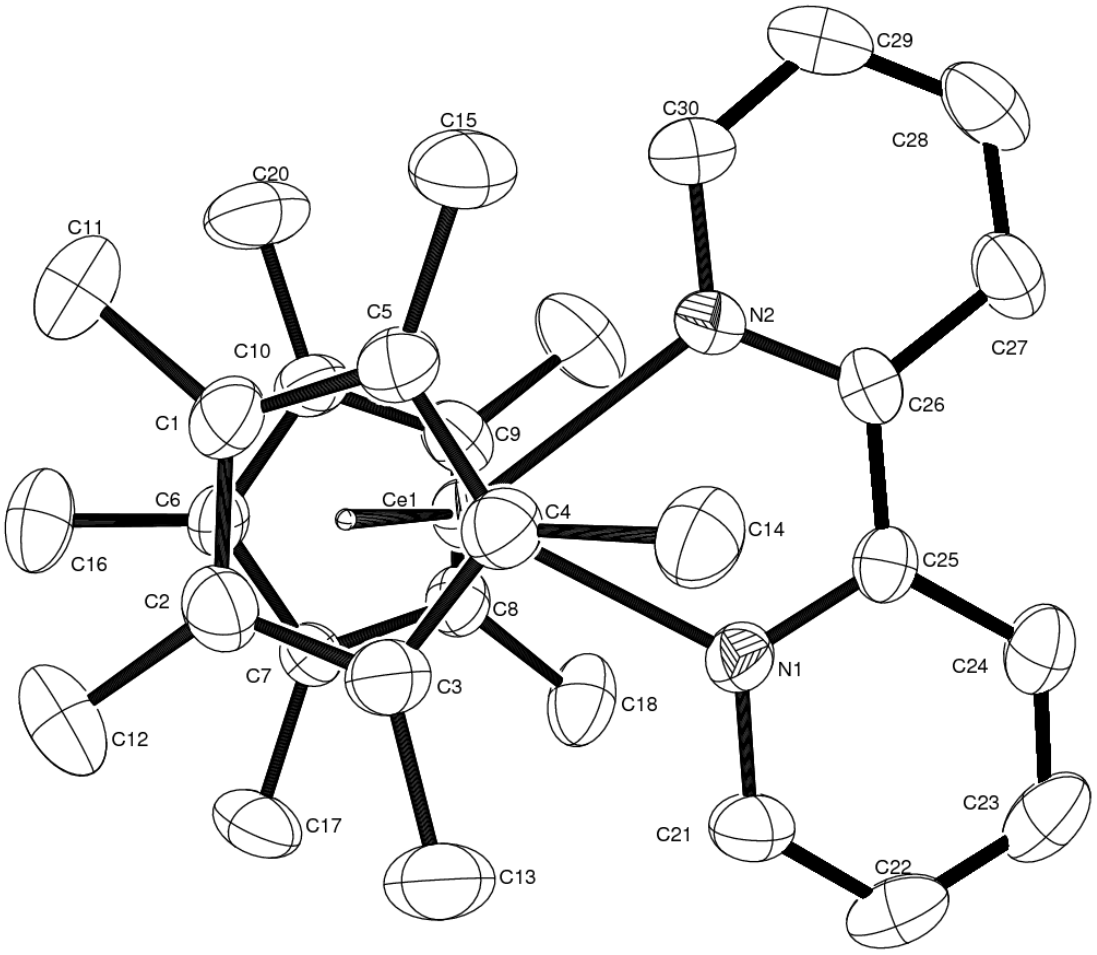

Figure 3.3.1: ORTEP diagram of $Cp^*_2Ce(bipy)$ (50% probability ellipsoids). All non-hydrogen atoms are refined anisotropically. Hydrogen atoms are placed and not refined and are not shown. Selected Bond Distances and Angles are given in Tables 3.3.1 and 3.3.2, respectively. The N1-C25-C26-N2 torsion angle is 0.9(4)°.

Table 3.3.1: Selected bond distances (Å) in $Cp^*_2Ce(bipy)$

Atom	atom	distance		atom	atom	Distance
Ce(1)	N(1)	2.496(3)		Ce(1)	N(2)	2.491(3)
Ce(1)	C(1)	2.788(3)		Ce(1)	C(2)	2.777(3)
Ce(1)	C(3)	2.762(3)		Ce(1)	C(4)	2.793(3)
Ce(1)	C(5)	2.800(3)		Ce(1)	C(6)	2.779(3)
Ce(1)	C(7)	2.804(3)		Ce(1)	C(8)	2.809(3)
Ce(1)	C(9)	2.792(3)		Ce(1)	C(10)	2.759(3)
Ce(1)	C(101)	2.51		Ce(1)	C(102)	2.51
C(25)	C(26)	1.426(4)				

Table 3.3.2: Selected bond angles in $Cp^*_2Ce(bipy)$

atom	atom	atom	angle		atom	atom	atom	Angle
N(1)	Ce(1)	N(2)	64.89(8)		C(101)	Ce(1)	C(102)	138.28

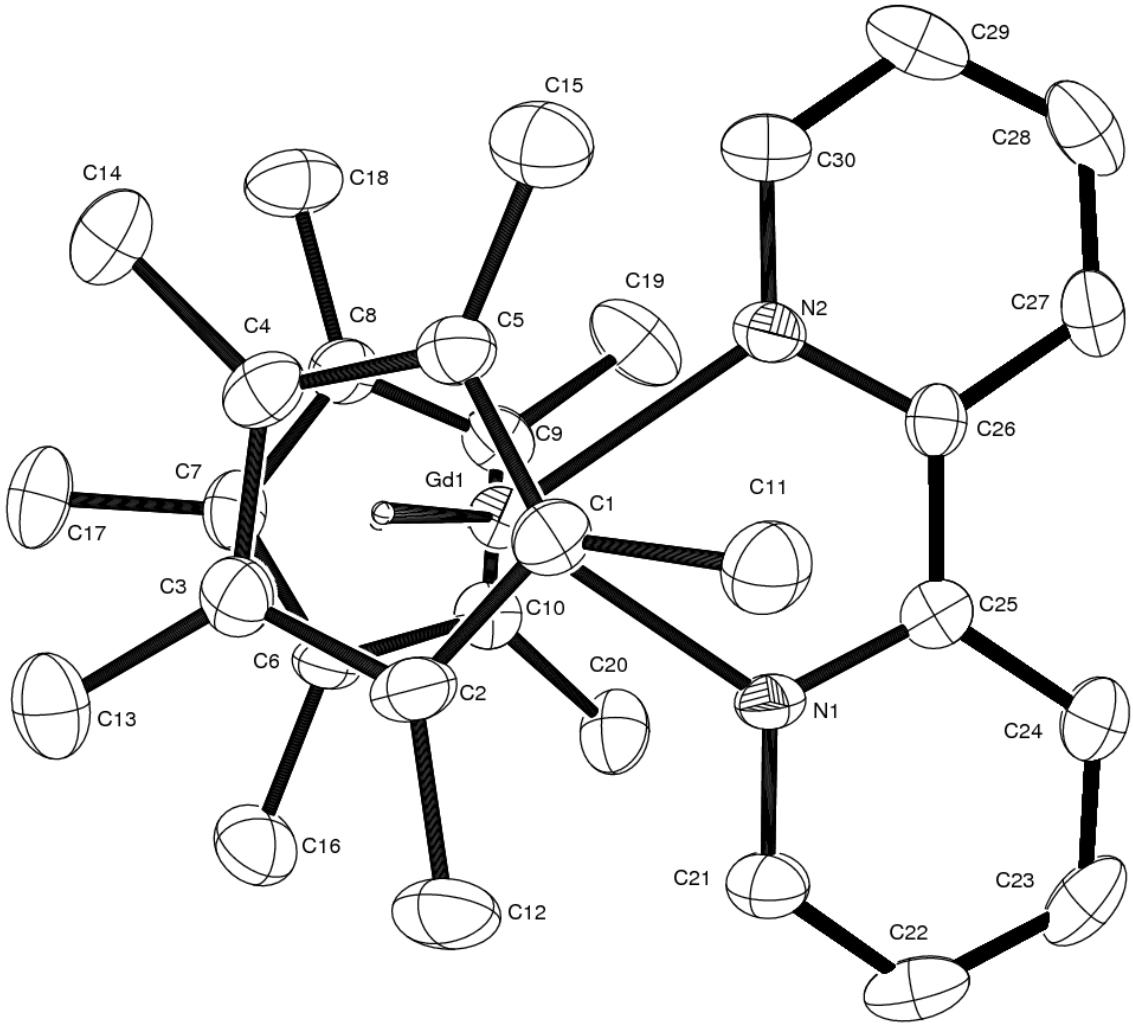

Figure 3.3.2: ORTEP diagram of $Cp^*_2Gd(bipy)$ (50% probability ellipsoids). All non-hydrogen atoms are refined anisotropically. Hydrogen atoms are placed and not refined and are not shown. Selected Bond Distances and Angles are given in Tables 3.3.3 and 3.3.4, respectively. The N1-C25-C26-N2 torsion angle is 0.4(7)°.

Table 3.3.3: Selected bond distances (Å) in $Cp^*_2Gd(bipy)$

atom	atom	distance		atom	atom	distance
Gd(1)	N(1)	2.398(4)		Gd(1)	N(2)	2.396(4)
Gd(1)	C(1)	2.693(5)		Gd(1)	C(2)	2.675(6)
Gd(1)	C(3)	2.684(5)		Gd(1)	C(4)	2.692(5)
Gd(1)	C(5)	2.698(5)		Gd(1)	C(6)	2.698(5)
Gd(1)	C(7)	2.688(5)		Gd(1)	C(8)	2.668(5)
Gd(1)	C(9)	2.694(5)		Gd(1)	C(10)	2.712(5)
Gd(1)	C(101)	2.40		Gd(1)	C(102)	2.41
C(25)	C(26)	1.421(7)				

Table 3.3.4: Selected bond angles in $Cp^*_2Gd(bipy)$

atom	atom	atom	angle		atom	atom	atom	angle
N(1)	Gd(1)	N(2)	68.6(1)		C(101)	Gd(1)	C(102)	138.1

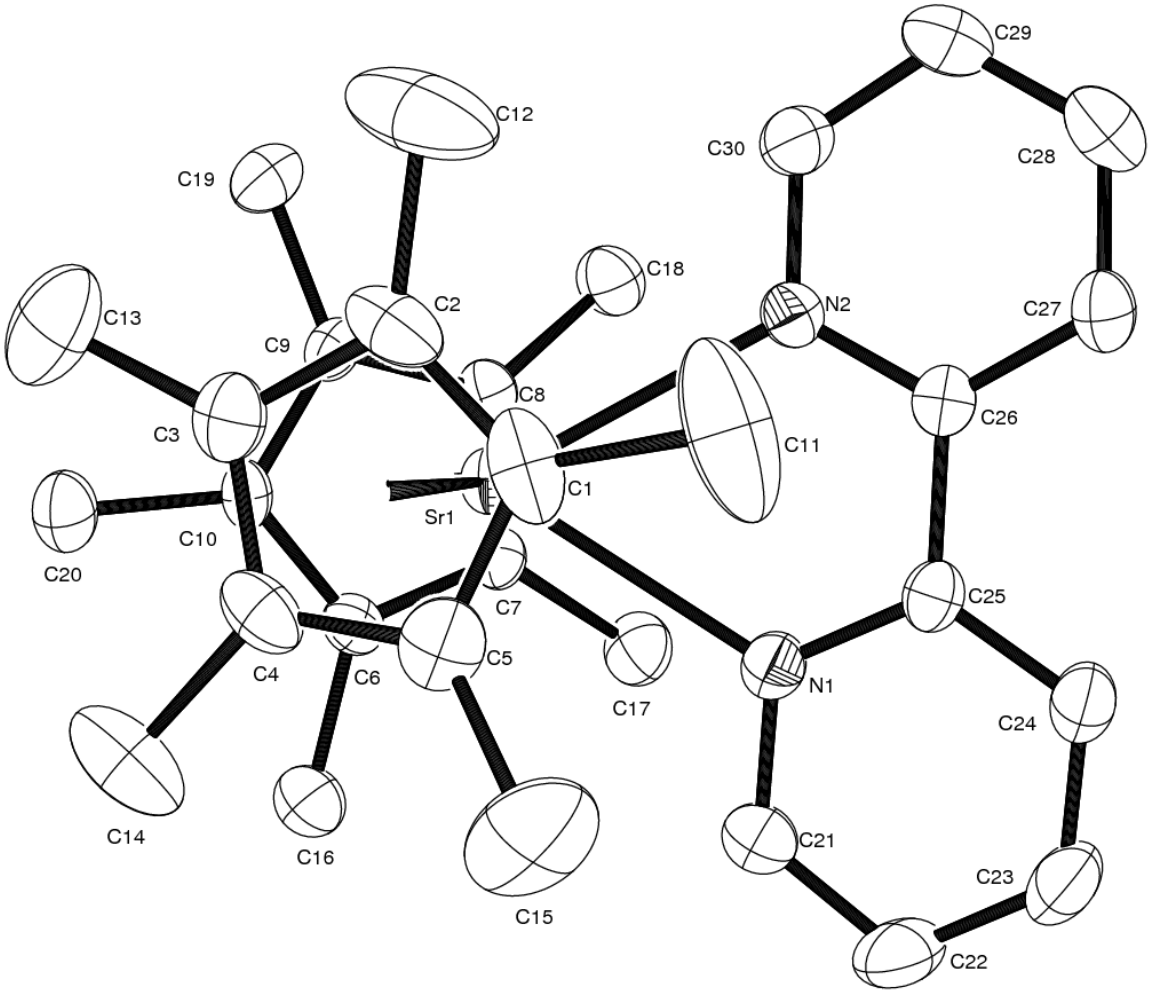

Figure 3.3.3: ORTEP diagram of $Cp^*_2Sr(bipy)$ (50% probability ellipsoids). All non-hydrogen atoms are refined anisotropically. Hydrogen atoms are placed and not refined and are not shown. Selected Bond Distances and Angles are given in Tables 3.3.5 and 3.3.6, respectively. The N1-C25-C26-N2 torsion angle is 2.2(4)°.

Table 3.3.5: Selected bond distances (Å) in $Cp^*_2Sr(bipy)$

atom	atom	distance		atom	atom	distance
Sr(1)	N(1)	2.624(3)		Sr(1)	N(2)	2.676(3)
Sr(1)	C(1)	2.841(3)		Sr(1)	C(2)	2.812(3)
Sr(1)	C(3)	2.819(3)		Sr(1)	C(4)	2.838(3)
Sr(1)	C(5)	2.869(3)		Sr(1)	C(6)	2.830(3)
Sr(1)	C(7)	2.840(3)		Sr(1)	C(8)	2.841(3)
Sr(1)	C(9)	2.818(3)		Sr(1)	C(10)	2.815(3)
Sr(1)	C(101)	2.57		Sr(1)	C(102)	2.56
C(25)	C(26)	1.495(4)				

Table 3.3.6: Selected bond angles in $Cp^*_2Sr(bipy)$

atom	atom	atom	angle		atom	atom	atom	angle
N(1)	Sr(1)	N(2)	61.32(8)		C(101)	Sr(1)	C(102)	141.4

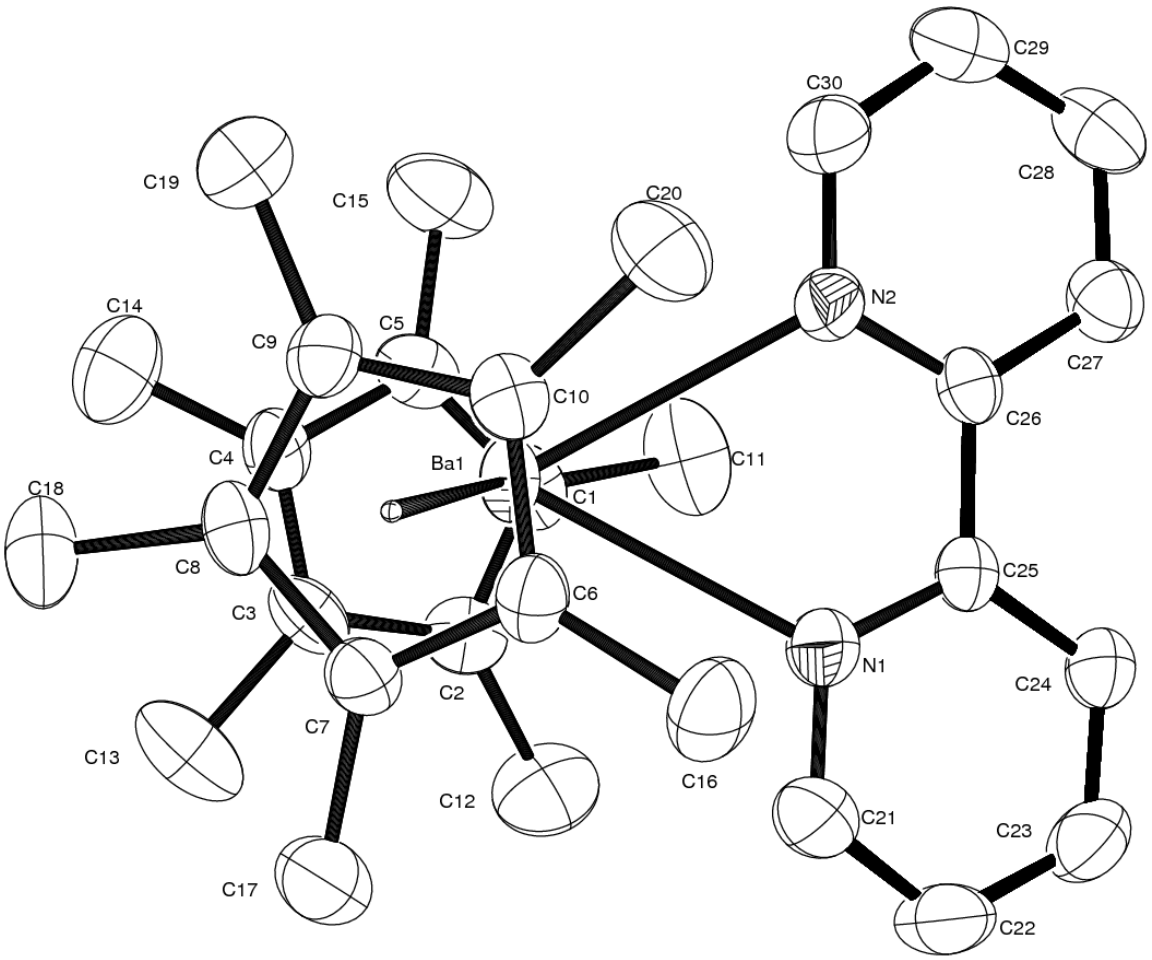

Figure 3.3.4: ORTEP diagram of $Cp^*_2Ba(bipy)$ (50% probability ellipsoids). All non-hydrogen atoms are refined anisotropically. Hydrogen atoms are placed and not refined and are not shown. Selected Bond Distances and Angles are given in Tables 3.3.7 and 3.3.8, respectively. The N1-C25-C26-N2 torsion angle is 1.6(4)°.

Table 3.3.7: Selected bond distances (Å) in $Cp^*_2Ba(bipy)$

Atom	atom	distance		atom	atom	distance
Ba(1)	N(1)	2.800(3)		Ba(1)	N(2)	2.886(3)
Ba(1)	C(1)	2.990(3)		Ba(1)	C(2)	3.044(3)
Ba(1)	C(3)	3.001(3)		Ba(1)	C(4)	2.940(3)
Ba(1)	C(5)	2.922(3)		Ba(1)	C(6)	2.995(3)
Ba(1)	C(7)	2.989(3)		Ba(1)	C(8)	2.964(3)
Ba(1)	C(9)	2.943(3)		Ba(1)	C(10)	2.971(3)
Ba(1)	C(101)	2.73		Ba(1)	C(102)	2.72
C(25)	C(26)	1.493(5)				

Table 3.3.8: Selected bond angles in $Cp^*_2Ba(bipy)$

atom	atom	atom	angle		atom	atom	atom	angle
N(1)	Ba(1)	N(2)	56.74(8)		C(101	Ba(1)	C(102)	140.8

In order to compare these two genres of molecules, molecules where bipy is present either as a neutral ligand or as a radical anion, it is important to understand the difference in electronic structure between bipy and bipy$^{\cdot -}$. A DFT calculation of the SOMO (SOMO = singly occupied molecular orbital) of bipy$^{\cdot -}$ is shown in Figure 3.3.5. This model is in good agreement with EPR studies on K(bipy), which show that the electron-nuclear coupling constant, a_H, of the hydrogen in the 6-position is about half that of the a_H value in the 4-postion, which is smaller than the coupling constant of all the other positions.[14,15,16]

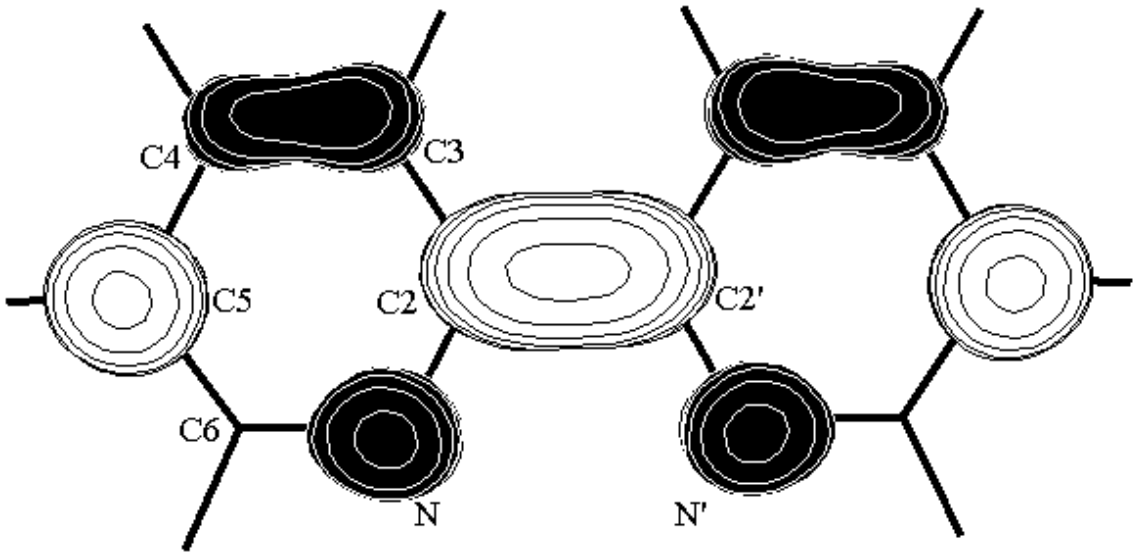

Figure 3.3.5: SOMO of bipy$^{\cdot -}$. Symmetry = C_{2v}. Exchange = B3LYP. Basis = 6-311+G*

When the SOMO of bipy$\cdot^-$ is occupied, the bond lengths will have a predictable lengthening or contraction depending on whether the molecular orbital of the SOMO has a bonding or anti-bonding contribution. A bond which in the SOMO of bipy$\cdot^-$ has an antibonding contribution, i.e. N-C2, C2-C3, and C4-C5, is expected to lengthen in $Cp^*_2M(bipy)$ molecules where bipy is a radical anion relative to $Cp^*_2M(bipy)$ molecules where bipy is neutral. The reverse is true for bonds in the SOMO of bipy$\cdot^-$ which have a bonding contribution, i.e. C2-C2' and C3-C4. In addition, the SOMO of bipy shows a π-bond between C2 and C2' which is expected to induce planarity between the two pyridine rings in bipy, whereas without electronic effects inducing planarity the steric interactions between the protons in the 3,3'-position is expected to induce a torque in the N-C2-C2'-N' torsion angle. Figure 3.3.6 shows the energy as a function of the N-C-C'-N' torsion angles in bipy and bipy$\cdot^-$. As expected, a planar configuration is a local maximum for bipy neutral and a local minimum for bipy radical anion. A comparison of bond lengths and the N-C2-C2'-N' torsion angles of $Cp^*_2Ce(bipy\cdot^-)$, $Cp^*_2Gd(bipy\cdot^-)$, $[Cp^*_2Ce(bipy)][BPh_4]$, $[Cp^*_2Gd(bipy)][BPh_4]$, $Cp^*_2Sr(bipy)$, $Cp^*_2Ba(bipy)$, and the average value of the distances and angles of $Cp^*_2M(bipy\cdot^-)$ minus $Cp^*_2M(bipy)$ is presented in Table 3.3.9. The atomic numbering scheme is that used in Figure 3.3.5. As predicted, every bond which has an antibonding contribution in the calculated SOMO of bipy$\cdot^-$ lengthens in $Cp^*_2M(bipy\cdot^-)$ relative to $Cp^*_2M(bipy)$, and every bond which has a bonding contribution shrinks. In addition, the NCC'N' torsion angles of the neutral bipys are larger than those of the bipy radical anions.

	NCC'N' Dihedral angle	N-C2	C2-C3	C3-C4	C4-C5	C5-C6	N-C6	C2-C2'
$Cp^*_2Ce(bipy^{\cdot-})$	0.9(4)	1.382(6)	1.421(7)	1.354(8)	1.413(8)	1.357(8)	1.365(6)	1.426(4)
$Cp^*_2Gd(bipy^{\cdot-})$	0.4(7)	1.393(8)	1.42(1)	1.35(1)	1.40(1)	1.36(1)	1.35(1)	1.421(7)
$[Cp^*_2Ce(bipy)]^+$	6.0(3)	1.351(4)	1.392(6)	1.382(6)	1.378(9)	1.373(6)	1.344(6)	1.487(4)
$[Cp^*_2Gd(bipy)]^+$	5.7(4)	1.355(6)	1.394(6)	1.377(6)	1.378(6)	1.376(6)	1.349(6)	1.485(4)
$Cp^*_2Sr(bipy)$	2.2(4)	1.348(6)	1.393(6)	1.376(7)	1.375(7)	1.380(7)	1.337(6)	1.495(4)
$Cp^*_2Ba(bipy)$	1.6(4)	1.347(6)	1.389(6)	1.381(7)	1.372(8)	1.368(7)	1.338(6)	1.493(5)
Δ	-3.2 (11)	0.037 (15)	0.029 (17)	-0.027 (18)	0.031 (20)	-0.016 (18)	0.016 (17)	-0.067 (12)

Table 3.3.9: A comparison of bond lengths of torsion angles between $Cp^*_2M(II)(bipy)$ and $Cp^*_2M(III)(bipy^{\cdot-})$; Δ is the difference between the averaged values in the bipy and $bipy^{\cdot-}$.

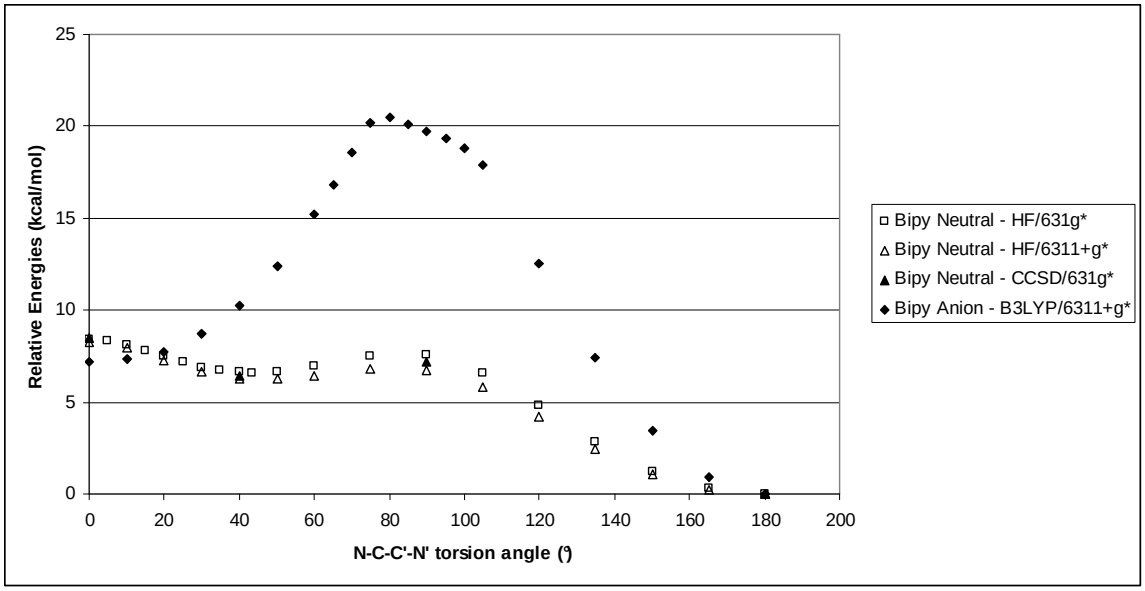

Figure 3.3.6: Computational studies of the energy of bipy neutral and $bipy^{\cdot-}$ as a function of the N-C-C'-N' torsion angle. The neutral molecules were optimized at HF/6-31g* and then their energies calculated at the described level of theory. All energies are given relative to the calculated energy of bipy with an N-C-C'-N' torsion angle of 180°.

The crystal structure of Cp^*_2Ce(iso-propyl-N-CH=CH-N=CMe_2) is unambiguous about the loss of the hydrogen atom and the formation of a C=N double bond (Figure 3.3.7). The angles defined by N1-C23-C25 and N1-C23-C24 are almost exactly 120 ° implying sp^2 hybridization. The effective magnetic moment also implies that the ligand is not a radical anion.

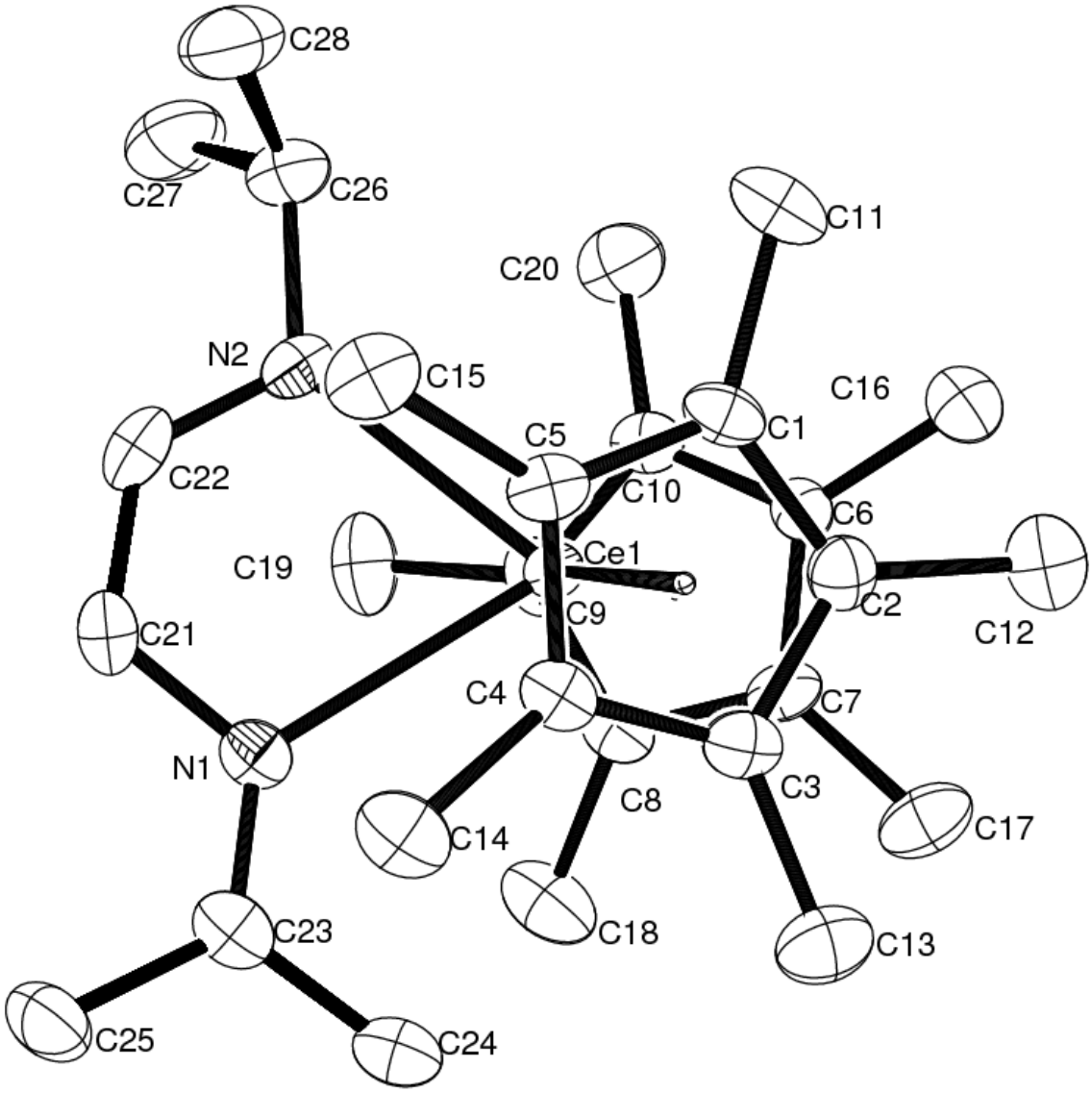

Figure 3.3.7: ORTEP diagram of Cp^*_2Ce(iso-propyl-N-CH=CH-N=CMe_2) (50% probability ellipsoids). All non-hydrogen atoms are refined anisotropically. Hydrogen

atoms are placed and not refined and are not shown. Selected Bond Distances and Angles are given in Tables 3.3.10 and 3.3.11, respectively.

Table 3.3.10: Selected bond distances (Å) in Cp^*_2Ce(iso-propyl-N-CH=CH-N=CMe_2)

atom	atom	distance		atom	atom	Distance
Ce(1)	N(1)	2.576(4)		Ce(1)	N(2)	2.426(4)
Ce(1)	C(1)	2.765(5)		Ce(1)	C(2)	2.784(5)
Ce(1)	C(3)	2.829(5)		Ce(1)	C(4)	2.836(5)
Ce(1)	C(5)	2.795(4)		Ce(1)	C(6)	2.825(4)
Ce(1)	C(7)	2.820(4)		Ce(1)	C(8)	2.821(4)
Ce(1)	C(9)	2.839(5)		Ce(1)	C(10)	2.835(5)
Ce(1)	C(101)	2.53		Ce(1)	C(102)	2.56
N(1)	C(21)	1.405(6)		N(1)	C(23)	1.294(6)
N(2)	C(22)	1.343(6)		N(2)	C(26)	1.476(6)
C(21)	C(22)	1.373(7)		C(23)	C(24)	1.501(7)
C(23)	C(25)	1.503(7)		C(26)	C(27)	1.519(8)
C(26)	C(28)	1.510(8)				

Table 3.3.11: Selected bond angles (°) in Cp^*_2Ce(iso-propyl-N-CH=CH-N=CMe_2)

atom	atom	atom	angle		atom	atom	atom	angle
N(1)	Ce(1)	N(2)	70.4(1)		C(101)	Ce(1)	C(102)	136.6
N(1)	C(23)	C(24)	119.3(5)		N(1)	C(23)	C(25)	123.3(5)

3.4 Solution Measurements: NMR Spectroscopy

The variable-temperature ^{1}H NMR spectra represented as a δ vs. 1/T plot of Cp^*_2Ce(bipy), Cp^*_2Ce(4,4'-dmb), and Cp^*_2Ce(6,6'-dmb) are shown in Figures 3.4.1, 3.4.2, and 3.4.3, respectively. The room-temperature ^{1}H NMR chemical shifts of Cp^*_2Ce(bipy), Cp^*_2Ce(4,4'-dmb), Cp^*_2Ce(5,5'-dmb), and Cp^*_2Ce(6,6'-dmb) are shown in Table 3.4.1.

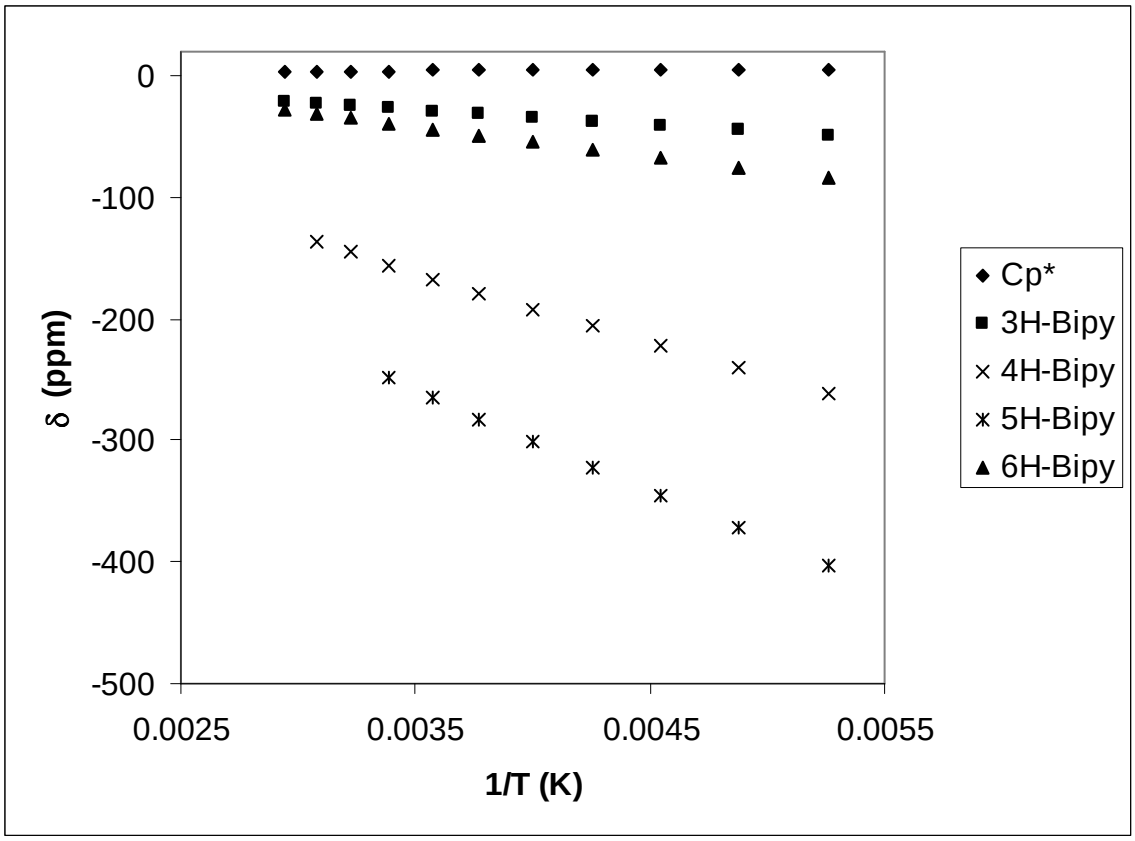

Figure 3.4.1: Variable Temperature ^{1}H NMR spectra represented as a δ vs. 1/T plot of $Cp^*_2Ce(bipy)$ in toluene-d_8.

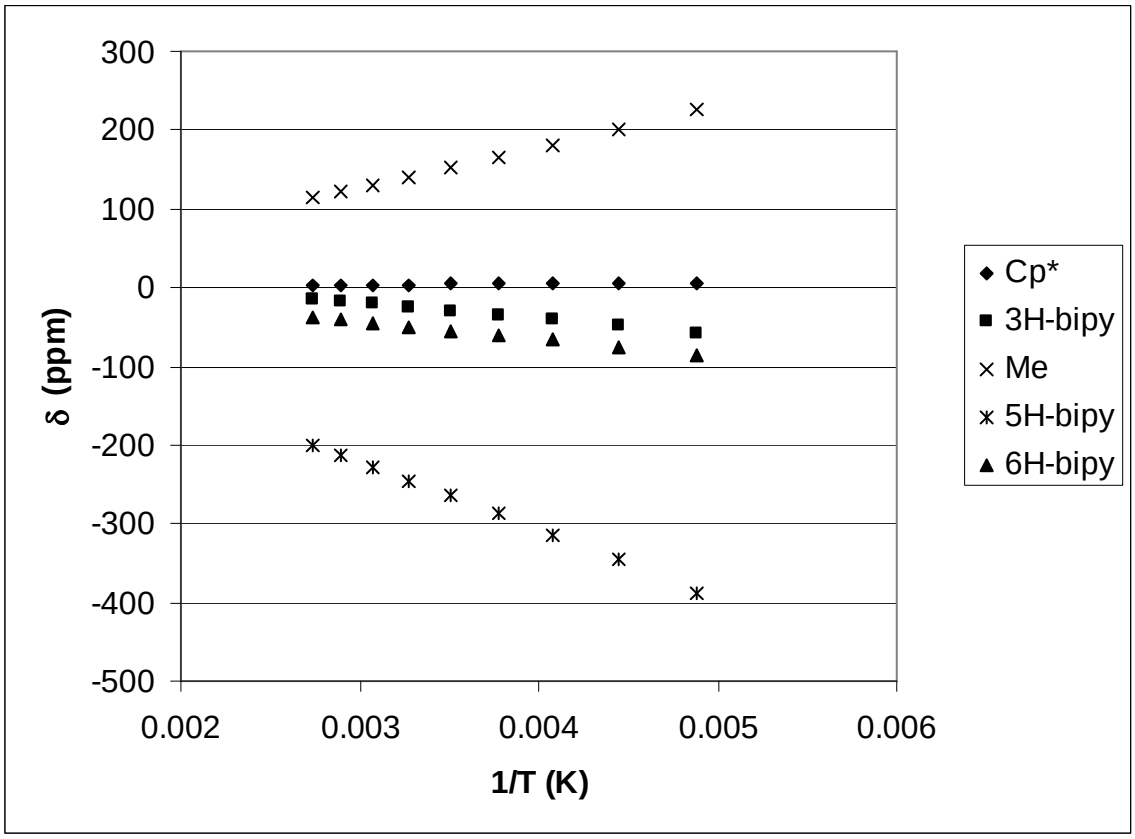

Figure 3.4.2: Variable Temperature ^{1}H NMR spectra represented as a δ vs. 1/T plot of $Cp^*_2Ce(4,4'\text{-dmb})$ in toluene-d_8.

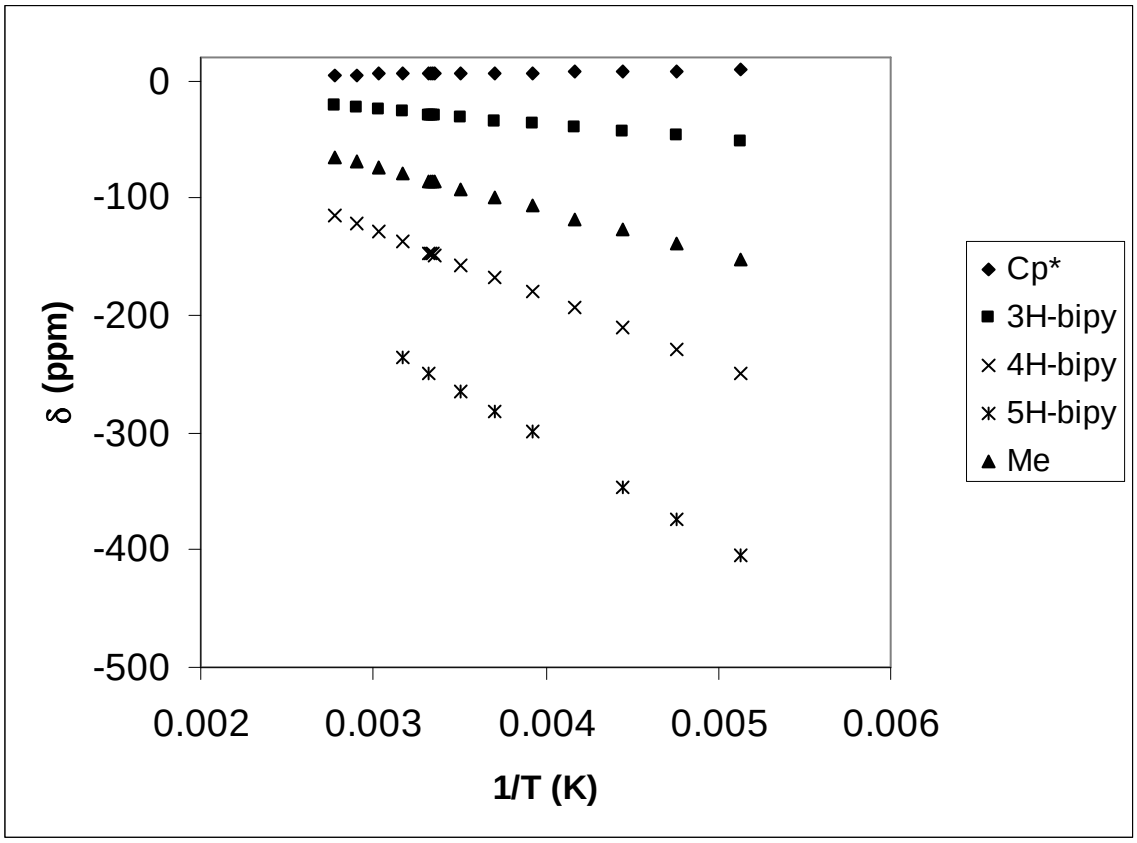

Figure 3.4.3: Variable Temperature ^{1}H NMR spectra represented as a δ vs. 1/T plot of Cp^*_2Ce(6,6'-dmb) in toluene-d_8.

	bipy	4,4'-dmb	5,5'-dmb	6,6'-dmb
3H	-27	-27	-1	-30
4H	-159	147	-171	-151
5H	-254	-256	226	-256
6H	-40	-52	-65	-89

Table 3.4.1: Room temperature ^{1}H NMR shifts of bipy in Cp^*_2Ce(bipy) and bipy analogues in toluene-d_8.

Clearly, the resonances in $Cp^*_2Ce(bipy)$ and $Cp^*_2Ce(x,x'\text{-dmb})$ (x=4,5,6) are strongly shifted from their diamagnetic values, and have a strong temperature dependence. As discussed in chapter one, there are two mechanisms by which a paramagnetic center can shift NMR resonances of atoms in a molecule. The first is through Fermi contact, which arises from the delocalization of unpaired electrons from the paramagnetic center through covalent interactions with the ligand orbitals.[17] The second is through a pseudocontact shift, which is due to direct dipolar coupling between the magnetic moment of the unpaired electrons on the paramagnetic center and the magnetic moment of the nucleus of interest. The magnitude of a pseudocontact shift has a $1/R^3$ dependence, where R is the distance between the paramagnetic center and the nucleus of interest.[18] In the case of molecules such $Cp^*_2Ce(bipy^{\cdot})$, where the bipy molecule carries unpaired electron density, the effects of the Fermi contact shift are qualitatively predictable. The unpaired electron density resides in a π^* orbital which is made up of p-orbitals localized on the ring carbon atoms (Figure 3.3.5). The unpaired electron density will align with magnetic field. By Hund's rule, in the case where a proton is bound to the ring carbons, unpaired electron density in the carbon p-orbital will result in polarization of the electron density in the CH bond, such that the electron density near to the carbon atom will also align with the unpaired electron in the p-orbital, and therefore with the magnetic field. Since the CH σ-bond consists of 2 electrons, one spin up and one spin down, the electron density near the hydrogen will be aligned against the magnetic field. This is pictorially represented by Bertini et al. and is reproduced in Figure 3.4.4.[19]

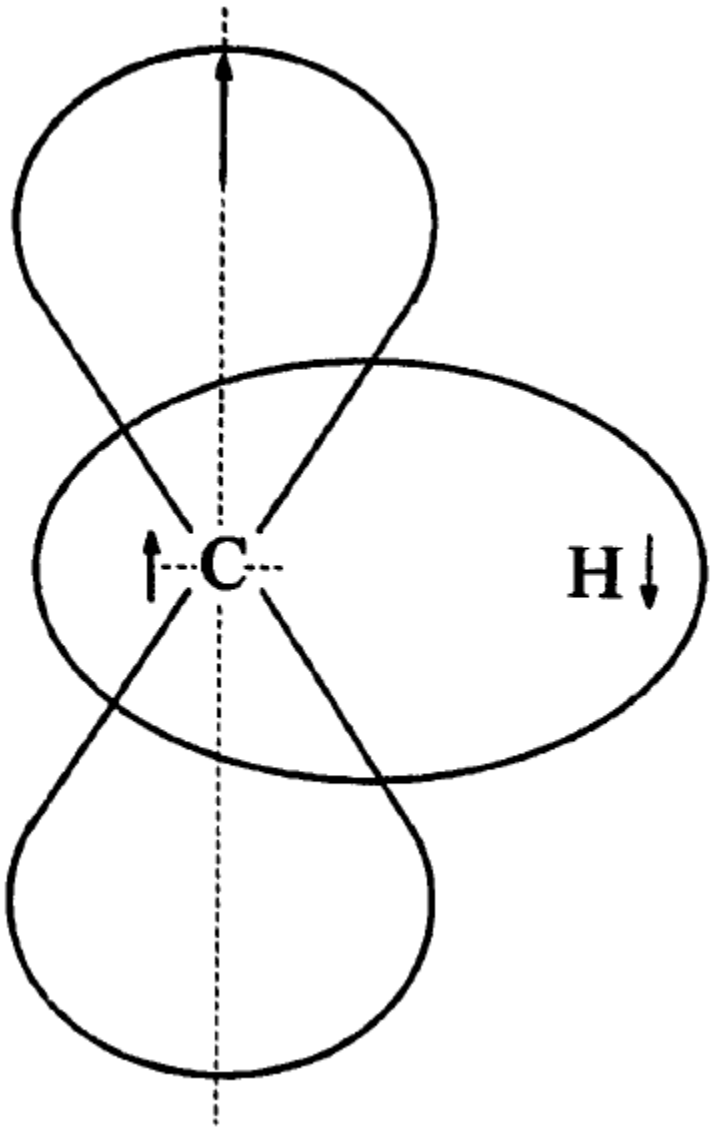

Figure 3.4.4: The spin density on protons has the opposite sign of that on the attached sp^2 carbon.

As a result, there is unpaired electron density at the proton aligned against the magnetic field and causing an upfield shift. On the other hand, if the ring carbon is attached to a methyl group, then by Hund's rule the unpaired electron density in the ring carbon p-orbital will polarize the electron density in the CC bond, such that the electron density

near to the ring carbon atom will also align with the magnetic field, and therefore the electron density near the methyl carbon will be aligned against the magnetic field. In turn, this will polarize the electron density in the CH σ-bond, such that the electron density near to the methyl carbon will also align against the magnetic field, while the electron density near the proton will align with the magnetic field, causing a strong downfield shift (Figure 3.4.5). In addition, the electron density on the H-atom is close to the unpaired electron density on the p-orbital of the ring carbon, and therefore there is a through-space polarization of the methyl CH bond, such that the unpaired electron density on the methyl hydrogens is aligned with the spin on the ring carbon, which is also aligned with the magnetic field.[20]

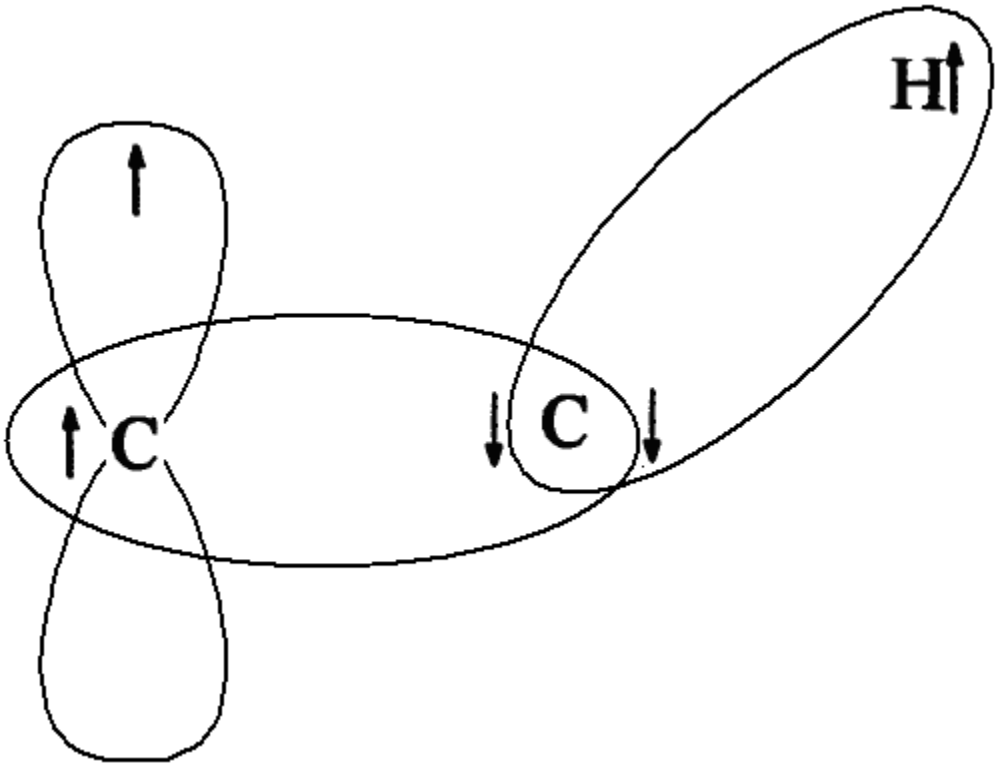

Figure 3.4.5: The spin density on methyl protons has same sign of that on the sp^2 carbon.

This phenomenon allows for an easy way to distinguish pseudo-contact shifts from contact shifts. If replacing a proton with a methyl group inverts the sign of the chemical shift, then the shift is predominantly contact in nature. If it does not, it is predominantly pseudocontact.[21] Interestingly, in the cases of Cp^*_2Ce(4,4'-dmb) and Cp^*_2Ce(5,5'-dmb), the ^1H NMR shift of the methyl peak changes sign relative to the same peak in Cp^*_2Ce(bipy), whereas in the case of Cp^*_2Ce(6,6'-dmb), the ^1H NMR chemical shift of the methyl peak does not (Table 3.4.1). The DFT calculation of the SOMO of bipy (Figure 3.3.5) shows that there is little unpaired electron density on the 6-position. The major contribution to the chemical shift in the ^1H NMR spectrum on the 6-position in Cp^*_2Ce(bipy) is, therefore, expected to be pseudo-contact in origin, whereas the shifts of the 4 and 5 positions, which have unpaired electron density in the SOMO of bipy, as well as being further away from the lanthanide center, are expected to be contact in nature, as is experimentally observed.

The accuracy of the assumption that the cerium atom is Ce(III), and therefore the bipy is $bipy^{\cdot -}$, is observed in the magnetism presented later in this thesis, as well as in the fact that the Cp* peaks in the variable-temperature ^1H NMR spectrum of Cp^*_2Ce(bipy) have essentially the same shifts as in $[Cp^*_2Ce(bipy)][BPh_4]$. The hypothesis that the ^1H NMR shift of the 6-position is mainly due to a pseudo-contact shift from the Ce(III) center is corroborated by a comparison of the 6 position in the variable temperature ^1H NMR spectrum of Cp^*_2Ce(bipy) with that of $[Cp^*_2Ce(bipy)][BPh_4]$ (Figure 3.4.6).

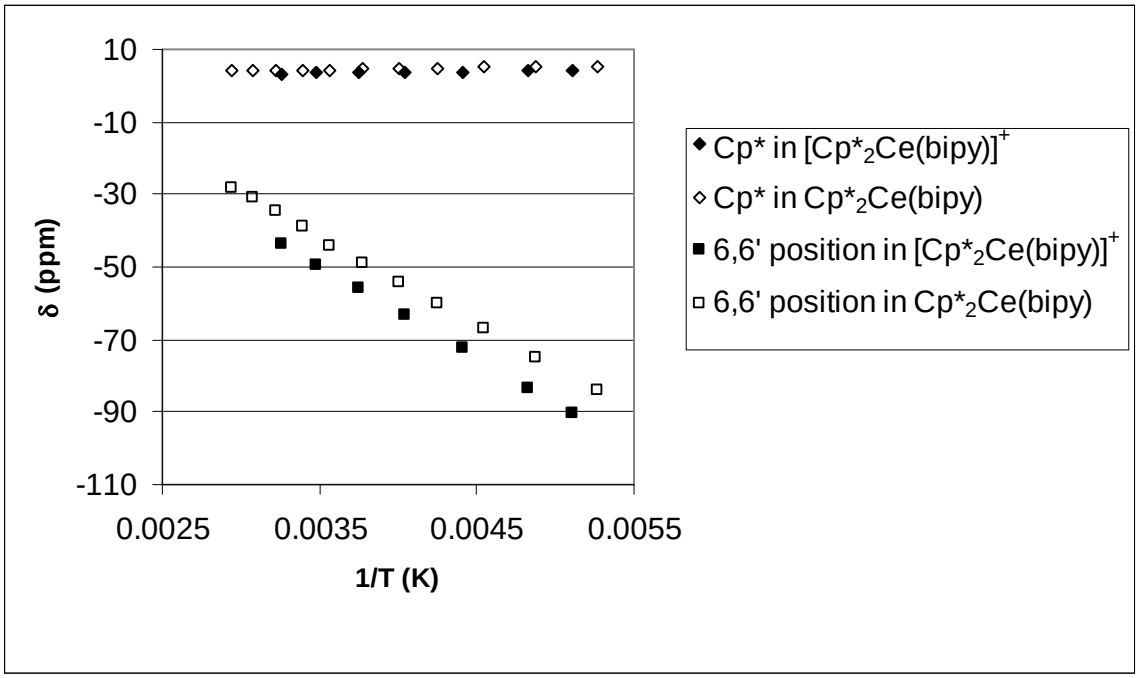

Figure 3.4.6: Comparison of the Cp* and the 6 position in the bipy in the variable temperature ^{1}H NMR spectra of $Cp^*_2Ce(bipy)$ (in toluene-d_8) and $[Cp^*_2Ce(bipy)][BPh_4]$ (in CD_2Cl_2)

The similarity of the shifts implies that the mechanism that determines the chemical shift at the 6-position is similar in these two molecules. The ^{1}H NMR shifts of the other bipy resonances in these two molecules vary wildly, consistent with the postulate that these shifts are predominantly contact in origin (Table 3.4.2).

	3	4	5	6
$Cp^*_2Ce(bipy)$	-27	-159	-254	-40
$[Cp^*_2Ce(bipy)]^+$	3.97	3.82	-2.04	-46

Table 3.4.2: Room temperature ^{1}H NMR shifts of $Cp^*_2Ce(bipy)$ (in toluene-d_8) and $[Cp^*_2Ce(bipy)][BPh_4]$ (in CD_2Cl_2)

This model is supported by the observation that the δ vs. 1/T plot of the ^{1}H NMR chemical shifts of the bipy resonances of Cp*$_2$Sm(bipy) is superimposable on that of Cp*$_2$Ce(bipy), with the exception of the proton in the 6-position (Figure 3.4.7).

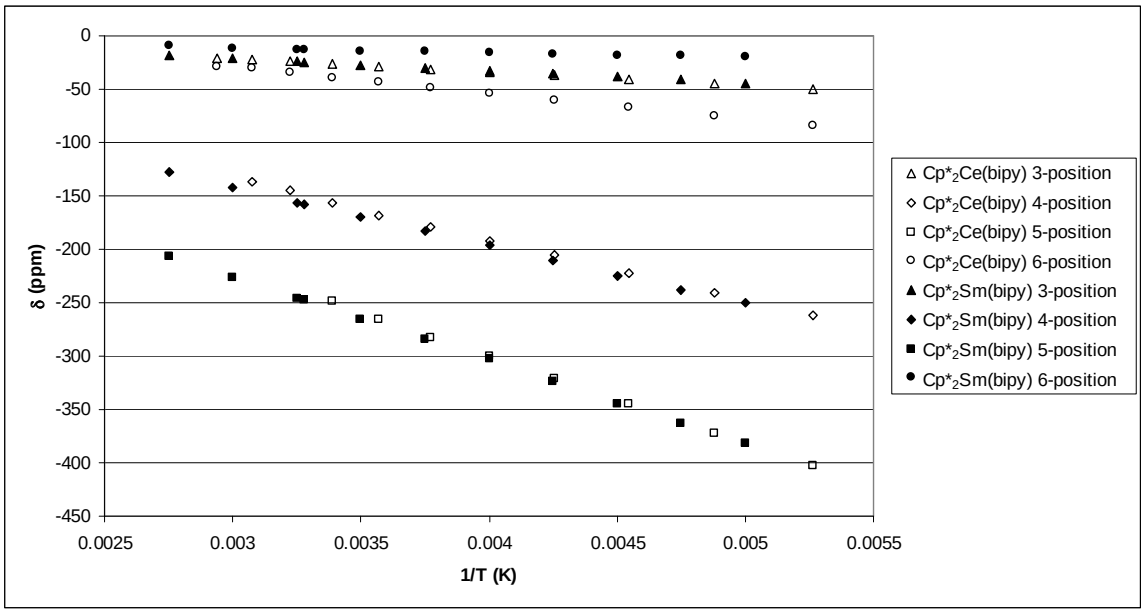

Figure 3.4.7: Comparison of the δ vs. 1/T plot of the bipy resonances in the ^{1}H NMR spectrum of Cp*$_2$Ce(bipy) and Cp*$_2$Sm(bipy) (in toluene-d_8).

Thus, the chemical shifts of the protons in the 3, 4, and 5-positions are due to the unpaired electron density on the ligand, which is similar in Cp*$_2$Ce(bipy) and Cp*$_2$Sm(bipy), whereas the chemical shift of the proton in the 6-position is due to the paramagnetic nature of the metal, which varies as the metal is changed. The ^{1}H NMR spectrum of Cp*$_2$Yb(bipy), where the electron density on the bipy ligand is significantly different (due to the Yb^{II}/Yb^{III} couple), looks completely different.[5]

The close relation of the ^{1}H NMR chemical shifts of the protons in the 3, 4, and 5 positions seems to indicate that the bipyridine ligand in Cp*$_2$Sm(bipy) has a similar

electronic configuration as that of $Cp^*_2Ce(bipy)$, that is, the molecule is well described as $Cp^*_2Sm(III)(bipy^{\cdot -})$. However, if this is the case, then the ^1H NMR spectrum of the Cp* ligand and the hydrogens in the 6,6'-position in the bipy ligands of $Cp^*_2Sm(bipy)$ should be similar to those of $[Cp^*_2Sm(bipy)][BPh_4]$, as observed in the case of cerium (Figure 3.4.6). This, however, is not the case (Figure 3.4.8). The crystal structure of $Cp^*_2Sm(bipy)$ is isomorphous with that of $Cp^*_2Ce(bipy)$. The crystal structure of $[Cp^*_2Sm(bipy)][BPh_4]$ has not been studied, however, the crystal structure of $[Cp^*_2Gd(bipy)][BPh_4]$ is isomorphous with that of $[Cp^*_2Ce(bipy)][BPh_4]$. Given that the radius of cerium is larger than samarium and that of gadolinium is smaller than samarium, it seems reasonable to assume that $[Cp^*_2Sm(bipy)][BPh_4]$ is isomorphous as well. It seems reasonable to postulate that the cause of the shift in the resonances in the ^1H NMR spectra is due to the presence $bipy^{\cdot -}$, reduced by the Cp^*_2Sm fragment, as in the case of $Cp^*_2Yb(bipy)$; XANES measurements will be obtained in future work in order to gather evidence for, or against, this conjecture.

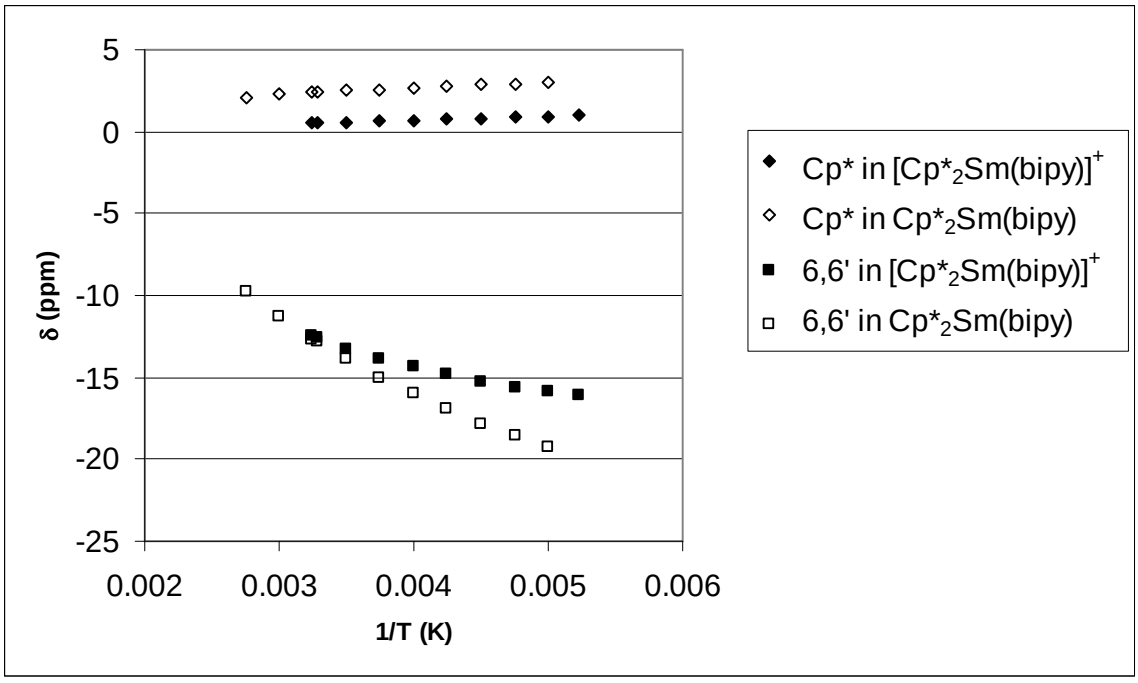

Figure 3.4.8: Comparison of the Cp* and the 6 position in the bipy in the variable temperature ^{1}H NMR spectrum of Cp*$_2$Sm(bipy) (in toluene-d_8) and [Cp*$_2$Sm(bipy)][BPh_4] (in CD_2Cl_2)

In the case of Cp*$_2$La(bipy), only one broad resonance, attributable to the Cp* group is visible in the ^{1}H NMR spectrum; the resonances due to bipy are broadened into the baseline. The Cp* resonance follows Curie behavior (Figure 3.4.9) and broadens into the baseline as the temperature is lowered (Figure 3.4.10). The y-intercept of the δ vs. 1/T plot of Cp*$_2$La(bipy) based on three points of highest temperature (where the Cp* peak has the largest width) is 1.97 ppm. In molecules where spin-orbit coupling is small, the intercept is expected to be the value of the diamagnetic shift. The ^{1}H NMR resonance of Cp* in Cp*$_2$Ca(bipy) at room temperature is 2.06, ppm, close to the value of that extrapolated for the lanthanum complex.

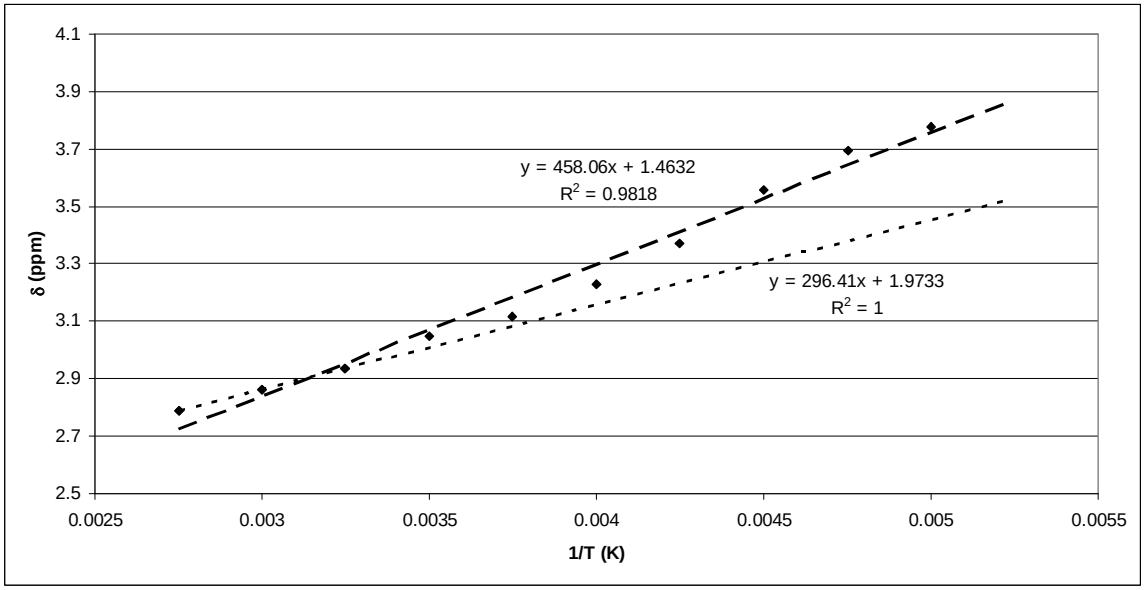

Figure 3.4.9: Variable Temperature ^{1}H NMR spectra represented as a δ vs. 1/T plot of Cp*$_2$La(bipy) in toluene-d$_8$. The dashed line is the least-squares fit of all the resonances. The dotted line is the least-squares fit of the resonances at the three highest temperatures.

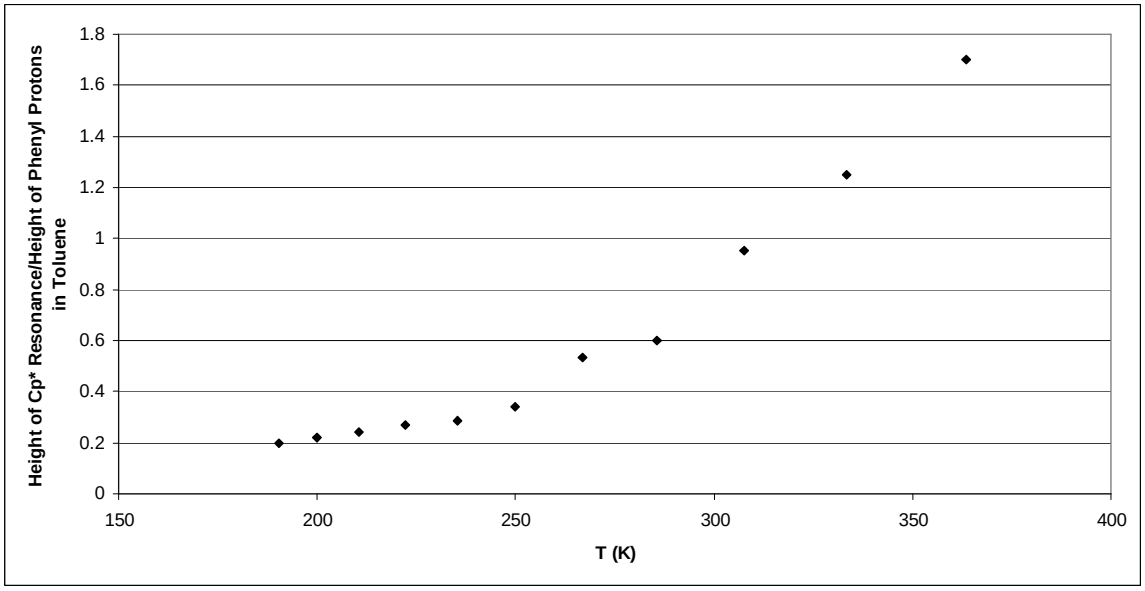

Figure 3.4.10: Ratio of the height of the Cp* resonance in Cp*$_2$La(bipy) to the height of the phenyl protons in toluene as a function of temperature in toluene-d$_8$.

The variable-temperature ^{1}H NMR spectra of Cp*$_2$Ce(N,N'-bis(iso-propyl)-1,4-diazadienyl) give a 30:6:3:3:1:1:1 area ratio at all temperatures, as expected (Figure 3.4.11).

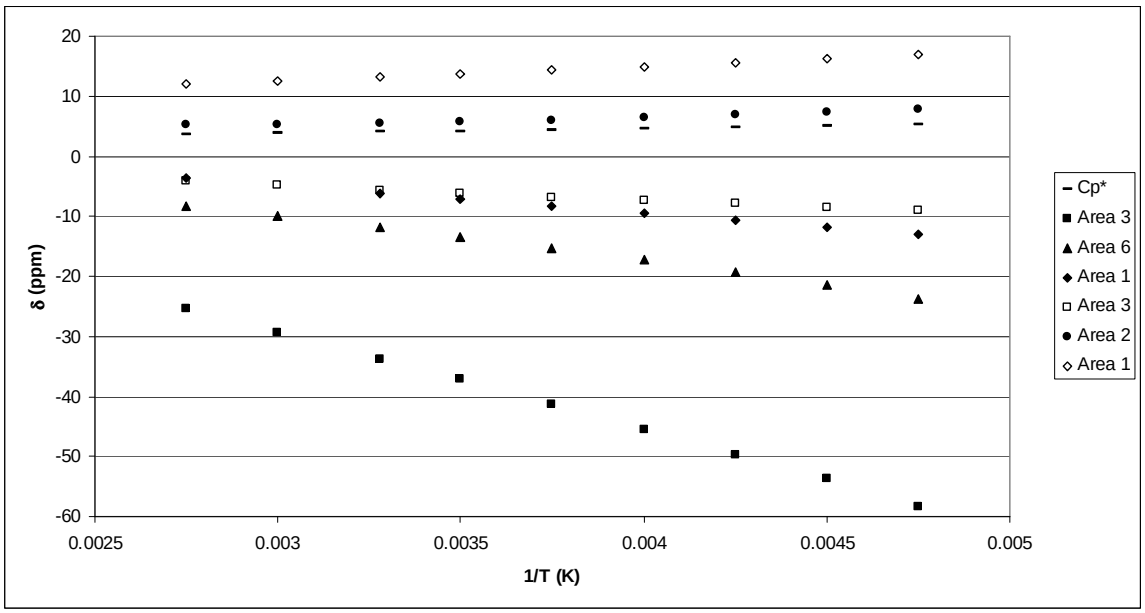

Figure 3.4.11: Variable Temperature ^{1}H NMR spectra represented as a δ vs. 1/T plot of Cp*$_2$Ce(N,N'-bis(iso-propyl)-1,4-diazadienyl) in toluene-d_8.

The variable temperature ^{1}H NMR spectra plotted as a δ vs. 1/T plot of Cp*$_2$Ce(2,2',6',2''-terpyridine) (Figure 3.4.12), and the published variable temperature ^{1}H NMR spectra plotted as a δ vs. 1/T plot of Cp*$_2$Sm(2,2',6',2''-terpyridine) (Figures 3.4.13 and 3.4.14)[22], are almost superimposable, except for the peaks marked with a dash, which in Cp*$_2$Ce(2,2',6',2''-terpyridine) is between -27 and -9 ppm, between 200 and 380K respectively, and in Cp*$_2$(2,2',6',2''-terpyridine) it is between -30 and 0 ppm between 210 and 293K respectively. As in the case of Cp*$_2$Ce(bipy) this seems to indicate that the shift of the dashed peak is due to a pseudocontact interaction with the

lanthanide center, whereas the shifts of the other peaks are due to a contact interaction with the unpaired electron in the 2,2',6',2''-terpyridine ligand. A DFT calculation on the SOMO of 2,2',6',2''-terpyridine$^{\cdot-}$ shows that the 6,6'' position has no electron density, while the other positions do (Figure 3.4.15). In 2003, Lyubimova and Baranovskii published an Open Shell Restricted Hartree Fock calculation of the SOMO of 2,2',6',2''-terpyridine$^{\cdot-}$, in which they claim that the 4' position does not contain unpaired spin density.[23] Their result is consistent with our Hartree Fock calculation of the HOMO of neutral 2,2',6',2''-terpyridine. This is in contrast with our calculation of SOMO of 2,2',6',2'', which shows unpaired spin density in the 4' position. The strong paramagnetic shift of the proton peak of area one indicates that unpaired spin-density is present in the 4' position.

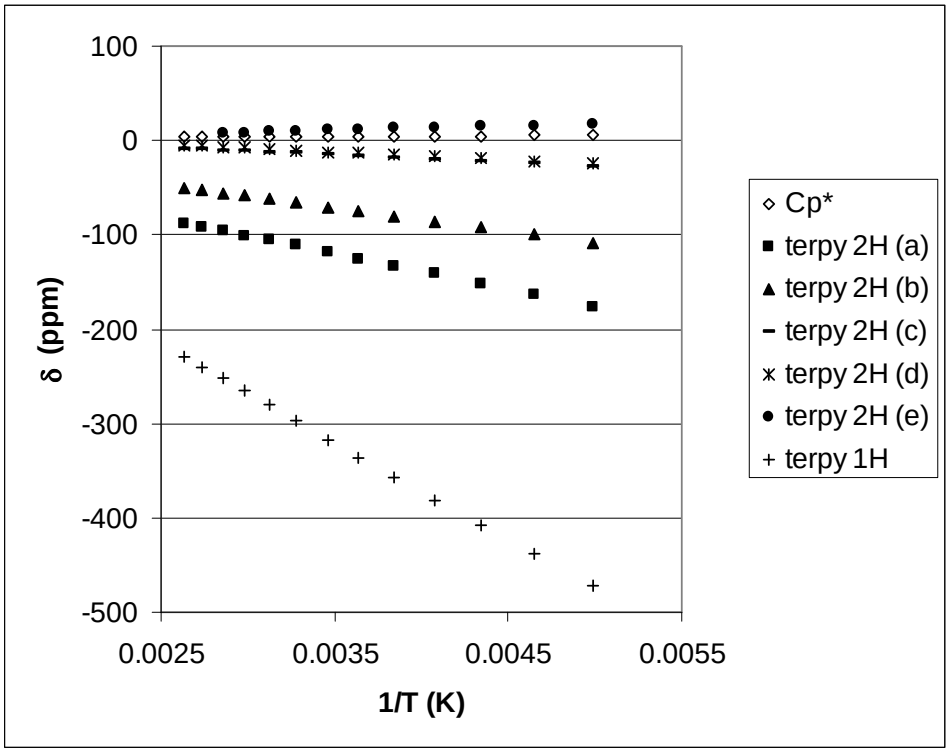

Figure 3.4.12: Variable Temperature ^{1}H NMR spectra represented as a δ vs. 1/T plot of Cp*$_2$Ce(2,2',6',2''-terpyridine) in toluene-d$_8$.

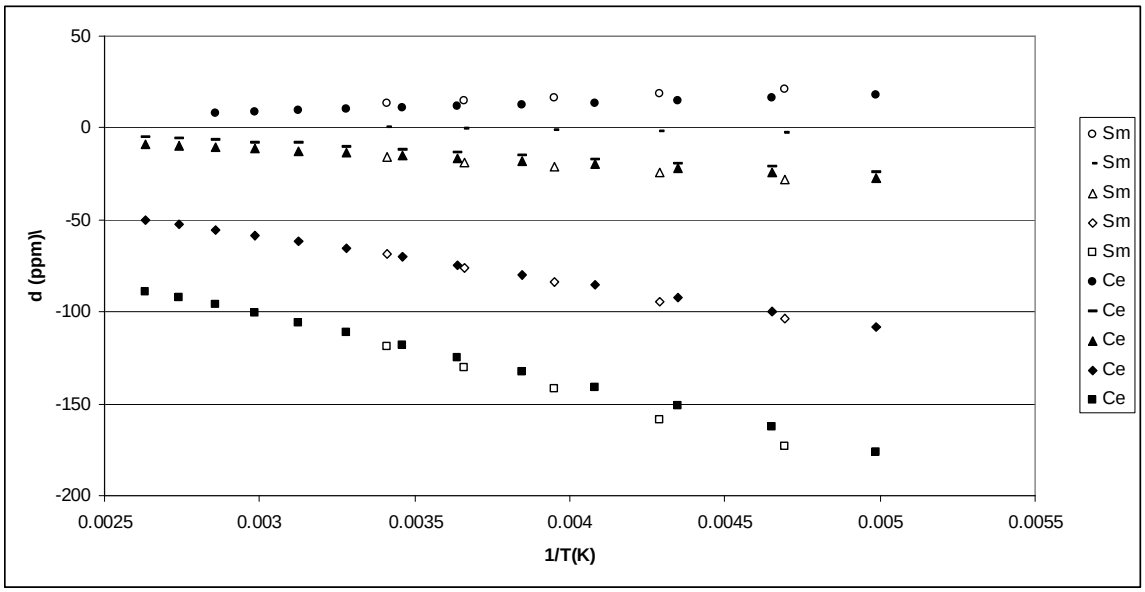

Figure 3.4.13: Variable Temperature ^{1}H NMR spectra represented as a δ vs. 1/T plot of Cp*$_2$Sm(2,2',6',2''-terpyridine) and the corresponding peaks in Cp*$_2$Ce(2,2',6',2''-terpyridine) in toluene-d_8. The peak between -200 and -500 ppm is shown in the next figure. The Cp* peaks have been omitted for clarity; they do not overlap.

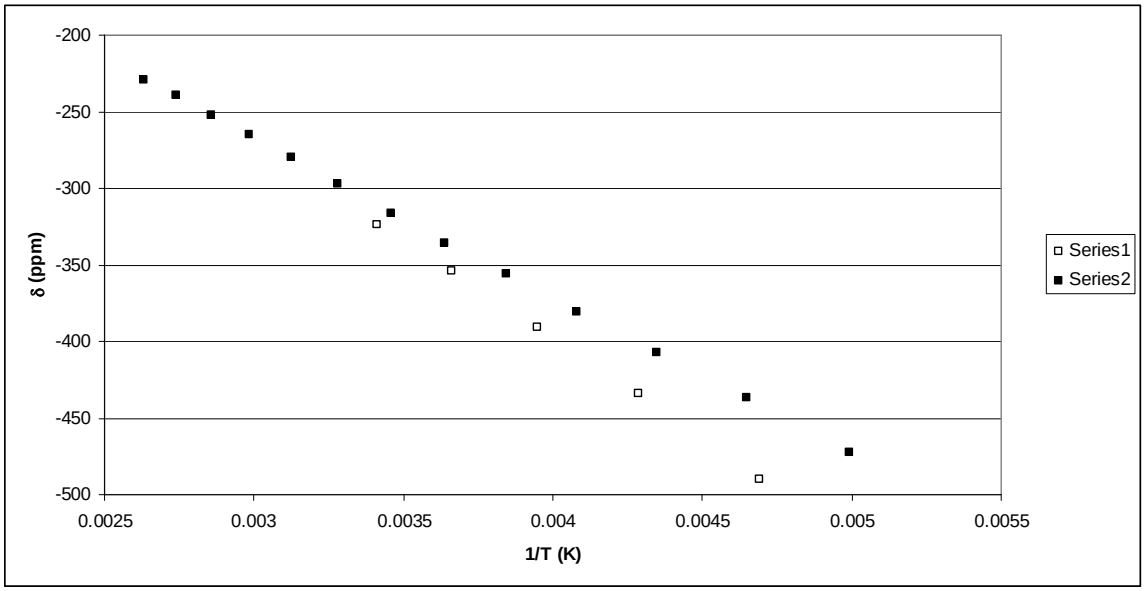

Figure 3.4.14: Variable Temperature ^{1}H NMR spectra represented as a δ vs. 1/T plot of the area one resonance between -200 and -500 ppm of Cp*$_2$Sm(2,2',6',2''-terpyridine) and Cp*$_2$Ce(2,2',6',2''-terpyridine) in toluene-d_8.

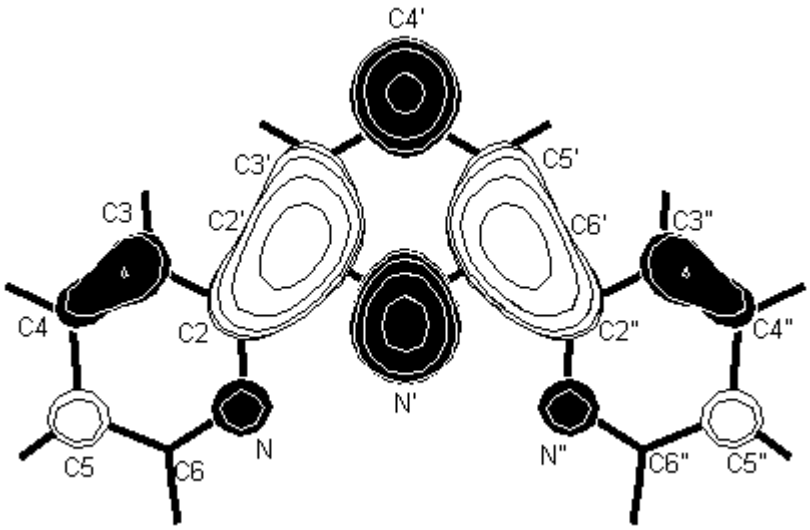

Figure 3.4.15: SOMO of 2,2',6',2''-terpyridine$^{\cdot-}$. Symmetry = C_{2v}. Exchange = B3LYP. Basis = 6-311+G*

3.5 Magnetism

To study the magnetic properties of systems of $Cp^*_2Ln(bipy^{\cdot -})$, where the unpaired electron on the ligand may couple with the unpaired electron on the cerium center, it is first necessary to understand the magnetic properties of the lanthanide ion in absence of the complication of the extra spin-carrier, as well as to understand the magnetic properties of the ligand in absence of the paramagnetic center. This is difficult, because at low temperatures the magnetic properties of lanthanide ions are ligand dependant. Kahn et al.[24] addressed this problem by synthesizing a molecule with an analogous ligand field around the lanthanide center, but one in which the ligands do not have an unpaired electron. In our case, $[Cp^*_2Ln(bipy)][BPh_4]$, where the bipy ligand is neutral, is representative of this class of molecules; a compound where the ligand carries an unpaired electron in absence of the paramagnetic center in a similar ligand field is $Cp^*_2La(bipy)$. We will use $Cp^*_2La(bipy)$ as a model for the unpaired spin on x,x'-dmb (x,x' = 4,5) radical anions as well.

The Pascal corrected values of χ, $1/\chi$, χT, and μ_{eff} at 300K of a series of $[Cp^*_2Ln(bipy)]$ cations, $Cp^*_2Ln(bipy)(X)$ (X = halide or triflate) and $Cp^*_2Ln(bipy)$ neutral molecules, and their substituted bipy analogues are given in Table 3.5.1.

Table 3.5.1: χ, $1/\chi$, χT, and μ_{eff} for molecules discussed in chapter 2 and 3.

Compound	χ (emu·mol^{-1}) * 10^{-3}	$1/\chi$ (emu^{-1}·mol)	χT (emu·K·mol^{-1})	μ_{eff}[a] (B.M.)
Cp*$_2$La(bipy)	1.10	912	0.329	1.62
Cp*$_2$Ce(bipy)(OTf)	2.61	383	0.784	2.50
Cp*$_2$Ce(bipy)(Cl)	2.54	394	0.761	2.47
Cp*$_2$Ce(4,4'-dmb)(OTf)	3.72	269	1.12	2.99
Cp*$_2$Ce(1,10-phenanthroline)(OTf)	2.95	339	0.885	2.66
[Cp*$_2$Ce(bipy)][BPh$_4$]	2.35	426	0.704	2.37
[Cp*$_2$Ce(4,4'-dmb)][BPh$_4$]	2.67	374	0.802	2.53
[Cp*$_2$Ce(5,5'-dmb)][BPh$_4$]	2.56	391	0.767	2.48
[Cp*$_2$Ce(6,6'-dmb)][BPh$_4$]	2.36	424	0.707	2.38
[Cp*$_2$Ce(terpy)][OTf]	2.39	418	0.717	2.40
Cp*$_2$Ce(bipy)	3.41	293	1.02	2.86
Cp*$_2$Ce(4,4'-dmb)	2.66	375	0.800	2.53
Cp*$_2$Ce(5,5'-dmb)	3.91	256	1.17	3.06
[Cp*$_2$Sm(bipy)][BPh$_4$]	1.08	925	0.324	1.61
Cp*$_2$Sm(bipy)	1.91	525	0.572	2.14
[Cp*$_2$Gd(bipy)][BPh$_4$]	22.8	43.9	6.83	7.39
[Cp*$_2$Gd(4,4'-dmb)][BPh$_4$]	21.2	47.1	6.36	7.13
Cp*$_2$Gd(bipy)	24.1	41.4	7.25	7.61
Cp*$_2$Gd(4,4'-dmb)	26.2	38.1	7.87	7.93
Cp*$_2$Ce(iso-propyl-N-CH=CH-N=CMe$_2$)	2.27	440	0.681	2.33

[a] μ_{eff} is defined as $2.828*\sqrt{(\chi T)}$, T = 300K.

The χ and $1/\chi$ vs. T plot of Cp*$_2$La(bipy) is shown in Figure 3.5.1.

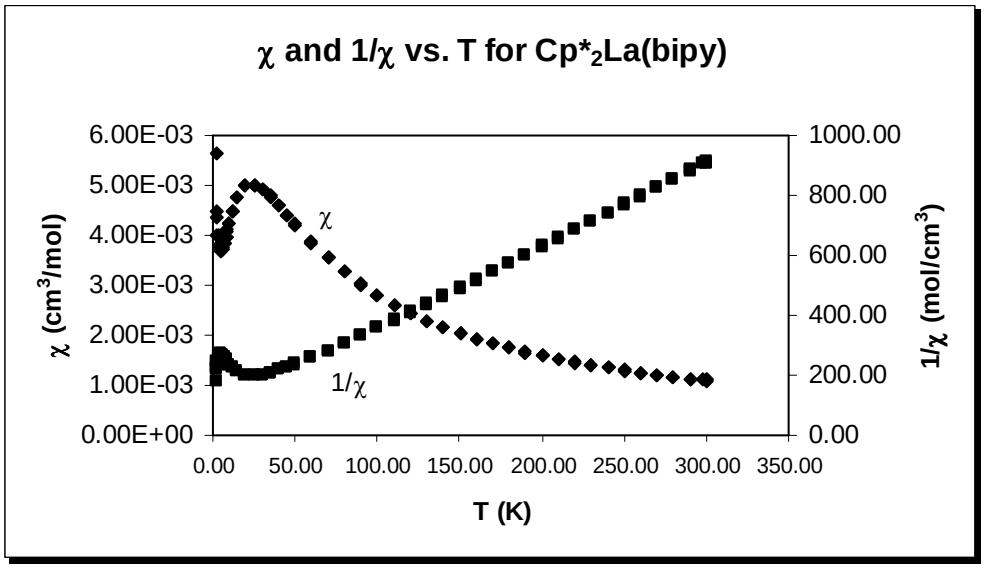

Figure 3.5.1: χ and $1/\chi$ vs. T plot of $Cp^*_2La(bipy)$

$Cp^*_2La(bipy^{\cdot-})$ shows antiferromagnetic coupling at low temperature, with a Néel temperature of 25 K. This coupling is presumably due to intermolecular coupling due to π-stacking of the bipyridine rings in the solid state.

At low temperatures, the χT value of $Cp^*_2Ce(bipy)$ and $Cp^*_2Ce(5,5'\text{-dmb})$ is lower than that of the corresponding cation (Figures 3.5.2 and 3.5.4) and at all temperatures the value of $Cp^*_2Ce(4,4'\text{-dmb})$ is lower than $[Cp^*_2Ce(4,4'\text{-dmb})]^+$ (Figure 3.5.3) even though the former two complexes have an extra unpaired electron. This implies that the unpaired electron on the bipy and 4,4'-dmb ligands are coupling antiferromagnetically with the unpaired electrons on the cerium center, which will lower the observed value of χT and μ_{eff}.

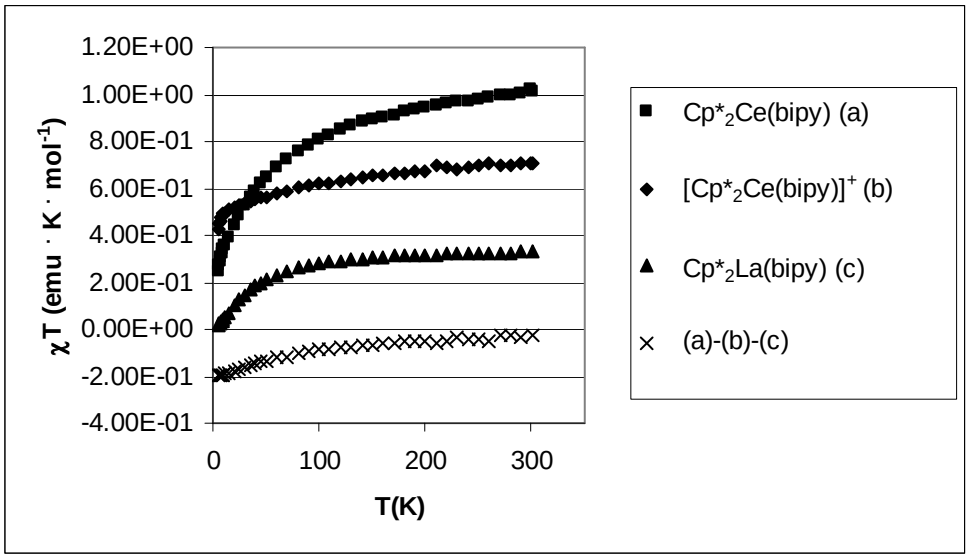

Figure 3.5.2: A plot of χT vs. T in $Cp^*_2Ce(bipy)$, $[Cp^*_2Ce(bipy)][BPh_4]$, and $Cp^*_2La(bipy)$, and the difference between $Cp^*_2Ce(bipy)$ and the other two curves.

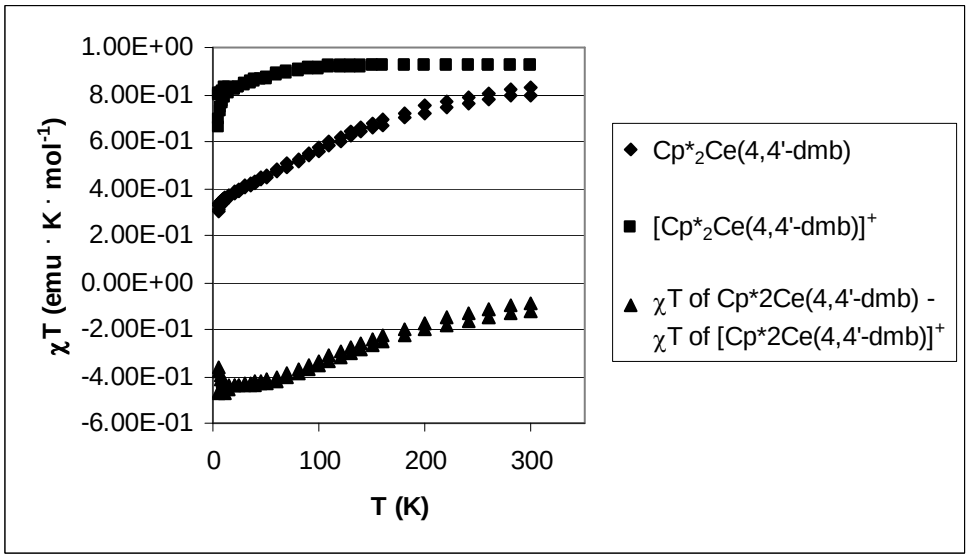

Figure 3.5.3: A plot of χT vs. T in $Cp^*_2Ce(4,4'\text{-dmb})$ and $[Cp^*_2Ce(4,4'\text{-dmb})][BPh_4]$ and the difference between the two curves.

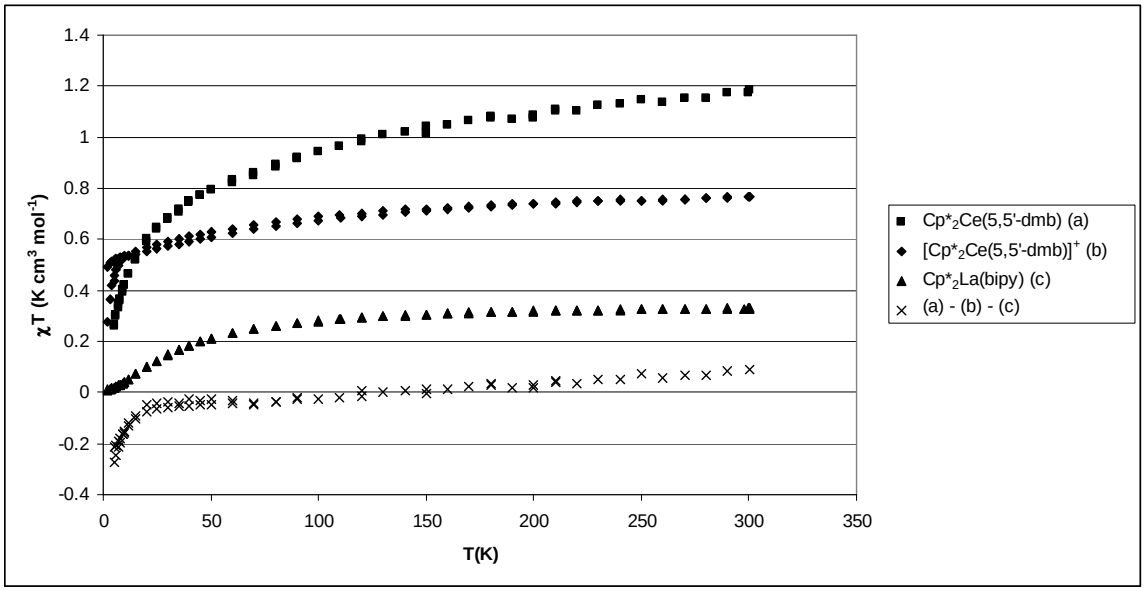

Figure 3.5.4: A plot of χT vs. T in $Cp^*_2Ce(5,5'\text{-dmb})$, $[Cp^*_2Ce(5,5'\text{-dmb})][BPh_4]$, and $Cp^*_2La(bipy)$, and the difference between $Cp^*_2Ce(5,5'\text{-dmb})$ and the other two curves.

In the case of $Cp^*_2Sm(bipy)$, the χT value of $Cp^*_2Sm(bipy)$ never falls below that of $[Cp^*_2Sm(bipy)]^+$, although the difference between the two begins to shrink at ~ 100 K (Figure 3.5.5) implying a small amount of antiferromagnetic coupling.

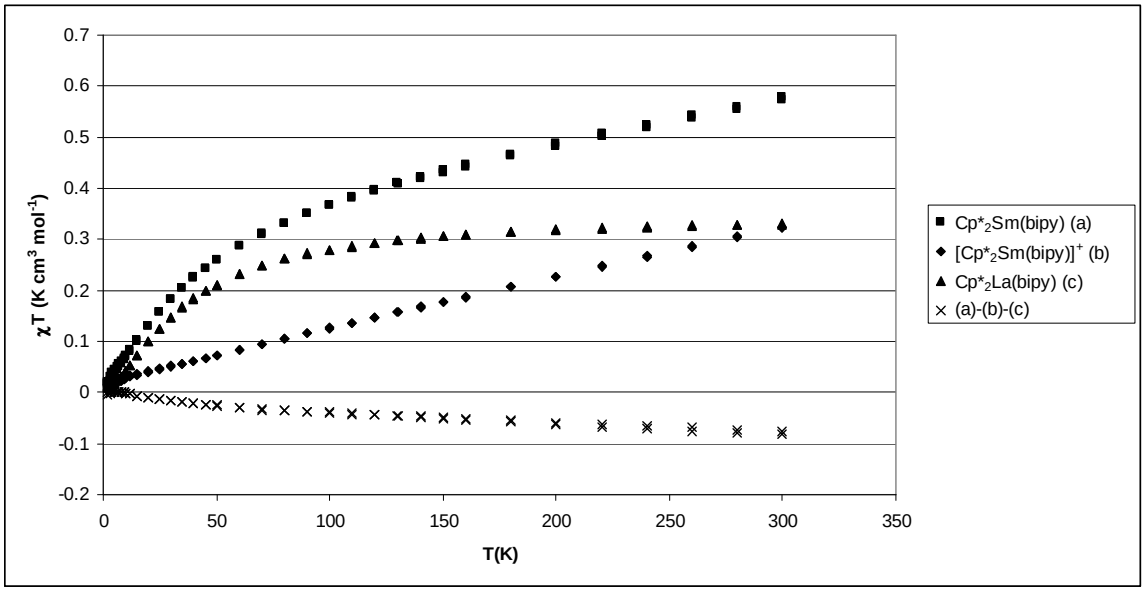

Figure 3.5.5: A plot of χT vs. T in $Cp^*_2Sm(bipy)$, $[Cp^*_2Sm(bipy)][BPh_4]$, and $Cp^*_2La(bipy)$ and the difference between $Cp^*_2Sm(bipy)$ and the other two curves.

However the χT vs. T plot of $Cp^*_2Sm(4,4'\text{-dmb})$ has a different form (Figure 3.5.6). XANES measurements are necessary to determine if there is mixed-configuration ground state in the $Cp^*_2Sm(bipy)$ and bipy analogues.

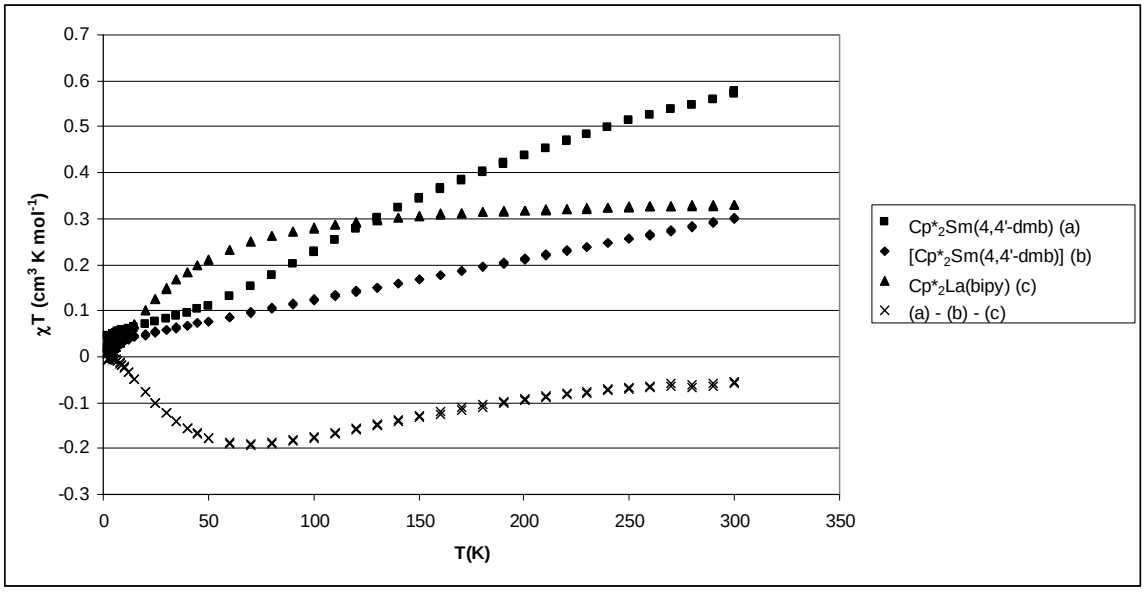

Figure 3.5.6: A plot of χT vs. T in $Cp^*_2Sm(4,4'\text{-dmb})$, $[Cp^*_2Sm(4,4'\text{-dmb})][BPh_4]$, and $Cp^*_2La(bipy)$ and the difference between $Cp^*_2Sm(4,4'\text{-dmb})$ and the other two curves.

On the other hand, in the case of $Cp^*_2Gd(bipy)$ and $Cp^*_2Gd(4,4'\text{-dmb})$ there is clearly strong coupling between the ligand and the metal. At low temperatures (T < 15K for $Cp^*_2Gd(bipy)$ and T<10K for $Cp^*_2Gd(4,4'\text{-dmb})$, the difference in χT values begins increasing again, implying that at very low temperatures there is some ferromagnetic coupling as well.

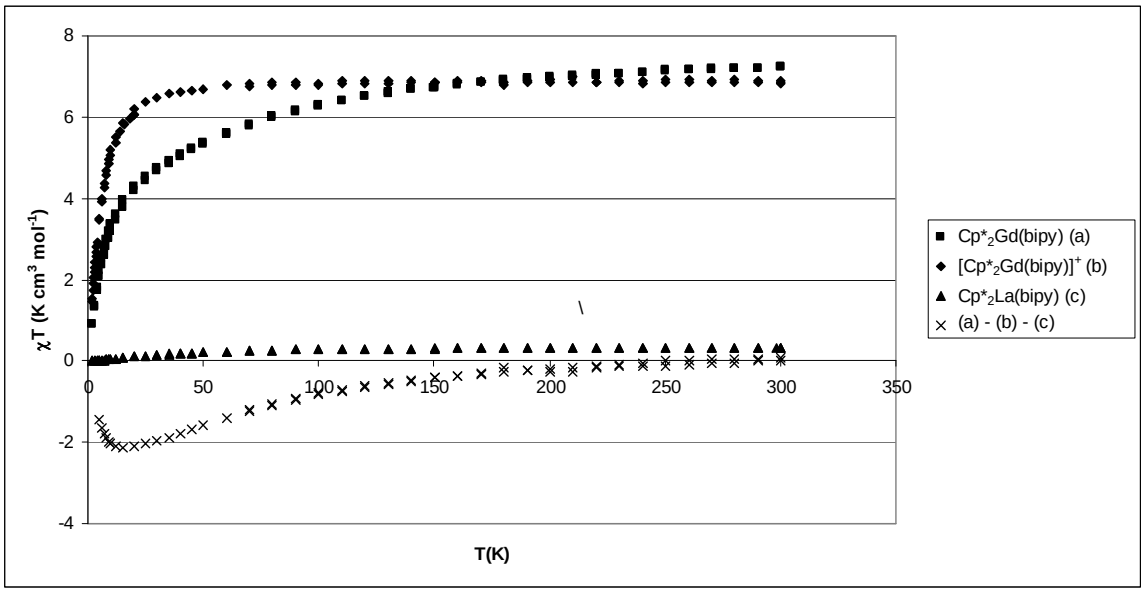

Figure 3.5.7: A plot of χT vs. T in $Cp^*_2Gd(bipy)$, $[Cp^*_2Gd(bipy)][BPh_4]$, and $Cp^*_2La(bipy)$ and the difference between $Cp^*_2Gd(bipy)$ and the other two curves.

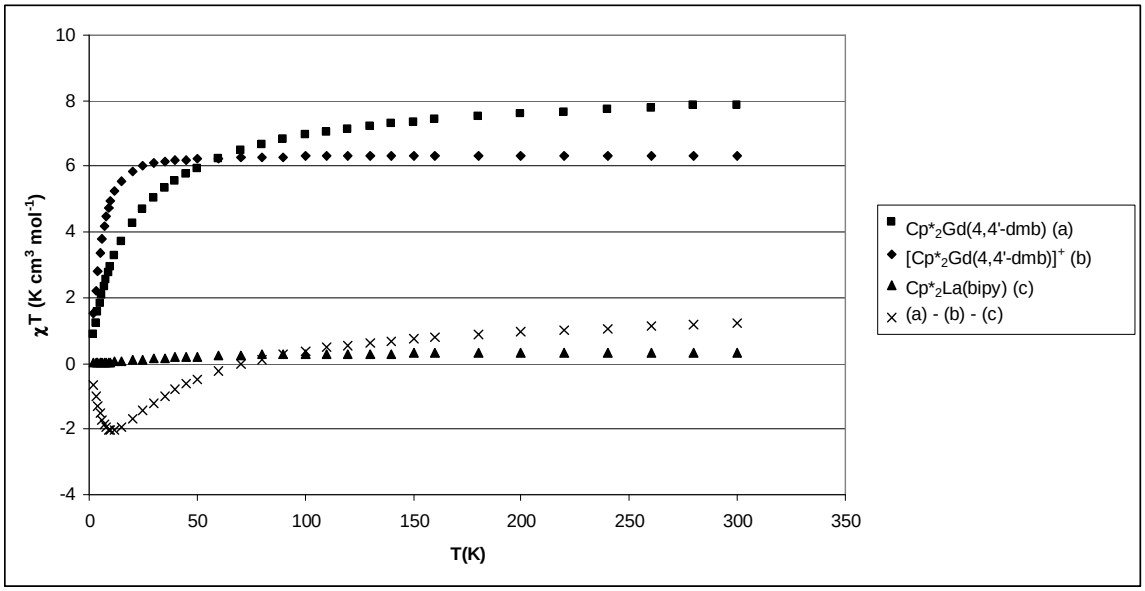

Figure 3.5.8: A plot of χT vs. T in $Cp^*_2Gd(4,4'\text{-dmb})$ and $[Cp^*_2Gd(4,4'\text{-dmb})][BPh_4]$ and the difference between the two curves.

Cp^*_2Yb(N,N'-bis(p-tolyl)-1,4-diazadiene) was prepared previously, and the magnetic moments was determined as a function of T, but without the corresponding cation, $[Cp^*_2Yb(N,N'\text{-bis(p-tolyl)-1,4-diazadiene})]^+$.[7] With $[Cp^*_2Yb(N,N'\text{-bis(p-tolyl)-1,4-diazadiene})][BPh_4]$ the magnetism can be analyzed more carefully (Figure 3.5.9). At all studied temperatures (T < 450K) the χT value of Cp^*_2Yb(N,N'-bis(p-tolyl)-1,4-diazadiene) is lower than that of $[Cp^*_2Yb(N,N'\text{-bis(p-tolyl)-1,4-diazadiene})][BPh_4]$ implying either strong coupling between the Yb(III) center and the N,N'-bis(p-tolyl)-1,4-diazadiene radical, a significant contribution from the electronic configuration Cp^*_2Yb(II)(N,N'-bis(p-tolyl)-1,4-diazadiene), where the N,N'-bis(p-tolyl)-1,4-diazadiene group is neutral, or both.

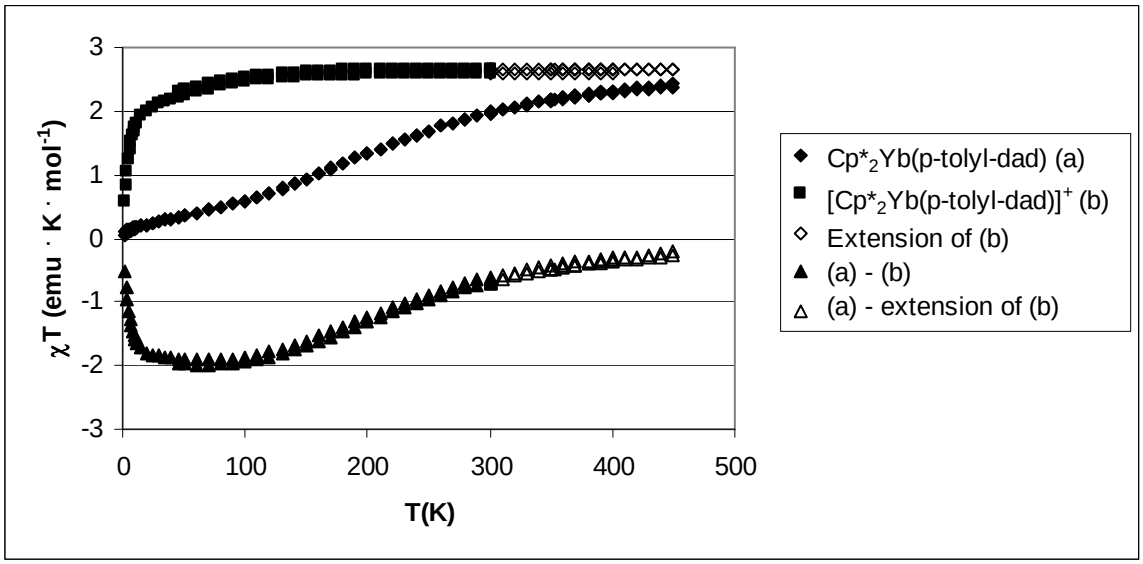

Figure 3.5.9: A plot of χT vs. T in Cp^*_2Yb(N,N'-bis(p-tolyl)-1,4-diazadienyl) and [Cp^*_2Yb(N,N'-bis(p-tolyl)-1,4-diazadiene)][BPh_4] and the difference between the two curves. The χT of [Cp^*_2Yb(N,N'-bis(p-tolyl)-1,4-diazadiene)][BPh_4] is stable at 2.6 B.M. above 190K, and the values above 300K were assumed to be constant.

In conclusion, Cp^*_2Ln(bipy) molecules have been synthesized and the X-ray crystal structures that were examined, as well as the ^1H NMR spectra indicate that there is an unpaired electron on the bipy ligand, and the electron density is distributed as shown in Figure 3.4.15.

The magnetism indicates that at low temperatures, the unpaired electron density on the bipy ligand couples with the unpaired electron(s) on the lanthanide center antiferromagnetically, except for gadolinium which couples antiferromagnetically at high temperatures, but ferromagnetically at low temperature. This conclusion is qualitative and the value of the coupling constant, J, cannot be evaluated, since the term-symbol of the crystal-field states cannot be determined.[24]

References:

1. Freeman, A.J.; Watson, R.E. *Phys. Rev. Series II*, **1962**, *127*, 2058
2. Van Vleck, J.H.; Frank, A. *Phys. Rev.*, **1929**, *34*, 1494
3. Van Vleck, J.H.; Frank, A. *Phys. Rev.*, **1929**, *34*, 1625
4. Van Vleck, J.H. *Theory of Electric and Magnetic Susceptibilities*, **1932**, p. 243.
5. Schultz, M.; Boncella, J.M.; Berg, D.J.; Tilley, T.D.; Andersen, R.A. *Organometallics*, **2002**, *21*, 460
6. Walter, M.D.; Berg, D.J.; Andersen, R.A. *Organometallics*, **2006**, *25*, 3228
7. Walter, M.D.; Berg, D.J.; Andersen, R.A. *Organometallics*, **2007**, *26*, 2296
8. Evans, W.J.; and Drummond, D.K. *J. Am. Chem. Soc.*, **1989**, *111*, 3329
9. Burns, C.J.; Andersen, R.A. *Journal of Organometallic Chemistry*, **1987**, *325*, 31
10. Franz, K.D.; Dieck, H.T.; Starzewski, K.A.O.; Hohmann, F. *Tetrahedron*, **1975**, *31*, 1465.
11. Chisholm, M.H.; Huffman, J.C.; Rothwell, I.P.; Bradley, P.G.; Kress, N.; Woodruff, W.H. *J. Am. Chem. Soc.*, **1981**, *103*, 4945
12. Fedushkin, I.L.; Petrovskaya, T.V.; Girgsdies, F.; Köhn, R.D.; Bochkarev, M.N.; Schumann, H. *Angew. Chem. Intl. Ed.* **1999**, *38*, 2262
13. Kazhdan, D.; Hu, Y.-J.; Kokai, A.; Levi, Z.; Rozenel, S. *Acta Cryst.*, **2008**, *E64*, m1134.
14. Takeshita, T.; Hirota, N. *J. Am. Chem. Soc.*, *93*, 6421
15. Kaim, W. *J. Am. Chem. Soc.*, **1982**, *104*, 3833
16. Kaim, W. *J. Am. Chem. Soc.*, **1982**, *104*, 7385
17. Proctor, W.G.; Yu, F.C. *Phys. Rev.*, **1950**, *77*, 717
18. Bloembergen, N.; Dickinson, W.C. *Phys. Rev.*, **1950**, *79*, 179
19. Bertini, I.; Luchinat, C.; Aime, S. *Coord. Chem. Rev.*, **1996**, *150*, R7
20. Karplus, M. *J. Am. Chem. Soc.*, **1963**, *85*, 2870
21. Eaton, D.R.; Josey, A.D.; Phillips, W.D.; Benson, R.E. *J. Chem. Phys.*, **1962**, *37*, 347
22. Veauthier, J.M.; Schelter, E.J.; Carlson, C.N.; Scott, B.L.; Da Re, R.E; Thompson, J. D.; Kiplinger, J.L.; Morris, D.E.; John, K.D. *Inorganic Chemistry*, **2008**, *47*, 5841.
23. Lyubimova, O.O.; Baranovskii, V.I. *Journal of Structural Chemistry*, **2003**, *44*, 728-735
24. Kahn, M.L.; Sutter, J.-P.; Golhen, S.; Guionneau, P.; Ouahab, L.; Kahn, O.; Chasseau, D. *J. Am. Chem. Soc.*, **2000**, *122*, 3413

Chapter 4: Synthesis, Properties, and Magnetism of Cp^*_2Yb(2,2'-bipyridine) analogues.

4.1 Introduction

Andersen and coworkers have shown that Cp^*_2Yb(bipy) has a magnetic susceptibility of $2.4\mu_B$.[1] The calculated magnetic moment for a Yb^{III} species is $4.5\mu_B$, whereas Yb^{II} is diamagnetic.[2,3] X-ray absorption near-edge spectroscopy shows that the cause of this intermediate magnetic moment is an intermediate ytterbium valence, with a temperature independant f-hole occupancy of 0.8 ± 0.03.[4] Further research in the Andersen group showed that symmetric substitution in the 4,4'-position has a pronounced effect on the magnetism. However, the valence of the ytterbium center in all the cases studied was still temperature independent.[5] This chapter outlines the synthesis and physical properties of complexes of the type Cp^*_2Yb(x,x'-Me_2-2,2'-bipyridine), where x = 5,6 and Cp^*_2Yb(x-Me-2,2'-bipyridine), where x = 4,5,6.

Results and Discussion

4.2 Synthesis of Cp^*_2Yb(x,x'-dimethyl-2,2'-bipyridine) (x = 5,6) and Cp^*_2Yb(x-methyl-2,2'bipyridine) (x = 4,5,6)

The substituted bipy adducts, Cp^*_2Yb(x,x'-dmb) (dmb = dimethyl-2,2'-bipyridine) and Cp^*_2Yb(x-mmb) (mmb = monomethyl-2,2'-bipyridine) are readily synthesized in a manner analogous to that used to synthesize Cp^*_2Yb(bipy) (bipy = 2,2'-bipyridine) and Cp^*_2Yb(4,4'-dmb).[1] Thus, the appropriate bipy derivative is added to $Cp^*_2Yb(OEt_2)$, and red crystals are grown by cooling a solution in toluene to -15 °C. The

melting points of $Cp^*_2Yb(bipy)$ and its derivatives are given in Table 4.2.1. $Cp^*_2Yb(6,6'$-dmb) can be crystallized from benzene giving crystals that have benzene incorporated into the crystal structure or from methyl-cyclohexane which have no solvent in the crystal structure.

Compound	Melting Point (°C)
$Cp^*_2Yb(bipy)$[1]	322-323
$Cp^*_2Yb(4,4'$-dmb) [1]	>330
$Cp^*_2Yb(5,5'$-dmb)	236-238
$Cp^*_2Yb(6,6'$-dmb)	336-339
Cp^*_2Yb(4-mmb)	282-284
Cp^*_2Yb(5-mmb)	318-320
Cp^*_2Yb(6-mmb)	333-335

4.3 Solid State Measurements: X-ray Crystallography

The X-ray structures of bipyridine complexes are used as evidence for the oxidation state of the bipyridine ligand, because donation of electron density into the LUMO of bipyridyl causes systematic changes to the bond lengths.[1,6,7] Therefore the crystal structures of $Cp^*_2Yb(bipy)$[1], $Cp^*_2Yb(4,4'$-dmb)[5], $Cp^*_2Yb(5,5'$-dmb), $Cp^*_2Yb(6,6'$-dmb), Cp^*_2Yb(6-mmb), and $[Cp^*_2Yb(bipy)][Cp^*_2YbCl_2]$[1] are determined. ORTEP diagrams of $Cp^*_2Yb(5,5'$-dmb), $Cp^*_2Yb(6,6'$-dmb)(C_6H_6), $Cp^*_2Yb(6,6'$-dmb), and Cp^*_2Yb(6-mmb) are shown in Figures 4.3.1-4.3.6. Table 4.3.9 compares selected bond distances and angles between various $Cp^*_2Yb(bipy)$ analogues.

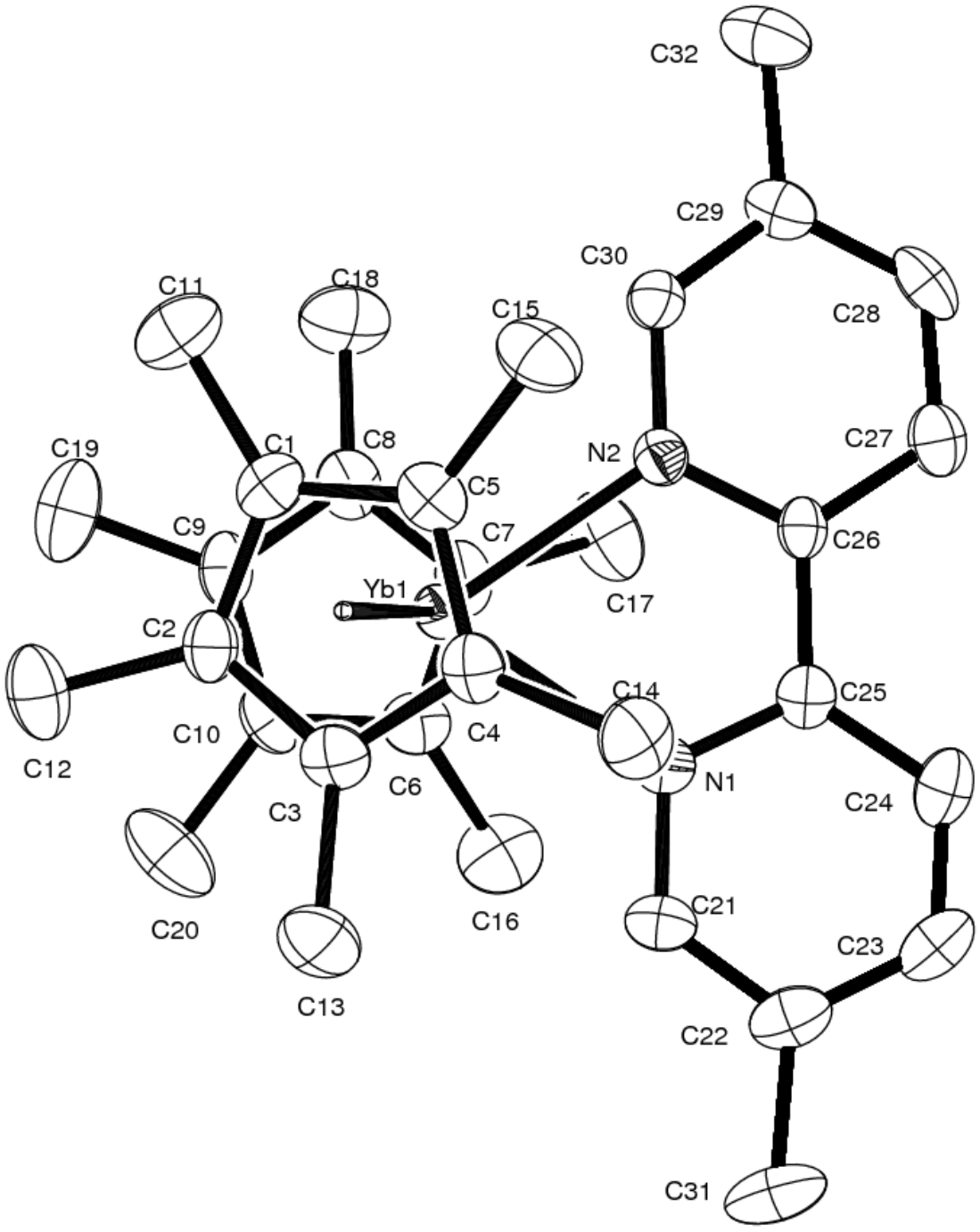

Figure 4.3.1: ORTEP diagram of Cp^*_2Yb(5,5'-dimethyl-2,2'-bipyridine) (50% probability ellipsoids). All non-hydrogen atoms are refined anisotropically. Hydrogen atoms are placed and not refined and are not shown. Selected Bond Distances and Angles

are given in Tables 4.3.1 and 4.3.2, respectively. The N1-C25-C26-N2 torsion angle is 3.9(6)°.

Table 4.3.1: Selected bond distances (Å) in $Cp^*_2Yb(5,5'\text{-dmb})$

Atom	atom	distance		Atom	atom	Distance
Yb(1)	N(1)	2.331(4)		Yb(1)	N(2)	2.347(4)
Yb(1)	C(1)	2.625(4)		Yb(1)	C(2)	2.649(4)
Yb(1)	C(3)	2.655(4)		Yb(1)	C(4)	2.659(4)
Yb(1)	C(5)	2.643(5)		Yb(1)	C(6)	2.651(5)
Yb(1)	C(7)	2.650(5)		Yb(1)	C(8)	2.637(5)
Yb(1)	C(9)	2.651(5)		Yb(1)	C(10)	2.643(5)
Yb(1)	C(101)	2.36		Yb(1)	C(102)	2.36
C(25)	C(26)	1.461(6)				

Table 4.3.2: Selected bond angles in $Cp^*_2Yb(5,5'\text{-dmb})$

atom	atom	atom	angle		atom	atom	atom	Angle
N(1)	Yb(1)	N(2)	69.4(1)		C(101)	Yb(1)	C(102)	140

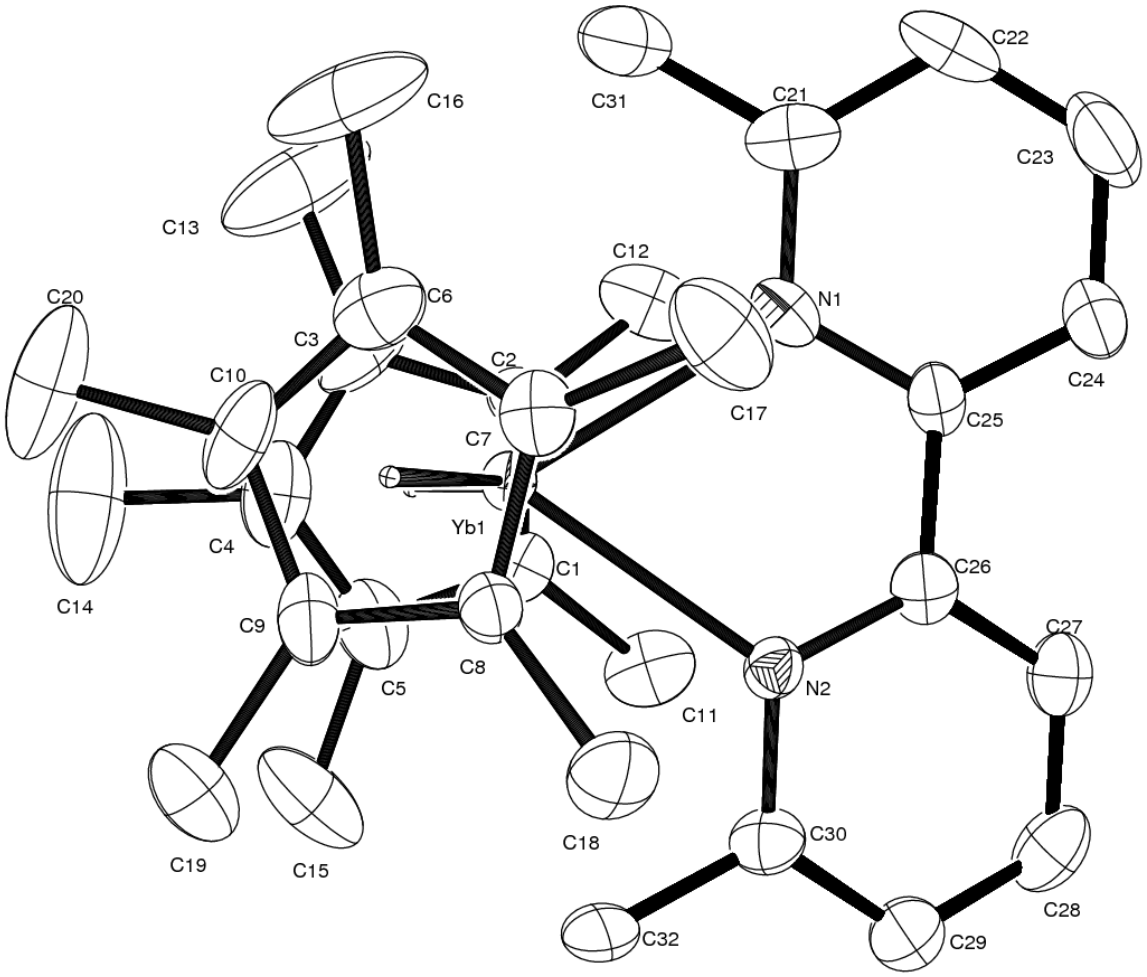

Figure 4.3.2: ORTEP diagram of $Cp^*_2Yb(6,6\text{-dmb})(C_6H_6)$ (50% probability ellipsoids). All the non-hydrogen atoms are refined anisotropically. Hydrogen atoms are placed and not refined and are not shown; benzene of crystallization is not shown. Selected Bond Distances and Angles are given in Tables 4.3.3 and 4.3.4, respectively. The N1-C25-C26-N2 torsion angle is 19.3(9)°.

Table 4.3.3: Selected bond distances (Å) in $Cp^*_2Yb(6,6'\text{-dmb})(C_6H_6)$

atom	atom	distance		Atom	atom	distance
Yb(1)	N(1)	2.510(6)		Yb(1)	N(2)	2.509(6)
Yb(1)	C(1)	2.749(7)		Yb(1)	C(2)	2.740(7)
Yb(1)	C(3)	2.725(8)		Yb(1)	C(4)	2.734(8)
Yb(1)	C(5)	2.746(7)		Yb(1)	C(6)	2.775(7)
Yb(1)	C(7)	2.743(7)		Yb(1)	C(8)	2.725(7)
Yb(1)	C(9)	2.711(8)		Yb(1)	C(10)	2.748(7)
Yb(1)	C(101)	2.46		Yb(1)	C(102)	2.46
C(25)	C(26)	1.487(9)				

Table 4.3.4: Selected bond angles in $Cp^*_2Yb(6,6'\text{-dmb})(C_6H_6)$

atom	atom	atom	angle		atom	atom	atom	angle
N(1)	Yb(1)	N(2)	66.7(2)		C(101)	Yb(1)	C(102)	141.

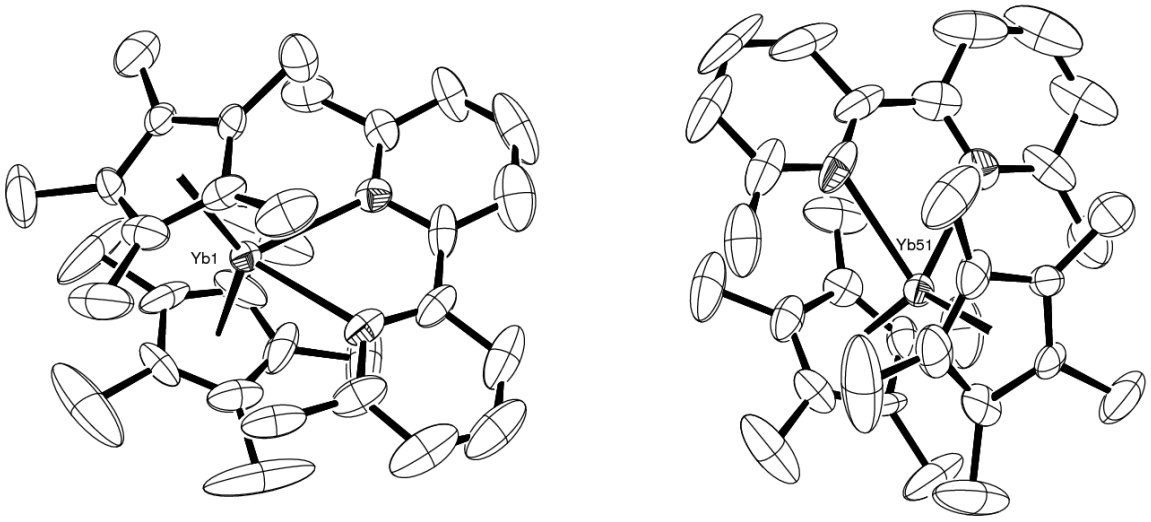

Figure 4.3.3: ORTEP diagram of $Cp^*_2Yb(6,6\text{-dmb})$ (50% probability ellipsoids) which contains two isolated molecules in the asymmetric unit. All the non-hydrogen atoms are refined anisotropically. Hydrogen atoms are placed and not refined and are not shown. The two individual molecules are shown separately in Figures 4.3.4 and 4.3.5.

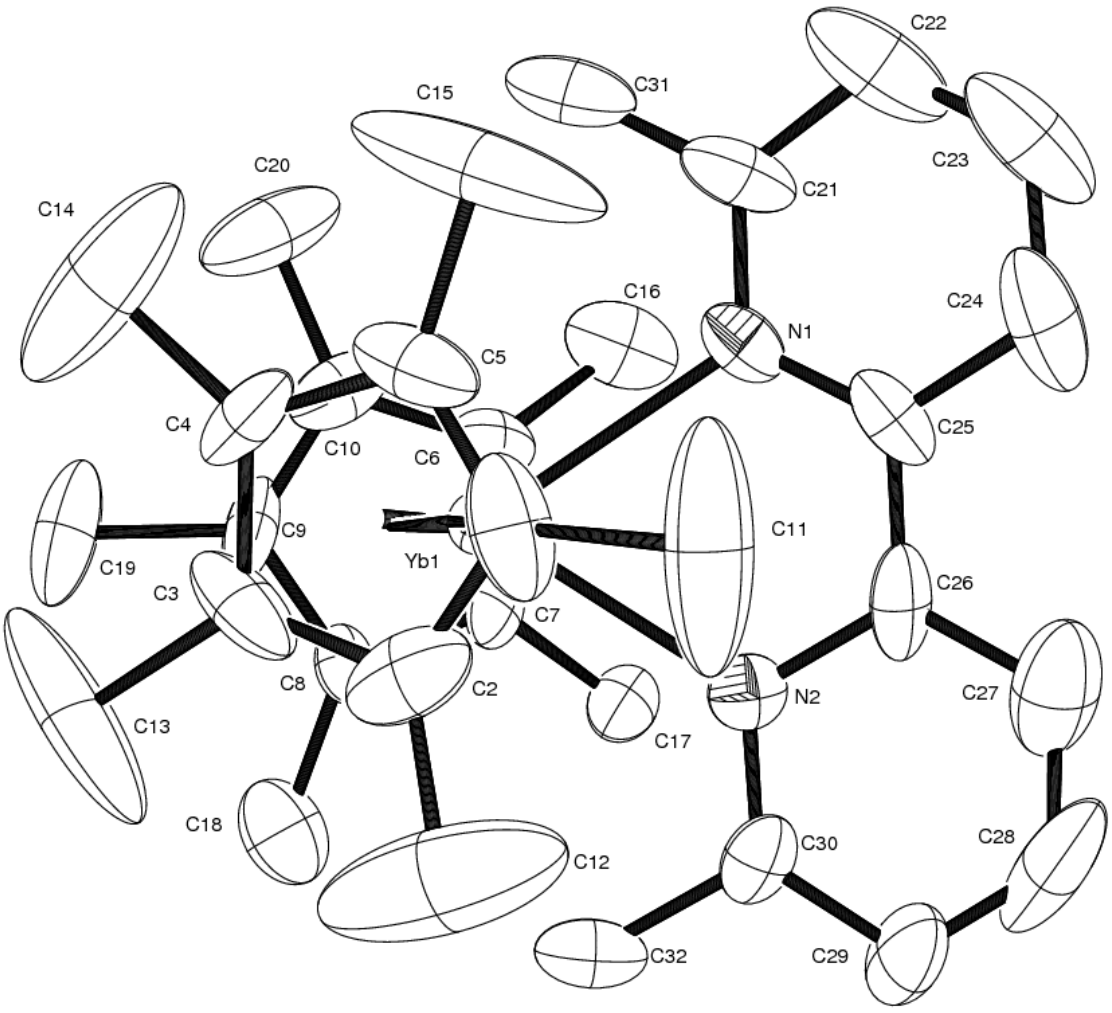

Figure 4.3.4: ORTEP diagram of one molecule of $Cp^*_2Yb(6,6\text{-dmb})$ in the asymmetric unit (50% probability ellipsoids). All the non-hydrogen atoms are refined anisotropically. Hydrogen atoms are placed and not refined and are not shown. Selected Bond Distances and Angles are given in Tables 4.3.5 and 4.3.6, respectively. The N1-C25-C26-N2 torsion angle is 13.(2)°.

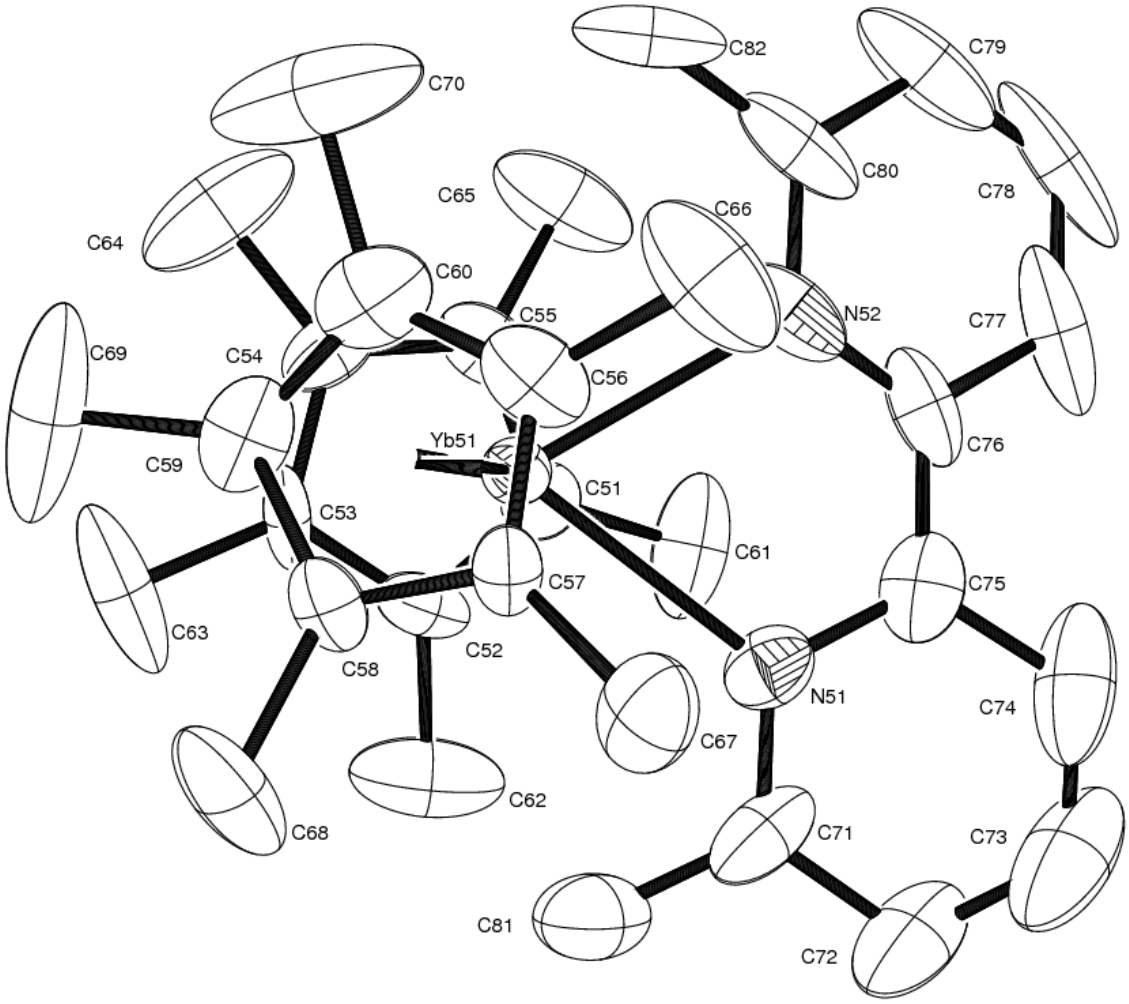

Figure 4.3.5: ORTEP diagram of the other molecule of $Cp^*_2Yb(6,6\text{-dmb})$ in the asymmetric unit (50% probability ellipsoids). All the non-hydrogen atoms are refined anisotropically. Hydrogen atoms are placed and not refined and are not shown. Selected Bond Distances and Angles are given in Tables 4.3.5 and 4.3.6, respectively. The N1-C25-C26-N2 torsion angle is 18.(2)°.

Table 4.3.5: Selected bond distances (Å) in $Cp^*_2Yb(6,6'\text{-dmb})$

atom	atom	distance		Atom	atom	distance
Yb(1)	N(1)	2.499(8)		Yb(1)	N(2)	2.484(8)
Yb(1)	C(1)	2.756(12)		Yb(1)	C(2)	2.725(12)
Yb(1)	C(3)	2.672(11)		Yb(1)	C(4)	2.734(11)
Yb(1)	C(5)	2.760(12)		Yb(1)	C(6)	2.731(11)
Yb(1)	C(7)	2.750(10)		Yb(1)	C(8)	2.798(10)
Yb(1)	C(9)	2.753(11)		Yb(1)	C(10)	2.760(11)
Yb(1)	C(101)	2.46		Yb(1)	C(102)	2.48
C(25)	C(26)	1.450(15)				
Yb(51)	N(51)	2.519(8)		Yb(51)	N(52)	2.513(9)
Yb(51)	C(51)	2.784(10)		Yb(51)	C(52)	2.717(11)
Yb(51)	C(53)	2.716(10)		Yb(51)	C(54)	2.716(11)
Yb(51)	C(55)	2.788(11)		Yb(51)	C(56)	2.723(10)
Yb(51)	C(57)	2.759(10)		Yb(51)	C(58)	2.766(9)
Yb(51)	C(59)	2.766(11)		Yb(51)	C(60)	2.722(12)
Yb(51)	C(103)	2.47		Yb(51)	C(104)	2.48
C(75)	C(76)	1.446(16)				

Table 4.3.6: Selected bond angles in $Cp^*_2Yb(6,6'\text{-dmb})$

atom	atom	atom	angle		Atom	atom	atom	angle
N(1)	Yb(1)	N(2)	66.9(3)		C(101)	Yb(1)	C(102)	140
N(51)	Yb(51)	N(52)	67.6(3)		C(103)	Yb(51)	C(104)	139

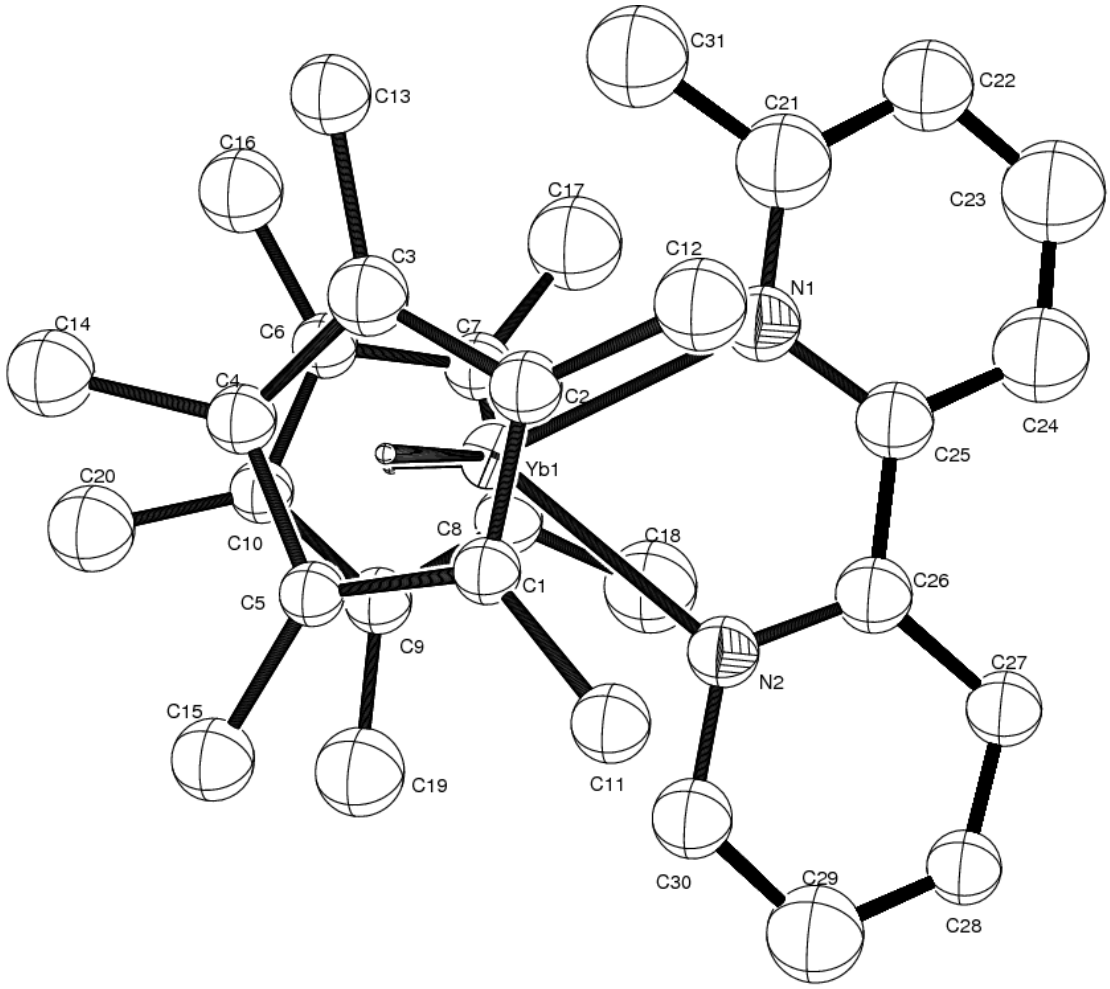

Figure 4.3.6: ORTEP diagram of Cp^*_2Yb(6-methyl-2,2'-bipyridine) (50% probability ellipsoids). The ytterbium atom is refined anisotropically while the rest of the non-hydrogen atoms are refined isotropically. Hydrogen atoms are placed and not refined and are not shown. Selected Bond Distances and Angles are given in Tables 4.2.3 and 4.2.4, respectively. The N1-C25-C26-N2 torsion angle is 2(2)°.

Table 4.3.7: Selected bond distances (Å) in Cp^*_2Yb(6-methyl-bipy)

atom	Atom	distance (Å)		atom	atom	distance (Å)
Yb(1)	N(1)	2.47(1)		Yb(1)	N(2)	2.46(1)
Yb(1)	C(1)	2.67(2)		Yb(1)	C(2)	2.71(1)
Yb(1)	C(3)	2.71(2)		Yb(1)	C(4)	2.70(1)
Yb(1)	C(5)	2.68(1)		Yb(1)	C(6)	2.66(1)
Yb(1)	C(7)	2.70(2)		Yb(1)	C(8)	2.68(2)
Yb(1)	C(9)	2.70(2)		Yb(1)	C(10)	2.71(1)
Yb(1)	C(101)	2.42		Yb(1)	C(102)	2.41
C(25)	C(26)	1.43(2)				

Table 4.3.8: Selected bond angles in Cp^*_2Yb(6-methyl-bipy)

atom	atom	atom	angle		Atom	atom	atom	Angle
N(1)	Yb(1)	N(2)	66.1(4)		C(101)	Yb(1)	C(102)	140

Table 4.3.9: Selected bond distances and torsion angles in Cp^*_2Yb(bipy) and related molecules. d is the distance from the plane defined by the Yb atom and two centroids to the bridging carbon of the bipyridine ligand which is nearest to the plane. d' is the distance from the plane defined by the Yb atom and two centroids to the bridging carbon of the bipyridine ligand which is further from the plane.

Molecule	Yb-N1 (Å)	Yb-N2 (Å)	Bridging Carbons of bipy (Å)	NCCN torsion angle (°)	d	d’	d'/d
Cp^*_2Yb(bipy) (molecule 1)	2.33	2.32	1.43	9	0.62	0.82	1.3
Cp^*_2Yb(bipy) (molecule 2)	2.31	2.33	1.43	5	0.65	0.77	1.2
Cp^*_2Yb(4,4’-dmb)	2.40	2.39	1.46	1	0.66	0.81	1.2
Cp^*_2Yb(5,5’-dmb)	2.33	2.35	1.46	4	0.68	0.77	1.1
Cp^*_2Yb(6,6’-dmb) (C_6H_6)	2.51	2.51	1.49	19	0.59	0.88	1.5
Cp^*_2Yb(6,6’-dmb) (molecule 1)	2.50	2.48	1.45	13	0.64	0.80	1.3
Cp^*_2Yb(6,6’-dmb) (molecule 2)	2.52	2.51	1.45	18	0.59	0.83	1.7
Cp^*_2Yb(6-mmb)	2.47	2.46	1.43	2	0.19	1.23	6.6
[Cp^*_2Yb(bipy)] [$Cp^*_2YbCl_2$]	2.36	2.38	1.492	7	0.68	0.81	1.2

The ratio of d'/d (Table 4.3.9) shows that in the case of 6-methyl-bipy, the bipy ligand skews the methylated side away from the Cp* rings, and in such a manner maintains an intermediate Yb-N distance between Cp^*_2Yb(bipy) and Cp^*_2Yb(6,6'-dmb), where the steric bulk of the methyl groups forces an elongation of the Yb-N distances. As discussed in Chapter 3, the SOMO (SOMO = singly occupied molecular orbital) of bipy$^{\cdot-}$ has a bonding contribution between the bridging carbons (Figure 4.3.7). As a result, the more unpaired electron density there is in the bipy ring, the smaller is the distance between the bridging carbons and the smaller is the N-C-C'-N' torsion angle. Based on this observation, Cp^*_2Yb(5,5'-dmb) and Cp^*_2Yb(6-methyl-bipy) should both have a significant amount of unpaired electron density on the bipy rings, whereas Cp^*_2Yb(6,6'-dmb), with the longest distances between the bridging carbons, and by far the largest N-C-C-N' torsion angles, has less electron density on the bipyridine ligand.

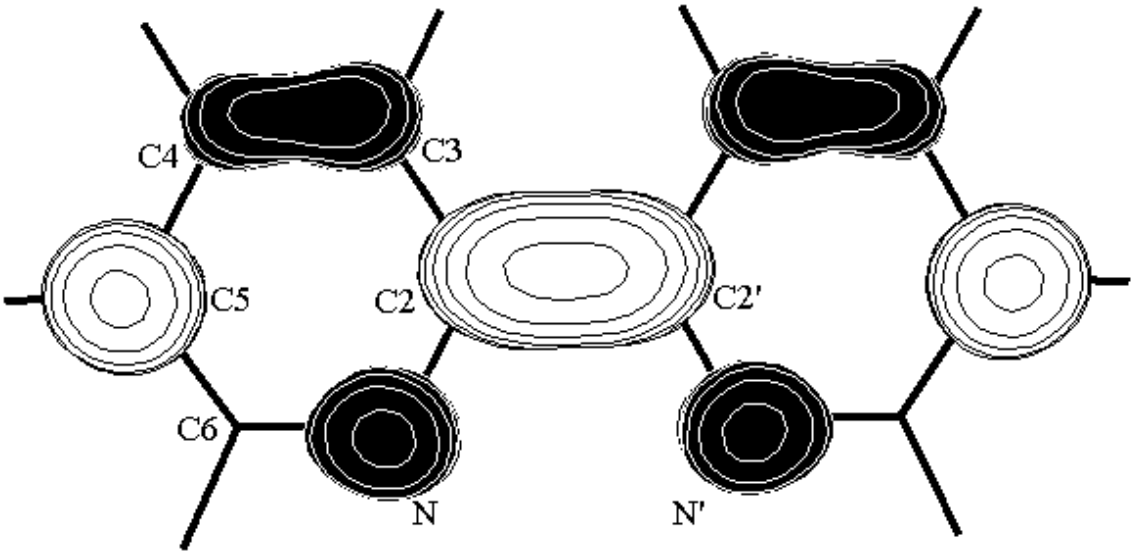

Figure 4.3.7: SOMO of bipy$^{\cdot-}$. Symmetry = C_{2v}. Exchange = B3LYP. Basis = 6-311+G*

4.4 Solution Measurements: NMR Spectroscopy

The variable temperature ^{1}H NMR spectra plotted as a δ vs. 1/T plot of $Cp^*_2Yb(bipy)$,[1] $Cp^*_2Yb(4\text{-mmb})$, $Cp^*_2Yb(4,4'\text{-dmb})$,[5] $Cp^*_2Yb(5\text{-mmb})$, $Cp^*_2Yb(5,5'\text{-dmb})$ and $Cp^*_2Yb(6\text{-mmb})$ are shown in Figures 4.2.1-4.2.6.

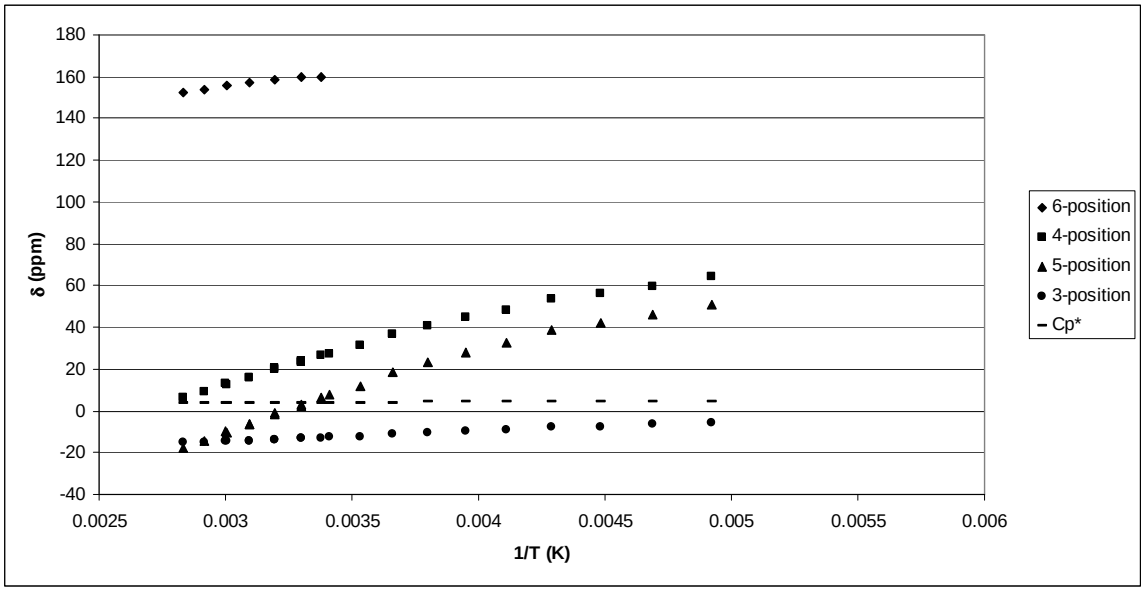

Figure 4.4.1: Variable Temperature ^{1}H NMR spectra represented as a δ vs. 1/T plot of $Cp^*_2Yb(bipy)$ in toluene-d_8.[1]

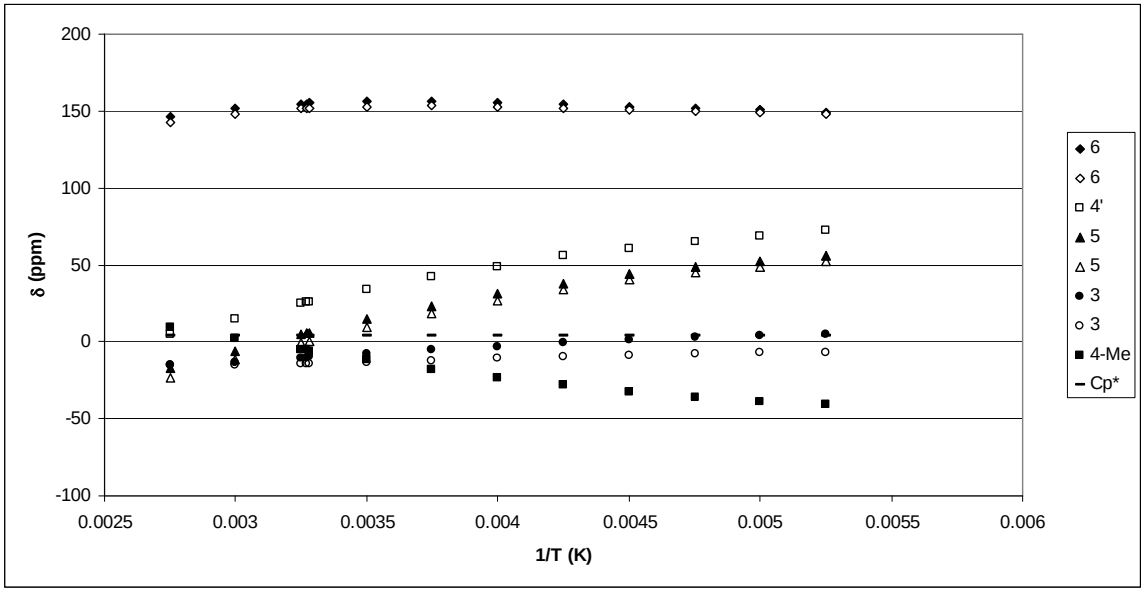

Figure 4.4.2: Variable Temperature ^{1}H NMR spectra represented as a δ vs. 1/T plot of Cp^*_2Yb(4-methyl-bipy) in toluene-d_8.

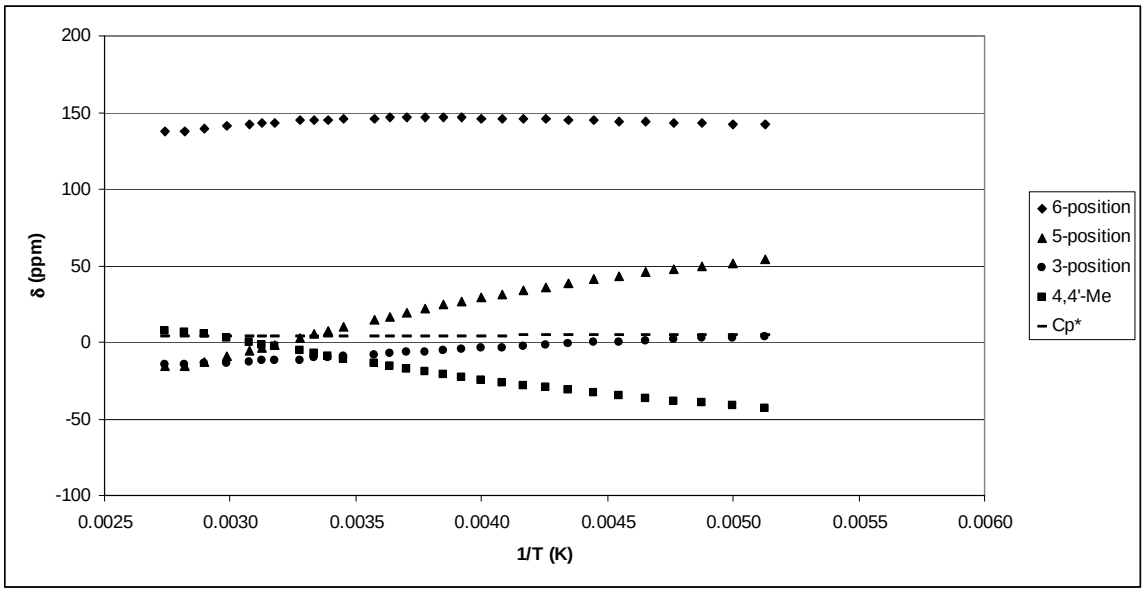

Figure 4.4.3: Variable Temperature ^{1}H NMR spectra represented as a δ vs. 1/T plot of Cp^*_2Yb(4,4-dmb) in toluene-d_8.[5]

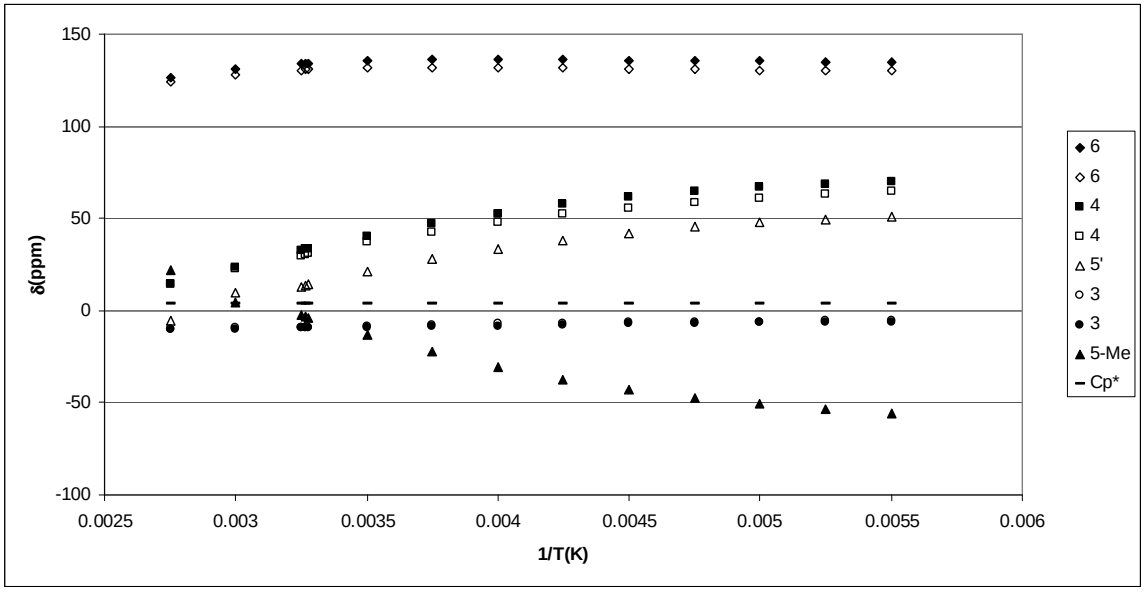

Figure 4.4.4: Variable Temperature ^{1}H NMR spectra represented as a δ vs. 1/T plot of Cp^*_2Yb(5-methyl-bipy) in toluene-d_8.

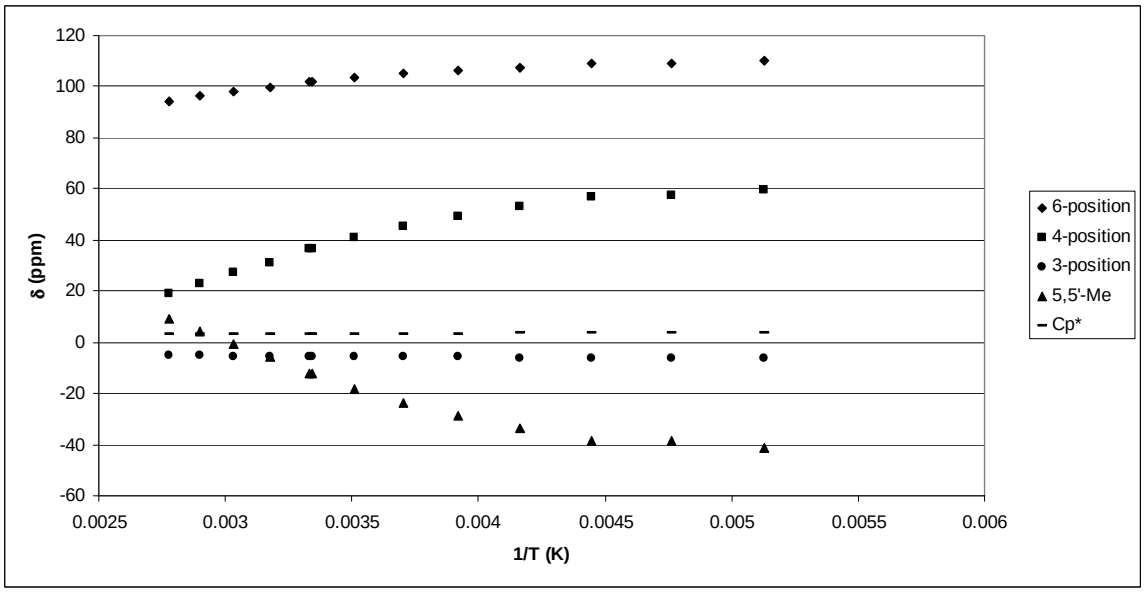

Figure 4.4.5: Variable Temperature ^{1}H NMR spectra represented as a δ vs. 1/T plot of Cp^*_2Yb(5,5'-dmb) in toluene-d_8.

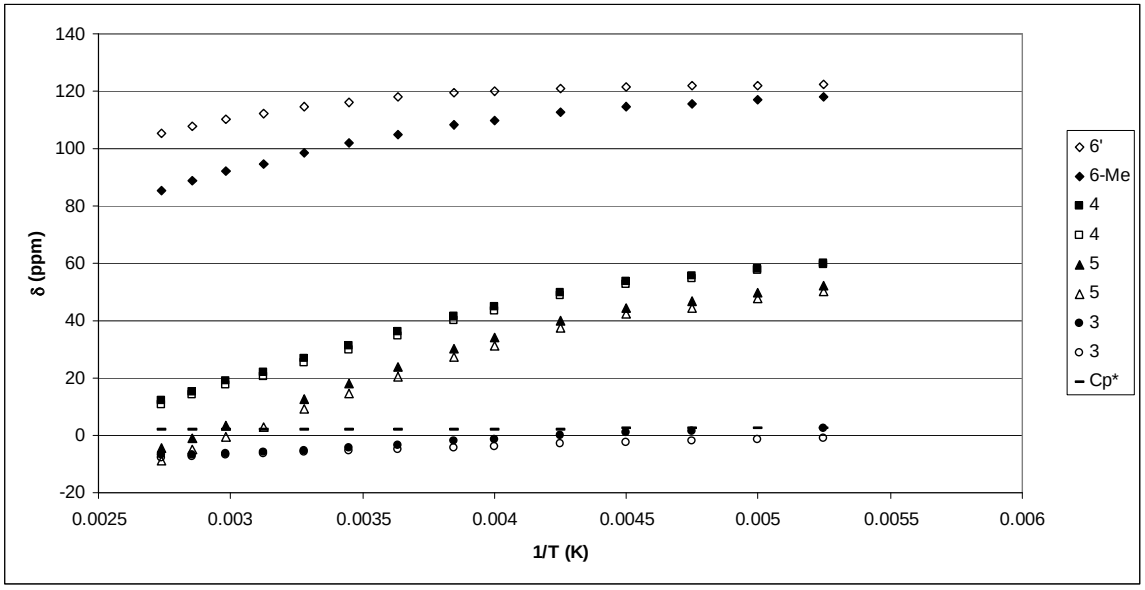

Figure 4.4.6: Variable Temperature ^{1}H NMR spectra represented as a δ vs. 1/T plot of Cp^*_2Yb(6-methyl-bipy) in toluene-d_8.

As discussed in the previous chapter, there are two mechanisms by which a paramagnetic center can shift NMR resonances of atoms in the molecule. The first is a Fermi contact shift, which arises from the delocalization of unpaired electrons from the paramagnetic center through covalent interactions with the ligand orbitals.[8] The second is a pseudocontact shift, which is due to direct dipolar coupling between the magnetic moment of the unpaired electrons on the paramagnetic center and the magnetic moment of the nucleus of interest. The magnitude of a pseudocontact shift has a $1/R^3$ dependence, where R is the distance between the paramagnetic center and the nucleus of interest.[9] The previous chapter shows that in a shift process which is predominantly contact in nature, replacement of a proton by a methyl group will change the sign of the shift, whereas in a predominantly pseudocontact shift replacement of a proton with a methyl group will not. In the case of both the monomethyl and dimethyl bipy substitutions in the 4 and 5

positions, the shift of the CH_3 group is of opposite sign and opposite slope to that of the H in the equivalent position in both Cp^*_2Yb(bipy) and Cp^*_2Yb(monomethyl-bipy). Thus, the contact shift dominates the dipolar shift in the 4 and 5 position. In the case of Cp^*_2Yb(6-methyl-bipy), the shift of the methyl group is similar in sign and slope to the shift of the 6'-H, indicating that the shift in the 4 and 5 positions is primarily contact in nature while the shift in the 6-position is dipolar in nature, as expected from the calculated electron density described in the previous chapter.

The room-temperature ^{1}H NMR spectra of Cp^*_2Yb(6-methyl-bipy) and Cp^*_2Yb(6,6'-dmb) are shown in Figures 4.2.7 and 4.2.8, respectively. Cp^*_2Yb(6,6'-dmb) is different from all the other substituted bipys studied, in that the peaks are only slightly shifted from their diamagnetic values.

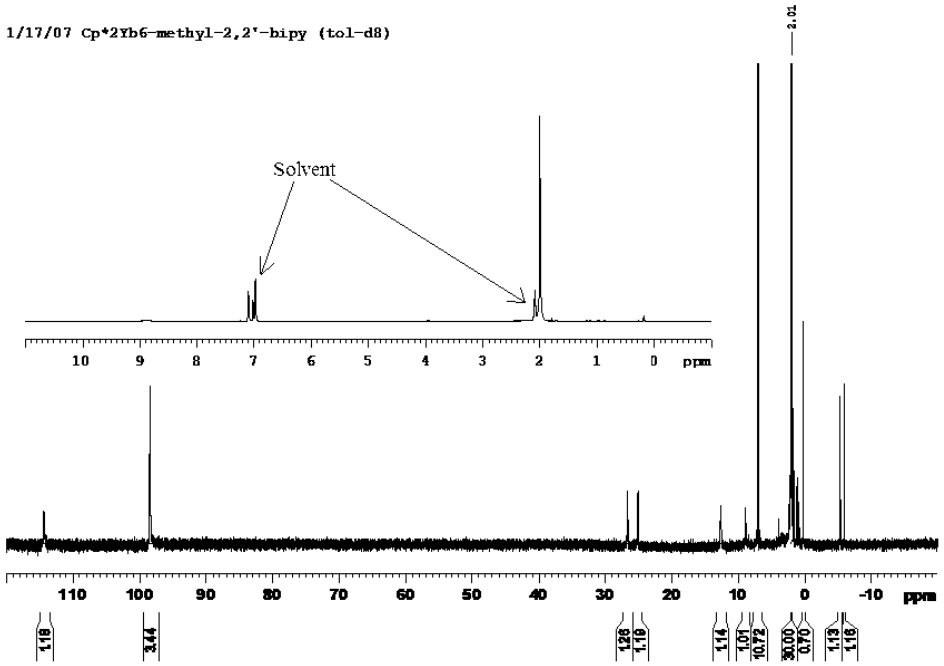

Figure 4.4.7: Room temperature ^{1}H NMR spectrum of Cp^*_2Yb(6-methyl-bipy) in toluene-d_8.

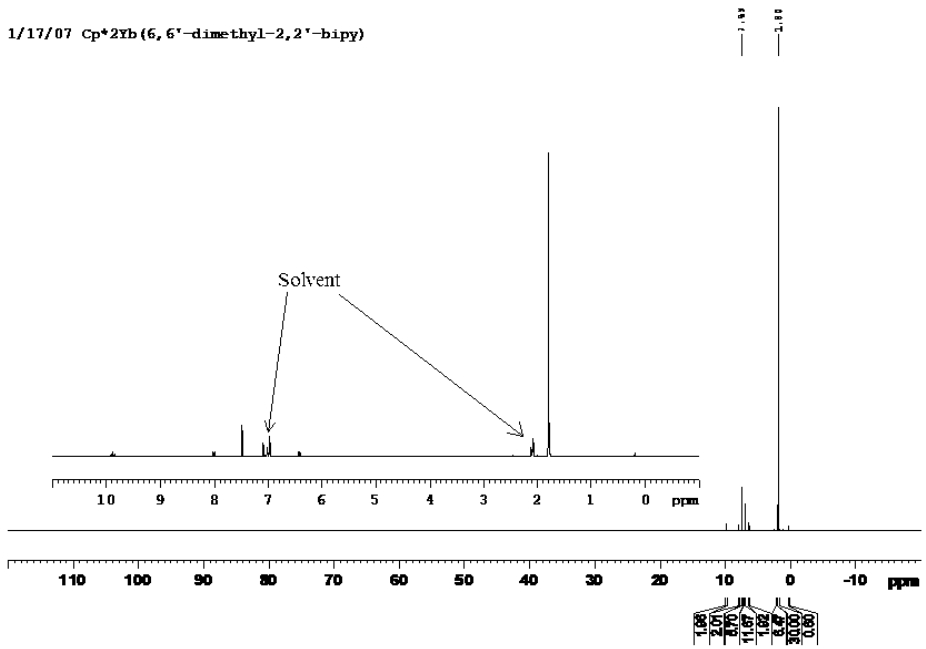

Figure 4.4.8: Room temperature ^{1}H NMR spectrum of Cp*$_2$Yb(6,6'-dimethyl-bipy) in toluene-d_8.

The variable temperature ^{1}H NMR spectra plotted as a δ vs. 1/T plot of Cp*$_2$Yb(6,6'-dmb) are shown in Figure 4.2.9. The plot of the variable temperature ^{1}H NMR spectra show that there is only a slight temperature dependence on the ^{1}H NMR resonances (the maximum shift is in the 6,6'-dimethyl position of 2.3 ppm) compared with the other substituted bipys which all show very strong temperature dependence (the average shift of the bipy resonances in the other Cp*$_2$Yb(x,x'-bipy) molecules over approximately the same temperature range is 35 ppm).

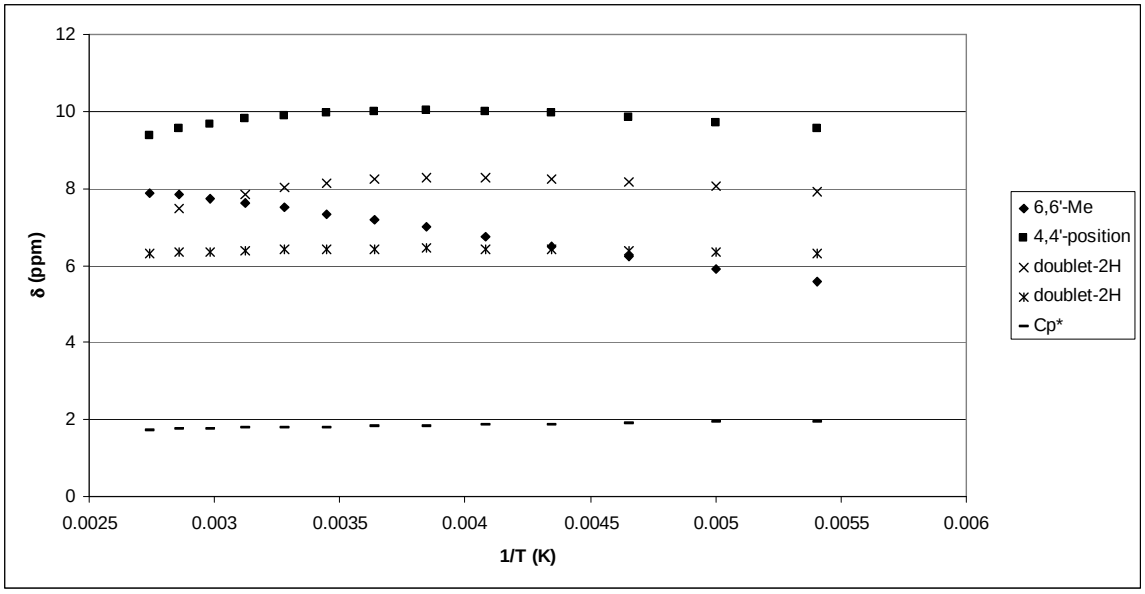

Figure 4.4.9: Variable Temperature ^{1}H NMR spectra represented as a δ vs. 1/T plot of Cp^*_2Yb(6,6'-dmb) in toluene-d_8.

Since the 6-position has relatively little unpaired electron density, it seems unlikely that electronic effects due to the donating ability of methyl groups are the cause of the sharp change. Based on the crystal structure we hypothesize, that while all Cp^*_2Yb(bipy) analogues are multi-configuration ground states, the elongation of the Yb-N distance as a result of the steric bulk of the methyl group in the 6-position destabilizes the configuration $Cp^*_2Yb(III)(bipy^{\cdot-})$, which has more ionic character and favors the more electronically neutral $Cp^*_2Yb(II)$(bipy) configuration. It still has both configurations in the ground state, but the weight of the $Cp^*_2Yb(II)$(bipy) configuration is greater than in the other bipy analogues. Evidence for this is that the even in the case of Cp^*_2Yb(6,6'-dmb), the 6,6'-dmb does not exchange with free 6,6'-dmb on the ^{1}H NMR time scale. Schultz et. al have shown that in the diamagnetic analogues of Cp^*_2Yb(bipy) the bipy is exchanging on the ^{1}H NMR time scale.[1]

4.5 Solid State Measurements: SQUID

Ytterbium has two stable oxidation states: +2 and +3. Ytterbium(II) has a filled f-shell and is diamagnetic. Ytterbium(III) is a paramagnetic $4f^{13}$ ion with a $^2F_{7/2}$ ground state. In a low-symmetry ligand field, the $^2F_{7/2}$ ground state is split into four Kramer doublets.[10] As a result, at temperatures from 2 to 30 K, a Yb(III) complex follows Curie law ($C = \chi T$) with a χT of 1.81 cm^3 K mol^{-1} and μ_{eff} ($\mu_{eff} = 2.828*\sqrt{(\chi T)}$) of 3.8 B.M. (B.M. = Bohr Magnetons). At temperatures above 30 K, thermal population of the third and fourth doublet levels becomes increasingly significant, and the contribution of these levels to the magnetic moment results in deviation from Curie behavior. By 90 K, both upper levels are easily accessible, while the next manifold of states, arising from the $^2F_{5/2}$ term, is 10,300 cm^{-1} higher in energy in the free ion and is not thermally accessible. Thus, from 90 – 300 K, the temperature dependence of the magnetic susceptibility follows the Curie-Weiss law ($C = \chi/(T-\theta)$) with a predicted χT of 2.53 cm^3 K mol^{-1} and μ_{eff} of 4.5 B.M..[11] The value of θ is typically between -20 and -50 K.

If there are two spin-carriers in a system, there are three possible outcomes. The first is that the two spin-carriers will not interact. In this case, the total magnetic moment, χ, and by extension χT, is simply the sum of the contributions of the two spin-carriers. Organic radicals have a term symbol of $^2S_{1/2}$, a χT of 0.37 cm^3 K mol^{-1} and a μ_{eff} of 1.73 B.M.. Thus, if a molecule has a non-interacting ytterbium(III) center and an organic radical, the predicted values of χT and μ_{eff} are 2.18 cm^3 K mol^{-1} and 4.18 B.M.,

respectively, between 2 – 30 K and 2.90 cm^3 K mol^{-1} and 4.8 B.M., respectively, between 90 – 300 K.

The second possibility is that the two spins align ferromagnetically, in which case the total magnetic moment will be larger that the sum of the contributions of the two spin-carriers. The term-symbol of a molecule with ferromagnetic coupling is $^{2S+2}L_{J+1/2}$. In the case of the coupling of trivalent ytterbium, which has a term symbol of $^2F_{7/2}$, and an organic radical, which has a term symbol $^2S_{1/2}$, the term symbol of a ferromagnetically coupled molecule is $^3F_4$. The associated value of χT and μ_{eff} are 3.91 cm^3 K mol^{-1} and 5.59 B.M., respectively. The final possibility is that the two spins align antiferromagnetically, and the total magnetic moment will be lower than the sum of the contributions of the two spin-carriers. The term-symbol of a molecule with antiferromagnetic coupling is $^{2S}L_{J-1/2}$. In the case of the coupling of trivalent ytterbium and an organic radical, the term symbol of an antiferromagnetically coupled molecule is $^1F_3$. The associated value of χT and μ_{eff} are 1.50 cm^3 K mol^{-1} and 3.46 B.M., respectively.[1]

In the case of $Cp^*_2Yb(bipy)$ and substituted bipy analogues, the situation is complicated by the additional factor that the total wave function of the molecule is a multi-configuration ground state due to a combination of the configuration $Cp^*_2Yb(II)(bipy)$ with a filled 4f shell, which is diamagnetic, and $Cp^*_2Yb(III)(bipy^{\cdot-})$, with 13 f-electrons, which is paramagnetic with two spin-carriers. The χT of $Cp^*_2Yb(bipy)$ is greater than zero, which would be the expected value for $Cp^*_2Yb(II)(bipy)$, but less than 1.50 cm^3 K mol^{-1}. The previously published χT vs. T curves of $Cp^*_2Yb(bipy)$ and $Cp^*_2Yb(4,4'\text{-dmb})$, along with the χT vs. T curves of the

complexes described in this thesis, Cp^*_2Yb(5,5'-dmb), Cp^*_2Yb(6,6'-dmb), Cp^*_2Yb(4-methyl-bipy), Cp^*_2Yb(5-methyl-bipy), and Cp^*_2Yb(6-methyl-bipy), at low and high magnetic fields (5 and 40 kG), are shown in Figures 4.5.1-4.5.7.

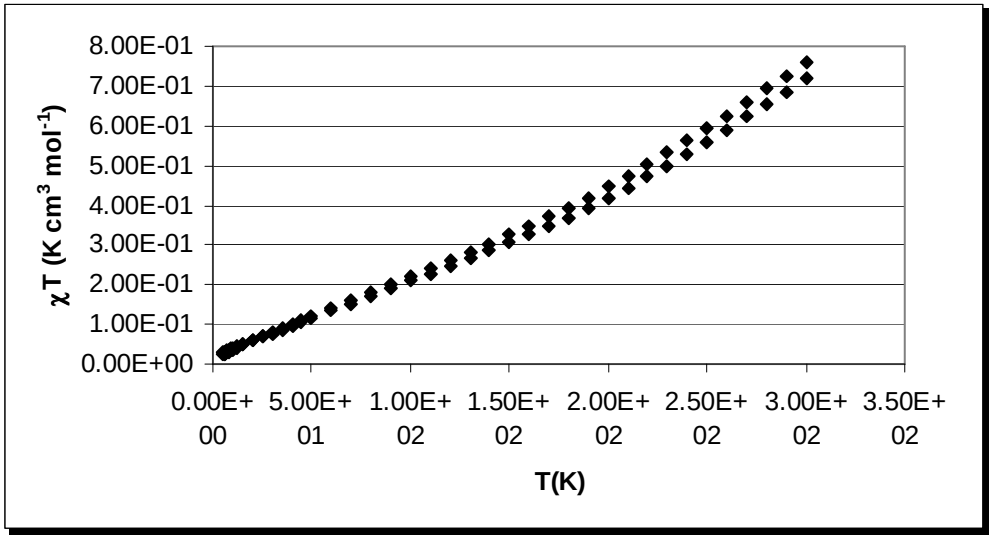

Figure 4.5.1: A plot of χT vs. T in Cp^*_2Yb(bipy)

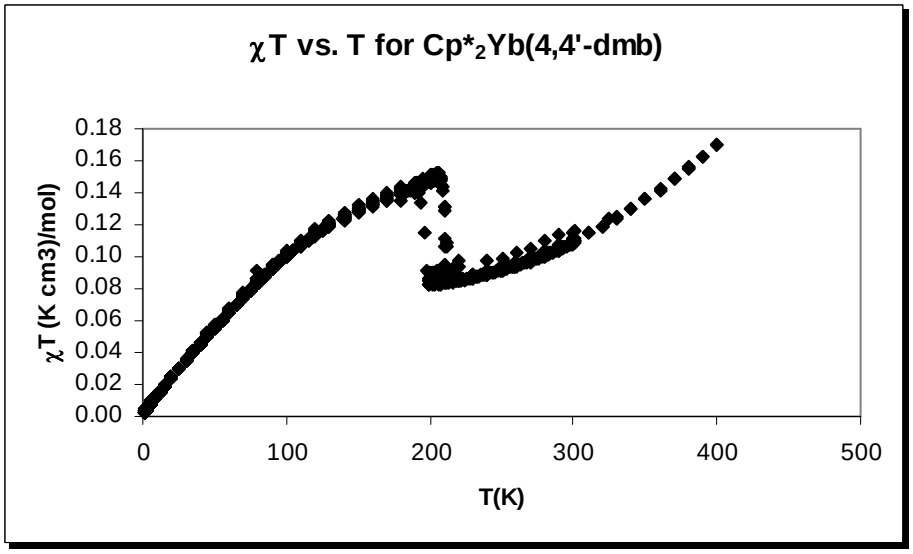

Figure 4.5.2: A plot of χT vs. T in Cp^*_2Yb(4,4'-dmb)

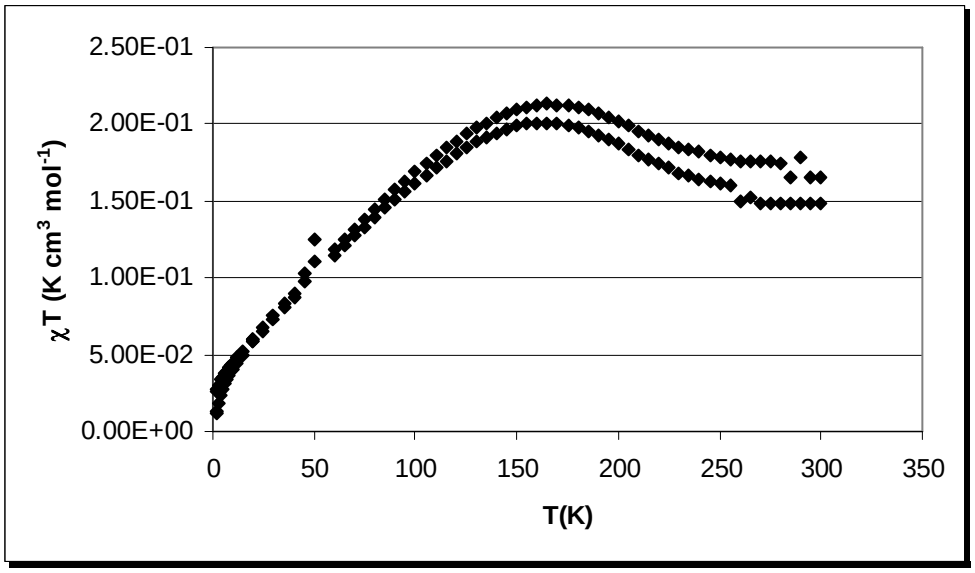

Figure 4.5.3: A plot of χT vs. T in Cp^*_2Yb(5,5'-dmb)

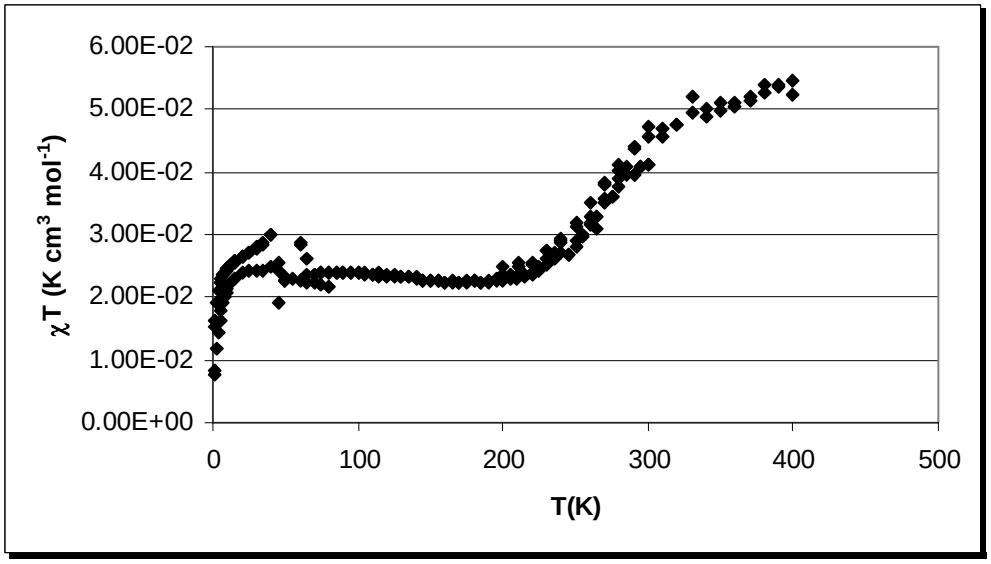

Figure 4.5.4: A plot of χT vs. T in Cp^*_2Yb(6,6'-dmb)

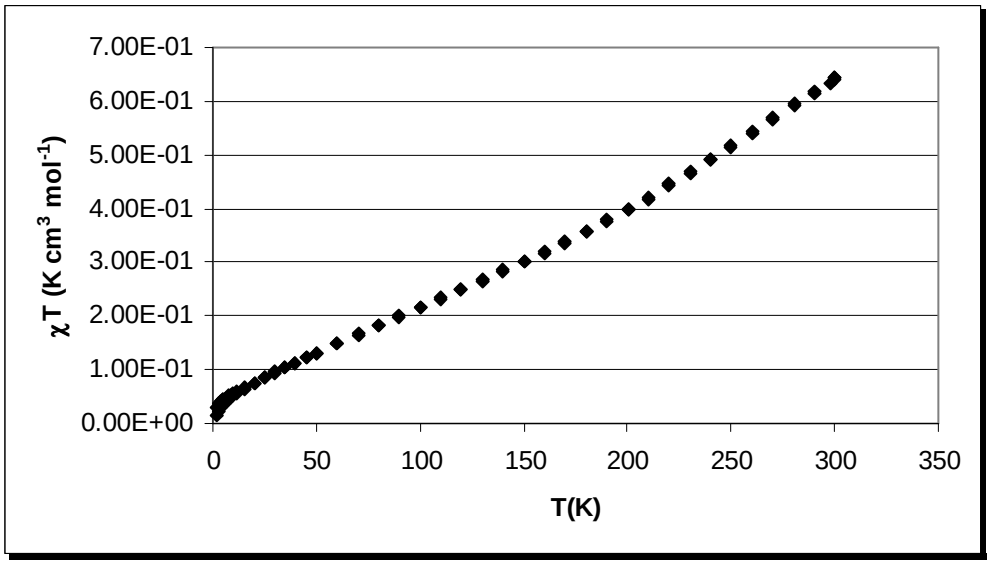

Figure 4.5.5: A plot of χT vs. T in Cp^*_2Yb(4-methyl-bipy)

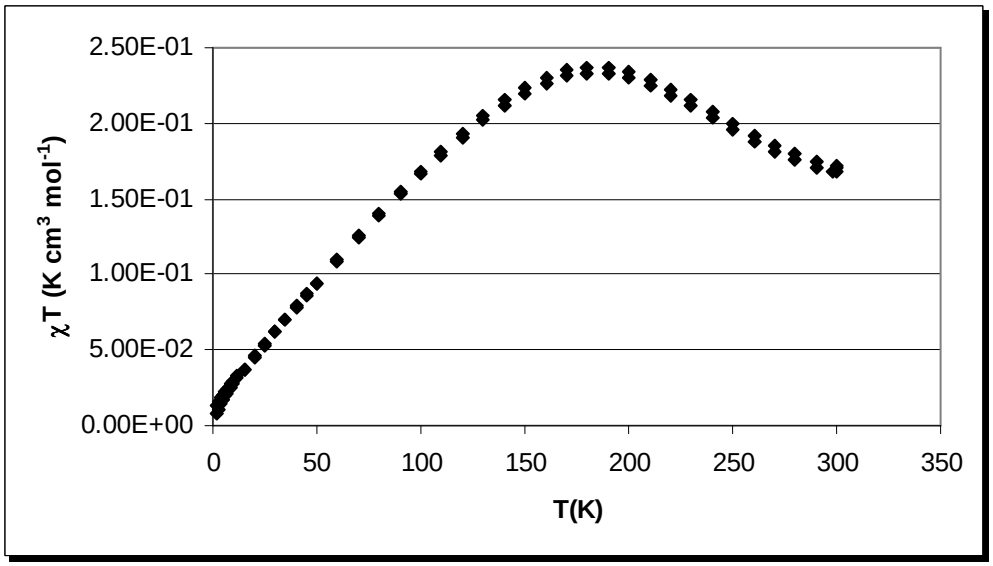

Figure 4.5.6: A plot of χT vs. T in Cp^*_2Yb(5-methyl-bipy)

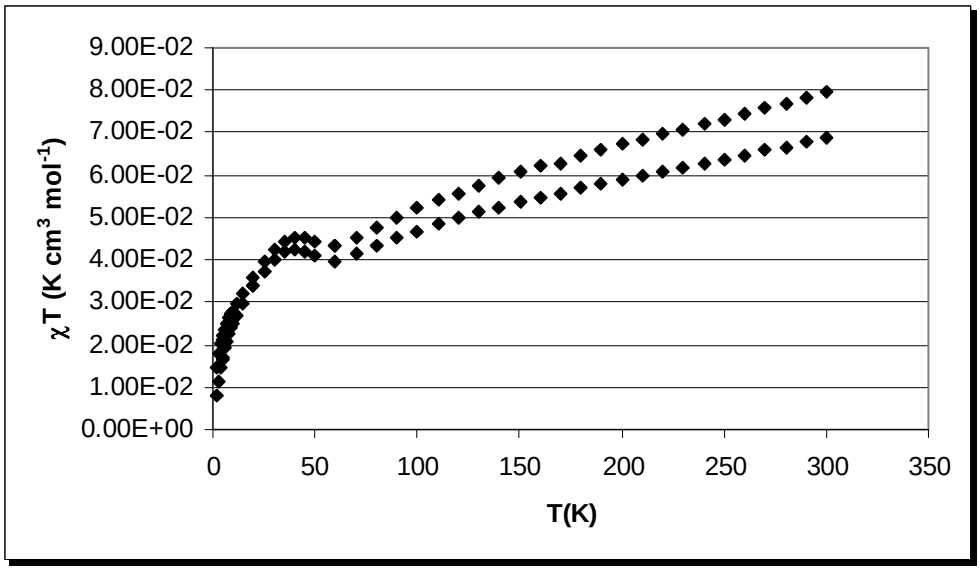

Figure 4.5.7: A plot of χT vs. T in Cp^*_2Yb(6-methyl-bipy)

The χT vs. T curve of Cp^*_2Yb(4-methyl-bipy) is similar to that of Cp^*_2Yb(bipy) (Figure 4.5.8) and the χT vs. T curve of Cp^*_2Yb(5-methyl-bipy) is similar to that of Cp^*_2Yb(5,5'-dmb) (Figure 4.5.9).

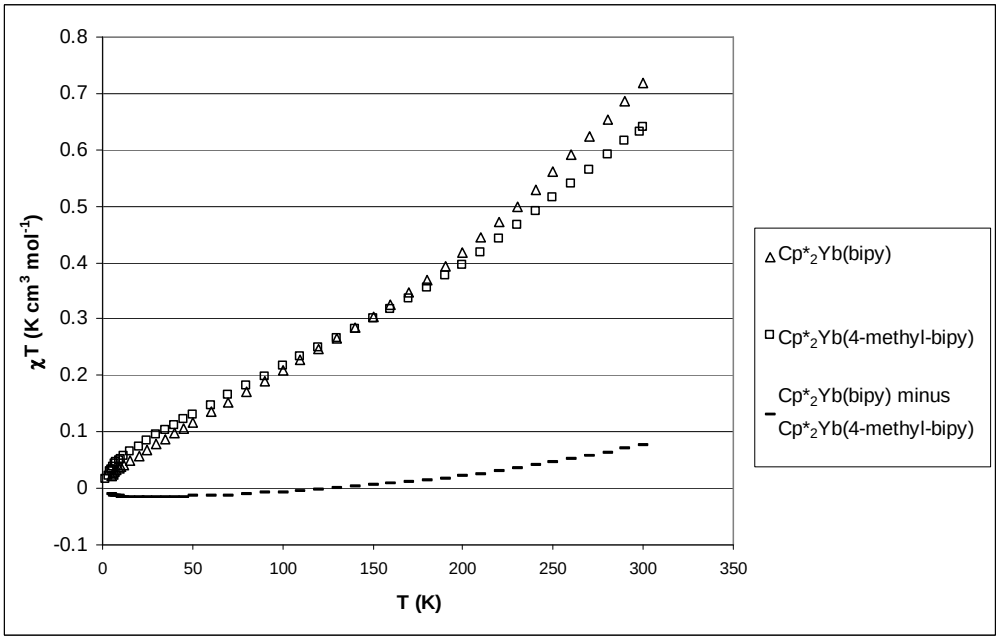

Figure 4.5.8: A plot of χT vs. T of Cp^*_2Yb(bipy), Cp^*_2Yb(4-methyl-bipy), and the difference between the two curves.

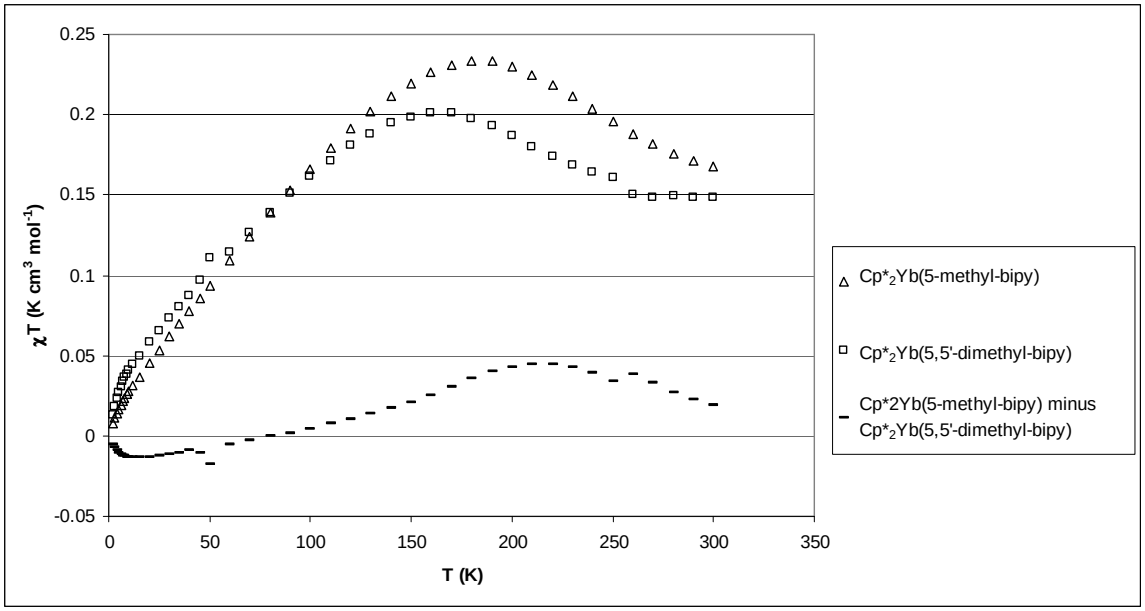

Figure 4.5.9: A plot of χT vs. T of Cp^*_2Yb(5-methyl-bipy), Cp^*_2Yb(5,5'-dmb), and the difference between the two curves.

As in Cp^*_2Yb(bipy), the magnetic moments of the methylated-bipys is higher than expected for Cp^*_2Yb(II)(bipy), where the bipy is neutral, but lower than expected for Cp^*_2Yb(III)(bipy$^{\cdot-}$), even with antiferromagnetic coupling. The implication is that the total wavefunction is a combination of the two oxidation states of Yb. The SQUID data corroborate the hypthesis deduced from the ^{1}H NMR spectra that Cp^*_2Yb(6,6'-dmb) is more diamagnetic than the other Cp^*_2Yb(bipy) analogues. As mentioned above, we think this is due to the steric bulk of the methyl groups causing an increase in the Yb-N distance, and favoring the more charge neutral Cp^*_2Yb(II)(bipy) over Cp^*_2Yb(III)(bipy$^{\cdot-}$).

The oxidation potential of Cp^*_2Sm is significantly higher than that of Cp^*_2Yb, so it is not surprising that Cp^*_2Sm(bipy) and Cp^*_2Sm(4,4'-dmb) the bipy and 4,4'-dmb carry a full unpaired electron and the samarium center is +3, as shown in the previous chapter.

4.6 Solid State Measurements: XANES (X-ray Absorption Near Edge Spectroscopy)

XANES data were collected at the Stanford Synchotron Radiation Laboratory, a national user facility operated by Stanford University on the behalf of the DOE/OBES, by Dr. Corwin Booth.

XANES spectroscopy allows for the measurement of the f-hole occupancy of ytterbium. The valence of a system is measured by comparing the position of a core x-ray absorption edge of the molecule of interest with that of model compounds. In the ytterbocene adduct, we compare the Yb L_{III} edge energy of $Cp^*_2Yb(bipy)$ and the substituted bipy analogues with that for $[Cp^*_2Yb(bipy)][I]$, which contains a true Yb(III) center, and $Cp^*_2Yb(OEt_2)$, which contains a true Yb(II) center. Yb(II) shows an absorption at about 8937 eV and Yb(III) shows an absorption at about 8943 eV. The XANES spectrum of $Cp^*_2Yb(bipy)$ has been previously published and is temperature independent.[4] The XANES spectra of $Cp^*_2Yb(5,5'\text{-dmb})$ and $Cp^*_2Yb(6\text{-methyl-bipy})$ are shown in Figures 4.6.1 and 4.6.2.

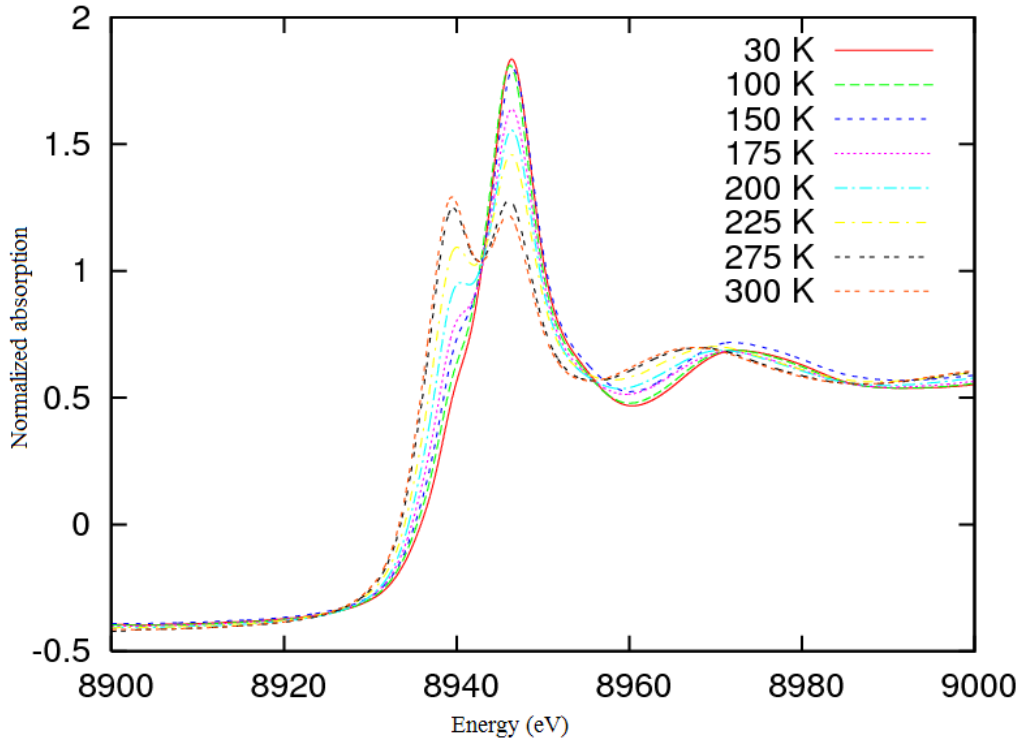

Figure 4.6.1: Yb L_{III} XANES for Cp*$_2$Yb(5,5'-dmb) as a function of temperature.

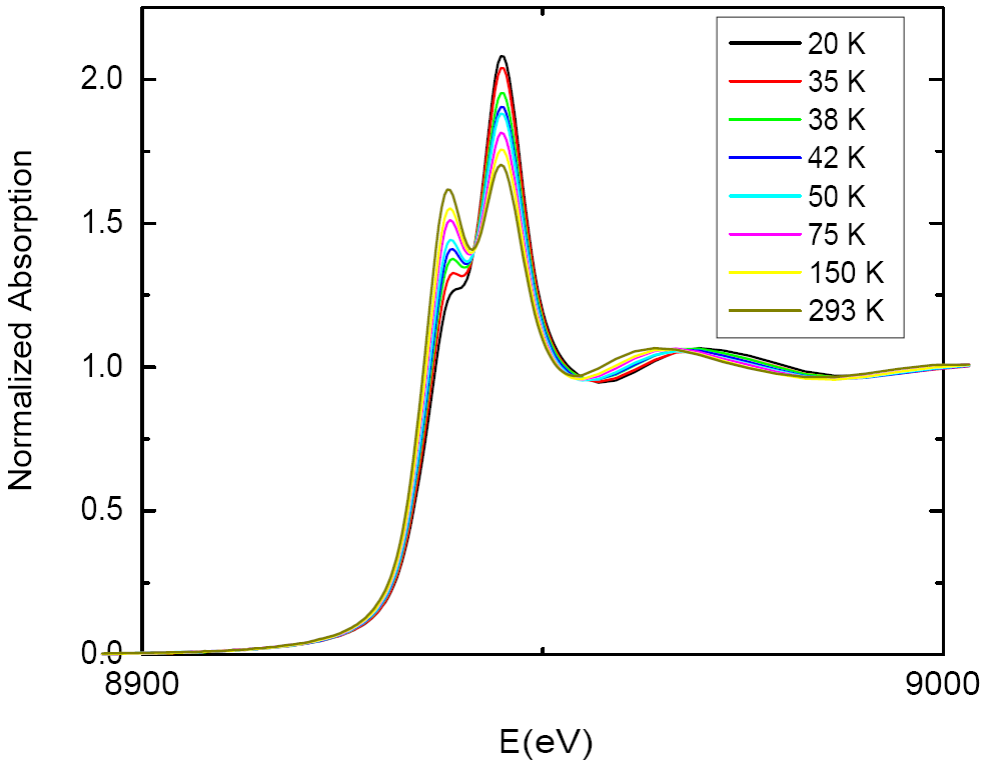

Figure 4.6.2: Yb L_{III} XANES for Cp*$_2$Yb(6-methyl-bipy) as a function of temperature.

The XANES spectrum of Cp^*_2Yb(bipy) is temperature independent, implying that the deviation of the magnetic susceptibility from Curie-Weiss law is due to a change in the coupling as a function of temperature. The magnetism of Cp^*_2Yb(5,5'-dmb) and Cp^*_2Yb(6-methyl-bipy) presumably still has temperature dependant coupling, but it is further complicated by temperature dependant oxidation state of the ytterbium center, as shown by the XANES spectra. The XANES spectra of both molecules indicate that the trivalent ytterbium contribution to the wave function of the molecule decreases as a function of temperature, although in the case of Cp^*_2Yb(5,5'-dmb) this change is more pronounced. The XANES spectra of Cp^*_2Yb(4-methyl-bipy), Cp^*_2Yb(5-methyl-bipy), and Cp^*_2Yb(6,6'-dmb) have not been obtained, but they will be examined in future studies. Hence, the electronic structure of these adducts and a general model for them is presently premature.

In conclusion, Cp^*_2Yb(bipy) analogues with methyl substituents have been synthesized. The variable-temperature ^1H NMR spectra of all the bipy analogues are similar to that of Cp^*_2Yb(bipy). The magnetism of Cp^*_2Yb(4-methyl-bipy) is similar to that of Cp^*_2Yb(bipy), but the magnetism of Cp^*_2Yb(5-methyl-bipy) and Cp^*_2Yb(5,5'-dimethyl-bipy) is more complicated with a maximum in the χT vs. T curve at about 170 K. The XANES data indicate that the f-weight of ytterbium in Cp^*_2Yb(5,5'-dmb) and Cp^*_2Yb(6-mmb) increase as the temperature is raised, and perhaps this is the cause of the maximum in the χT vs. T curve as a function of temperature. All the resonances of Cp^*_2Yb(6,6'-dmb) in the ^1H NMR spectrum are between 0 and 10 ppm, and the magnetic moment is low, indicating that the Cp^*_2Yb(II)(bipy) contribution to the wave function is larger than in the other bipy analogues. We hypothesize that this is due to the steric bulk

of the methyl groups which cause the Yb-N distance to lengthen, which disfavors the charge separation present in the $Cp^*_2Yb(III)(6,6'\text{-}dmb^{\cdot-})$ wave function.

References:

1. Schultz, M.; Boncella, J. M.; Berg, D. J.; Tilley, T. D.; Andersen, R. A. *Organometallics*, **2002**, *21*, 460.
2. Van Vleck, J.H.; Frank, A. *Phys. Rev.*, **1929**, *34*, 1494
3. Van Vleck, J.H.; Frank, A. *Phys. Rev.*, **1929**, *34*, 1625
4. Booth, C.H.; Walter, M.D.; Daniel, M.; Luken, W.W.; Andersen, R.A. *Phys. Rev. Lett.*, **2005**, *95*, 267202
5. Walter, M.D.; Berg, D.J.; Andersen, R.A. *Organometallics*, **2006**, *25*, 3228.
6. Chisholm, M.H.; Huffman, J.C.; Rothwell, I.P.; Bradley, P.G.; Kress, N.; Woodruff, W.H. *J. Am. Chem. Soc.*, **1981**, *103*, 4945
7. Fedushkin, I.L.; Petrovskaya, T.V.; Girgsdies, F.; Köhn, R.D.; Bochkarev, M.N.; Schumann, H. *Angew. Chem. Intl. Ed.* **1999**, *38*, 2262
8. Proctor, W.G.; Yu, F.C. *Phys. Rev.*, **1950**, *77*, 717
9. Bloembergen, N.; Dickinson, W.C. *Phys. Rev.*, **1950**, *79*, 179
10. Boudreaux, E.A.; Mulay, L.N. *Theory and Applications of Molecular Paramagnetism*; Wiley-Interscience: New York, 1976.
11. Gerloch, M.; Constable, E.C.; *Transition Metal Chemistry*; VCH: Weinheim, 1995.

Chapter 5: Synthesis of $[X_3Ln]_2\mu$-L where X = Cp and MeC_5H_4, Ln = Ce and Tb, and L = 1,4-benzoquinone and 4,4-bipyridine

5.1 Introduction

In lanthanide ions, the valence 4f orbitals do not penetrate radially the electron density of the 5s and 5p orbitals.[1] As a result the 4f electrons are relatively unaffected by the ion's external environment, and therefore the magnetic moment of lanthanide ions is nearly independent of its ligands. Van Vleck and Frank derived an equation that predicts the value of the ground state effective magnetic moment of a free metal ion with quantum number *J*,

$$\mu_{eff} = g[J(J+1)]^{1/2} \text{ (B.M.)},^{2,3} \quad (1)$$

where

$$g = 1 + [S(S+1) - L(L+1) + J(J+1)]/[2J(J+1)].$$

Cerium has two commonly accessed oxidation states: Ce(III) and Ce(IV). Trivalent cerium has a $4f^1$ electronic configuration and a term symbol $^2F_{5/2}$. The calculated magnetic moment of 2.54 B.M. (B.M. = Bohr magnetons) is in good agreement with experimental values for a series of Ce(III) salts.[4] Tetravelent cerium has a $4f^0$ electronic configuration and a term symbol $^1S_0$ and is diamagnetic. Walter has made $[Ce(N(SiMe_3)_2)_3]_2\mu$-1,4-benzoquinone, and the magnetic moment is higher than expected for diamagnetic Ce(IV) but lower than expected for Ce(III).[5] The μ_{eff} vs. T plot is shown in Figure 5.1.

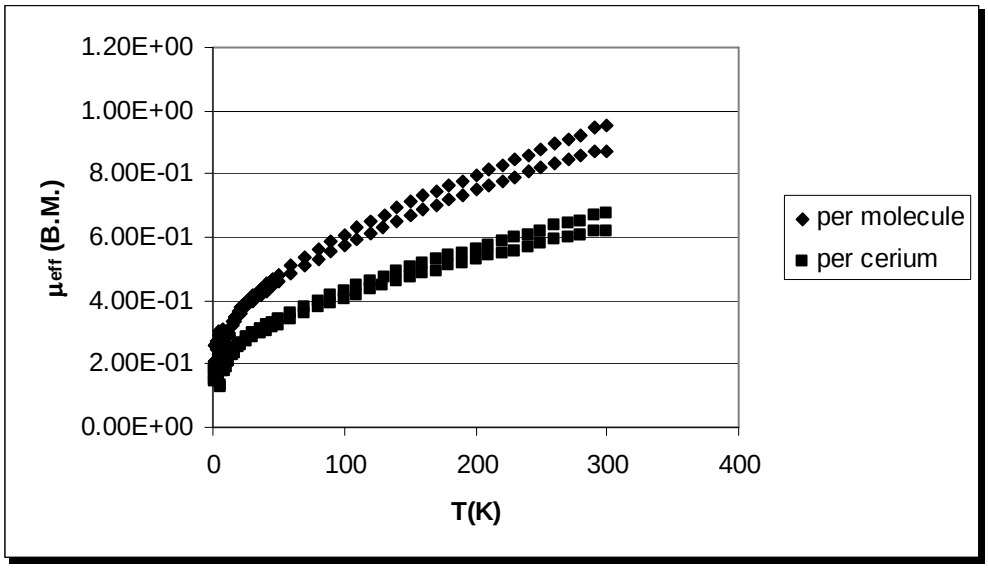

Figure 5.1: μ_{eff} vs. T plot for $[Ce(N(SiMe_3)_2)_3]_2\mu$-1,4-benzoquinone.

It is interesting to expand the series of molecules by changing the ligand on the lanthanide, the bridging ligand, and the lanthanide metal itself. In this chapter the synthesis of a series of molecules of the general formula $[X_3Ln]_2(\mu\text{-}L)$, where X = Cp and MeC_5H_4, Ln = Ce and Tb, and L = 1,4-benzoquinone and 4,4'-bipyridine is described and the magnetic properties are discussed.

Results and Discussion

5.2 Synthesis and properties of $Cp_3CeO{=}(NC_5H_5)$, $(MeC_5H_4)_3CeO{=}(NC_5H_5)$, and $(MeC_5H_4)_3TbO{=}(NC_5H_5)$

Addition of pyridine-N-oxide to (1,2,4-tri-tert-butyl-cyclopentadienyl)$_2$U(2,2'-bipyridine) gives (1,2,4-tri-tert-butyl-cyclopentadienyl)$_2$U=O(pyridine).[6] A potential synthesis of $(Cp_3Ce)_2(\mu\text{-}O)$ is then the addition of pyridine-N-oxide to Cp_3Ce. Addition of pyridine-N-oxide gives the red adduct Cp_3Ce(pyridine-N-oxide). Cp_3Ce(pyridine-N-oxide) is not soluble in hydrocarbon solvents, but is soluble in CH_2Cl_2, from which crystals are obtained. The variable-temperature ^{1}H NMR spectra plotted as a δ vs. 1/T plot are shown in Figure 5.2.1. Interestingly, the resonances do not follow Curie-Weiss behavior; the shifts plotted against 1/T are not linear. Excess pyridine-N-oxide exchanges with bound pyridine-N-oxide in solution, so the deviation from Curie-Weiss behavior may be due to intermolecular interactions.

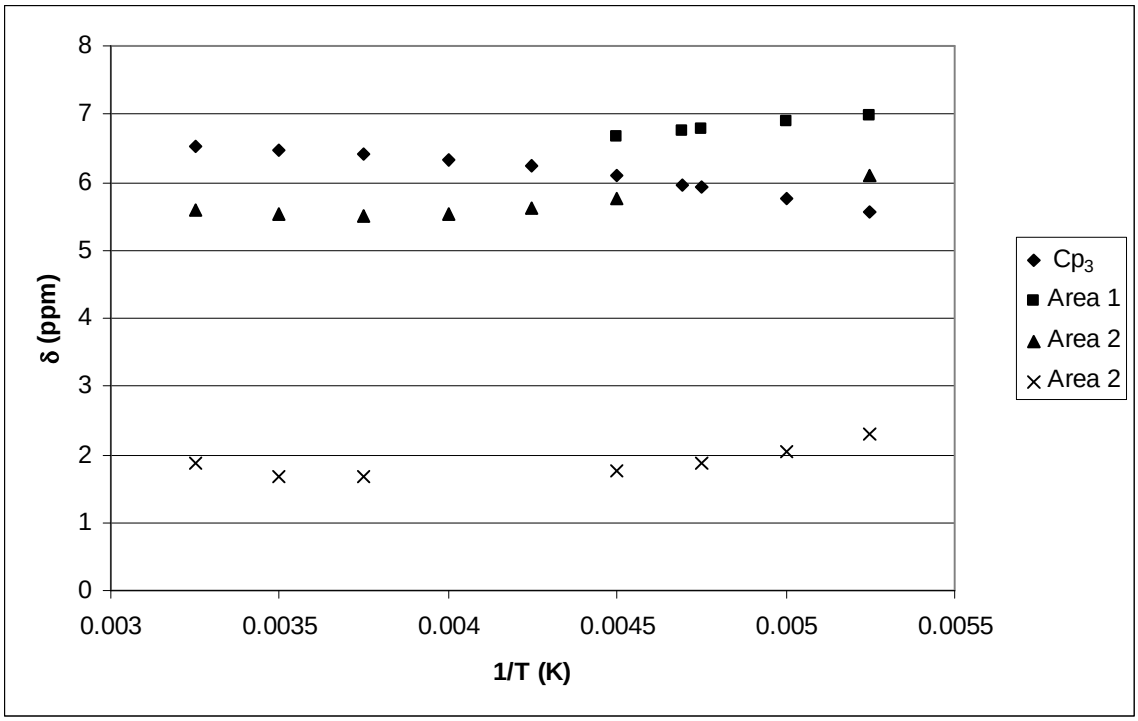

Figure 5.2.1: Variable Temperature ^{1}H NMR spectra represented as a δ vs. 1/T plot of Cp_3Ce(pyridine-N-oxide) in CD_2Cl_2.

The crystal structure of Cp_3Ce(pyridine-N-oxide) is shown Figure 5.2.2.

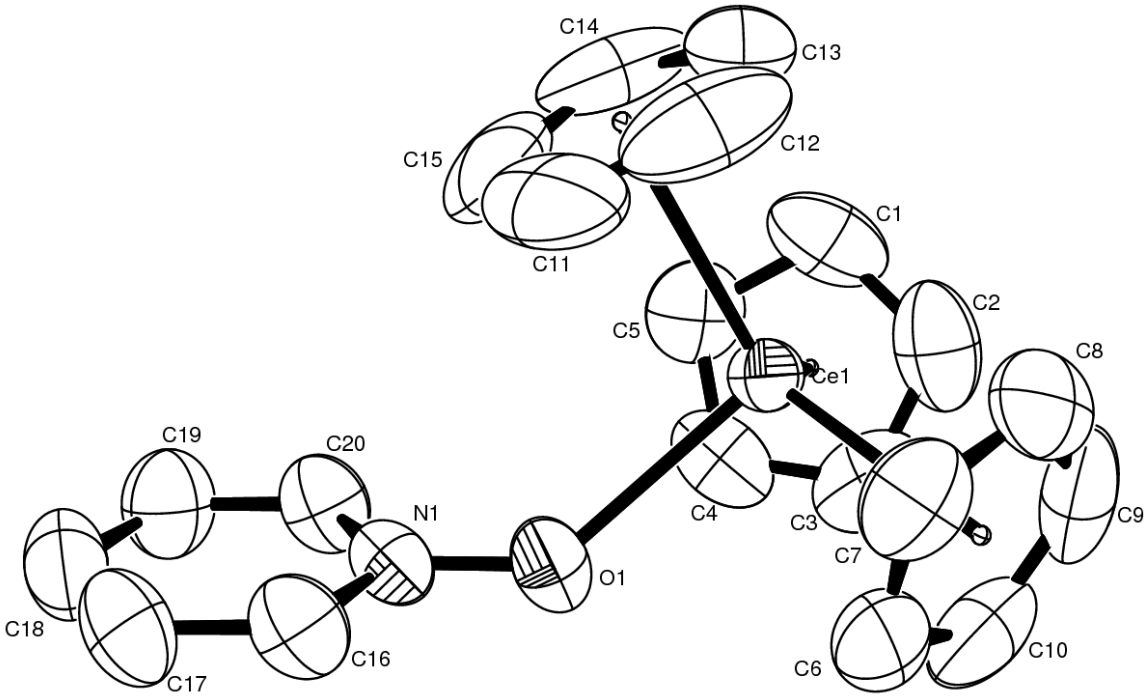

Figure 5.2.2: ORTEP diagram of Cp_3Ce(pyridine-N-oxide) (50% probability ellipsoids). All non-hydrogen atoms are refined anisotropically. Hydrogen atoms are placed and not refined and are not shown. Selected Bond Distances and Angles are given in Tables 5.2.1 and 5.2.2, respectively.

Table 5.2.1: Selected bond distances (Å) in Cp_3Ce(pyridine-N-oxide)

atom	Atom	distance		Atom	atom	distance
Ce(1)	O(1)	2.393(2)		Ce(1)	C(1)	2.816(3)
Ce(1)	C(2)	2.840(3)		Ce(1)	C(3)	2.849(3)
Ce(1)	C(4)	2.833(3)		Ce(1)	C(5)	2.811(3)
Ce(1)	C(6)	2.823(3)		Ce(1)	C(7)	2.807(3)
Ce(1)	C(8)	2.795(3)		Ce(1)	C(9)	2.800(3)
Ce(1)	C(10)	2.807(3)		Ce(1)	C(11)	2.812(4)
Ce(1)	C(12)	2.803(3)		Ce(1)	C(13)	2.798(3)
Ce(1)	C(14)	2.839(3)		Ce(1)	C(15)	2.849(4)
O(1)	N(1)	1.329(2)		N(1)	C(16)	1.345(3)
N(1)	C(20)	1.329(3)		C(1)	C(2)	1.389(4)
C(1)	C(5)	1.388(4)		C(2)	C(3)	1.377(4)
C(3)	C(4)	1.379(4)		C(4)	C(5)	1.374(4)
C(6)	C(7)	1.349(4)		C(6)	C(10)	1.370(4)
C(7)	C(8)	1.383(4)		C(8)	C(9)	1.402(4)
C(9)	C(10)	1.377(4)		C(11)	C(12)	1.326(6)
C(11)	C(15)	1.337(7)		C(12)	C(13)	1.338(5)
C(13)	C(14)	1.355(5)		C(14)	C(15)	1.385(7)
C(16)	C(17)	1.375(4)		C(17)	C(18)	1.353(4)
C(18)	C(19)	1.370(4)		C(19)	C(20)	1.359(4)
Ce(1)	C(101)	2.58		Ce(1)	C(102)	2.55
Ce(1)	C(103)	2.58				

Table 5.2.2: Selected bond angles in Cp_3Ce(pyridine-N-oxide)

atom	Atom	atom	angle		atom	atom	atom	angle
O(1)	Ce(1)	C(101)	101.2		O(1)	Ce(1)	C(102)	97.9
O(1)	Ce(1)	C(103)	99.1		C(101)	Ce(1)	C(102)	117.3
C(101)	Ce(1)	C(103)	117.2		C(102)	Ce(1)	C(103)	117.5
Ce(1)	O(1)	N(1)	137.9(1)					

The crystal structure of Cp_3Ce(pyridine-N-oxide) shows cerium bound in an almost tetrahedral fashion assuming the centroids of the three cyclopentadiene rings occupy a coordination site along with the oxygen atom. The cyclopentadiene rings, which have some steric bulk distort this tetrahedral geometry to keep away from the other cyclopentadiene rings and at the expense of decreasing the centroid-Ce-oxygen angles.

$(MeC_5H_4)_3Ce$(pyridine-N-oxide) is synthesized in a manner analogous to that used to make Cp_3Ce(pyridine-N-oxide). The variable temperature ^1H NMR spectra plotted as a δ vs. 1/T plot again show deviation from Curie-Weiss behavior (Figure 5.2.3). Again, pyridine-N-oxide exchanges in the presence of excess pyridine-N-oxide. The methyl resonance of the cyclopentadiene ring has the opposite sign and slope of the ring proton resonances and, as described in previous chapters, this implies that the shift is primarily contact in nature.

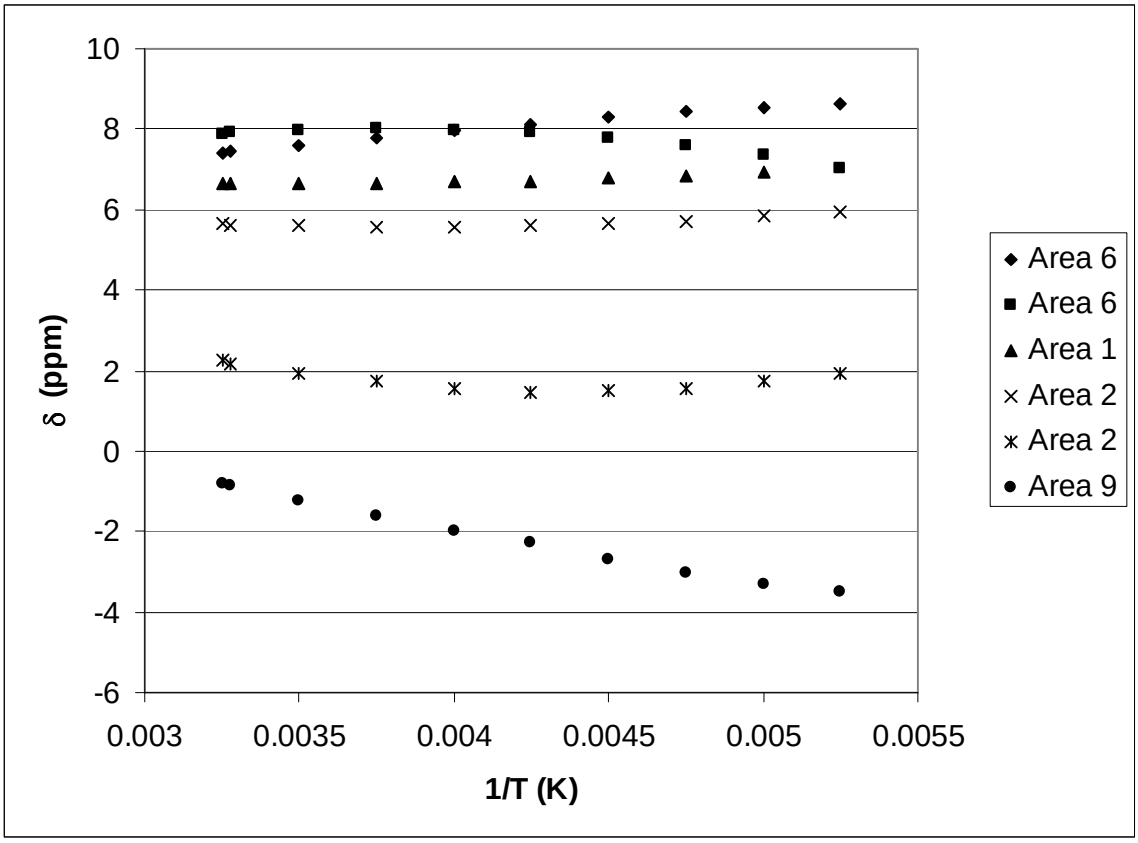

Figure 5.2.3: Variable Temperature ^{1}H NMR spectra represented as a δ vs. 1/T plot of $(MeC_5H_4)_3Ce$(pyridine-N-oxide) in CD_2Cl_2.

Given that both Cp_3Ce(pyridine-N-oxide) and $(MeC_5H_4)_3Ce$(pyridine-N-oxide) are isolable, it should be possible, in principal, to synthesize a molecule with mixed Cp rings, i.e. $Cp_x(MeC_5H_4)_{3-x}Ce$(pyridine-N-oxide). However, mixing a small amount of Cp_3Ce(THF) with $(MeC_5H_4)_3Ce$(THF) in an NMR tube gives new resonances in the ^{1}H NMR spectrum that may be assigned to $Cp_2(MeC_5H_4)Ce$(THF) and $Cp(MeC_5H_4)_2Ce$(THF) based on their relative integrals and their similarity to the ^{1}H NMR shifts to those of Cp_3Ce(THF) and $(MeC_5H_4)_3Ce$(THF). Addition of more Cp_3Ce(THF) increases the amount of $Cp_2(MeC_5H_4)Ce$(THF) relative to $Cp(MeC_5H_4)_2Ce$(THF). In this fashion, the ^{1}H NMR resonances of all molecules of the

type $Cp_x(MeC_5H_4)_{3-x}Ce(THF)$ are assigned. The ^1H NMR resonances of these compounds in C_6D_6 are in Table 5.2.3. The fact that rings exchange freely in solution means that it is not possible to isolate pure mixed-ring compounds of the type $Cp_x(MeC_5H_4)_{3-x}Ce$ for a given x.

Table 5.2.3: ^1H NMR resonances of the Cp and MeC_5H_4 rings in molecules of the type $Cp_x(MeC_5H_4)_{3-x}Ce(THF)$.

	Area 3	Area 2	Area 2	Cp
$Cp_3Ce(THF)$	NA	NA	NA	7.65
$Cp_2(MeC_5H_4)Ce(THF)$	-1.06	8.97	11.74	7.15
$Cp(MeC_5H_4)_2Ce(THF)$	-1.22	8.80	10.95	6.68
$(MeC_5H_4)_3Ce(THF)$	-1.53	8.53	10.36	NA

Terbium also has an accessible +4 oxidation state, and the synthesis of the pyridine-N-oxide adduct with $(MeC_5H_4)Tb$ was attempted. $Tb(MeC_5H_4)_3(THF)$ can be synthesized in a manner similar to that used to synthesize $Ce(MeC_5H_4)_3(THF)$. A solution of $NaMeC_5H_4$ in thf is added to a suspension of $TbCl_3$ in thf. The thf is removed under vacuum. However, unlike the cerium analogue, this reaction does not go to completion, and therefore, the $Tb(MeC_5H_4)_3(THF)$ is separated from $(MeC_5H_4)_2TbCl$ by extraction and crystallization from toluene. The presence of $(MeC_5H_4)_2TbCl$ is ascertained by dissolving/decomposing the compound in distilled water, filtering and adding $AgNO_3$, and is also confirmed by Electron Impact (EI) mass spectroscopy where a molecular ion with m/z of 704 and 706 are observed ($[(MeCp)_2TbCl]_2$). Tetrahydrofuran is removed from $Tb(MeC_5H_4)_3(THF)$ by sublimation under dynamic vacuum. Crystals of $Tb(MeC_5H_4)_3$ are grown by heating a sealed ampule with $Tb(MeC_5H_4)_3$ at 120 °C for a week. The unit cell is determined to have dimensions a = 8.2039(4), b = 14.1555(8), c =

26.3360(14), $\alpha = 90$, $\beta = 94.483(1)$, $\gamma = 90$. This is similar to the unit cell of $Yb(MeC_5H_4)_3$ which has a = 8.075(2), b = 13.935(3), c = 26.390(5), $\alpha = 90$, $\beta = 94.55(2)$, $\gamma = 90$.[7] $Yb(MeC_5H_4)_3$ is a monomer in the solid state. This is in contrast to the larger lanthanides, $Ln(MeC_5H_4)_3$ (Ln = La[8], Ce[9], Pr[10], Nd[11]), which have unit cells of a = 9.478 +/- 0.2, b = 12.498 +/- 0.009, c = 26.462 +/- 0.46, $\alpha = \beta = 90$, $\gamma = 98.50$ +/- 1.17, which are tetramers in the solid state. The effective magnetic moment also shows no intermolecular coupling (Figure 5.2.4).

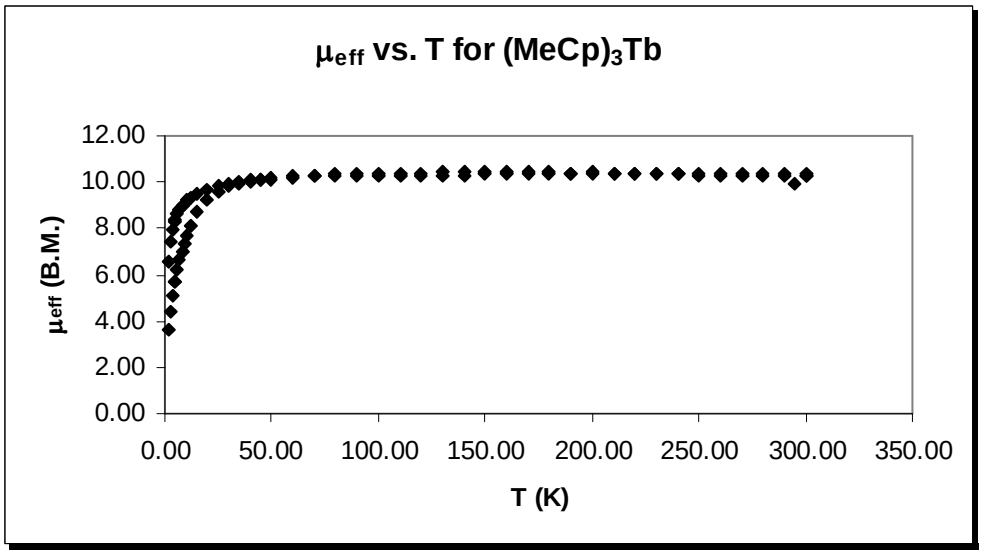

Figure 5.2.4: μ_{eff} vs. T plot of $(MeC_5H_4)_3Tb$

The variable-temperature ^1H NMR spectra plotted as a δ vs. 1/T plot of $Tb(MeC_5H_4)_3$ is shown in Figure 5.2.5. The protons follow Curie-Weiss behavior and show very large shifts, as expected for terbium.[12] The two sets of resonances attributable to the ring protons are of opposite sign and slope of the methyl resonance, implying that the shift is primarily contact in nature.

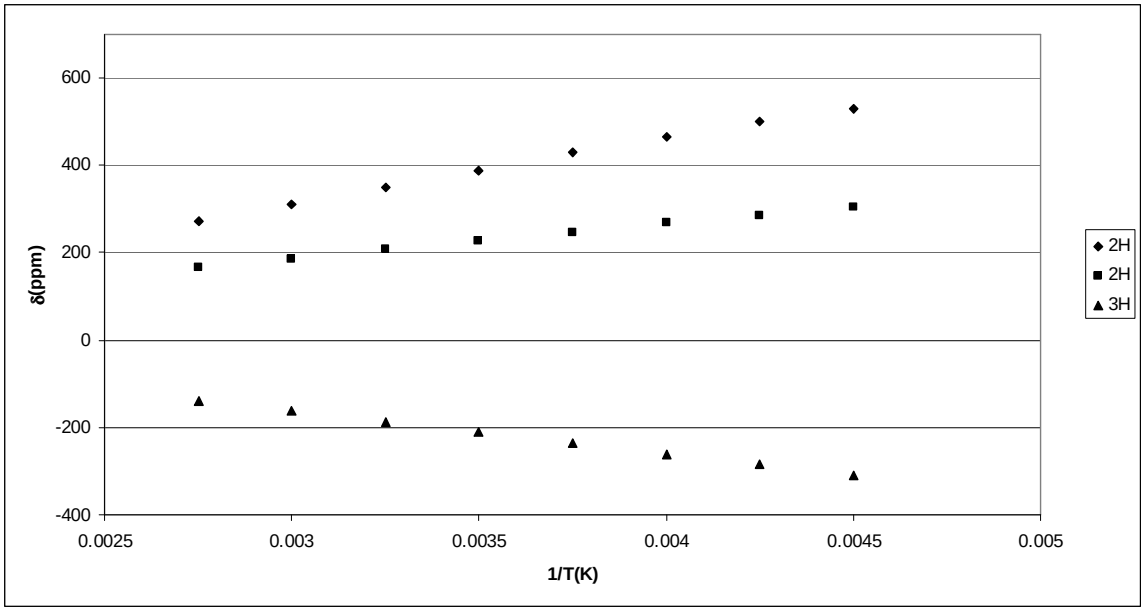

Figure 5.2.5: Variable Temperature ^{1}H NMR spectra represented as a δ vs. 1/T plot of $(MeC_5H_4)_3Tb$ in toluene-d_8.

Addition of pyridine-N-oxide to $(MeC_5H_4)_3Tb$ gives the pyridine-N-oxide adduct. The ^{1}H NMR spectra represented as a δ vs. 1/T plot are shown in Figure 5.2.6. Again the methyl resonance has the opposite sign and slope of the ring proton resonances, implying that the shift is contact in nature. All the resonances follow Curie-Weiss behavior, as opposed to the resonances in the cerium case which are not linear as a function of 1/T. This means either that the exchange is rapid on the ^{1}H NMR time scale so that averaged resonances are observed over the temperature range studied, or that the pyridine-N-oxide is not undergoing exchange over the temperature range.

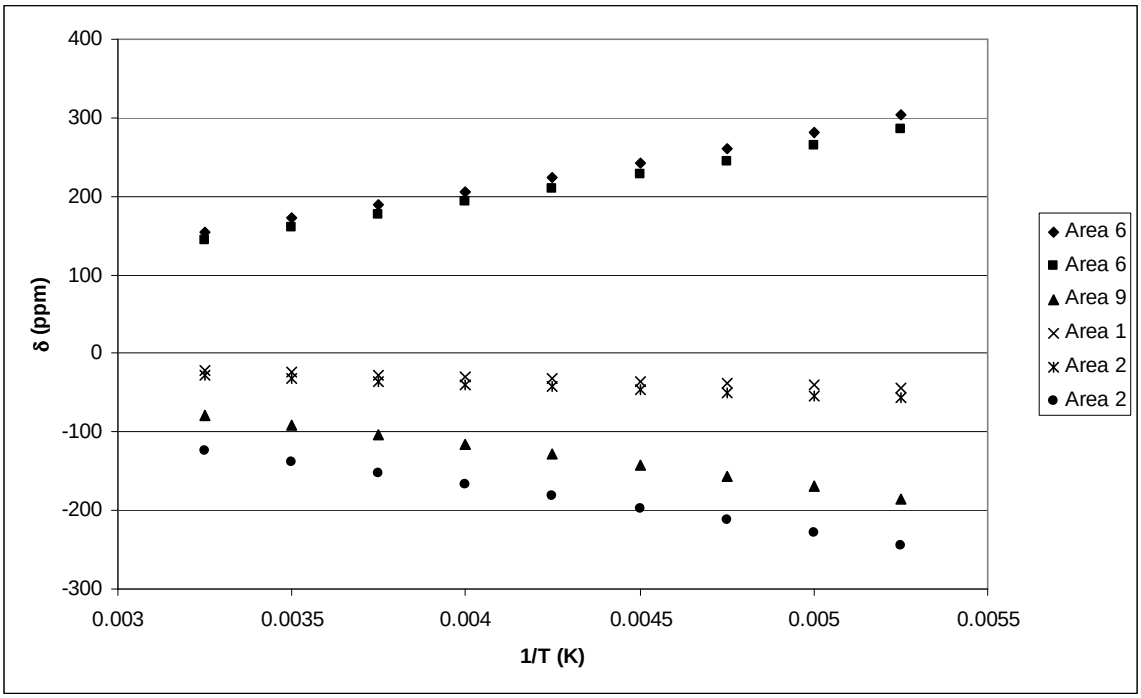

Figure 5.2.6: Variable Temperature ^{1}H NMR spectra represented as a δ vs. 1/T plot of $(MeC_5H_4)_3Tb$(pyridine-N-oxide) in CD_2Cl_2.

5.3 Synthesis and properties of $[(MeC_5H_4)_3Ln]$(4,4'-bipyridine) (Ln = Ce, Tb)

Addition of one equivalent of 4,4'-bipyridine to two equivalents of $(MeC_5H_4)_3Ce(THF)$ gives a dark green compound that can be crystallized from thf. The same reaction with $Cp_3Ce(THF)$ gives an insoluble purple powder, which in the presence of CH_2Cl_2 or thf reverts to $Cp_3Ce(THF)$. The fact that in CH_2Cl_2 the molecule reverts to $Cp_3Ce(THF)$ implies that the purple powder still has tetrahydrofuran bound. The variable-temperature ^{1}H NMR spectra plotted as a δ vs. 1/T plot (Figure 5.3.2) shows that C2, C6, C2' and C6' are equivalent and C3, C5, C3', and C5' are equivalent in the 4,4'-bipyridine (Figure 5.3.1); the molecule has averaged C_{2v} symmetry in solution.

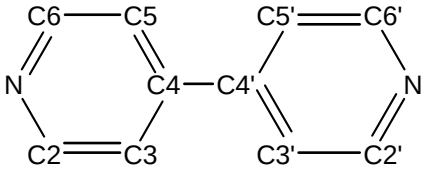

Figure 5.3.1: Numbering scheme of 4,4'-bipyridine

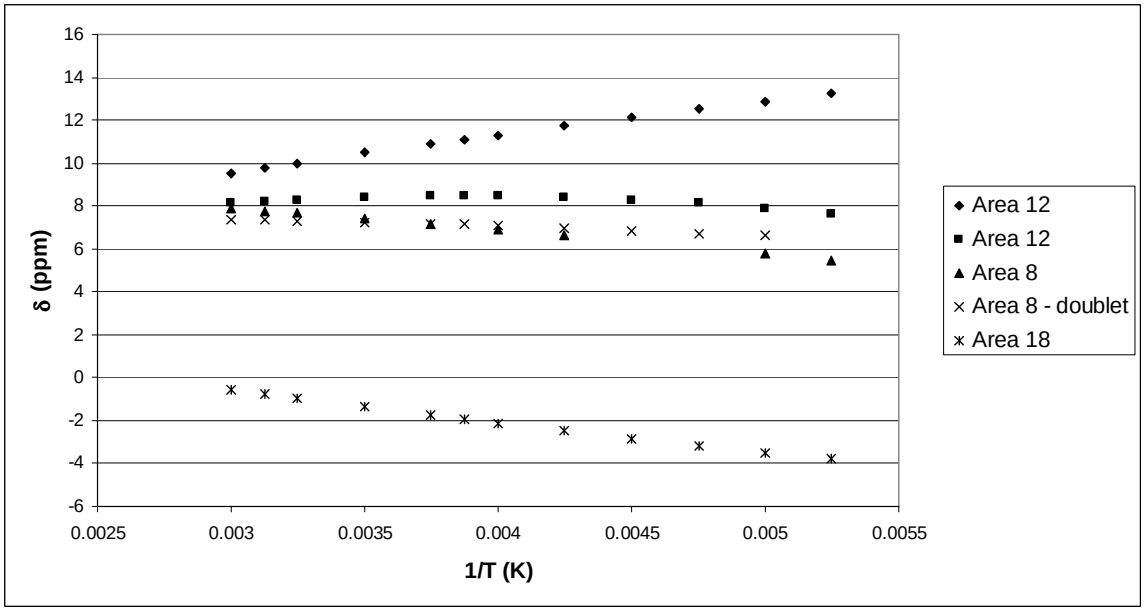

Figure 5.3.2: Variable Temperature ^{1}H NMR spectra represented as a δ vs. 1/T plot of $[(MeC_5H_4)_3Ce]_2$(4,4'-bipyridine) in thf-d_8.

The solid state crystal structure shows that the two pyridine rings are equivalent in the solid state as well (Figure 5.3.3). The structure has a crystallographic inversion center between C(21) and C(21_2). A comparison between the bond distances and angles of the 4,4'-bipyridine in $[(MeC_5H_4)_3Ce]$(4,4'-bipyridine) and free 4,4'-bipyridine will be given in the next section.

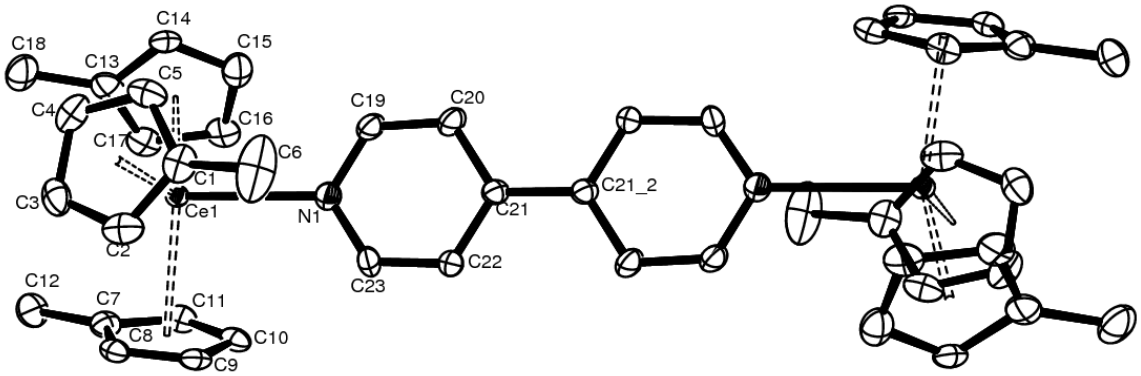

Figure 5.3.3: ORTEP diagram of $[(MeC_5H_4)_3Ce]_2$(4,4'-bipyridine) (50% probability ellipsoids). All non-hydrogen atoms are refined anisotropically. Hydrogen atoms are placed and not refined and are not shown. Selected Bond Distances and Angles are given in Tables 5.3.1 and 5.3.2, respectively. The C22-C21-C21_2-C22_2 torsion angle is 180°. There is an inversion center between C21 and C21_2.

Table 5.3.1: Selected bond distances (Å) in $[(MeC_5H_4)_3Ce]_2$(4,4'-bipyridine)

atom	Atom	distance		atom	Atom	Distance
Ce(1)	C(101)	2.54		Ce(1)	C(102)	2.56
Ce(1)	C(103)	2.58		Ce(1)	C(1)	2.898(6)
Ce(1)	C(2)	2.819(6)		Ce(1)	C(3)	2.751(6)
Ce(1)	C(4)	2.751(7)		Ce(1)	C(5)	2.832(7)
Ce(1)	C(7)	2.872(6)		Ce(1)	C(8)	2.818(6)
Ce(1)	C(9)	2.782(6)		Ce(1)	C(10)	2.809(6)
Ce(1)	C(11)	2.868(7)		Ce(1)	C(13)	2.852(6)
Ce(1)	C(14)	2.884(6)		Ce(1)	C(15)	2.870(7)
Ce(1)	C(16)	2.826(6)		Ce(1)	C(17)	2.815(6)
Ce(1)	N(1)	2.673(5)		N(1)	C(19)	1.357(8)
C(19)	C(20)	1.380(8)		C(20)	C(21)	1.403(8)
C(21)	C(22)	1.394(8)		C(22)	C(23)	1.382(8)
C(23)	N(1)	1.339(8)		C(21)	C(21_2)	1.480(11)

Table 5.3.2: Selected bond angles (°) in $[(MeC_5H_4)_3Ce]_2$(4,4'-bipyridine)

atom	Atom	atom	angle		atom	atom	atom	angle
C(101)	Ce(1)	C(102)	117.5		C(101)	Ce(1)	C(103)	119.0
C(102)	Ce(1)	C(103)	115.3		C(101)	Ce(1)	N(1)	94.9
C(102)	Ce(1)	N(1)	99.3		C(103)	Ce(1)	N(1)	104.3
N(1)	C(19)	C(20)	124.2(6)		C(19)	C(20)	C(21)	119.6(6)
C(20)	C(21)	C(22)	116.6(5)		C(21)	C(22)	C(23)	119.3(6)
C(22)	C(23)	N(1)	125.1(6)		C(20)	C(21)	C(21_2)	122.3(7)
C(22)	C(21)	C(21_2)	121.1(6)					

Addition of one equivalent of 4,4'-bipyridine to two equivalents of $Tb(MeC_5H_4)_3$ gives the orange compound $[(MeC_5H_4)_3Tb]_2$(4,4'-bipyridine), which unlike the cerium analogue is insoluble in thf, though it is soluble in dichloromethane. The 4,4'-bipyridine resonances are not visible in the ^{1}H NMR spectrum, but the resonances due to the MeC_5H_4 are significantly shifted relative to those in $Tb(MeC_5H_4)_3$ at all temperatures (Figure 5.3.4). The resonances that are observable follow Curie-Weiss behavior. The observation that the 4,4'-bipyridine resonances are silent means either that they are undergoing exchange that is rapid on the ^{1}H NMR time scale and the resonances are broadened into the base line, or that the presence of two terbium centers in the vicinity of the 4,4'-bipyridine ligand broadens the lines into the baseline.

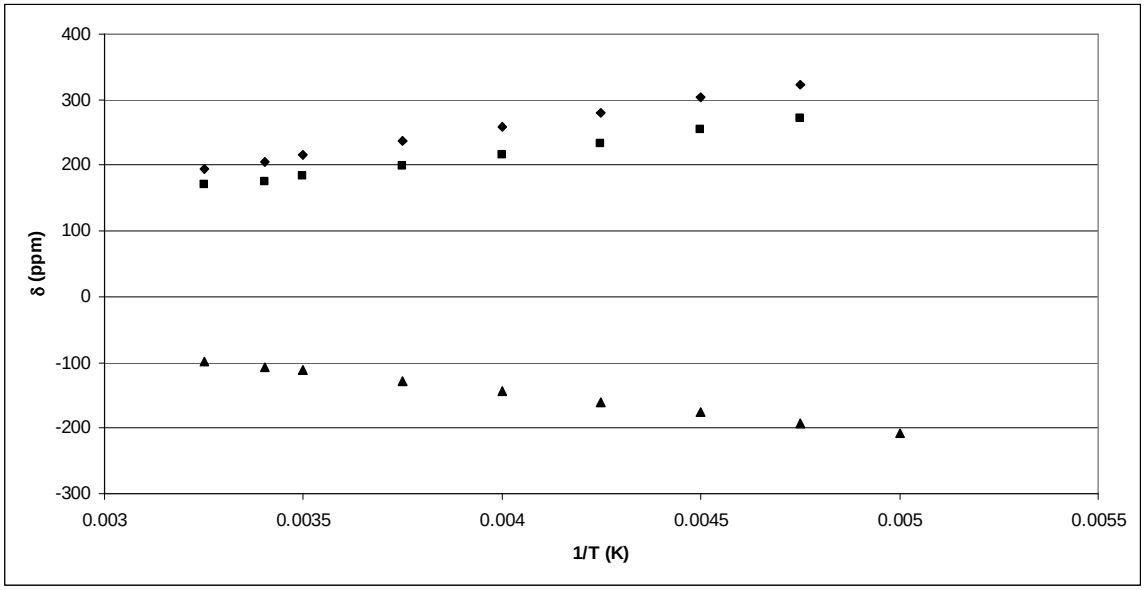

Figure 5.3.4: Variable Temperature ^{1}H NMR spectra represented as a δ vs. 1/T plot of $[(MeC_5H_4)_3Tb]_2$(4,4'-bipyridine) in CD_2Cl_2.

5.4 Synthesis and properties of $[Cp^*_2CeOTf]_2$(4,4'-bipyridine)

By analogy with $[(MeC_5H_4)_3Ce]_2$(4,4'-bipyridine), $[Cp^*_2CeOTf]_2$(4,4'-bipyridine) is synthesized by addition of 1 equivalent of 4,4'-bipyridine to two equivalents of Cp^*_2CeOTf. Crystals are grown by layering pentane on a concentrated solution of the complex in dichloromethane. The variable-temperature ^{1}H NMR spectra plotted as a δ vs. 1/T plot (Figure 5.4.1) shows two peaks attributable to 4,4'-bipyridine, indicating that the molecule has either averaged C_{2v} or C_{2h} symmetry. The variable temperature ^{1}H and ^{19}F NMR spectra plotted as a δ vs. 1/T plot are shown in Figures 5.4.1 and 5.4.2. At high temperatures, two peaks are visible in the ^{19}F NMR spectra, and at all temperatures there is a small Cp* peak as well the expected large Cp* peak in the ^{1}H NMR spectra.

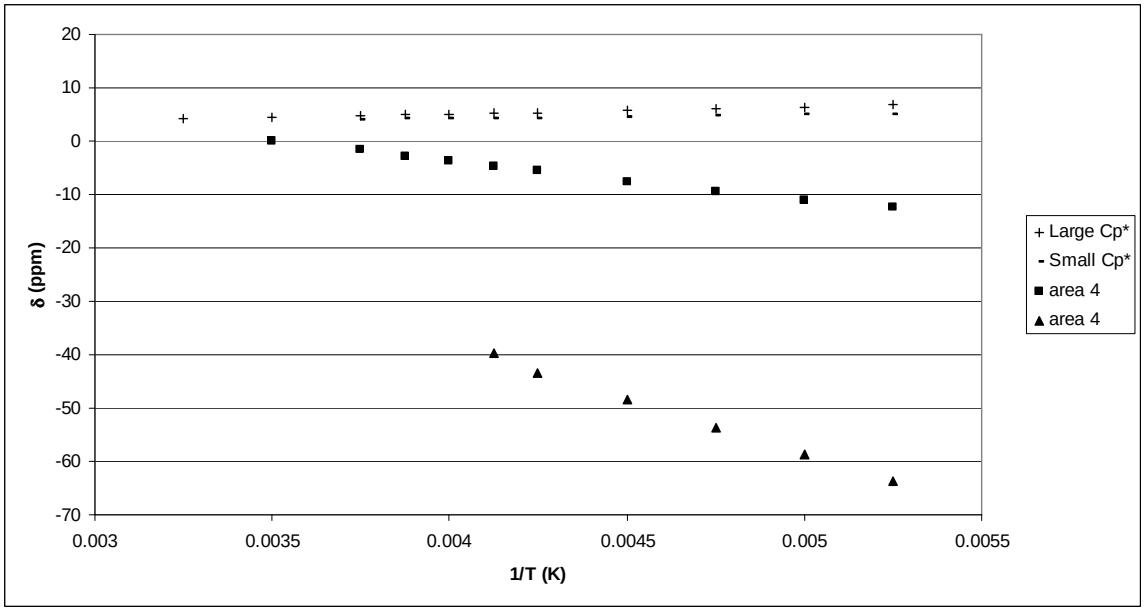

Figure 5.4.1: Variable Temperature ^{1}H NMR spectra represented as a δ vs. 1/T plot of $[Cp^*_2CeOTf]_2$(4,4'-bipyridine) in CD_2Cl_2. The "Small Cp*" peak is ~ 1/20th the size of the "Large Cp*" peak.

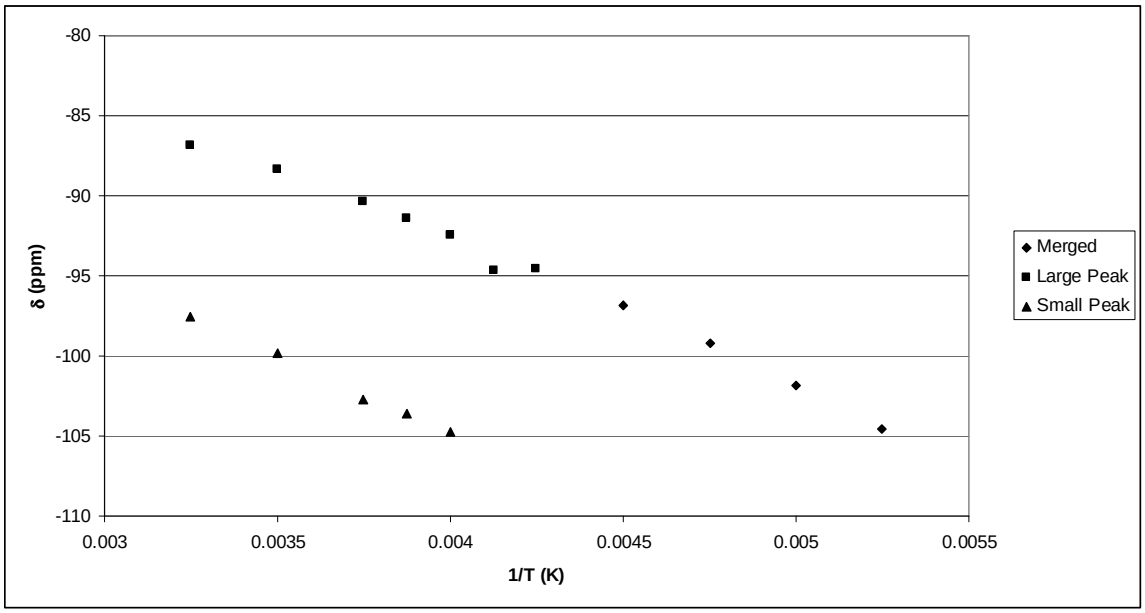

Figure 5.4.2: Variable Temperature ^{19}F NMR spectra represented as a δ vs. 1/T plot of $[Cp^*_2CeOTf]_2$(4,4'-bipyridine) in CD_2Cl_2. The relative integrals can not be obtained with confidence as the area of the larger peak relative to that of the smaller peak decreases as

the temperature is raised and the ratio is not stabilized by 35 °C (the boiling point of CD_2Cl_2 is 40 °C).

It is unclear why there are two peaks in the ^{19}F NMR spectra at high temperatures and why there is what seems like an extra Cp* peak in the ^{1}H NMR spectra at all temperatures. Addition of free 4,4'-bipyridine causes the small peak in the ^{19}F NMR spectra to disappear, and in the ^{1}H NMR spectra the peaks attributed to 4,4-bipyridine shift towards the diamagnetic region. The extra Cp* peak in the ^{1}H NMR spectrum is unaffected. Perhaps it is an impurity. The variable temperature ^{19}F NMR spectra of the small peak in the ^{19}F NMR spectra are at almost the exact same chemical shift as in Cp^*_2CeOTf (Figure 5.4.3), although the extra ^{1}H NMR resonance in $[Cp^*_2CeOTf]_2$(4,4'-bipy) does not track with the ^{1}H NMR resonance in Cp^*_2CeOTf (Figure 5.4.4).

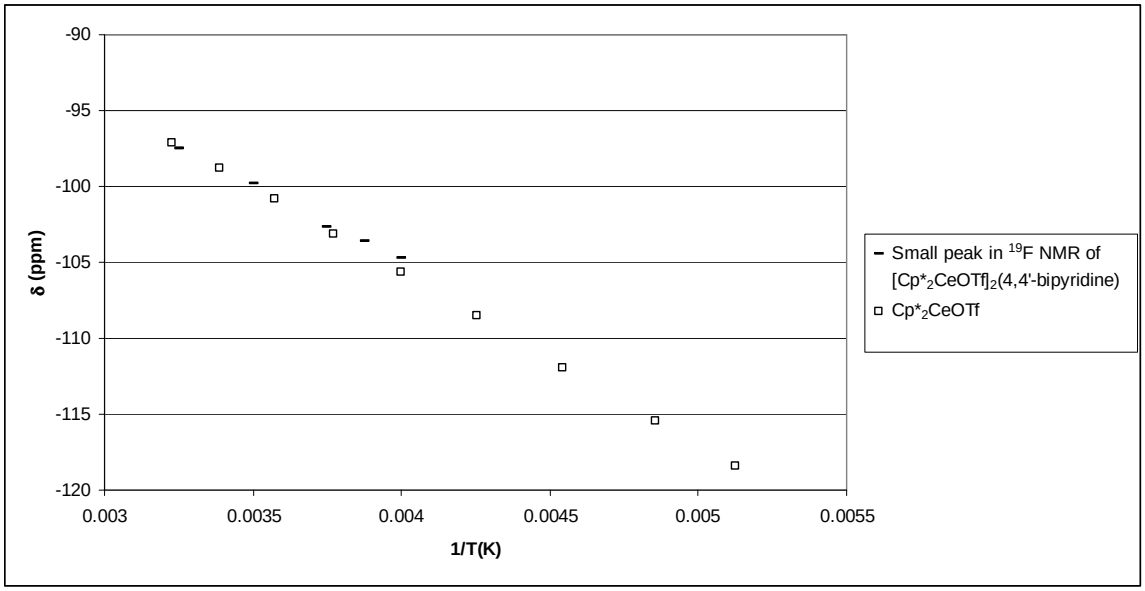

Figure 5.4.3: Variable Temperature ^{19}F NMR spectra represented as a δ vs. 1/T plot of the small peak in$[Cp^*_2CeOTf]_2$(4,4'-bipyridine) and Cp^*_2CeOTf in CD_2Cl_2.

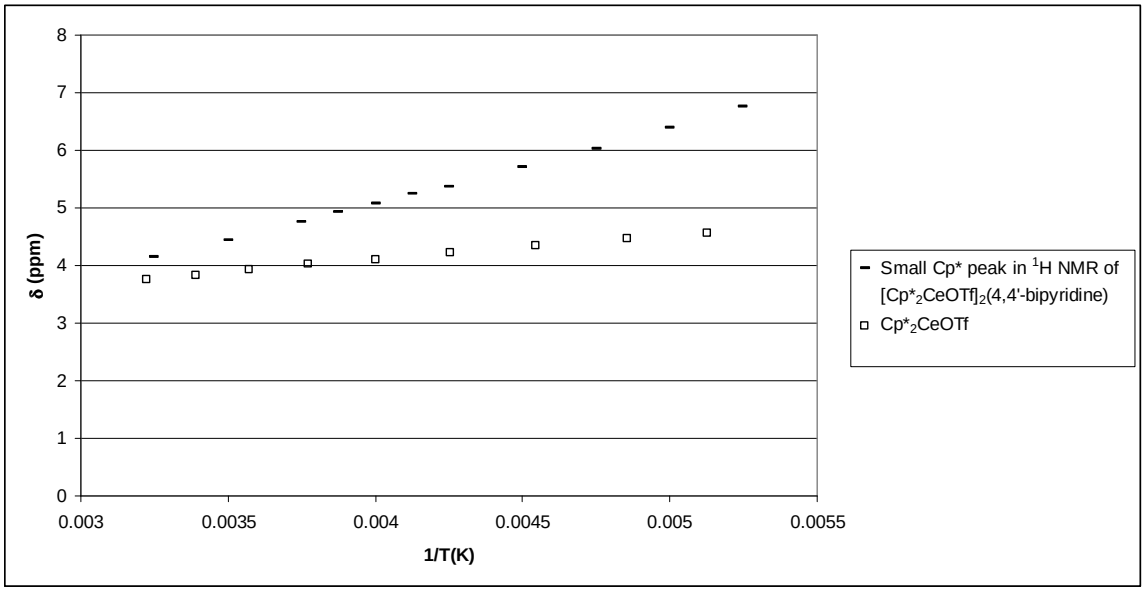

Figure 5.4.4: Variable Temperature ^{1}H NMR spectra represented as a δ vs. 1/T plot of the small peak in[Cp*$_2$CeOTf]$_2$(4,4'-bipyridine) and Cp*$_2$CeOTf in CD_2Cl_2.

As in [(MeC_5H_4)$_3$Ce]$_2$(4,4'-bipyridine), the X-ray crystal structure of [Cp*$_2$CeOTf]$_2$(4,4'-bipyridine) has a crystallographic inversion center in between the two bridging carbons of the bipyridine ring (Figure 5.4.5).

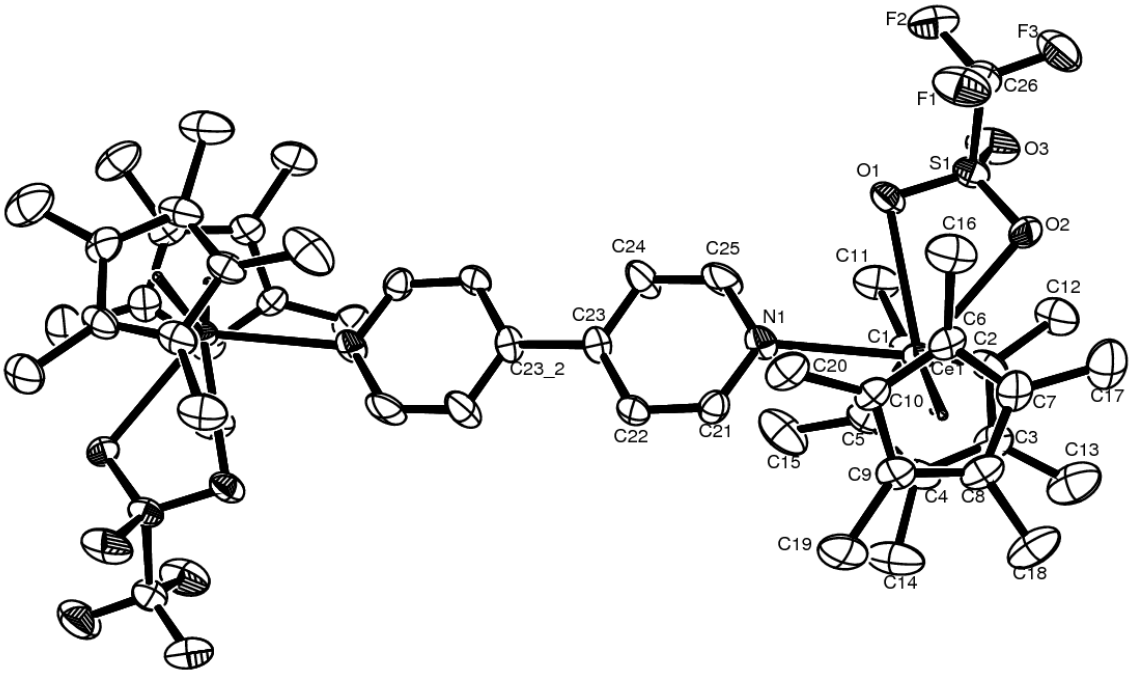

Figure 5.4.5: ORTEP diagram of $[Cp^*_2CeOTf]_2$(4,4'-bipyridine) (50% probability ellipsoids). All non-hydrogen atoms are refined anisotropically. Hydrogen atoms are placed and not refined and are not shown. Selected Bond Distances and Angles are given in Tables 5.4.1 and 5.4.2, respectively. The C22-C23-C23_2-C22_2 torsion angle is 180°. There is an inversion center between C22 and C22_2.

Table 5.4.1: Selected bond distances (Å) in $[Cp^*_2CeOTf]_2$(4,4'-bipyridine)

atom	atom	distance		Atom	Atom	distance
Ce(1)	O(1)	2.734(5)		Ce(1)	O(2)	2.713(5)
Ce(1)	N(1)	2.627(7)		Ce(1)	C(1)	2.853(8)
Ce(1)	C(2)	2.827(8)		Ce(1)	C(3)	2.786(8)
Ce(1)	C(4)	2.817(8)		Ce(1)	C(5)	2.865(8)
Ce(1)	C(6)	2.788(8)		Ce(1)	C(7)	2.772(8)
Ce(1)	C(8)	2.843(8)		Ce(1)	C(9)	2.892(7)
Ce(1)	C(10)	2.868(7)		Ce(1)	C(101)	2.56
Ce(1)	C(102)	2.56		N(1)	C(21)	1.357(10)
N(1)	C(25)	1.371(10)		C(21)	C(22)	1.38(1)
C(22)	C(23)	1.39(1)		C(23)	C(23)	1.55(2)
C(23)	C(24)	1.38(1)		C(24)	C(25)	1.37(1)

Table 5.4.2: Selected bond angles (°) in $[Cp^*_2CeOTf]_2$(4,4'-bipyridine)

Atom	atom	atom	angle		atom	atom	atom	angle
O(1)	Ce(1)	O(2)	52.1(2)		O(1)	Ce(1)	N(1)	74.2(2)
O(1)	Ce(1)	C(101)	103.7		O(1)	Ce(1)	C(102)	121.0
O(2)	Ce(1)	C(101)	102.3		O(2)	Ce(1)	C(102)	99.7
N(1)	Ce(1)	C(101)	97.1		N(1)	Ce(1)	C(102)	101.4
C(101)	Ce(1)	C(102)	134.7		N(1)	C(21)	C(22)	125.0(7)
C(21)	C(22)	C(23)	119.0(7)		C(22)	C(23)	C(23)	122.2(9)
C(22)	C(23)	C(24)	117.6(7)		C(23)	C(23)	C(24)	120.2(9)
C(23)	C(24)	C(25)	120.4(8)		N(1)	C(25)	C(24)	123.8(8)

Table 5.4.3 is a comparison of the bond lengths of $[(MeC_5H_4)_3Ce]_2$(4,4'-bipyridine), $[Cp^*_2CeOTf]$(4,4'-bipyridine), and the previously published crystal structure of 4,4'-bipyridine.[13] The C4-C4' bond lengths in free 4,4'-bipyridine is shorter than in $[(MeC_5H_4)_3Ce]_2$(4,4'-bipyridine) and $[Cp^*_2CeOTf]_2$(4,4'-bipyridine). Calculations on 4,4'-bipyridine show that the radical anion should in fact have a shorter C4-C4' bond as there is a bonding interaction between C4 and C4' in the SOMO (SOMO = singly occupied molecular orbital) of 4,4'-bipyridine.[14] The bond length comparison indicates that the 4,4'-bipyridine is neutral in these molecules and, by extension, that the cerium atoms are Ce(III).

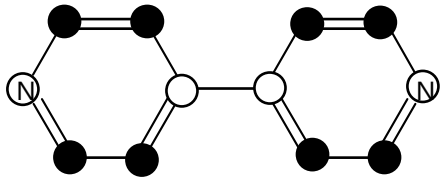

Figure 5.4.6: Cartoon drawing of the SOMO of 4,4'-bipyridine as calculated in reference 14.

Table 5.4.3: A comparison of bond-lengths (Å) between $[(MeC_5H_4)_3Ce]_2$(4,4'-bipyridine), $[Cp^*_2CeOTf]$(4,4'-bipyridine), and free 4,4'-bipyridine. In the crystal structure of 4,4'-bipyridine there are two molecules in the asymmetric unit, and the two pyridine rings in each are crystallographically unique. The average bond length is given in each case, along with the standard deviation.[1] The numbering scheme is as shown in Figure 5.3.1. 4,4'-bipyridine is abbreviated as 4,4'-bipy for the purpose of this table.

	$[(MeC_5H_4)_3Ce]_2$(4,4'-bipy)	$[Cp^*_2CeOTf]_2$(4,4'-bipy)	4,4'-bipy
N1-C2	1.357(8)	1.36(1)	1.331 (6)
C2-C3	1.380(8)	1.38(1)	1.381 (6)
C3-C4	1.403(8)	1.39(1)	1.384 (8)
C4-C5	1.394(8)	1.38(1)	1.384 (8)
C5-C6	1.382(8)	1.37(1)	1.381 (6)
C6-N1	1.339(8)	1.37(1)	1.331 (6)
C4-C4	1.480(11)	1.55(1)	1.489 (9)

[1] Note that in free 4,4'-bipyridine N1-C2 is the same as N2-C6

5.5 Synthesis and properties of $[(MeC_5H_4)_3Ce]_2$(1,4-benzoquinone) and $[Cp^*_2Yb]_2$(benzoquinone)

The reduction potential of 4,4'-bipyridine is -1.91 V vs. SCE,[15] whereas the reduction potential of 1,4-benzoquinone is -0.51 V vs. SCE[16]; 1,4-benzoquinone is a much better oxidizing agent. Addition of one equivalent of 1,4-benzoquinone to two equivalents of $(MeC_5H_4)_3Ce(THF)$ in toluene gives the black adduct $[(MeC_5H_4)_3Ce]_2$(1,4-benzoquinone), analogous to synthesis of $[(N(SiMe_3)_2)_3Ce]_2$(1,4-benzoquinone).[5] The variable-temperature ^1H NMR spectra are plotted as a δ vs. 1/T plot in Figure 5.5.1. The chemical shifts are not large, and they show almost no temperature dependence, indicative of a diamagnetic molecule, implying that both cerium centers have been oxidized to Ce(IV), and the 1,4-benzoquinone is doubly reduced, i.e. $[(MeC_5H_4)_3Ce(IV)]^+_2$[1,4-benzoquinone]$^{2-}$. The silyl amide, $[(N(SiMe_3)_2)_3Ce]_2$(1,4-benzoquinone), was synthesized according to literature procedures, and its variable temperature ^1H NMR spectra are plotted as a δ vs. 1/T plot in Figure 5.5.2, and the chemical shifts of $[(N(SiMe_3)_2)_3Ce]_2$(1,4-benzoquinone) show slight temperature dependence, also implying that its electronic configuration is $[(N(SiMe_3)_2)_3Ce(IV)]^+_2$[1,4-benzoquinone]$^{2-}$, analogous to the MeC_5H_4 derivative. The Cp derivative, $[Cp_3Ce]_2$(1,4-benzoquinone], is insoluble in all solvents and could not be obtained as a pure material.

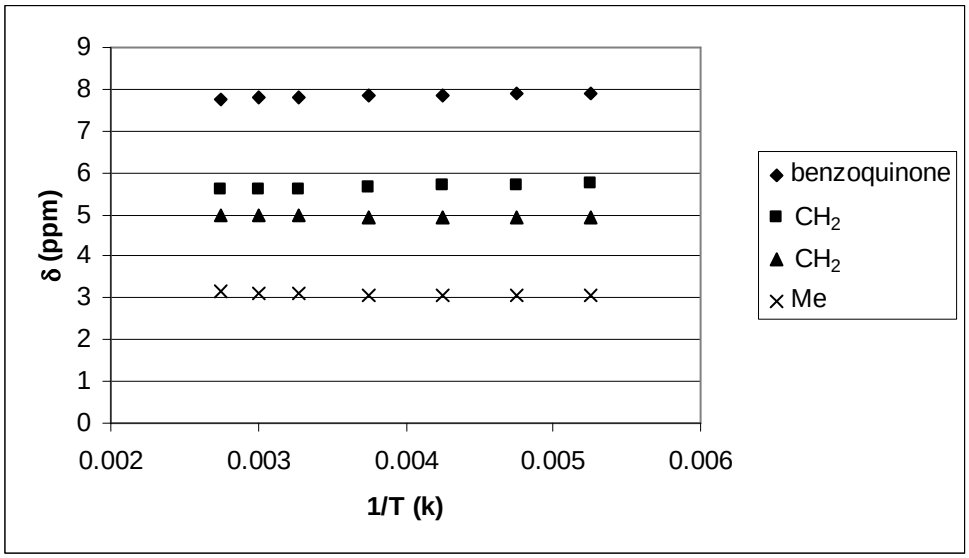

Figure 5.5.1: Variable Temperature ^{1}H NMR spectra represented as a δ vs. 1/T plot of $[(MeC_5H_4)_3Ce]_2$(1,4-benzoquinone) in toluene-d_8.

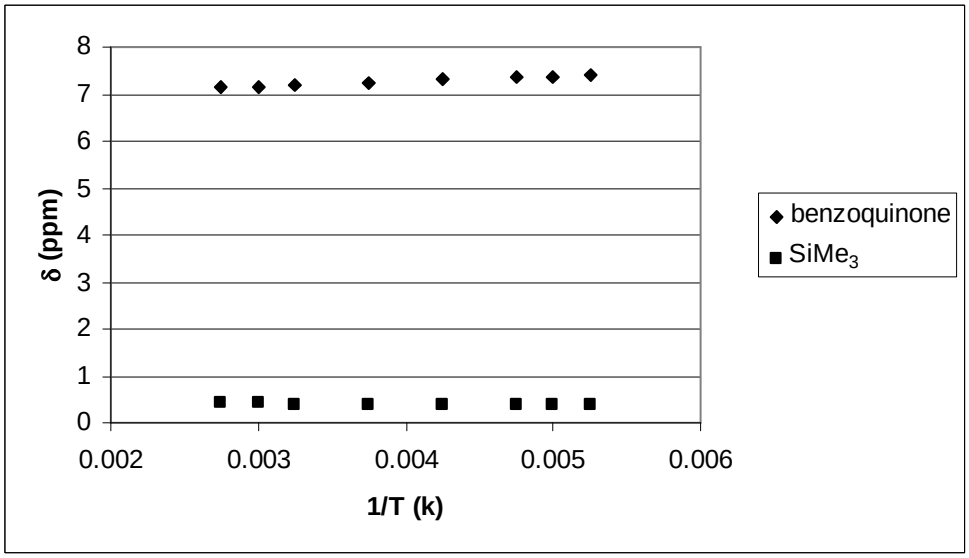

Figure 5.5.2: Variable Temperature ^{1}H NMR spectra represented as a δ vs. 1/T plot of $[(N(SiMe_3)_2)_3Ce]_2$(1,4-benzoquinone) in toluene-d_8.

Crystals suitable for X-ray diffraction of $[(MeCp)_3Ce]_2$(1,4-benzoquinone) were obtained from toluene and the ORTEP diagram is shown in Figure 5.5.3. The crystal structure of the related $[(^tBu_3CO)_3Ce]_2$(1,4-benzoquinone) is also known.[17] A comparison of the bond lengths of free 1,4-benzoquinone[18] with the bond lengths of $[(^tBu_3CO)_3Ce]_2$(1,4-benzoquinone) and $[(MeCp)_3Ce]_2$(1,4-benzoquinone) is shown in Table 5.5.3. The HOMO (HOMO = highest occupied molecular orbital) of [1,4-benzoquinone]$^{2-}$ is shown in Figure 5.5.4. The molecular orbital shows that a two electron reduction of 1,4-benzoquinone leads to a bonding interaction between C1 and C2 and between C1 and C6, and an antibonding interaction between C1 and O1 and C2 and C3. The differences in bond lengths show a lengthening of the bond between C1 and O1 and between C2 and C3 in $[(MeCp)_3Ce]_2$(1,4-benzoquinone) and $[(^tBu_3CO)_3Ce]_2$(1,4-benzoquinone), as expected if there is added electron density into the 1,4-benzoquinone π-system.

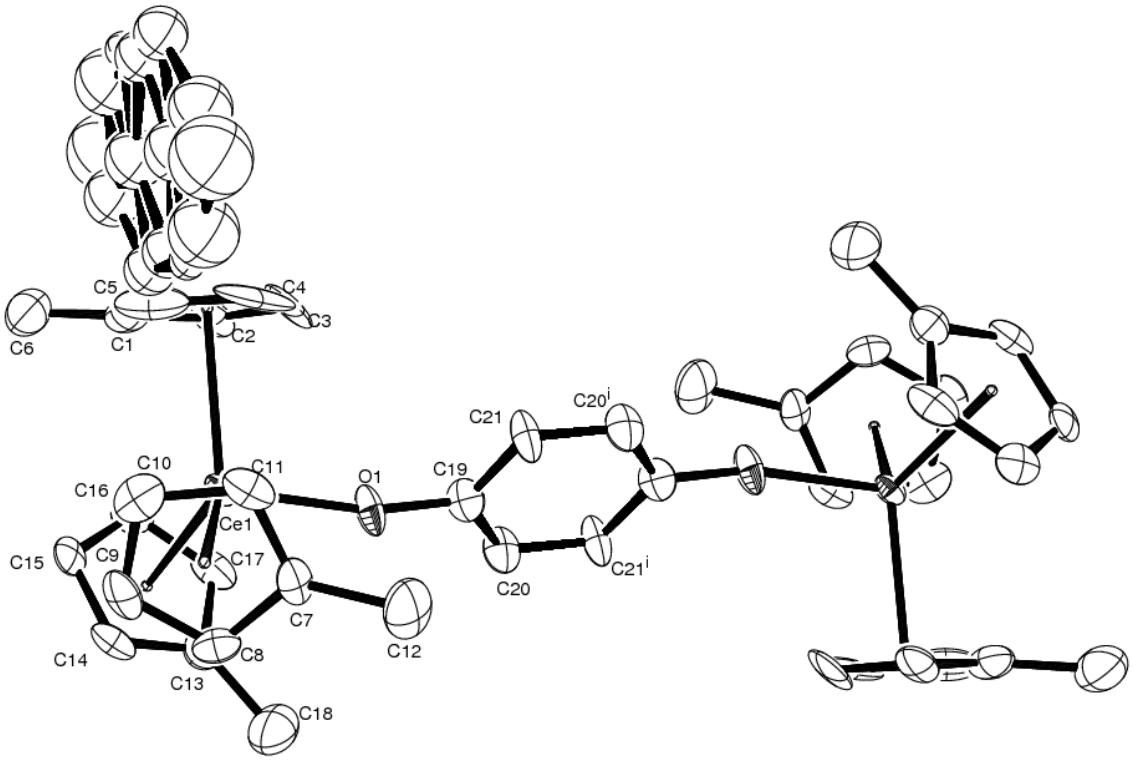

Figure 5.5.3: ORTEP diagram of $[(MeC_5H_4)_3Ce]_2$(1,4-benzoquinone) (50% probability ellipsoids). Toluene of crystallization is refined isotropically and modeled as two separate toluene molecules, each with 50% occupancy. All other non-hydrogen atoms are refined anisotropically. Hydrogen atoms are placed and not refined and are not shown. Selected Bond Distances and Angles are given in Tables 5.5.1 and 5.5.2, respectively. There is an inversion center in the middle of the benzoquinone ring.

Table 5.5.1: Selected bond distances (Å) in $[(MeCp)_3Ce]_2$(1,4-benzoquinone)

atom	atom	distance		atom	atom	distance
Ce(1)	O(1)	2.107(4)		Ce(1)	C(1)	2.800(5)
Ce(1)	C(2)	2.768(5)		Ce(1)	C(3)	2.731(5)
Ce(1)	C(4)	2.729(6)		Ce(1)	C(5)	2.758(6)
Ce(1)	C(7)	2.787(5)		Ce(1)	C(8)	2.770(5)
Ce(1)	C(9)	2.747(5)		Ce(1)	C(10)	2.756(5)
Ce(1)	C(11)	2.760(5)		Ce(1)	C(13)	2.792(5)
Ce(1)	C(14)	2.769(5)		Ce(1)	C(15)	2.744(4)

Ce(1)	C(16)	2.754(5)		Ce(1)	C(17)	2.765(5)
O(1)	C(19)	1.367(6)		C(19)	C(20)	1.395(7)
C(19)	C(21)	1.377(7)		C(20)	C(21)	1.401(7)
Ce(1)	C(101)	2.49		Ce(1)	C(102)	2.50
Ce(1)	C(103)	2.50				

Table 5.5.2: Selected bond angles (°) in $[(MeCp)_3Ce]_2$(1,4-benzoquinone)

atom	atom	atom	angle		atom	atom	atc	an
Ce(1)	O(1)	C(19)	166.6(3)		C(101)	Ce(1)	C(	11
C(101)	Ce(1)	C(103)	116		C(102)	Ce(1)	C(	11

Table 5.5.3: Bond lengths of 1,4-benzoquinone in free 1,4-benzoquinone,

$[(MeCp)_3Ce]_2$(1,4-benzoquinone) and $[(^tBu_3CO)_3Ce]_2$(1,4-benzoquinone).

	Free 1,4-benzoquinone	$[(^tBu_3CO)_3Ce]_2$(1,4-bq)	$[(^tBu_3CO)_3Ce]_2$(1,4-bq)
C1-O1	1.222(3)	1.367(6)	1.38(2)
C1-C2	1.477(3)	1.395(7)	1.37(2)
C2-C3	1.334(3)	1.401(7)	1.40(2)
C6-C1	1.470(3)	1.377(7)	1.35(4)

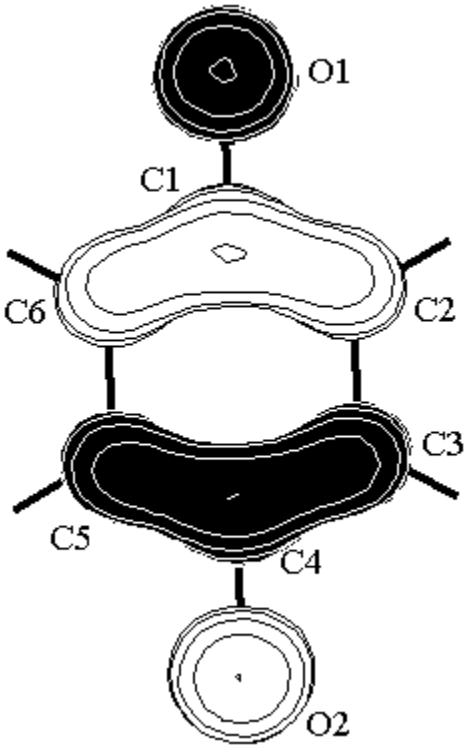

Figure 5.5.4: HOMO of [1,4-benzoquinone]$^{2-}$. Symmetry = C_{2v}. Exchange = B3LYP. Basis = 6-311+G*

Upon addition of one equivalent of 1,4-benzoquinone to two equivalents of $(MeC_5H_4)_3Tb$ or $(MeC_5H_4)_3Pr(THF)$ in toluene, the solution turns black, presumably implying a redox reaction, but no isolable product could be obtained.

Addition of two equivalents of $Cp^*_2Yb(OEt_2)$ to one equivalent of 1,4-benzoquinone gives a dark purple powder which is insoluble in pentane, toluene, OEt_2, and thf.

5.6 Magnetism of the Dimers

Cerium has two stable oxidation states: +3 and +4. Ce(IV) has an empty f-shell and is diamagnetic whereas Ce(III) is a paramagnetic $4f^1$ ion with a $^2F_{5/2}$ ground state. The magnetic moment, when corrected for the diamagnetic susceptibility of the atoms using Pascal's constants of a diamagnetic molecule is 0 B.M. (B.M. = Bohr Magnetons), while the magnetic moment, when corrected for the diamagnetic susceptibility of the atoms using Pascal's constants of a Ce(III) ion is calculated to be 2.54 B.M.. Thus, in molecules of the type $[X_3Ce]_2(L)$ ($X = MeC_5H_4$, $N(SiMe_3)_2$) (L = 4,4'-bipyridine, 1,4-benzoquinone) there are four possibilities. The first is that both cerium atoms are Ce(III), f^1, and L remains neutral, i.e. $[X_3Ce(III)]_2(L)$, and the f^1 spins are isolated or not. The second possibility is one in which a cerium atom is Ce(III), the other cerium atom is Ce(IV), and L is a radical anion, i.e. $[Ce(IV)X_3]^+[L]^-Ce(III)X_3$, again the spin carriers may be isolated or not. The third possibility is that both cerium atoms are Ce(IV) and L is a dianion, i.e. $[X_3Ce(IV)]^+_2[L]^{2-}$. The fourth possibility is that it is similar to the ytterbium case and has an intermediate valence ground state. The Pascal-corrected effective magnetic moments at room temperature of the previous possibilities assuming the spin carriers are non-interacting gives the following values of the effective magnetic moment at 300K: $[X_3Ce(III)]_2(L)$, μ_{eff} = 3.59 B.M., $[Ce(IV)X_3]^+[L]^-Ce(III)X_3$, μ_{eff} = 3.07 B.M., $[X_3Ce(IV)]^+_2[L]^{2-}$, μ_{eff} = 0 B.M..

The reported μ_{eff} vs. T plot of $[(N(SiMe_3)_2)_3Ce]_2$(1,4-benzoquinone) along with the μ_{eff} vs. T plot of $[(MeC_5H_4)_3Ce]_2$(1,4-benzoquinone), $[(MeC_5H_4)_3Ce]_2$(4,4'-bipyridine), and $[Cp^*_2CeOTf]_2$(4,4'-bipyridine) are shown in Figures 5.6.1-5.6.4, respectively. The effective magnetic moment of $[(MeC_5H_4)_3Ce]_2$(4,4'-bipyridine) clearly identifies it as a

molecule with two non-interacting Ce(III) centers, i.e., $[(MeC_5H_4)_3Ce(III)]_2$(4,4'-bipyridine). In the case of the 1,4-benzoquinone adducts the situation is more complicated. The moment is too low for it to be $[X_3Ce(III)]_2$(1,4-benzoquinone) (X = $N(SiMe_3)_2$, MeC_5H_4) or even $[Ce(IV)X_3]^+[L]^-Ce(III)X_3$, but it is greater than zero, and therefore it is not diamagnetic $[X_3Ce(IV)]^+{}_2[1,4\text{-benzoquinone}]^{2-}$. It seems that this case is related to the situation in $Cp^*{}_2Yb$(2,2'-bipyridine), that is, an intermediate valence ground state. The lower reduction potential of 4,4-bipyridine, relative to 1,4-benzoquinone, allows 4,4'-bipyridine to remain a neutral ligand when bound to two Ce(III) centers, whereas 1,4-benzoquinone accept two electrons, one from each Ce(III) center, so that the net result is that the cerium fragments have an intermediate valence.

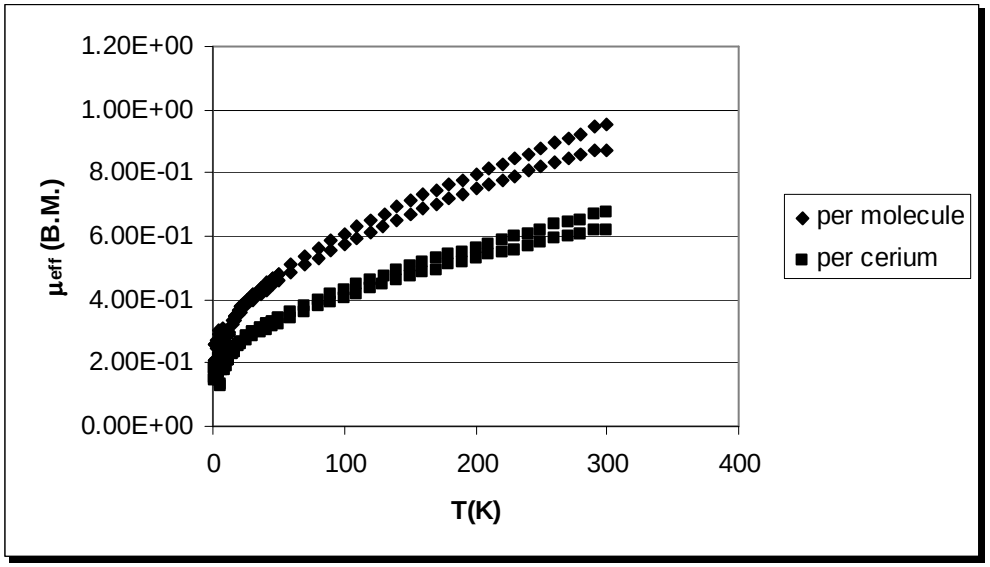

Figure 5.6.1: A plot of μ_{eff} vs. T in $[(N(SiMe_3)_2)_3Ce]_2$(1,4-benzoquinone)

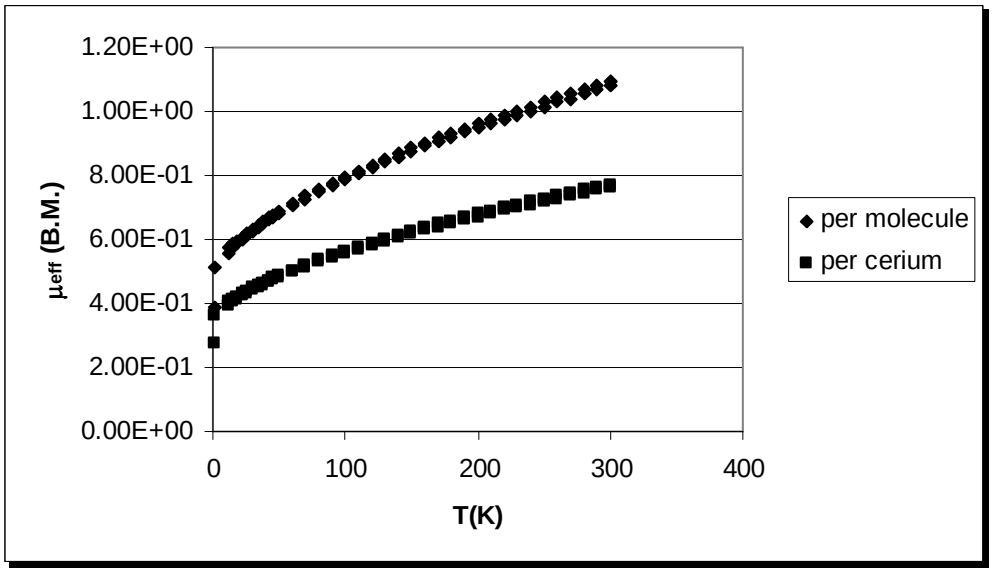

Figure 5.6.2: A plot of μ_{eff} vs. T in $[(MeC_5H_4)_3Ce]_2$(1,4-benzoquinone)

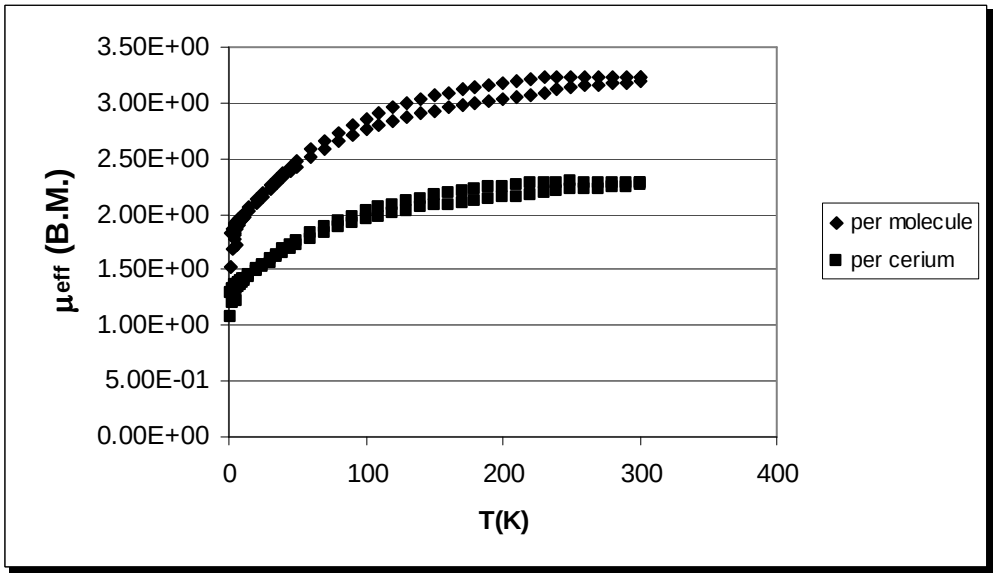

Figure 5.6.3: A plot of μ_{eff} vs. T in $[(MeC_5H_4)_3Ce]_2$(4,4'-bipyridine)

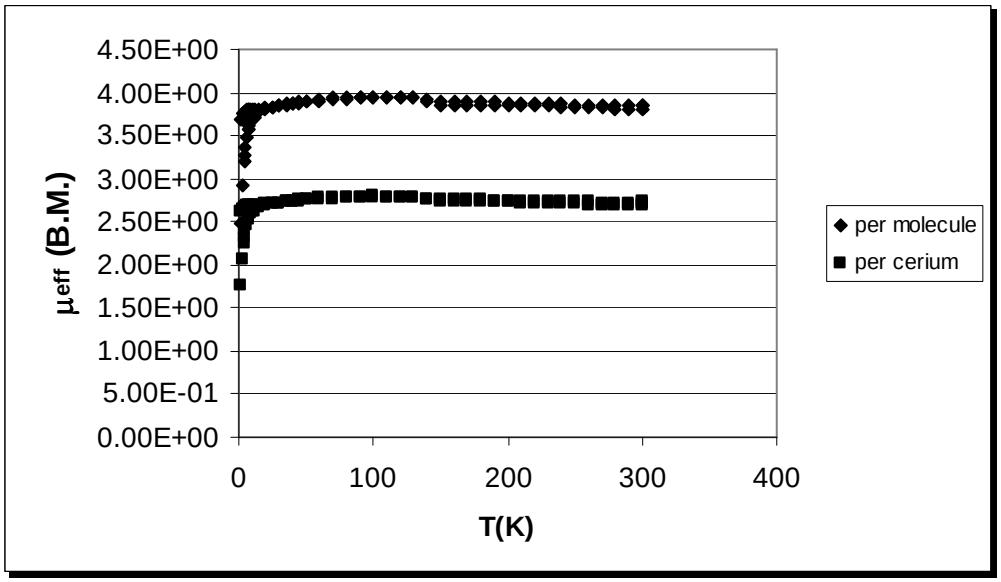

Figure 5.6.4: A plot of μ_{eff} vs. T in $[Cp^*_2CeOTf]_2$(4,4'-bipyridine)

Not surprisingly 4,4'-bipyridine does not oxidize the terbium centers to Tb(IV). However, there may be slight ferromagnetic coupling as seen in the μ_{eff} vs. T plot shown in Figure 5.6.5, since μ_{eff} comes to a maximum at T = 80K.

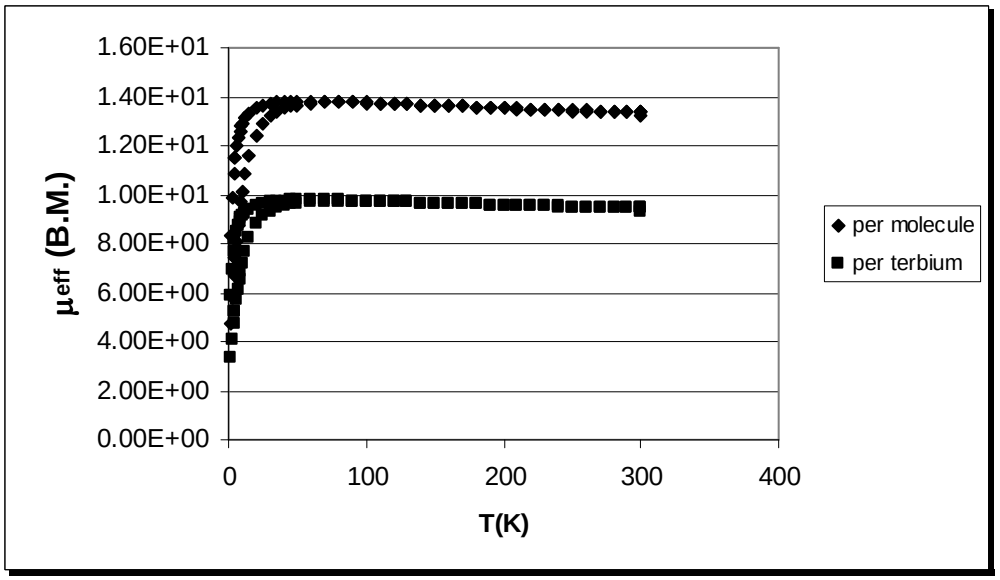

Figure 5.6.5: A plot of μ_{eff} vs. T in $[(MeC_5H_4)_3Tb]_2$(4,4'-bipyridine)

The effective magnetic moment vs. T of the 2:1 adduct of $Cp^*_2Yb(OEt_2)$ and 1,4-benzoquinone is shown in Figure 5.6.6, which indicates that the two Yb(III) centers are isolated paramagnets at all temperatures.

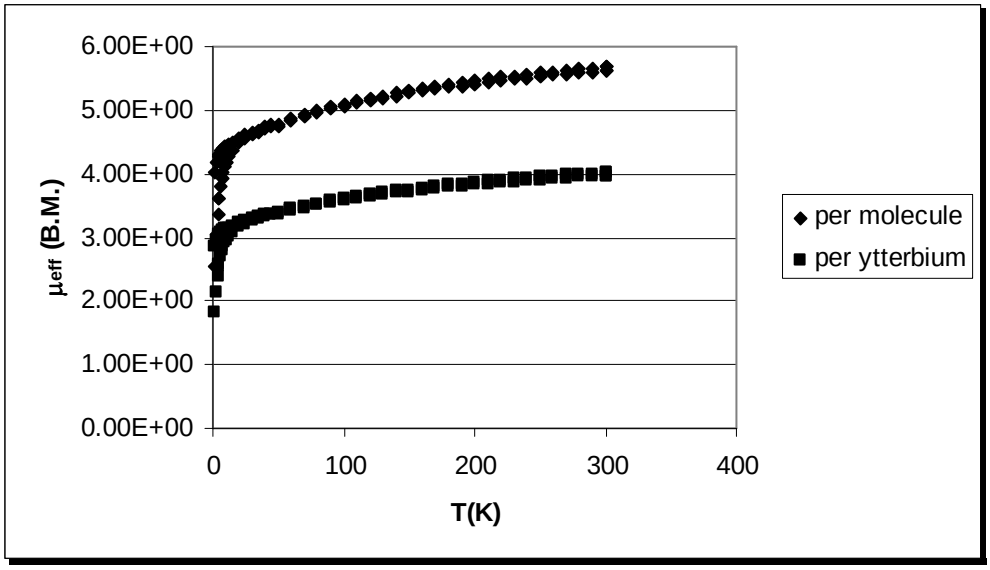

Figure 5.6.6: A plot of μ_{eff} vs. T in $[Cp^*_2Yb]_2$(1,4-benzoquinone)

5.7 Solid State Measurements: XANES (X-ray Absorption Near Edge Spectroscopy)

XANES data were collected at the Stanford Synchotron Radiation Laboratory and analyzed by Dr. Corwin Booth. XANES spectroscopy allows for the measurement of the f-electron occupancy of metal ions. The valence of a system is measured by comparing the position of a core x-ray absorption edge of the molecule of interest with that of model compounds. In the case of cerium compounds, the Ce L_{III} edge ionization energy of $[(MeC_5H_4)_3Ce]_2$(1,4-benzoquinone) is compared to that of CeO_2 and CeF_4, as a model for a Ce(IV) center and for the excited state of a Ce(IV) center with charge transfer back from the ligand, and CeF_3 which contains a Ce(III) center. CeO_2 and CeF_4 show two absorptions: 5726.8 eV due to a Ce(IV) center excited state in which it oxidizes its ligands, and 5736.6 eV due to a Ce(IV) center. CeF_3 shows one at 5723.8 eV. The XANES spectrum of $[(MeC_5H_4)_3Ce]_2$(1,4-benzoquinone) is shown in Figures 5.7.1. The XANES spectrum shows that $[(MeC_5H_4)_3Ce]_2$(1,4-benzoquinone) contains signiatures of the Ce(III) and Ce(IV) configurations and therefore both configurations contribute to the overall wavefunction. Figure 5.7.2 compares the XANES data for $[(MeC_5H_4)_3Ce]_2$(1,4-benzoquinone) with that of the previously published spectrum for cerocene[19]. The comparison shows a smaller Ce(IV) contribution in $[(MeC_5H_4)_3Ce]_2$(1,4-benzoquinone) than in cerocene. The XANES spectrum of $[(N(SiMe_3)_2)_3Ce]_2$(1,4-benzoquinone) and $[(MeC_5H_4)_3Ce]_2$(4,4'-bipyridine) will be determined in the future and a correlation between the magnetic properties of the Synchotron data will provide a unified model for these dimetal systems. The formal f count of $[(MeCp)_3Ce]_2$(1,4-benzoquinone) is 0.6 ± 0.1.

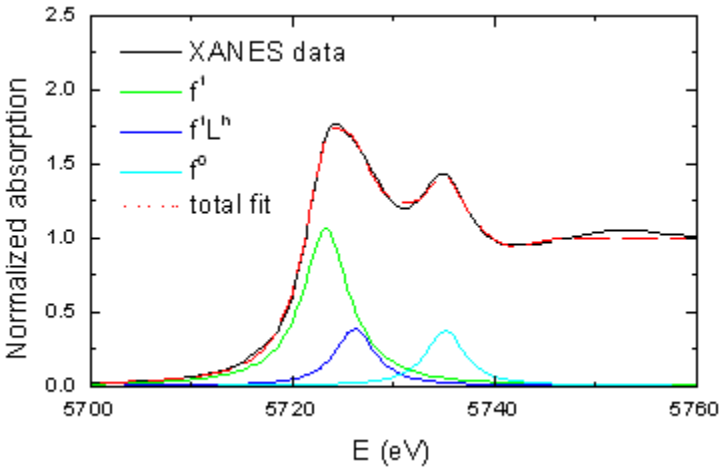

Figure 5.7.1: Ce L_{III} XANES for $[(MeC_5H_4)_3Ce]_2$(1,4-benzoquinone) decomposed into its Ce(III), Ce(IV) excited state, and Ce(IV).

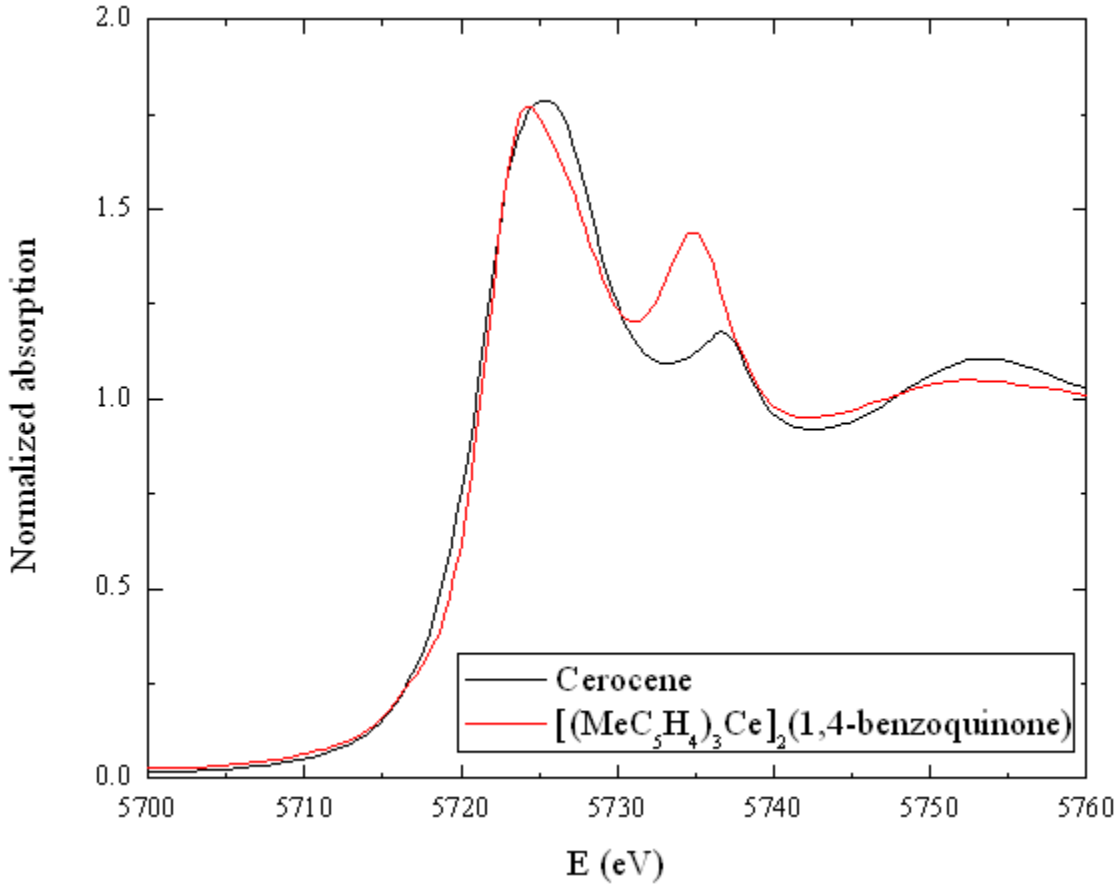

Figure 5.7.2: Ce L_{III} XANES for $[(MeC_5H_4)_3Ce]_2$(1,4-benzoquinone) and cerocene.

In conclusion, molecules analogous to Walter's $[(N(SiMe_3)_2)_3Ce]_2$(1,4-benzoquinone) have been synthesized and depending on the reduction potential of the ligands the cerium center can be in the +3 or +4 oxidation state.

References:

1. Freeman, A.J.; Watson, R.E. *Phys. Rev. Series II*, **1962**, *127*, 2058
2. Van Vleck, J.H.; Frank, A. *Phys. Rev.*, **1929**, *34*, 1494
3. Van Vleck, J.H.; Frank, A. *Phys. Rev.*, **1929**, *34*, 1625
4. Van Vleck, J.H. *Theory of Electric and Magnetic Susceptibilities*, **1932**, p. 243
5. Walter, M.D., Ph.D. Thesis, Technische Universität Kaiserlautern Fachbereich Chemie, **2005**
6. Zi, G.; Jia, L.; Werkema, E.L.; Walter, M.D.; Gottfriedsen, J.P.; Andersen, R.A., *Organometallics*, **2005**, *24*, 4251
7. Hammel, A.; Schwarz, W.; Weidlein, J. *J. Organomet. Chem.*, **1989**, *363*, c29
8. Xie, Z.; Ekkehardt Hahn, F.; Qian, C. *J. Organomet. Chem.*, **1991**, *414*, c12
9. Stults, S.D.; Andersen, R.A.; Zalkin, A. *Organometallics*, **1990**, *9*, 115
10. Xi-Geng, Z.; Zu-En, H.; Rui-Fang, C.; Sheng-Nan, Y.; Ziao-Ying, H. *Chinese J. Struct. Chem.*, **1997**, *16*, 384
11. Burns, J.H.; Baldwin, W.H.; Fink, F.H. *Inorganic Chemistry*, **1974**, *13*, 1916
12. Bleaney, B. *J. Magn. Reson.*,**1972**, *8*, 91
13. Boag, N.M.; Coward, K.M.; Jones, A.C.; Pemble, M.E.; Thompson, J.R. *Acta Cryst.* **1999**, *C55*, 672.
14. Castellà-Ventura, M.; Kassab, E. *J. Raman Spectrosc.*, **1998**, *29*, 511.
15. Tabner, B.J.; Yandle, J.R. *J. Chem. Soc. A.*, **1968**, 381.
16. Connelly, N.G.; Geiger, W.E. *Chem. Rev.*, **1996**, *96*, 877
17. Sen, A.; Stecher, H.A.; Rheingold, A.L. *Inorg. Chem.*, **1992**, *31*, 473.
18. van Bolhuis, F.; Kiers, C.T. *Acta Cryst.*, **1978**, *B34*, 1015
19. Booth, C.H.; Walter, M.D.; Daniel, M.; Lukens, W.W.; Andersen, R.A. *Phys. Rev. Lett.*, **2005**, *95*, 267202.

Chapter 6: Experimental Section

General Procedures. All reactions and product manipulations were carried out under dry nitrogen using standard Schlenk and drybox techniques. Dry, oxygen-free solvents were employed throughout. Pentane and toluene were dried over sodium. OEt_2 and THF were dried over Na/benzophenone. CH_2Cl_2 and CH_3CN were dried over molecular sieves. Cp*H,[1] $MgCp^*_2$,[2] $Ce(OTf)_3$,[3] and $CeI_3(THF)_3$[4] were made according to literature preparations. 1,2-Diaminobenzene, 2,2'-bipyridine, 4,4'-dimethyl-2,2'-bipyridine, 5,5'-dimethyl-2,2'-bipyridine, 6,6'-dimethyl-2,2'-bipyridyl, 4-methyl-2,2'-bipyridine, 1,10-phenanthroline, 2,2',6',2''-terpyridine, and 4,4'-bipyridine were purified by vacuum sublimation onto a water cooled probe at temperatures of approximately 100 °C. 6-methyl-2,2'-bipyridine, $[NEt_4][OTf]$, and $[NBu_4][OTf]$ were obtained from Sigma-Aldrich and were melted under dynamic vacuum to remove the water. Upon melting, 6-methyl-2,2'-bipyridine became an oil and was left to sit for a few days to solidify. 5-methyl-2,2'-bipyridine was stirred with calcium hydride and then distilled under diffusion pump vacuum. $[NMe_4][OH]$ and $NaBPh_4$ were obtained from Sigma-Aldrich and used as bought. Some batches of $NaBPh_4$ were either pink or yellow and had a strong odor. These batches are impure and were not used. Infrared spectra were obtained as Nujol mulls using either KBr or CsI plates. ^1H and ^{19}F NMR spectra were recorded on Bruker AVB-400, AVQ-400, AV-300 and DPX-300 spectrometers. The chemical shifts are reported at 20 °C unless otherwise reported. All chemical shifts are reported in δ units with reference to the residual protons of deuterated solvents for proton chemical shifts. All ^{19}F chemical shifts are relative to $CFCl_3$ and calculated against C_6F_6 at -163 ppm.[5] All

^{11}B chemical shifts are relative to $BF_3 \cdot (OEt_2)$. Magnetic susceptibility data were obtained on a Quantum Design MPMS XL7 SQUID magnetometer according to literature procedures.[6] Melting points were measured on a Thomas-Hoover melting point apparatus in sealed capillaries and are uncorrected. Elemental analysis was performed by the analytical laboratories at the University of California, Berkeley.

Chapter 1

Preparation of $CeCl_3$

Concentrated HCl (200 mL, 2.5 mol) was added to cerium oxide (20 g, 0.07 mol) in an evaporating dish. The solution was heated to a slow boil and covered with a glass plate until there were only 20 mL of solvent. 30 mL of distilled water were added and the solution was concentrated to 20 mL again. This process was repeated (3-4 times) till the odor of HCl was no longer detectable. The solvent was then all boiled off and the grayish residue was put in a round bottom flask and was placed under dynamic vacuum overnight. The grey solid was the ground in a mortar and pestle, put back in the round bottom flask and heated to 160 °C under dynamic vacuum for 12 hours. Thionyl chloride (150 mL, 1.37 mol) was added to the flask through a plastic cannula and the thionyl chloride was refluxed for a week. The thionyl chloride was then distilled off and the $CeCl_3$ was heated at 140 °C overnight under dynamic vacuum. Yield 28.5 g (~90%).

Preparation of $Ce(OTf)_3$

Triflic acid (0.90 L of a 0.37 M solution, 0.33 mol) was added to cerium carbonate hydrate (24 g, 0.052 mol). Cerium carbonate was added until the pH was five. The water was then boiled off and the $CeOTf_3 \cdot (xH_2O)$ was heated at 160 °C under dynamic vacuum until the OH stretch in the IR spectrum disappeared (approximately two weeks). Yield 52 g (~ 85%).

Preparation of $LnOTf_3$ (Ln ≠ Ce)

The preparation was the same as for cerium except that lanthanide oxides were used. Sometimes the lanthanide oxide does not react immediately with the triflic acid. In these cases it is necessary to heat the solution before adding excess Ln_2O_3.

Preparation of $Cp^*_2CeCl\cdot(CH_3CN)_2$

$CeCl_3$ (2.0g, 8.1 mmol) and $MgCp^*_2$ (2.4g, 8.1 mmol) were dissolved in approximately 50 mL of THF and stirred under reflux overnight. The THF was removed under reduced pressure from the pink-orange solution and acetonitrile was added to the residue and the MeCN was removed under reduced pressure until a precipitate began to form. The solution was warmed to re-dissolve the precipitate then cooled to -20 °C yielding yellow crystals. The mother liquor was concentrated and cooled, but $MgCl_2$ (white crystals) cocrystallized with the product. The $Cp^*_2CeCl\cdot(CH_3CN)_2$ crystals were separated from the $MgCl_2$ crystals using tweezers. Yield 0.5 g (12%). ^{1}H NMR (C_6D_6): δ -3.72 (6H, $\upsilon_{1/2}$ = 8 Hz), 2.97 (30H, $\upsilon_{1/2}$ = 12 Hz). IR (Nujol mull): 2920 (vs), 2298 (m), 2282 (s), 1518 (vs), 1380 (s), 1368 (w), 1020 (w), 720 (w) cm^{-1}. Anal. Calcd for $C_{24}H_{36}CeN_2Cl$: C, 54.58; H, 6.87; N, 5.30. Found C, 54.21; H, 6.86; N, 5.12. M.P.: 290-291 °C. The sample changes color reversibly to pinkish red at 124-126 °C. When heated under vacuum the yellow color does not return upon cooling to room temperature.

Preparation of $Cp^*_2CeI\cdot(CH_3CN)_2$

$CeI_3(THF)_3$ [7] (5.9g, 8.00 mmol) and $MgCp^*_2$ (2.4g, 8.14 mmol) were dissolved in approximately 50 mL of THF and stirred under reflux overnight. The THF was removed under reduced pressure from the pink-orange solution and acetonitrile was added to the residue and the MeCN was removed under reduced pressure until a precipitate began to form. The solution was warmed to re-dissolve the precipitate then cooled to -20 °C yielding yellow crystals. The mother liquor was concentrated and cooled three twim, until MgI_2 (white crystals) also crystallized. The $Cp^*_2CeI\cdot(CH_3CN)_2$ crystals were separated from the MgI_2 crystals using tweezers. Yield 3.98 g (80%). ^{1}H NMR (CD_2Cl_2): δ -5.54 (7.4H, $\upsilon_{1/2}$ = 12 Hz), 4.94 (30H, $\upsilon_{1/2}$ = 46 Hz). IR (Nujol mull): 2920 (vs), 2298 (m), 2282 (s), 2115 (w), 1460 (s), 1380 (s), 1365 (w), 1196 (s), 1026 (s), 935 (w), 870 (w), 800 (s), 725 (w), 600 (w), 475 (w), 400 (s), 306 (s) cm^{-1}. Anal. Calcd for $C_{24}H_{36}CeN_2I$: C, 46.53; H, 5.86; N, 4.52. Found C, 46.41; H, 5.50; N, 4.39. M.P.: greater than 360 °C. The sample changed color reversibly to pinkish red at 118-120 °C. When heated under vacuum the yellow color does not return upon cooling. This compound was synthesized accidentally and the crystal structure was reported.[4]

Preparation of Cp^*_2CeI

$Cp^*_2CeI\cdot(CH_3CN)_2$ (1.0 g, 1.6 mmol) was sublimed at 160 °C in a diffusion-pump vacuum to give a pink powder. Yield 0.74 g (85%). ^{1}H NMR (THF-d_8): δ 5.362 ($\upsilon_{1/2}$ = 54 Hz). Anal. Calcd for $C_{20}H_{30}CeI$: C, 44.69; H, 5.63. Found C, 44.58; H, 5.48. The E.I. mass spectrum showed a molecular ion at m/e = 537 amu. The parent isotopic cluster was simulated: (Calcd %, observd. %): 537 (100, 100), 538 (23,23), 539 (15,14), 540 (3, 4).

Preparation of $Cp^*_2Ce(OTf)$[3]

$Ce(OTf)_3$ (11.2 g, 19.0 mmol) and $MgCp^*_2$ (5.6g, 19 mmol) were dissolved in approximately 50 mL THF and the mixture was heated at reflux overnight. The yellow solution was cooled to room temperature and the solvent was removed. The resulting orange powder was extracted with 100 mL of toluene and filtered. The filtrate was evaporated under reduced pressure to 50 mL when a precipitate began to form. The solution was warmed to re-dissolve the precipitate, and then cooled to -20 °C, yielding orange plates. Yield 7.3g (69%). ^{1}H NMR (CD_2Cl_2): δ 3.83 ($\upsilon_{1/2}$ = 38 Hz). ^{19}F NMR (CD_2Cl_2): δ -98.8 (s). IR (Nujol mull): 2920 (vs), 2880 (w), 2730 (w), 2140 (w), 1460 (s), 1380 (s), 1320 (s), 1220 (s), 1192 (m), 1028 (s), 804 (w), 770 (vw), 724 (m), 631 (s), 581 (w), 520 (m), 390 (w), 370 (w), 320 (s), 280 (w) cm^{-1}. Anal. Calcd for $C_{21}H_{30}CeF_3O_3S$: C, 45.07; H, 5.40. Found C, 44.76; H, 5.13. M.P.: 347-349 °C. (VT done)

Preparation of $Cp^*_2CeN(SiMe_3)_2$

Cp^*_2CeOTf (0.74 g, 1.3 mmol) and $NaN(SiMe_3)_2$ (0.23 g, 1.3 mmol) were dissolved in 100 mL pentane and the mixture was stirred overnight. The red suspension was filtered and the filtrate was concentrated under reduced pressure to 50 mL when a precipitate began to form. The solution was warmed to re-dissolve the precipitate, and then cooled to -20 °C, yielding red plates. Yield 0.6g (81%). The ^{1}H NMR spectrum was identical to the literature value.[8] Crystals suitable for X-ray diffraction were grown from cyclohexene by Dr. C.F. Choi.

Preparation of (1,3-di-tert-butylcyclopentadienyl)$_2$CeN(SiMe$_3$)$_2$[9]

Bis(di-t-butylcyclopentadienyl)cerium triflate[3] (8.4 g, 13 mmol) was stirred with sodium bis(trimethylsilyl)amide (2.4 g, 13 mmol) in 75 mL of diethyl ether for 30 hours at room temperature. The solvent was removed under reduced pressure, and the solid was triturated twice with hexane to remove most of the residual diethyl ether. The solids were extracted with hexane, concentrated, and chilled to -40 °C. At first, only deep blue crystals of tris(di-t-butylcyclopentadienyl)cerium were produced. After filtration, the filtrate was concentrated to approximately 5 mL and cooled to -40 °C. Deep red crystals formed. Yield 3.7 g (44%). Mp 220-223 °C. IR: 1250 (s), 1205 (w), 1170 (w), 1060 (m), 1010 (s), 935 (w), 870 (s), 840 (w), 820 (m), 810 (s), 770 (w), 750 (m), 725 (w), 680 (w), 660 (w), 395 (w), 375 (w) cm^{-1}. ^{1}H NMR: -5.8 (18H, $\nu_{1/2}$ = 28 Hz), -3.3 (36H, $\nu_{1/2}$ = 14 Hz), 23.5 (4H, $\nu_{1/2}$ = 95 Hz). MS (EI): m/z 654 (M+). Parent ion isotopic cluster simulation: (calc. %, obs. %); 654 (100, 100), 655 (47, 45), 656 (30, 29), 657 (10, 10), 658 (3, 3). Anal Calcd for $C_{22}H_{60}CeNSi_2$: C, 58.7; H, 9.2; N, 2.14. Found: C, 58.5; H, 9.5; N, 2.15.

Preparation of Cp*$_2$Ce(1-amido-2-amido-benzene)

Cp*$_2$CeN(SiMe$_3$)$_2$ (0.44 g, 0.78 mmol) and 1,2-diaminobenzene (0.084 g, 0.78 mmol) were stirred in 30 mL of pentane overnight. A white solid precipitated from the purple solution. The purple suspension was filtered and the filtrate was concentrated under reduced pressure until a solid began to precipitate; the solution was not reheated to dissolve the solid, but the solution was cooled to -20 °C overnight. Purple crystals formed. Yield 0.08 g (20%). ^{1}H NMR (C_6D_6): δ -29.30 (2H, $\nu_{1/2}$ = 200 Hz), -9.32 (1H, $\nu_{1/2}$ = 200 Hz), -0.07 (1H, $\nu_{1/2}$ = 30 Hz), 2.38 (30H, $\nu_{1/2}$ = 20 Hz), 5.08 (1H, $\nu_{1/2}$ = 25 Hz),

5.31 (1H, $v_{1/2}$ = 25 Hz). The half-life ($t_{½}$) in C_6D_6 is 21 days at room temperature. The pure solid decomposed at 150 °C and in tol-d_8 it decomposed at 60° C. (Crystal structure and VT done)

Preparation of (1,3-di-tert-butyl-cyclopentadienyl)$_2$Ce(1-amido-2-amido-benzene)

(1,3-ditbutyl-cyclopentadiene) $_2$CeN(SiMe$_3$)$_2$ (0.58 g, 0.88 mmol) and 1,2-diaminobenzene (0.096 g, 0.88 mmol) were stirred in 30 mL of pentane overnight. The red-purple solution was filtered and the filtrate was concentrated under reduced pressure until a solid began to precipitate. The solution was reheated to dissolve the solid, then the solution was cooled to -20 °C overnight. Red crystals formed. Yield 0.35 g (66%). ^{1}H NMR (C_6D_6): δ -7.13 (36H, $v_{1/2}$ = 30 Hz), -1.82 (2H, $v_{1/2}$ = 60 Hz), 6.82 (1H, $v_{1/2}$ = 9 Hz), 7.97 (2H, $v_{1/2}$ = 30 Hz), 9.18 (1H, $v_{1/2}$ = 9 Hz), 12.10 (1H, $v_{1/2}$ = 9 Hz), 22 (1H, $v_{1/2}$ = 900 Hz), 29.02 (1H, $v_{1/2}$ = 300 Hz). The solid decomposes at 107 °C. Anal. Calcd for $C_{32}H_{49}CeN_2$: C, 63.86; H, 8.21; N, 4.65. Found: C, 63.85; H, 8.38; N, 5.00.

Preparation of Cp*$_2$La(OTf)(pyridine)

MgCp*$_2$ (6.11 g, 2.7 mmol) and dry La(OTf)$_3$ (12.15 g, 2.7 mmol) in 50 mL of a 1:10 pyridine:toluene were stirred overnight. The green-yellow solution was then taken to dryness and the green-yellow residue was dissolved in 300 mL of diethylether. The suspension was filtered, and the filtrate was concentrated to 100 mL, then warmed to re-dissolve the precipitate and the solution was cooled to -20 °C. Light green crystals of Cp*$_2$La(OTf)(pyridine) formed. Yield 2.40 g (18 %). ^{1}H NMR (C_6D_6): δ 1.92 (s, 30H), 6.56 (t, 1H, J = 7 Hz), 6.84 (t, 2H, J = 8 Hz), 8.32 (d, 2H, J = 5 Hz). ^{19}F NMR (C_6D_6): δ -76.7 (s). Anal. Calcd for $C_{26}H_{35}NF_3LaO_3S$: C, 48.98; H, 5.53; N, 2.20. Found C, 49.12; H, 5.26; N, 2.20. M.P.: 363-367 °C.

Preparation of $Cp^*_2Sm(OTf)(pyridine)$

$MgCp^*_2$ (2.0 g, 6.7 mmol) and dry $Sm(OTf)_3$ (1.97 g, 6.7 mmol) in 50 mL of a 1:10 pyridine:toluene mixture were stirred overnight. The red solution was taken to dryness the residue was dissolved in 100 mL of diethylether. The suspension was filtered, concentrated to 50 mL, warmed to re-dissolve the precipitate then cooled to -20 °C. Light yellow crystals of $Cp^*_2Sm(OTf)(pyridine)$ formed. Yield 3.3 g (75%). ^1H NMR (C_6D_6): δ 0.87 (30H, $\upsilon_{1/2}$ = 40 Hz), 4.90 (2H, $\upsilon_{1/2}$ = 200 Hz), 5.67 (1H, $\upsilon_{1/2}$ = 120 Hz). The ortho hydrogen was not observed at 20 °C. ^{19}F NMR (C_6D_6): δ -78.0. Anal. Calcd for $C_{26}H_{35}NF_3LaO_3S$: C, 48.12; H, 5.44; N, 2.16. Found C, 48.32; H, 5.40; N, 2.30. M.P.: 212-214 °C.

Preparation of $Cp^*_2Sm(OTf)$

$MgCp^*_2$ (12.4 g, 42.1 mmol) was stirred with dry $Sm(OTf)_3$ (25.2 g, 42.2 mmol) in 80 mL of refluxing di-n-butylether for two weeks. The deep maroon solution was taken to dryness and heated at 80 °C for 6 hours to remove all of the ether. The red powder was extracted with 300 mL of diethyl-ether and then again with 150 mL of diethylether and the combined extracts were filtered and the filtrate was concentrated to 300 mL. The solution was heated to dissolve the $Cp^*_2Sm(OTf)$ and the solution was cooled to -20 °C overnight. Dark red crystals of $Cp^*_2Sm(OTf)$ formed. The mother liquor was filtered and concentrated to 50 mL to get a second crop of crystals. Yield 18.7 g (78%) Anal. Calcd for $C_{21}H_{30}SmF_3O_3S$: C, 44.26; H, 5.31. Found C, 44.25; H, 5.31. ^1H NMR (C_6D_6): δ 0.95. ^{19}F NMR (C_6D_6): δ -82.41. M.P. 348 °C.

Preparation of $Cp^*_2Gd(OTf)$

$MgCp^*_2$ (7.4 g, 25.2 mmol) was stirred with dry $Gd(OTf)_3$ (15.3g, 25.2 mmol) in 50 mL of refluxing di-n-butylether for two weeks. The orange solution was taken to dryness and heated at 80 °C for 6 hours to remove all of the ether. The light orange powder was extracted with 300 mL diethylether and then again with 150 mL ether, and the combined extracts were filtered and concentrated to 150 mL. The solution was heated to dissolve the $Cp^*_2Gd(OTf)$ and cooled to -20 °C overnight. Very pale orange crystals of $Cp^*_2Gd(OTf)$ formed. The mother liquor was filtered and concentrated to 50 mL to get a second crop of crystals. Yield 10.2 g (70%). Anal. Calcd for $C_{21}H_{30}GdF_3O_3S$: C, 43.73; H, 5.24. Found C, 42.38; H, 4.98. IR (Nujol mull): 2930 (vs), 2849 (vs), 2425 (w), 2730 (w), 1457 (s), 1378 (s), 1327 (m), 1272(m), 1224 (s), 1033 (s), 801 (w), 723 (w), 632 (m), 519 (w) cm^{-1}. M.P. >360 °C.

Preparation of $Cp^*_2Yb(OTf)(pyridine)$

$MgCp^*_2$ (6.1 g, 20.8 mmol) was stirred with dry $Yb(OTf)_3$ (12.9g, 20.8 mmol) in 50 mL of a 1:10 mixture of pyridine:toluene. The purple solution warmed and was stirred overnight. The solution was then taken to dryness and the purple powder was dissolved in 100 mL of diethylether. The suspension was filtered and the filtrate was concentrated to 50 mL, warmed to dissolve the $Cp^*_2Yb(OTf)(pyridine)$ and cooled to -20 °C overnight. Dark purple block crystals of $Cp^*_2Yb(OTf)(pyridine)$ formed. Yield 12.6g (90%). ^1H NMR (C_6D_6): δ 3.83 (30H, $\upsilon_{1/2}$ = 60 Hz), 25.54 (1H, $\upsilon_{1/2}$ = 80 Hz). The ortho and meta hydrogens were not observed at 20 °C. ^{19}F NMR (C_6D_6): δ -51.0 (s) Anal. Calcd for

$C_{26}H_{35}NF_3O_3SYb$: C, 46.49; H, 5.25; N, 2.09. Found C, 46.35; H, 4.94; N, 2.43. M.P.: 211 °C. (VT done)

Preparation of Cp*$_2$Yb(OTf)(dimethylaminopyridine)

Cp*$_2$Yb(OTf)(pyridine) (0.28g, 0.42 mmol) and dimethylaminopyridine (0.10g, 0.84 mmol) were stirred in 50 mL of toluene. The purple solution was concentrated to 30 mL, warmed to dissolve the Cp*$_2$Yb(OTf)(dimethylaminopyridine) and then cooled at -20 °C overnight. Dark purple crystals formed. Yield 0.19 g (63%). ^{1}H NMR (tol-d_8): δ 3.54 (30H, $\upsilon_{1/2}$ = 60 Hz), 9.46 (6H, $\upsilon_{1/2}$ = 150 Hz) (see text). ^{19}F NMR (tol-d_8): δ -37.3 (s) Anal. Calcd for $C_{28}H_{40}N_2F_3O_3SYb$: C, 47.05; H, 5.64; N, 3.92. Found C, 47.44; H, 5.81; N, 3.93. M.P.: 240-241 °C. (VT done)

Preparation of Cp*$_2$Yb(OTf)

Cp*$_2$Yb(OTf)(pyridine) (5.0 g, 9.6 mmol) was heated at 160 °C in diffusion-pump vacuum for a week. The compound remained purple. The purple powder was dissolved in 200 mL toluene, filtered and the filtrate was concentrated to 70 mL and then cooled to -20 °C overnight. Dark purple block crystals of base-free Cp*$_2$YbOTf formed. Yield 4.6 g (82%). ^{1}H NMR (C_6D_6): δ 3.83 ($\upsilon_{1/2}$ = 2400 Hz). ^{19}F NMR (C_6D_6): δ 13.34. Anal. Calcd for $C_{21}H_{30}F_3O_3SYb$: C, 42.57; H, 5.10. Found C, 42.25; H, 5.13. M.P.: 250-252 °C. (VT done in toluene, THF and CD_2Cl_2)

Preparation of $[NMe_4][Cp^*_2CeOTf_2]\cdot$(0.5 toluene)

$[NMe_4][OTf]$ was prepared by titrating an aqueous tetramethylammonium hydroxide solution with an aqueous trifluoromethanesulfonic acid solution. It was purified by multiple crystallizations from acetone.[10] Water was removed by heating at 60 °C until the OH stretch in the IR spectrum disappeared (approximately 2 days). Cp^*_2CeOTf (1.0g, 1.8 mmol) and $[NMe_4][OTf]$ (0.4g, 1.8 mmol) were stirred in 30 mL of toluene overnight. The toluene was filtered and the yellow powder was dissolved in 10 mL of CH_2Cl_2, filtered and the filtrate was layered with pentane. Small yellow block crystals formed over the period of a week. Yield 0.3g (21%). ^{1}H NMR (CD_2Cl_2): δ 1.32 (12H, $\upsilon_{1/2}$ = 10 Hz), 4.40 (30H, $\upsilon_{1/2}$ = 40 Hz) . ^{19}F NMR (CD_2Cl_2): δ -87.6. Anal. Calcd for $C_{29.5}H_{46}CeF_6NO_6S_2$: C, 42.75; H, 5.59; N, 1.69. Found C, 42.92; H, 5.58; N, 1.64. (Crystal structure done)

Preparation of $[NEt_4][Cp^*_2CeOTf_2]$

Cp^*_2CeOTf (1.0g, 1.8 mmol) and $[NEt_4][OTf]$ (0.5g, 1.8 mmol) were stirred in 30 mL of toluene overnight. The toluene was filtered and the yellow powder was dissolved in 10 mL of CH_2Cl_2, filtered and the filtrate was layered with pentane. Small yellow block crystals formed over the period of a week. Yield (0.6g, 40%). ^{1}H NMR (CD_2Cl_2): δ 0.67 (12H, $\upsilon_{1/2}$ = 40 Hz), 2.31 (8H, $\upsilon_{1/2}$ = 40 Hz), 4.51 (30H, $\upsilon_{1/2}$ = 60 Hz) . ^{19}F NMR (CD_2Cl_2): δ -79.4. Anal. Calcd for $C_{30}H_{50}CeF_6NO_6S_2$: C, 42.95; H, 6.00; N, 1.67. Found C, 42.94; H, 6.16; N, 1.83. (Crystal structure and VT done)

Preparation of [NBu_4][$Cp^*_2CeOTf_2$]

Cp^*_2CeOTf (0.75g, 1.3 mmol) and [NBu_4][OTf] (0.48g, 1.2 mmol) were stirred in 30 mL of toluene overnight. The toluene was removed under reduced pressure, and the yellow powder was washed with pentane. Yield (1.0g, 90%). ^{1}H NMR (CD_2Cl_2): δ 0.67 (t, 12H, J = 7 Hz), 0.86 (t, 8H, J = 7 Hz), 1.90 (t, 8H, J = 8 Hz), 4.43 (30H, $\upsilon_{1/2}$ = 80 Hz) . ^{19}F NMR (CD_2Cl_2): δ -87.50 ($\upsilon_{1/2}$ = 320 Hz). Anal. Calcd for $C_{38}H_{66}CeF_6NO_6S_2$: C, 47.98; H, 6.99; N, 1.47. Found C, 47.67; H, 6.91; N, 1.56. M.P. 124-127 °C.

Preparation of [NEt_4][$Cp^*_2YbOTf_2$]

$Cp^*_2YbOTf(pyr)$ (1.14g, 1.70 mmol) and [NEt_4][OTf] (0.47g, 1.70 mmol) were stirred in 30 mL of toluene. The toluene was filtered and the purple powder was dissolved in 10 mL of CH_2Cl_2, filtered, and the filtrate was layered with pentane. Small purple block crystals formed over the period of a week. Yield 1.3 g (88%). ^{1}H NMR (CD_2Cl_2): δ -0.09 (12H, $\upsilon_{1/2}$ = 10 Hz), 1.77 (8H, $\upsilon_{1/2}$ = 10 Hz), 7.66 (30H, $\upsilon_{1/2}$ = 40 Hz) . ^{19}F NMR (CD_2Cl_2): δ -46.9. Anal. Calcd for $C_{30}H_{50}F_6NO_6S_2Yb$: C, 41.33; H, 5.78; N, 1.61. Found C, 41.23; H, 5.75; N, 1.56. (VT done)

Chapter 2

Preparation of Cp^*_2Ce(2,2'-bipyridine)(OTf)

$Cp^*_2Ce(OTf)$ (1.4g, 2.4 mmol) and 2,2'-bipyridine (0.41g, 2.6 mmol) were mixed in 50 mL of pentane. After stirring the suspension overnight, the solvent was filtered and the yellow-red powder was dissolved in a minimum amount of CH_2Cl_2 and the filtrate was layered with pentane to give red crystals. The product is insoluble in pentane and toluene, and decomposes in THF. Yield 0.58g (33%). ^{1}H NMR (CD_2Cl_2): δ 4.90 ($\upsilon_{1/2}$ = 16 Hz). None of the bipy resonances were observed at 20 °C (see text). ^{19}F NMR (CD_2Cl_2): δ -82.05 (s). IR (Nujol mull): 2920 (vs), 2710(w), 1600 (s), 1592(s), 1570 (m), 1490 (w), 1478 (w), 1460 (s), 1430 (w), 1380 (s), 1318 (m), 1300 (s), 1280 (m), 1260 (w), 1230 (s), 1210 (s), 1181 (m), 1155 (s), 1099 (w), 1063 (w), 1020 (s), 1010 (w), 800 (m), 769 (s), 740 (m), 720 (w), 635 (s) cm^{-1}. Anal. Calcd for $C_{31}H_{38}CeF_3N_2O_3S$: C, 52.02; H, 5.35; N, 3.91. Found C, 52.03; H 5.37; N, 3.91. M.P.: 210-212 °C. (Crystal structure and VT done)

Preparation of Cp^*_2Ce(4,4'-dimethyl-2,2'-bipyridine)(OTf)

$Cp^*_2Ce(OTf)$ (1.2g, 2.14 mmol) and 4,4'-dimethyl-2,2'-bipyridine (0.44 g, 2.4 mmol) were mixed in 50 mL of pentane. After stirring the suspension overnight, the solvent was filtered and the yellow-red powder was dissolved in a minimum amount of CH_2Cl_2 and the filtrate was layered with pentane to give reddish-brown crystals. Yield 1.34g (84%). ^{1}H NMR (CD_2Cl_2): δ 0.07 (6H, $\upsilon_{1/2}$ = 79 Hz), 4.80 (30H, $\upsilon_{1/2}$ = 48 Hz). Not all the 4,4'-dimethyl-2,2'-bipyridyl resonances were observed at 25 °C (see text). ^{19}F NMR (CD_2Cl_2): δ -82.16 (s). IR (Nujol mull): 2920 (vs), 2855 (w), 2720 (w), 2670 (w),

1615 (w), 1520 (s), 1379 (s), 1312 (w), 1262 (m), 1230 (w), 1210 (m), 1168 (w), 1090 (w), 1020 (m), 800 (s), 720 (m) cm^{-1}. Anal. Calcd for $C_{33}H_{42}CeF_3N_2O_3S$: C, 53.28; H, 5.69; N, 3.77. Found C, 53.10; H, 5.53; N, 3.64. M.P.: 250-252 °C. (VT done)

NMR tube reaction of Cp*$_2$Ce(2,2'-bipyridine)(OTf) and 4,4'-dimethyl-2,2'-bipyridine

2,2'-Bipyridyl was added to half an equivalent of Cp*$_2$Ce(2,2'-bipyridine)(OTf) and dissolved in CD_2Cl_2. The ^{1}H NMR indicates no exchange. 5 equivalents of 4,4'-dimethyl-2,2'-bipyridine were added to this mixture. ^{1}H NMR (CD_2Cl_2): δ 2.42 (4,4'-dimethyl-2,2'-bipyridine, s, 12H), 4.79 (Cp*$_2$Ce(4,4'-dimethyl-2,2'-bipyridine)(OTf), 30H, $\upsilon_{1/2}$ = 14 Hz), 4.88 (Cp*$_2$Ce(2,2'-bipyridine)(OTf), 3H, $\upsilon_{1/2}$ = 25 Hz), 7.13 (4,4'-dimethyl-2,2'-bipyridine, d, 4H, *J*=5 Hz), 7.31 (2,2'-bipyridine, t, 2H, *J*=8 Hz), 7.81 (bipy, t, 2H, *J*=9 Hz), 8.25 (4,4'-dimethyl-2,2'-bipyridine, s, 2H), 8.41 (bipy, d, 2H, *J*=8 Hz), 8.48 (4,4'-dimethyl-2,2'-bipyridine, d, 4H, *J* = 5 Hz), 8.64 (bipy, d, 2H, *J*=8 Hz). Another 10.5 equivalents of bipy were added. ^{1}H NMR (CD_2Cl_2): δ 2.42 (4,4'-dimethyl-2,2'-bipyridine, s, 15H), 4.77 (Cp*$_2$Ce(4,4'-dimethyl-2,2'-bipyridine)(OTf), 24H, $\upsilon_{1/2}$ = 11 Hz), 4.87 (Cp*$_2$Ce(2,2'-bipyridine)(OTf), 9H, $\upsilon_{1/2}$ = 13 Hz), 7.13 (4,4'-dimethyl-2,2'-bipyridine, d, 5H, *J*=5 Hz), 7.30 (bipy, t, 14H, *J* = 6 Hz), 7.81 (bipy, t, 14H, *J* = 8 Hz), 8.02 (4,4'-dimethyl-2,2'-bipyridine, s, 5H), 8.23 (bipy, d, 14H, *J*=12 Hz), 8.48 (4,4'-dimethyl-2,2'-bipyridine, d, 5H, *J* = 5 Hz), 8.64 (bipy, d, 14H, *J*=8 Hz).

Preparation of Cp^*_2Ce(1,10-phenanthroline)(OTf)

Cp^*_2CeOTf (1.42g, 2.54 mmol) and 1,10-phenanthroline (0.47g, 2.6 mmol) were mixed in 50 mL of pentane. After stirring the suspension overnight, the solvent was filtered and the yellow-red powder was dissolved in a minimum amount of CH_2Cl_2 and the filtrate was layered with pentane to give brown crystals. Yield 0.95g (51%). ^{1}H NMR (CD_2Cl_2): δ -17.37 (1H, $\upsilon_{1/2}$ = 690 Hz), -13.40 (1H, $\upsilon_{1/2}$ = 115 Hz), 4.74 (30H, $\upsilon_{1/2}$ = 32 Hz), 5.70(1H, $\upsilon_{1/2}$ = 64 Hz) (see text). ^{19}F NMR (CD_2Cl_2): δ -81.57 (s). IR (Nujol mull): 2920 (vs), 2855 (w), 2720 (w), 1625 (w), 1592 (w), 1578 (w), 1518 (m), 1510 (s), 1420 (w), 1379 (s), 1312 (s), 1261 (s), 1232 (s), 1210 (s), 1162 (m), 1100 (m), 1020 (s), 862 (w), 842 (m), 800 (s), 730 (m), 720 (w), 632 (s), 588 (w), 521 (m), 480 (w), 390 (m), 303 (m) cm^{-1}. Anal. Calcd for $C_{33}H_{38}CeF_3N_2O_3S$: C, 53.57; H, 5.18; N, 3.79. Found C, 53.22; H, 5.19; N, 3.71. M.P.: 335-337 ˚C. (VT done)

Preparation of Cp^*_2Ce(4,4'-dicarbomethoxy-2,2'-bipyridine)(OTf)

Cp^*_2CeOTf (0.45 g, 0.80 mmol) and 4,4'-dicarbomethoxy-2,2'-bipyridine (0.22 g, 0.80 mmol) were mixed in 50 mL of pentane. After stirring the suspension overnight, the solvent was filtered and the dark purple-brown powder was dissolved in a minimum amount of CH_2Cl_2 and the filtrate was layered with pentane to give dark brown crystals. Yield 0.20g (30%). ^{1}H NMR (CD_2Cl_2): δ -20 (2H, $\upsilon_{1/2}$ = 3000 Hz), 2.81 (6H, $\upsilon_{1/2}$ = 8 Hz), 3.85 (2H, $\upsilon_{1/2}$ = 40 Hz), 5.02 (30H, $\upsilon_{1/2}$ = 32 Hz). ^{19}F NMR (CD_2Cl_2): δ -82.11 (s). Anal. Calcd for C_{35}, H_{42}, Ce, F_3, N_2, O_7, S: C, 50.53; N, 5.09; H, 2.37. Found: C, 49.21; H, 4.96; N, 3.24. M.P. 200-212 °C. IR (Nujol mull): 2916 (vs), 2726 (w), 1737 (s), 1613 (w), 1560 (w), 1459 (vs), 1378 (s), 1316 (s), 1279 (s), 1228 (s), 1207 (s), 1160 (m), 1132

(w), 1117 (w), 1018 (s), 987 (w), 961 (w), 807 (w), 870 (w), 786 (w), 761 (s), 721 (m), 695 (w), 666 (w), 634 (s), 577 (w), 514 (m). (VT done)

Preparation of Cp*$_2$Ce(2,2',6',2''-terpyridine)(OTf)

Cp*$_2$CeOTf (0.86g, 1.5 mmol) and 2,2',6',2''-terpyridine (0.36g, 1.5 mmol) were mixed in 50 mL pentane. After stirring the suspension overnight, the solvent was filtered and the red powder was dissolved in a minimum amount of CH_2Cl_2 and the filtrate was the filtrate was layered with pentane to give a red powder. Yield 0.95g (53%). The compound is insoluble in pentane and toluene. Crystals suitable for X-ray crystallography were grown by dissolving the powder in 10 mL of dichloromethane and adding pentane until a precipitate formed. A small amount of dichloromethane was added with stirring to dissolve the precipitate, a layer of dichloromethane was added without stirring, and then the solution was layered with pentane. ^{1}H NMR (CD_2Cl_2): δ -17.92 (2H, $\upsilon_{1/2}$ = 23 Hz), 2.42 (d, 2H, J = 8 Hz), 3.63 (d, 2 H, J = 8 Hz), 3.69 (d, 2H, J = 8 Hz), 4.40 (d, 30H, $\upsilon_{1/2}$ = 12 Hz), 5.58 (d, 2H, J = 8 Hz), 5.87 (t, 1H, J = 8 Hz). ^{19}F NMR (CD_2Cl_2): δ -79.87. IR (Nujol mull): 2920 (vs), 2710(w), 1596 (s), 1570 (m), 1460 (s), 1378 (s), 1308 (w), 1266 (s), 1237 (w), 1150 (s), 1090 (w), 1033 (s), 1010 (w), 800 (s), 780 (s), 722 (s), 640 (s) cm^{-1}. Anal. Calcd for $C_{36}H_{41}CeF_3N_2O_3S$: C, 54.40; H, 5.20; N, 5.29. Found C, 54.10; H, 5.07; N, 5.29. M.P.: 288-292 $^{\circ}$C. (Crystal structure and VT done)

NMR tube reaction of Cp*$_2$Ce(terpy)(OTf) and Cp*$_2$CeOTf

Cp*$_2$CeOTf was dissolved in CD_2Cl_2 in an NMR tube, and Cp*$_2$Ce(terpy)(OTf) was added. ^{1}H NMR (CD_2Cl_2): δ -18.40 (2H, $\upsilon_{1/2}$ = 40 Hz), 2.294 (4H, $\upsilon_{1/2}$ = 15 Hz), 3.022 (d, 2H, J = 8 Hz), 3.070 (d, 2H, J = 8 Hz), 4.193 (new Cp*$_2$Ce(L)(X) peak, 21H, $\upsilon_{1/2}$ = 19 Hz), 4.385 (Cp*$_2$Ce(terpy)(OTf) 30H, $\upsilon_{1/2}$ = 8 Hz). ^{19}F NMR (CD_2Cl_2): δ -87.64

($\upsilon_{1/2}$ = 576 Hz). Comparison of the ^{19}F VT NMR spectra of the mixture with those of the ^{19}F VT NMR of [NEt_4][$Cp^*_2CeOTf_2$] indicate that [Cp^*_2Ce(terpy)][$Cp^*_2CeOTf_2$] is formed.

Preparation of Cp^*_2Ce(2,2'-bipyridine)(Cl)

$Cp^*_2CeCl\cdot(CH_3CN)_2$ (0.22g, 0.4 mmol) was sublimed to remove the coordinated CH_3CN. 2,2'-Bipyridine (0.07 g, 0.4 mmol) was added and the mixture was stirred in 50 mL of pentane overnight. The solvent was then filtered and the yellow powder was dissolved in a minimum amount of CH_2Cl_2 and the filtrate was layered with pentane to give a brown-yellow crystals. Yield 0.17 g (68%). ^{1}H NMR (CD_2Cl_2): δ -16.527 (1H, $\upsilon_{1/2}$ = 40 Hz), -0.550 (1H, $\upsilon_{1/2}$ = 40 Hz), 0.393 (d, 1H, J = 6Hz), 2.955 (d, 1H, J = 8Hz), 4.109 (30H, $\upsilon_{1/2}$ = 80 Hz), 4.791 (d, 1H, J = 8Hz), 6.536 (d, 1H, J = 7Hz), 7.682 (t, 1H, J = 8Hz). One of the bipy resonances was not located. IR (Nujol mull): 2920 (vs), 1598 (w), 1460 (s), 1379 (m), 1320 (w), 1260 (m), 1178 (w), 1158 (m), 1048 (m), 1010 (w), 900 (w), 800 (m), 770 (s), 740 (w), 720 (w), 640 (m), 300 (m) cm^{-1}. Anal. Calcd for $C_{30}H_{38}CeN_2Cl$: C, 59.83; H, 6.36; N, 4.65. Found C, 59.45; H, 6.36; N, 4.58. M.P.: 261-265 $^\circ$C. (Crystal structure done)

Preparation of Cp^*_2Ce(2,2'-bipyridine)(I)

$Cp^*_2CeI\cdot(CH_3CN)_2$ (2.4g, 3.9 mmol) was ground and dried *in vacuo* overnight at 95 $^\circ$C. 2,2'-Bipyridine (0.58g, 3.7mmol) was added and mixed in dichloromethane. The dark brown liquid was filtered, taken to dryness, washed with pentane, and crystallized by layering pentane on dichloromethane. Yield 1.8g (70%). ^{1}H NMR (CD_2Cl_2): δ -21.58 (2H, $\upsilon_{1/2}$ = 300 Hz), 1.50 (2H, $\upsilon_{1/2}$ = 30 Hz), 4.21 (d, 2H, J = 8 Hz), 5.24 (2H, $\upsilon_{1/2}$ = 22 Hz), 5.43 (30H, $\upsilon_{1/2}$ = 20 Hz). The ^{1}H NMR is similar to that reported in THF-d_8 in which

the crystal structure is also presented. [14] Anal. Calcd for $C_{30}H_{38}CeN_2I$: C, 51.95; H, 5.52; N, 4.04. Found C, 52.08; H, 5.55; N, 4.01. M.P.: 240-243 °C.

Preparation of [Cp*$_2$Ce(2,2'-bipyridine)][BPh$_4$]

Cp*$_2$Ce(2,2'-bipyridine)(OTf) (0.60 g, 0.84 mmol) and $NaBPh_4$ (0.57 g,1.6 mmol) were stirred in pentane overnight. The pentane was filtered and the green powder was dissolved in 10 mL CH_2Cl_2 filtered and the filtrate was layered with pentane. Green plate crystals formed. Yield 0.50 g (67%). Anal. Calcd for $C_{54}H_{58}N_2BCe$: C, 73.21; H, 6.60; N, 3.16. Found C, 71.80; H, 6.39; N, 3.22.[11] ^{1}H NMR (CD_2Cl_2): δ -46.13 (2H, $\upsilon_{1/2}$ = 320 Hz), -2.04 (d, 2H, J = 7 Hz), 3.40 (30H, $\upsilon_{1/2}$ = 120 Hz), 3.82 (d, 2H, J = 9 Hz), 3.97 (t, 2H, J = 8), 6.55 (12H), 6.69 (d, 8H, J = 2 Hz). ^{11}B NMR (CD_2Cl_2): δ -7.42. IR (Nujol mull): 2883 (vs), 1593 (m), 1559 (w), 1464 (s), 1376 (s), 1313 (w), 1261 (w), 1159 (w), 1091 (w), 1017 (m), 844 (w), 771 (m), 732 (s), 706 (s), 611 (s). (Crystal structure and VT done).

Preparation of [Cp*$_2$Ce(4,4'-dimethyl-2,2'-bipyridine)][BPh$_4$]:

Cp*$_2$Ce(4,4'-dimethyl-2,2'-bipyridine)(OTf) (1.1 g, 1.5 mmol) and $NaBPh_4$ (1.0 g, 3.0 mmol) were stirred in 50 mL of pentane overnight. The pentane was filtered and the green powder was dissolved in 10 mL CH_2Cl_2, filtered, and the filtrate was layered with pentane. Green plate-like crystals formed. Yield 1.3 g (93%). Anal. Calcd for $C_{56}H_{62}N_2BCe$: C, 73.59; H, 6.84; N, 3.07. Found C, 68.31; H, 6.44; N, 2.94.[11] ^{1}H NMR (CD_2Cl_2): δ -49.72 (2H, $\upsilon_{1/2}$ = 60 Hz), -2.78 (2H, $\upsilon_{1/2}$ = 30 Hz), -0.75 (6H, $\upsilon_{1/2}$ = 20 Hz), 3.38 (30H, $\upsilon_{1/2}$ = 90 Hz), 3.96 (2H, $\upsilon_{1/2}$ = 20 Hz), 6.52 (12H), 6.70 (8H). (VT done)

Preparation of [Cp*$_2$Ce(5,5'-dimethyl-2,2'-bipyridine)][BPh$_4$]

Cp*$_2$Ce(OTf) (0.40 g, 0.71 mmol), 5,5'-dimethyl-2,2'-bipyridine (0.13 g, 0.71 mmol) and $NaBPh_4$ (0.24 g, 1.4 mmol) were stirred in 50 mL of pentane overnight. The pentane was filtered and the green powder was dissolved in CH_2Cl_2, filtered, and the filtrate was layered with pentane. Green plate-like crystals formed. Yield 0.3 g (39%). Anal. Calcd for $C_{56}H_{62}N_2BCe$: C, 73.59; H, 6.84; N, 3.07. Found C, 73.36; H, 6.61; N, 3.41.[11] ^{1}H NMR (CD_2Cl_2): δ -48.27 (2H, $\upsilon_{1/2}$ = 200 Hz), -5.07 (6H, $\upsilon_{1/2}$ = 16 Hz), 3.41 (30H, $\upsilon_{1/2}$ = 60 Hz), 3.71 (d, 2H, J = 8 Hz), 3.84 (d, 2H, J = 9 Hz), 6.76 (12H $\upsilon_{1/2}$ = 16 Hz), 6.90 (8H, $\upsilon_{1/2}$ = 16 Hz). IR (Nujol Mull): 2891 (vs), 2724 (w), 1604 (w), 1573 (m), 1463 (s), 1377 (s), 1312 (m), 1229 (m), 1207 (m), 1162 (m), 1097 (w), 1044 (w), 1019 (m), 824 (m), 733 (m), 704 (m), 634 (m), 605 (w), 530 (w), 466 (w). (VT done)

Preparation of [Cp*$_2$Ce(6,6'-dimethyl-2,2'-bipyridine)][BPh$_4$]

Cp*$_2$Ce(OTf) (1.10 g, 2.0 mmol), 6,6'-dimethyl-2,2'-bipyridine (0.36 g, 2.0 mmol) and $NaBPh_4$ (1.0 g, 3.0 mmol) were stirred in 50 mL of pentane for two days. The pentane was filtered and the red powder was dissolved in CH_2Cl_2, filtered, and the filtrate was layered with pentane. Red plate crystals formed. Yield 0.9 g (49%). Anal. Calcd for $C_{56}H_{62}N_2BCe$: C, 73.59; H, 6.84; N, 3.07. Found C, 67.72; H, 6.01; N, 3.15.[11] ^{1}H NMR (CD_2Cl_2): δ -48.99 (6H, $\upsilon_{1/2}$ = 150 Hz), -1.74 (d, 2H, J = 9 Hz), 4.91 (t, 2H, J = 8 Hz), 5.44 (30H, $\upsilon_{1/2}$ = 60 Hz), 5.94 (d, 2H, J = 8 Hz), 6.66 (12H), 6.92 (8H). (VT done)

Preparation of Cp*$_2$La(2,2'-bipyridine)(OTf)

Cp*$_2$LaOTf(pyridine) (1.2g, 1.9 mmol) and bipy (0.29g, 1.9 mmol) were mixed in 50 mL of pentane with stirring. After stirring the suspension overnight, the solvent was filtered, the red powder was dissolved in 5 mL of CH_2Cl_2 and the filtrate was layered

with pentane. Red crystals form over the course of a week. Yield 0.48g (36%). ^{1}H NMR (CD_2Cl_2): δ 1.73 (s, 30H), 7.70 (t, 2H, J = 6 Hz), 8.14 (td, 2H, J = 8 Hz, J = 2 Hz), 8.26 (d, 2H, J = 8 Hz), 8.92 (2H, $\upsilon_{1/2}$ = 40 Hz). ^{19}F NMR (CD_2Cl_2): δ -76.99 (s). Anal. Calcd for $C_{31}H_{38}N_2F_3LaO_3$: C, 52.10; H, 5.36; N, 3.92. Found C, 51.74; H, 5.00; N, 3.81.

Preparation of Cp*$_2$Sm(2,2'-bipyridine)(OTf)

Cp*$_2$Sm(OTf) (0.60 g, 1.1 mmol) and 2,2'-bipyridine (0.16 g, 1.1 mmol) were stirred in 50 mL of pentane overnight. The pentane was filtered, the red powder was dissolved in CH_2Cl_2, filtered, and the filtrate was layered with pentane. Red block crystals formed. Yield 0.59 g (74%). Anal. Calcd for $C_{31}H_{38}N_2F_3SSmO_3$: C, 51.28; H, 5.28; N, 3.86. Found C, 51.67; H, 5.29; N, 3.89. ^{1}H NMR (CD_2Cl_2): δ 0.76 (2H, $\upsilon_{1/2}$ = 16 Hz) 0.94 (30H), 6.20 (dd, 2H, J = 2.4 Hz), 7.66 (t, 2H, J = 8 Hz), 8.43 (d, 2H, J = 8 Hz). ^{19}F NMR (CD_2Cl_2): δ -77.84. (Crystal structure and VT done)

Preparation of Cp*$_2$Sm(4,4'-dimethyl-2,2'-bipyridine)(OTf)

Cp*$_2$Sm(OTf) (0.73 g, 1.3 mmol) and 4,4'-dimethyl-2,2'-bipyridine (0.24 g, 1.3 mmol) were stirred in 50 mL of pentane overnight. The pentane was filtered, the red powder was dissolved in CH_2Cl_2, filtered, and the filtrate was layered with pentane. Red block crystals formed. Yield 0.83 g (86%). Anal. Calcd for $C_{33}H_{42}N_2F_3SSmO_3$: C, 52.56; H, 5.61; N, 3.71. Found: C, 52.33; H, 5.64; N, 3.82. ^{1}H NMR (CD_2Cl_2): δ -0.103 (2H, $\upsilon_{1/2}$ = 20 Hz) 0.88 (30H), 2.52 (6H, $\upsilon_{1/2}$ = 12 Hz), 5.92 (2H, $\upsilon_{1/2}$ = 8 Hz), 7.99 (2H, $\upsilon_{1/2}$ = 4 Hz). ^{19}F NMR (CD_2Cl_2): δ -77.69. M.P. 206-210 °C. IR (Nujol mull): 2872 (vs), 2726 (w), 2359 (w), 2331 (w), 1615 (s), 1557 (w), 1462 (s), 1377 (s), 1311 (s), 1227 (s), 1212 (s), 1166 (s), 1020 (s), 921 (m), 849 (m), 825 (m), 723 (w), 632 (s), 577 (w), 517 (m). (VT done).

Preparation of [Cp*$_2$Sm(2,2'-bipyridine)][BPh$_4$]

Cp*$_2$Sm(2,2'-bipyridine)(OTf) (0.51 g, 0.7 mmol) and NaBPh$_4$ (0.34 g, 1.0 mmol) were stirred in 50 mL of pentane overnight. The pentane was filtered, the orange powder was dissolved in CH_2Cl_2, filtered, and the filtrate was layered with pentane. Red block crystals formed. Yield 0.50 g (80%). Anal. Calcd for $C_{54}H_{58}N_2BSm$: C, 72.37; H, 6.52; N, 3.13. Found C, 72.05; H, 6.42; N, 3.11. ^{1}H NMR (CD_2Cl_2): δ -12.91 (2H, $\upsilon_{1/2}$ = 20 Hz) 0.56 (30H), 4.42 (d, 2H, J = 5 Hz), 6.88 (t, 4H, J = 7 Hz), 7.03 (t, 8H, J = 7 Hz), 7.38 (8H, $\upsilon_{1/2}$ = 30 Hz), 7.74 (t, 2H, J = 8 Hz), 9.31 (d, 2H, J = 8 Hz). Decomposes at 298-300 °C. (VT done)

Preparation of [Cp*$_2$Sm(4,4'-dimethyl-2,2'-bipyridine)][BPh$_4$]

Cp*$_2$Sm (OTf) (1.06 g, 1.9 mmol), 4,4'-dimethyl-2,2'-bipyridine (0.34 g, 1.8 mmol) and NaBPh$_4$ (1.27 g, 3.7 mmol) were stirred in 50 mL of pentane overnight. The pentane was filtered, the orange powder was dissolved in CH_2Cl_2, filtered, and the filtrate was layered with pentane. Red block crystals formed. Yield 1.10 g (62%). ^{1}H NMR (CD_2Cl_2): δ -12.86 (2H, $\upsilon_{1/2}$ = 30 Hz), 0.61 (30H), 2.66 (6H), 4.29 (s, 2H), 6.79 (t, 4H, J = 7 Hz), 6.92 (t, 8H, J = 7 Hz), 7.23 (8H, $\upsilon_{1/2}$ = 30 Hz), 9.48 (2H). ^{11}B NMR (CD_2Cl_2): δ -6.73 ($\upsilon_{1/2}$ = 30 Hz). IR (Nujol mull): 2875 (vs), 2729 (w), 2406 (w), 1952 (w), 1883 (w), 1815 (w), 1608 (m), 1579 (w), 1552 (w), 1456 (m), 1378 (m), 1306 (m), 1265 (m), 1182 (w), 1138 (m), 1032 (w), 1011 (m), 918 (m), 895 (m), 836 (s), 742 (s), 738 (s), 702 (s), 611 (s), 547 (s), 520 (s), 490 (m), 468 (m), 428 (m).

Preparation of [Cp*$_2$Sm(5,5'-dimethyl-2,2'-bipyridine)][BPh$_4$]

Cp*$_2$Sm (OTf) (0.49 g, 0.86 mmol), 5,5'-dimethyl-2,2'-bipyridine (0.16 g, 0.86 mmol) and NaBPh$_4$ (0.59 g, 1.7 mmol) were stirred in 50 mL of pentane overnight. The pentane was filtered, the orange powder was dissolved in CH_2Cl_2, filtered, and the filtrate was layered with pentane. Red block crystals formed. Yield 0.51 g (63%). ^{1}H NMR (CD_2Cl_2): δ -13.20 (2H, $\upsilon_{1/2}$ = 10 Hz), -0.23 (6H, $\upsilon_{1/2}$ = 3 Hz), 0.61 (30H), 6.98 (t, 4H, J = 7 Hz), 7.14 (t, 8H, J = 7 Hz), 7.50 (8H, $\upsilon_{1/2}$ = 12 Hz), 7.56 (d, 2H, J = 8 Hz), 9.15 (d, 2H, J = 8 Hz). ^{11}B NMR (CD_2Cl_2): δ -6.55 ($\upsilon_{1/2}$ = 3 Hz).

NMR tube addition of 5,5'-dimethyl-2,2'-bipyridine to [Cp*$_2$Sm(4,4'-dimethyl-2,2'-bipyridine)][BPh$_4$]

Addition of 5,5'-dimethyl-2,2'-bipyridine to an NMR tube containing [Cp*$_2$Sm(4,4'-dimethyl-2,2'-bipyridine)][BPh$_4$] shows that there is no exchange on the NMR time scale, but there is exchange on the chemical time scale. Four new peaks attributable to the bipyridine ring in [Cp*$_2$Sm(5,5'-dimethyl-2,2'-bipyridine)][BPh$_4$] appear after 2 hours.

Preparation of Cp*$_2$Gd(2,2'-bipyridine)(Cl)

Cp*$_2$GdCl$_2$Na[12] (0.50 g, 0.96 mmol) and bipy (0.15 g, 0.96 mmol) were stirred in 50 mL pentane. The pentane was filtered, the red powder was dissolved in 10 mL of CH_2Cl_2, filtered, and the filtrate was layered with 100 mL of pentane to grow red crystals suitable for X-ray diffraction. Yield 0.15 g (25 %). (Crystal structure done)

Preparation of [Cp*$_2$Gd(2,2'-bipyridine)][BPh$_4$]

Method 1: Cp*$_2$GdOTf (1.0 g, 1.7 mmol), bipy (0.36 g, 1.7 mmol), and NaBPh$_4$ (1.0 g, 2.9 mmol) were stirred in 20 mL of CH_2Cl_2 overnight. The yellow suspension was

filtered and the filtrate was layered with 80 mL of pentane. Yellow crystals of [Cp^*_2Gd(2,2'-bipyridine)][BPh_4] formed. Yield 1.1 g (68 %). Anal. Calcd for $C_{54}H_{58}BGdN_2$: C, 71.82; H, 6.47; 3.10. Found C, 69.39; H, 6.22; N, 3.13.[11] Decomposes at 268-271 °C. (Crystal structure done)

Method 2: Cp^*_2Gd(2,2'-bipyridine)(Cl) (0.20 g, 0.32 mmol) and $NaBPh_4$ (0.75 g, 2.2 mmol) were stirred in 5 mL CH_2Cl_2 overnight. The suspension was filtered and the filtrate was layered with pentane. Yellow crystals formed. Yield 0.12 g (42%).

Preparation of [Cp^*_2Gd(4,4'-dimethyl-2,2'-bipyridine)][BPh_4]

Cp^*_2GdOTf (1.14 g, 2.0 mmol), 4,4'-dimethyl-2,2'-bipyridine (0.36 g, 2.0 mmol), and $NaBPh_4$ (1.6 g, 4.8 mmol) were stirred in 20 mL of CH_2Cl_2 overnight. The yellow suspension was filtered and the filtrate was layered with 80 mL of pentane. Yellow crystals of [Cp^*_2Gd(4,4'-dimethyl-2,2'-bipyridine)][BPh_4] formed. Anal. Calcd for $C_{56}H_{62}BGdN_2$: C, 72.23; H, 6.71; N, 3.01. Found C, 67.73; H, 6.29; N, 3.04.[11]

Preparation of [Cp^*_2Yb(2,2'-bipyridine)][OTf]/[Cp*2Yb(2,2'-bipyridine)][Cp*2YbOTf$_2$] (see text)

Cp^*_2YbOTf(pyridine) (0.89 g, 1.3 mmol) and bipy (0.21 g, 1.3 mmol) were stirred in 20 mL of pentane overnight. The color changed from dark purple to brown. The pentane was filtered and the brown powder was dissolved in CH_2Cl_2, filtered, and the filtrate was layered with pentane. Brown block crystals formed. Yield 0.69 g (70% yield assuming [Cp^*_2Yb(2,2'-bipyridine)][OTf]; 78% yield assuming [Cp^*_2Yb(2,2'-bipyridine)][Cp^*_2YbOTf$_2$]). ^{1}H NMR (CD_2Cl_2): δ -16.26 (2H, $\upsilon_{1/2}$ = 40 Hz) 3.39 (30H, $\upsilon_{1/2}$ = 120 Hz), 7.69 (2.64H, $\upsilon_{1/2}$ = 80 Hz), 9.03 (2H, $\upsilon_{1/2}$ = 40 Hz), 57.71 (2H, $\upsilon_{1/2}$ = 120

Hz), 338.46 (2H, $\upsilon_{1/2}$ = 400 Hz). ^{19}F NMR (CD_2Cl_2): δ -76.19 (6F, $\upsilon_{1/2}$ = 800 Hz), -51.87 (1.2F, $\upsilon_{1/2}$ = 40 Hz). (VT done)

Preparation of [Cp*2Yb(4,4'-dimethyl-2,2'-bipyridine)][Cp*2YbOTf$_2$]

Cp*$_2$YbOTf(pyridine) (0.48 g, 0.72 mmol) and 4,4'-dimethyl-2,2'-bipyridine (0.13 g, 0.72 mmol) were stirred in 20 mL of pentane overnight. The color changed from dark purple to brown. The pentane was filtered and the brown powder was dissolved in 5 mL of CH_2Cl_2 filtered, and the filtrate was layered with pentane. Brown block crystals formed. Yield 0.33 g (67%). ^{1}H NMR (CD_2Cl_2): δ -16.75 (2H, $\upsilon_{1/2}$ = 40 Hz), 3.48 (30H, $\upsilon_{1/2}$ = 120 Hz), 7.45 (6H, $\upsilon_{1/2}$ = 40 Hz), 8.02 (30H, $\upsilon_{1/2}$ = 80 Hz), 57.19 (2H, $\upsilon_{1/2}$ = 160 Hz), 336.30 (2H, $\upsilon_{1/2}$ = 400 Hz). ^{19}F NMR (CD_2Cl_2): δ -51.10 ($\upsilon_{1/2}$ = 40 Hz). Anal.Calcd for $C_{54}H_{72}F_6N_2O_6S_2Yb_2$: C, 47.36; H, 5.30; N 2.05. Found C, 47.01; H, 5.19; N, 2.08. (VT done)

Preparation of [Cp*$_2$Yb(2,2'-bipyridine)][BPh$_4$]

Cp*$_2$Yb(OTf)(pyridine) (0.89g 1.33 mmol) and bipy (0.21g, 1.35 mmol) were stirred in pentane overnight. The pentane was filtered, the brown powder was taken to dryness and heated at 50 $^\circ$C for one hour. The brown powder was dissolved in 100 mL CH_2Cl_2 and filtered into a flask containing $NaBPh_4$ (0.90 g, 2.7 mmol). The two were stirred overnight, and the solution was filtered, the filtrate was concentrated to 10 mL and layered with pentane. Dark brown crystals are formed. Yield 0.70 g (56%). ^{1}H NMR (CD_2Cl_2): δ -17.06 (2H, $\upsilon_{1/2}$ = 80 Hz), 3.32 (30H, $\upsilon_{1/2}$ = 120 Hz), 6.69 (4H, $\upsilon_{1/2}$ = 60 Hz), 7.08 (8H, $\upsilon_{1/2}$ = 60 Hz), 7.81 (8H, $\upsilon_{1/2}$ = 60 Hz), 8.45 (2H, $\upsilon_{1/2}$ = 40 Hz), 56.86 (2H, $\upsilon_{1/2}$ = 80 Hz), 336.86 (2H, $\upsilon_{1/2}$ = 1200 Hz). Anal.Calcd for $C_{56}H_{62}BN_2Yb$: C, 70.58; H, 6.36; N 3.05. Found C, 70.26; H, 6.13; N, 3.05. (VT done)

Preparation of [Cp*$_2$Yb(4,4'-dimethyl-2,2'-bipyridine)][BPh$_4$]

Cp*$_2$Yb(OTf)(pyridine) (0.85 g, 1.3 mmol), 4,4'-dimethyl-2,2'-bipyridine (0.23 g, 1.3 mmol) and $NaBPh_4$ (0.9 g, 2.6 mmol) were stirred in pentane overnight. The pentane was filtered and the black powder was dissolved in 10 mL of CH_2Cl_2, filtered, and the filtrate was layered with 50 mL pentane. Black plate crystals of [Cp*$_2$Yb(4,4'-dimethyl-2,2'-bipyridine)][BPh_4] formed. Yield 0.36g (37%). ^{1}H NMR (CD_2Cl_2): δ -17.78 (2H, $\upsilon_{1/2}$ = 40 Hz), 3.45 (30H, $\upsilon_{1/2}$ = 120 Hz), 7.43 (4H, $\upsilon_{1/2}$ = 40 Hz), 7.51 (6H, $\upsilon_{1/2}$ = 40 Hz), 7.87 (8H, $\upsilon_{1/2}$ = 40 Hz), 8.58 (12H, $\upsilon_{1/2}$ = 40 Hz), 57.19 (2H, $\upsilon_{1/2}$ = 160 Hz), 335.82 (2H, $\upsilon_{1/2}$ = 400 Hz). ^{11}B NMR (CD_2Cl_2): -δ 4.96. Anal.Calcd for $C_{56}H_{62}BN_2Yb$: C, 71.03; H, 6.60; N 2.96. Found C, 71.19; H, 6.68; N, 3.04.

Preparation of [Cp*$_2$Yb(N,N'-bis(p-tolyl)-1,4-diazadienyl)][BPh$_4$]

N,N'-Bis-(p-tolyl)-1,4-diazadiene was prepared by the Schiff base condensation of glyoxal and p-toluidine as reported. The crude product was recrystallized twice from hot isopropanol.[13] Cp*$_2$Yb(OTf)(pyridine) (0.65 g, 0.97 mmol), N,N'-bis-(p-tolyl)-1,4-diazadiene (0.24 g, 0.97 mmol) and $NaBPh_4$ (1.0 g, 2.8 mmol) were stirred in 50 mL of pentane overnight. The pentane was filtered, the brown powder was dissolved in 10 mL of CH_2Cl_2, filtered and the filtrate was layered with 50 mL of pentane. Brown plate-like crystals of [Cp*$_2$Yb(p-tolyl-dad)][BPh_4] formed. Yield 0.36g (37%). ^{1}H NMR (CD_2Cl_2): δ -35.53 (2H, $\upsilon_{1/2}$ = 80 Hz), -3.21 (30H, $\upsilon_{1/2}$ = 200 Hz), -0.649 (4H, $\upsilon_{1/2}$ = 60 Hz), 1.19 (8H, $\upsilon_{1/2}$ = 40 Hz), 2.24 (8H, $\upsilon_{1/2}$ = 40 Hz), 24.54 (6H, $\upsilon_{1/2}$ = 4 Hz), 53.92 (2H, $\upsilon_{1/2}$ = 800 Hz). ^{11}B NMR (CD_2Cl_2): δ -12.78 ($\upsilon_{1/2}$ = 8 Hz). Anal.Calcd for $C_{60}H_{66}N_2BYb$: C, 72.14; H, 6.66; N 2.80. Found C, 69.82; H, 6.26; N, 2.97. (Crystal structure and VT done)

Preparation of [Cp*$_2$Yb(N,N'-bis(p-anisyl)-1,4-diazadienyl)][BPh$_4$]

N,N'-Bis-(p-anisyl)-1,4-diazadiene was prepared by the Schiff base condensation of glyoxal and p-toluidine as reported.[13] The crude product was sublimed under reduced pressure at 160 °C. Cp*$_2$Yb(OTf) (0.14 g, 0.24 mmol), N,N'-bis-(p-anisyl)-1,4-diazadiene (0.13 g, 0.49 mmol) and NaBPh$_4$ (0.17 g, 0.49 mmol) were stirred in 50 mL of ether overnight. The ether was filtered, the brown powder was dissolved in 10 mL of CH_2Cl_2, filtered and the filtrate was layered with 50 mL of pentane. Brown plate-like crystals of [Cp*$_2$Yb(p-anisyl-dad)][BPh$_4$] formed. The crystals were crushed and heated at 120 °C under reduced pressure to sublime off excess N,N'-bis(p-anisyl)-1,4-diazadienyl. Yield 0.08 g (28%). ^{1}H NMR (CD_2Cl_2): δ -36.71 (2H, $\upsilon_{1/2}$ = 80 Hz), -3.40 (30H, $\upsilon_{1/2}$ = 180 Hz), -0.01 (4H, $\upsilon_{1/2}$ = 40 Hz), 1.70 (8H, $\upsilon_{1/2}$ = 40 Hz), 2.69 (8H, $\upsilon_{1/2}$ = 40 Hz), 6.87 (4H, $\upsilon_{1/2}$ = 40 Hz), 23.13 (6H, $\upsilon_{1/2}$ = 120 Hz). ^{11}B NMR (CD_2Cl_2): δ -12.18 ($\upsilon_{1/2}$ = 8 Hz). (VT done)

Preparation of [Cp*$_2$Yb(N,N'-bis(p-anisyl)-2,3-dimethyl-1,4-diazadienyl)][BPh$_4$]

Cp*$_2$Yb(OTf) (0.40 g, 0.68 mmol), N,N'-bis-(p-anisyl)-2,3-dimethyl-1,4-diazadiene (0.40 g, 1.3 mmol) and NaBPh$_4$ (0.46 g, 1.3 mmol) were stirred in 50 mL of ether overnight. The ether was filtered, the brown powder was dissolved in 10 mL of CH_2Cl_2, filtered and the filtrate was layered with 50 mL of pentane. Brown plate-like crystals of [Cp*$_2$Yb(p-anisyl-dad)][BPh$_4$] formed. The crystals were crushed and heated at 120 °C under reduced pressure to sublime off excess N,N'-bis(p-anisyl)-1,4-diazadienyl. Yield 0.05 g (7%). ^{1}H NMR (CD_2Cl_2): δ -11.34 (6H, $\upsilon_{1/2}$ = 120 Hz), -3.31 (30H, $\upsilon_{1/2}$ = 200 Hz), 4.93 (4H, $\upsilon_{1/2}$ = 20 Hz), 5.30 (8H, $\upsilon_{1/2}$ = 40 Hz), 5.55 (8H, $\upsilon_{1/2}$ = 40

Hz), 26.19 (6H, $\upsilon_{1/2}$ = 80 Hz), 60.38 (4H, $\upsilon_{1/2}$ = 120 Hz). ^{11}B NMR (CD_2Cl_2): δ -8.60 ($\upsilon_{1/2}$ = 6 Hz). (VT done)

Preparation of [Cp*$_2$Yb(4,4'-CO_2Me-2,2'-bipyridine)][BPh_4]

Cp*$_2$Yb(OTf) (0.40 g, 0.68 mmol), 4,4'-CO_2Me-2,2'-bipyridine (0.17 g, 0.67 mmol) and $NaBPh_4$ (0.4 g, 1.2 mmol) were stirred in 50 mL of pentane overnight. The pentane was filtered, the brown powder was dissolved in 20 mL of CH_2Cl_2, filtered, and the filtrate was layered with pentane. Brown crystals formed. Yield 0.32 g (47%). ^{1}H NMR (CD_2Cl_2): δ -14.12 (2H, $\upsilon_{1/2}$ = 40 Hz), 3.31 (30H, $\upsilon_{1/2}$ = 160 Hz), 6.00 (6H, $\upsilon_{1/2}$ = 40 Hz), 8.29 (4H, $\upsilon_{1/2}$ = 40 Hz), 8.73 (8H, $\upsilon_{1/2}$ = 60 Hz), 9.44 (8H, $\upsilon_{1/2}$ = 60 Hz), 57.13 (2H, $\upsilon_{1/2}$ = 40 Hz), 332.60 (2H, $\upsilon_{1/2}$ = 700 Hz). ^{11}B NMR (CD_2Cl_2): δ -4.44 ($\upsilon_{1/2}$ = 15 Hz). Anal. Calcd for $C_{56}H_{62}BN_2O_4Yb$: C, 66.53; H, 6.18; 2.77. Found C, 66.07; H, 5.76; N, 2.56. (VT done)

Preparation of [Cp*$_2$Yb(4,4'-CO_2Et-2,2'-bipyridine)][BPh_4]

Cp*$_2$Yb(OTf)(pyridine) (0.63 g, 0.94 mmol), 4,4'-CO_2Et-2,2'-bipyridine (0.31 g, 0.94 mmol) and $NaBPh_4$ (0.7 g, 2.1 mmol) were stirred in 50 mL of pentane overnight. The pentane was filtered, the brown powder was dissolved in 20 mL of CH_2Cl_2, filtered and the filtrate was crystallized by layering with pentane. Yield 0.42 g (42%). ^{1}H NMR (CD_2Cl_2): δ -14.11 (2H, $\upsilon_{1/2}$ = 30 Hz), 3.39 (30H, $\upsilon_{1/2}$ = 160 Hz), 3.84 (6H, $\upsilon_{1/2}$ = 40 Hz), 6.53 (4H, $\upsilon_{1/2}$ = 80 Hz), 9.45 (4H, $\upsilon_{1/2}$ = 120 Hz), 10.15 (8H, $\upsilon_{1/2}$ = 120 Hz), 11.18 (8H, $\upsilon_{1/2}$ = 120 Hz), 57.28 (2H, $\upsilon_{1/2}$ = 160 Hz), 333.39 (2H, $\upsilon_{1/2}$ = 400 Hz). Anal. Calcd for $C_{60}H_{66}N_2BO_4Yb$: C, 67.79; H, 6.26; 2.64. Found C, 67.54; H, 5.91; N, 2.63.

Preparation of [Cp*$_2$Lu(2,2'-bipyridine)][Cp*$_2$LuCl$_2$]

Cp*$_2$LuCl$_2$Na[12] (0.56 g, 1.0 mmol) and 2,2'-bipyridine (0.16 g, 1.0 mmol) were stirred in 50 mL of pentane overnight. The pentane was filtered, the yellow-orange powder was dissolved in 5 mL CH_2Cl_2. The suspension was filtered and the filtrate was layered with pentane. Yield 0.56 g (96%). ^{1}H NMR (CD_2Cl_2): δ 1.68 (s, 30H), 1.93 (s, 30H), 7.78 (d, 2H, J = 4 Hz), 7.88 (td, 2H, J = 6 Hz, J = 1 Hz), 8.47 (td, 2H, J = 8 Hz, J = 2Hz), 8.91 (d, 2H, J = 8 Hz). Anal. Calcd for $C_{50}H_{68}N_2Cl_2Lu_2$: C, 53.72; H, 6.13; N, 2.51. Found C, 53.35; H, 6.37; N, 2.66.

Preparation of [Cp*$_2$Lu(4,4'-dimethyl-2,2'-bipyridine)][Cp*$_2$LuCl$_2$]

Cp*$_2$LuCl$_2$Na[12] (0.83 g, 1.5 mmol) and 4,4'-dimethyl-2,2'-bipyridine (0.28 g, 1.5 mmol) were stirred in 50 mL of pentane overnight. The pentane was filtered, the yellow-orange powder was dissolved in 5 mL CH_2Cl_2. The suspension was filtered and the filtrate was layered with pentane. Yield 0.81 g (92%). ^{1}H NMR (CD_2Cl_2): δ 1.68 (30H, s), 1.92 (30H, s), 2.73 (s, 6H), 7.65 (d, 2H, J = 5 Hz), 7.70 (d, 2H, J = 3 Hz), 8.48 (s, 2H). ^{13}C NMR (CD_2Cl_2): 11.15 (s), 12.13 (s), 22.41 (s), 115.49 (s), 119.43 (s), 125.53 (s), 128.03 (s), 147.39 (s), 151.20 (s), 155.50 (s). Anal. Calcd for $C_{52}H_{72}N_2Cl_2Lu_2$: C, 54.50; H, 6.33; N, 2.44. Found: C, 51.98; H, 6.09; N, 2.35.

Preparation of [Cp*$_2$Lu(2,2'-bipyridine)][BPh$_4$]

[Cp*$_2$Lu(2,2'-bipyridine)][Cp*$_2$LuCl$_2$] (0.54 g, 0.48 mmol), 2,2'-bipyridine (0.08 g, 0.50 mmol) and $NaBPh_4$ (0.66 g, 1.9 mmol) were stirred in 50 mL of pentane overnight. The pentane was filtered, the yellow powder was dissolved in 10 mL of CH_2Cl_2, filtered, and the filtrate was layered with pentane. Yellow crystals formed. Yield 0.67 g (75%). ^{1}H NMR (CD_2Cl_2): δ 1.65 (s, 30H), 6.88 (t, 4H, J = 7 Hz), 7.05 (t, 8H, J =

7.5 Hz), 7.43 (t, 8H, *J* = 1.5 Hz), 7.60 (t, 2H, *J* = 5.5 Hz), 7.65 (d, 2H, *J* = 4 Hz), 7.83 (d, 2H, J = 8 Hz), 7.90 (td, 2H, *J* = 8.3 Hz, *J* = 1.5 Hz). ^{11}B NMR (CD_2Cl_2): δ -6.62. ^{13}C NMR (CD_2Cl_2): δ 11.13 (s), 119.58 (s), 122.45 (s), 125.02 (s), 126.34 (q, *J* = 11 Hz), 136.51 (s), 142.53 (s), 147.55 (s), 151.07 (s), 164.64 (q, *J* = 200 Hz). There is no temperature dependence to the ^{1}H and ^{11}B NMR peaks. Anal. Calcd for $C_{54}H_{58}BLuN_2$: C, 70.43; H, 6.35; N, 3.04. Found: C, 69.89; H, 6.47; N, 3.03.

Chapter 3

Preparation of $Cp^*_2La(2,2'\text{-bipyridine})$

$Cp^*_2La(2,2'\text{-bipyridine})(OTf)$ (1.1 g, 1.6 mmol) was added on sodium amalgam formed by dissolving Na (0.04 g, 1.9 mmol) in Hg (38 g, 188 mmol). Toluene (100 mL) was added and the dark red solution was stirred overnight. The toluene suspension was filtered and the filtrate was taken to dryness. The dark red powder was dissolved in 60 mL of pentane, the suspension was filtered, and the filtrate was concentrated to 20 mL, heated to dissolve the $Cp^*_2La(2,2'\text{-bipyridine})$ and cooled to -20 °C. Dark red crystals were obtained. Yield 0.70 g (79%). ^{1}H NMR (C_6D_6): 3.39 ($\upsilon_{1/2}$ = 120 Hz). The 2,2'-bipyridine resonances are not found. Anal. Calcd for $C_{30}H_{38}LaN_2$: C, 63.71; H, 6.77; N, 4.95. Found: C, 63.45; H, 6.97; N, 4.87. M.P. 310-312 °C. IR (Nujol mull): 2917 (vs), 2724 (w), 1539 (w), 1463 (s), 1417 (w), 1377 (s), 1276 (m), 1260 (m), 1205 (m), 1169 (w), 1146 (m), 1076 (m), 998 (m), 942 (s), 822 (w), 743 (w), 715 (s), 676 (m), 642 (m), 604 (w).

Preparation of $Cp^*_2Ce(2,2'\text{-bipyridine})$

Method 1: $Cp^*_2Ce(2,2'\text{-bipyridine})(OTf)$ (1.1 g, 1.5 mmol) was added on sodium amalgam formed by dissolving Na (0.04 g, 1.7 mmol) in Hg (2.65 mL, 17.9 mmol). Toluene (100 mL) was added and the dark red solution was stirred overnight. The toluene suspension was filtered and the filtrate was taken to dryness. The dark red powder was dissolved in 60 mL of pentane, concentrated to 20 mL, heated to dissolve the $Cp^*_2Ce(2,2'\text{-bipyridine})$ and cooled to -20 °C. Dark red crystals were obtained. Yield 0.30 g (34 %). ^{1}H NMR (C_6D_6): δ -253.55 (2H, $\upsilon_{1/2}$ = 800 Hz), -159.11 (2H, $\upsilon_{1/2}$ = 400 Hz), -40.38 (2H, $\upsilon_{1/2}$ = 80 Hz), -27.11 (2H, $\upsilon_{1/2}$ = 40 Hz), 4.30 (30H, $\upsilon_{1/2}$ = 40 Hz). Anal.

Calcd for $C_{30}H_{38}CeN_2$: C, 63.58; H, 6.76; N, 4.94. Found C, 63.35; H, 6.71; N, 4.78. M.P. 290-292 °C. (Crystal structure and VT done)

Method 2: 2,2'-Bipyridine (0.27 g, 1.7 mmol) was stirred with an excess of Na in THF overnight. The purple solution was decanted and the THF was removed under reduced pressure. Cp^*_2CeOTf (0.90 g, 1.6 mmol) was dissolved in 100 mL of toluene, added to Na(2,2'-bipyridine) prepared as above, and stirred overnight. The red solution was taken to dryness, and the red powder was dissolved in 100 mL of pentane, filtered, the filtrate was concentrated to 20 mL, heated to reddisolve the precipitated solid, and cooled to -20 °C overnight. Dark red crystals were obtained. Yield 0.65 g (71%). The NMR was identical to that obtained in method 1.

Preparation of Cp^*_2Ce(4,4'-dimethyl-2,2'-bipyridine)

Napthalene (0.26 g, 2.0 mmol) was stirred in an excess of Na overnight. The green solution was decanted into a flask containing 4,4'-dimethyl-2,2'-bipyridine (0.37 g, 2.0 mmol) and the solution was stirred overnight. The purple solution was taken to dryness and heated to 50 °C under reduced pressure for 2 hours to remove the naphthalene. Cp^*_2CeOTf (1.1 g, 2.0 mmol) dissolved in 75 mL of toluene was added to the Na(4,4'-dimethyl-2,2'-bipyridine) and stirred overnight. The suspension was taken to dryness and extracted with 100 mL of pentane, the extract was concentrated to 15 mL, heated to reddisolve the solid, and cooled to -20 °C overnight. Dark red crystals were obtained. Yield 0.45 g (38%). ^1H NMR (C_6D_6): δ -255.63 (2H, $\upsilon_{1/2}$ = 1000 Hz), -52.46 (2H, $\upsilon_{1/2}$ = 80 Hz), -26.62 (2H, $\upsilon_{1/2}$ = 80 Hz), 4.16 (30H, $\upsilon_{1/2}$ = 40 Hz), 147.39 (6H, $\upsilon_{1/2}$ = 400 Hz). Anal. Calcd for $C_{32}H_{42}CeN_2$: C, 64.62; H, 7.12; N, 4.71. Found C, 63.95; H, 7.19; N, 4.15. IR (Nujol mull): 2930 (vs), 1600 (w), 1569 (w), 1490 (w), 1460 (s), 1380

(s), 1265 (m), 1210 (w), 1100 (w), 960 (w), 821 (w), 800 (w), 620 (vw), 310 (w). M.P. 254-256 °C. (VT done)

Preparation of Cp*$_2$Ce(5,5'-dimethyl-2,2'-bipyridine)

Napthalene (0.30 g, 2.3 mmol) was stirred with an excess of Na overnight. The green solution was decanted into a flask containing 5,5'-dimethyl-2,2'-bipyridine (0.43 g, 2.3 mmol) and the solution was stirred overnight. The purple solution was taken to dryness and heated to 50 °C under reduced pressure for 2 hours to remove the naphthalene. Cp*$_2$CeOTf (1.3 g, 2.3 mmol) was dissolved in 75 mL of toluene, added to the Na(5,5'-dimethyl-2,2'-bipyridine) and stirred overnight. The suspension was taken to dryness, and the residue was extracted with 100 mL of pentane, concentrated to 15 mL, heated to reddisolve the solid, and cooled to -20 °C overnight. Dark red crystals were obtained. Yield 0.42 g (31%). ^{1}H NMR (C_6D_6): δ -171.15 (2H, $\upsilon_{1/2}$ = 400 Hz), -64.94 (2H, $\upsilon_{1/2}$ = 160 Hz), -0.88 (2H, $\upsilon_{1/2}$ = 40 Hz), 4.45 (30H, $\upsilon_{1/2}$ = 40 Hz), 226.47 (6H, $\upsilon_{1/2}$ = 800 Hz). Anal. Calcd for $C_{32}H_{42}CeN_2$: C, 64.62; H, 7.12; N, 4.71. Found C, 64.26; H, 7.45; N, 4.50. M.P. >360 °C.

Preparation of Cp*$_2$Ce(6,6'-dimethyl-2,2'-bipyridine)

Napthalene (0.29 g, 2.3 mmol) was stirred with an excess of Na overnight. The green solution was decanted into a flask containing 6,6'-dimethyl-2,2'-bipyridine (0.38 g, 2.1 mmol) and the solution was stirred overnight. The purple solution was taken to dryness and heated to 50 °C under reduced pressure for 2 hours to remove the naphthalene. Cp*$_2$CeOTf (1.18 g, 2.1 mmol) was dissolved in 75 mL of toluene, added to the Na(6,6'-dimethyl-2,2'-bipyridine) and stirred overnight. The solution was taken to dryness, dissolved in 100 mL pentane, filtered, and the filtrate was concentrated to 10

mL, heated to reddisolve the solid, and cooled to -20 °C overnight. Dark red crystals were obtained. Yield 0.15 g (12%). ^{1}H NMR (C_6D_6): δ -256.01 (2H, $\upsilon_{1/2}$ = 1200 Hz), -151.30 (2H, $\upsilon_{1/2}$ = 200 Hz), -88.57 (6H, $\upsilon_{1/2}$ = 80 Hz), -30.27 (2H, $\upsilon_{1/2}$ = 80 Hz), 6.40 (30H, $\upsilon_{1/2}$ = 40 Hz). M.P. >360 °C. (VT done)

Preparation of Cp*$_2$Ce(2,2':6',2''-terpyridyl)

[Cp*$_2$Ce(2,2',6',2''-terpyridyl)][OTf] (0.29 g, 0.37 mmol) was added on a sodium amalgam by dissolving Na (0.009 g, 0.39 mmol) in Hg (0.7 mL, 47 mmol). Toluene (100 mL) was added and the green solution was stirred overnight. The toluene suspension was filtered, the filtrate was taken to dryness, dissolved in 100 mL pentane, concentrated to 5 mL, heated to redissolve the solid and cooled to -20 °C overnight. A green powder was obtained. Yield 0.07 g (29%). ^{1}H NMR (tol-d_8): δ -116.26 (2H, $\upsilon_{1/2}$ = 400 Hz), -68.50 (2H, $\upsilon_{1/2}$ = 200 Hz), -14.66 (2H, $\upsilon_{1/2}$ = 40 Hz), -11.35 (2H, $\upsilon_{1/2}$ = 40 Hz), 4.30 (30H, $\upsilon_{1/2}$ = 20 Hz), 10.36 (2H, $\upsilon_{1/2}$ = 10 Hz), which is similar to the literature values in THF-d_8[14]. (VT done)

Preparation of Cp*$_2$Ce(iso-propyl-N-CH=CH-N=CMe$_2$):

N,N'-Bis(iso-propyl)-1,4-diazadiene was prepared according to literature procedure.[15] Napthalene (0.40 g, 3.1 mmol) was stirred with an excess of Na overnight. The green solution was decanted into a flask containing N,N'-bis(iso-propyl)-1,4-diazadiene (0.39 g, 2.8 mmol) and the mixture was stirred overnight. The red solution was taken to dryness and heated to 50 °C under reduced pressure for 2 hours to remove the naphthalene. Cp*$_2$CeOTf (1.6 g, 2.8 mmol) was dissolved in 75 mL of toluene and added to the Na(N,N'-bis(iso-propyl)-1,4-diazadiene) and the mixture was stirred overnight. The suspension was taken to dryness, dissolved in 100 mL of pentane, filtered,

and the filtrate was concentrated to 10 mL, heated to reddisolve the solid, and cooled to -20 °C overnight. Red crystals were obtained. The crystals were sublimed in a diffusion pump vacuum at 120-140 °C and then crystallized from pentane. Yield 0.7 g (45%). ^{1}H NMR (C_6D_6): δ -36.01 (3H, $\upsilon_{1/2}$ = 30 Hz), -12.74 (6H, $\upsilon_{1/2}$ = 30 Hz), -6.74 (1H, $\upsilon_{1/2}$ = 60 Hz), -6.02 (3H, $\upsilon_{1/2}$ = 30 Hz), 4.15 (30H, $\upsilon_{1/2}$ = 15 Hz), 5.85 (1H, $\upsilon_{1/2}$ = 15 Hz), 13.74 (1H, $\upsilon_{1/2}$ = 30 Hz). Anal. Calcd for $C_{28}H_{45}CeN_2$: C, 61.17; H, 8.25; N, 5.10. Found C, 61.18; H, 8.59; N, 4.92. M.P. 310-312 °C. (VT done)

Cp*$_2$Sr(2,2'-bipyridine) and Cp*$_2$Ba(2,2'-bipyridine) were prepared according to literature procedure.[16]

Preparation of Cp*$_2$Sm(2,2'-bipyridine)

Cp*$_2$Sm(2,2'-bipyridine)(OTf) (0.88 g, 1.2 mmol) was added on a sodium amalgam by dissolving Na (0.031 g, 1.33 mmol) in Hg (3.1 g, 15.3 mmol). Toluene (100 mL) was added and the dark red solution was stirred overnight. The toluene suspension was filtered, the filtrate was taken to dryness, dissolved in 60 mL pentane, concentrated to 5 mL, heated to redissolve the solid and cooled to -20 °C overnight. Dark brown crystals were obtained. Yield 0.06 g (9 %). ^{1}H NMR (C_6D_6): δ -258.09 (2H, $\upsilon_{1/2}$ = 800 Hz), -164.38 (2H, $\upsilon_{1/2}$ = 400 Hz), -26.19 (2H, $\upsilon_{1/2}$ = 40 Hz), -13.41 (2H, $\upsilon_{1/2}$ = 20 Hz), 2.50 (30H, $\upsilon_{1/2}$ = 40 Hz). The ^{1}H NMR was identical to the literature value.[17] (VT done)

Preparation of Cp*$_2$Sm(4,4'-dimethyl-2,2'-bipyridine)

Sodium metal (0.10g, 4.4 mmol) was added to a solution of napthalene (0.16 g, 1.2 mmol) in 50 mL of THF and the solution was stirred overnight. The green solution was added onto 4,4'-dimethyl-2,2'-bipyridine (0.21 g, 1.1 mmol) and the red solution of Na(4,4'dimethyl-2,2'-bipyridine) was stirred overnight. The THF was removed under reduced pressure and the residue was heated at 80 °C for 2 hours to remove the excess THF. Cp*$_2$Sm(OTf) (0.65 g, 1.1 mmol) was dissolved in 100 mL of toluene and added to the Na(4,4'-dimethyl-2,2'-bipyridine). The suspension was stirred overnight, filtered and the filtrate was taken to dryness. The dark red powder was dissolved in 100 mL of pentane, concentrated to 20 mL, heated to dissolve the solid and cooled to -20 °C overnight. The red-black crystals of Cp*$_2$Sm(4,4'-dimethyl-2,2'-bipyridine) were collected by filtration. Yield 0.6 g (87 %). ^{1}H NMR (C_6D_6): δ -260.93 (2H, $\upsilon_{1/2}$ = 370 Hz), -52.53 (2H, $\upsilon_{1/2}$ = 30 Hz), -0.40 (2H, $\upsilon_{1/2}$ = 10 Hz), 2.38 (30H, $\upsilon_{1/2}$ = 7 Hz), 156.42 ($\upsilon_{1/2}$ = 200 Hz). Anal. Calcd for $C_{32}H_{42}SmN_2$: C, 63.52; H, 7.00; N, 4.63. Found C, 63.33; H, 6.72; N, 4.62. M.P. 263-265 °C.

Preparation of Cp*$_2$Sm(5,5'-dimethyl-2,2'-bipyridine)

Cp*$_2$SmOTf(pyridine) (1.18 g, 1.8 mmol) and 5,5'-dimethyl-2,2'-bipyridine (0.33 g, 1.8 mmol) were stirred in ether overnight. The ether was filtered off and the orange powder was taken to dryness and was added on a sodium amalgam by dissolving Na (0.037 g, 1.6 mmol) in Hg (32.18 g, 160 mmol). Toluene (100 mL) was added and the brown solution was stirred overnight. The toluene suspension was filtered, the filtrate was taken to dryness, dissolved in 100 mL pentane, concentrated to 5 mL, heated to redissolve the solid and cooled to -20 °C overnight. A brown powder was obtained. Yield

0.09 g (9%). ^{1}H NMR (C_6D_6): δ -180.56 (2H, $\upsilon_{1/2}$ = 370 Hz), -41.56 (2H, $\upsilon_{1/2}$ = 15 Hz), 0.34 (2H, $\upsilon_{1/2}$ = 14 Hz), 2.56 (30H, $\upsilon_{1/2}$ = 9 Hz), 237.45 ($\upsilon_{1/2}$ = 520 Hz). Anal. Calcd for $C_{32}H_{42}SmN_2$: C, 63.52; H, 7.00; N, 4.63. Found ?. M.P. 248-250 °C.

Preparation of Cp*$_2$Gd(2,2'-bipyridine)

Sodium metal (0.15g, 6.5 mmol) was added to a solution of bipy (0.43 g, 2.8 mmol) in 50 mL of THF and the solution was stirred overnight. The red solution of Na(2,2'-bipyridine) was stirred overnight and then all of the THF was removed under reduced pressure. It was then heated at 80 °C under reduced pressure for 2 hours to remove the excess THF. Cp*$_2$Gd(OTf) (1.6 g, 2.8 mmol) was dissolved in 100 mL of toluene and added to the solid Na(2,2'-bipyridine). The suspension was stirred overnight, filtered, and the concentrate was taken to dryness. The dark red powder was dissolved in 100 mL of pentane, concentrated to 40 mL, heated to dissolve the solid and cooled to -20 °C overnight. The red-black crystals of Cp*$_2$Gd(2,2'-bipyridine) were collected by filtration and the mother liquor was concentrated to 10 mL to obtain a second crop. Yield 1.1 g (67 %). Anal. Calcd for $C_{30}H_{38}GdN_2$: C, 61.71; H, 6.56; N, 4.89. Found C, 61.76; H, 6.02; N, 4.88. M.P. 332-334 °C. (Crystal structure done)

Preparation of Cp*$_2$Gd(4,4'-dimethyl-2,2'-bipyridine)

Sodium metal (0.10g, 4.4 mmol) was added to a solution of napthalene (0.18 g, 1.4 mmol) in 50 mL of THF and the solution was stirred overnight. The green solution was added onto 4,4'-dimethyl-2,2'-bipyridine (0.23 g, 1.2 mmol) and the red solution of Na(4,4'dimethyl-2,2'-bipyridine) was stirred overnight. The THF was removed under reduced pressure and the residue was heated at 80 °C for 2 hours to remove the excess THF. Cp*$_2$Gd(OTf) (0.72 g, 1.2 mmol) was dissolved in 100 mL of toluene and added to

the Na(4,4'-dimethyl-2,2'-bipyridine). The suspension was stirred overnight, filtered and the filtrate was taken to dryness. The dark red powder was dissolved in 100 mL of pentane, concentrated to 20 mL, heated to dissolve the solid and cooled to -20 °C overnight. The red-black crystals of Cp^*_2Gd(4,4'-dimethyl-2,2'-bipyridine) were collected by filtration. Yield 0.2 g (27 %). Anal. Calcd for $C_{32}H_{42}GdN_2$: C, 62.81; H, 6.92; N, 4.58. Found C, 62.58; H, 6.76; N, 4.84. M.P. 221-226 °C.

Preparation of Cp^*_2Yb(2,2'-bipyridine)

Sodium metal (0.05 g, 2 mmol) was added to a solution of naphthalene (0.22 g, 1.7 mmol) in 50 mL of THF. The green solution was stirred overnight then added to 2,2'-bipyridine (0.245 g, 1.57 mmol). The red solution was stirred overnight and the THF was removed under reduced pressure. The red powder was heated at 50 °C under reduced pressure for 2 hours to remove the naphthalene and THF. $Cp^*_2Yb(OTf)$(pyridine) (1.05 g, 1.57 mmol), dissolved in 50 mL of toluene was added to the Na(2,2'-bipyridine) and the solution was stirred overnight. The suspension was filtered and the filtrate was concentrated to 30 mL, yielding dark red-brown crystals. Yield 0.21 g (22 %). ^{1}H NMR (C_6D_6): -12.48 (2H, $\upsilon_{1/2}$ = 12 Hz), 3.99 (30H, $\upsilon_{1/2}$ = 8 Hz), 8.70 (2H, $\upsilon_{1/2}$ = 80 Hz), 27.82 ($\upsilon_{1/2}$ = 40 Hz), 161.93 (2H, $\upsilon_{1/2}$ = 60 Hz). The ^{1}H NMR spectrum and melting point were similar to the literature value.[18]

Chapter 4

Preparation of Cp^*_2Yb(5,5'-dimethyl-2,2'-bipyridine)

$Cp^*_2YbOEt_2$ (0.65 g, 1.25 mmol) and 5,5'-dimethyl-2,2'-bipyridine (0.23 g, 1.3 mmol) were stirred in 50 mL of toluene overnight. The solution was concentrated to 30 mL, warmed to dissolve the solid and cooled to -20 °C overnight. Black crystals formed. The crystals were collected by filtration and the mother liquor was concentrated to 5 mL and cooled to -20 °C to give a second crop of crystals. Yield 0.52 g (66 %). ^{1}H NMR (tol-d_8): δ -14.54 (6H, $\upsilon_{1/2}$ = 80 Hz), -5.78 (2H, $\upsilon_{1/2}$ = 20 Hz), 3.19 (30H, $\upsilon_{1/2}$ = 20 Hz), 38.22 (2H, $\upsilon_{1/2}$ = 40 Hz), 102.71 (2H, $\upsilon_{1/2}$ = 80 Hz). Anal.Calcd for $C_{32}H_{42}N_2Yb$: C, 61.23; H, 6.74; N, 4.46. Found C, 61.51; H, 6.87; N, 4.78. M.P. 236-237 °C (Crystal structure and VT done)

Preparation of Cp^*_2Yb(6,6'-dimethyl-2,2'-bipyridine)

$Cp^*_2YbOEt_2$ (0.62 g, 1.20 mmol) and 6,6'-dimethyl-2,2'-bipyridine (0.22 g, 1.2 mmol) were stirred in 50 mL of toluene overnight. The solution was concentrated to 30 mL, warmed to dissolve the solid and cooled to -20 °C overnight. Black crystals formed. The mother liquor was concentrated to 5 mL and cooled to -20 °C overnight to give a second crop of crystals. Yield 0.40 g (53 %). ^{1}H NMR (C_6D_6): δ 1.88 (s, 30H), 6.47 (d, 2H, J = 8 Hz), 6.93 (s, 6H), 7.92 (d, 2H, J = 8 Hz), 9.66 (t, 2H, J = 8 Hz). Anal.Calcd for $C_{32}H_{42}N_2Yb$: C, 61.23; H, 6.74; N, 4.46. Found C, 61.24; H, 6.78; N, 4.94. M.P. 336-339 °C. (Crystal structure and VT done)

Preparation of Cp^*_2Yb(4-methyl-2,2'-bipyridine)

$Cp^*_2YbOEt_2$ (2.50 g, 4.83 mmol) and 4-methyl-2,2'-bipyridine (0.80 g, 4.83 mmol) were stirred in 200 mL of toluene overnight. The solution was concentrated to 60 mL, warmed to dissolve the solid and cooled to -20 °C overnight. Black crystals formed. The mother liquor was concentrated to 10 mL and cooled to -20 °C overnight to give a second crop of crystals. Yield 1.46 g (49%). ^{1}H NMR (C_6D_6): δ -13.33 (1H, $\upsilon_{1/2}$ = 80 Hz), -9.33 (3H, $\upsilon_{1/2}$ = 160 Hz), -8.62 (1H, $\upsilon_{1/2}$ = 60 Hz), 3.92 (30H, $\upsilon_{1/2}$ = 60 Hz), 5.97 (1H, $\upsilon_{1/2}$ = 40 Hz), 11.12 (1H, $\upsilon_{1/2}$ = 40 Hz), 30.49 (1H, $\upsilon_{1/2}$ = 60 Hz), 151.60 (1H, $\upsilon_{1/2}$ = 80 Hz), 154.82 (1H, $\upsilon_{1/2}$ = 80 Hz). Anal.Calcd for $C_{31}H_{40}N_2Yb$: C, 60.67; H, 6.57; N, 4.56. Found C, 61.04; H, 6.73; N, 4.60. M.P. 282-284 °C. (VT done)

Preparation of Cp^*_2Yb(5-methyl-2,2'-bipyridine)

$Cp^*_2YbOEt_2$ (0.60 g, 1.16 mmol) and 5-methyl-2,2'-bipyridine (0.20 g, 1.17 mmol) were stirred in 20 mL of toluene overnight. The solution was concentrated to 10 mL, warmed to dissolve the solid and cooled to -20 °C overnight. Black crystals formed. The mother liquor was concentrated to 5 mL and cooled to -20 °C overnight to give a second crop of crystals. Yield 0.42 g (59 %). ^{1}H NMR (C_6D_6): δ -9.33 (1H, $\upsilon_{1/2}$ = 20 Hz), -9.13 (3H, $\upsilon_{1/2}$ = 400 Hz), -8.36 (1H, $\upsilon_{1/2}$ = 20 Hz), 3.61 (30H, $\upsilon_{1/2}$ = 40 Hz), 18.32 (1H, $\upsilon_{1/2}$ = 200 Hz), 34.34 (1H, $\upsilon_{1/2}$ = 20 Hz), 37.57 (1H, $\upsilon_{1/2}$ = 20 Hz), 130.43 (1H, $\upsilon_{1/2}$ = 200 Hz), 134.04 (1H, $\upsilon_{1/2}$ = 200 Hz). Anal.Calcd for $C_{31}H_{40}N_2Yb$: C, 60.67; H, 6.57; N, 4.56. Found C, 60.35; H, 6.34; N, 4.72. M.P. 318-320 °C. (VT done)

Preparation of Cp^*_2Yb(6-methyl-2,2'-bipyridine)

$Cp^*_2YbOEt_2$ (0.44 g, 0.85 mmol) and 6-methyl-2,2'-bipyridine (0.14 g, 0.82 mmol) were stirred in 30 mL of toluene overnight. The solution was concentrated to 10 mL, warmed to dissolve the solid and cooled to -20 °C overnight. Black crystals formed. Yield 0.24 g (48 %). ^{1}H NMR (C_6D_6): δ -5.20 (1H, $\upsilon_{1/2}$ = 80 Hz), -4.32 (1H, $\upsilon_{1/2}$ = 80 Hz), 2.06 (30H, $\upsilon_{1/2}$ = 120 Hz), 12.74 (1H, $\upsilon_{1/2}$ = 120 Hz), 16.22 (1H, $\upsilon_{1/2}$ = 120 Hz), 27.84 (1H, $\upsilon_{1/2}$ = 60 Hz), 29.21 (1H, $\upsilon_{1/2}$ = 60 Hz), 97.64 (3H, $\upsilon_{1/2}$ = 80 Hz), 112.34 (1H, $\upsilon_{1/2}$ = 80 Hz). Anal.Calcd for $C_{31}H_{40}N_2Yb$: C, 60.67; H, 6.57; N, 4.56. Found: C, 60.55; H, 6.80; N, 4.40. M.P. 333-335 °C. (Crystal structure and VT done)

Chapter 5

Preparation of $Cp_3Ce(THF)$

Sodium cyclopentadienide (60 mL of a 2.45 M solution in tetrahydrofuran, 147 mmol) was added to a suspension of cerium trichloride (9.19 g, 37.3 mmol) in tetrahydrofuran (60 mL). The yellow-red suspension was stirred for 12 h. The solvent was removed under reduced pressure. The golden residue was extracted with toluene in a Soxhlet extractor. Yield 13.60 g (88%). ^{1}H NMR (C_6D_6): δ -12.68 (4H, $\nu_{1/2}$ = 210 Hz), -5.45 (4H, $\nu_{1/2}$ = 120 Hz), 7.65 (15H, $\nu_{1/2}$ = 30 Hz). The ^{1}H NMR spectrum was identical to the literature value.[19]

NMR tube reaction of $Cp_3Ce(THF)$ and $(MeC_5H_4)_3Ce(THF)$

$(MeC_5H_4)_3Ce(THF)$ was prepared according to literature procedure.[20] A small amount of $(MeC_5H_4)_3Ce(THF)$ was added to $Cp_3Ce(THF)$ and the ^{1}H NMR spectrum was measured. A small amount of $Cp_3Ce(THF)$ was added to the mixture and the ^{1}H NMR was measured again. More $Cp_3Ce(THF)$ was added to the mixture and the ^{1}H NMR was measured again. Based on the peaks that grew in it was possible to identify the ^{1}H NMR spectrum of the Cp and MeC_5H_4 rings of $Cp_2(MeC_5H_4)Ce(THF)$ and $Cp(MeC_5H_4)_2Ce(THF)$. $Cp_2(MeC_5H_4)Ce(THF)$ ^{1}H NMR (C_6D_6): δ -1.06 (Me from MeC_5H_4, $\nu_{1/2}$ = 3 Hz), 7.15[1] (Cp, $\nu_{1/2}$ = 9 Hz), 8.97 (ring ^{1}H from MeC_5H_4, $\nu_{1/2}$ = 9 Hz), 11.74 (ring ^{1}H from MeC_5H_4). $Cp(MeC_5H_4)_2Ce(THF)$ ^{1}H NMR (C_6D_6): δ -1.22 (Me from MeC_5H_4, $\nu_{1/2}$ = 3 Hz), 6.68 (Cp, $\nu_{1/2}$ = 9 Hz), 8.80 (ring ^{1}H from MeC_5H_4, $\nu_{1/2}$ = 9 Hz), 10.95 (ring ^{1}H from MeC_5H_4, $\nu_{1/2}$ = 9 Hz).

[1] It overlaps with the C_6D_5H impurity in the C_6D_6

Preparation of Cp_3Ce

$Cp_3Ce(THF)$ (2.0 g, 4.9 mmol) was heated at 190 °C in a diffusion-pump vacuum for one week. A small amount of Cp_3Ce sublimed, but most of it remained at the bottom of the flask. Yield 1.56 g (95%). ^1H NMR (CD_2Cl_2): δ 9.73 ($\nu_{1/2}$ = 120 Hz).

$[(MeC_5H_4)_3Ce]_2$(4,4'-bipyridine)

$(MeC_5H_4)_3Ce(THF)$ (1.2 g, 2.7 mmol) and 4,4'-bipyridine (0.21 g, 1.3 mmol) were stirred in 50 mL of pentane overnight. The green suspension was filtered and the green powder was dissolved in 50 mL of tetrahydrofuran, filtered and concentrated under reduced pressure until a solid began to precipitate. The solution was reheated to dissolve the solid, then the solution was cooled to -20 °C overnight. Green crystals formed. The mother liquor was filtered off, concentrated and cooled to -20 °C. Yield 0.80 g (65%). ^1H NMR (thf-d_8): δ -1.23 (18H, $\nu_{1/2}$ = 15 Hz), 7.27 (d, 4H, J = 4 Hz), 7.52 (4H, $\nu_{1/2}$ = 30 Hz), 8.36 (12H, $\nu_{1/2}$ = 30 Hz), 10.28 (12H, $\nu_{1/2}$ = 30 Hz). M.P. 314-315 °C. Anal. Calcd for $C_{46}H_{50}Ce_2N_2$: C, 60.64; H, 5.53; N, 3.07. Found: C, 60.35; H, 5.26; N, 3.07.

$[Cp^*_2CeOTf]_2$(4,4'-bipyridine)

Cp^*_2CeOTf (0.91 g, 1.6 mmol) and 4,4'-bipyridine (0.13 g, 0.8 mmol) were stirred in 50 mL of pentane overnight. The brown suspension was filtered and the brown powder was dissolved in 50 mL CH_2Cl_2, filtered, concentrated to 10 mL, and layered with pentane. Brown crystals formed. Yield 0.40 g (38%). ^1H NMR (CD_2Cl_2): δ -1.23 (18H, $\nu_{1/2}$ = 15 Hz), 7.27 (d, 4H, J = 4 Hz), 7.52 (4H, $\nu_{1/2}$ = 30 Hz), 8.36 (12H, $\nu_{1/2}$ = 30 Hz), 10.28 (12H, $\nu_{1/2}$ = 30 Hz). Anal. Calcd for $C_{52}H_{48}Ce_2F_6N_2O_2S_2$: C, 48.97; H, 5.37; N, 2.20. Found: C, 48.91; H, 5.35; N, 2.17.

$(MeC_5H_4)_3Tb(THF)$

$(MeC_5H_4)_3Tb(THF)$ was synthesized by a modification of the method used for $(MeC_5H_4)_3Ce(THF)$.[20] Sodium methyl-cyclopentadienide (63.5 mL of a 0.86 M solution in tetrahydrofuran, 54.6 mmol) was added to a suspension of terbium trichloride (4.83 g, 18.2 mmol) in tetrahydrofuran (60 mL). The white suspension was stirred for 12 h. The solvent was removed under reduced pressure, the off-white residue was extracted with toluene (200 mL), filtered, and the toluene was removed under reduced pressure. The off-white residue was dissolved in 150 mL ether, filtered, and concentrated until a white precipitate began to form. The solution was heated to redissolve the precipitate and cooled to -20 °C. Off-white crystals formed. Yield 4.0 g (65%). ^{1}H NMR (C_6D_6): δ -312.61 (8H, $\nu_{1/2}$ = 2000 Hz), -145.71 (8H, $\nu_{1/2}$ = 400 Hz), -105.92 (9H, $\nu_{1/2}$ = 400 Hz), 189.40 (6H, $\nu_{1/2}$ = 1200 Hz), 245.61 (6H, $\nu_{1/2}$ = 1200 Hz). Anal. Calcd for $C_{22}H_{29}OTb$: C, 56.41; H, 6.24; N, 0. Found: C, 56.19; H, 6.12; N, 0. M.P. 150-151 °C.

$(MeC_5H_4)_3Tb$

$(MeC_5H_4)_3Tb(THF)$ (5.0 g, 10.7) mmol was heated under diffusion-pump vacuum for two days at 110 °C. A yellow powder sublimed onto the walls. The powder was removed, placed in another flask and sublimed again. Yield 3.8 g (90% yield). ^{1}H NMR (C_7D_8): -203.21 (9H, $\nu_{1/2}$ = 800 Hz), 220.34 (6H, $\nu_{1/2}$ = 400 Hz), 377.27 (6H, $\nu_{1/2}$ = 400 Hz).[2]

$[(MeC_5H_4)_3Tb]_2$(4,4'-bipyridine)

$(MeC_5H_4)_3Tb$ (0.89 g, 2.2 mmol) and 4,4'-bipyridine (0.18 g, 1.2 mmol) were stirred in 50 mL of pentane overnight. The red-orange suspension was filtered and the powder was dissolved in 50 mL of CH_2Cl_2, filtered, concentrated under reduced pressure

[2]

to 5 mL, and layered with pentane. Red-orange crystals formed. Yield 0.60 g (55%). ^{1}H NMR (CD_2Cl_2): δ -106.14 (18H, $v_{1/2}$ = 400 Hz), 176.22 (12H, $v_{1/2}$ = 200 Hz), 205.77 (12H, $v_{1/2}$ = 200 Hz). Anal. Calcd for $C_{46}H_{50}Tb_2N_2$: C, 58.23; H, 5.31; N, 2.95. Found: C, 57.87; H, 5.14; N, 2.86.

UV-vis

Optical Spectra of Bipyridyl Complexes

Complex	Solvent	λ_{max} in nm (ε x 10^{-3} in L mol^{-1} cm^{-1})
$(C_5Me_5)_2La$(2,2'-bipyridine)	C_6H_{12}	930 (1.36), 812 (2.07), 368 (10.10)
$(C_5Me_5)_2Ce$(2,2'-bipyridine)	C_6H_{12}	920 (0.53), 820 (0.50), 520 (1.29), 490 (1.06), 380 (6.64)
$(C_5Me_5)_2Ce$(N,N'-bis(iso-propyl)-1,4-diazadienyl)	C_6H_{12}	936 (0.69), 826 (1.09), 816 (1.22), 368 (3.86), 364 (4.47), 358 (3.42), 351 (3.05), 341 (2.22), 336 (2.28), 284 (4.16)
$(C_5Me_5)_2Gd$(4,4'-dimethyl-2,2'-bipyridine)	C_6H_{12}	923 (0.20), 803 (0.13), 534 (0.41), 499 (0.06), 394 (0.67)
$[(C_5Me_5)_2Ce$(2,2'-bipyridine)$][BPh_4]$	(CH_2Cl_2)	884 (0.04), 591 (0.24), 385 (2.12)
$(C_5Me_5)_2Ce$(2,2'-bipyridine)(OTf)	(CH_2Cl_2)	884 (0.04), 385 (0.29)
$(C_5Me_5)_2Ce$(4,4'-dimethyl-2,2'-bipyridine)(OTf)	(CH_2Cl_2)	885 (0.10), 365 (4.74)
$(C_5Me_5)_2Ce$(phen)(OTf)	(CH_2Cl_2)	885 (0.02), 385 (0.69)
$[(C_5Me_5)_2Ce$(terpy)$][(OTf)]$	(CH_2Cl_2)	885 (0.02), 390 (0.24)
$(C_5H_5)_3Ce$(O=pyridine)	(CH_2Cl_2)	1022 (17.47), 884 (20.62), 538 (0.12)
$(C_5Me_5)_2Yb$(4-methyl-2,2'-bipyridine)	C_6H_{12}	786 (3.13), 384 (7.65), 355 (6.90), 258 (12.19)
$(C_5Me_5)_2Yb$(5-methyl-2,2'-bipyridine)	C_6H_{12}	778 (4.05), 379 (7.02), 359 (6.52), 261 (12.04)
$(C_5Me_5)_2Yb$(6-methyl-2,2'-bipyridine)	C_6H_{12}	785 (3.34), 368 (9.99), 257 (10.97)
$(C_5Me_5)_2Yb$(5,5'-dimethyl-2,2'-bipyridine)	C_6H_{12}	783 (1.63), 369 (4.33)
$(C_5Me_5)_2Yb$(6,6'-dimethyl-2,2'-bipyridine)	C_6H_{12}	929 (0.98), 811 (1.65), 369 (9.40)
$[(MeCp)_3Ce]_2$(1,4-benzoquinone)	C_6H_{12}	475 (6.17), 297 (8.15), 274 (11.53)

References:

1. Threlkel, R. S.; Bercaw, J. E.; Seidler, P. F. *Organic Synthesis, Collective Volume 8 505*.
2. Andersen, R. A.; Blum, R.; Boncella, J. M.; Burns, C. J.; Volden, H. V. *Acta Chemica Scand. A*, **1987**, *41*, 24.
3. Sofield, C. D. Ph.D. Thesis; University of California at Berkeley: Berkeley, CA, 2000.
4. Hazin, P.N.; Lakshminarayan, C.; Brinen, L.S.; Knee, J.L.; Bruno, J.W.; Streib, W.E.; Folting, K. *Inorg. Chem.*, **1988**, *27*, 1393
5. Dungan, C. H.; VanWazer, J. R. *Compilation of Reported F-19 Chemical Shifts*, Wiley-Interscience, New York, **1970**.
6. Walter, M.D.; Schultz, M.; Andersen, R.A. *New J. Chem.*, **2006**, *30*, 238
7. Hazin, P.N.; Huffman, J.C.; Bruno, J.W. *Organometallics*, **1987**, *6*, 23.
8. Heeres, H.J.; Renkema, J.; Booij, M.; Meetsma, A.; Teuben, J.H. *Organometallics*, **1988**, *7*, 2495
9. Taken from the first year report of Dr. Evan Werkema
10. Li, L.; Loveday, D.C.; Mudigonda, D.S.K.; Ferraris, J.P. *Journal of the Electrochemical Society*, **2002**, *149*, A1201
11. It is unclear why we had so much difficulty obtaining accurate elemental analysis for our [BPh4] salts. However, the 1H NMR and crystal structure seem quite convincing. Elemental analysis which are not quite accurate with [BPh4] salts are also reported in Evans, W.J.; Ulibarri, T.A.; Chamberlain, L.R.; Ziller, J.W.; Alvarez, D. *Organometallics*, **1990**, *9*, 2124 and Evans, W.J.; Seibel, C.A.; Ziller, J.W. *J. Am. Chem. Soc.*, **1998**, *120*, 6745
12. Schumann, H.; Albrecht, I.; Loebel, J.; Hahn, E.; Hossain, M.B.; van der Helm, D. *Organometallics*, **1986**, *5*, 1296.
13. Kliegman, J.M.; Barnes, R.K., *J. Org. Chem.*, **1970**, *35*, 3140
14. Mehdoui, T.; Berthet, J.C.; Thuèry, P.; Salmon, L.; Rivière, E.; Ephritikhine, M. *Chem. Eur. J.*, **2005**, *11*, 6994.
15. Tom Dieck, H.; Franz, K.-D.; Majunke, W., *Z. Naturforsch.*, **1975**, *30b*, 922
16. Burns, C.J.; Andersen, R.A. *Journal of Organometallic Chemistry*, **1987**, *325*, 31
17. Evans, W.J.; Drummond, D.K. *J. Am. Chem. Soc.*, **1989**, *111*, 3329
18. Schultz, M.; Boncella, J. M.; Berg, D. J.; Tilley, T. D.; Andersen, R. A. *Organometallics*, **2002**, *21*, 460.
19. Gradeff, P.S.; Yunlu, K.; Deming, T.J.; Olofson, J.M.; Ziller, J.W.; Evans, W.J. *Inorg. Chem.*, **1989**, *28*, 2600.
20. Brennan, J.G.; Stults, S.D.; Andersen, R.A.; Zalkin, A. *Organometallics*, **1988**, *7*, 1329

Chapter 7: Magnetic Susceptibility Measurements

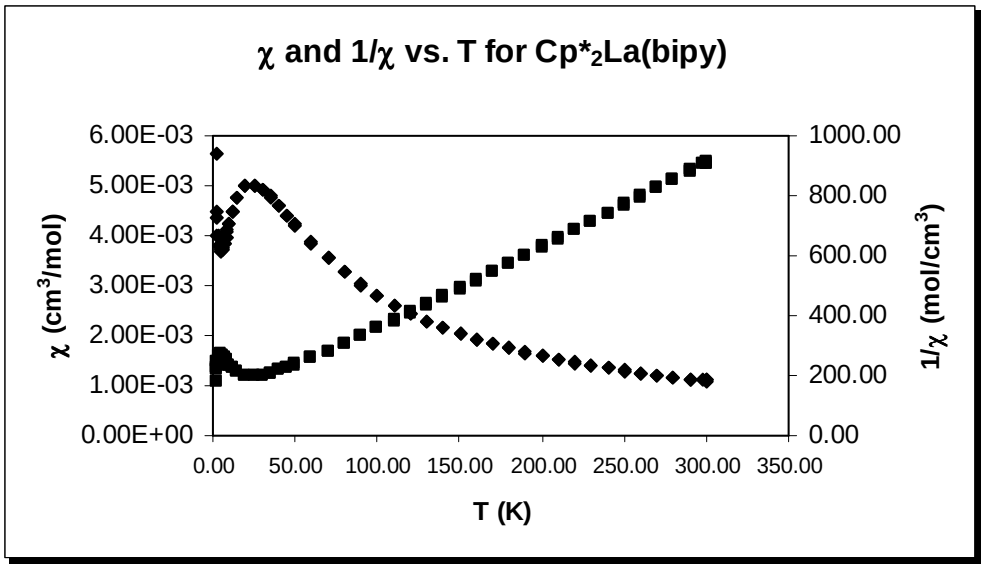
χ and 1/χ vs. T for Cp*2La(bipy)
6.00E-03
5.00E-03
4.00E-03
3.00E-03
2.00E-03
1.00E-03
0.00E+00
χ (cm3/mol)
1000.00
800.00
600.00
400.00
200.00
0.00
1/χ (mol/cm3)
0.00
50.00
100.00
150.00
200.00
250.00
300.00
350.00
T (K)

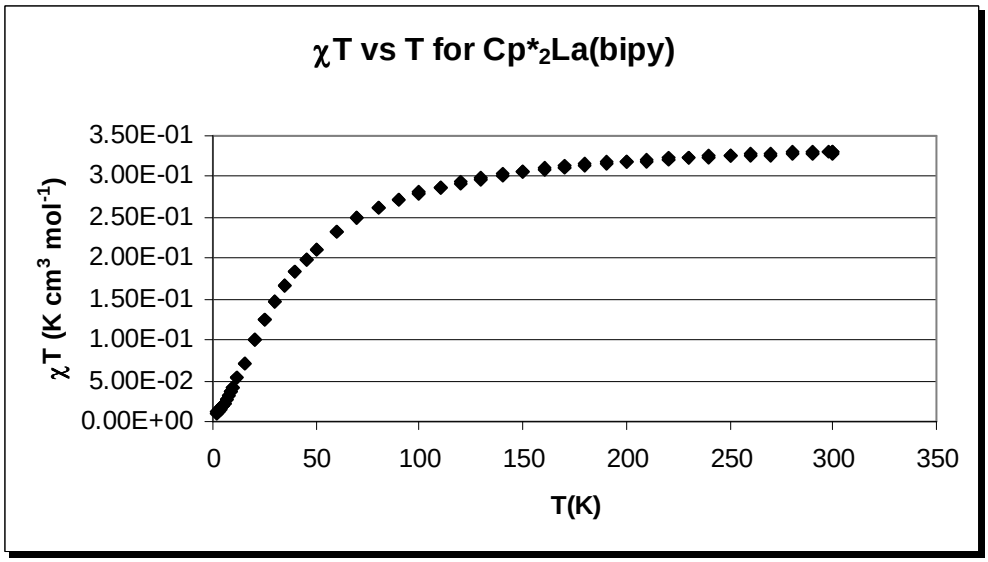
χT vs T for Cp*2La(bipy)
3.50E-01
3.00E-01
2.50E-01
2.00E-01
1.50E-01
1.00E-01
5.00E-02
0.00E+00
χT (K cm3 mol-1)
0
50
100
150
200
250
300
350
T(K)

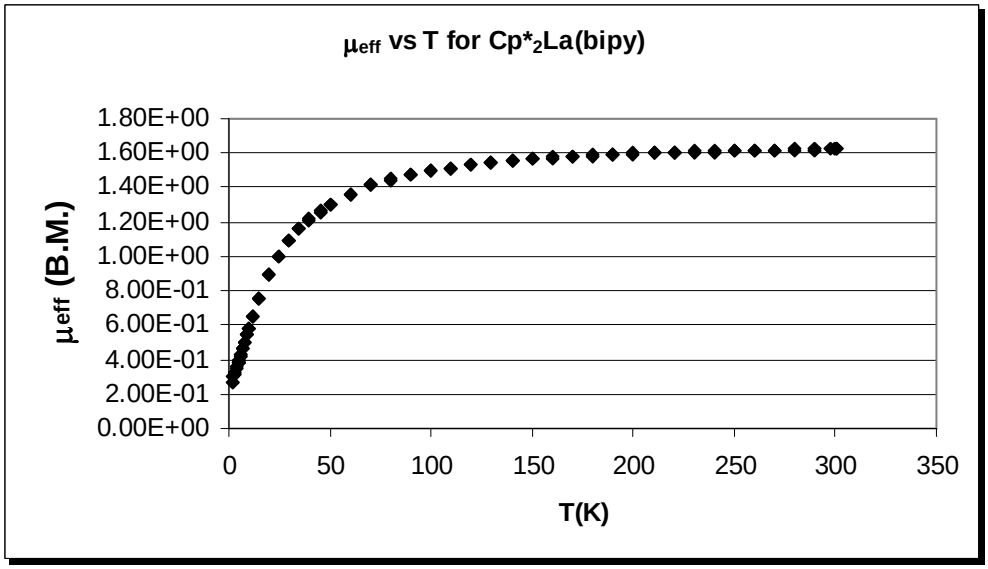
μeff vs T for Cp*2La(bipy)
1.80E+00
1.60E+00
1.40E+00
1.20E+00
1.00E+00
8.00E-01
6.00E-01
4.00E-01
2.00E-01
0.00E+00
μeff (B.M.)
0
50
100
150
200
250
300
350
T(K)

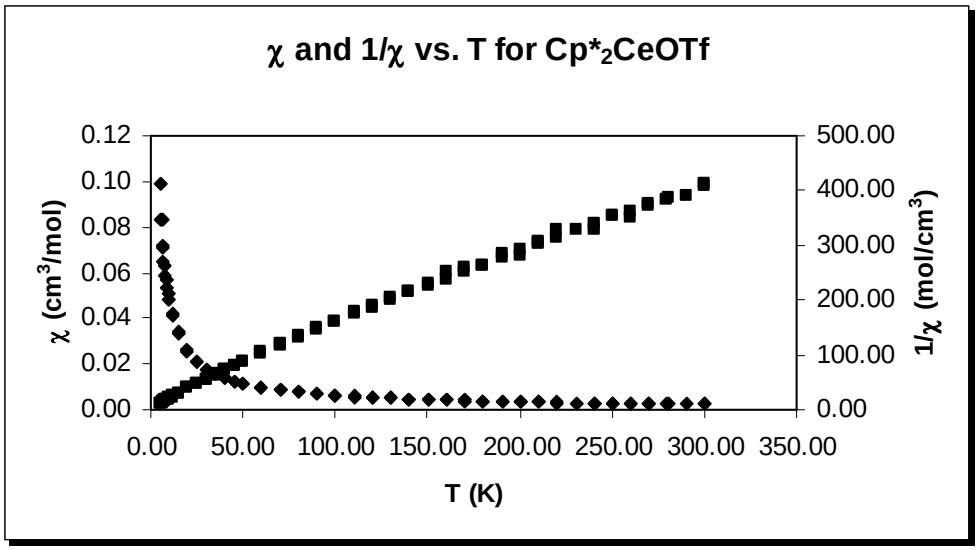
χ and 1/χ vs. T for Cp*2CeOTf
χ (cm3/mol)
1/χ (mol/cm3)
0.12
0.10
0.08
0.06
0.04
0.02
0.00
500.00
400.00
300.00
200.00
100.00
0.00
0.00 50.00 100.00 150.00 200.00 250.00 300.00 350.00
T (K)

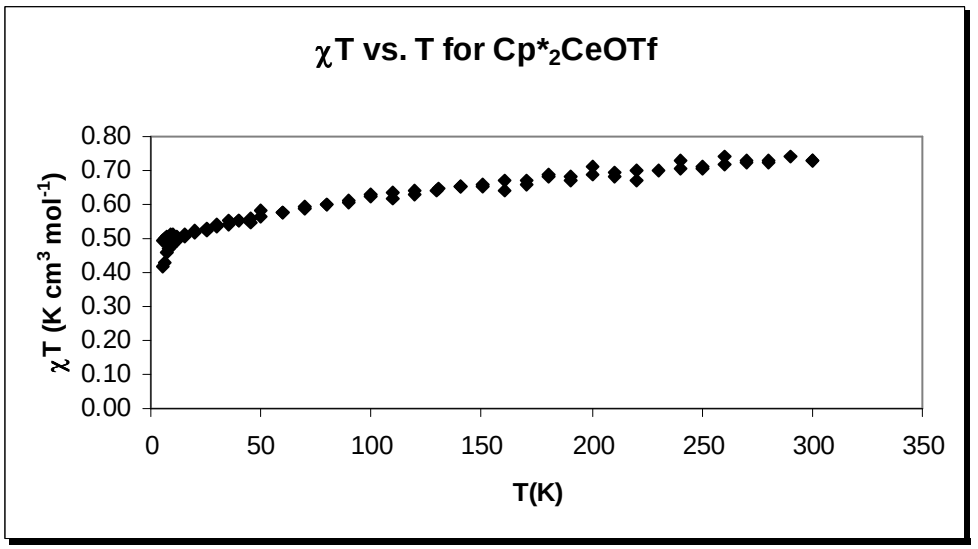
χT vs. T for Cp*2CeOTf
χT (K cm3 mol-1)
0.80
0.70
0.60
0.50
0.40
0.30
0.20
0.10
0.00
0 50 100 150 200 250 300 350
T(K)

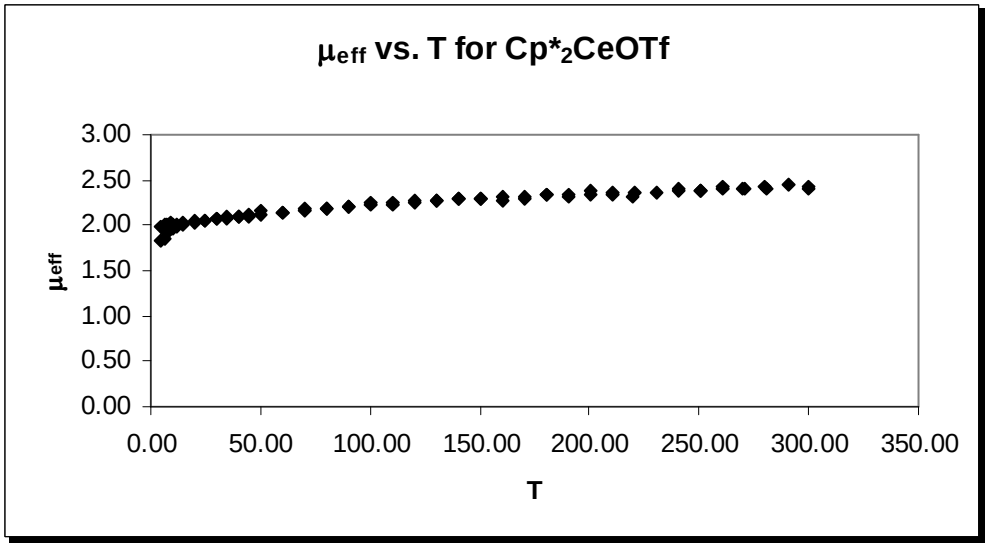
μeff vs. T for Cp*2CeOTf
μeff
3.00
2.50
2.00
1.50
1.00
0.50
0.00
0.00 50.00 100.00 150.00 200.00 250.00 300.00 350.00
T

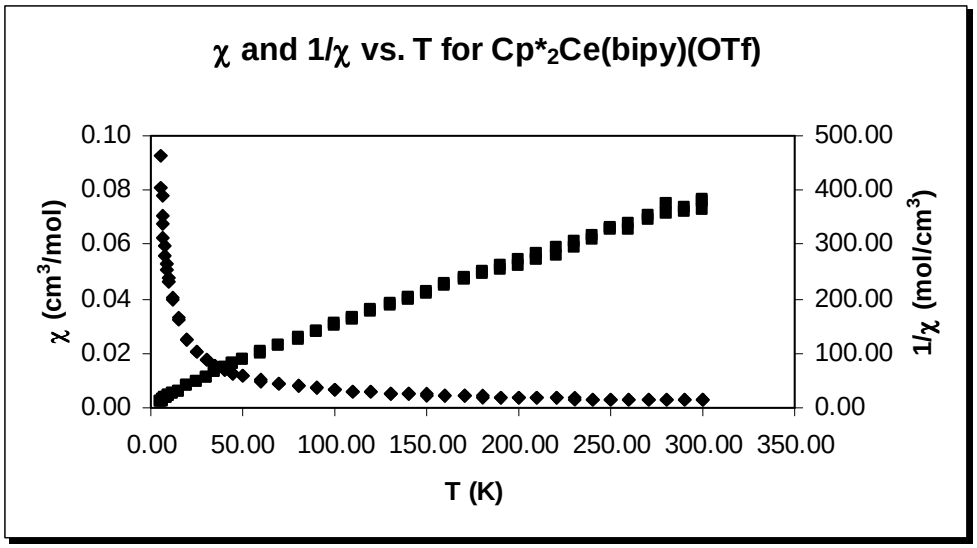
χ and 1/χ vs. T for Cp*2Ce(bipy)(OTf)
χ (cm3/mol)
1/χ (mol/cm3)
0.10
0.08
0.06
0.04
0.02
0.00
500.00
400.00
300.00
200.00
100.00
0.00
0.00 50.00 100.00 150.00 200.00 250.00 300.00 350.00
T (K)

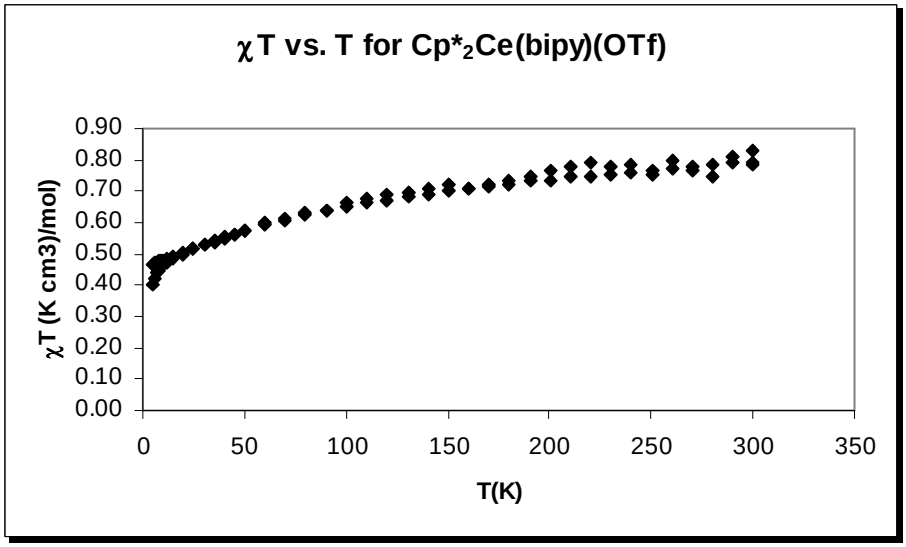
χT vs. T for Cp*2Ce(bipy)(OTf)
χT (K cm3)/mol)
0.90
0.80
0.70
0.60
0.50
0.40
0.30
0.20
0.10
0.00
0 50 100 150 200 250 300 350
T(K)

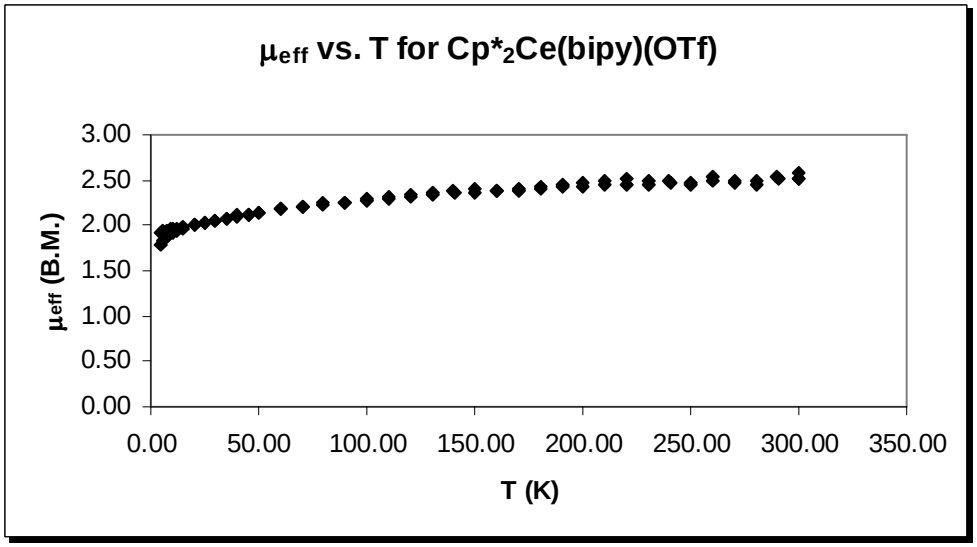
μeff vs. T for Cp*2Ce(bipy)(OTf)
μeff (B.M.)
3.00
2.50
2.00
1.50
1.00
0.50
0.00
0.00 50.00 100.00 150.00 200.00 250.00 300.00 350.00
T (K)

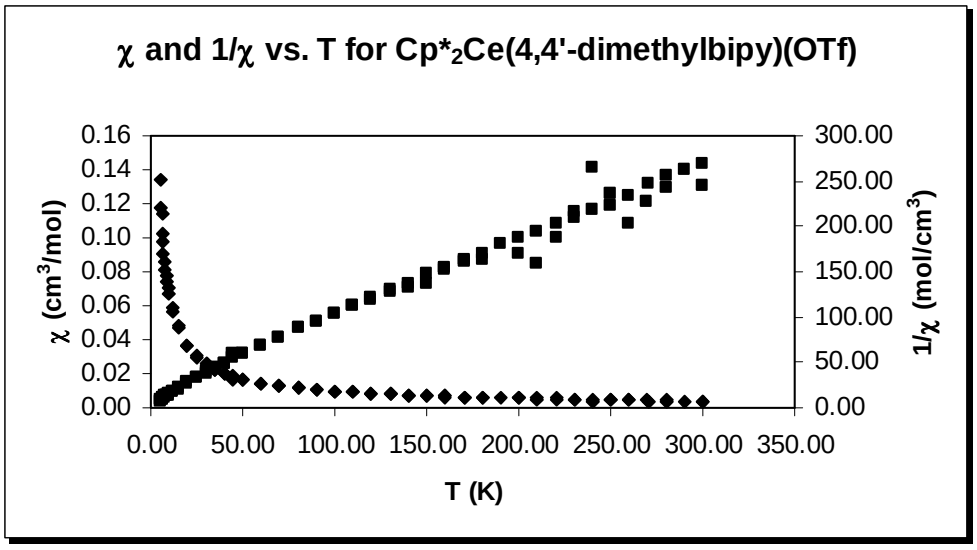
χ and 1/χ vs. T for Cp*2Ce(4,4'-dimethylbipy)(OTf)
χ (cm3/mol)
1/χ (mol/cm3)
T (K)
0.16
0.14
0.12
0.10
0.08
0.06
0.04
0.02
0.00
300.00
250.00
200.00
150.00
100.00
50.00
0.00
0.00 50.00 100.00 150.00 200.00 250.00 300.00 350.00

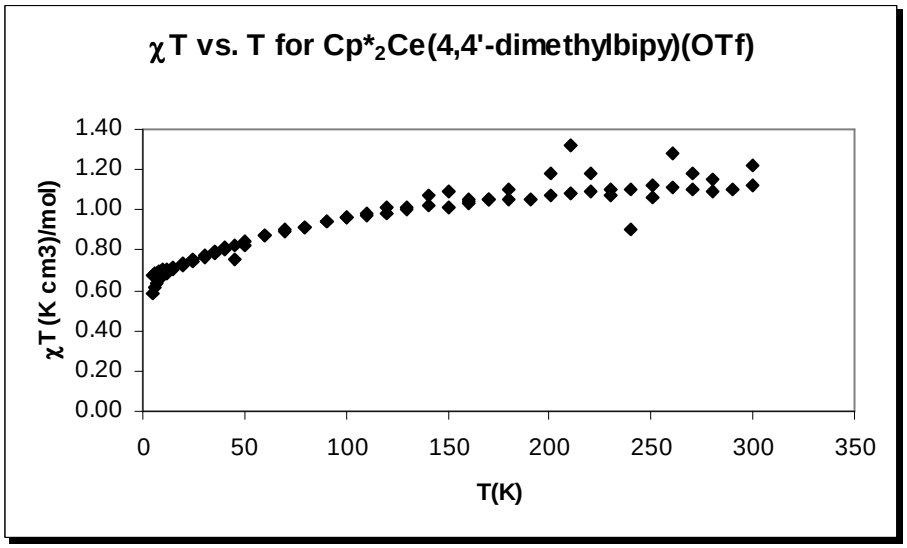
χT vs. T for Cp*2Ce(4,4'-dimethylbipy)(OTf)
χT (K cm3)/mol
T(K)
1.40
1.20
1.00
0.80
0.60
0.40
0.20
0.00
0 50 100 150 200 250 300 350

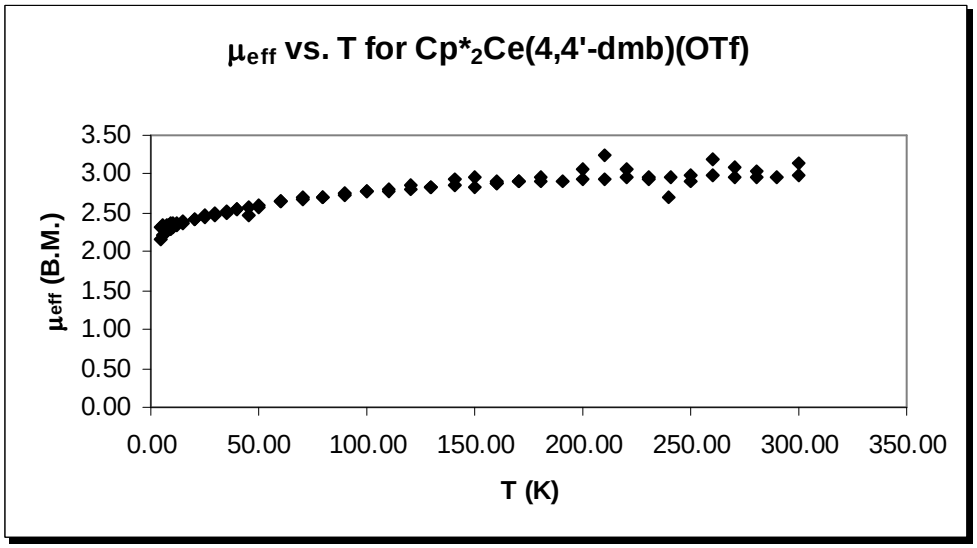
μeff vs. T for Cp*2Ce(4,4'-dmb)(OTf)
μeff (B.M.)
T (K)
3.50
3.00
2.50
2.00
1.50
1.00
0.50
0.00
0.00 50.00 100.00 150.00 200.00 250.00 300.00 350.00

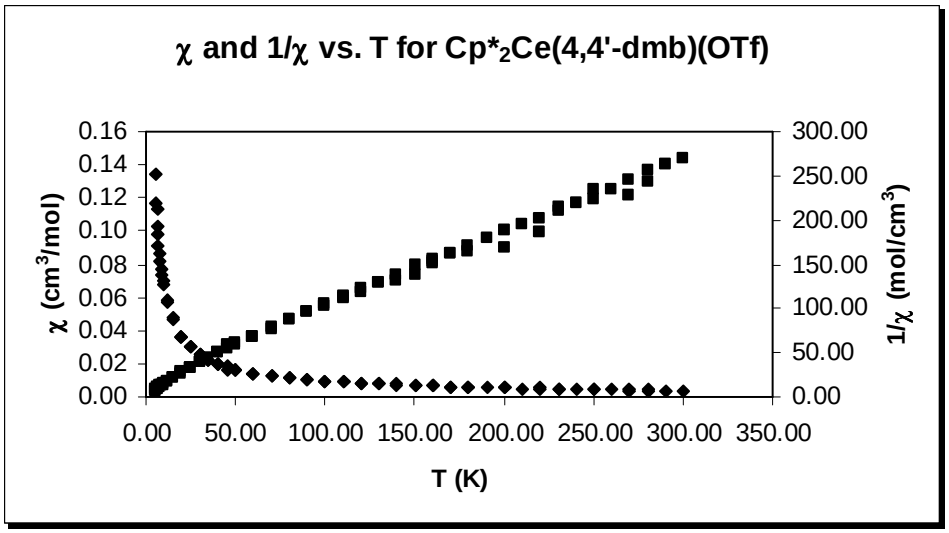
χ and 1/χ vs. T for Cp*2Ce(4,4'-dmb)(OTf)
χ (cm3/mol)
1/χ (mol/cm3)
T (K)
0.16
0.14
0.12
0.10
0.08
0.06
0.04
0.02
0.00
300.00
250.00
200.00
150.00
100.00
50.00
0.00
0.00 50.00 100.00 150.00 200.00 250.00 300.00 350.00

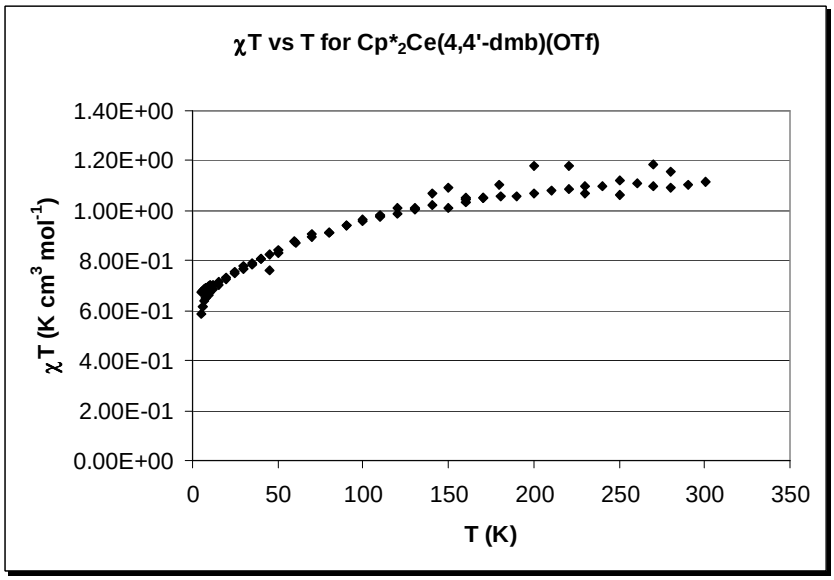
χT vs T for Cp*2Ce(4,4'-dmb)(OTf)
χT (K cm3 mol-1)
T (K)
1.40E+00
1.20E+00
1.00E+00
8.00E-01
6.00E-01
4.00E-01
2.00E-01
0.00E+00
0 50 100 150 200 250 300 350

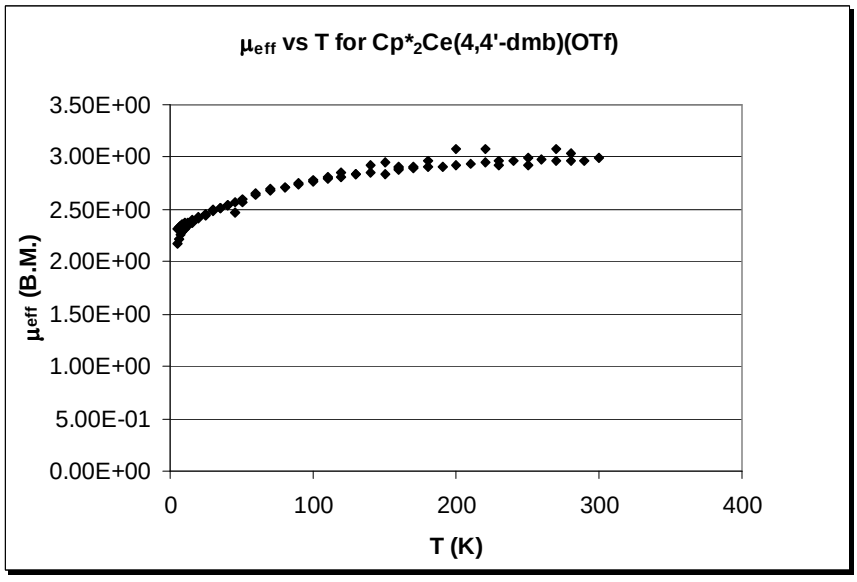
μeff vs T for Cp*2Ce(4,4'-dmb)(OTf)
μeff (B.M.)
T (K)
3.50E+00
3.00E+00
2.50E+00
2.00E+00
1.50E+00
1.00E+00
5.00E-01
0.00E+00
0 100 200 300 400

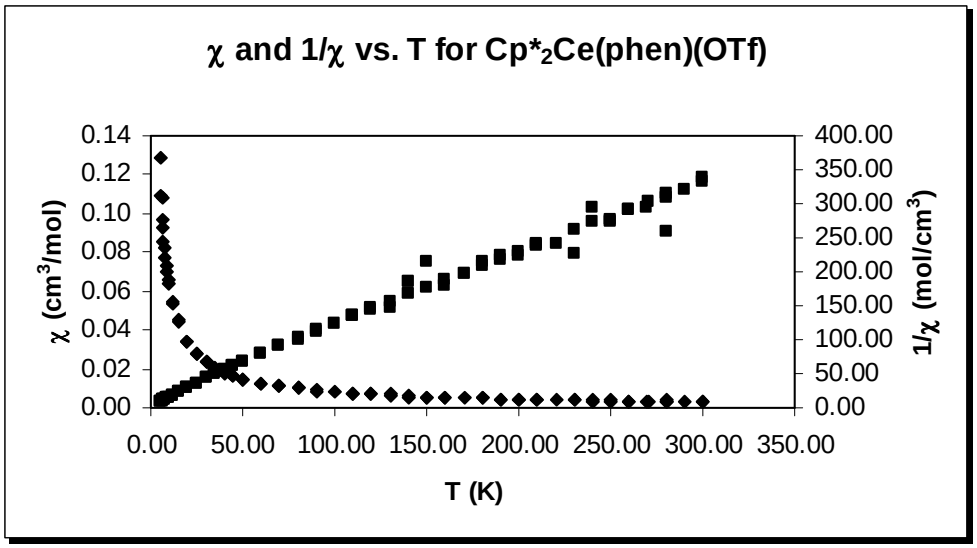
χ and 1/χ vs. T for Cp*2Ce(phen)(OTf)
χ (cm3/mol)
1/χ (mol/cm3)
T (K)
0.14
0.12
0.10
0.08
0.06
0.04
0.02
0.00
400.00
350.00
300.00
250.00
200.00
150.00
100.00
50.00
0.00
0.00 50.00 100.00 150.00 200.00 250.00 300.00 350.00

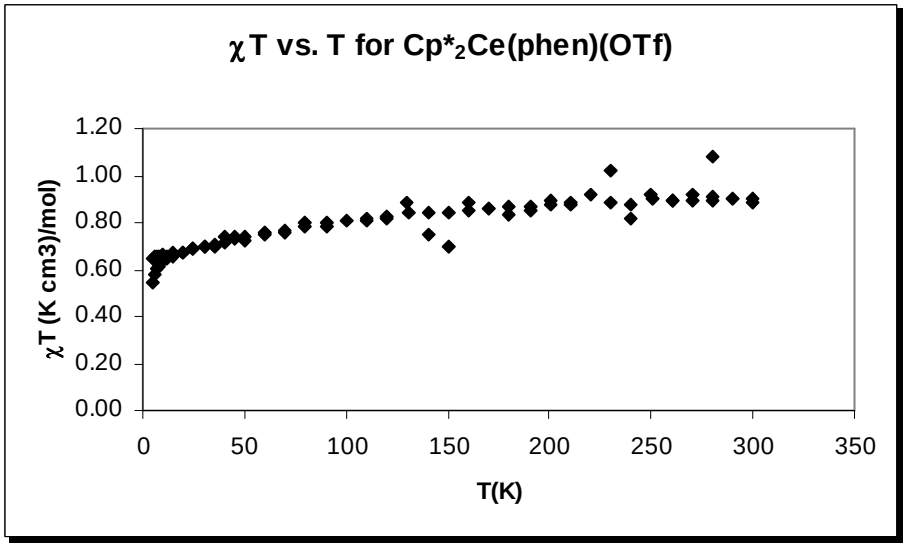
χT vs. T for Cp*2Ce(phen)(OTf)
χT (K cm3)/mol)
T(K)
1.20
1.00
0.80
0.60
0.40
0.20
0.00
0 50 100 150 200 250 300 350

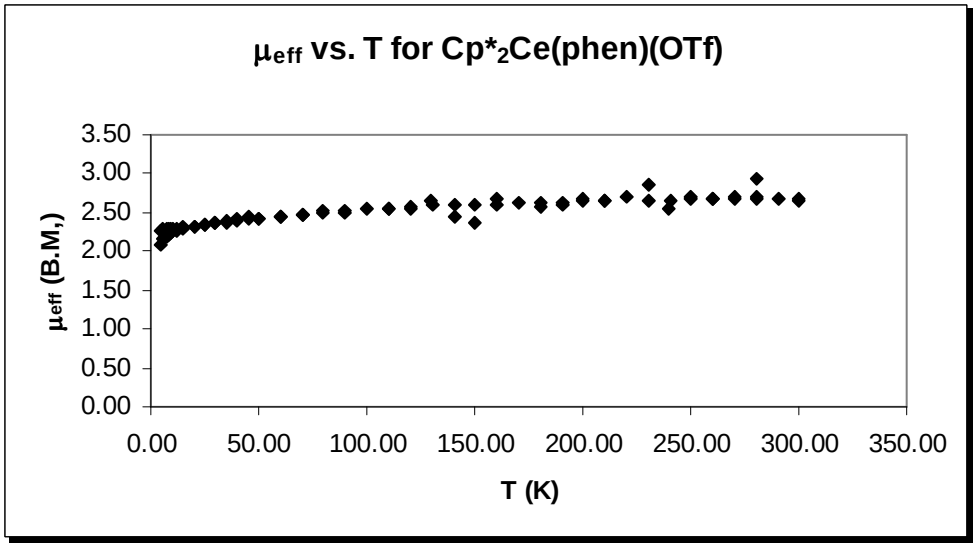
μeff vs. T for Cp*2Ce(phen)(OTf)
μeff (B.M.,)
T (K)
3.50
3.00
2.50
2.00
1.50
1.00
0.50
0.00
0.00 50.00 100.00 150.00 200.00 250.00 300.00 350.00

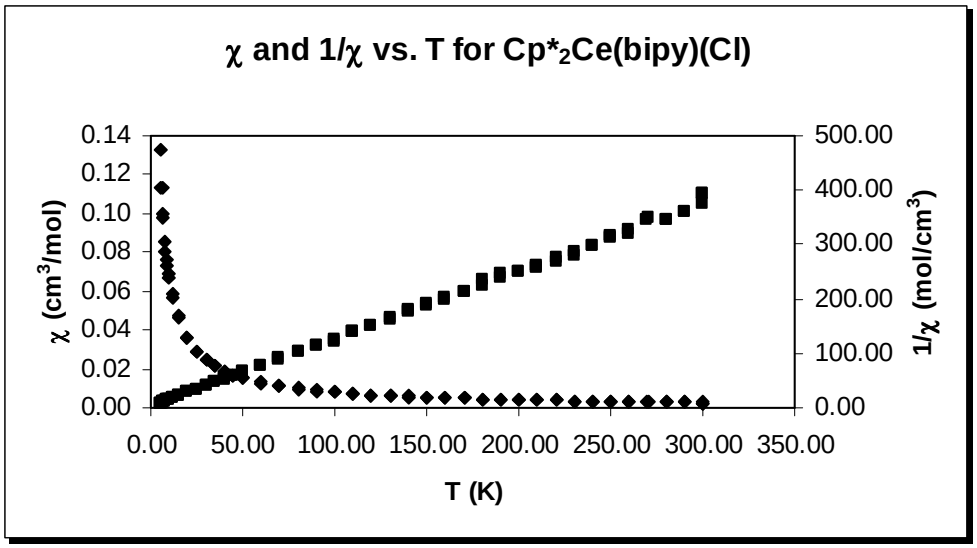
χ and 1/χ vs. T for Cp*2Ce(bipy)(Cl)
χ (cm3/mol)
1/χ (mol/cm3)
0.14
0.12
0.10
0.08
0.06
0.04
0.02
0.00
500.00
400.00
300.00
200.00
100.00
0.00
0.00 50.00 100.00 150.00 200.00 250.00 300.00 350.00
T (K)

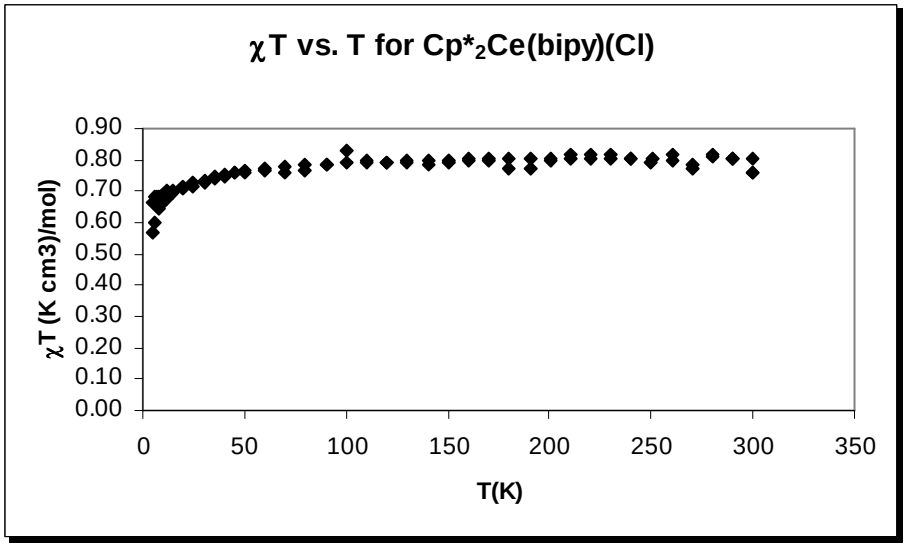
χT vs. T for Cp*2Ce(bipy)(Cl)
χT (K cm3)/mol)
0.90
0.80
0.70
0.60
0.50
0.40
0.30
0.20
0.10
0.00
0 50 100 150 200 250 300 350
T(K)

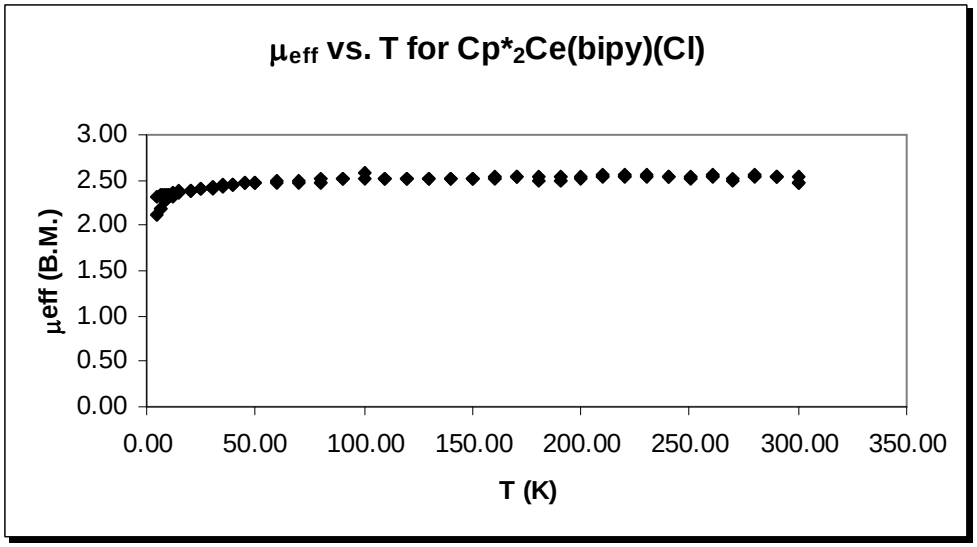
μeff vs. T for Cp*2Ce(bipy)(Cl)
μeff (B.M.)
3.00
2.50
2.00
1.50
1.00
0.50
0.00
0.00 50.00 100.00 150.00 200.00 250.00 300.00 350.00
T (K)

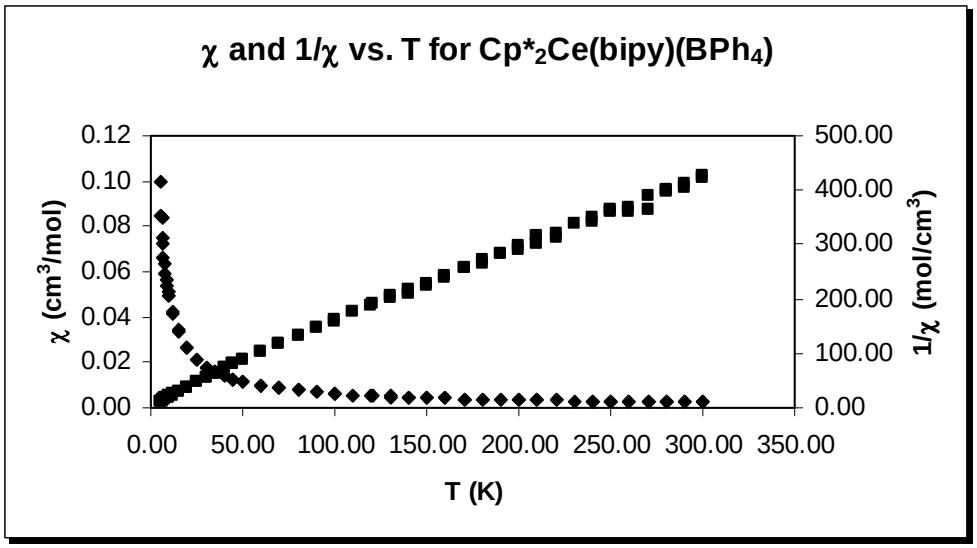
χ and 1/χ vs. T for Cp*2Ce(bipy)(BPh4)
χ (cm3/mol)
1/χ (mol/cm3)
0.12
0.10
0.08
0.06
0.04
0.02
0.00
500.00
400.00
300.00
200.00
100.00
0.00
0.00 50.00 100.00 150.00 200.00 250.00 300.00 350.00
T (K)

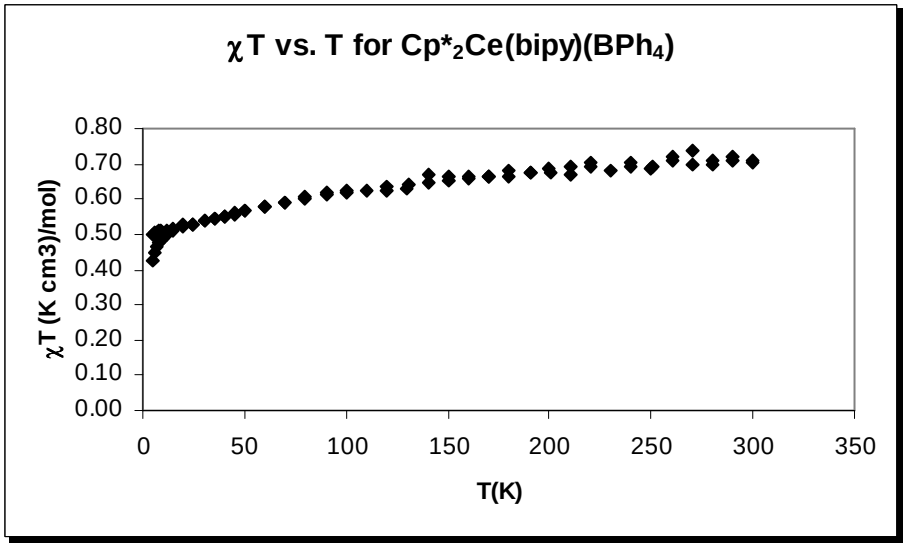
χT vs. T for Cp*2Ce(bipy)(BPh4)
χT (K cm3)/mol)
0.80
0.70
0.60
0.50
0.40
0.30
0.20
0.10
0.00
0 50 100 150 200 250 300 350
T(K)

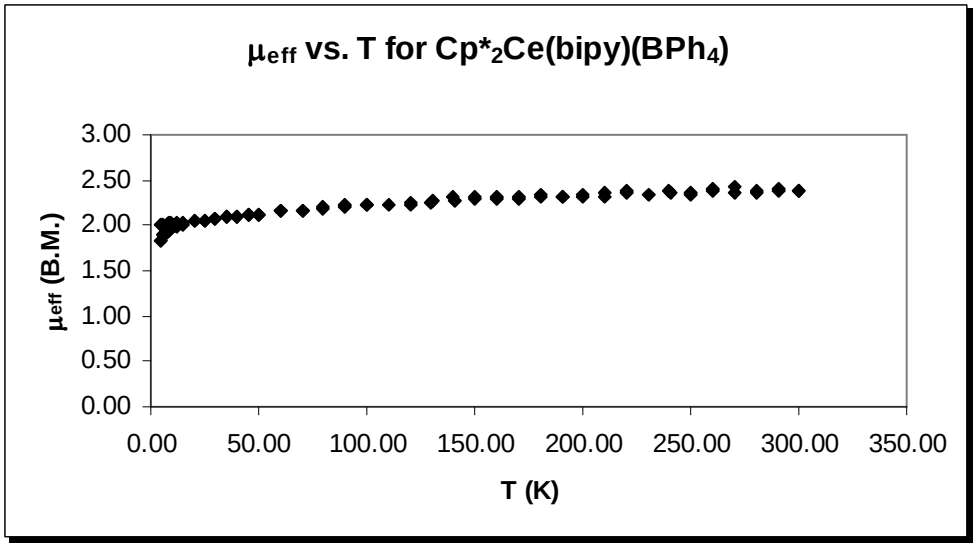
μeff vs. T for Cp*2Ce(bipy)(BPh4)
μeff (B.M.)
3.00
2.50
2.00
1.50
1.00
0.50
0.00
0.00 50.00 100.00 150.00 200.00 250.00 300.00 350.00
T (K)

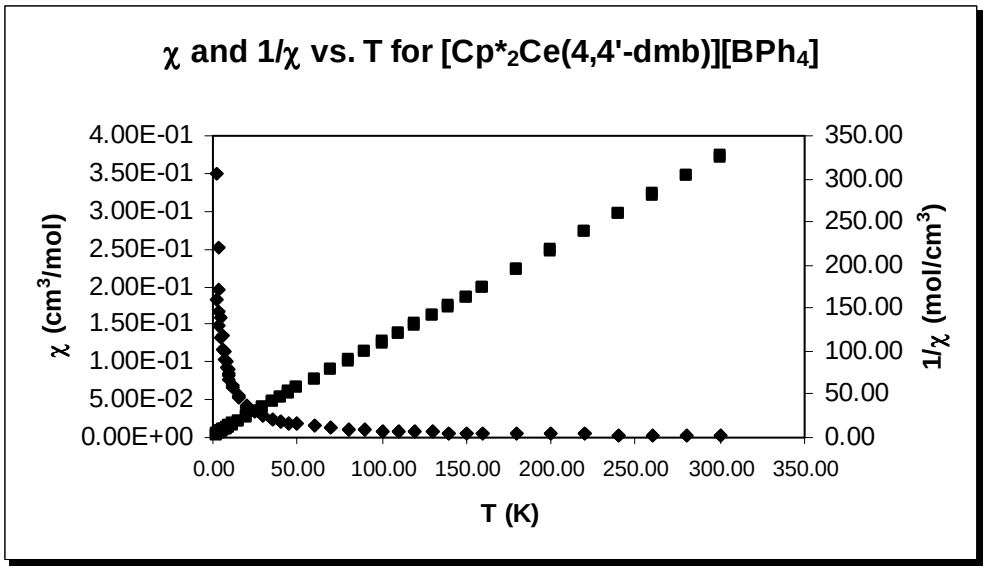
χ and 1/χ vs. T for [Cp*2Ce(4,4'-dmb)][BPh4]
4.00E-01
3.50E-01
3.00E-01
2.50E-01
2.00E-01
1.50E-01
1.00E-01
5.00E-02
0.00E+00
χ (cm3/mol)
350.00
300.00
250.00
200.00
150.00
100.00
50.00
0.00
1/χ (mol/cm3)
0.00
50.00
100.00
150.00
200.00
250.00
300.00
350.00
T (K)

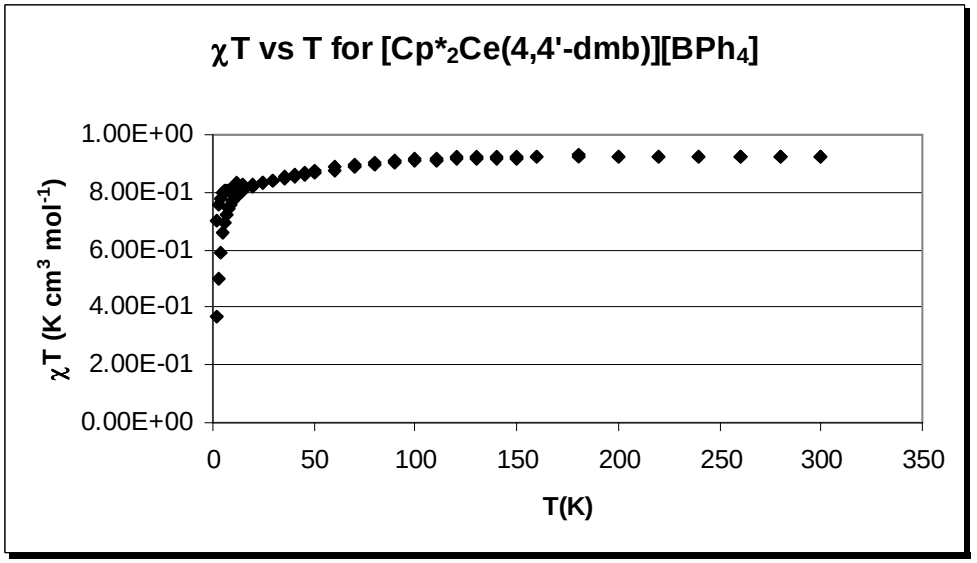
χT vs T for [Cp*2Ce(4,4'-dmb)][BPh4]
1.00E+00
8.00E-01
6.00E-01
4.00E-01
2.00E-01
0.00E+00
χT (K cm3 mol-1)
0
50
100
150
200
250
300
350
T(K)

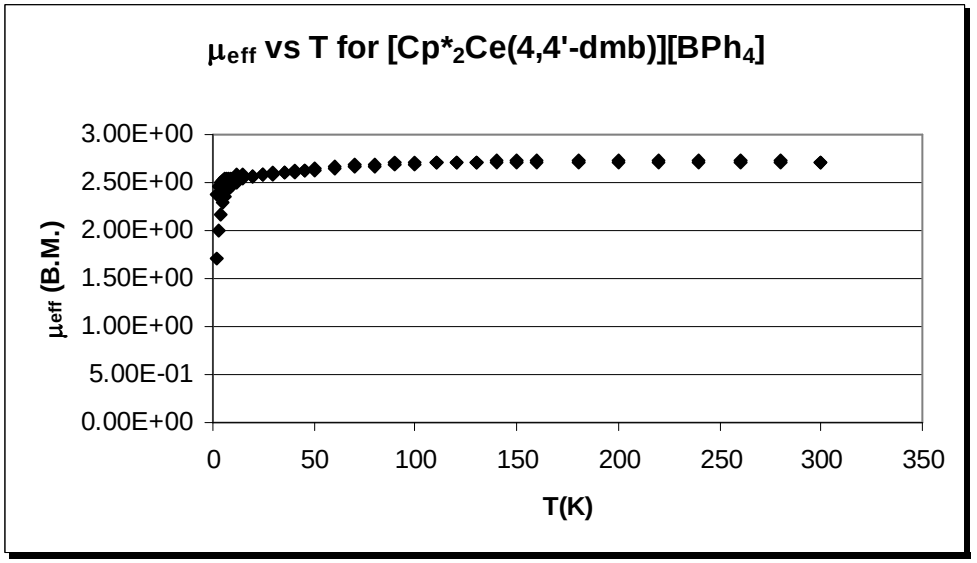
μeff vs T for [Cp*2Ce(4,4'-dmb)][BPh4]
3.00E+00
2.50E+00
2.00E+00
1.50E+00
1.00E+00
5.00E-01
0.00E+00
μeff (B.M.)
0
50
100
150
200
250
300
350
T(K)

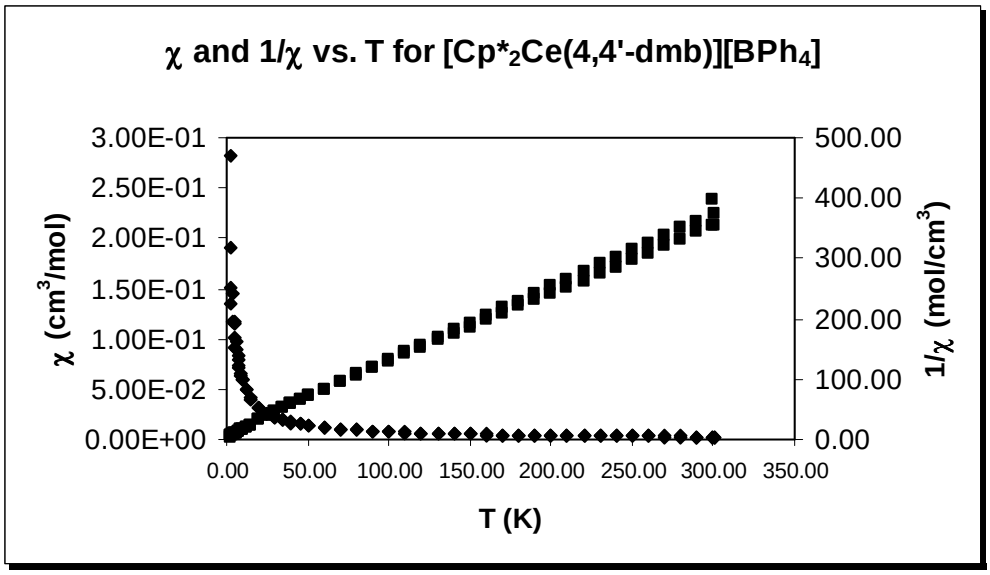
χ and 1/χ vs. T for [Cp*2Ce(4,4'-dmb)][BPh4]
3.00E-01
2.50E-01
2.00E-01
1.50E-01
1.00E-01
5.00E-02
0.00E+00
χ (cm3/mol)
500.00
400.00
300.00
200.00
100.00
0.00
1/χ (mol/cm3)
0.00 50.00 100.00 150.00 200.00 250.00 300.00 350.00
T (K)

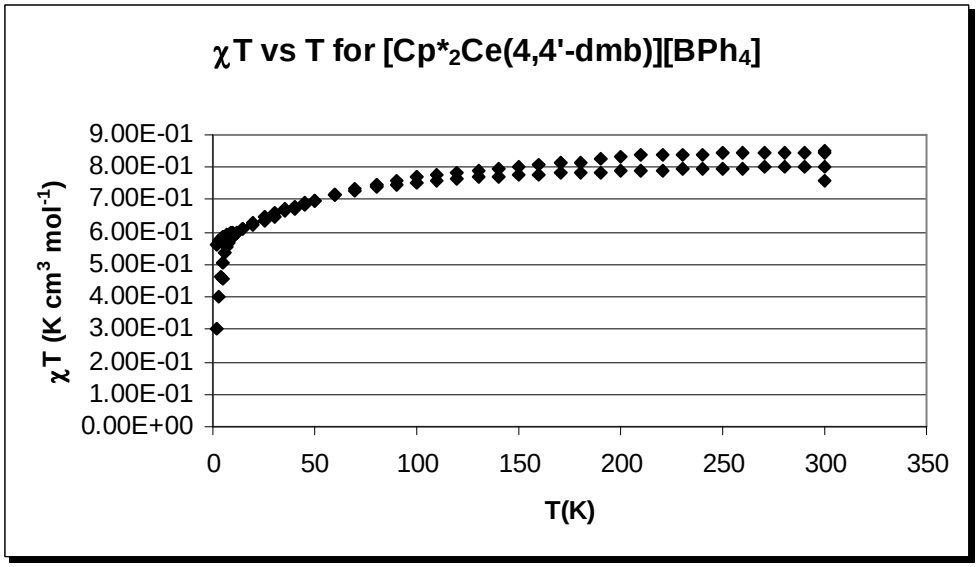
χT vs T for [Cp*2Ce(4,4'-dmb)][BPh4]
9.00E-01
8.00E-01
7.00E-01
6.00E-01
5.00E-01
4.00E-01
3.00E-01
2.00E-01
1.00E-01
0.00E+00
χT (K cm3 mol-1)
0 50 100 150 200 250 300 350
T(K)

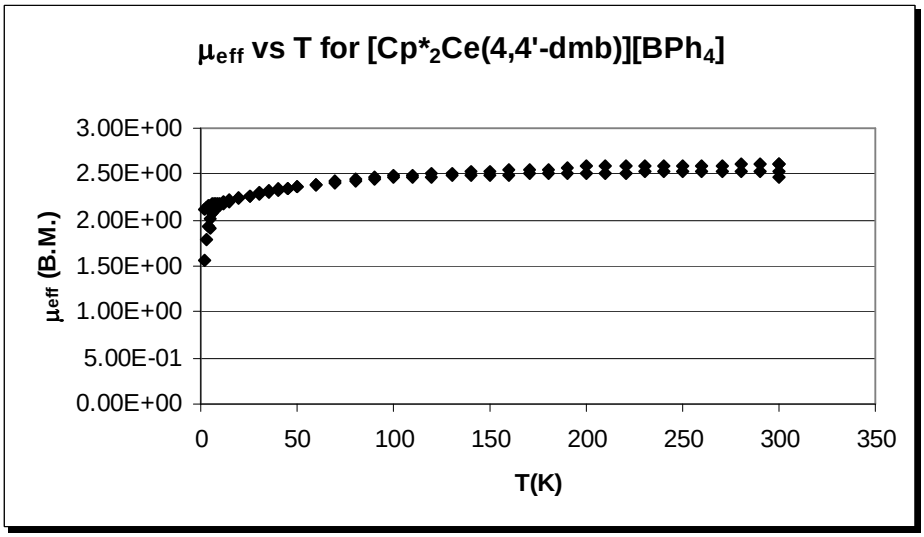
μeff vs T for [Cp*2Ce(4,4'-dmb)][BPh4]
3.00E+00
2.50E+00
2.00E+00
1.50E+00
1.00E+00
5.00E-01
0.00E+00
μeff (B.M.)
0 50 100 150 200 250 300 350
T(K)

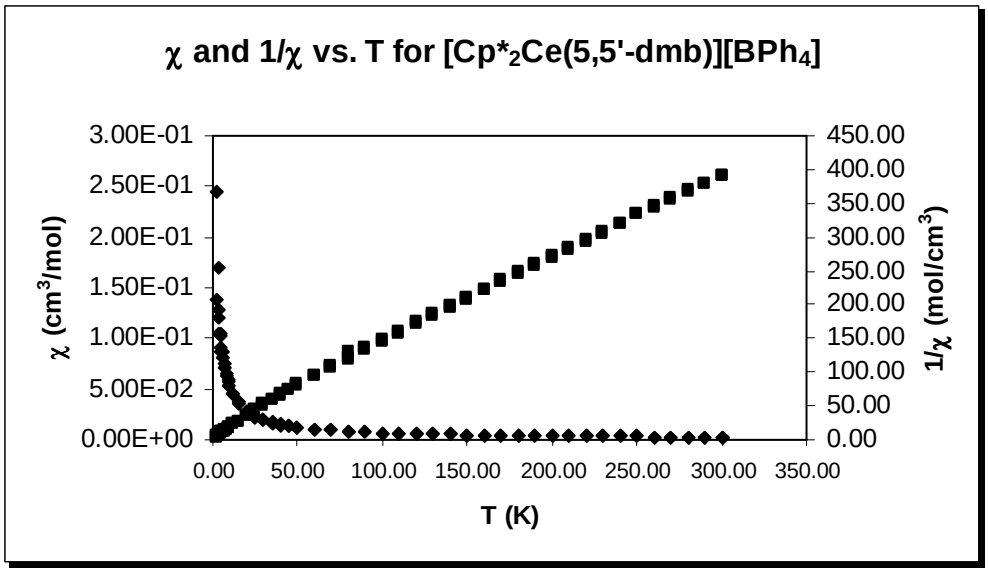
χ and 1/χ vs. T for [Cp*2Ce(5,5'-dmb)][BPh4]
3.00E-01
2.50E-01
2.00E-01
1.50E-01
1.00E-01
5.00E-02
0.00E+00
χ (cm3/mol)
450.00
400.00
350.00
300.00
250.00
200.00
150.00
100.00
50.00
0.00
1/χ (mol/cm3)
0.00
50.00
100.00
150.00
200.00
250.00
300.00
350.00
T (K)

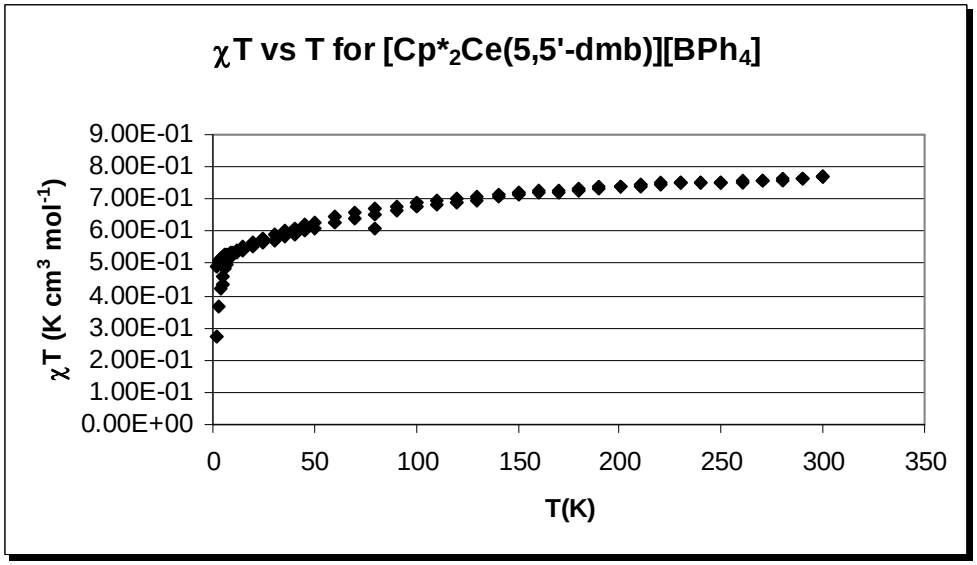
χT vs T for [Cp*2Ce(5,5'-dmb)][BPh4]
9.00E-01
8.00E-01
7.00E-01
6.00E-01
5.00E-01
4.00E-01
3.00E-01
2.00E-01
1.00E-01
0.00E+00
χT (K cm3 mol-1)
0
50
100
150
200
250
300
350
T(K)

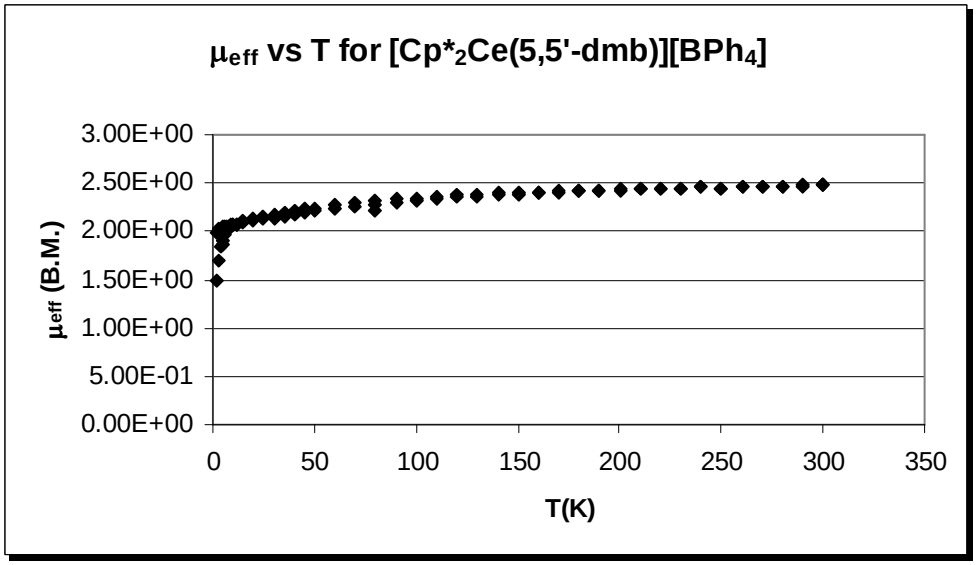
μeff vs T for [Cp*2Ce(5,5'-dmb)][BPh4]
3.00E+00
2.50E+00
2.00E+00
1.50E+00
1.00E+00
5.00E-01
0.00E+00
μeff (B.M.)
0
50
100
150
200
250
300
350
T(K)

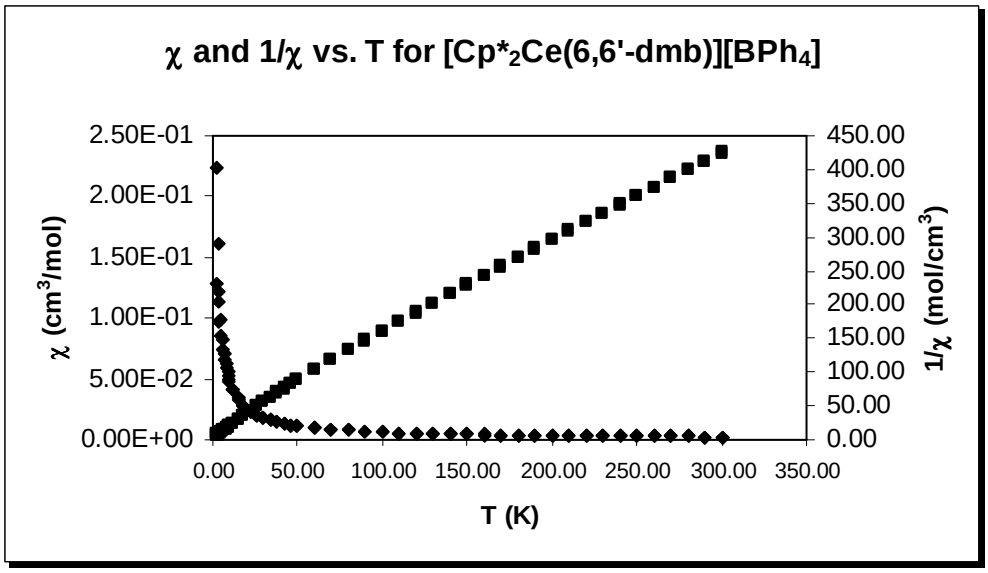
χ and 1/χ vs. T for [Cp*2Ce(6,6'-dmb)][BPh4]
2.50E-01
2.00E-01
1.50E-01
1.00E-01
5.00E-02
0.00E+00
χ (cm3/mol)
450.00
400.00
350.00
300.00
250.00
200.00
150.00
100.00
50.00
0.00
1/χ (mol/cm3)
0.00
50.00
100.00
150.00
200.00
250.00
300.00
350.00
T (K)

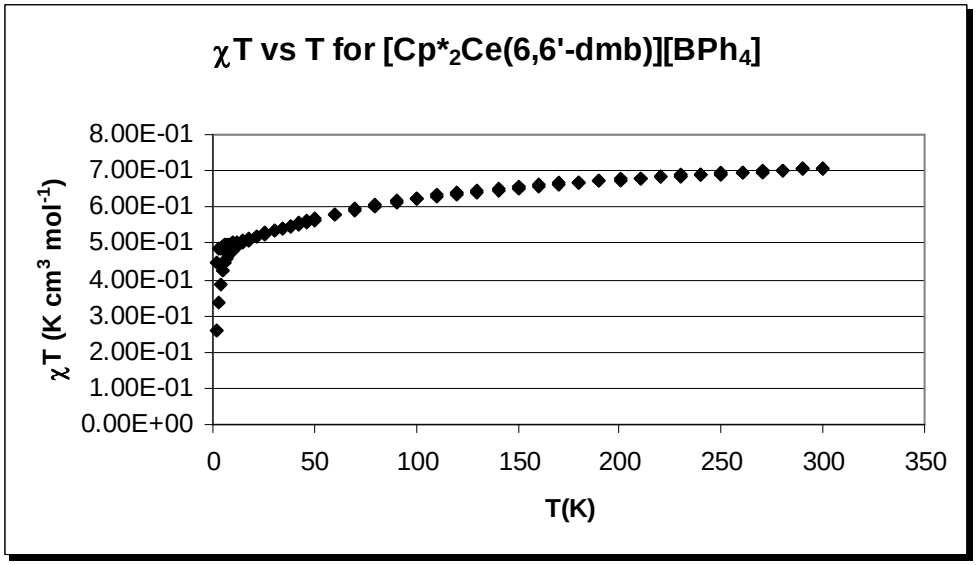
χT vs T for [Cp*2Ce(6,6'-dmb)][BPh4]
8.00E-01
7.00E-01
6.00E-01
5.00E-01
4.00E-01
3.00E-01
2.00E-01
1.00E-01
0.00E+00
χT (K cm3 mol-1)
0
50
100
150
200
250
300
350
T(K)

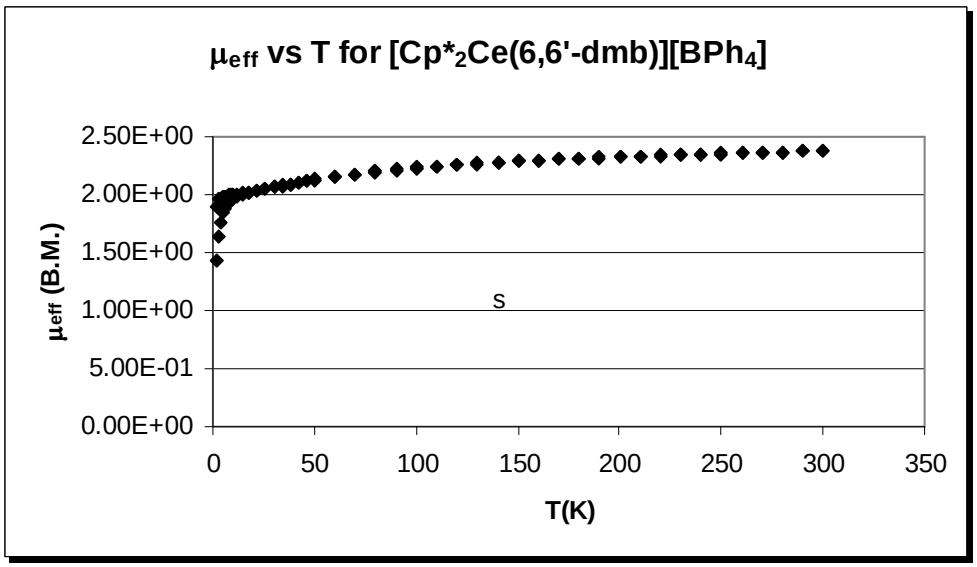
μeff vs T for [Cp*2Ce(6,6'-dmb)][BPh4]
2.50E+00
2.00E+00
1.50E+00
1.00E+00
5.00E-01
0.00E+00
μeff (B.M.)
0
50
100
150
200
250
300
350
T(K)

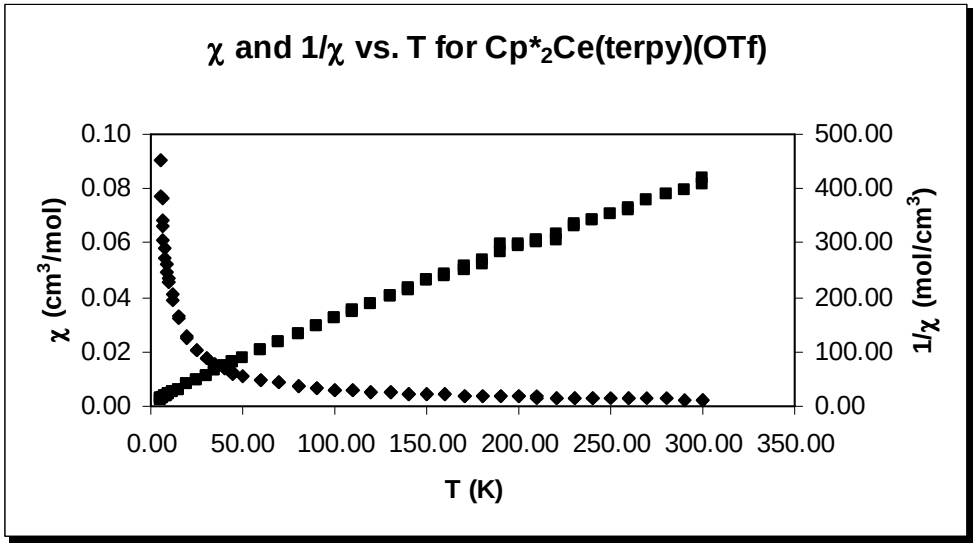
χ and 1/χ vs. T for Cp*2Ce(terpy)(OTf)
0.10
0.08
0.06
0.04
0.02
0.00
χ (cm3/mol)
500.00
400.00
300.00
200.00
100.00
0.00
1/χ (mol/cm3)
0.00 50.00 100.00 150.00 200.00 250.00 300.00 350.00
T (K)

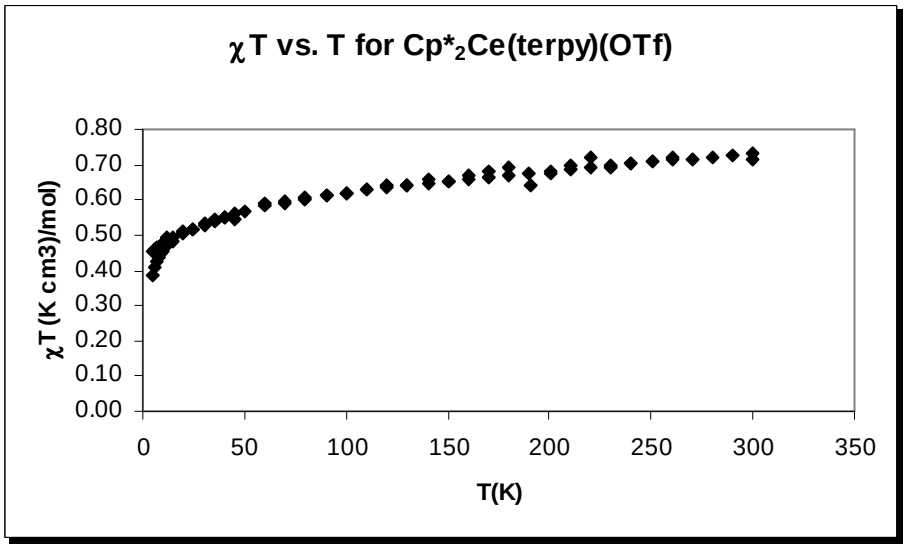
χT vs. T for Cp*2Ce(terpy)(OTf)
0.80
0.70
0.60
0.50
0.40
0.30
0.20
0.10
0.00
χT (K cm3)/mol)
0 50 100 150 200 250 300 350
T(K)

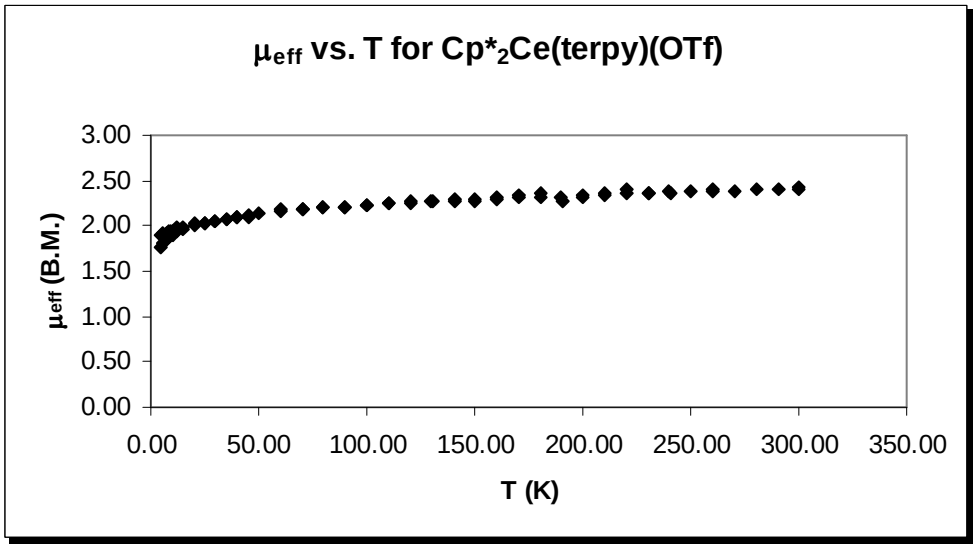
μeff vs. T for Cp*2Ce(terpy)(OTf)
3.00
2.50
2.00
1.50
1.00
0.50
0.00
μeff (B.M.)
0.00 50.00 100.00 150.00 200.00 250.00 300.00 350.00
T (K)

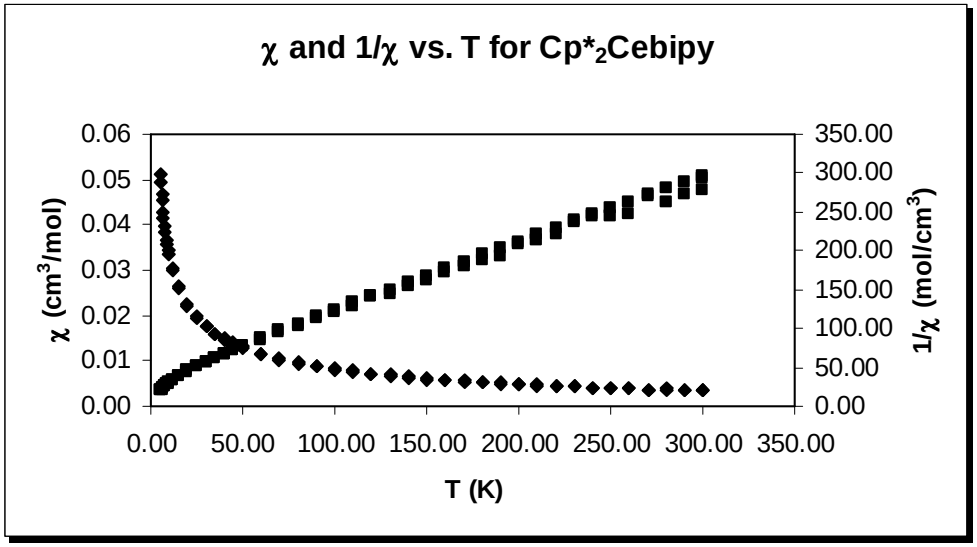
χ and 1/χ vs. T for Cp*2Cebipy
χ (cm3/mol)
1/χ (mol/cm3)
T (K)
0.06
0.05
0.04
0.03
0.02
0.01
0.00
350.00
300.00
250.00
200.00
150.00
100.00
50.00
0.00
0.00 50.00 100.00 150.00 200.00 250.00 300.00 350.00

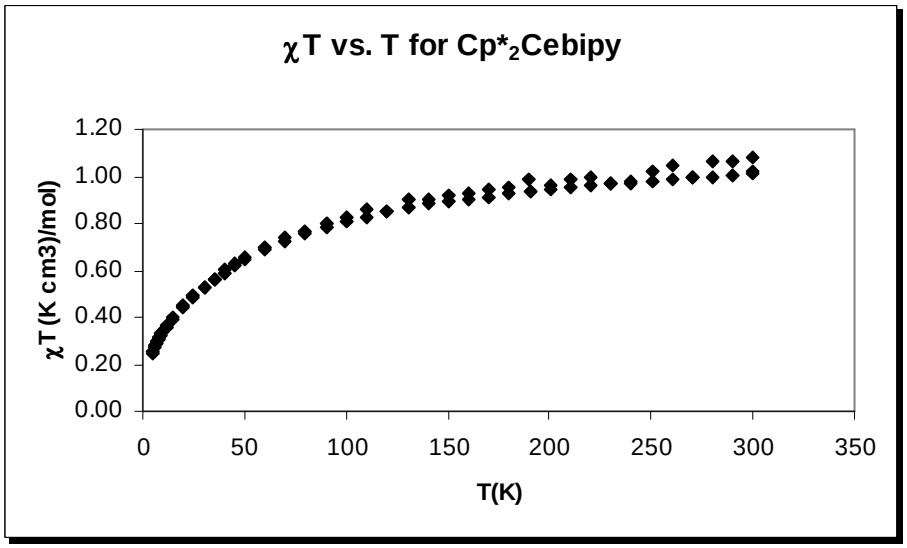
χT vs. T for Cp*2Cebipy
χT (K cm3)/mol
T(K)
1.20
1.00
0.80
0.60
0.40
0.20
0.00
0 50 100 150 200 250 300 350

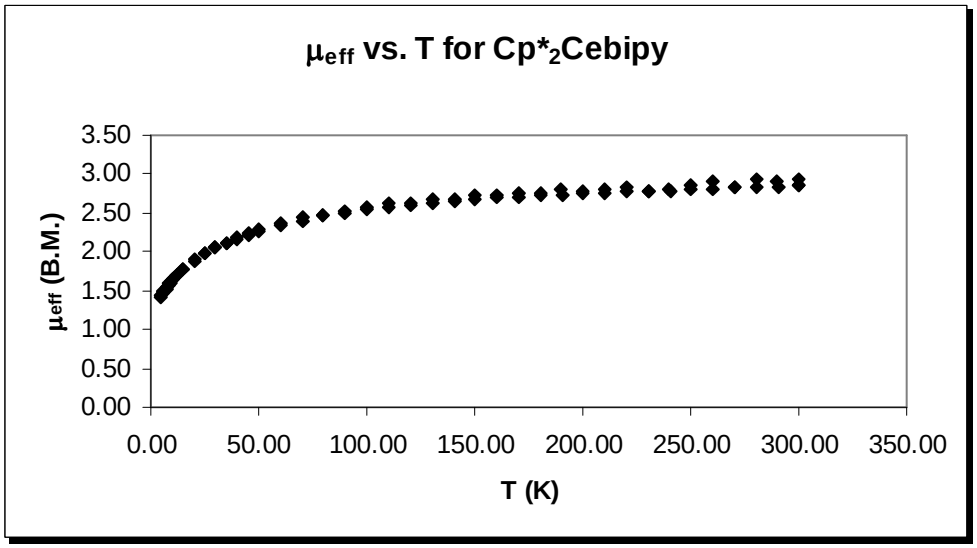
μeff vs. T for Cp*2Cebipy
μeff (B.M.)
T (K)
3.50
3.00
2.50
2.00
1.50
1.00
0.50
0.00
0.00 50.00 100.00 150.00 200.00 250.00 300.00 350.00

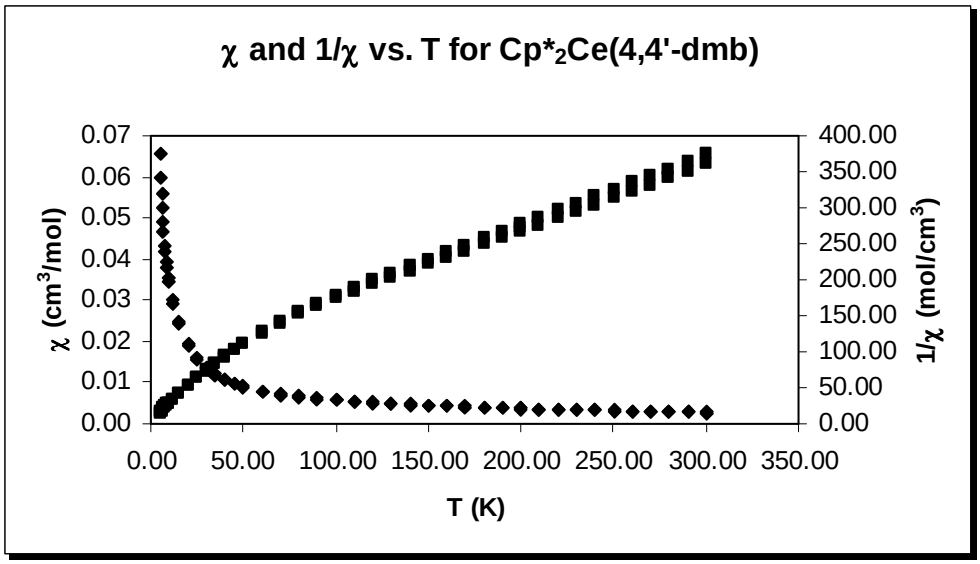
χ and 1/χ vs. T for Cp*2Ce(4,4'-dmb)
χ (cm3/mol)
1/χ (mol/cm3)
T (K)
0.07
0.06
0.05
0.04
0.03
0.02
0.01
0.00
400.00
350.00
300.00
250.00
200.00
150.00
100.00
50.00
0.00
0.00 50.00 100.00 150.00 200.00 250.00 300.00 350.00

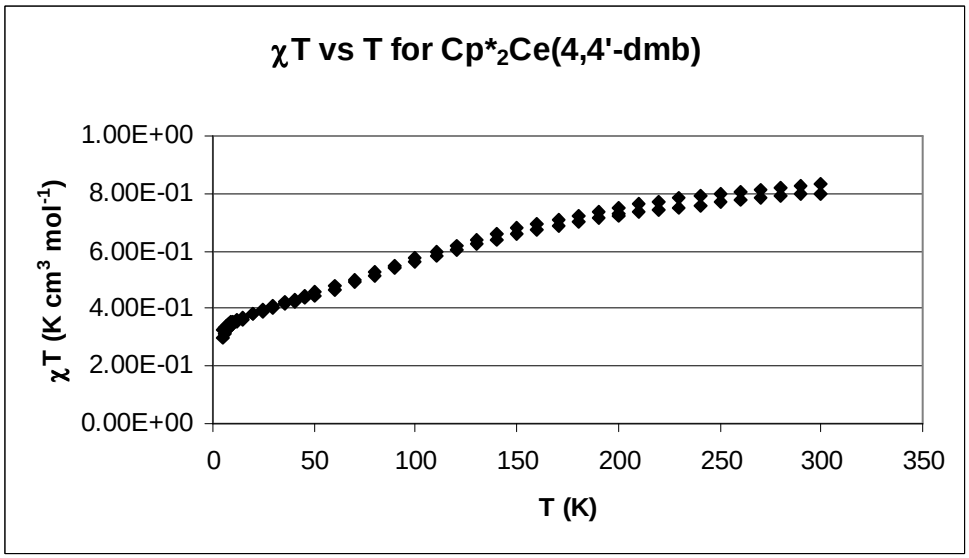
χT vs T for Cp*2Ce(4,4'-dmb)
χT (K cm3 mol-1)
T (K)
1.00E+00
8.00E-01
6.00E-01
4.00E-01
2.00E-01
0.00E+00
0 50 100 150 200 250 300 350

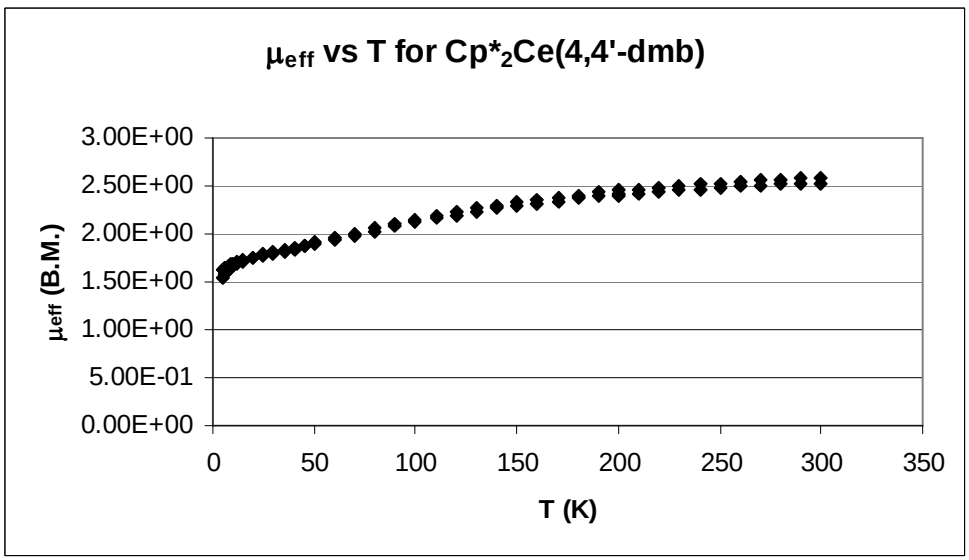
μeff vs T for Cp*2Ce(4,4'-dmb)
μeff (B.M.)
T (K)
3.00E+00
2.50E+00
2.00E+00
1.50E+00
1.00E+00
5.00E-01
0.00E+00
0 50 100 150 200 250 300 350

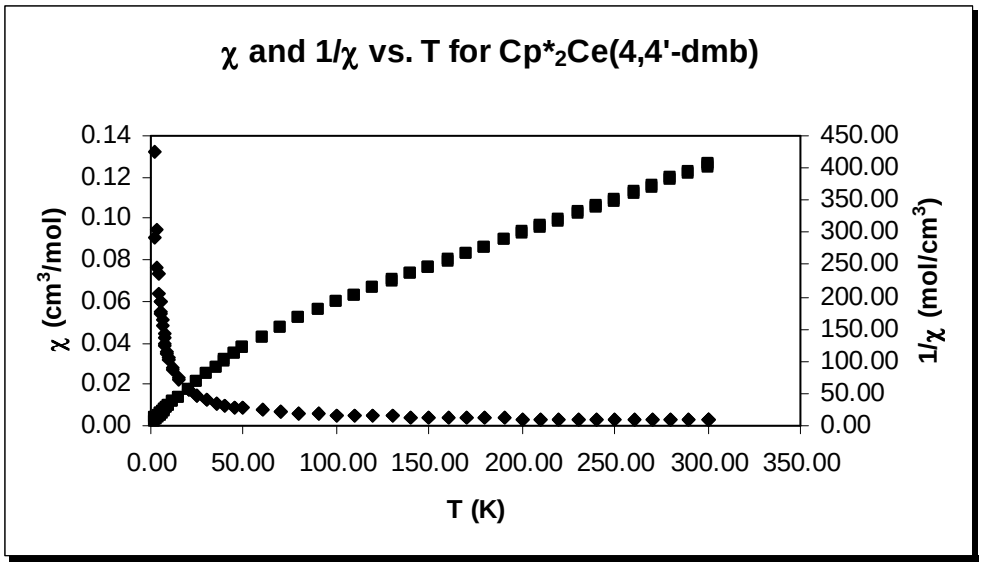
χ and 1/χ vs. T for Cp*2Ce(4,4'-dmb)
χ (cm3/mol)
1/χ (mol/cm3)
T (K)
0.14
0.12
0.10
0.08
0.06
0.04
0.02
0.00
450.00
400.00
350.00
300.00
250.00
200.00
150.00
100.00
50.00
0.00
0.00 50.00 100.00 150.00 200.00 250.00 300.00 350.00

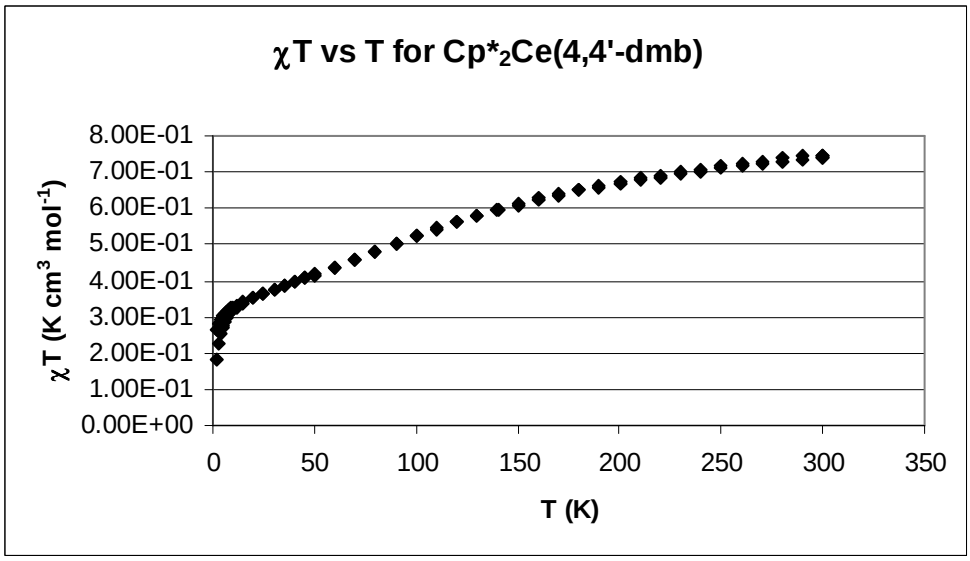
χT vs T for Cp*2Ce(4,4'-dmb)
χT (K cm3 mol-1)
T (K)
8.00E-01
7.00E-01
6.00E-01
5.00E-01
4.00E-01
3.00E-01
2.00E-01
1.00E-01
0.00E+00
0 50 100 150 200 250 300 350

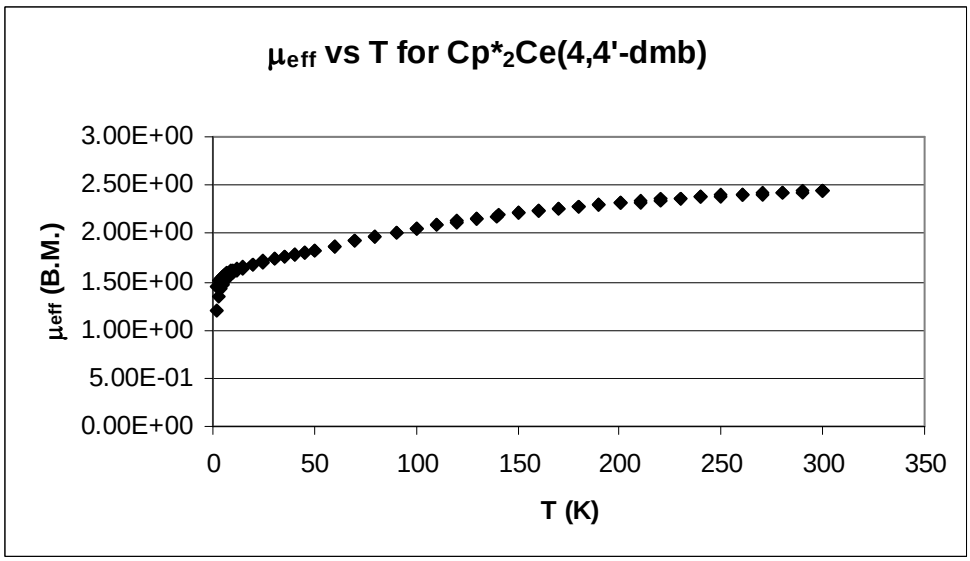
μeff vs T for Cp*2Ce(4,4'-dmb)
μeff (B.M.)
T (K)
3.00E+00
2.50E+00
2.00E+00
1.50E+00
1.00E+00
5.00E-01
0.00E+00
0 50 100 150 200 250 300 350

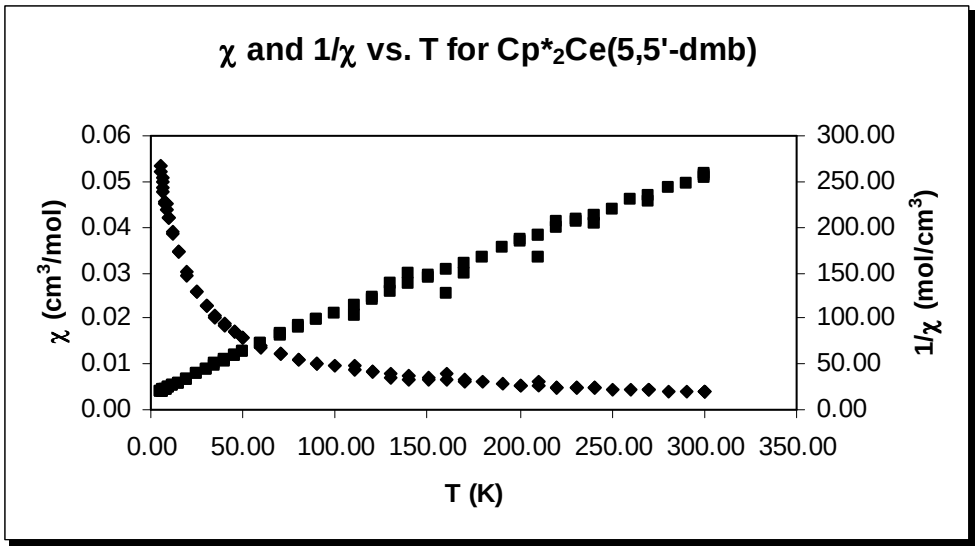
χ and 1/χ vs. T for Cp*2Ce(5,5'-dmb)
χ (cm3/mol)
1/χ (mol/cm3)
T (K)
0.06
0.05
0.04
0.03
0.02
0.01
0.00
300.00
250.00
200.00
150.00
100.00
50.00
0.00
0.00 50.00 100.00 150.00 200.00 250.00 300.00 350.00

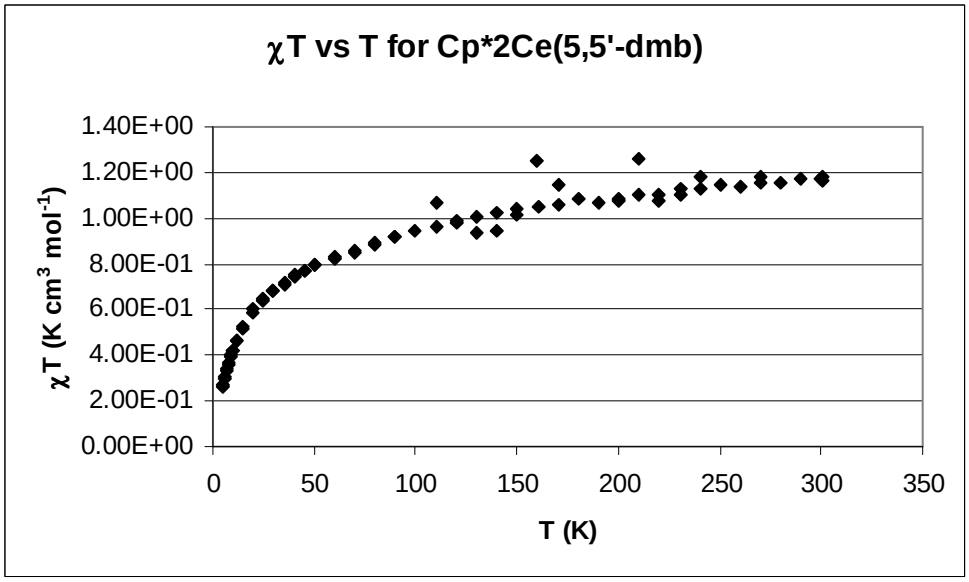
χT vs T for Cp*2Ce(5,5'-dmb)
χT (K cm3 mol-1)
T (K)
1.40E+00
1.20E+00
1.00E+00
8.00E-01
6.00E-01
4.00E-01
2.00E-01
0.00E+00
0 50 100 150 200 250 300 350

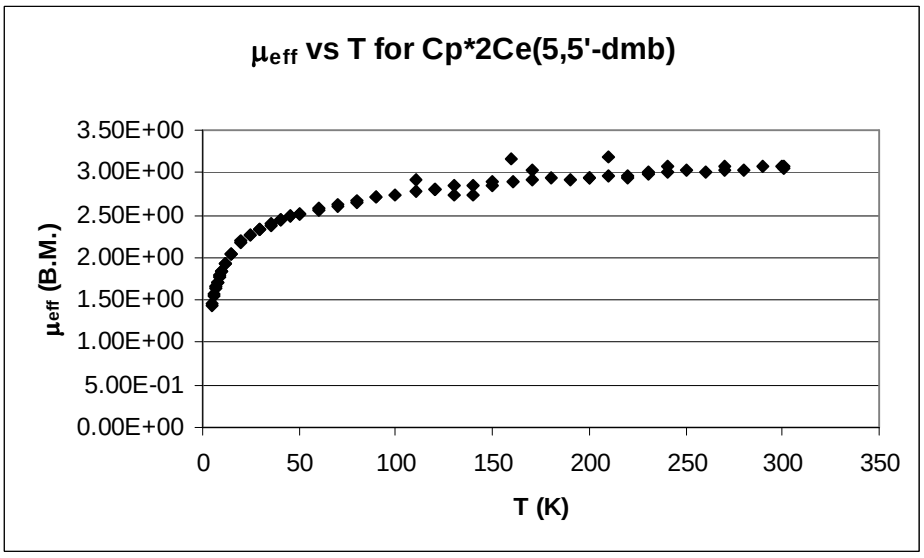
μeff vs T for Cp*2Ce(5,5'-dmb)
μeff (B.M.)
T (K)
3.50E+00
3.00E+00
2.50E+00
2.00E+00
1.50E+00
1.00E+00
5.00E-01
0.00E+00
0 50 100 150 200 250 300 350

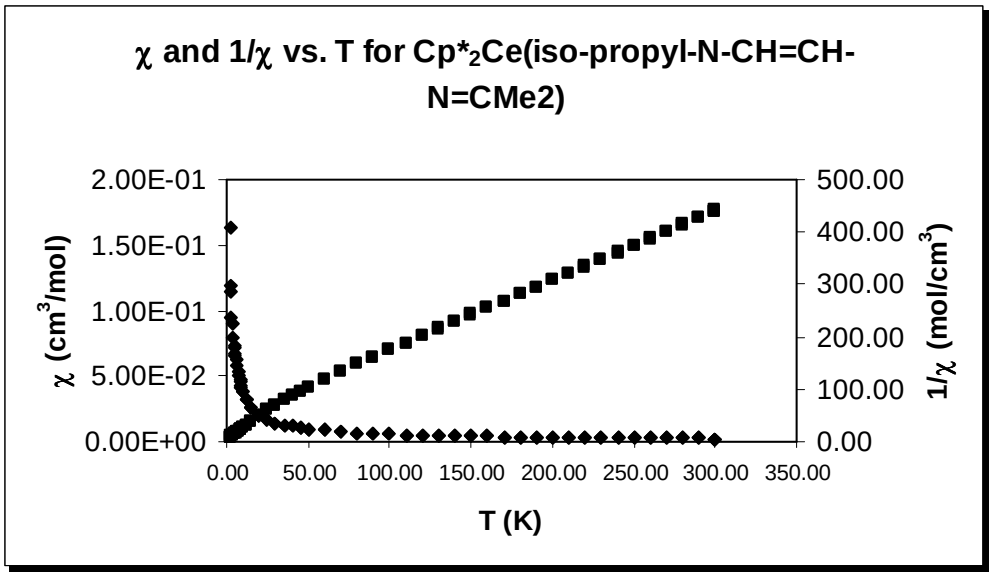
χ and 1/χ vs. T for Cp*2Ce(iso-propyl-N-CH=CH-N=CMe2)
2.00E-01
1.50E-01
1.00E-01
5.00E-02
0.00E+00
χ (cm3/mol)
500.00
400.00
300.00
200.00
100.00
0.00
1/χ (mol/cm3)
0.00
50.00
100.00
150.00
200.00
250.00
300.00
350.00
T (K)

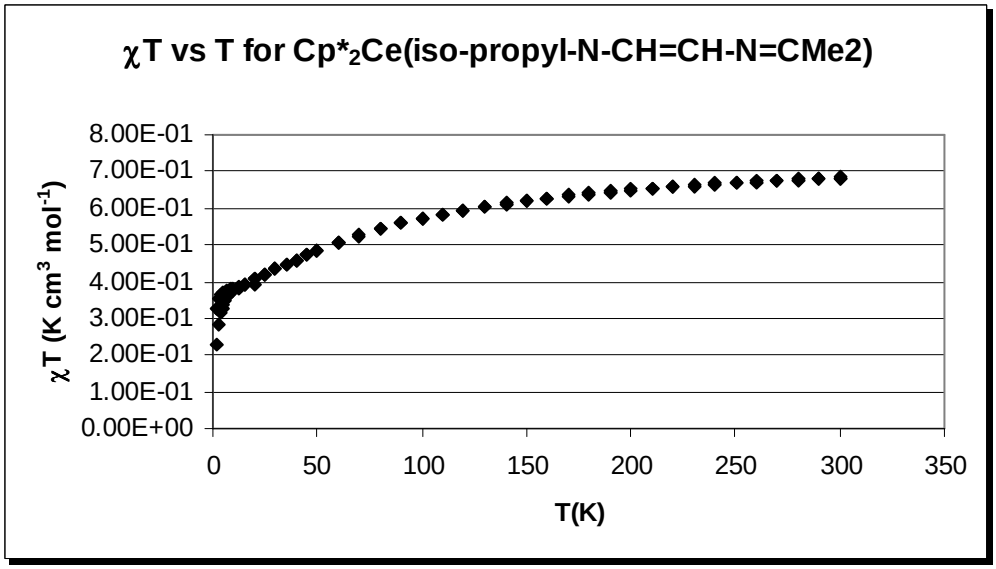
χT vs T for Cp*2Ce(iso-propyl-N-CH=CH-N=CMe2)
8.00E-01
7.00E-01
6.00E-01
5.00E-01
4.00E-01
3.00E-01
2.00E-01
1.00E-01
0.00E+00
χT (K cm3 mol-1)
0
50
100
150
200
250
300
350
T(K)

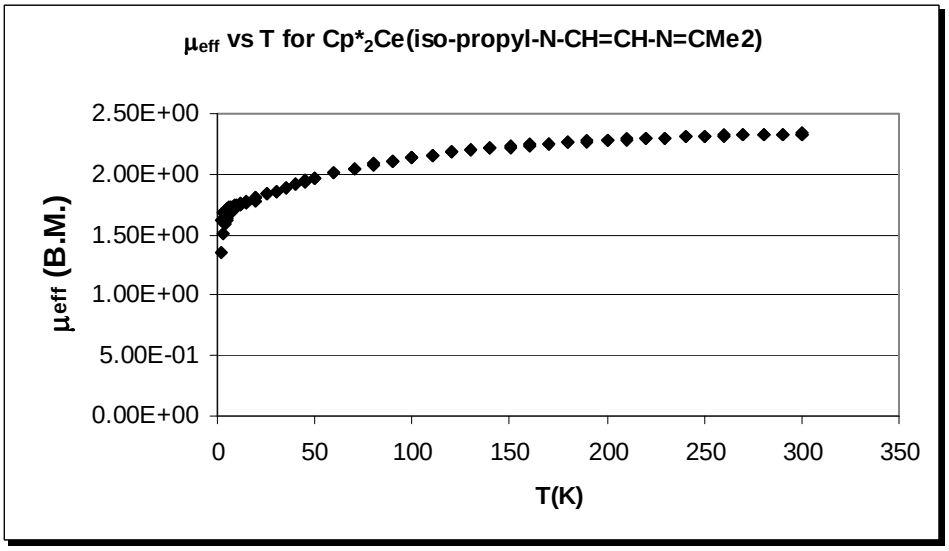
μeff vs T for Cp*2Ce(iso-propyl-N-CH=CH-N=CMe2)
2.50E+00
2.00E+00
1.50E+00
1.00E+00
5.00E-01
0.00E+00
μeff (B.M.)
0
50
100
150
200
250
300
350
T(K)

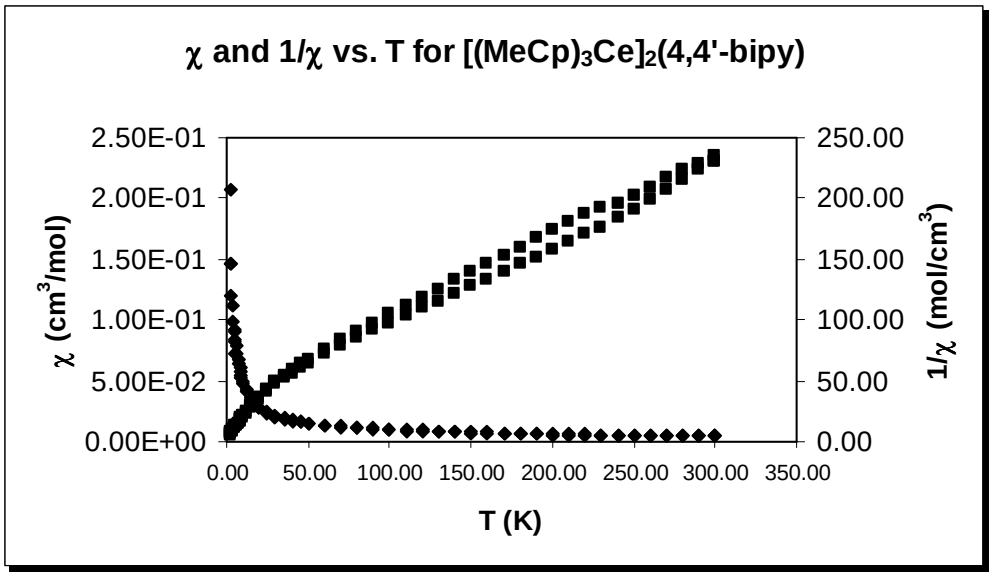
χ and 1/χ vs. T for [(MeCp)3Ce]2(4,4'-bipy)
2.50E-01
2.00E-01
1.50E-01
1.00E-01
5.00E-02
0.00E+00
χ (cm3/mol)
250.00
200.00
150.00
100.00
50.00
0.00
1/χ (mol/cm3)
0.00 50.00 100.00 150.00 200.00 250.00 300.00 350.00
T (K)

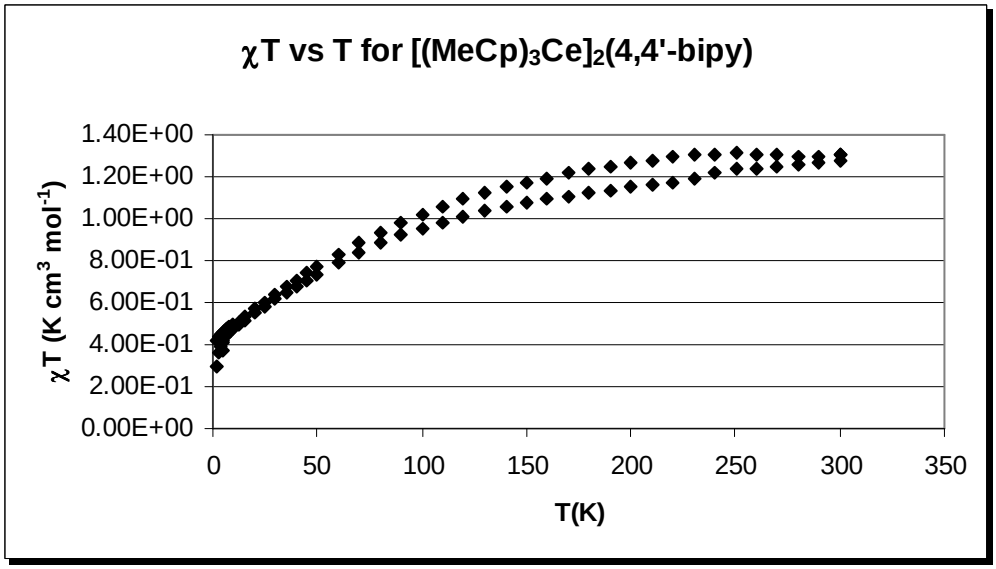
χT vs T for [(MeCp)3Ce]2(4,4'-bipy)
1.40E+00
1.20E+00
1.00E+00
8.00E-01
6.00E-01
4.00E-01
2.00E-01
0.00E+00
χT (K cm3 mol-1)
0 50 100 150 200 250 300 350
T(K)

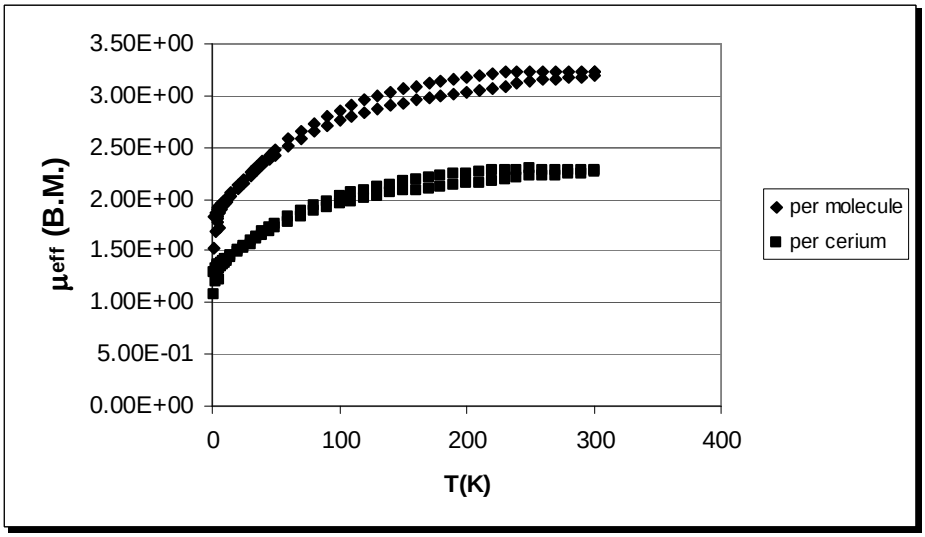
3.50E+00
3.00E+00
2.50E+00
2.00E+00
1.50E+00
1.00E+00
5.00E-01
0.00E+00
μeff (B.M.)
0 100 200 300 400
T(K)
per molecule
per cerium

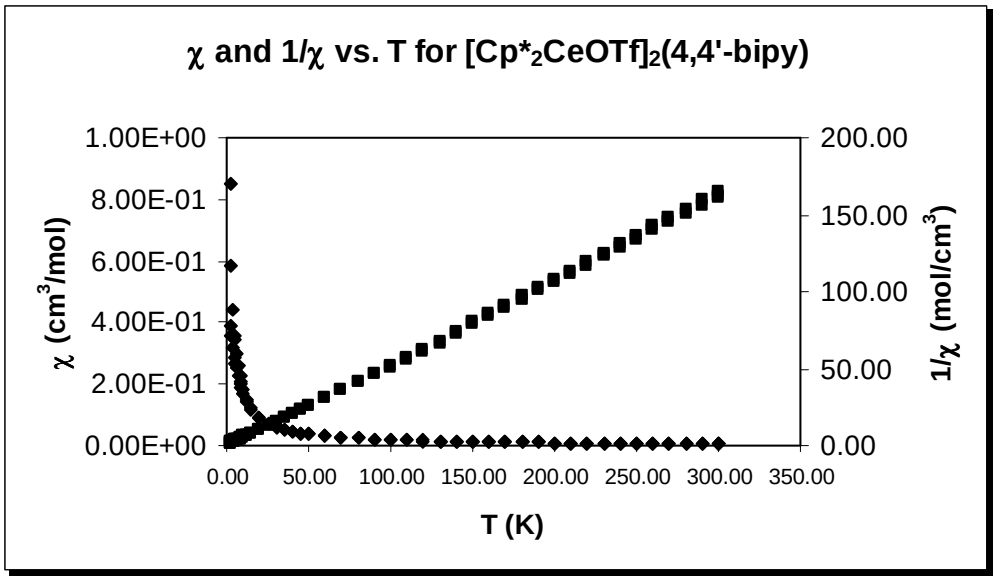
χ and 1/χ vs. T for [Cp*2CeOTf]2(4,4'-bipy)
1.00E+00
8.00E-01
6.00E-01
4.00E-01
2.00E-01
0.00E+00
χ (cm3/mol)
200.00
150.00
100.00
50.00
0.00
1/χ (mol/cm3)
0.00
50.00
100.00
150.00
200.00
250.00
300.00
350.00
T (K)

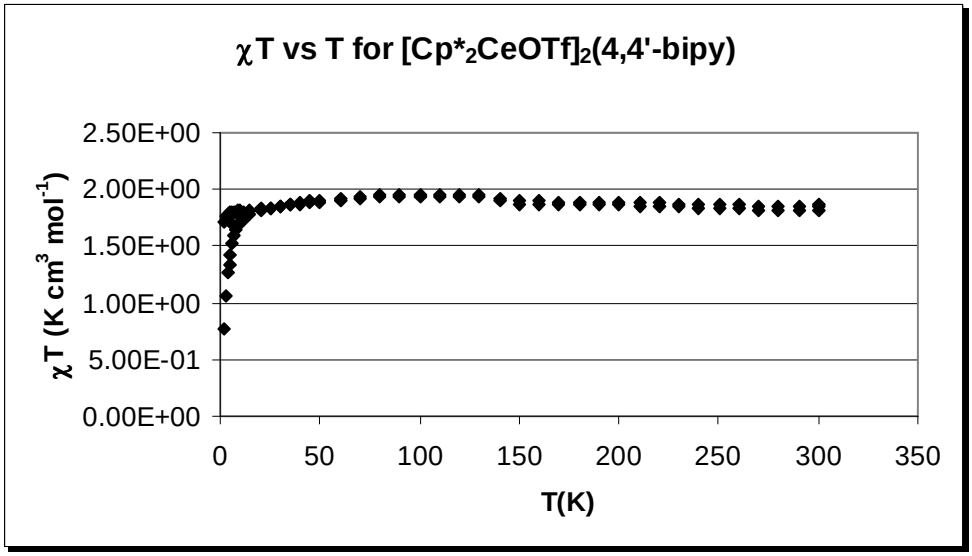
χT vs T for [Cp*2CeOTf]2(4,4'-bipy)
2.50E+00
2.00E+00
1.50E+00
1.00E+00
5.00E-01
0.00E+00
χT (K cm3 mol-1)
0
50
100
150
200
250
300
350
T(K)

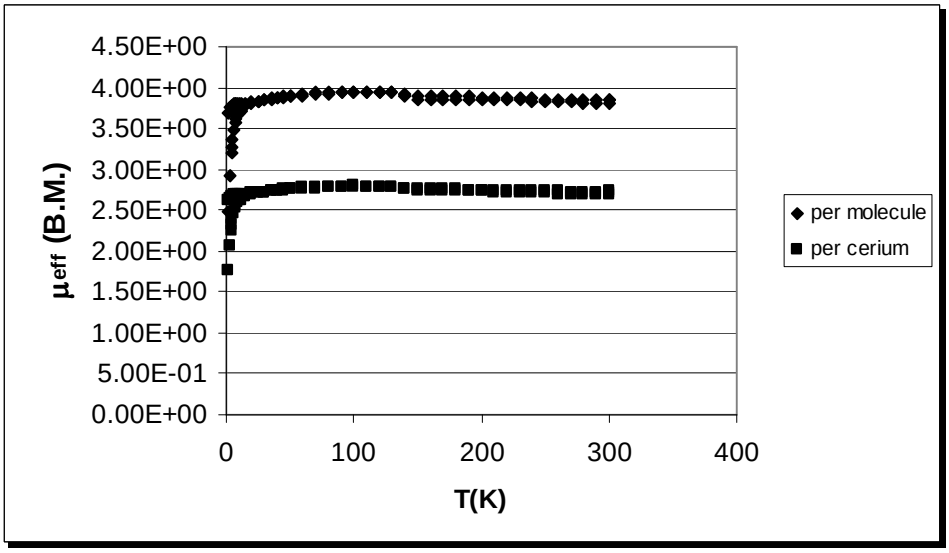
4.50E+00
4.00E+00
3.50E+00
3.00E+00
2.50E+00
2.00E+00
1.50E+00
1.00E+00
5.00E-01
0.00E+00
μeff (B.M.)
0
100
200
300
400
T(K)
per molecule
per cerium

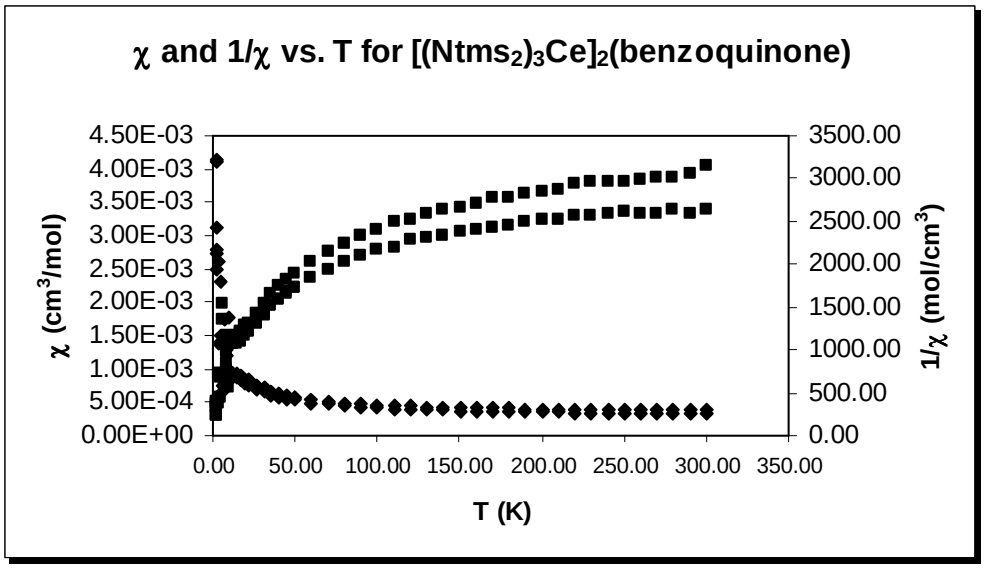
χ and 1/χ vs. T for [(Ntms2)3Ce]2(benzoquinone)
4.50E-03
4.00E-03
3.50E-03
3.00E-03
2.50E-03
2.00E-03
1.50E-03
1.00E-03
5.00E-04
0.00E+00
χ (cm3/mol)
3500.00
3000.00
2500.00
2000.00
1500.00
1000.00
500.00
0.00
1/χ (mol/cm3)
0.00 50.00 100.00 150.00 200.00 250.00 300.00 350.00
T (K)

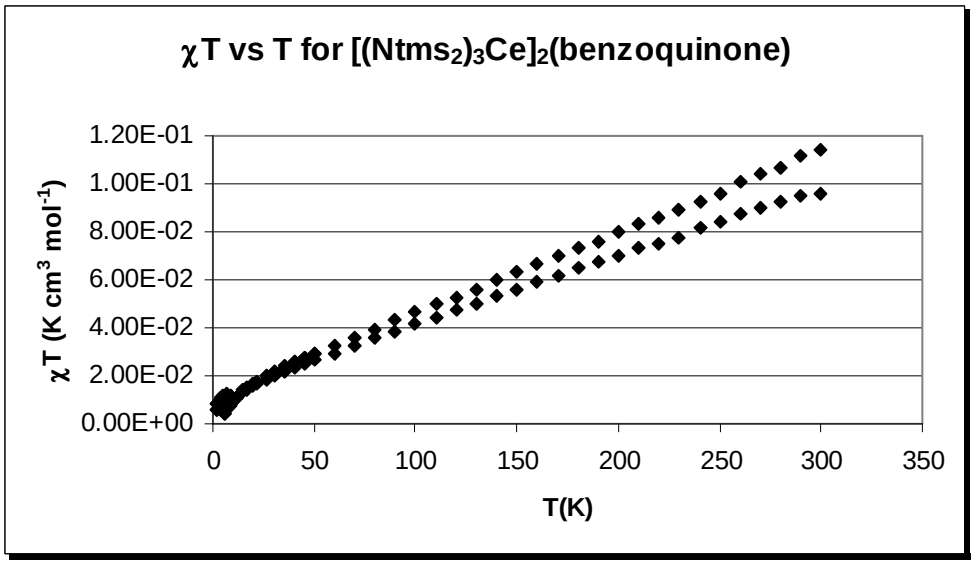
χT vs T for [(Ntms2)3Ce]2(benzoquinone)
1.20E-01
1.00E-01
8.00E-02
6.00E-02
4.00E-02
2.00E-02
0.00E+00
χT (K cm3 mol-1)
0 50 100 150 200 250 300 350
T(K)

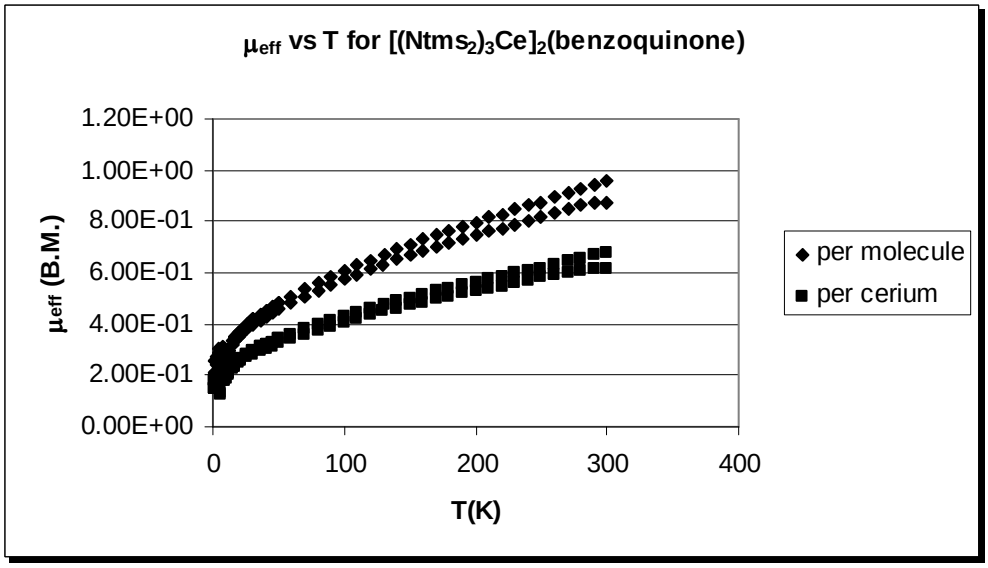
μeff vs T for [(Ntms2)3Ce]2(benzoquinone)
1.20E+00
1.00E+00
8.00E-01
6.00E-01
4.00E-01
2.00E-01
0.00E+00
μeff (B.M.)
0 100 200 300 400
T(K)
per molecule
per cerium

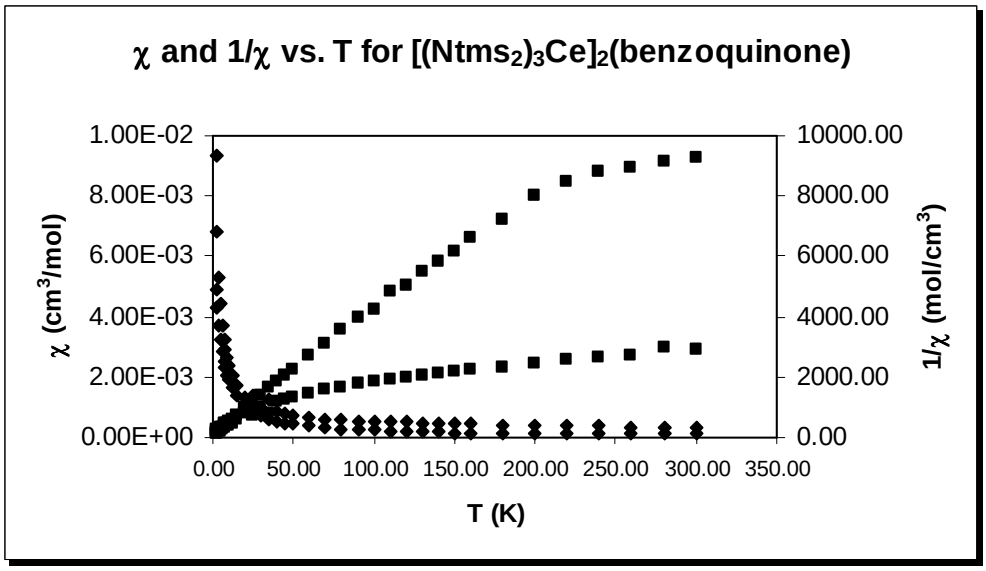
χ and 1/χ vs. T for [(Ntms2)3Ce]2(benzoquinone)
1.00E-02
8.00E-03
6.00E-03
4.00E-03
2.00E-03
0.00E+00
χ (cm3/mol)
10000.00
8000.00
6000.00
4000.00
2000.00
0.00
1/χ (mol/cm3)
0.00
50.00
100.00
150.00
200.00
250.00
300.00
350.00
T (K)

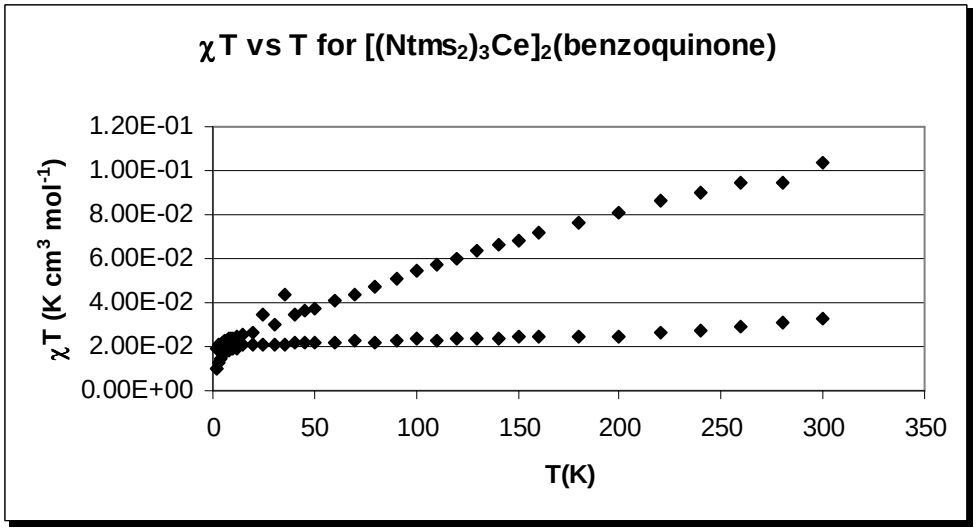
χT vs T for [(Ntms2)3Ce]2(benzoquinone)
1.20E-01
1.00E-01
8.00E-02
6.00E-02
4.00E-02
2.00E-02
0.00E+00
χT (K cm3 mol-1)
0
50
100
150
200
250
300
350
T(K)

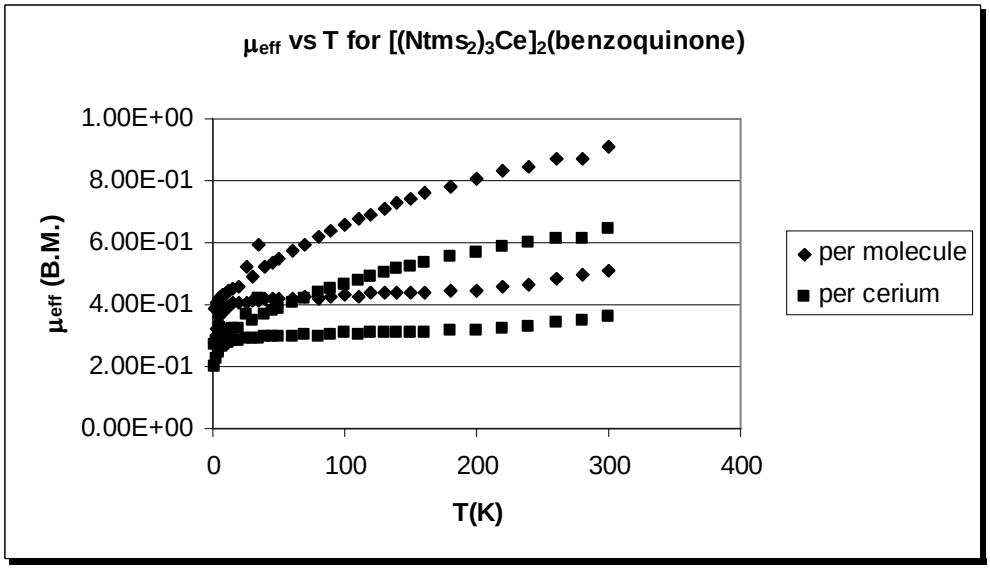
μeff vs T for [(Ntms2)3Ce]2(benzoquinone)
1.00E+00
8.00E-01
6.00E-01
4.00E-01
2.00E-01
0.00E+00
μeff (B.M.)
0
100
200
300
400
T(K)
per molecule
per cerium

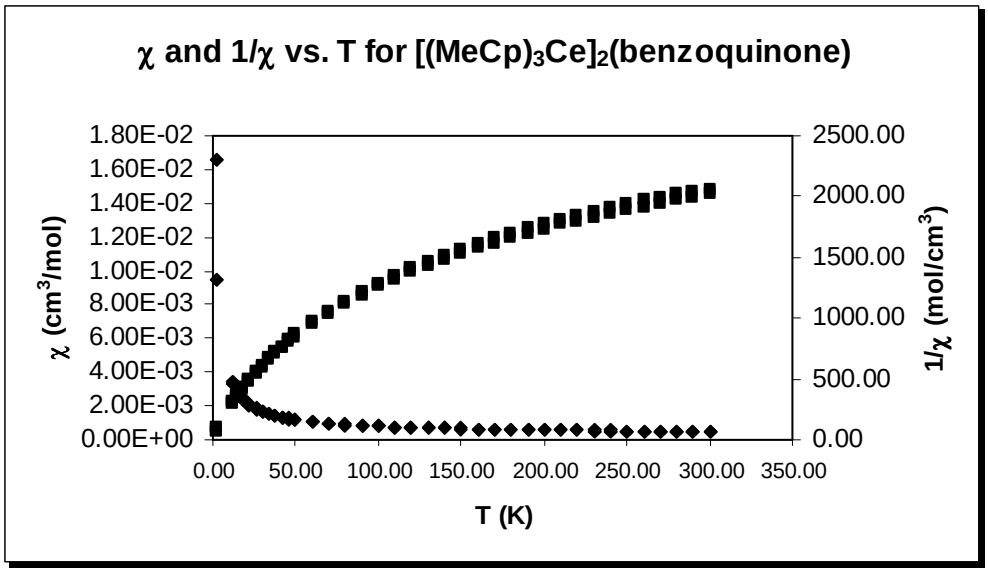
χ and 1/χ vs. T for [(MeCp)3Ce]2(benzoquinone)
1.80E-02
1.60E-02
1.40E-02
1.20E-02
1.00E-02
8.00E-03
6.00E-03
4.00E-03
2.00E-03
0.00E+00
χ (cm3/mol)
2500.00
2000.00
1500.00
1000.00
500.00
0.00
1/χ (mol/cm3)
0.00
50.00
100.00
150.00
200.00
250.00
300.00
350.00
T (K)

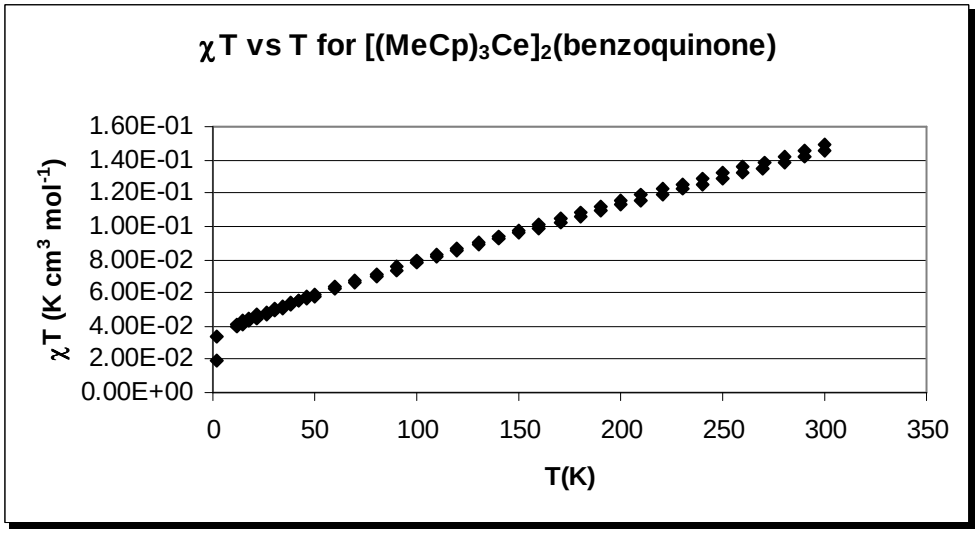
χT vs T for [(MeCp)3Ce]2(benzoquinone)
1.60E-01
1.40E-01
1.20E-01
1.00E-01
8.00E-02
6.00E-02
4.00E-02
2.00E-02
0.00E+00
χT (K cm3 mol-1)
0
50
100
150
200
250
300
350
T(K)

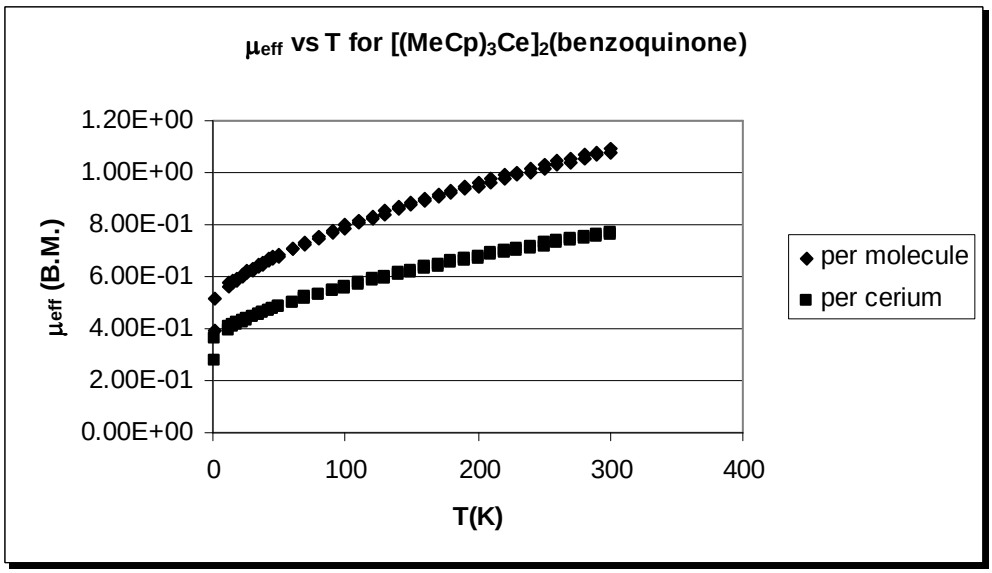
μeff vs T for [(MeCp)3Ce]2(benzoquinone)
1.20E+00
1.00E+00
8.00E-01
6.00E-01
4.00E-01
2.00E-01
0.00E+00
μeff (B.M.)
0
100
200
300
400
T(K)
per molecule
per cerium

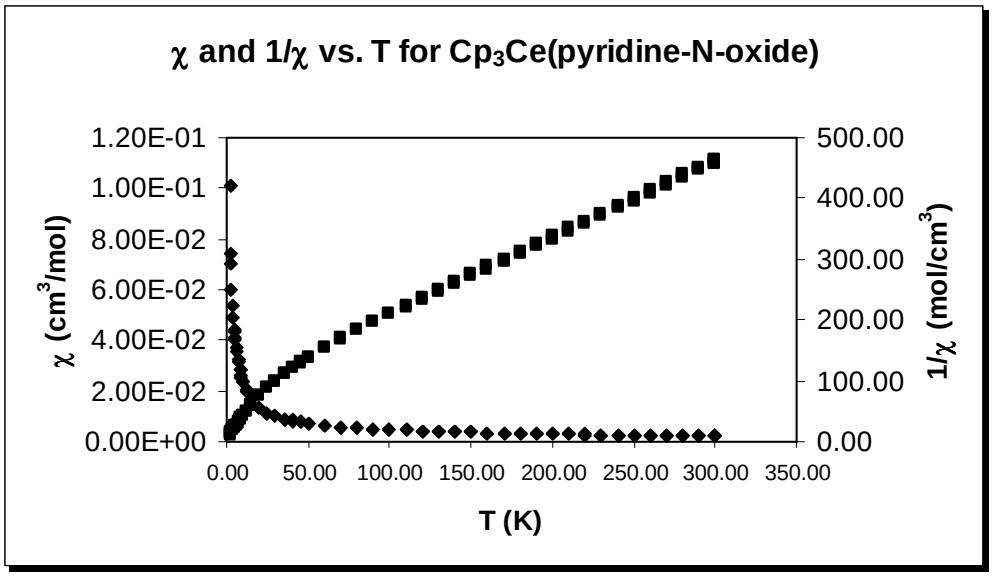
χ and 1/χ vs. T for Cp3Ce(pyridine-N-oxide)
1.20E-01
1.00E-01
8.00E-02
6.00E-02
4.00E-02
2.00E-02
0.00E+00
χ (cm3/mol)
500.00
400.00
300.00
200.00
100.00
0.00
1/χ (mol/cm3)
0.00 50.00 100.00 150.00 200.00 250.00 300.00 350.00
T (K)

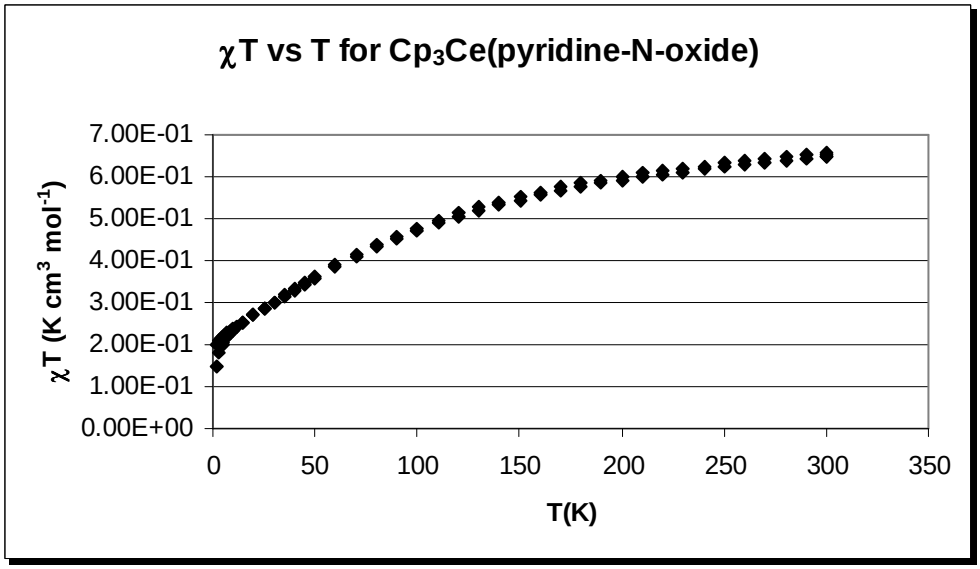
χT vs T for Cp3Ce(pyridine-N-oxide)
7.00E-01
6.00E-01
5.00E-01
4.00E-01
3.00E-01
2.00E-01
1.00E-01
0.00E+00
χT (K cm3 mol-1)
0 50 100 150 200 250 300 350
T(K)

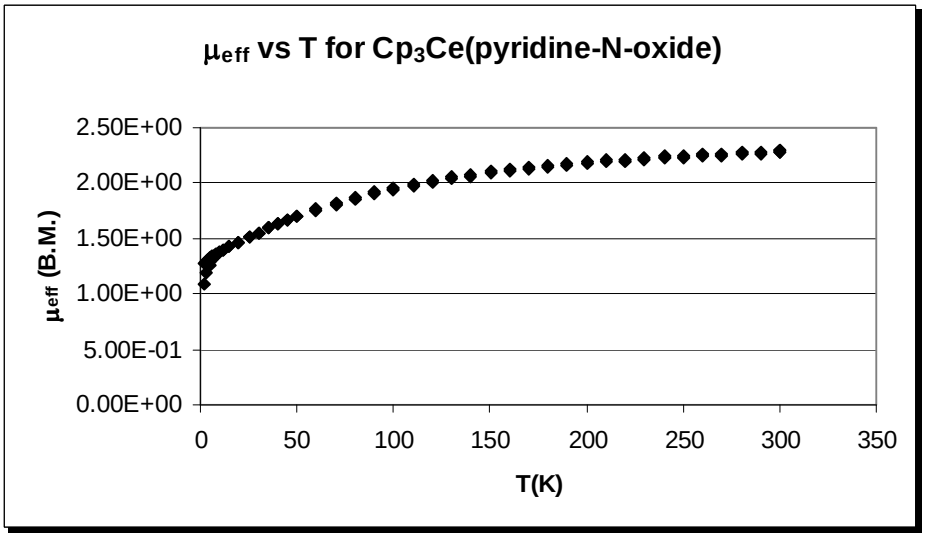
μeff vs T for Cp3Ce(pyridine-N-oxide)
2.50E+00
2.00E+00
1.50E+00
1.00E+00
5.00E-01
0.00E+00
μeff (B.M.)
0 50 100 150 200 250 300 350
T(K)

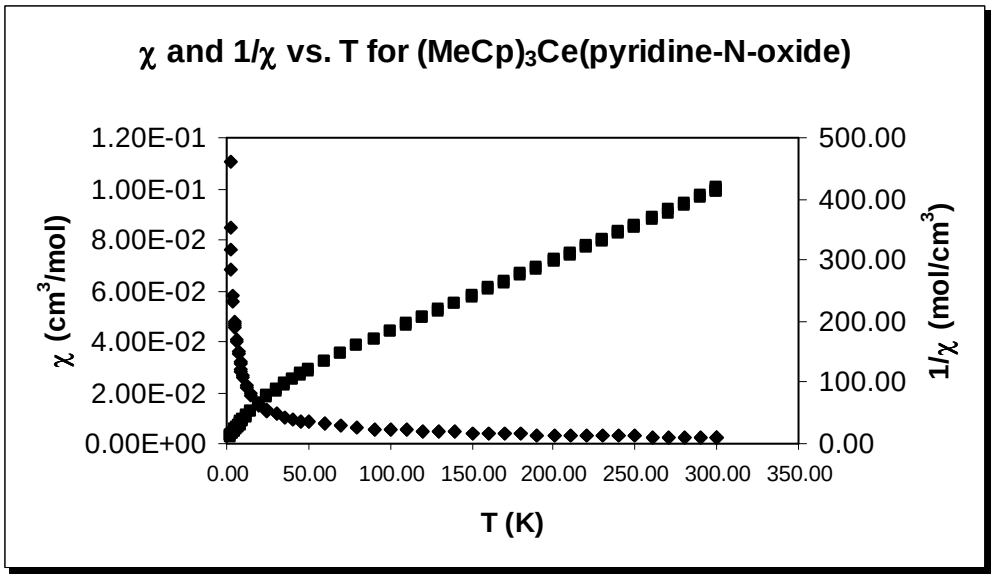
χ and 1/χ vs. T for (MeCp)3Ce(pyridine-N-oxide)
1.20E-01
1.00E-01
8.00E-02
6.00E-02
4.00E-02
2.00E-02
0.00E+00
χ (cm3/mol)
500.00
400.00
300.00
200.00
100.00
0.00
1/χ (mol/cm3)
0.00 50.00 100.00 150.00 200.00 250.00 300.00 350.00
T (K)

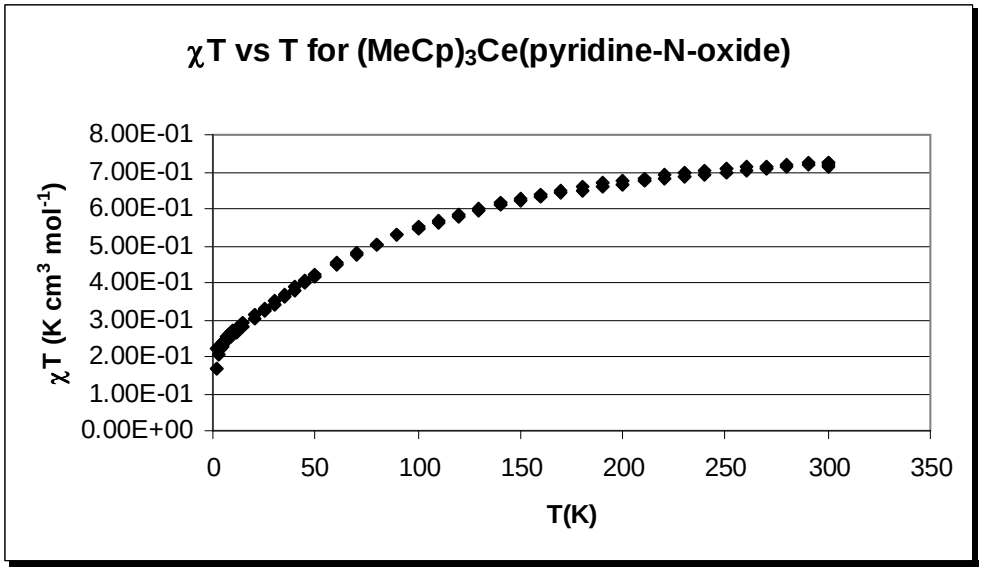
χT vs T for (MeCp)3Ce(pyridine-N-oxide)
8.00E-01
7.00E-01
6.00E-01
5.00E-01
4.00E-01
3.00E-01
2.00E-01
1.00E-01
0.00E+00
χT (K cm3 mol-1)
0 50 100 150 200 250 300 350
T(K)

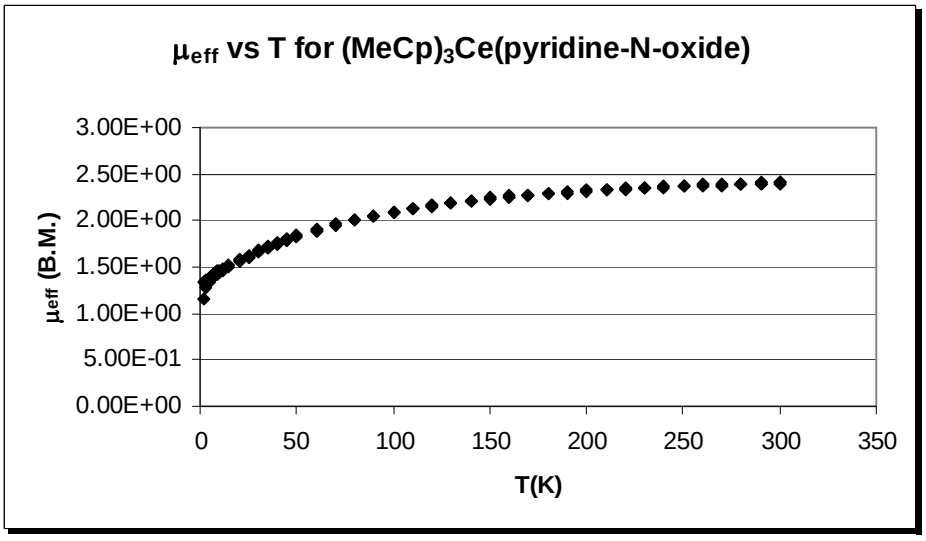
μeff vs T for (MeCp)3Ce(pyridine-N-oxide)
3.00E+00
2.50E+00
2.00E+00
1.50E+00
1.00E+00
5.00E-01
0.00E+00
μeff (B.M.)
0 50 100 150 200 250 300 350
T(K)

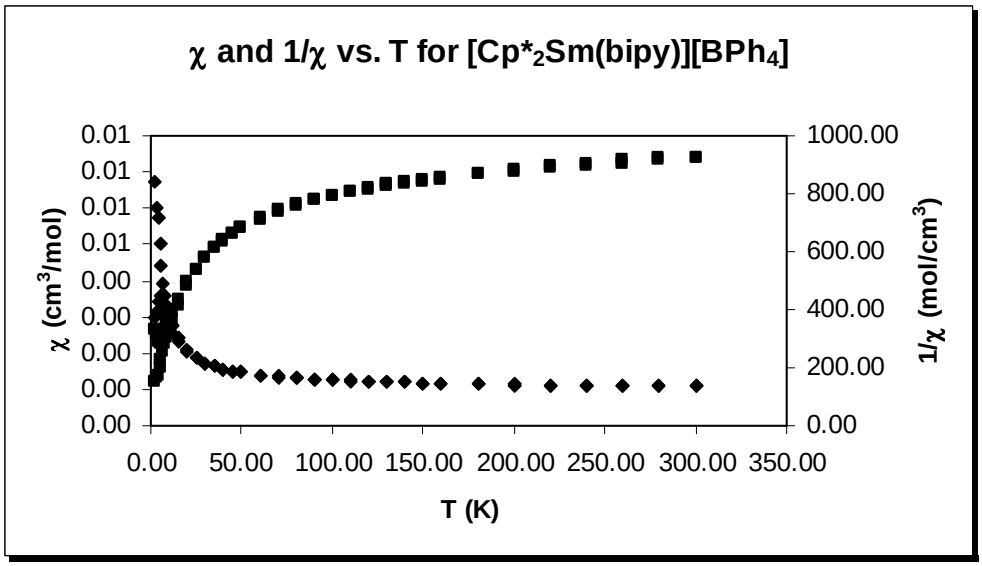
χ and 1/χ vs. T for [Cp*2Sm(bipy)][BPh4]
χ (cm3/mol)
1/χ (mol/cm3)
T (K)
0.01
0.01
0.01
0.01
0.00
0.00
0.00
0.00
1000.00
800.00
600.00
400.00
200.00
0.00
0.00
50.00
100.00
150.00
200.00
250.00
300.00
350.00

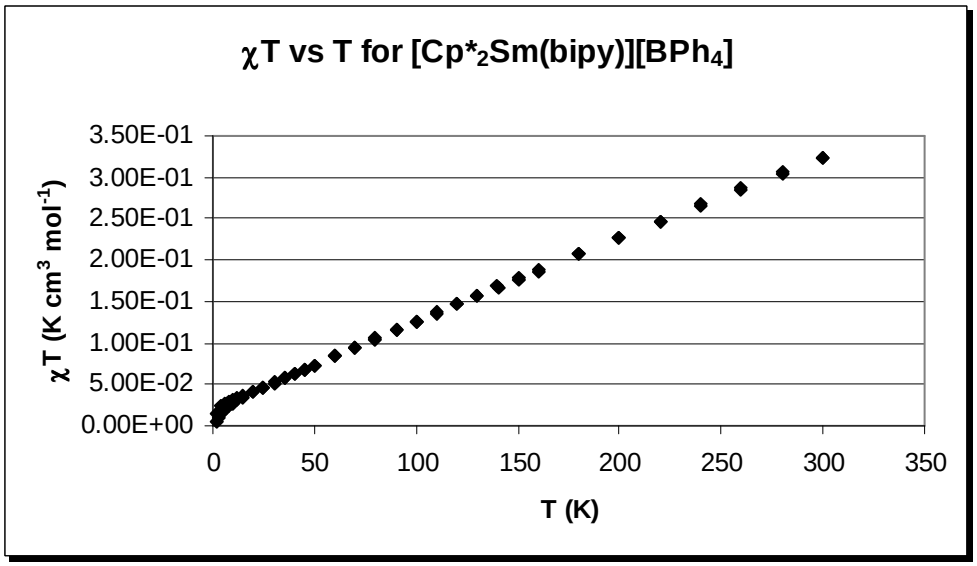
χT vs T for [Cp*2Sm(bipy)][BPh4]
χT (K cm3 mol-1)
T (K)
3.50E-01
3.00E-01
2.50E-01
2.00E-01
1.50E-01
1.00E-01
5.00E-02
0.00E+00
0
50
100
150
200
250
300
350

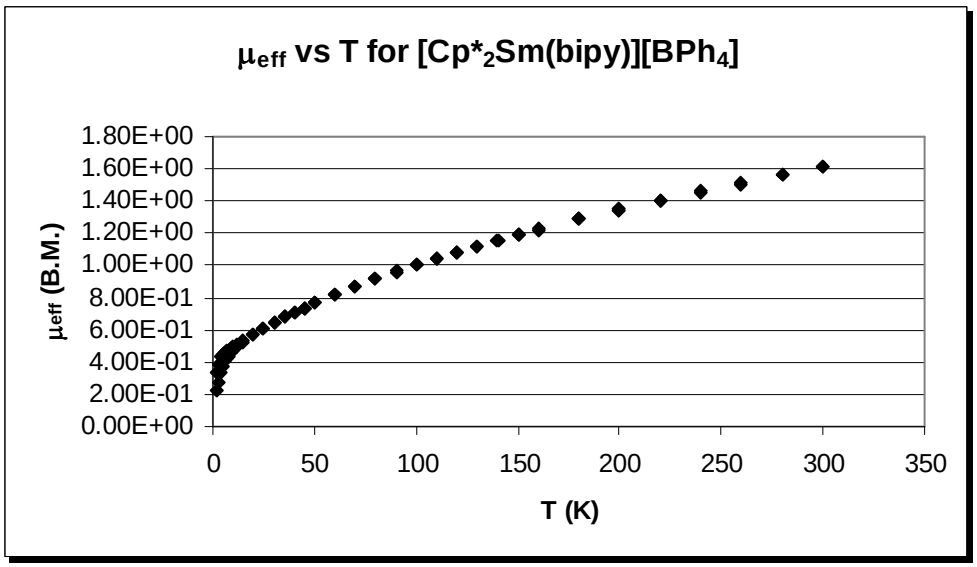
μeff vs T for [Cp*2Sm(bipy)][BPh4]
μeff (B.M.)
T (K)
1.80E+00
1.60E+00
1.40E+00
1.20E+00
1.00E+00
8.00E-01
6.00E-01
4.00E-01
2.00E-01
0.00E+00
0
50
100
150
200
250
300
350

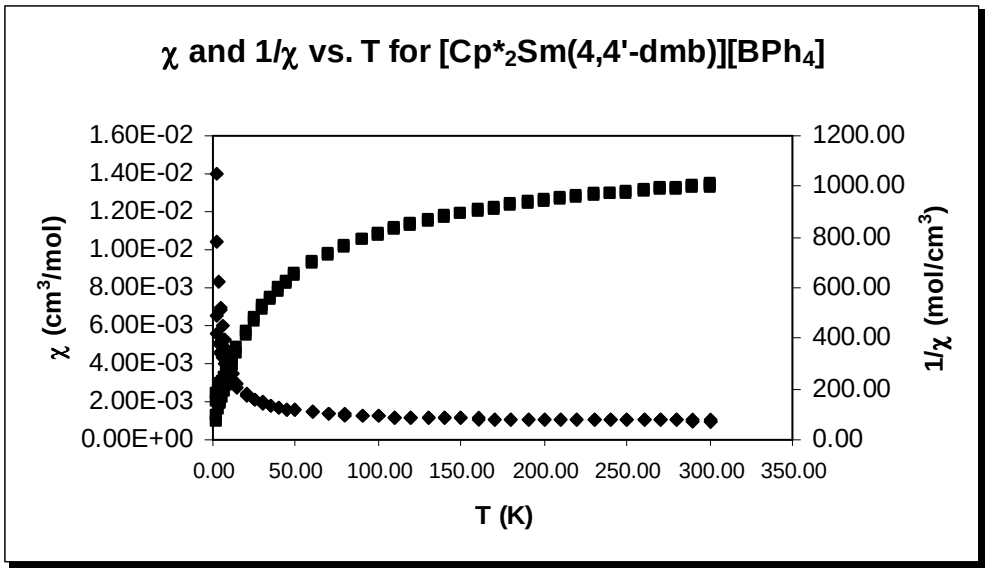
χ and 1/χ vs. T for [Cp*2Sm(4,4'-dmb)][BPh4]
1.60E-02
1.40E-02
1.20E-02
1.00E-02
8.00E-03
6.00E-03
4.00E-03
2.00E-03
0.00E+00
χ (cm3/mol)
1200.00
1000.00
800.00
600.00
400.00
200.00
0.00
1/χ (mol/cm3)
0.00
50.00
100.00
150.00
200.00
250.00
300.00
350.00
T (K)

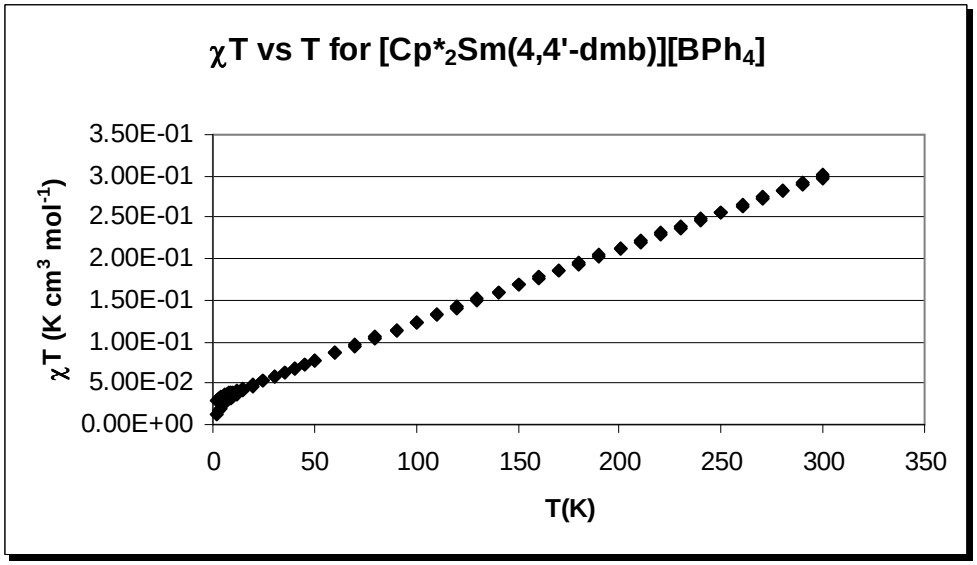
χT vs T for [Cp*2Sm(4,4'-dmb)][BPh4]
3.50E-01
3.00E-01
2.50E-01
2.00E-01
1.50E-01
1.00E-01
5.00E-02
0.00E+00
χT (K cm3 mol-1)
0
50
100
150
200
250
300
350
T(K)

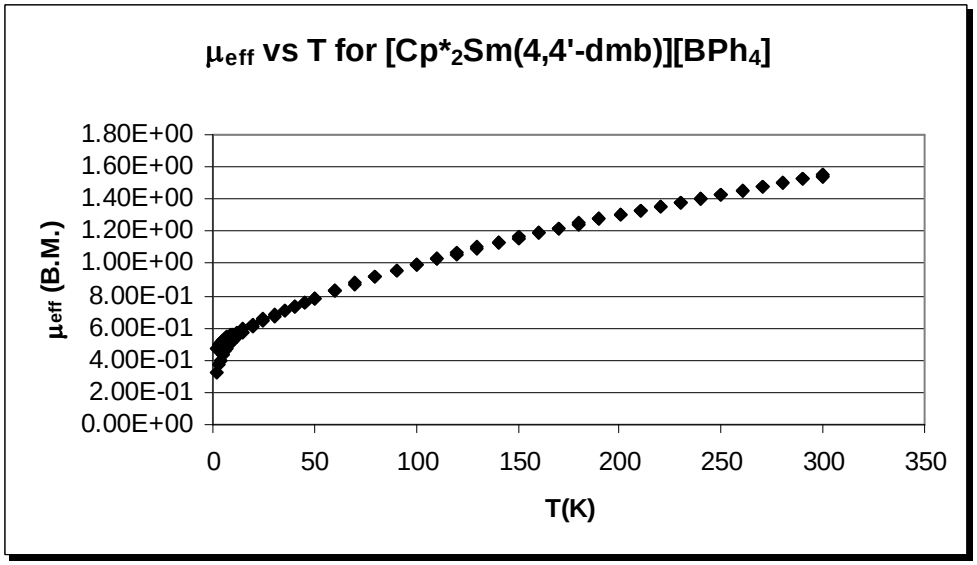
μeff vs T for [Cp*2Sm(4,4'-dmb)][BPh4]
1.80E+00
1.60E+00
1.40E+00
1.20E+00
1.00E+00
8.00E-01
6.00E-01
4.00E-01
2.00E-01
0.00E+00
μeff (B.M.)
0
50
100
150
200
250
300
350
T(K)

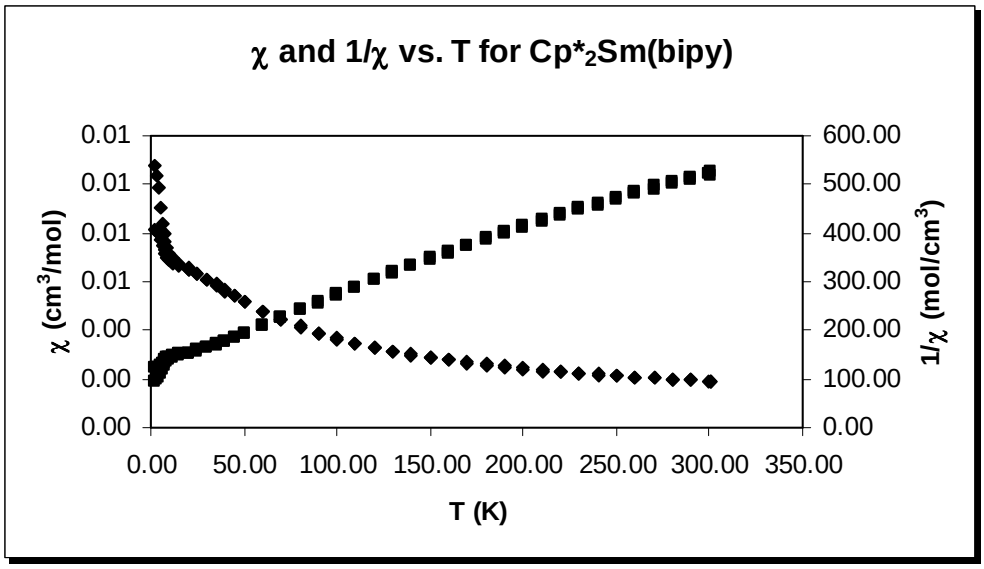
χ and 1/χ vs. T for Cp*2Sm(bipy)
χ (cm3/mol)
1/χ (mol/cm3)
T (K)
0.01
0.01
0.01
0.01
0.00
0.00
0.00
600.00
500.00
400.00
300.00
200.00
100.00
0.00
0.00
50.00
100.00
150.00
200.00
250.00
300.00
350.00

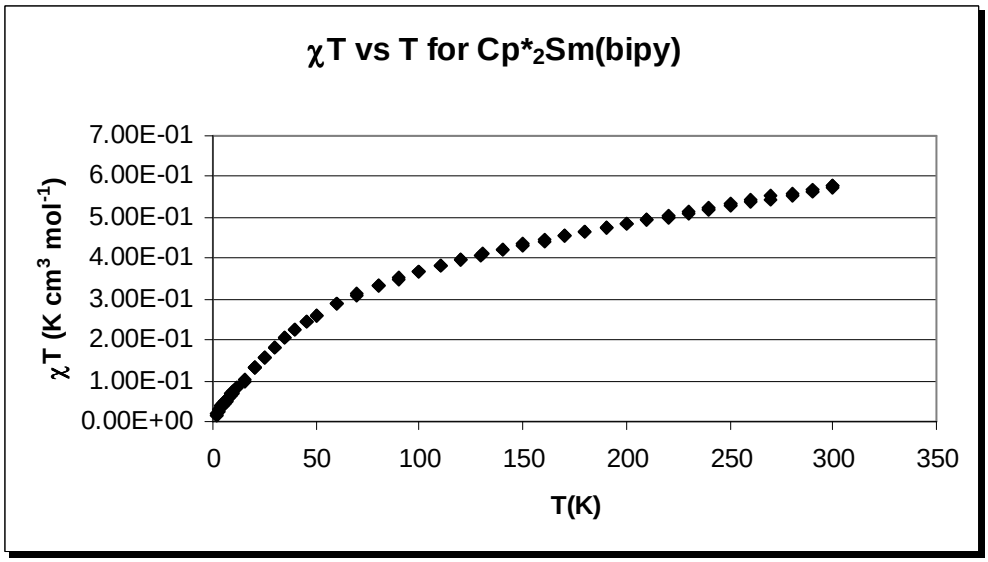
χT vs T for Cp*2Sm(bipy)
χT (K cm3 mol-1)
T(K)
7.00E-01
6.00E-01
5.00E-01
4.00E-01
3.00E-01
2.00E-01
1.00E-01
0.00E+00
0
50
100
150
200
250
300
350

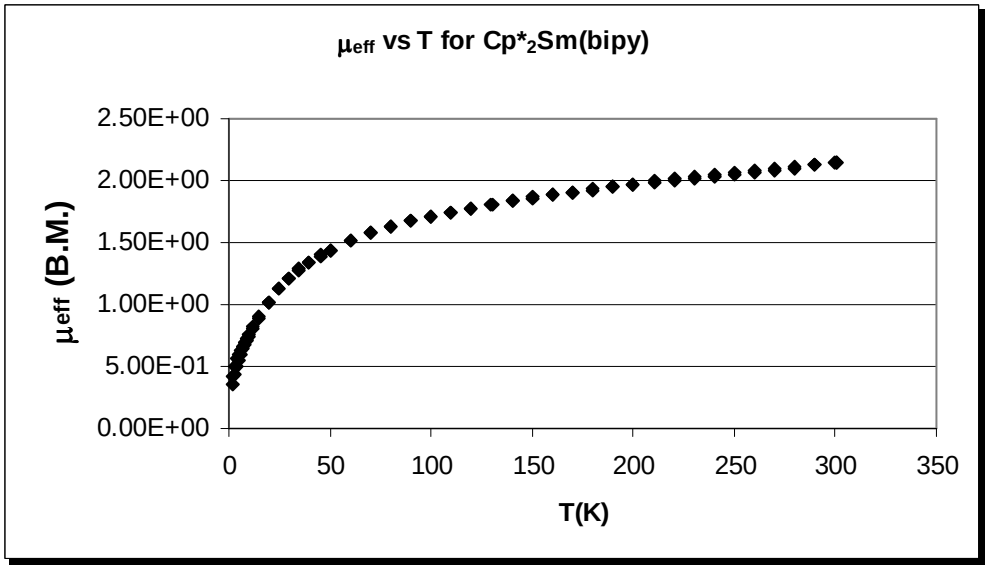
μeff vs T for Cp*2Sm(bipy)
μeff (B.M.)
T(K)
2.50E+00
2.00E+00
1.50E+00
1.00E+00
5.00E-01
0.00E+00
0
50
100
150
200
250
300
350

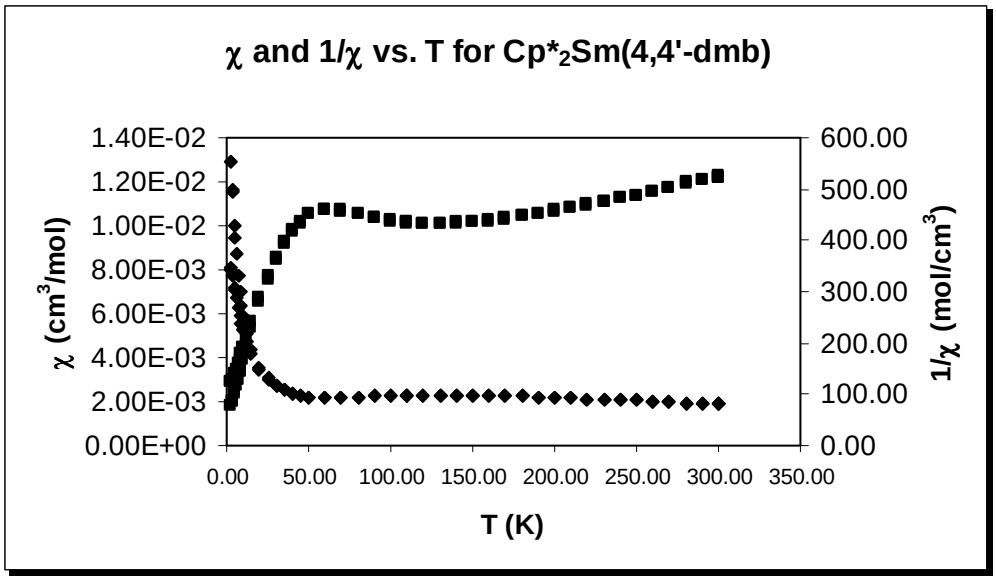
χ and 1/χ vs. T for Cp*2Sm(4,4'-dmb)
1.40E-02
1.20E-02
1.00E-02
8.00E-03
6.00E-03
4.00E-03
2.00E-03
0.00E+00
χ (cm3/mol)
600.00
500.00
400.00
300.00
200.00
100.00
0.00
1/χ (mol/cm3)
0.00
50.00
100.00
150.00
200.00
250.00
300.00
350.00
T (K)

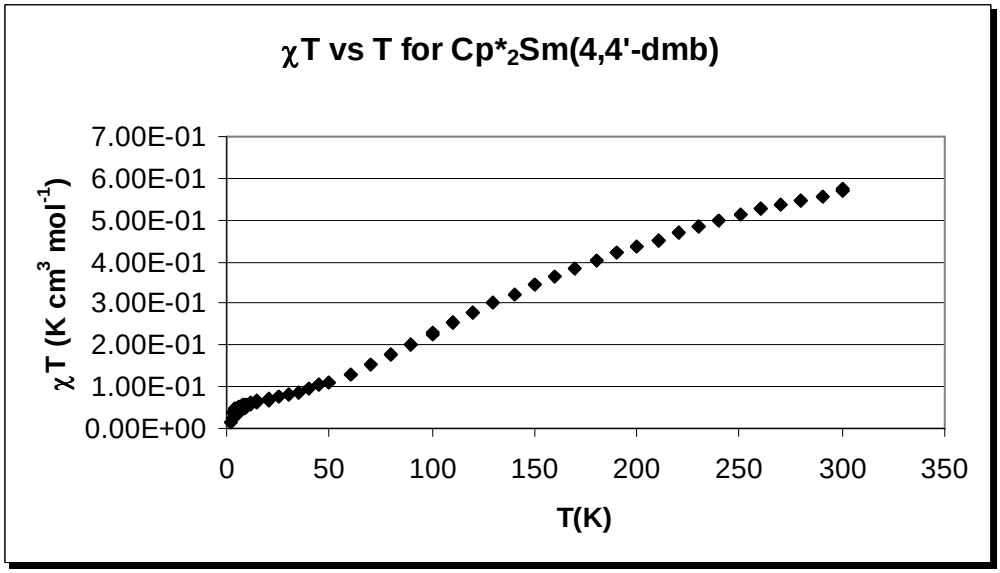
χT vs T for Cp*2Sm(4,4'-dmb)
7.00E-01
6.00E-01
5.00E-01
4.00E-01
3.00E-01
2.00E-01
1.00E-01
0.00E+00
χT (K cm3 mol-1)
0
50
100
150
200
250
300
350
T(K)

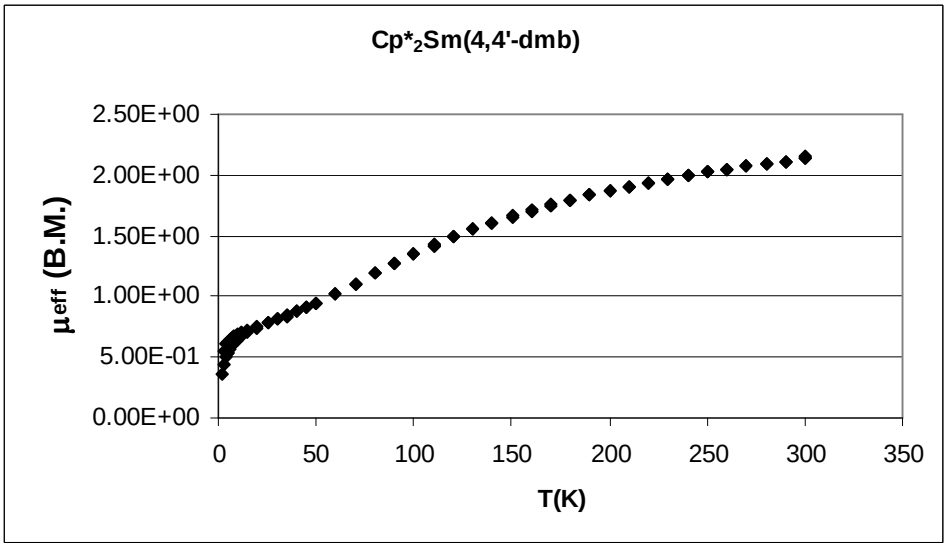
Cp*2Sm(4,4'-dmb)
2.50E+00
2.00E+00
1.50E+00
1.00E+00
5.00E-01
0.00E+00
μeff (B.M.)
0
50
100
150
200
250
300
350
T(K)

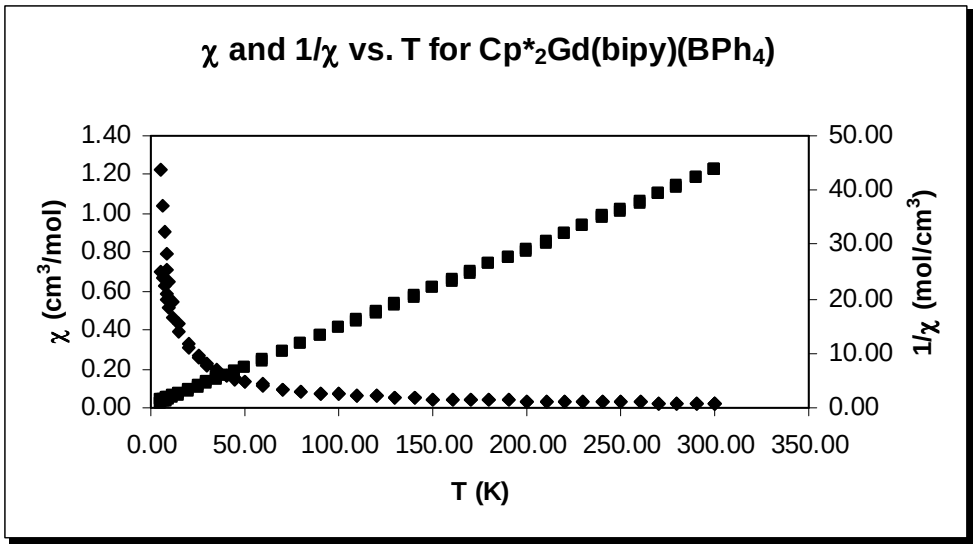
χ and 1/χ vs. T for Cp*2Gd(bipy)(BPh4)
χ (cm3/mol)
1/χ (mol/cm3)
T (K)
1.40
1.20
1.00
0.80
0.60
0.40
0.20
0.00
50.00
40.00
30.00
20.00
10.00
0.00
0.00
50.00
100.00
150.00
200.00
250.00
300.00
350.00

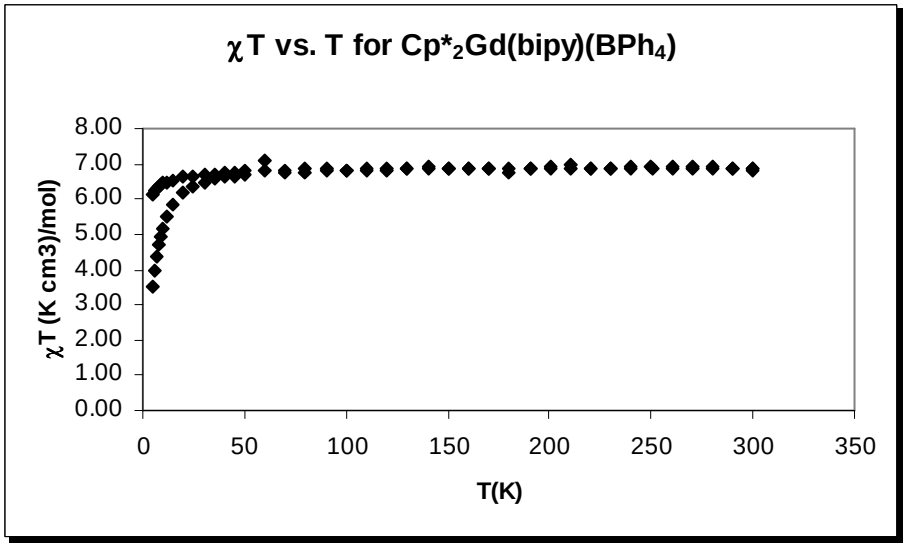
χT vs. T for Cp*2Gd(bipy)(BPh4)
χT (K cm3)/mol)
T(K)
8.00
7.00
6.00
5.00
4.00
3.00
2.00
1.00
0.00
0
50
100
150
200
250
300
350

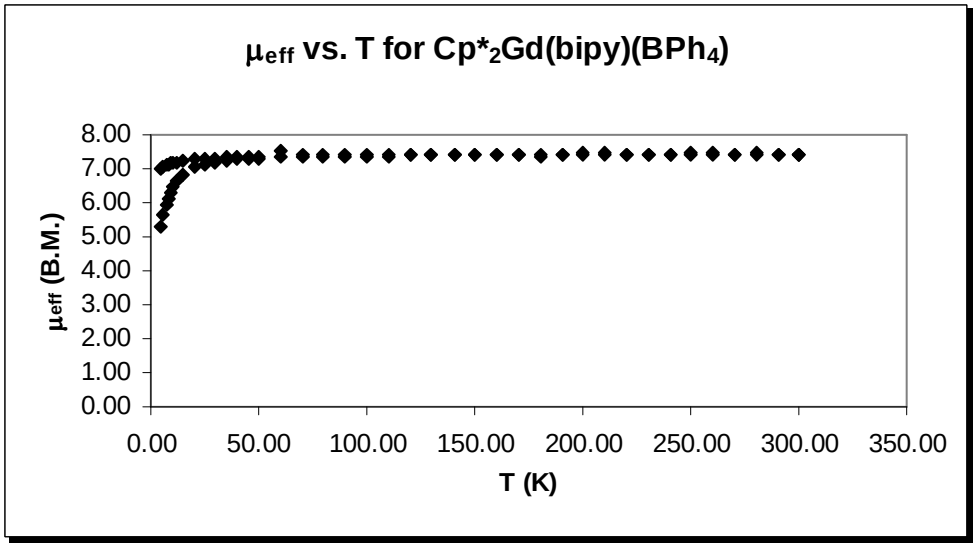
μeff vs. T for Cp*2Gd(bipy)(BPh4)
μeff (B.M.)
T (K)
8.00
7.00
6.00
5.00
4.00
3.00
2.00
1.00
0.00
0.00
50.00
100.00
150.00
200.00
250.00
300.00
350.00

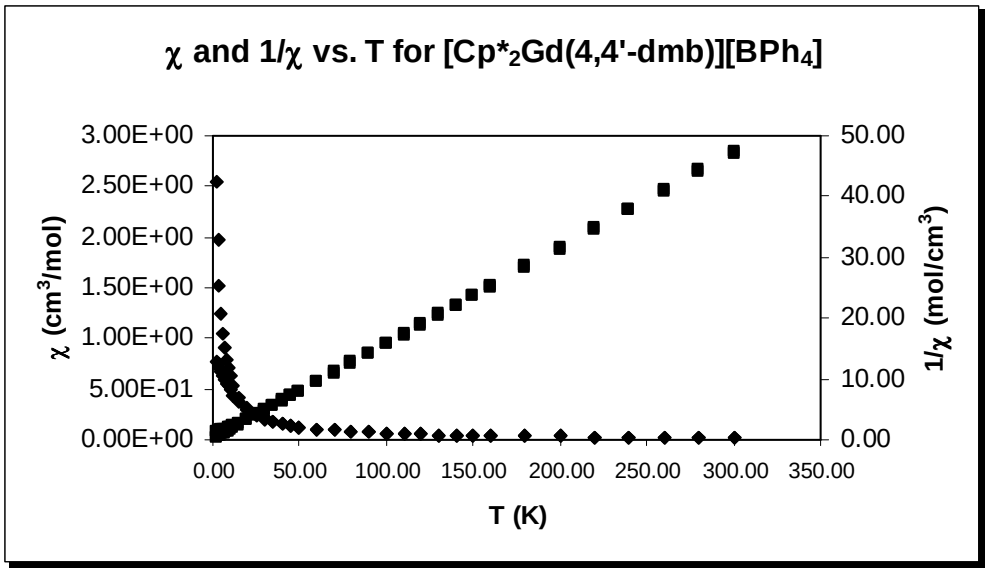
χ and 1/χ vs. T for [Cp*2Gd(4,4'-dmb)][BPh4]
3.00E+00
2.50E+00
2.00E+00
1.50E+00
1.00E+00
5.00E-01
0.00E+00
χ (cm3/mol)
50.00
40.00
30.00
20.00
10.00
0.00
1/χ (mol/cm3)
0.00
50.00
100.00
150.00
200.00
250.00
300.00
350.00
T (K)

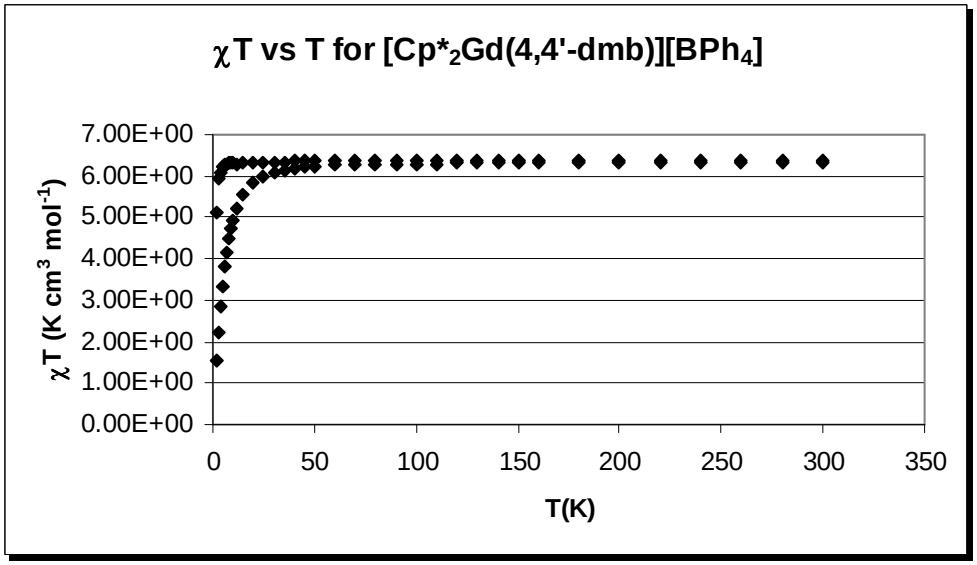
χT vs T for [Cp*2Gd(4,4'-dmb)][BPh4]
7.00E+00
6.00E+00
5.00E+00
4.00E+00
3.00E+00
2.00E+00
1.00E+00
0.00E+00
χT (K cm3 mol-1)
0
50
100
150
200
250
300
350
T(K)

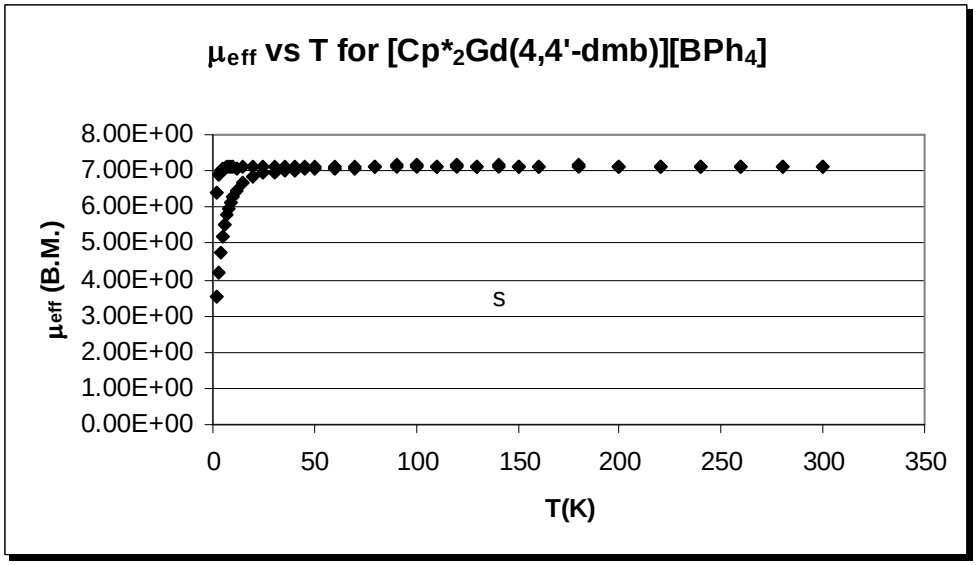
μeff vs T for [Cp*2Gd(4,4'-dmb)][BPh4]
8.00E+00
7.00E+00
6.00E+00
5.00E+00
4.00E+00
3.00E+00
2.00E+00
1.00E+00
0.00E+00
μeff (B.M.)
s
0
50
100
150
200
250
300
350
T(K)

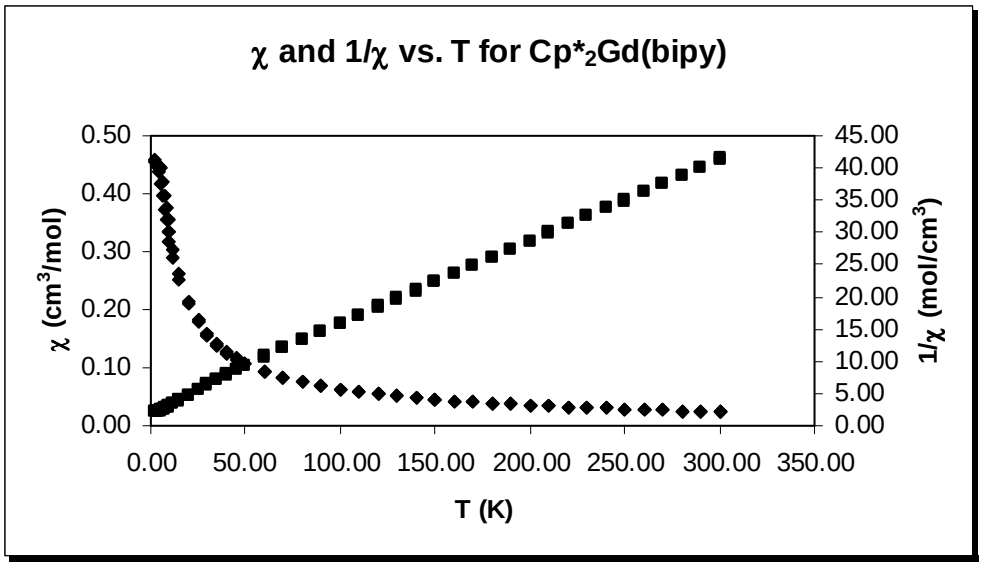
χ and 1/χ vs. T for Cp*2Gd(bipy)
χ (cm3/mol)
1/χ (mol/cm3)
T (K)
0.50
0.40
0.30
0.20
0.10
0.00
45.00
40.00
35.00
30.00
25.00
20.00
15.00
10.00
5.00
0.00
0.00
50.00
100.00
150.00
200.00
250.00
300.00
350.00

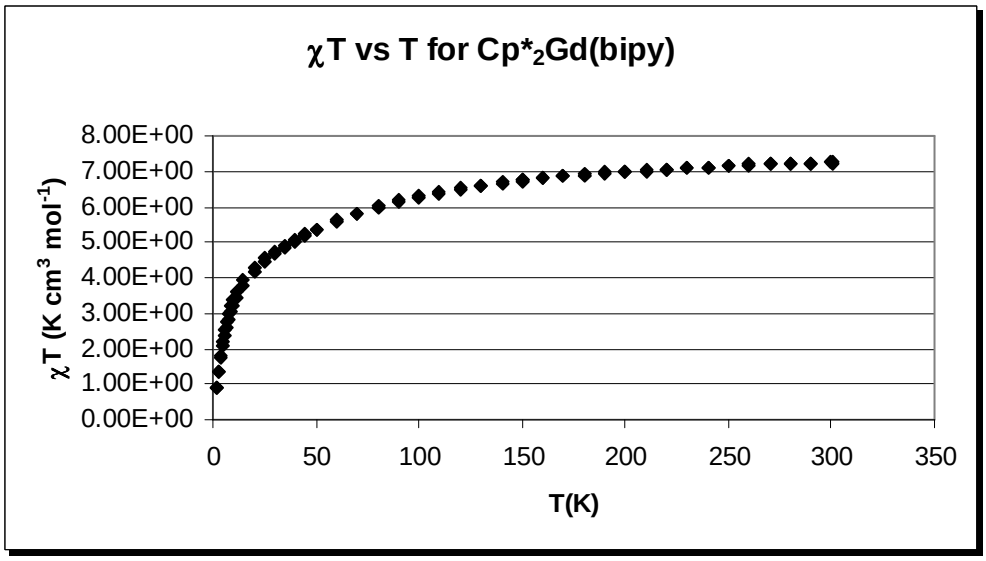
χT vs T for Cp*2Gd(bipy)
χT (K cm3 mol-1)
T(K)
8.00E+00
7.00E+00
6.00E+00
5.00E+00
4.00E+00
3.00E+00
2.00E+00
1.00E+00
0.00E+00
0
50
100
150
200
250
300
350

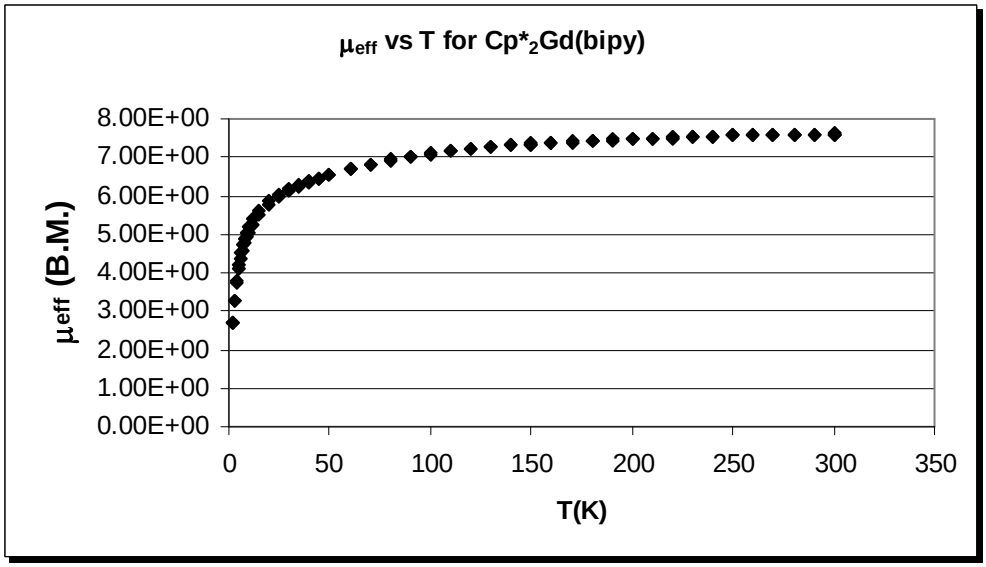
μeff vs T for Cp*2Gd(bipy)
μeff (B.M.)
T(K)
8.00E+00
7.00E+00
6.00E+00
5.00E+00
4.00E+00
3.00E+00
2.00E+00
1.00E+00
0.00E+00
0
50
100
150
200
250
300
350

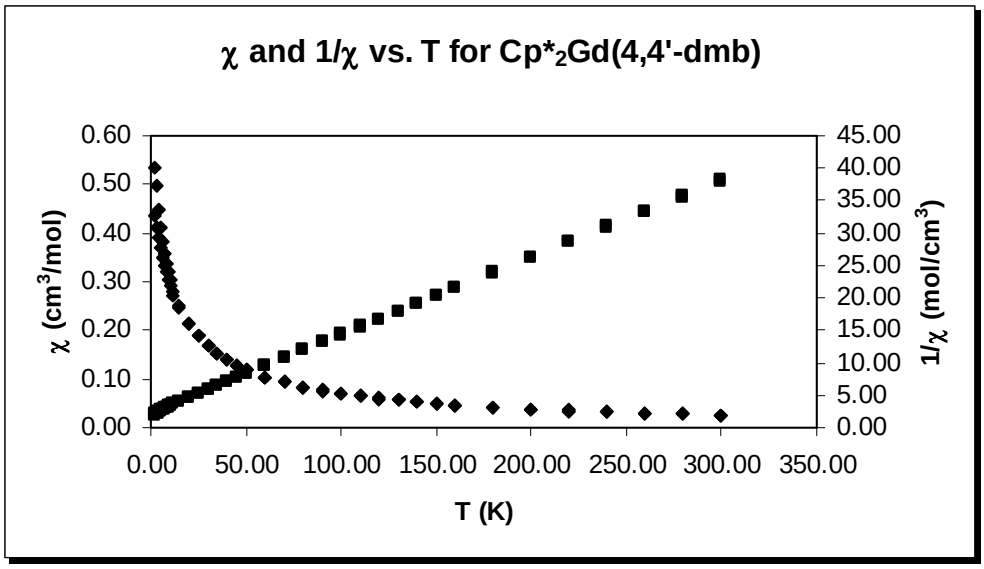
χ and 1/χ vs. T for Cp*2Gd(4,4'-dmb)
χ (cm3/mol)
1/χ (mol/cm3)
T (K)
0.60
0.50
0.40
0.30
0.20
0.10
0.00
45.00
40.00
35.00
30.00
25.00
20.00
15.00
10.00
5.00
0.00
0.00
50.00
100.00
150.00
200.00
250.00
300.00
350.00

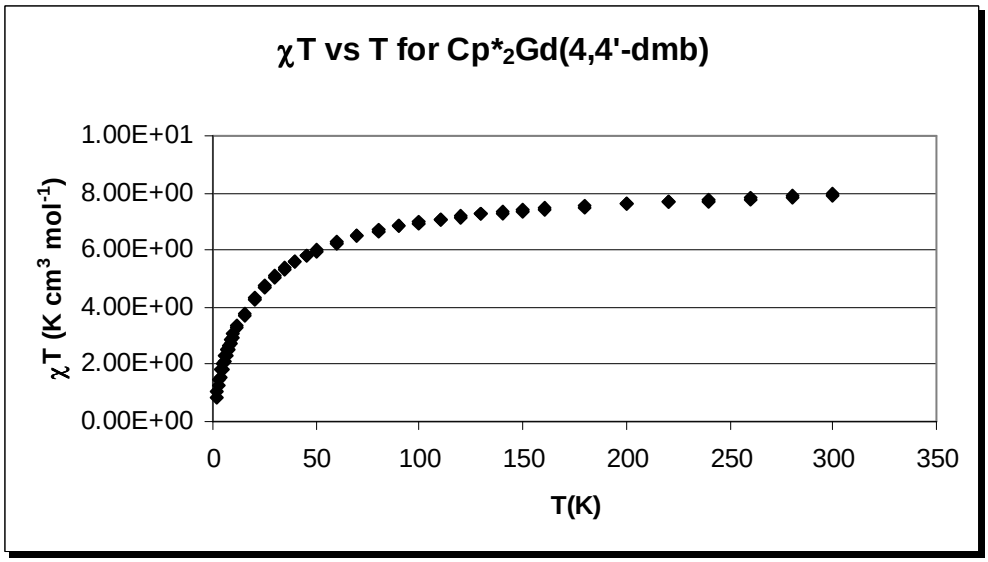
χT vs T for Cp*2Gd(4,4'-dmb)
χT (K cm3 mol-1)
T(K)
1.00E+01
8.00E+00
6.00E+00
4.00E+00
2.00E+00
0.00E+00
0
50
100
150
200
250
300
350

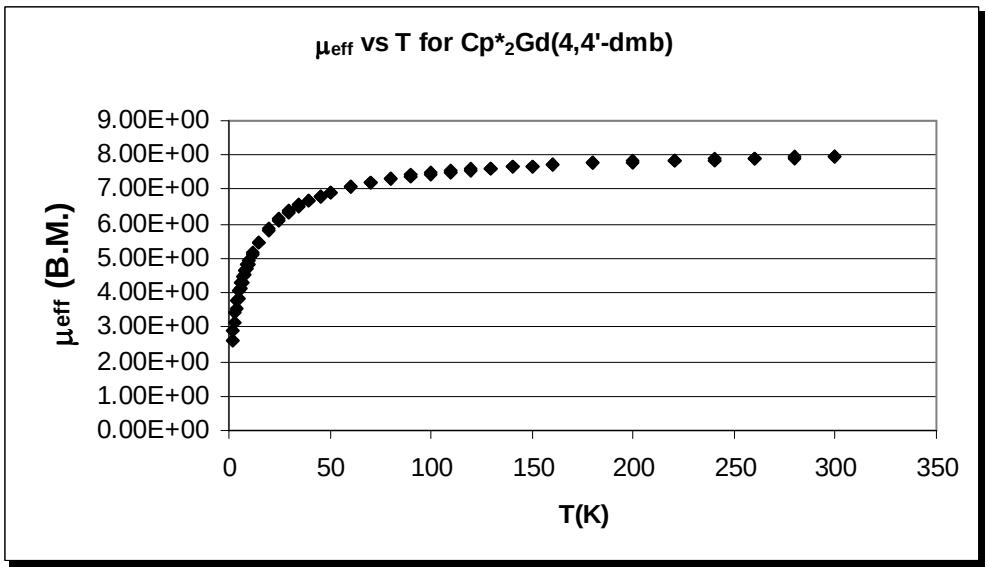
μeff vs T for Cp*2Gd(4,4'-dmb)
μeff (B.M.)
T(K)
9.00E+00
8.00E+00
7.00E+00
6.00E+00
5.00E+00
4.00E+00
3.00E+00
2.00E+00
1.00E+00
0.00E+00
0
50
100
150
200
250
300
350

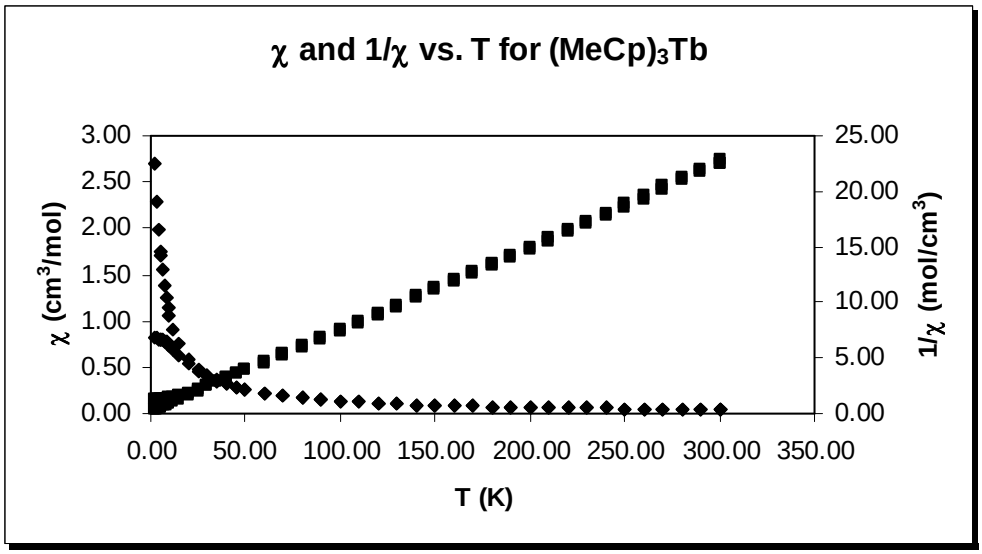
χ and 1/χ vs. T for (MeCp)3Tb
χ (cm3/mol)
1/χ (mol/cm3)
T (K)
3.00
2.50
2.00
1.50
1.00
0.50
0.00
25.00
20.00
15.00
10.00
5.00
0.00
0.00
50.00
100.00
150.00
200.00
250.00
300.00
350.00

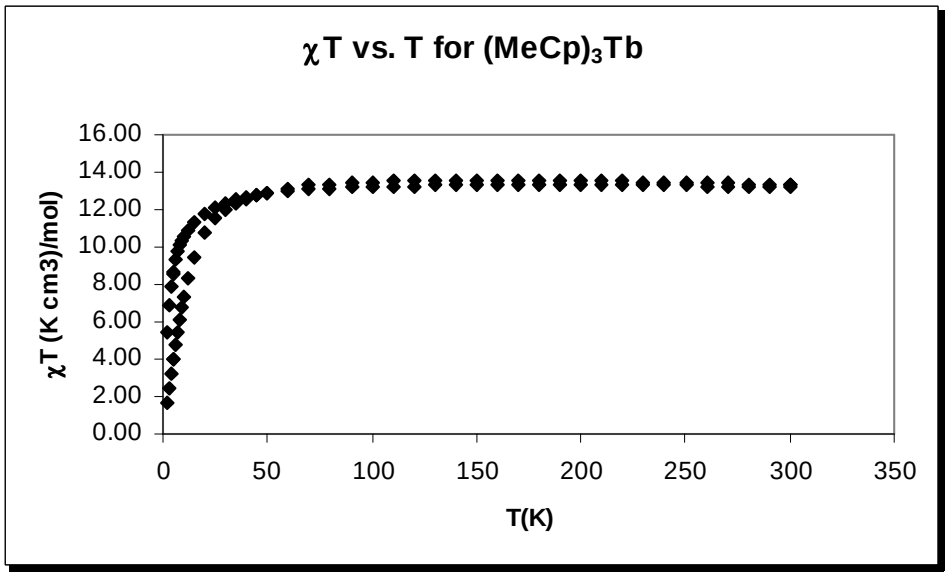
χT vs. T for (MeCp)3Tb
χT (K cm3)/mol
T(K)
16.00
14.00
12.00
10.00
8.00
6.00
4.00
2.00
0.00
0
50
100
150
200
250
300
350

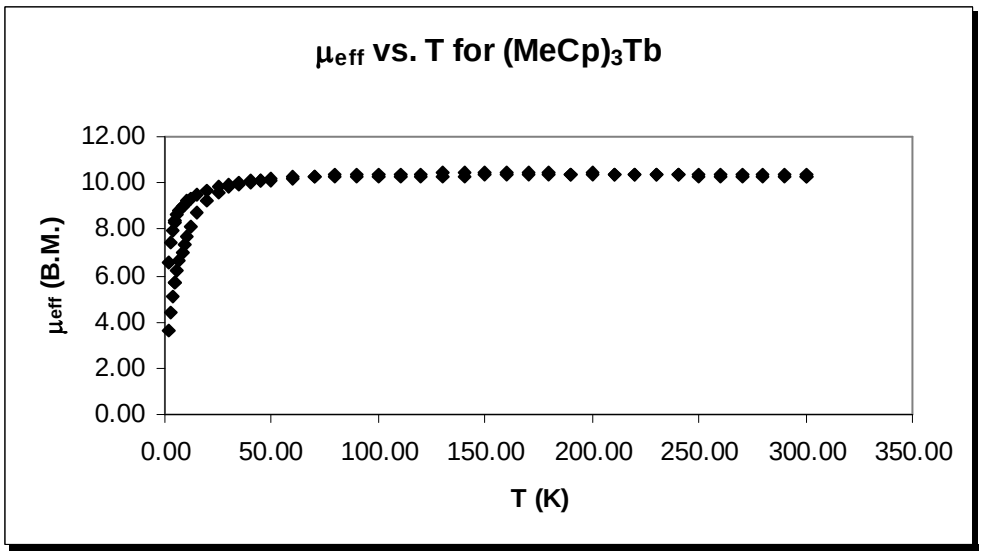
μeff vs. T for (MeCp)3Tb
μeff (B.M.)
T (K)
12.00
10.00
8.00
6.00
4.00
2.00
0.00
0.00
50.00
100.00
150.00
200.00
250.00
300.00
350.00

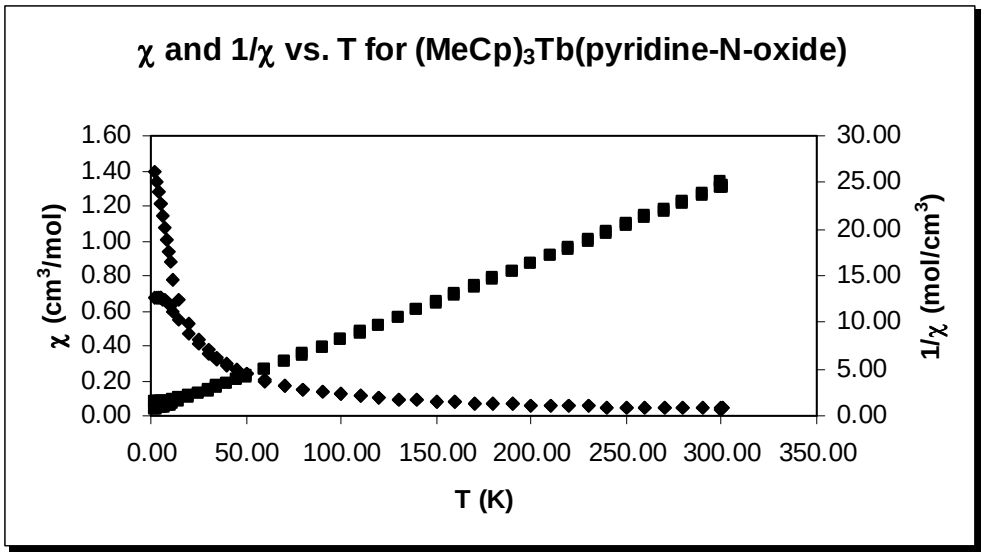
χ and 1/χ vs. T for (MeCp)3Tb(pyridine-N-oxide)
χ (cm3/mol)
1/χ (mol/cm3)
T (K)
1.60
1.40
1.20
1.00
0.80
0.60
0.40
0.20
0.00
30.00
25.00
20.00
15.00
10.00
5.00
0.00
0.00
50.00
100.00
150.00
200.00
250.00
300.00
350.00

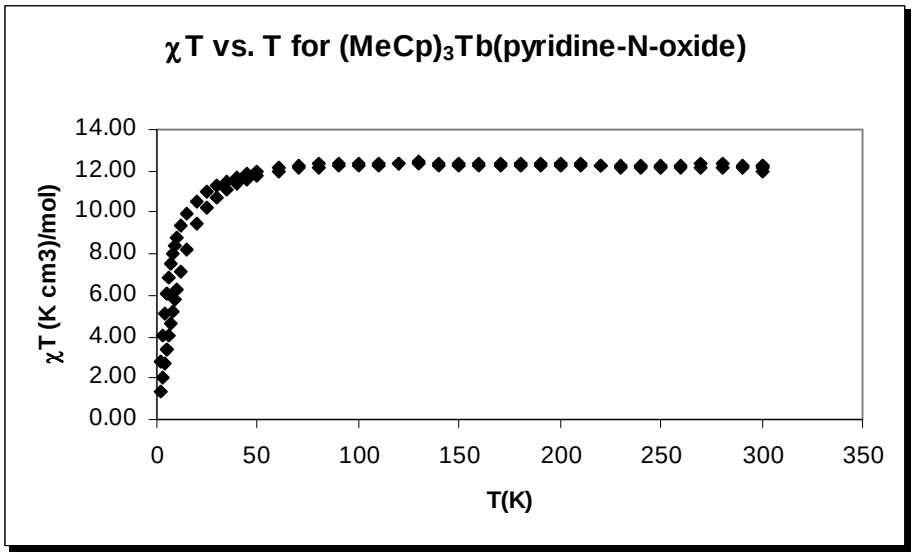
χT vs. T for (MeCp)3Tb(pyridine-N-oxide)
χT (K cm3)/mol
T(K)
14.00
12.00
10.00
8.00
6.00
4.00
2.00
0.00
0
50
100
150
200
250
300
350

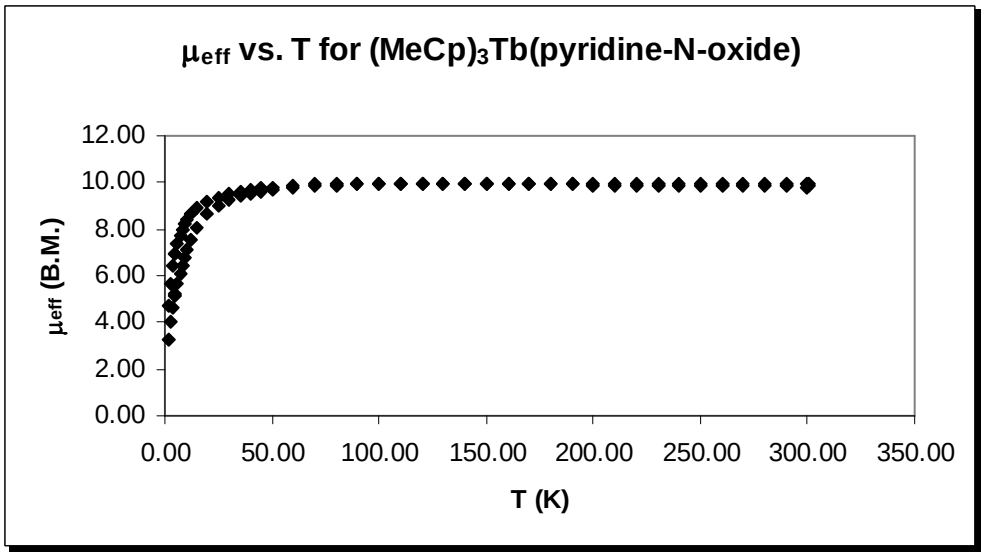
μeff vs. T for (MeCp)3Tb(pyridine-N-oxide)
μeff (B.M.)
T (K)
12.00
10.00
8.00
6.00
4.00
2.00
0.00
0.00
50.00
100.00
150.00
200.00
250.00
300.00
350.00

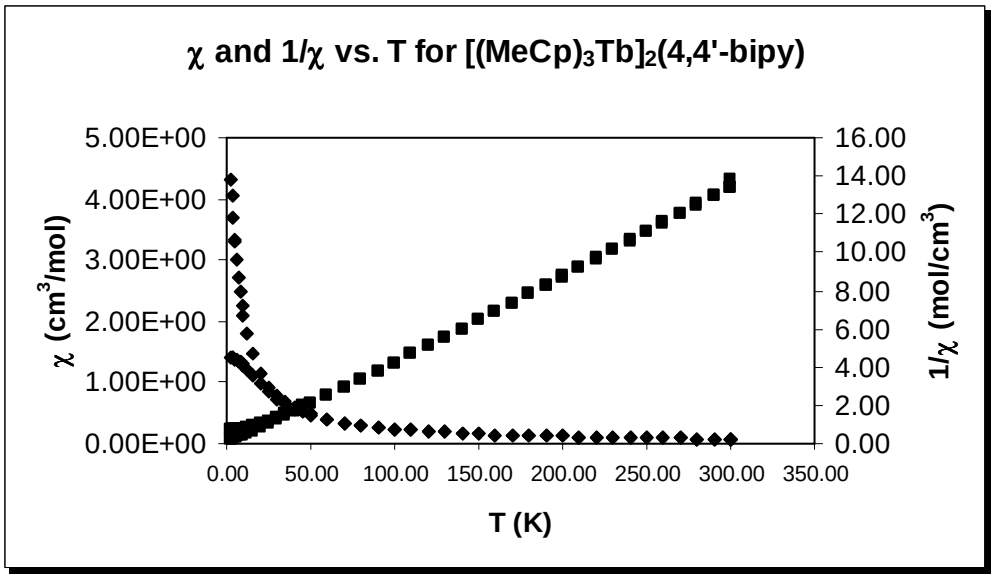
χ and 1/χ vs. T for [(MeCp)3Tb]2(4,4'-bipy)
5.00E+00
4.00E+00
3.00E+00
2.00E+00
1.00E+00
0.00E+00
χ (cm3/mol)
16.00
14.00
12.00
10.00
8.00
6.00
4.00
2.00
0.00
1/χ (mol/cm3)
0.00
50.00
100.00
150.00
200.00
250.00
300.00
350.00
T (K)

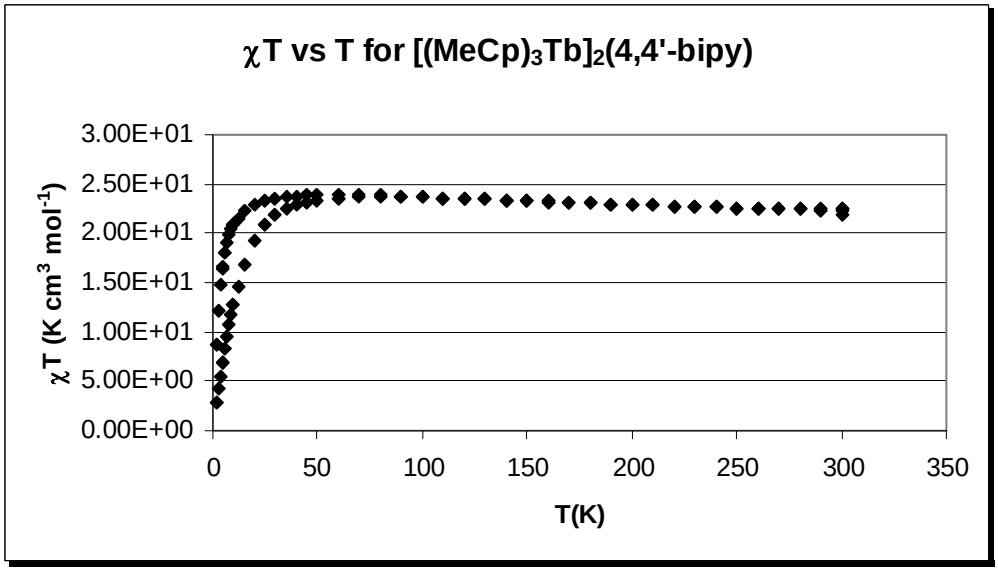
χT vs T for [(MeCp)3Tb]2(4,4'-bipy)
3.00E+01
2.50E+01
2.00E+01
1.50E+01
1.00E+01
5.00E+00
0.00E+00
χT (K cm3 mol-1)
0
50
100
150
200
250
300
350
T(K)

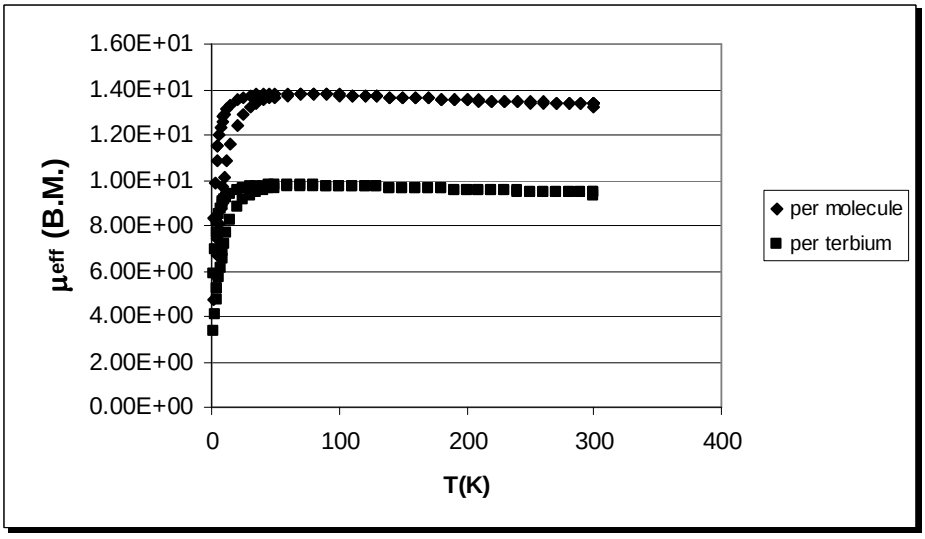
1.60E+01
1.40E+01
1.20E+01
1.00E+01
8.00E+00
6.00E+00
4.00E+00
2.00E+00
0.00E+00
μeff (B.M.)
0
100
200
300
400
T(K)
per molecule
per terbium

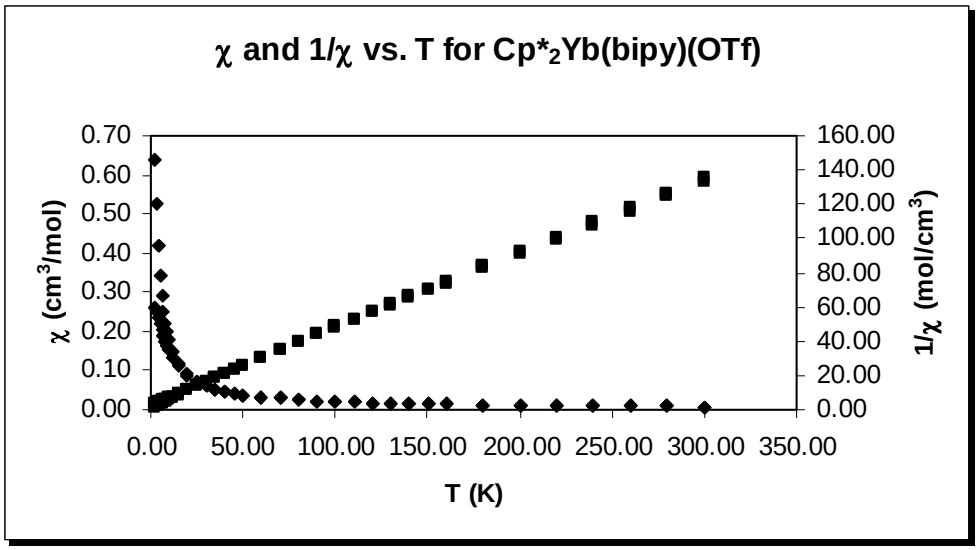
χ and 1/χ vs. T for Cp*2Yb(bipy)(OTf)
χ (cm3/mol)
1/χ (mol/cm3)
T (K)
0.70
0.60
0.50
0.40
0.30
0.20
0.10
0.00
160.00
140.00
120.00
100.00
80.00
60.00
40.00
20.00
0.00
0.00
50.00
100.00
150.00
200.00
250.00
300.00
350.00

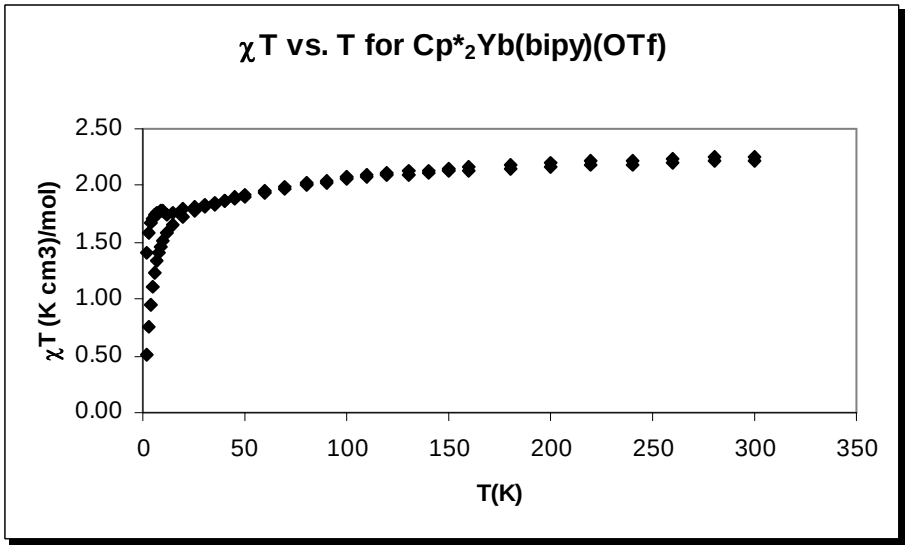
χT vs. T for Cp*2Yb(bipy)(OTf)
χT (K cm3)/mol)
T(K)
2.50
2.00
1.50
1.00
0.50
0.00
0
50
100
150
200
250
300
350

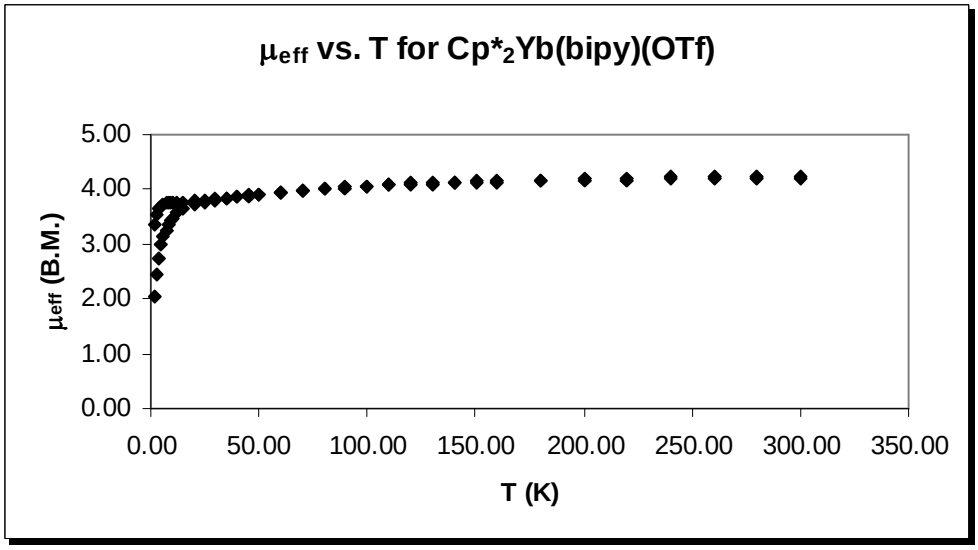
μeff vs. T for Cp*2Yb(bipy)(OTf)
μeff (B.M.)
T (K)
5.00
4.00
3.00
2.00
1.00
0.00
0.00
50.00
100.00
150.00
200.00
250.00
300.00
350.00

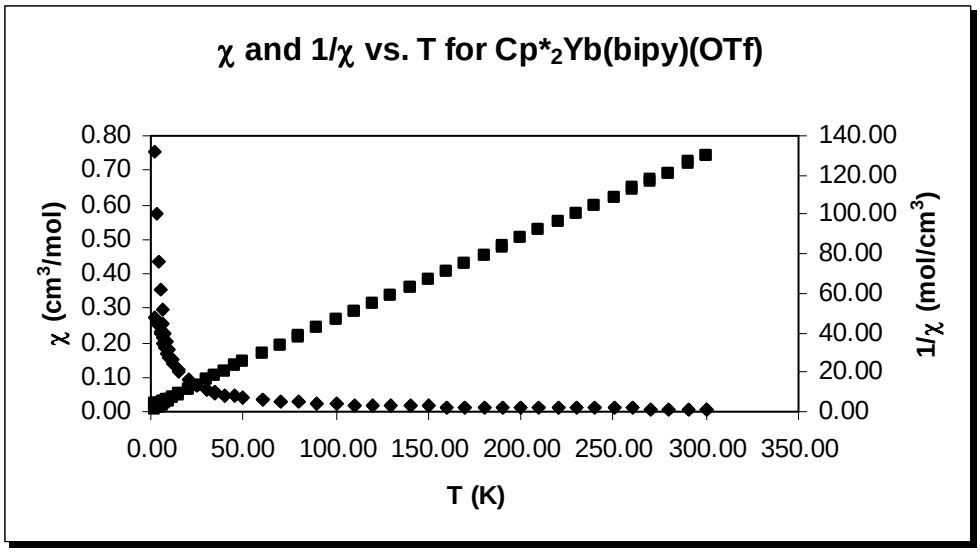
χ and 1/χ vs. T for Cp*2Yb(bipy)(OTf)
χ (cm3/mol)
1/χ (mol/cm3)
T (K)
0.80
0.70
0.60
0.50
0.40
0.30
0.20
0.10
0.00
140.00
120.00
100.00
80.00
60.00
40.00
20.00
0.00
0.00
50.00
100.00
150.00
200.00
250.00
300.00
350.00

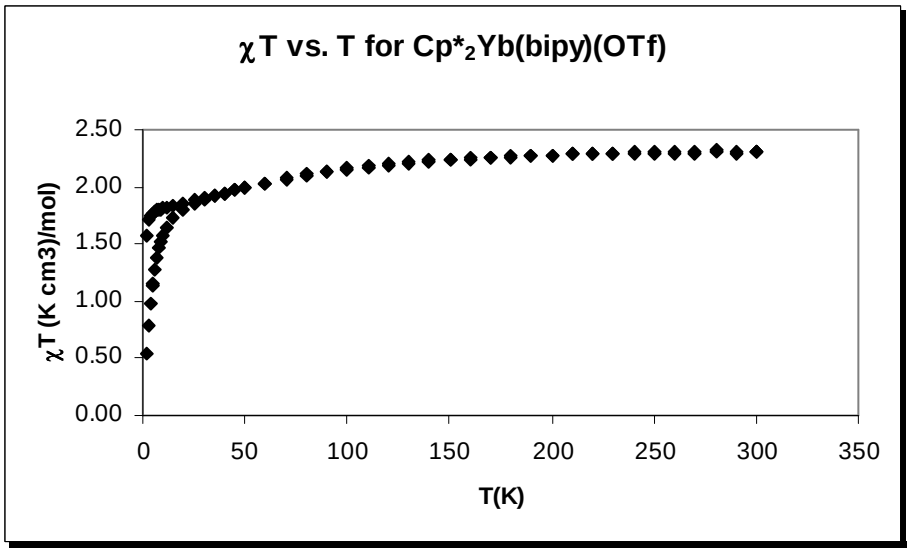
χT vs. T for Cp*2Yb(bipy)(OTf)
χT (K cm3)/mol)
T(K)
2.50
2.00
1.50
1.00
0.50
0.00
0
50
100
150
200
250
300
350

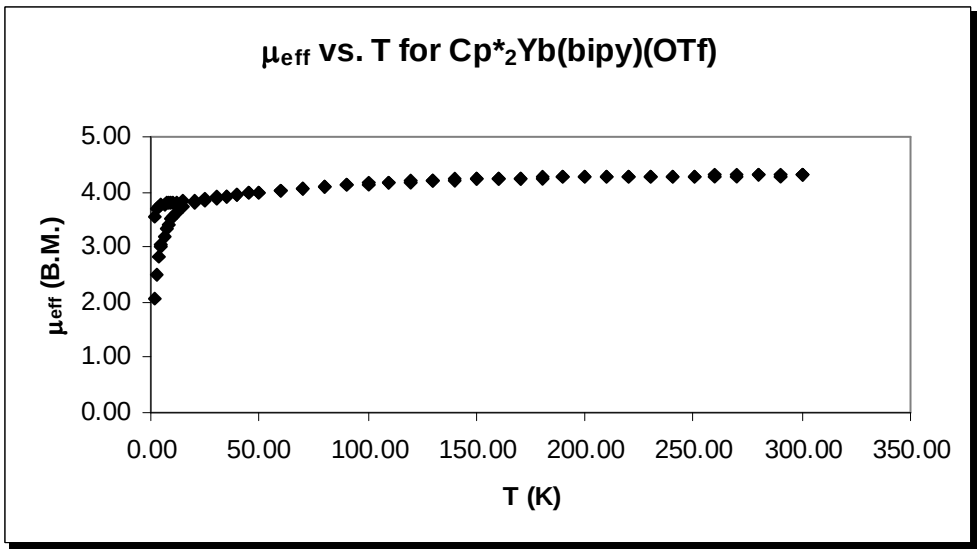
μeff vs. T for Cp*2Yb(bipy)(OTf)
μeff (B.M.)
T (K)
5.00
4.00
3.00
2.00
1.00
0.00
0.00
50.00
100.00
150.00
200.00
250.00
300.00
350.00

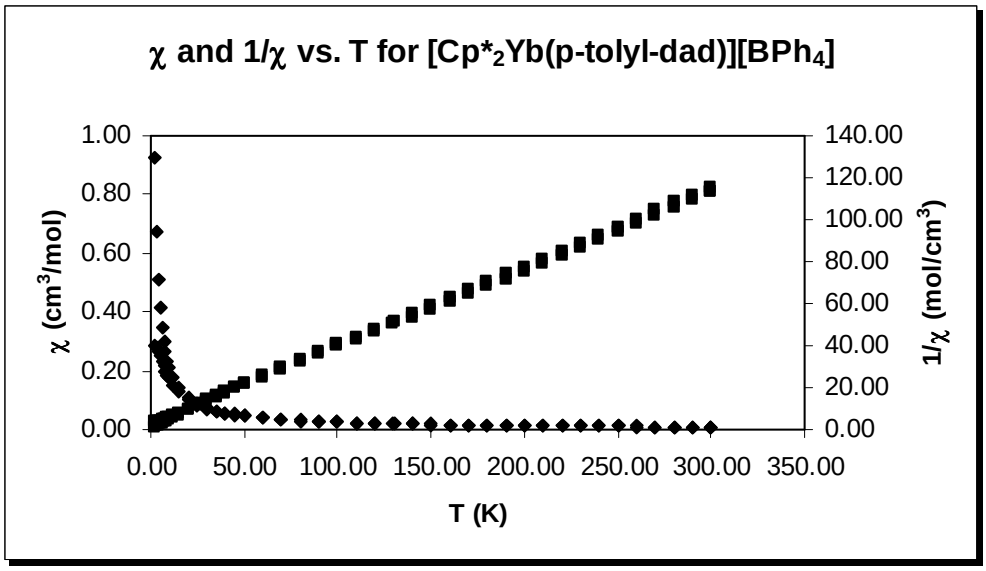
χ and 1/χ vs. T for [Cp*2Yb(p-tolyl-dad)][BPh4]
χ (cm3/mol)
1/χ (mol/cm3)
T (K)
1.00
0.80
0.60
0.40
0.20
0.00
140.00
120.00
100.00
80.00
60.00
40.00
20.00
0.00
0.00
50.00
100.00
150.00
200.00
250.00
300.00
350.00

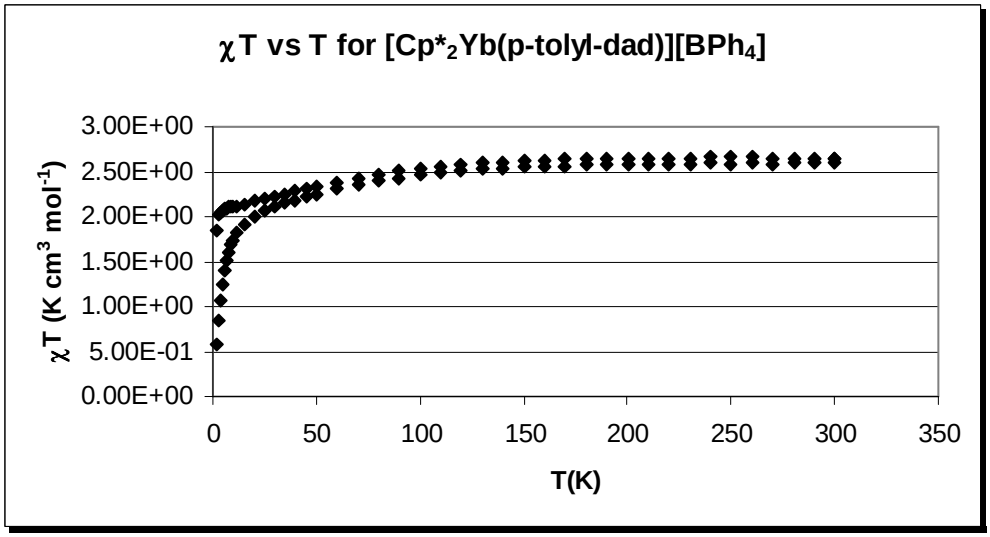
χT vs T for [Cp*2Yb(p-tolyl-dad)][BPh4]
χT (K cm3 mol-1)
T(K)
3.00E+00
2.50E+00
2.00E+00
1.50E+00
1.00E+00
5.00E-01
0.00E+00
0
50
100
150
200
250
300
350

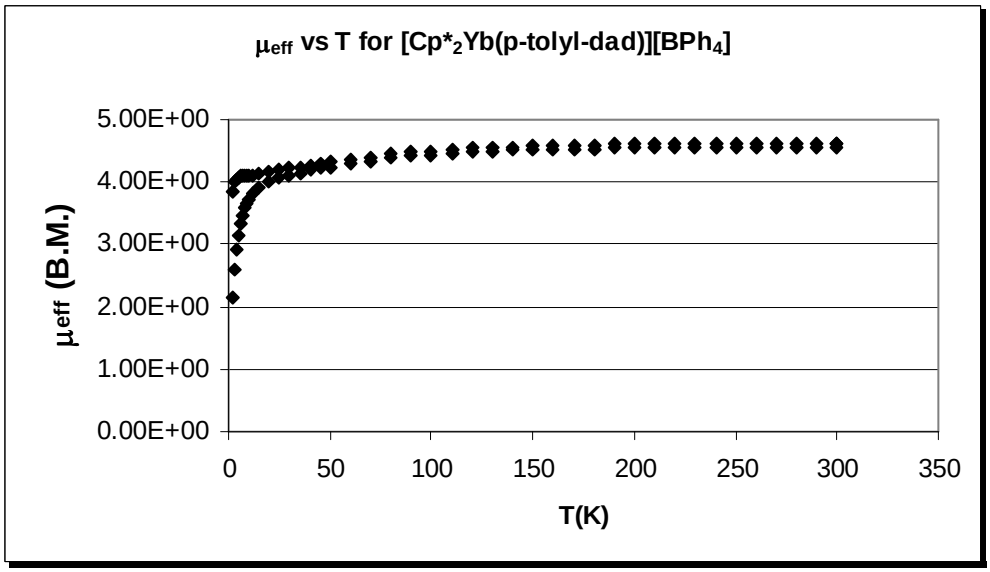
μeff vs T for [Cp*2Yb(p-tolyl-dad)][BPh4]
μeff (B.M.)
T(K)
5.00E+00
4.00E+00
3.00E+00
2.00E+00
1.00E+00
0.00E+00
0
50
100
150
200
250
300
350

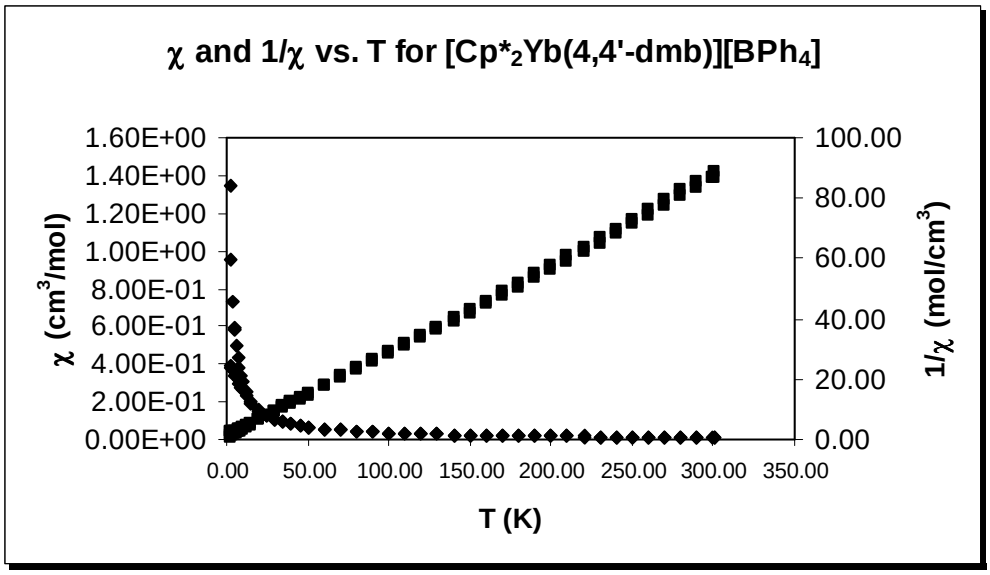
χ and 1/χ vs. T for [Cp*2Yb(4,4'-dmb)][BPh4]
1.60E+00
1.40E+00
1.20E+00
1.00E+00
8.00E-01
6.00E-01
4.00E-01
2.00E-01
0.00E+00
χ (cm3/mol)
100.00
80.00
60.00
40.00
20.00
0.00
1/χ (mol/cm3)
0.00
50.00
100.00
150.00
200.00
250.00
300.00
350.00
T (K)

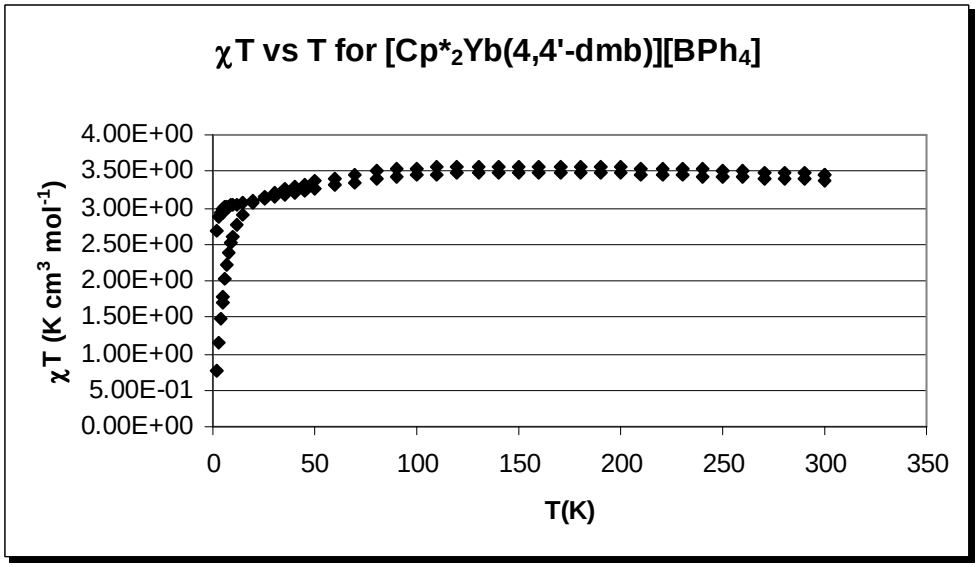
χT vs T for [Cp*2Yb(4,4'-dmb)][BPh4]
4.00E+00
3.50E+00
3.00E+00
2.50E+00
2.00E+00
1.50E+00
1.00E+00
5.00E-01
0.00E+00
χT (K cm3 mol-1)
0
50
100
150
200
250
300
350
T(K)

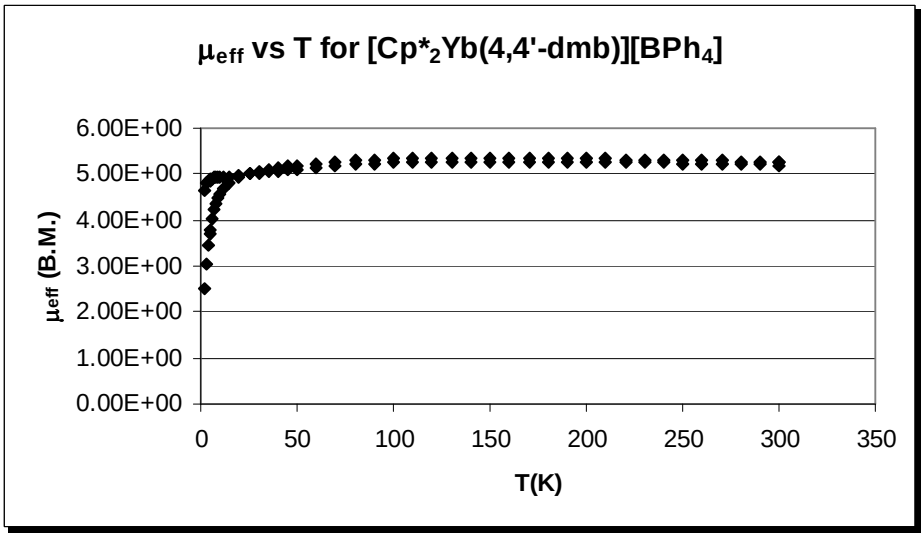
μeff vs T for [Cp*2Yb(4,4'-dmb)][BPh4]
6.00E+00
5.00E+00
4.00E+00
3.00E+00
2.00E+00
1.00E+00
0.00E+00
μeff (B.M.)
0
50
100
150
200
250
300
350
T(K)

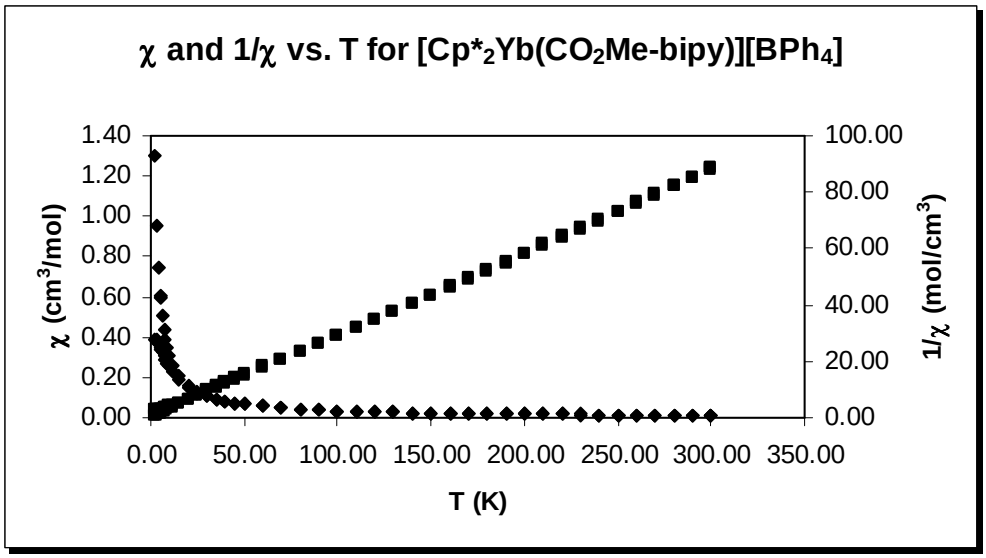
χ and 1/χ vs. T for [Cp*2Yb(CO2Me-bipy)][BPh4]
χ (cm3/mol)
1/χ (mol/cm3)
T (K)
1.40
1.20
1.00
0.80
0.60
0.40
0.20
0.00
100.00
80.00
60.00
40.00
20.00
0.00
0.00
50.00
100.00
150.00
200.00
250.00
300.00
350.00

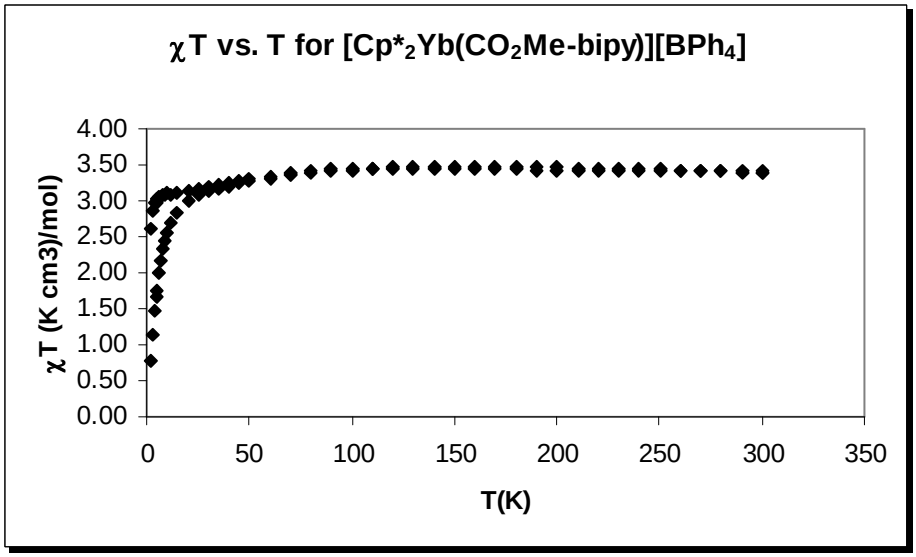
χT vs. T for [Cp*2Yb(CO2Me-bipy)][BPh4]
χT (K cm3)/mol)
T(K)
4.00
3.50
3.00
2.50
2.00
1.50
1.00
0.50
0.00
0
50
100
150
200
250
300
350

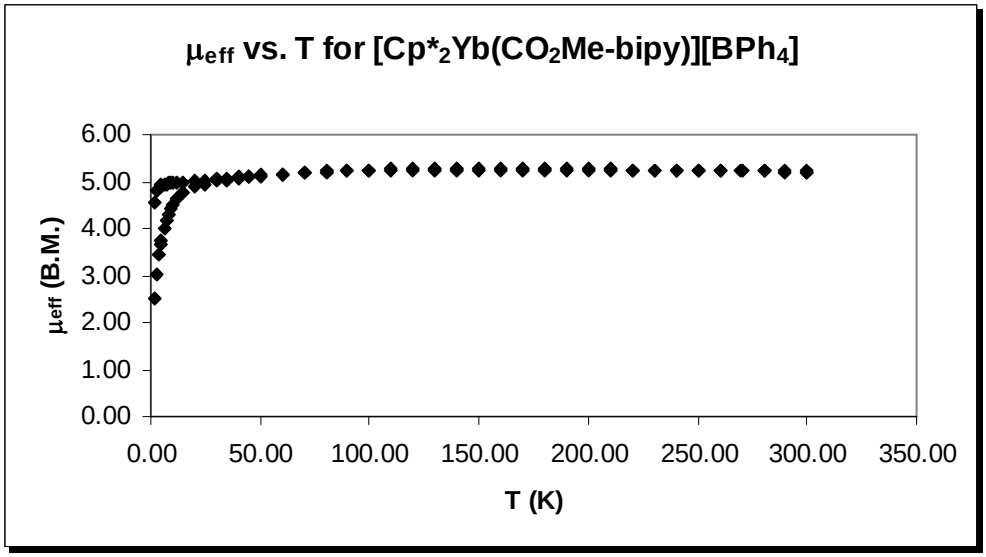
μeff vs. T for [Cp*2Yb(CO2Me-bipy)][BPh4]
μeff (B.M.)
T (K)
6.00
5.00
4.00
3.00
2.00
1.00
0.00
0.00
50.00
100.00
150.00
200.00
250.00
300.00
350.00

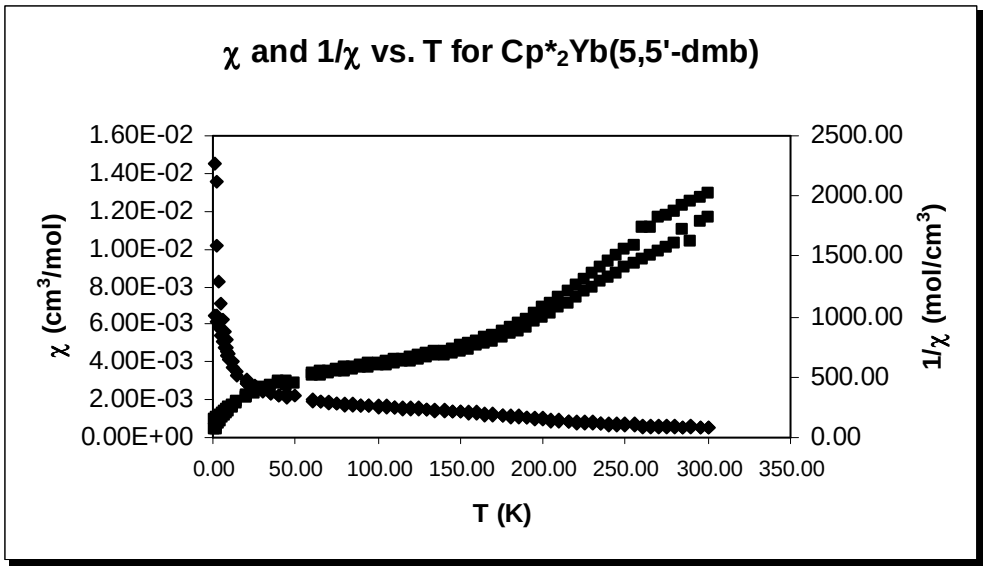
χ and 1/χ vs. T for Cp*2Yb(5,5'-dmb)
1.60E-02
1.40E-02
1.20E-02
1.00E-02
8.00E-03
6.00E-03
4.00E-03
2.00E-03
0.00E+00
χ (cm3/mol)
2500.00
2000.00
1500.00
1000.00
500.00
0.00
1/χ (mol/cm3)
0.00
50.00
100.00
150.00
200.00
250.00
300.00
350.00
T (K)

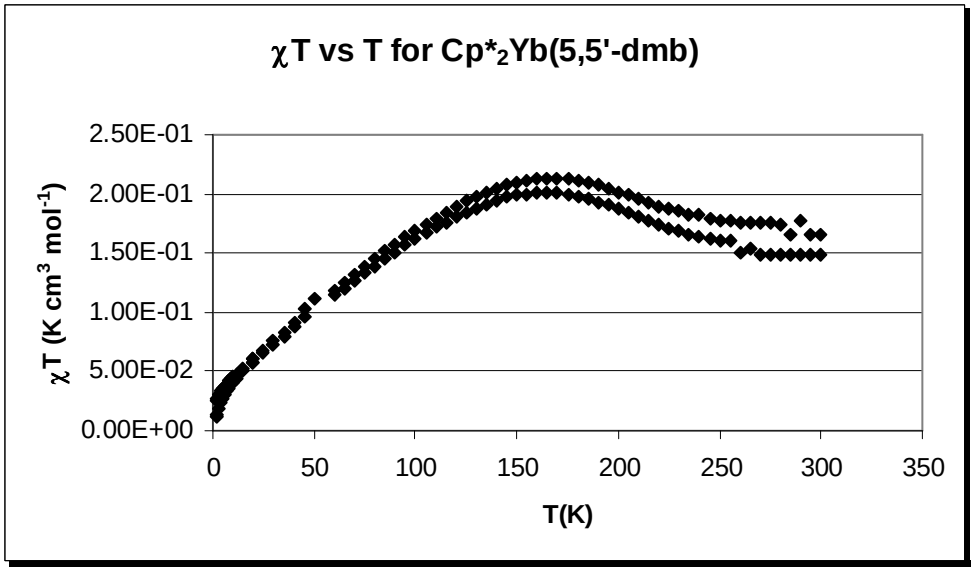
χT vs T for Cp*2Yb(5,5'-dmb)
2.50E-01
2.00E-01
1.50E-01
1.00E-01
5.00E-02
0.00E+00
χT (K cm3 mol-1)
0
50
100
150
200
250
300
350
T(K)

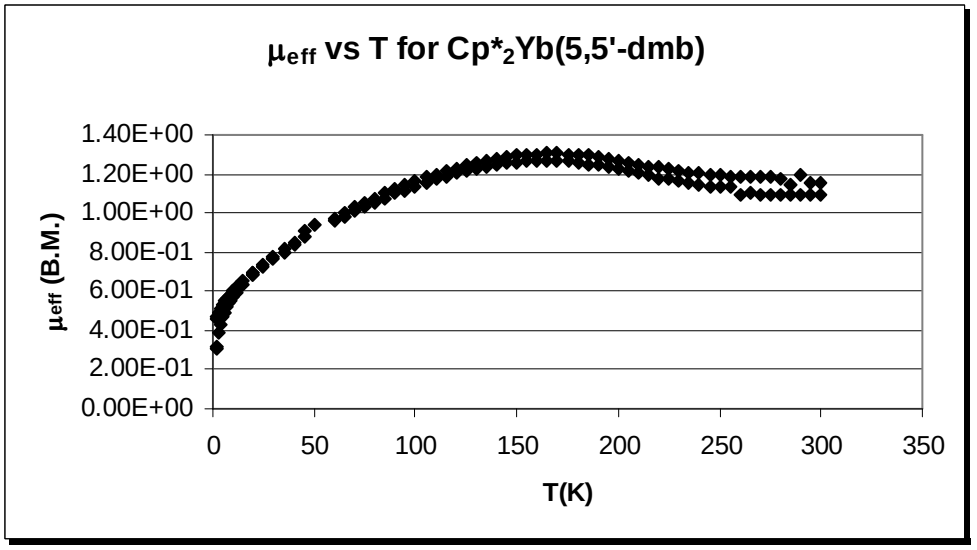
μeff vs T for Cp*2Yb(5,5'-dmb)
1.40E+00
1.20E+00
1.00E+00
8.00E-01
6.00E-01
4.00E-01
2.00E-01
0.00E+00
μeff (B.M.)
0
50
100
150
200
250
300
350
T(K)

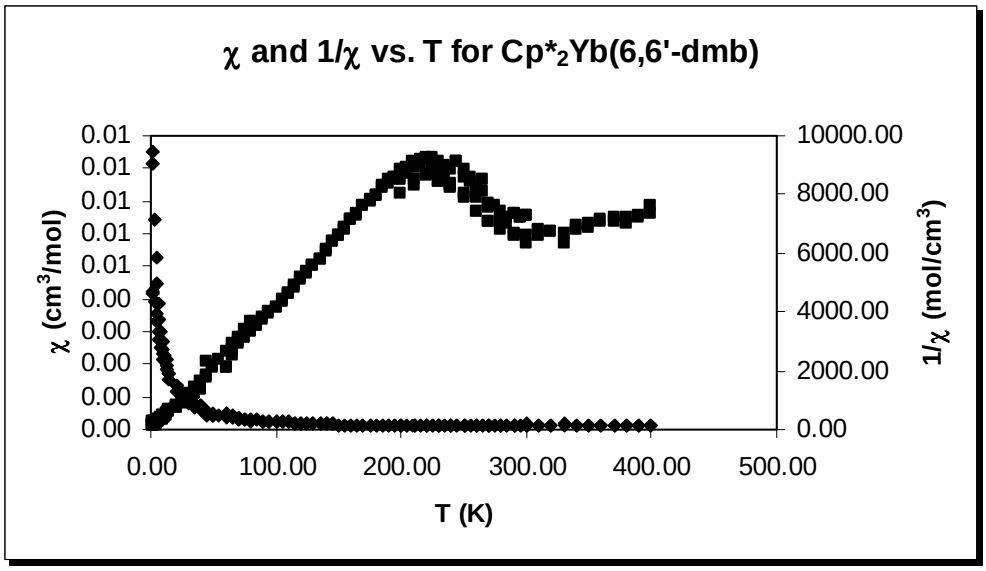
χ and 1/χ vs. T for Cp*2Yb(6,6'-dmb)
χ (cm3/mol)
1/χ (mol/cm3)
T (K)
0.01
0.01
0.01
0.01
0.01
0.00
0.00
0.00
0.00
0.00
10000.00
8000.00
6000.00
4000.00
2000.00
0.00
0.00
100.00
200.00
300.00
400.00
500.00

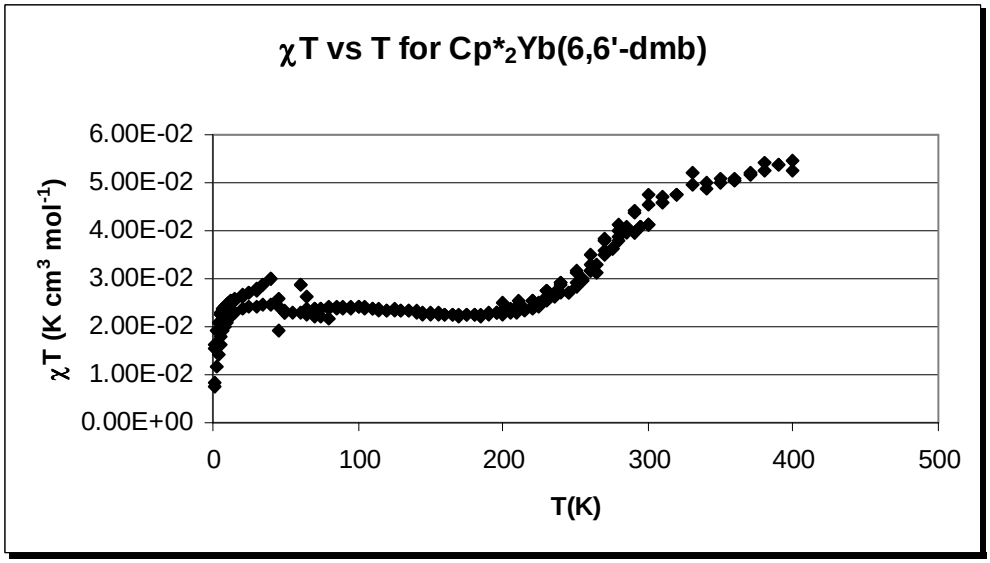
χT vs T for Cp*2Yb(6,6'-dmb)
χT (K cm3 mol-1)
T(K)
6.00E-02
5.00E-02
4.00E-02
3.00E-02
2.00E-02
1.00E-02
0.00E+00
0
100
200
300
400
500

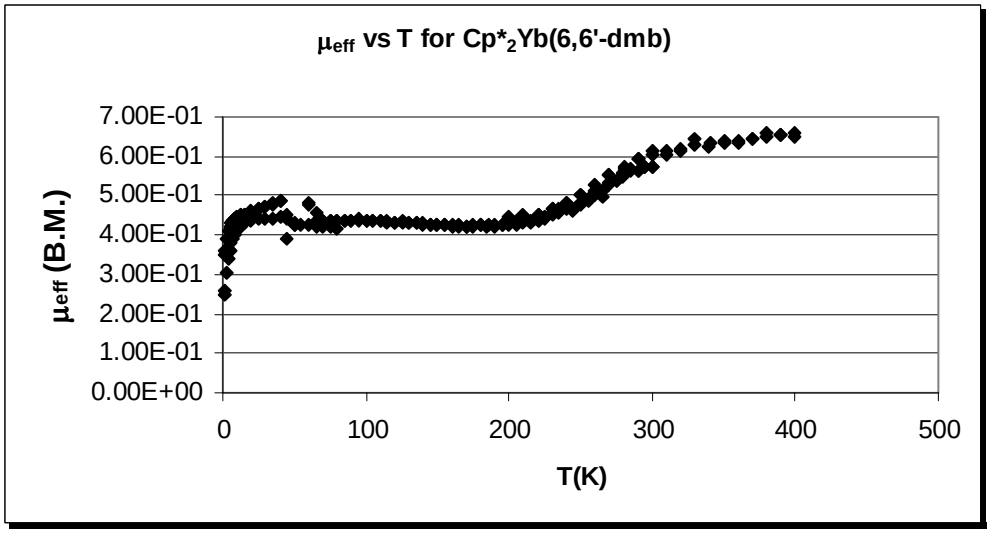
μeff vs T for Cp*2Yb(6,6'-dmb)
μeff (B.M.)
T(K)
7.00E-01
6.00E-01
5.00E-01
4.00E-01
3.00E-01
2.00E-01
1.00E-01
0.00E+00
0
100
200
300
400
500

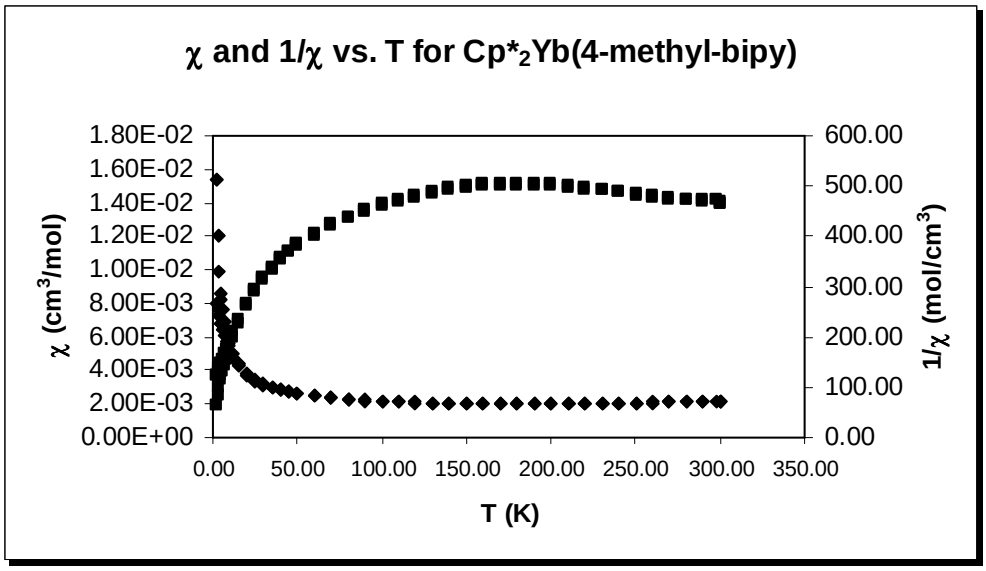
χ and 1/χ vs. T for Cp*2Yb(4-methyl-bipy)
1.80E-02
1.60E-02
1.40E-02
1.20E-02
1.00E-02
8.00E-03
6.00E-03
4.00E-03
2.00E-03
0.00E+00
χ (cm3/mol)
600.00
500.00
400.00
300.00
200.00
100.00
0.00
1/χ (mol/cm3)
0.00
50.00
100.00
150.00
200.00
250.00
300.00
350.00
T (K)

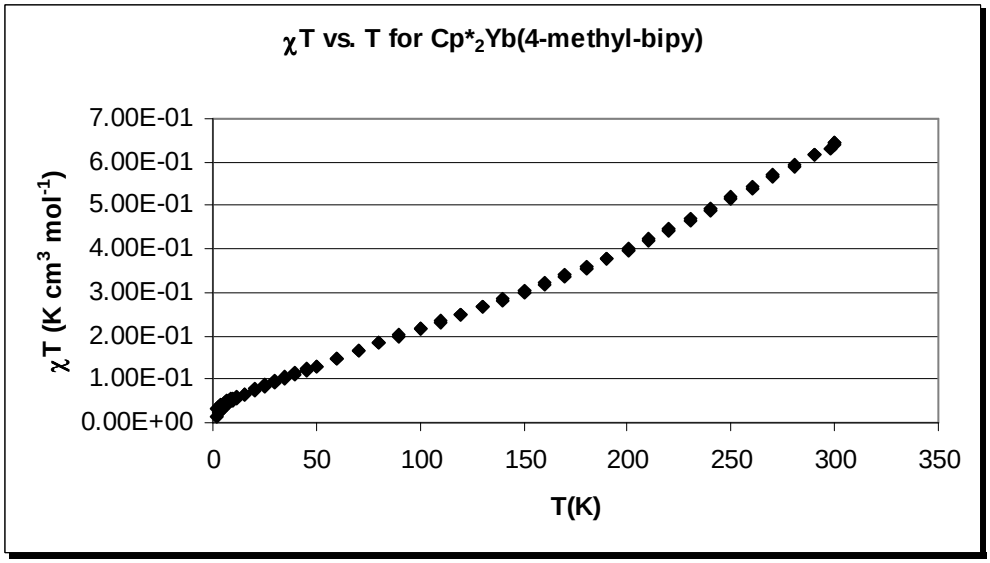
χT vs. T for Cp*2Yb(4-methyl-bipy)
7.00E-01
6.00E-01
5.00E-01
4.00E-01
3.00E-01
2.00E-01
1.00E-01
0.00E+00
χT (K cm3 mol-1)
0
50
100
150
200
250
300
350
T(K)

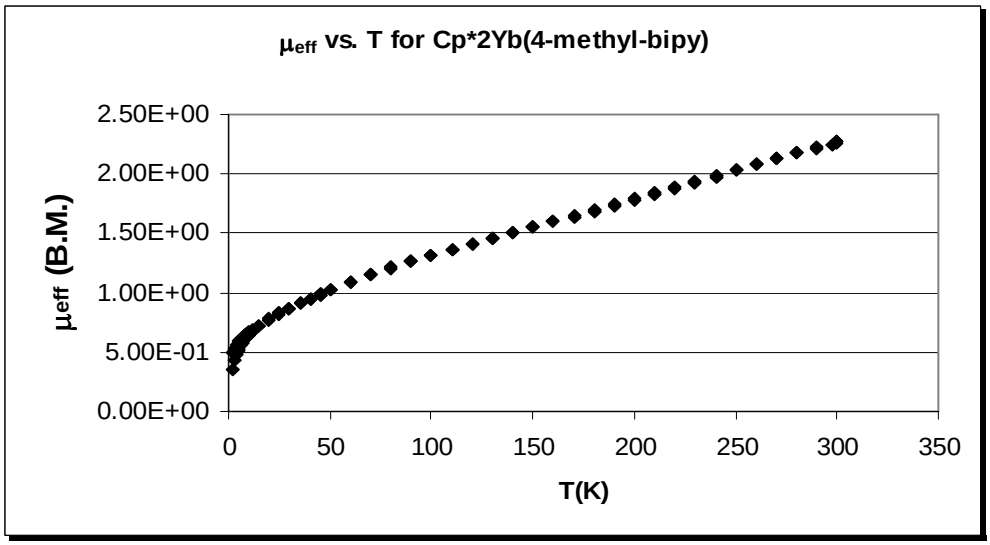
μeff vs. T for Cp*2Yb(4-methyl-bipy)
2.50E+00
2.00E+00
1.50E+00
1.00E+00
5.00E-01
0.00E+00
μeff (B.M.)
0
50
100
150
200
250
300
350
T(K)

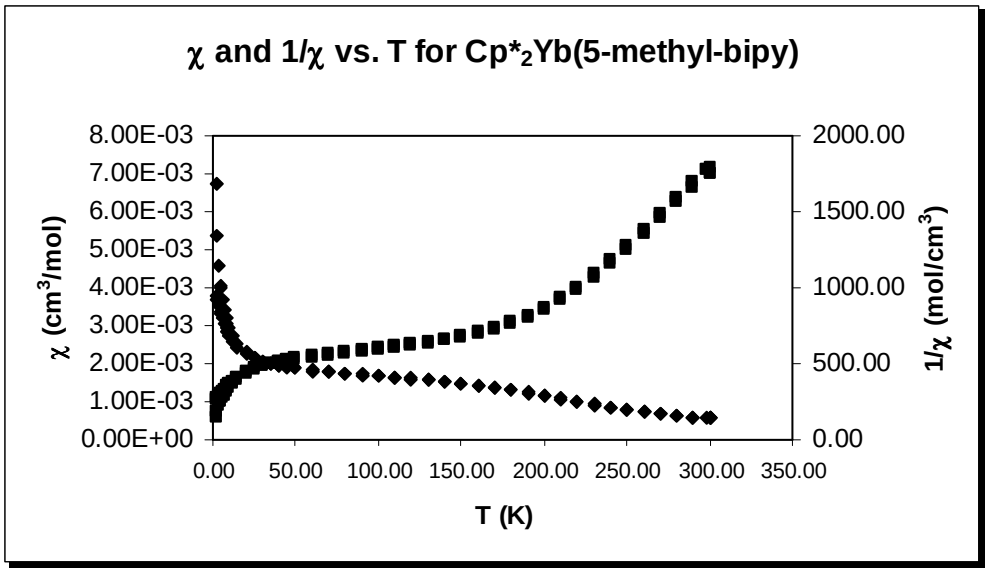
χ and 1/χ vs. T for Cp*2Yb(5-methyl-bipy)
8.00E-03
7.00E-03
6.00E-03
5.00E-03
4.00E-03
3.00E-03
2.00E-03
1.00E-03
0.00E+00
χ (cm3/mol)
2000.00
1500.00
1000.00
500.00
0.00
1/χ (mol/cm3)
0.00
50.00
100.00
150.00
200.00
250.00
300.00
350.00
T (K)

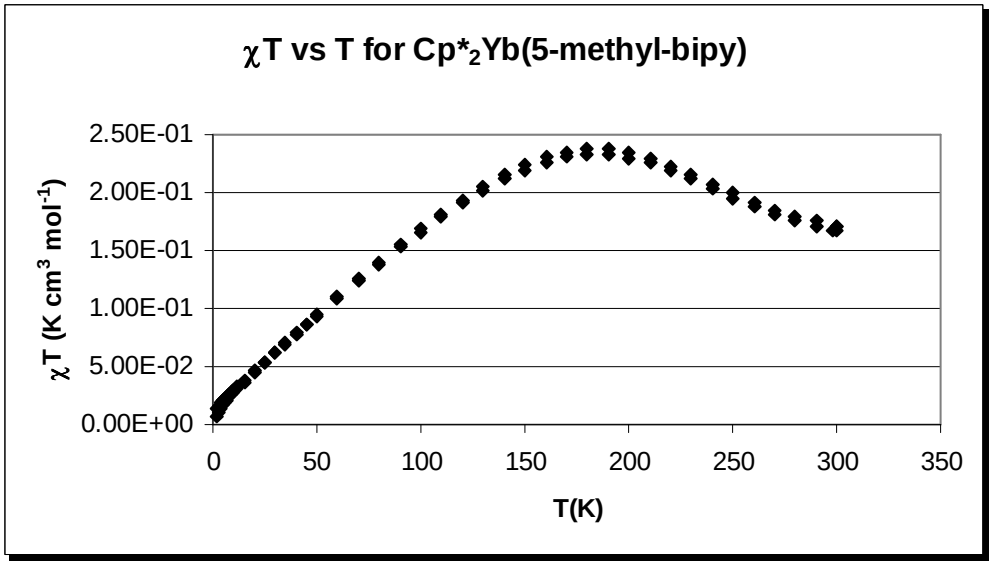
χT vs T for Cp*2Yb(5-methyl-bipy)
2.50E-01
2.00E-01
1.50E-01
1.00E-01
5.00E-02
0.00E+00
χT (K cm3 mol-1)
0
50
100
150
200
250
300
350
T(K)

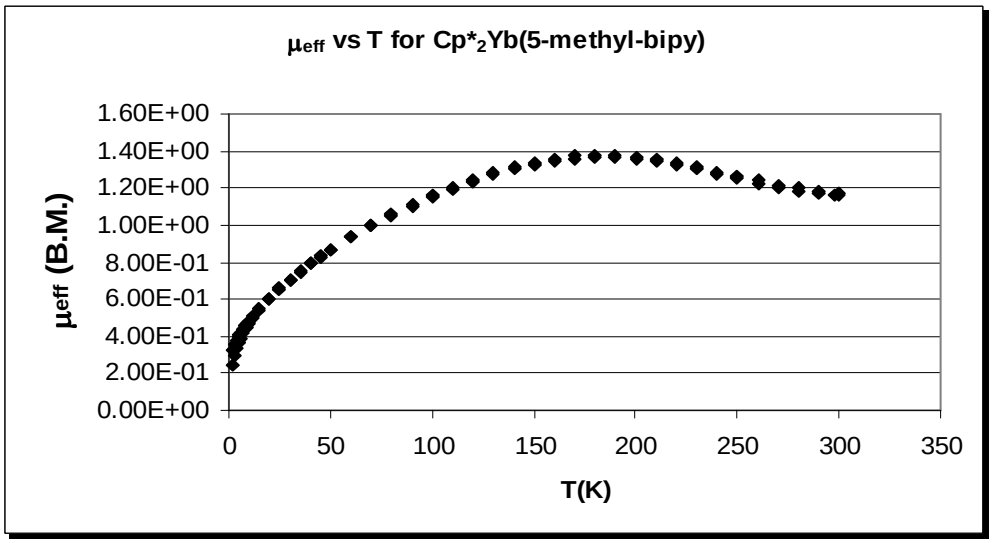
μeff vs T for Cp*2Yb(5-methyl-bipy)
1.60E+00
1.40E+00
1.20E+00
1.00E+00
8.00E-01
6.00E-01
4.00E-01
2.00E-01
0.00E+00
μeff (B.M.)
0
50
100
150
200
250
300
350
T(K)

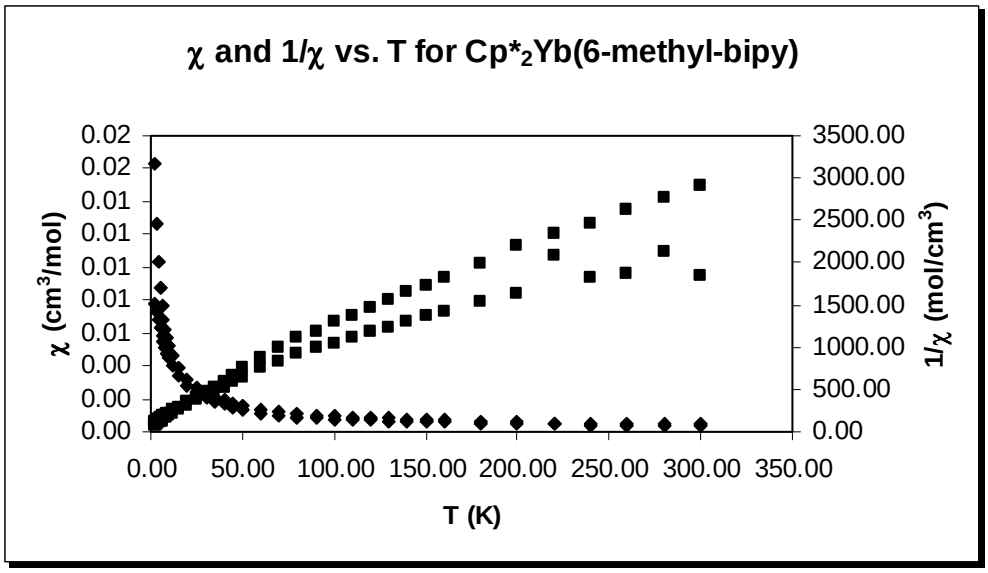
χ and 1/χ vs. T for Cp*2Yb(6-methyl-bipy)
χ (cm3/mol)
1/χ (mol/cm3)
T (K)
0.02
0.02
0.01
0.01
0.01
0.01
0.01
0.00
0.00
0.00
3500.00
3000.00
2500.00
2000.00
1500.00
1000.00
500.00
0.00
0.00
50.00
100.00
150.00
200.00
250.00
300.00
350.00

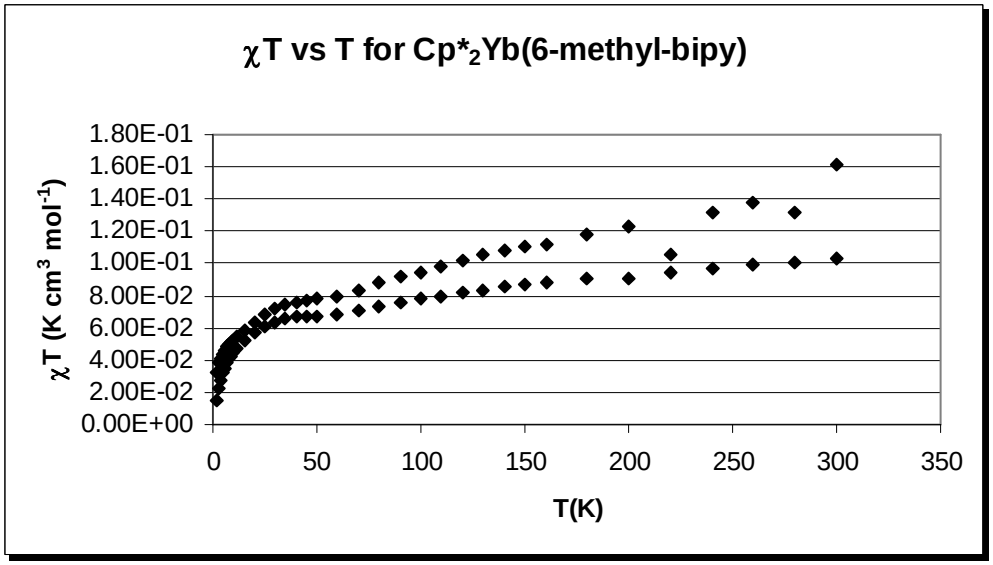
χT vs T for Cp*2Yb(6-methyl-bipy)
χT (K cm3 mol-1)
T(K)
1.80E-01
1.60E-01
1.40E-01
1.20E-01
1.00E-01
8.00E-02
6.00E-02
4.00E-02
2.00E-02
0.00E+00
0
50
100
150
200
250
300
350

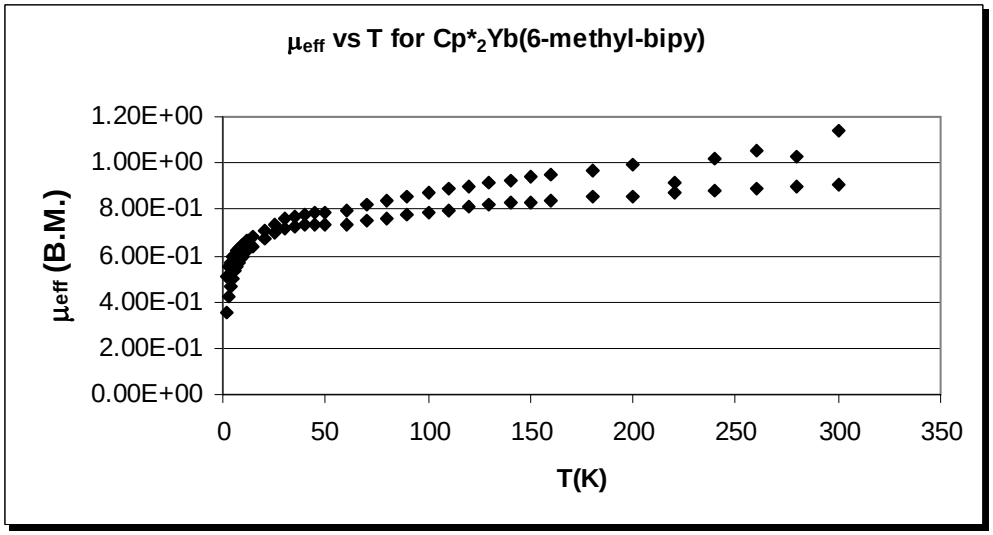
μeff vs T for Cp*2Yb(6-methyl-bipy)
μeff (B.M.)
T(K)
1.20E+00
1.00E+00
8.00E-01
6.00E-01
4.00E-01
2.00E-01
0.00E+00
0
50
100
150
200
250
300
350

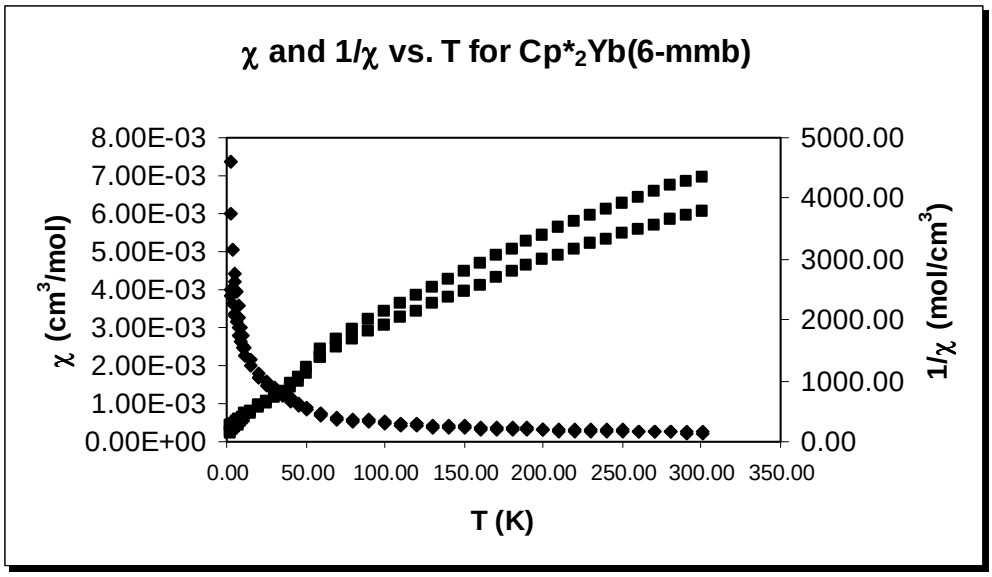
χ and 1/χ vs. T for Cp*2Yb(6-mmb)
8.00E-03
7.00E-03
6.00E-03
5.00E-03
4.00E-03
3.00E-03
2.00E-03
1.00E-03
0.00E+00
χ (cm3/mol)
5000.00
4000.00
3000.00
2000.00
1000.00
0.00
1/χ (mol/cm3)
0.00
50.00
100.00
150.00
200.00
250.00
300.00
350.00
T (K)

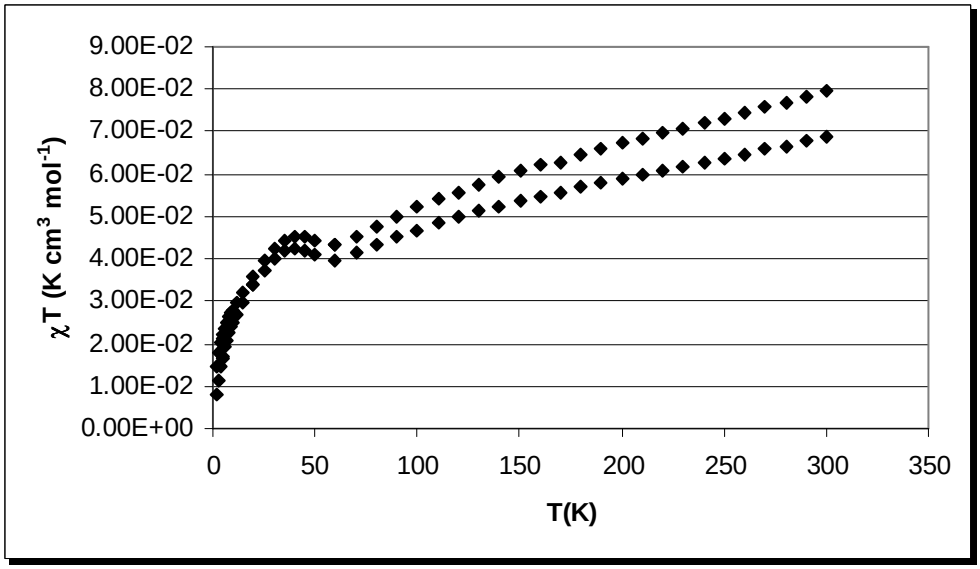
9.00E-02
8.00E-02
7.00E-02
6.00E-02
5.00E-02
4.00E-02
3.00E-02
2.00E-02
1.00E-02
0.00E+00
χT (K cm3 mol-1)
0
50
100
150
200
250
300
350
T(K)

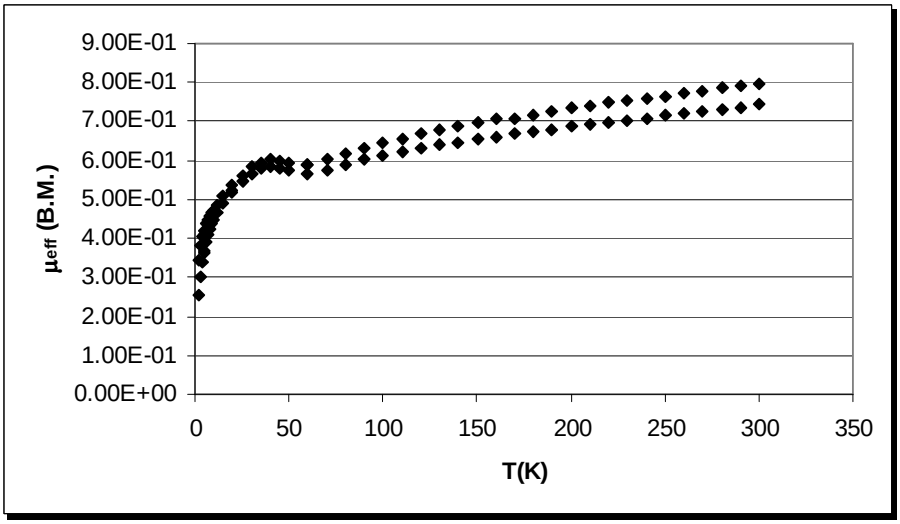
9.00E-01
8.00E-01
7.00E-01
6.00E-01
5.00E-01
4.00E-01
3.00E-01
2.00E-01
1.00E-01
0.00E+00
μeff (B.M.)
0
50
100
150
200
250
300
350
T(K)

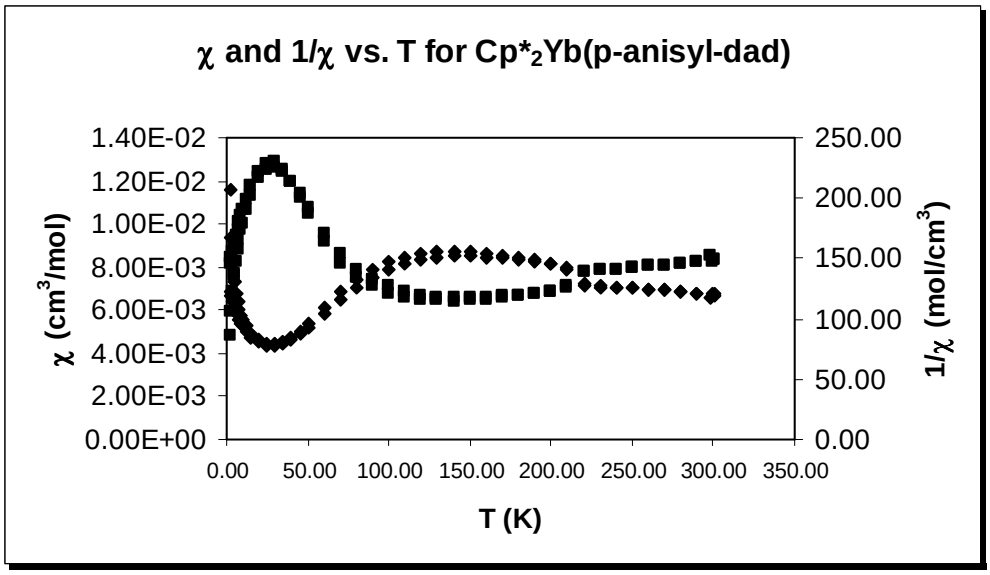
χ and 1/χ vs. T for Cp*2Yb(p-anisyl-dad)
1.40E-02
1.20E-02
1.00E-02
8.00E-03
6.00E-03
4.00E-03
2.00E-03
0.00E+00
χ (cm3/mol)
250.00
200.00
150.00
100.00
50.00
0.00
1/χ (mol/cm3)
0.00 50.00 100.00 150.00 200.00 250.00 300.00 350.00
T (K)

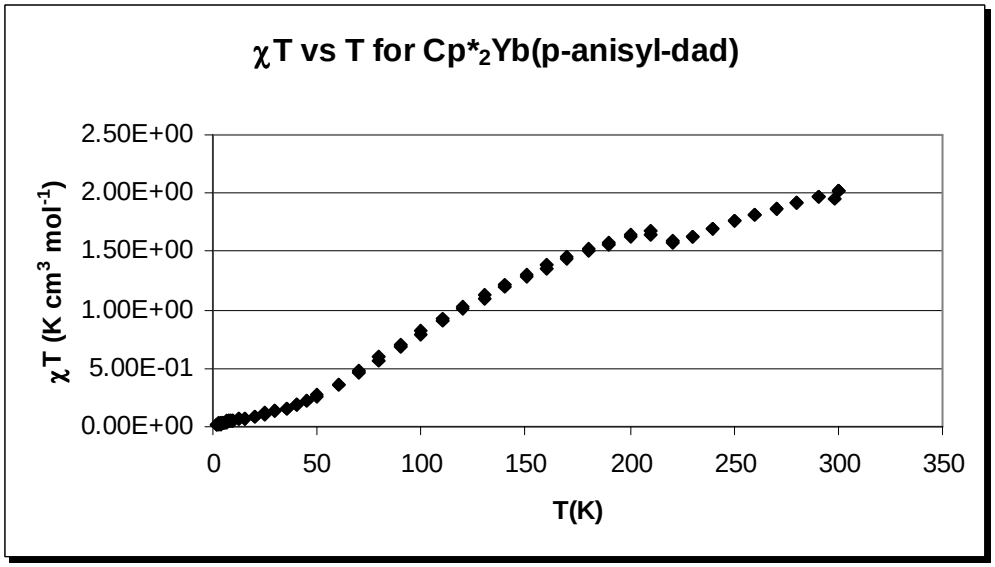
χT vs T for Cp*2Yb(p-anisyl-dad)
2.50E+00
2.00E+00
1.50E+00
1.00E+00
5.00E-01
0.00E+00
χT (K cm3 mol-1)
0 50 100 150 200 250 300 350
T(K)

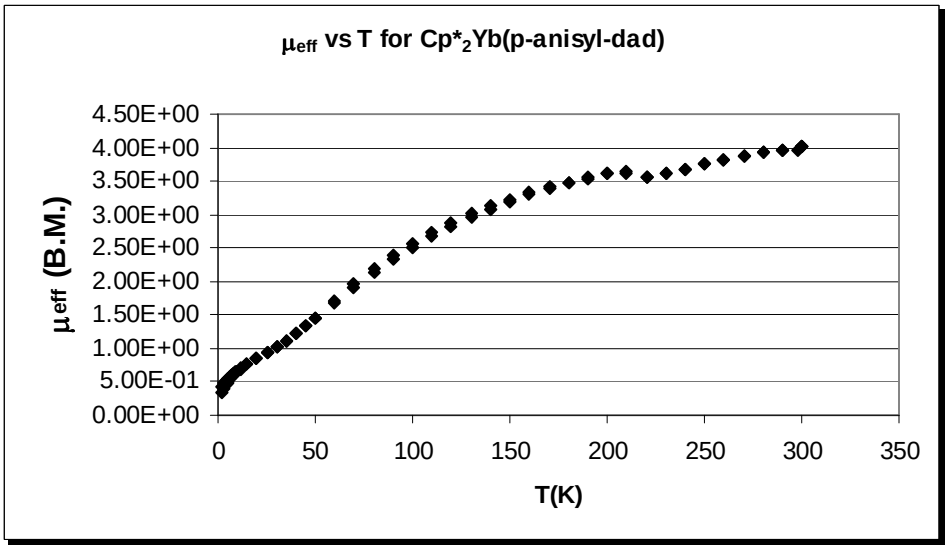
μeff vs T for Cp*2Yb(p-anisyl-dad)
4.50E+00
4.00E+00
3.50E+00
3.00E+00
2.50E+00
2.00E+00
1.50E+00
1.00E+00
5.00E-01
0.00E+00
μeff (B.M.)
0 50 100 150 200 250 300 350
T(K)

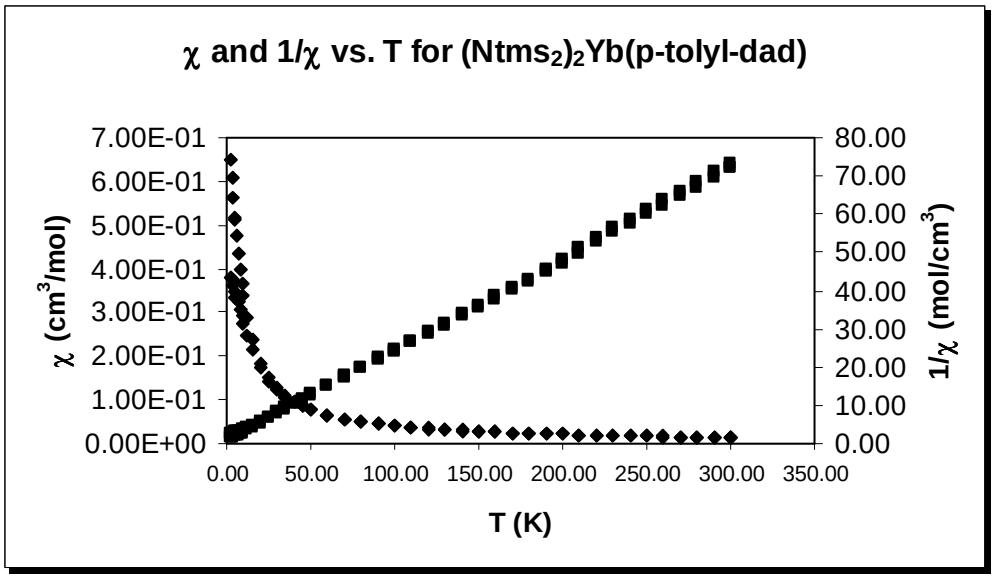
χ and 1/χ vs. T for (Ntms2)2Yb(p-tolyl-dad)
7.00E-01
6.00E-01
5.00E-01
4.00E-01
3.00E-01
2.00E-01
1.00E-01
0.00E+00
χ (cm3/mol)
80.00
70.00
60.00
50.00
40.00
30.00
20.00
10.00
0.00
1/χ (mol/cm3)
0.00
50.00
100.00
150.00
200.00
250.00
300.00
350.00
T (K)

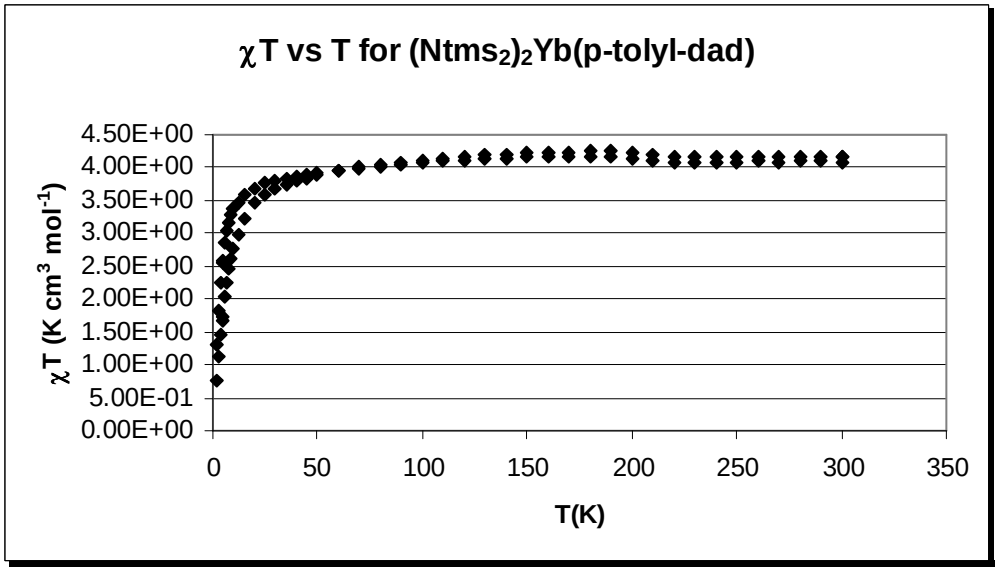
χT vs T for (Ntms2)2Yb(p-tolyl-dad)
4.50E+00
4.00E+00
3.50E+00
3.00E+00
2.50E+00
2.00E+00
1.50E+00
1.00E+00
5.00E-01
0.00E+00
χT (K cm3 mol-1)
0
50
100
150
200
250
300
350
T(K)

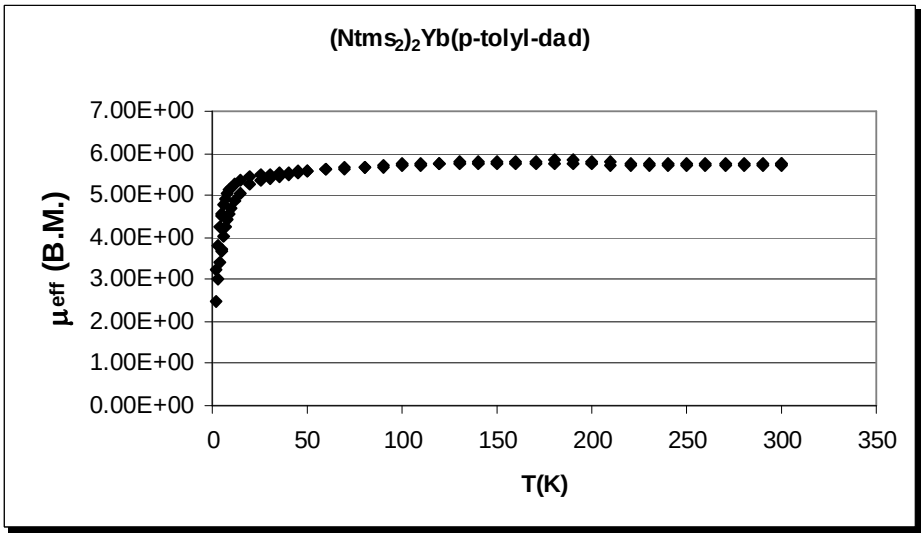
(Ntms2)2Yb(p-tolyl-dad)
7.00E+00
6.00E+00
5.00E+00
4.00E+00
3.00E+00
2.00E+00
1.00E+00
0.00E+00
μeff (B.M.)
0
50
100
150
200
250
300
350
T(K)

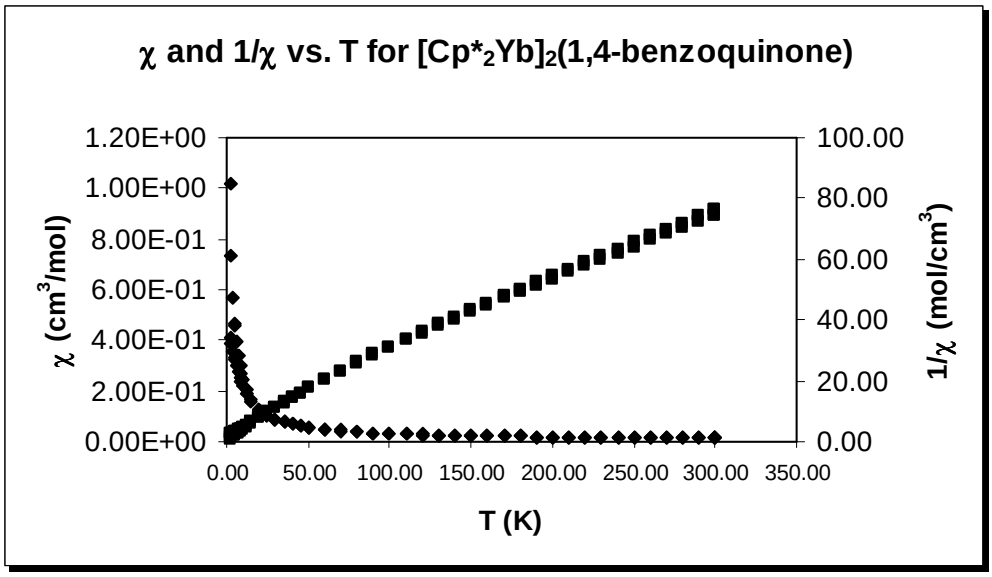
χ and 1/χ vs. T for [Cp*2Yb]2(1,4-benzoquinone)
1.20E+00
1.00E+00
8.00E-01
6.00E-01
4.00E-01
2.00E-01
0.00E+00
χ (cm3/mol)
100.00
80.00
60.00
40.00
20.00
0.00
1/χ (mol/cm3)
0.00
50.00
100.00
150.00
200.00
250.00
300.00
350.00
T (K)

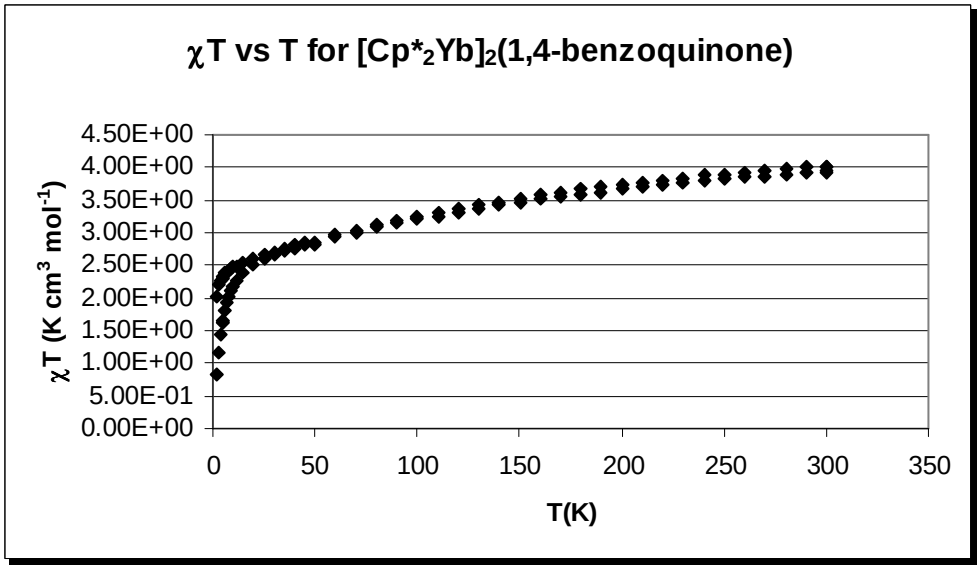
χT vs T for [Cp*2Yb]2(1,4-benzoquinone)
4.50E+00
4.00E+00
3.50E+00
3.00E+00
2.50E+00
2.00E+00
1.50E+00
1.00E+00
5.00E-01
0.00E+00
χT (K cm3 mol-1)
0
50
100
150
200
250
300
350
T(K)

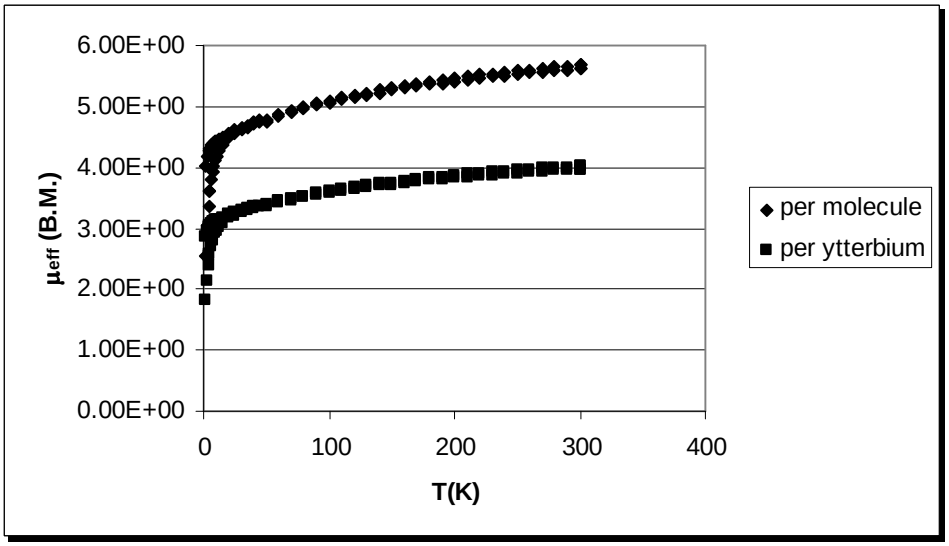
6.00E+00
5.00E+00
4.00E+00
3.00E+00
2.00E+00
1.00E+00
0.00E+00
μeff (B.M.)
0
100
200
300
400
T(K)
per molecule
per ytterbium

Chapter 8: X-ray Crystallography Details

General

A crystal of appropriate dimension was mounted on a glass fiber using Paratone N hydrocarbon oil. All measurements were made on a Bruker SMART or Apex CCD area detector[1] with graphite monochromated Mo-Kα radiation. Cell constants and an orientation matrix were obtained of the measured positions of reflections with $I > 10\ \sigma$ to give the unit cell. The systematic absences uniquely determined the space group in each case. An arbitrary hemisphere of data was collected at low temperature (see Experimental Details) using the ω scan technique with 0.3° scans counted for 10-30 seconds per frame. Data were integrated using SAINT[2] and corrected for Lorentz and polarization effects. The data were analyzed for agreement and absorption using XPREP,[3] and an empirical absorption correction was applied based on comparison of redundant and equivalent reflections using SADABS.[4] The structure was solved by direct methods[5] and expanded using Fourier techniques.[6] Non-hydrogen atoms were refined anisotropically (unless stated otherwise), and the hydrogen atoms were included in calculated position using a riding model, but not refined. The least squares was run to minimize the function $\Sigma w (|F_o|-|F_c|)^2$. The weighting scheme was based on counting statistics and included a factor ($p = 0.030$) to downweight the intense reflections. Plots of $\Sigma w (|Fo| - |Fc|)^2$ versus $|Fo|$, reflection order in data collection, $\sin\theta/\lambda$ and various classes of indices showed no unusual trends. Neutral atom scattering factors were taken from Cromer and Waber.[7] Anomalous dispersion effects were included in Fcalc[8]; the values for $\Delta f'$ and $\Delta f''$ were those of Creagh and McAuley.[9] The values for the mass attenuation coefficients are those of Creagh and Hubbel.[10] All calculations were performed using the teXsan[11]

crystallographic software package of Molecular Structure Corporation, unless explicitly stated that SHELXS-97 (structure solution)[12] and SHELXL-97 (refinement)[13] were used.

$Cp^*_2Sr(2,2'\text{-bipyridine})$

EXPERIMENTAL DETAILS

A. Crystal Data

Empirical Formula	$C_{30}H_{38}N_2Sr$
Formula Weight	514.26
Crystal Color, Habit	red, plate
Crystal Dimensions	0.10 X 0.09 X 0.03 mm
Crystal System	orthorhombic
Lattice Type	Primitive
Lattice Parameters	a = 15.5489(9)Å
	b = 16.7821(9) Å
	c = 20.561(1) Å
	V = 5365.4(5) $Å^3$
Space Group	Pbca (#61)
Z value	8
D_{calc}	1.273 g/cm^3
F_{000}	2160.00
μ(MoKα)	20.26 cm^{-1}

B. Intensity Measurements

Diffractometer	Bruker APEX CCD
Radiation	MoKα (λ = 0.71069 Å) graphite monochromated
Detector Position	60.00 mm
Exposure Time	20.0 seconds per frame.
Scan Type	ω (0.3 degrees per frame)
$2\theta_{max}$	52.7^o
No. of Reflections Measured	
Total: 30804	Unique: 3262 (R_{int} = 0.034)
Corrections	Lorentz-polarization
Absorption	(Tmax = 1.00 Tmin = 0.82)

C. Structure Solution and Refinement

Structure Solution	Direct Methods (SIR97)
Refinement	Full-matrix least-squares
Function Minimized	Σ w (|Fo| - |Fc|)^2
Least Squares Weights	$1/\sigma^2(Fo) = 4Fo^2/\sigma^2(Fo^2)$
p-factor	0.0300
Anomalous Dispersion	All non-hydrogen atoms
No. Observations (I>3.00σ(I))	3494
No. Variables	298
Reflection/Parameter Ratio	11.72
Residuals: R; Rw; Rall	0.034 ; 0.039; 0.068
Goodness of Fit Indicator	1.57
Max Shift/Error in Final Cycle	0.00
Maximum peak in Final Diff. Map	0.53 $e^-/Å^3$
Minimum peak in Final Diff. Map	-0.30 $e^-/Å^3$

Table 1. Atomic coordinates and B_{iso}/B_{eq} and occupancy

atom	x	y	z	B_{eq}	occ
Sr1	0.88103(2)	0.21813(2)	0.12421(1)	1.801(6)	
N1	0.9677(2)	0.3503(2)	0.1051(1)	2.45(6)	
N2	0.8425(2)	0.3460(1)	0.1963(1)	2.11(6)	
C1	1.0006(3)	0.1935(2)	0.2267(2)	3.22(9)	
C2	0.9339(2)	0.1399(2)	0.2383(2)	3.15(9)	
C3	0.9370(2)	0.0800(2)	0.1897(2)	2.65(8)	
C4	1.0066(2)	0.0990(2)	0.1483(2)	2.65(8)	
C5	1.0460(2)	0.1682(2)	0.1715(2)	2.98(9)	
C6	0.8290(2)	0.1915(2)	-0.0059(2)	2.10(7)	
C7	0.7927(2)	0.2655(2)	0.0097(2)	1.89(7)	
C8	0.7266(2)	0.2531(2)	0.0561(2)	2.01(7)	
C9	0.7230(2)	0.1706(2)	0.0694(2)	2.10(7)	
C10	0.7861(2)	0.1323(2)	0.0310(2)	2.00(7)	
C11	1.0229(4)	0.2649(3)	0.2689(2)	6.7(1)	
C12	0.8676(4)	0.1433(3)	0.2921(2)	6.9(1)	
C13	0.8814(3)	0.0067(3)	0.1861(2)	5.0(1)	
C14	1.0366(3)	0.0512(3)	0.0904(2)	4.8(1)	
C15	1.1271(3)	0.2059(3)	0.1456(3)	5.9(1)	
C16	0.8986(2)	0.1763(2)	-0.0554(2)	3.07(9)	
C17	0.8158(2)	0.3448(2)	-0.0202(2)	3.05(9)	
C18	0.6675(2)	0.3164(2)	0.0822(2)	2.97(9)	
C19	0.6609(2)	0.1307(2)	0.1157(2)	3.11(9)	
C20	0.7986(2)	0.0439(2)	0.0234(2)	3.04(9)	
C21	1.0290(2)	0.3505(2)	0.0594(2)	3.08(9)	
C22	1.0872(3)	0.4116(3)	0.0512(2)	3.65(10)	
C23	1.0803(3)	0.4764(2)	0.0915(2)	3.8(1)	
C24	1.0177(2)	0.4781(2)	0.1389(2)	2.90(9)	
C25	0.9619(2)	0.4137(2)	0.1450(2)	2.10(7)	
C26	0.8938(2)	0.4108(2)	0.1962(2)	1.99(7)	
C27	0.8846(2)	0.4709(2)	0.2424(2)	2.59(8)	
C28	0.8216(2)	0.4643(2)	0.2889(2)	3.23(9)	
C29	0.7689(2)	0.3982(2)	0.2896(2)	3.16(9)	
C30	0.7819(2)	0.3412(2)	0.2421(2)	2.73(8)	
C101	0.9850	0.1362	0.1948	0.0038	0.000
C102	0.7716	0.2026	0.0320	0.0038	0.000
H1	0.9904	0.2628	0.3080	7.9961	
H2	1.0825	0.2640	0.2789	7.9961	
H3	1.0096	0.3126	0.2461	7.9961	
H4	0.8535	0.0907	0.3054	8.2403	

Table 1. Atomic coordinates and B_{iso}/B_{eq} and occupancy (continued)

atom	x	y	z	B_{eq}	occ
H5	0.8903	0.1720	0.3280	8.2403	
H6	0.8173	0.1692	0.2766	8.2403	
H7	0.8961	-0.0285	0.2205	5.9786	
H8	0.8227	0.0215	0.1899	5.9786	
H9	0.8904	-0.0193	0.1456	5.9786	
H10	1.0396	-0.0035	0.1019	5.7138	
H11	0.9971	0.0578	0.0556	5.7138	
H12	1.0919	0.0692	0.0773	5.7138	
H13	1.1757	0.1814	0.1653	7.0870	
H14	1.1270	0.2612	0.1555	7.0870	
H15	1.1297	0.1988	0.0998	7.0870	
H16	0.9326	0.1322	-0.0419	3.6850	
H17	0.8732	0.1649	-0.0963	3.6850	
H18	0.9340	0.2222	-0.0591	3.6850	
H19	0.8724	0.3422	-0.0375	3.6587	
H20	0.7764	0.3569	-0.0541	3.6587	
H21	0.8132	0.3852	0.0121	3.6587	
H22	0.6148	0.2926	0.0954	3.5604	
H23	0.6937	0.3418	0.1184	3.5604	
H24	0.6565	0.3546	0.0492	3.5604	
H25	0.6716	0.1488	0.1587	3.7342	
H26	0.6036	0.1436	0.1036	3.7342	
H27	0.6686	0.0746	0.1138	3.7342	
H28	0.7707	0.0170	0.0582	3.6470	
H29	0.8583	0.0319	0.0241	3.6470	
H30	0.7746	0.0270	-0.0168	3.6470	
H31	1.0326	0.3060	0.0310	3.6992	
H32	1.1306	0.4089	0.0188	4.3790	
H33	1.1186	0.5201	0.0867	4.5494	
H34	1.0127	0.5227	0.1671	3.4849	
H35	0.9215	0.5160	0.2417	3.1031	
H36	0.8143	0.5051	0.3205	3.8717	
H37	0.7252	0.3920	0.3215	3.7948	
H38	0.7454	0.2958	0.2420	3.2705	

$B_{eq} = 8/3\ \pi^2(U_{11}(aa^*)^2 + U_{22}(bb^*)^2 + U_{33}(cc^*)^2 + 2U_{12}(aa^*bb^*)\cos\gamma + 2U_{13}(aa^*cc^*)\cos\beta + 2U_{23}(bb^*cc^*)\cos\alpha)$

Table 2. Anisotropic Displacement Parameters

atom	U_{11}	U_{22}	U_{33}	U_{12}	U_{13}	U_{23}
Sr1	0.0253(1)	0.0195(1)	0.0236(1)	-0.0008(1)	-0.0028(1)	-0.0020(1)
N1	0.035(2)	0.029(2)	0.029(2)	-0.006(1)	0.003(1)	-0.002(1)
N2	0.027(1)	0.025(1)	0.028(2)	0.002(1)	0.001(1)	-0.001(1)
C1	0.053(3)	0.032(2)	0.037(2)	0.013(2)	-0.022(2)	-0.007(2)
C2	0.053(3)	0.044(2)	0.023(2)	0.024(2)	0.005(2)	0.007(2)
C3	0.036(2)	0.027(2)	0.038(2)	0.005(2)	-0.007(2)	0.006(2)
C4	0.037(2)	0.036(2)	0.028(2)	0.016(2)	-0.003(2)	-0.002(2)
C5	0.027(2)	0.038(2)	0.048(2)	0.004(2)	-0.010(2)	0.004(2)
C6	0.029(2)	0.030(2)	0.021(2)	0.000(1)	-0.002(1)	-0.004(1)
C7	0.030(2)	0.021(2)	0.021(2)	-0.001(1)	-0.003(1)	0.002(1)
C8	0.023(2)	0.026(2)	0.028(2)	0.004(1)	-0.004(2)	-0.001(1)
C9	0.027(2)	0.024(2)	0.029(2)	-0.006(1)	-0.002(1)	0.000(1)
C10	0.027(2)	0.020(2)	0.029(2)	-0.001(1)	-0.007(1)	-0.005(1)
C11	0.115(5)	0.061(3)	0.077(4)	0.033(3)	-0.066(3)	-0.032(3)
C12	0.115(4)	0.097(4)	0.049(3)	0.066(3)	0.038(3)	0.037(3)
C13	0.064(3)	0.043(3)	0.082(3)	-0.005(2)	-0.012(3)	0.024(2)
C14	0.063(3)	0.074(3)	0.044(3)	0.035(2)	-0.007(2)	-0.015(2)
C15	0.030(2)	0.081(4)	0.114(4)	0.002(2)	-0.011(2)	0.024(3)
C16	0.043(3)	0.040(2)	0.034(2)	-0.001(2)	0.003(2)	-0.006(2)
C17	0.048(2)	0.032(2)	0.036(2)	0.002(2)	0.000(2)	0.006(2)
C18	0.036(2)	0.034(2)	0.043(2)	0.008(2)	0.003(2)	-0.000(2)
C19	0.037(2)	0.037(2)	0.044(2)	-0.008(2)	0.005(2)	0.004(2)
C20	0.039(2)	0.031(2)	0.045(2)	-0.002(2)	-0.005(2)	-0.006(2)
C21	0.044(2)	0.040(2)	0.033(2)	-0.004(2)	0.009(2)	-0.006(2)
C22	0.046(2)	0.060(3)	0.033(2)	-0.017(2)	0.011(2)	0.001(2)
C23	0.053(3)	0.041(3)	0.050(3)	-0.022(2)	0.008(2)	0.001(2)
C24	0.043(2)	0.028(2)	0.040(2)	-0.007(2)	0.001(2)	-0.002(2)
C25	0.028(2)	0.023(2)	0.029(2)	-0.001(1)	-0.004(1)	0.002(1)
C26	0.026(2)	0.024(2)	0.025(2)	0.001(1)	-0.006(1)	0.002(1)
C27	0.034(2)	0.029(2)	0.036(2)	-0.002(2)	-0.006(2)	-0.006(1)
C28	0.041(2)	0.046(2)	0.035(2)	0.009(2)	-0.003(2)	-0.013(2)
C29	0.034(2)	0.052(2)	0.035(2)	0.008(2)	0.006(2)	-0.004(2)
C30	0.033(2)	0.033(2)	0.038(2)	-0.001(2)	0.005(2)	0.002(2)

The general temperature factor expression:
$\exp(-2\pi^2(a^{*2}U_{11}h^2 + b^{*2}U_{22}k^2 + c^{*2}U_{33}l^2 + 2a^*b^*U_{12}hk + 2a^*c^*U_{13}hl + 2b^*c^*U_{23}kl))$

$Cp^*_2Ba(2,2'\text{-bipyridine})$

EXPERIMENTAL DETAILS

A. Crystal Data

Empirical Formula	$H_{38}C_{30}BaN_2$
Formula Weight	563.97
Crystal Color, Habit	red, block
Crystal Dimensions	0.18 X 0.15 X 0.12 mm
Crystal System	orthorhombic
Lattice Type	Primitive
Lattice Parameters	a = 15.551(7)Å
	b = 17.022(7) Å
	c = 20.865(9) Å
	V = 5523(4) $Å^3$
Space Group	Pbca (#61)
Z value	8
D_{calc}	1.356 g/cm^3
F_{000}	2304.00
μ(MoKα)	14.56 cm^{-1}

B. Intensity Measurements

Diffractometer	Bruker SMART CCD
Radiation	MoKα (λ = 0.71069 Å) graphite monochromated
Detector Position	60.00 mm
Exposure Time	20.0 seconds per frame.
Scan Type	ω (0.3 degrees per frame)
$2\theta_{max}$	48.2^o
No. of Reflections Measured	
Total: 15800	Unique: 3218 (R_{int} = 0.022)
Corrections	Lorentz-polarization
Absorption	(Tmax = 1.00 Tmin = 0.85)

C. Structure Solution and Refinement

Structure Solution	Direct Methods (SIR97)
Refinement	Full-matrix least-squares
Function Minimized	Σ w (|Fo| - |Fc|)^2
Least Squares Weights	$1/\sigma^2(Fo) = 4Fo^2/\sigma^2(Fo^2)$
p-factor	0.0300
Anomalous Dispersion	All non-hydrogen atoms
No. Observations (I>3.00σ(I))	3307
No. Variables	298
Reflection/Parameter Ratio	11.10
Residuals: R; Rw; Rall	0.026 ; 0.036; 0.038
Goodness of Fit Indicator	1.69
Max Shift/Error in Final Cycle	0.00
Maximum peak in Final Diff. Map	0.99 $e^-/Å^3$
Minimum peak in Final Diff. Map	-0.37 $e^-/Å^3$

Table 1. Atomic coordinates and B_{iso}/B_{eq} and occupancy

atom	x	y	z	B_{eq}	occ
Ba(1)	0.86670(1)	0.28031(1)	0.12506(1)	2.581(6)	
N(1)	0.9559(2)	0.1384(2)	0.1115(1)	3.33(7)	
N(2)	0.8342(2)	0.1442(2)	0.2039(1)	3.04(7)	
C(1)	1.0017(2)	0.3091(2)	0.2244(2)	3.40(9)	
C(2)	1.0445(2)	0.3332(2)	0.1683(2)	3.38(9)	
C(3)	1.0038(2)	0.4017(2)	0.1461(2)	3.34(9)	
C(4)	0.9366(2)	0.4208(2)	0.1883(2)	3.20(9)	
C(5)	0.9350(2)	0.3625(2)	0.2370(2)	3.39(9)	
C(6)	0.7805(2)	0.2315(2)	0.0030(2)	2.69(8)	
C(7)	0.8178(2)	0.3045(2)	-0.0120(2)	2.70(8)	
C(8)	0.7723(2)	0.3636(2)	0.0220(2)	2.81(8)	
C(9)	0.7074(2)	0.3262(2)	0.0587(2)	2.65(8)	
C(10)	0.7121(2)	0.2445(2)	0.0466(2)	2.63(8)	
C(11)	1.0254(3)	0.2381(3)	0.2651(2)	5.4(1)	
C(12)	1.1233(3)	0.2933(3)	0.1396(3)	5.5(1)	
C(13)	1.0308(3)	0.4485(3)	0.0873(2)	5.4(1)	
C(14)	0.8791(3)	0.4912(3)	0.1846(2)	5.4(1)	
C(15)	0.8692(3)	0.3563(3)	0.2895(2)	5.9(1)	
C(16)	0.8069(3)	0.1534(2)	-0.0241(2)	3.83(9)	
C(17)	0.8903(3)	0.3186(2)	-0.0582(2)	4.02(10)	
C(18)	0.7879(3)	0.4508(2)	0.0164(2)	4.03(10)	
C(19)	0.6456(2)	0.3652(3)	0.1043(2)	4.1(1)	
C(20)	0.6543(2)	0.1816(2)	0.0744(2)	3.93(10)	
C(21)	1.0158(3)	0.1373(2)	0.0659(2)	4.26(10)	
C(22)	1.0742(3)	0.0782(3)	0.0572(2)	4.4(1)	
C(23)	1.0702(3)	0.0160(2)	0.0987(2)	4.22(10)	
C(24)	1.0096(2)	0.0150(2)	0.1471(2)	3.41(9)	
C(25)	0.9526(2)	0.0771(2)	0.1524(2)	2.47(7)	
C(26)	0.8861(2)	0.0809(2)	0.2040(2)	2.59(8)	
C(27)	0.8788(2)	0.0224(2)	0.2503(2)	3.50(9)	
C(28)	0.8178(3)	0.0298(2)	0.2979(2)	4.3(1)	
C(29)	0.7652(2)	0.0946(2)	0.2984(2)	4.3(1)	
C(30)	0.7753(2)	0.1491(2)	0.2507(2)	4.02(9)	
C(101)	0.9843	0.3654	0.1928	0.2000	0.000
C(102)	0.7580	0.2941	0.0237	0.2000	0.000
H(1)	1.0482	0.1980	0.2384	6.4930	
H(2)	1.0672	0.2530	0.2960	6.4930	
H(3)	0.9756	0.2191	0.2864	6.4930	
H(4)	1.1249	0.2399	0.1527	6.6188	

Table 1. Atomic coordinates and B_{iso}/B_{eq} and occupancy (continued)

atom	x	y	z	B_{eq}	occ
H(5)	1.1204	0.2958	0.0941	6.6188	
H(6)	1.1738	0.3193	0.1539	6.6188	
H(7)	1.0896	0.4385	0.0781	6.4810	
H(8)	0.9966	0.4333	0.0517	6.4810	
H(9)	1.0230	0.5030	0.0953	6.4810	
H(10)	0.8906	0.5250	0.2198	6.4226	
H(11)	0.8895	0.5184	0.1456	6.4226	
H(12)	0.8208	0.4747	0.1861	6.4226	
H(13)	0.8954	0.3356	0.3270	7.0380	
H(14)	0.8240	0.3226	0.2762	7.0380	
H(15)	0.8466	0.4070	0.2985	7.0380	
H(16)	0.8073	0.1152	0.0091	4.5914	
H(17)	0.8629	0.1575	-0.0421	4.5914	
H(18)	0.7673	0.1381	-0.0564	4.5914	
H(19)	0.9248	0.2726	-0.0611	4.8182	
H(20)	0.9245	0.3612	-0.0435	4.8182	
H(21)	0.8676	0.3308	-0.0993	4.8182	
H(22)	0.8474	0.4614	0.0219	4.8379	
H(23)	0.7560	0.4777	0.0484	4.8379	
H(24)	0.7701	0.4684	-0.0248	4.8379	
H(25)	0.6446	0.4202	0.0962	4.9118	
H(26)	0.6637	0.3561	0.1471	4.9118	
H(27)	0.5897	0.3441	0.0982	4.9118	
H(28)	0.6333	0.1983	0.1149	4.7194	
H(29)	0.6861	0.1343	0.0796	4.7194	
H(30)	0.6074	0.1726	0.0463	4.7194	
H(31)	1.0181	0.1807	0.0373	5.1176	
H(32)	1.1157	0.0802	0.0238	5.2463	
H(33)	1.1092	-0.0266	0.0941	5.0622	
H(34)	1.0071	-0.0277	0.1763	4.0889	
H(35)	0.9156	-0.0221	0.2492	4.1952	
H(36)	0.8122	-0.0095	0.3300	5.1458	
H(37)	0.7231	0.1015	0.3309	5.2151	
H(38)	0.7380	0.1933	0.2507	4.8287	

$B_{eq} = 8/3\ \pi^2(U_{11}(aa^*)^2 + U_{22}(bb^*)^2 + U_{33}(cc^*)^2 + 2U_{12}(aa^*bb^*)\cos\gamma + 2U_{13}(aa^*cc^*)\cos\beta + 2U_{23}(bb^*cc^*)\cos\alpha)$

Table 2. Anisotropic Displacement Parameters

atom	U_{11}	U_{22}	U_{33}	U_{12}	U_{13}	U_{23}
Ba(1)	0.0365(2)	0.0243(2)	0.0372(1)	0.00060(8)	-0.00962(8)	0.00257(9)
N(1)	0.047(2)	0.038(2)	0.042(2)	0.009(1)	0.004(1)	0.007(1)
N(2)	0.032(2)	0.032(2)	0.051(2)	0.001(1)	0.004(1)	0.001(1)
C(1)	0.052(2)	0.044(2)	0.033(2)	-0.010(2)	-0.015(2)	0.003(2)
C(2)	0.029(2)	0.053(2)	0.047(2)	-0.008(2)	-0.007(2)	-0.003(2)
C(3)	0.045(2)	0.047(2)	0.035(2)	-0.017(2)	-0.004(2)	0.006(2)
C(4)	0.049(2)	0.029(2)	0.044(2)	-0.008(2)	-0.004(2)	-0.003(2)
C(5)	0.050(2)	0.048(2)	0.031(2)	-0.016(2)	0.000(2)	-0.008(2)
C(6)	0.043(2)	0.028(2)	0.031(2)	0.002(2)	-0.005(1)	-0.001(1)
C(7)	0.035(2)	0.035(2)	0.033(2)	0.002(2)	0.002(1)	0.006(1)
C(8)	0.040(2)	0.029(2)	0.038(2)	-0.000(2)	-0.009(2)	0.009(2)
C(9)	0.031(2)	0.034(2)	0.036(2)	0.007(1)	-0.004(1)	0.004(1)
C(10)	0.032(2)	0.033(2)	0.036(2)	-0.003(1)	-0.005(2)	0.002(1)
C(11)	0.084(4)	0.064(3)	0.057(3)	-0.012(2)	-0.038(2)	0.010(2)
C(12)	0.036(3)	0.088(4)	0.086(4)	-0.001(2)	-0.003(2)	-0.005(3)
C(13)	0.076(3)	0.080(3)	0.049(3)	-0.038(3)	-0.006(2)	0.016(2)
C(14)	0.075(3)	0.047(3)	0.081(3)	0.004(2)	-0.008(2)	-0.016(2)
C(15)	0.104(4)	0.067(3)	0.051(3)	-0.032(3)	0.029(2)	-0.023(2)
C(16)	0.063(3)	0.037(2)	0.045(2)	0.003(2)	-0.003(2)	-0.010(2)
C(17)	0.051(2)	0.055(3)	0.047(2)	-0.001(2)	0.008(2)	0.010(2)
C(18)	0.054(3)	0.033(2)	0.067(3)	0.002(2)	-0.010(2)	0.011(2)
C(19)	0.045(2)	0.052(3)	0.059(3)	0.009(2)	0.005(2)	0.001(2)
C(20)	0.043(2)	0.050(3)	0.056(2)	-0.015(2)	-0.001(2)	0.005(2)
C(21)	0.065(3)	0.053(2)	0.044(2)	0.009(2)	0.011(2)	0.012(2)
C(22)	0.052(3)	0.070(3)	0.044(2)	0.013(2)	0.014(2)	0.002(2)
C(23)	0.057(3)	0.048(2)	0.055(2)	0.019(2)	0.007(2)	-0.002(2)
C(24)	0.050(2)	0.034(2)	0.045(2)	0.007(2)	0.002(2)	0.005(2)
C(25)	0.031(2)	0.027(2)	0.035(2)	-0.000(1)	-0.005(1)	0.001(1)
C(26)	0.033(2)	0.029(2)	0.036(2)	-0.005(1)	-0.005(1)	0.002(1)
C(27)	0.041(2)	0.042(2)	0.050(2)	0.002(2)	-0.002(2)	0.009(2)
C(28)	0.047(3)	0.064(3)	0.052(2)	-0.009(2)	0.000(2)	0.021(2)
C(29)	0.046(3)	0.066(3)	0.053(2)	-0.011(2)	0.012(2)	0.002(2)
C(30)	0.039(2)	0.045(2)	0.069(3)	0.001(2)	0.010(2)	-0.003(2)

The general temperature factor expression:
$\exp(-2\pi^2(a^{*2}U_{11}h^2 + b^{*2}U_{22}k^2 + c^{*2}U_{33}l^2 + 2a^*b^*U_{12}hk + 2a^*c^*U_{13}hl + 2b^*c^*U_{23}kl))$

$Cp^*_2CeN(SiMe_3)_2$

EXPERIMENTAL DETAILS

A. Crystal Data

Empirical Formula	$C_{26}H_{48}NCeSi_2$
Formula Weight	570.96
Crystal Color, Habit	red, block
Crystal Dimensions	0.30 X 0.19 X 0.15 mm
Crystal System	trigonal
Lattice Type	R-centered
Lattice Parameters	a = 17.813(1)Å
	c = 47.197(3) Å
	V = 12969(1) $Å^3$
Space Group	R-3 (#148)
Z value	18
D_{calc}	1.316 g/cm^3
F_{000}	5346.00
μ(MoKα)	16.75 cm^{-1}

B. Intensity Measurements

Diffractometer	Bruker APEX CCD
Radiation	MoKα (λ = 0.71069 Å) graphite monochromated
Detector Position	60.00 mm
Exposure Time	20.0 seconds per frame.
Scan Type	ω (0.3 degrees per frame)
$2\theta_{max}$	52.8^o
No. of Reflections Measured	
Total: 28159	Unique: 4290 (R_{int} = 0.046)
Corrections	Lorentz-polarization
Absorption	(Tmax = 1.00 Tmin = 0.84)

C. Structure Solution and Refinement

Structure Solution	Direct Methods (SIR97)
Refinement	Full-matrix least-squares
Function Minimized	Σ w (|Fo| - |Fc|)^2
Least Squares Weights	$1/\sigma^2(Fo) = 4Fo^2/\sigma^2(Fo^2)$
p-factor	0.0300
Anomalous Dispersion	All non-hydrogen atoms
No. Observations (I>3.00σ(I))	4492
No. Variables	271
Reflection/Parameter Ratio	16.58
Residuals: R; Rw; Rall	0.034 ; 0.041; 0.050
Goodness of Fit Indicator	1.38
Max Shift/Error in Final Cycle	0.00
Maximum peak in Final Diff. Map	1.85 $e^-/Å^3$
Minimum peak in Final Diff. Map	-0.36 $e^-/Å^3$

Table 1. Atomic coordinates and B_{iso}/B_{eq} and occupancy

atom	x	y	z	B_{eq}	occ
Ce(1)	0.62452(1)	-0.00473(1)	0.415693(4)	1.539(5)	
Si(1)	0.82191(8)	0.07509(8)	0.44884(3)	2.95(3)	
Si(2)	0.82095(8)	0.06158(7)	0.38355(3)	2.55(3)	
N(1)	0.7759(2)	0.0495(2)	0.41610(7)	2.02(7)	
C(1)	0.6517(3)	0.1647(3)	0.40645(9)	2.36(9)	
C(2)	0.5789(3)	0.1083(3)	0.38966(8)	2.06(9)	
C(3)	0.5085(2)	0.0571(3)	0.40814(9)	2.10(9)	
C(4)	0.5385(3)	0.0805(3)	0.43608(9)	2.6(1)	
C(5)	0.6268(3)	0.1468(3)	0.43499(9)	2.7(1)	
C(6)	0.6014(2)	-0.1717(2)	0.42391(8)	1.93(8)	
C(7)	0.5738(3)	-0.1736(2)	0.39582(9)	2.21(9)	
C(8)	0.4963(3)	-0.1712(2)	0.39663(9)	2.36(9)	
C(9)	0.4743(3)	-0.1689(2)	0.42504(9)	2.29(9)	
C(10)	0.5402(3)	-0.1678(2)	0.44203(8)	2.13(9)	
C(11)	0.7363(3)	0.2375(3)	0.3959(1)	4.4(1)	
C(12)	0.5705(3)	0.1115(3)	0.35797(10)	3.5(1)	
C(13)	0.4161(3)	-0.0002(3)	0.3987(1)	3.6(1)	
C(14)	0.4838(4)	0.0471(4)	0.4626(1)	4.4(1)	
C(15)	0.6786(4)	0.2019(4)	0.4600(1)	5.5(2)	
C(16)	0.6766(3)	-0.1823(3)	0.4332(1)	3.8(1)	
C(17)	0.6122(3)	-0.1915(3)	0.3701(1)	4.3(1)	
C(18)	0.4400(3)	-0.1825(3)	0.3710(1)	4.3(1)	
C(19)	0.3884(3)	-0.1838(3)	0.4361(1)	4.5(1)	
C(20)	0.5344(4)	-0.1781(3)	0.47380(10)	4.2(1)	
C(21)	0.7295(3)	0.0360(3)	0.47483(10)	3.9(1)	
C(22)	0.8963(3)	0.1937(3)	0.4544(1)	4.6(1)	
C(23)	0.8842(4)	0.0207(4)	0.4588(1)	6.4(2)	
C(24)	0.7320(3)	0.0373(3)	0.35731(9)	3.0(1)	
C(25)	0.8639(3)	-0.0135(3)	0.3763(1)	4.1(1)	
C(26)	0.9124(3)	0.1737(3)	0.3757(1)	4.0(1)	
C(101)	0.5809	0.1115	0.4151	0.2000	0.000
C(102)	0.5372	-0.1706	0.4167	0.2000	0.000
H(1)	0.7428	0.2290	0.3764	5.3330	
H(2)	0.7825	0.2388	0.4063	5.3330	
H(3)	0.7372	0.2909	0.3983	5.3330	
H(4)	0.6261	0.1475	0.3499	4.2529	
H(5)	0.5338	0.1344	0.3536	4.2529	
H(6)	0.5463	0.0547	0.3504	4.2529	
H(7)	0.3938	0.0348	0.3917	4.3078	

Table 1. Atomic coordinates and B_{iso}/B_{eq} and occupancy (continued)

atom	x	y	z	B_{eq}	occ
H(8)	0.4143	-0.0378	0.3841	4.3078	
H(9)	0.3821	-0.0335	0.4143	4.3078	
H(10)	0.4246	0.0117	0.4575	5.3125	
H(11)	0.4905	0.0946	0.4736	5.3125	
H(12)	0.5020	0.0139	0.4733	5.3125	
H(13)	0.7369	0.2395	0.4543	6.6461	
H(14)	0.6774	0.1654	0.4749	6.6461	
H(15)	0.6541	0.2355	0.4664	6.6461	
H(16)	0.7140	-0.1351	0.4450	4.5992	
H(17)	0.7077	-0.1834	0.4170	4.5992	
H(18)	0.6555	-0.2351	0.4433	4.5992	
H(19)	0.6726	-0.1684	0.3728	5.1649	
H(20)	0.5851	-0.2523	0.3672	5.1649	
H(21)	0.6030	-0.1652	0.3540	5.1649	
H(22)	0.4758	-0.1503	0.3555	5.1426	
H(23)	0.4078	-0.2421	0.3660	5.1426	
H(24)	0.4012	-0.1621	0.3753	5.1426	
H(25)	0.3496	-0.2442	0.4381	5.4024	
H(26)	0.3648	-0.1602	0.4232	5.4024	
H(27)	0.3968	-0.1563	0.4540	5.4024	
H(28)	0.5203	-0.1378	0.4818	5.0628	
H(29)	0.4907	-0.2354	0.4785	5.0628	
H(30)	0.5886	-0.1675	0.4811	5.0628	
H(31)	0.6987	-0.0255	0.4752	4.6400	
H(32)	0.6916	0.0563	0.4692	4.6400	
H(33)	0.7518	0.0576	0.4932	4.6400	
H(34)	0.8647	0.2234	0.4524	5.4842	
H(35)	0.9204	0.2032	0.4729	5.4842	
H(36)	0.9415	0.2148	0.4408	5.4842	
H(37)	0.9102	0.0409	0.4769	7.6532	
H(38)	0.9282	0.0338	0.4451	7.6532	
H(39)	0.8462	-0.0402	0.4595	7.6532	
H(40)	0.7079	0.0733	0.3611	3.6534	
H(41)	0.6880	-0.0218	0.3589	3.6534	
H(42)	0.7551	0.0481	0.3386	3.6534	
H(43)	0.8852	-0.0241	0.3934	4.8613	
H(44)	0.9096	0.0122	0.3629	4.8613	
H(45)	0.8187	-0.0668	0.3690	4.8613	
H(46)	0.9526	0.1932	0.3909	4.7639	

Table 1. Atomic coordinates and B_{iso}/B_{eq} and occupancy (continued)

atom	x	y	z	B_{eq}	occ
H(47)	0.9407	0.1727	0.3587	4.7639	
H(48)	0.8901	0.2119	0.3734	4.7639	

$B_{eq} = 8/3\ \pi^2(U_{11}(aa^*)^2 + U_{22}(bb^*)^2 + U_{33}(cc^*)^2 + 2U_{12}(aa^*bb^*)\cos\gamma + 2U_{13}(aa^*cc^*)\cos\beta + 2U_{23}(bb^*cc^*)\cos\alpha)$

Table 2. Anisotropic Displacement Parameters

atom	U_{11}	U_{22}	U_{33}	U_{12}	U_{13}	U_{23}
Ce(1)	0.0175(1)	0.0168(1)	0.0247(1)	0.00892(10)	-0.00063(9)	-0.00034(9)
Si(1)	0.0266(7)	0.0328(7)	0.0470(8)	0.0105(6)	-0.0141(6)	-0.0056(6)
Si(2)	0.0259(6)	0.0237(6)	0.0441(8)	0.0100(5)	0.0082(5)	-0.0027(5)
N(1)	0.021(2)	0.022(2)	0.032(2)	0.009(1)	-0.001(1)	-0.003(1)
C(1)	0.029(2)	0.020(2)	0.043(3)	0.014(2)	-0.003(2)	0.001(2)
C(2)	0.034(2)	0.025(2)	0.025(2)	0.019(2)	-0.003(2)	0.003(2)
C(3)	0.025(2)	0.029(2)	0.035(2)	0.020(2)	-0.002(2)	0.001(2)
C(4)	0.049(3)	0.039(3)	0.030(2)	0.035(2)	0.001(2)	-0.001(2)
C(5)	0.044(3)	0.032(2)	0.039(3)	0.029(2)	-0.019(2)	-0.020(2)
C(6)	0.020(2)	0.014(2)	0.037(2)	0.007(2)	-0.003(2)	-0.001(2)
C(7)	0.028(2)	0.016(2)	0.033(2)	0.005(2)	0.006(2)	-0.004(2)
C(8)	0.025(2)	0.019(2)	0.037(3)	0.006(2)	-0.008(2)	0.001(2)
C(9)	0.022(2)	0.019(2)	0.043(3)	0.008(2)	0.005(2)	0.000(2)
C(10)	0.036(2)	0.016(2)	0.021(2)	0.008(2)	-0.002(2)	-0.001(2)
C(11)	0.043(3)	0.021(2)	0.100(4)	0.012(2)	0.000(3)	0.008(3)
C(12)	0.055(3)	0.060(3)	0.035(3)	0.040(3)	-0.001(2)	0.007(2)
C(13)	0.031(3)	0.041(3)	0.068(4)	0.021(2)	-0.003(2)	0.007(2)
C(14)	0.072(4)	0.079(4)	0.040(3)	0.055(3)	0.019(3)	0.007(3)
C(15)	0.093(5)	0.071(4)	0.070(4)	0.059(4)	-0.045(3)	-0.046(3)
C(16)	0.034(3)	0.027(3)	0.088(4)	0.019(2)	-0.016(3)	-0.005(2)
C(17)	0.064(4)	0.024(2)	0.058(3)	0.009(2)	0.030(3)	-0.004(2)
C(18)	0.058(3)	0.036(3)	0.056(3)	0.014(3)	-0.031(3)	-0.003(2)
C(19)	0.035(3)	0.038(3)	0.095(4)	0.017(2)	0.028(3)	0.010(3)
C(20)	0.075(4)	0.031(3)	0.029(3)	0.008(3)	-0.000(2)	0.000(2)
C(21)	0.050(3)	0.040(3)	0.033(3)	0.004(2)	-0.010(2)	0.002(2)
C(22)	0.044(3)	0.048(3)	0.059(3)	0.006(3)	-0.009(3)	-0.021(3)
C(23)	0.063(4)	0.069(4)	0.118(5)	0.038(4)	-0.055(4)	-0.022(4)
C(24)	0.046(3)	0.030(2)	0.036(3)	0.016(2)	0.009(2)	-0.000(2)
C(25)	0.037(3)	0.040(3)	0.080(4)	0.021(2)	0.013(3)	-0.010(3)
C(26)	0.041(3)	0.034(3)	0.065(3)	0.010(2)	0.021(3)	-0.001(2)

The general temperature factor expression:
$\exp(-2\pi^2(a^{*2}U_{11}h^2 + b^{*2}U_{22}k^2 + c^{*2}U_{33}l^2 + 2a^*b^*U_{12}hk + 2a^*c^*U_{13}hl + 2b^*c^*U_{23}kl))$

Table 3. Bond Lengths(Å)

atom	atom	distance	atom	atom	distance
Ce(1)	N(1)	2.366(3)	Ce(1)	C(1)	2.841(4)
Ce(1)	C(2)	2.804(4)	Ce(1)	C(3)	2.809(4)
Ce(1)	C(4)	2.813(4)	Ce(1)	C(5)	2.830(4)
Ce(1)	C(6)	2.818(4)	Ce(1)	C(7)	2.833(4)
Ce(1)	C(8)	2.836(4)	Ce(1)	C(9)	2.842(4)
Ce(1)	C(21)	3.233(5)	Ce(1)	C(24)	3.222(4)
Ce(1)	C(10)	2.807(4)	Ce(1)	C(101)	2.5495(2)
Ce(1)	C(102)	2.5604(2)	Si(1)	N(1)	1.701(3)
Si(1)	C(21)	1.885(5)	Si(1)	C(22)	1.867(5)
Si(1)	C(23)	1.862(6)	Si(2)	N(1)	1.697(3)
Si(2)	C(24)	1.883(5)	Si(2)	C(25)	1.875(5)
Si(2)	C(26)	1.878(5)	C(1)	C(2)	1.420(6)
C(1)	C(5)	1.404(6)	C(1)	C(11)	1.499(6)
C(1)	C(101)	1.208(4)	C(2)	C(3)	1.422(5)
C(2)	C(12)	1.507(6)	C(2)	C(101)	1.202(4)
C(3)	C(4)	1.406(6)	C(3)	C(13)	1.506(6)
C(3)	C(101)	1.209(4)	C(4)	C(5)	1.419(6)
C(4)	C(14)	1.513(6)	C(4)	C(101)	1.200(4)
C(5)	C(15)	1.517(6)	C(5)	C(101)	1.196(4)
C(6)	C(7)	1.408(6)	C(6)	C(10)	1.414(5)
C(6)	C(16)	1.508(6)	C(6)	C(102)	1.202(4)
C(7)	C(8)	1.402(6)	C(7)	C(17)	1.504(6)
C(7)	C(102)	1.198(4)	C(8)	C(9)	1.403(6)
C(8)	C(18)	1.521(6)	C(8)	C(102)	1.192(4)
C(9)	C(10)	1.414(6)	C(9)	C(19)	1.510(6)
C(9)	C(102)	1.202(4)	C(10)	C(20)	1.508(6)
C(10)	C(102)	1.196(4)			

Cp^*_2Ce(1,2-phenylenediamine)

EXPERIMENTAL DETAILS

A. Crystal Data

Empirical Formula	$C_{27}N_2H_{37}Ce$
Formula Weight	529.72
Crystal Color, Habit	purple, block
Crystal Dimensions	0.08 X 0.07 X 0.07 mm
Crystal System	monoclinic
Lattice Type	C-centered
Lattice Parameters	a = 30.426(6)Å
	b = 10.914(2) Å
	c = 14.996(2) Å
	β = 96.837(4)^o
	V = 4944(1) Å^3
Space Group	C2/c (#15)
Z value	8
D_{calc}	1.423 g/cm^3
F_{000}	2168.00
μ(MoKα)	18.56 cm^{-1}

B. Intensity Measurements

Diffractometer	Bruker APEX CCD
Radiation	MoKα (λ = 0.71069 Å) graphite monochromated
Detector Position	600.00 mm
Exposure Time	10.0 seconds per frame.
Scan Type	ω (0.3 degrees per frame)
$2\theta_{max}$	52.7^o
No. of Reflections Measured	
Total: 13199	Unique: 3623 (R_{int} = 0.027)
Corrections	Lorentz-polarization
Absorption	(Tmax = 1.00 Tmin = 0.80)

C. Structure Solution and Refinement

Structure Solution	Direct Methods (SIR97)
Refinement	Full-matrix least-squares
Function Minimized	Σ w (|Fo| - |Fc|)^2
Least Squares Weights	$1/\sigma^2(Fo) = 4Fo^2/\sigma^2(Fo^2)$
p-factor	0.0300
Anomalous Dispersion	All non-hydrogen atoms
No. Observations (I>3.00σ(I))	3725
No. Variables	274
Reflection/Parameter Ratio	13.59
Residuals: R; Rw; Rall	0.031 ; 0.038; 0.046
Goodness of Fit Indicator	1.40
Max Shift/Error in Final Cycle	0.01
Maximum peak in Final Diff. Map	0.82 $e^-/Å^3$
Minimum peak in Final Diff. Map	-0.40 $e^-/Å^3$

Table 1. Atomic coordinates and B_{iso}/B_{eq} and occupancy

atom	x	y	z	B_{eq}	occ
Ce(1)	0.869685(7)	0.32143(2)	0.29925(2)	2.444(5)	
N(1)	0.9372(1)	0.1830(5)	0.2900(3)	4.0(1)	
N(2)	0.9099(1)	0.3656(4)	0.1723(3)	3.79(10)	
C(1)	0.7869(1)	0.2611(4)	0.2149(3)	2.92(9)	
C(2)	0.7820(1)	0.2484(4)	0.3059(3)	3.3(1)	
C(3)	0.8074(2)	0.1482(4)	0.3400(3)	3.8(1)	
C(4)	0.8275(1)	0.0959(4)	0.2684(4)	4.0(1)	
C(5)	0.8142(1)	0.1667(4)	0.1895(3)	3.4(1)	
C(6)	0.8995(2)	0.5530(4)	0.3557(3)	3.5(1)	
C(7)	0.8604(2)	0.5360(4)	0.3967(3)	3.8(1)	
C(8)	0.8683(1)	0.4455(4)	0.4624(3)	3.3(1)	
C(9)	0.9124(1)	0.4031(4)	0.4621(3)	2.82(9)	
C(10)	0.9318(1)	0.4707(4)	0.3972(3)	2.93(9)	
C(11)	0.7646(2)	0.3585(5)	0.1546(4)	4.7(1)	
C(12)	0.7502(2)	0.3197(6)	0.3569(4)	6.1(2)	
C(13)	0.8120(2)	0.0963(6)	0.4334(4)	6.9(2)	
C(14)	0.8544(2)	-0.0204(5)	0.2727(5)	6.9(2)	
C(15)	0.8232(2)	0.1416(6)	0.0956(4)	6.0(2)	
C(16)	0.9076(2)	0.6469(4)	0.2861(4)	5.9(2)	
C(17)	0.8193(2)	0.6138(6)	0.3783(5)	6.7(2)	
C(18)	0.8382(2)	0.4071(6)	0.5312(4)	5.6(1)	
C(19)	0.9345(2)	0.3043(4)	0.5209(3)	4.4(1)	
C(20)	0.9788(2)	0.4629(5)	0.3766(3)	4.6(1)	
C(21)	0.9401(1)	0.1643(4)	0.1956(3)	3.05(10)	
C(22)	0.9544(1)	0.0531(4)	0.1637(3)	4.1(1)	
C(23)	0.9571(2)	0.0379(5)	0.0722(4)	4.9(1)	
C(24)	0.9459(2)	0.1336(6)	0.0145(4)	4.8(1)	
C(25)	0.9310(2)	0.2434(5)	0.0457(3)	4.2(1)	
C(26)	0.9267(1)	0.2602(4)	0.1367(3)	3.3(1)	
C(101)	0.8036	0.1840	0.2638	0.2000	0.000
C(102)	0.8945	0.4817	0.4148	0.2000	0.000
H(1)	0.7735	0.4370	0.1774	5.6832	
H(2)	0.7728	0.3493	0.0959	5.6832	
H(3)	0.7334	0.3505	0.1527	5.6832	
H(4)	0.7659	0.3542	0.4095	7.3678	
H(5)	0.7371	0.3841	0.3197	7.3678	
H(6)	0.7277	0.2669	0.3729	7.3678	
H(7)	0.7957	0.1461	0.4701	8.3011	
H(8)	0.8005	0.0154	0.4317	8.3011	

Table 1. Atomic coordinates and B_{iso}/B_{eq} and occupancy (continued)

atom	x	y	z	B_{eq}	occ
H(9)	0.8422	0.0954	0.4574	8.3011	
H(10)	0.8368	-0.0871	0.2885	8.1416	
H(11)	0.8641	-0.0357	0.2158	8.1416	
H(12)	0.8794	-0.0118	0.3167	8.1416	
H(13)	0.8426	0.0732	0.0952	7.1490	
H(14)	0.7962	0.1237	0.0593	7.1490	
H(15)	0.8366	0.2113	0.0724	7.1490	
H(16)	0.9300	0.7021	0.3107	7.0991	
H(17)	0.9171	0.6067	0.2354	7.0991	
H(18)	0.8811	0.6905	0.2683	7.0991	
H(19)	0.8264	0.6966	0.3935	8.0875	
H(20)	0.8084	0.6088	0.3163	8.0875	
H(21)	0.7974	0.5851	0.4132	8.0875	
H(22)	0.8512	0.4301	0.5897	6.6604	
H(23)	0.8103	0.4467	0.5184	6.6604	
H(24)	0.8341	0.3209	0.5290	6.6604	
H(25)	0.9144	0.2734	0.5591	5.3054	
H(26)	0.9435	0.2399	0.4845	5.3054	
H(27)	0.9598	0.3372	0.5563	5.3054	
H(28)	0.9939	0.4009	0.4129	5.5247	
H(29)	0.9791	0.4427	0.3150	5.5247	
H(30)	0.9931	0.5392	0.3890	5.5247	
H(31)	0.9624	-0.0123	0.2044	4.9028	
H(32)	0.9667	-0.0379	0.0500	5.8207	
H(33)	0.9483	0.1241	-0.0477	5.7958	
H(34)	0.9235	0.3085	0.0046	4.9916	
H(35)	0.954(2)	0.217(4)	0.314(3)	3(1)	
H(36)	0.951(2)	0.109(7)	0.322(5)	10(1)	
H(37)	0.904(2)	0.407(4)	0.133(3)	3(1)	

$B_{eq} = 8/3\ \pi^2(U_{11}(aa^*)^2 + U_{22}(bb^*)^2 + U_{33}(cc^*)^2 + 2U_{12}(aa^*bb^*)\cos\gamma + 2U_{13}(aa^*cc^*)\cos\beta + 2U_{23}(bb^*cc^*)\cos\alpha)$

Table 2. Anisotropic Displacement Parameters

atom	U_{11}	U_{22}	U_{33}	U_{12}	U_{13}	U_{23}
Ce(1)	0.0266(1)	0.0348(1)	0.0319(1)	-0.0025(1)	0.00549(9)	-0.0039(1)
N(1)	0.040(2)	0.057(3)	0.054(3)	0.005(2)	0.003(2)	-0.010(2)
N(2)	0.046(2)	0.041(2)	0.058(3)	0.006(2)	0.011(2)	0.001(2)
C(1)	0.024(2)	0.044(2)	0.041(2)	-0.005(2)	-0.001(2)	0.003(2)
C(2)	0.029(2)	0.056(3)	0.042(3)	-0.013(2)	0.008(2)	-0.004(2)
C(3)	0.043(3)	0.054(3)	0.046(3)	-0.018(2)	0.005(2)	0.012(2)
C(4)	0.036(3)	0.027(2)	0.086(4)	-0.009(2)	-0.012(2)	-0.001(2)
C(5)	0.035(2)	0.050(3)	0.045(3)	-0.019(2)	0.005(2)	-0.014(2)
C(6)	0.067(3)	0.030(2)	0.036(2)	-0.002(2)	0.008(2)	-0.005(2)
C(7)	0.050(3)	0.040(2)	0.054(3)	0.013(2)	0.004(2)	-0.012(2)
C(8)	0.042(3)	0.048(3)	0.038(2)	-0.005(2)	0.010(2)	-0.016(2)
C(9)	0.041(2)	0.036(2)	0.029(2)	-0.003(2)	-0.000(2)	-0.008(2)
C(10)	0.036(2)	0.038(2)	0.037(2)	-0.010(2)	0.008(2)	-0.013(2)
C(11)	0.045(3)	0.064(3)	0.068(4)	-0.002(2)	-0.005(3)	0.022(3)
C(12)	0.036(3)	0.134(6)	0.064(4)	-0.011(3)	0.019(2)	-0.022(3)
C(13)	0.085(4)	0.105(5)	0.067(4)	-0.044(4)	-0.015(3)	0.039(4)
C(14)	0.060(3)	0.038(3)	0.160(7)	-0.007(3)	0.004(4)	0.003(3)
C(15)	0.058(4)	0.109(5)	0.061(4)	-0.031(3)	0.012(3)	-0.044(3)
C(16)	0.132(6)	0.038(3)	0.052(3)	-0.011(3)	0.006(3)	0.001(2)
C(17)	0.081(4)	0.075(4)	0.098(5)	0.041(4)	0.005(4)	-0.016(4)
C(18)	0.063(4)	0.101(4)	0.053(3)	-0.023(3)	0.026(3)	-0.027(3)
C(19)	0.072(4)	0.049(3)	0.044(3)	-0.007(2)	-0.008(3)	0.003(2)
C(20)	0.042(3)	0.075(3)	0.057(3)	-0.021(3)	0.005(2)	-0.018(3)
C(21)	0.030(2)	0.038(2)	0.048(3)	0.000(2)	0.007(2)	-0.008(2)
C(22)	0.040(3)	0.046(3)	0.070(3)	0.000(2)	0.011(2)	-0.013(2)
C(23)	0.051(3)	0.057(3)	0.081(4)	-0.004(3)	0.020(3)	-0.037(3)
C(24)	0.060(3)	0.080(4)	0.047(3)	-0.008(3)	0.017(3)	-0.019(3)
C(25)	0.047(3)	0.065(3)	0.049(3)	-0.005(2)	0.018(2)	-0.001(3)
C(26)	0.030(2)	0.045(3)	0.051(3)	-0.008(2)	0.009(2)	-0.005(2)

The general temperature factor expression:
$\exp(-2\pi^2(a^{*2}U_{11}h^2 + b^{*2}U_{22}k^2 + c^{*2}U_{33}l^2 + 2a^*b^*U_{12}hk + 2a^*c^*U_{13}hl + 2b^*c^*U_{23}kl))$

$[NMe_4][Cp^*_2CeOTf_2]\cdot$(toluene)

EXPERIMENTAL DETAILS

A. Crystal Data

Empirical Formula	$CeNS_2F_6O_6C_{26}H_{42}$
Formula Weight	782.85
Crystal Color, Habit	yellow, small block
Crystal Dimensions	0.20 X 0.20 X 0.20 mm
Crystal System	monoclinic
Lattice Type	C-centered
Lattice Parameters	a = 33.538(5)Å
	b = 11.003(2) Å
	c = 21.191(3) Å
	β = 95.075(3)^o
	V = 7789(2) Å^3
Space Group	C2/c (#15)
Z value	8
D_{calc}	1.335 g/cm^3
F_{000}	3176.00
μ(MoKα)	13.36 cm^{-1}

B. Intensity Measurements

Diffractometer	Bruker APEX CCD
Radiation	MoKα (λ = 0.71069 Å)
	graphite monochromated
Detector Position	60.00 mm
Exposure Time	10.0 seconds per frame.
Scan Type	ω (0.3 degrees per frame)
$2\theta_{max}$	48.8^o
No. of Reflections Measured	Total: 18621
	Unique: 6746 (R_{int} = 0.036)
Corrections	Lorentz-polarization
Absorption	(Tmax = 1.00 Tmin = 0.82)

C. Structure Solution and Refinement

Structure Solution	Direct Methods (SIR92)
Refinement	Full-matrix least-squares
Function Minimized	Σ w (|Fo| - |Fc|)^2
Least Squares Weights	$1/\sigma^2(Fo) = 4Fo^2/\sigma^2(Fo^2)$
p-factor	0.0300
Anomalous Dispersion	All non-hydrogen atoms
No. Observations (I>3.00σ(I))	4789
No. Variables	434
Reflection/Parameter Ratio	11.03
Residuals: R; Rw; Rall	0.043 ; 0.053; 0.062
Goodness of Fit Indicator	1.83
Max Shift/Error in Final Cycle	0.01
Maximum peak in Final Diff. Map	0.82 $e^-/Å^3$
Minimum peak in Final Diff. Map	-0.67 $e^-/Å^3$

Table 1. Atomic coordinates and B_{iso}/B_{eq} and occupancy

atom	x	y	z	B_{eq}	occ
Ce(1)	0.118183(9)	0.48016(3)	0.63032(2)	2.725(8)	
S(1)	0.19240(5)	0.5219(2)	0.50706(8)	3.92(4)	
S(2)	0.17457(8)	0.1902(3)	0.6820(1)	3.83(6)	0.598
S(3)	0.1772(1)	0.2516(5)	0.6818(2)	4.6(1)	0.402
F(1)	0.2215(1)	0.6640(4)	0.4241(2)	7.2(1)	
F(2)	0.1589(1)	0.6869(4)	0.4317(2)	7.2(1)	
F(3)	0.2008(1)	0.7576(4)	0.5023(2)	6.8(1)	
F(4)	0.1571(2)	0.0732(9)	0.5774(4)	5.9(2)	0.598
F(5)	0.2078(2)	0.1940(7)	0.5759(4)	7.2(2)	0.598
F(6)	0.2111(3)	0.0256(8)	0.6273(4)	7.1(2)	0.598
F(7)	0.1659(5)	0.025(1)	0.6675(9)	10.7(4)	0.402
F(8)	0.2176(5)	0.094(1)	0.6121(7)	8.2(3)	0.402
F(9)	0.1541(5)	0.122(2)	0.5773(8)	8.7(5)	0.402
O(1)	0.1593(1)	0.5411(4)	0.5464(2)	3.83(10)	
O(2)	0.2304(1)	0.5165(5)	0.5416(3)	6.1(1)	
O(3)	0.1839(2)	0.4341(5)	0.4588(3)	6.4(1)	
O(4)	0.1522(2)	0.2974(7)	0.6560(4)	4.6(2)	0.598
O(5)	0.1491(2)	0.1033(7)	0.7093(4)	5.1(2)	0.598
O(6)	0.2137(3)	0.2181(7)	0.7151(4)	4.7(2)	0.598
O(7)	0.1875(3)	0.3469(10)	0.6387(5)	4.9(2)	0.402
O(8)	0.1366(3)	0.2708(9)	0.6931(5)	4.3(2)	0.402
O(9)	0.2038(4)	0.224(1)	0.7359(6)	4.1(3)	0.402
N(1)	0.1822(1)	0.1024(5)	0.3639(3)	4.0(1)	
C(1)	0.1227(2)	0.7093(5)	0.6836(3)	4.2(2)	
C(2)	0.1627(2)	0.6681(6)	0.6917(3)	4.1(2)	
C(3)	0.1645(2)	0.5745(6)	0.7357(3)	4.1(2)	
C(4)	0.1259(2)	0.5573(6)	0.7557(3)	4.3(2)	
C(5)	0.1005(2)	0.6410(6)	0.7241(3)	4.3(2)	
C(6)	0.0396(2)	0.5138(5)	0.5778(3)	3.2(1)	
C(7)	0.0380(2)	0.4086(6)	0.6156(3)	3.6(1)	
C(8)	0.0587(2)	0.3143(5)	0.5879(3)	3.3(1)	
C(9)	0.0737(2)	0.3619(5)	0.5325(3)	3.1(1)	
C(10)	0.0620(2)	0.4834(6)	0.5272(3)	3.4(1)	
C(11)	0.1079(3)	0.8152(7)	0.6438(5)	8.8(3)	
C(12)	0.1982(3)	0.7185(8)	0.6621(4)	7.5(3)	
C(13)	0.2013(3)	0.5095(7)	0.7639(6)	8.6(3)	
C(14)	0.1147(3)	0.4687(9)	0.8063(4)	9.1(3)	
C(15)	0.0583(2)	0.6705(9)	0.7404(5)	8.4(3)	
C(16)	0.0164(2)	0.6309(6)	0.5825(4)	4.9(2)	

Table 1. Atomic coordinates and B_{iso}/B_{eq} and occupancy (continued)

atom	x	y	z	B_{eq}	occ
C(17)	0.0142(2)	0.3918(7)	0.6722(3)	4.8(2)	
C(18)	0.0603(2)	0.1844(6)	0.6105(3)	4.8(2)	
C(19)	0.0957(2)	0.2915(6)	0.4861(3)	4.6(2)	
C(20)	0.0690(2)	0.5672(7)	0.4724(3)	5.0(2)	
C(21)	0.1933(2)	0.6652(7)	0.4642(3)	4.9(2)	
C(22)	0.1899(4)	0.115(1)	0.6110(7)	4.2(3)	0.598
C(23)	0.1791(6)	0.123(2)	0.636(1)	5.4(5)	0.402
C(24)	0.1815(4)	0.116(2)	0.4300(7)	20.1(7)	
C(25)	0.2161(3)	0.161(2)	0.346(1)	25.8(9)	
C(26)	0.1856(4)	-0.021(1)	0.356(1)	17.8(7)	
C(27)	0.1449(2)	0.1532(10)	0.3334(5)	8.6(3)	
C(28)	0.0593(4)	-0.065(1)	0.4142(6)	10.0(4)	
C(29)	0.0753(3)	-0.1368(7)	0.3751(5)	6.4(2)	
C(30)	0.0715(3)	-0.1183(9)	0.3099(6)	8.7(3)	
C(31)	0.0509(3)	-0.029(1)	0.2826(5)	8.9(3)	
C(32)	0.0314(3)	0.050(1)	0.3318(10)	10.5(4)	
C(33)	0.0341(4)	0.037(1)	0.3906(9)	11.1(5)	
C(34)	0.0606(5)	-0.067(1)	0.4790(7)	14.6(6)	
C(100)	0.1353	0.6299	0.7182	0.2000	0.000
C(101)	0.0544	0.4164	0.5682	0.2000	0.000
H(1)	0.1213	0.8867	0.6583	10.6273	
H(2)	0.1136	0.8007	0.6005	10.6273	
H(3)	0.0800	0.8236	0.6450	10.6273	
H(4)	0.2103	0.6563	0.6394	9.0678	
H(5)	0.1895	0.7821	0.6332	9.0678	
H(6)	0.2169	0.7506	0.6938	9.0678	
H(7)	0.1982	0.4258	0.7584	10.4576	
H(8)	0.2236	0.5379	0.7428	10.4576	
H(9)	0.2056	0.5295	0.8076	10.4576	
H(10)	0.1059	0.5139	0.8411	10.7788	
H(11)	0.0936	0.4179	0.7894	10.7788	
H(12)	0.1372	0.4215	0.8205	10.7788	
H(13)	0.0593	0.7028	0.7820	10.0488	
H(14)	0.0474	0.7319	0.7112	10.0488	
H(15)	0.0422	0.6012	0.7366	10.0488	
H(16)	0.0342	0.6982	0.5819	5.9130	
H(17)	-0.0032	0.6371	0.5470	5.9130	
H(18)	0.0035	0.6318	0.6204	5.9130	
H(19)	0.0026	0.4672	0.6825	5.7314	

Table 1. Atomic coordinates and B_{iso}/B_{eq} and occupancy (continued)

atom	x	y	z	B_{eq}	occ
H(20)	-0.0066	0.3341	0.6620	5.7314	
H(21)	0.0312	0.3632	0.7070	5.7314	
H(22)	0.0339	0.1525	0.6079	5.7390	
H(23)	0.0762	0.1380	0.5845	5.7390	
H(24)	0.0716	0.1817	0.6531	5.7390	
H(25)	0.0998	0.2105	0.5014	5.4587	
H(26)	0.0800	0.2891	0.4465	5.4587	
H(27)	0.1205	0.3287	0.4814	5.4587	
H(28)	0.0826	0.6382	0.4883	5.8958	
H(29)	0.0849	0.5267	0.4439	5.8958	
H(30)	0.0441	0.5894	0.4509	5.8958	
H(31)	0.2059	0.0843	0.4500	24.8321	
H(32)	0.1794	0.1993	0.4396	24.8321	
H(33)	0.1597	0.0723	0.4434	24.8321	
H(34)	0.2394	0.1217	0.3667	32.4964	
H(35)	0.2171	0.1502	0.3010	32.4964	
H(36)	0.2158	0.2424	0.3562	32.4964	
H(37)	0.1632	-0.0603	0.3730	20.9278	
H(38)	0.1859	-0.0407	0.3132	20.9278	
H(39)	0.2094	-0.0493	0.3795	20.9278	
H(40)	0.1433	0.2366	0.3434	10.1176	
H(41)	0.1448	0.1437	0.2886	10.1176	
H(42)	0.1228	0.1108	0.3477	10.1176	
H(43)	0.0900	-0.2046	0.3913	7.6488	
H(44)	0.0851	-0.1739	0.2843	10.6134	
H(45)	0.0480	-0.0155	0.2382	10.7417	
H(46)	0.0156	0.1161	0.3139	11.9365	
H(47)	0.0208	0.0908	0.4173	11.8937	
H(48)	0.0346	-0.0770	0.4912	17.8306	
H(49)	0.0771	-0.1335	0.4937	17.8306	
H(50)	0.0720	0.0066	0.4947	17.8306	

$B_{eq} = 8/3\ \pi^2(U_{11}(aa^*)^2 + U_{22}(bb^*)^2 + U_{33}(cc^*)^2 + 2U_{12}(aa^*bb^*)\cos\gamma + 2U_{13}(aa^*cc^*)\cos\beta + 2U_{23}(bb^*cc^*)\cos\alpha)$

Table 2. Anisotropic Displacement Parameters

atom	U_{11}	U_{22}	U_{33}	U_{12}	U_{13}	U_{23}
Ce(1)	0.0292(2)	0.0412(2)	0.0326(2)	-0.0056(1)	-0.0003(1)	-0.0019(2)
S(1)	0.0395(9)	0.0628(10)	0.0474(10)	-0.0007(7)	0.0078(7)	0.0067(8)
F(1)	0.079(3)	0.134(4)	0.064(3)	-0.028(3)	0.025(2)	0.021(3)
F(2)	0.067(3)	0.115(4)	0.085(3)	-0.017(2)	-0.020(3)	0.050(3)
F(3)	0.109(4)	0.073(3)	0.075(3)	-0.030(3)	0.007(3)	0.005(2)
O(1)	0.034(2)	0.065(3)	0.046(3)	-0.005(2)	0.003(2)	0.008(2)
O(2)	0.038(3)	0.111(4)	0.084(4)	0.010(2)	-0.000(3)	0.036(3)
O(3)	0.094(4)	0.077(3)	0.075(4)	-0.013(3)	0.032(3)	-0.018(3)
N(1)	0.036(3)	0.062(4)	0.054(4)	0.001(2)	-0.001(3)	0.021(3)
C(1)	0.066(5)	0.037(4)	0.053(4)	-0.005(3)	-0.019(4)	-0.005(3)
C(2)	0.045(4)	0.063(4)	0.047(4)	-0.018(3)	0.009(3)	-0.023(3)
C(3)	0.043(4)	0.058(4)	0.052(4)	0.002(3)	-0.016(3)	-0.013(3)
C(4)	0.067(5)	0.066(4)	0.030(4)	-0.021(4)	0.000(3)	-0.005(3)
C(5)	0.043(4)	0.062(4)	0.055(5)	-0.010(3)	-0.002(3)	-0.019(3)
C(6)	0.022(3)	0.052(4)	0.046(4)	-0.006(2)	-0.007(2)	0.001(3)
C(7)	0.026(3)	0.068(4)	0.041(4)	-0.010(3)	-0.003(3)	0.001(3)
C(8)	0.033(3)	0.048(4)	0.041(4)	-0.011(3)	-0.005(3)	-0.004(3)
C(9)	0.029(3)	0.057(4)	0.031(3)	-0.008(3)	-0.003(3)	-0.004(3)
C(10)	0.034(3)	0.060(4)	0.033(3)	-0.009(3)	-0.007(3)	0.010(3)
C(11)	0.148(9)	0.054(5)	0.119(8)	-0.019(5)	-0.062(7)	0.011(5)
C(12)	0.098(6)	0.119(7)	0.073(6)	-0.071(5)	0.027(5)	-0.035(5)
C(13)	0.071(6)	0.082(6)	0.16(1)	0.009(4)	-0.062(6)	-0.038(6)
C(14)	0.163(10)	0.133(8)	0.049(5)	-0.067(7)	-0.003(6)	0.016(5)
C(15)	0.045(5)	0.147(8)	0.126(8)	-0.004(5)	0.012(5)	-0.085(7)
C(16)	0.039(4)	0.066(5)	0.077(5)	0.004(3)	-0.011(3)	-0.001(4)
C(17)	0.043(4)	0.093(5)	0.050(4)	-0.016(3)	0.013(3)	-0.001(4)
C(18)	0.057(4)	0.060(4)	0.064(5)	-0.020(3)	-0.002(4)	0.001(4)
C(19)	0.048(4)	0.081(5)	0.046(4)	-0.006(3)	0.001(3)	-0.014(3)
C(20)	0.046(4)	0.082(5)	0.061(5)	-0.008(3)	-0.012(3)	0.024(4)
C(21)	0.044(4)	0.088(6)	0.052(5)	-0.019(4)	-0.005(4)	0.007(4)
C(24)	0.15(1)	0.45(3)	0.14(1)	0.21(2)	-0.09(1)	-0.15(2)
C(25)	0.040(6)	0.45(3)	0.49(3)	0.001(10)	0.03(1)	0.38(3)
C(26)	0.12(1)	0.13(1)	0.40(3)	0.054(8)	-0.12(1)	-0.12(1)
C(27)	0.055(5)	0.165(9)	0.103(7)	0.020(5)	-0.008(5)	0.078(7)
C(28)	0.17(1)	0.124(9)	0.090(8)	-0.084(9)	0.039(8)	-0.024(7)
C(29)	0.097(7)	0.069(5)	0.074(7)	-0.019(4)	0.004(5)	-0.008(5)
C(30)	0.100(8)	0.097(7)	0.13(1)	-0.009(6)	-0.002(7)	0.007(7)
C(31)	0.086(7)	0.145(10)	0.104(9)	0.009(7)	-0.007(6)	0.036(7)
C(32)	0.059(6)	0.069(7)	0.27(2)	-0.000(5)	0.002(10)	0.01(1)

Table 2. Anisotropic Displacement Parameters (continued)

atom	U_{11}	U_{22}	U_{33}	U_{12}	U_{13}	U_{23}
C(33)	0.084(8)	0.094(9)	0.24(2)	-0.032(6)	-0.02(1)	0.08(1)
C(34)	0.25(2)	0.20(1)	0.10(1)	-0.11(1)	0.02(1)	-0.03(1)

The general temperature factor expression:
$\exp(-2\pi^2(a^{*2}U_{11}h^2 + b^{*2}U_{22}k^2 + c^{*2}U_{33}l^2 + 2a^*b^*U_{12}hk + 2a^*c^*U_{13}hl + 2b^*c^*U_{23}kl))$

$[NEt_4][Cp^*_2CeOTf_2]\cdot 1/4(toluene)$

EXPERIMENTAL DETAILS

A. Crystal Data

Empirical Formula	$Ce_2N_2S_4F_{12}O_{12}C_{67.50}H_{104}$
Formula Weight	1772.03
Crystal Color, Habit	yellow, plate
Crystal Dimensions	0.20 X 0.20 X 0.20 mm
Crystal System	triclinic
Lattice Type	Primitive
Lattice Parameters	a = 13.9637(9)Å
	b = 16.668(1) Å
	c = 18.789(1) Å
	α = 110.877(1)^o
	β = 107.690(1)^o
	γ = 90.310(1)^o
V = 3861.0(4) Å^3	
Space Group	P-1 (#2)
Z value 4	
D_{calc} 3.048 g/cm^3	
F_{000} 3628.00	
μ(MoKα) 27.15 cm^{-1}	

B. Intensity Measurements

Diffractometer	Bruker APEX CCD
Radiation	MoKα (λ = 0.71069 Å) graphite monochromated
Detector Position	60.00 mm
Exposure Time	20.0 seconds per frame.
Scan Type	ω (0.3 degrees per frame)
$2\theta_{max}$	50.8^o
No. of Reflections Measured (R_{int} = 0.027)	Total: 23333 Unique: 8331
Corrections	Lorentz-polarization

Absorption (Tmax = 1.00 Tmin = 0.80)

C. Structure Solution and Refinement

Structure Solution	Direct Methods (SIR97)
Refinement	Full-matrix least-squares
Function Minimized	Σ w (|Fo| - |Fc|)^2
Least Squares Weights	$1/\sigma^2(Fo) = 4Fo^2/\sigma^2(Fo^2)$
p-factor	0.0300
Anomalous Dispersion	All non-hydrogen atoms
No. Observations (I>3.00σ(I))	8490
No. Variables	849
Reflection/Parameter Ratio	10.00
Residuals: R; Rw; Rall	0.041 ; 0.040; 0.087
Goodness of Fit Indicator	1.34
Max Shift/Error in Final Cycle	0.01
Maximum peak in Final Diff. Map	1.00 $e^-/Å^3$
Minimum peak in Final Diff. Map	-0.54 $e^-/Å^3$

Table 1. Atomic coordinates and B_{iso}/B_{eq} and occupancy

atom	x	y	z	B_{eq}	occ
Ce(1)	0.49569(3)	0.01563(2)	0.26166(2)	1.843(9)	
Ce(2)	-0.12014(3)	-0.36346(2)	0.31646(2)	2.440(10)	
S(1)	0.2847(1)	0.0895(1)	0.1332(1)	2.78(4)	
S(2)	0.3807(1)	-0.1760(1)	0.14963(10)	2.67(4)	
S(3)	0.0401(1)	-0.5468(1)	0.2514(1)	3.63(5)	
S(4)	-0.1112(1)	-0.2736(1)	0.1546(1)	3.44(5)	
F(1)	0.3624(4)	0.2306(3)	0.1303(3)	6.8(2)	
F(2)	0.2815(4)	0.2530(3)	0.2145(3)	7.1(2)	
F(3)	0.2013(4)	0.2112(3)	0.0887(3)	7.2(2)	
F(4)	0.4053(4)	-0.1884(3)	0.0136(3)	6.9(1)	
F(5)	0.4304(4)	-0.3012(3)	0.0441(3)	7.1(1)	
F(6)	0.2808(3)	-0.2711(3)	0.0005(2)	5.1(1)	
F(7)	0.0570(3)	-0.6587(3)	0.1192(3)	6.7(1)	
F(8)	-0.0951(3)	-0.6380(3)	0.1127(3)	6.8(1)	
F(9)	0.0029(4)	-0.5433(3)	0.1076(3)	6.5(1)	
F(10)	0.0271(6)	-0.3703(5)	0.1292(6)	14.1(3)	
F(11)	0.0200(4)	-0.2725(4)	0.0824(3)	7.4(2)	
F(12)	0.0845(4)	-0.2437(6)	0.2065(4)	11.0(2)	
O(1)	0.3786(3)	0.0967(3)	0.1982(2)	2.7(1)	
O(2)	0.2897(3)	0.0450(3)	0.0538(3)	3.6(1)	
O(3)	0.1949(3)	0.0690(3)	0.1479(3)	4.2(1)	
O(4)	0.4882(3)	-0.1512(3)	0.1947(2)	2.8(1)	
O(5)	0.3341(3)	-0.0995(3)	0.1480(3)	3.2(1)	
O(6)	0.3300(4)	-0.2367(3)	0.1675(3)	4.0(1)	
O(7)	0.0253(4)	-0.6142(3)	0.2783(3)	5.6(2)	
O(8)	0.1418(3)	-0.5097(3)	0.2712(3)	4.5(1)	
O(9)	-0.0300(3)	-0.4819(3)	0.2643(3)	4.0(1)	
O(10)	-0.1068(3)	-0.3024(3)	0.2198(3)	3.8(1)	
O(11)	-0.1805(5)	-0.3271(4)	0.0797(3)	7.9(2)	
O(12)	-0.1097(5)	-0.1821(3)	0.1777(4)	6.1(2)	
N(1)	0.0681(4)	-0.0879(3)	-0.1730(3)	3.0(1)	
N(2)	0.3539(4)	-0.4943(3)	0.1667(3)	2.5(1)	
C(1)	0.5364(5)	0.0277(4)	0.4193(3)	2.6(2)	
C(2)	0.4568(5)	-0.0397(4)	0.3745(4)	2.7(2)	
C(3)	0.3685(5)	-0.0041(4)	0.3458(4)	2.6(2)	
C(4)	0.3941(5)	0.0855(4)	0.3729(4)	2.4(2)	
C(5)	0.4985(5)	0.1054(4)	0.4180(4)	2.5(2)	
C(6)	0.6972(4)	0.0107(4)	0.2668(4)	2.3(2)	
C(7)	0.6941(4)	0.0971(4)	0.3126(4)	2.1(1)	

Table 1. Atomic coordinates and B_{iso}/B_{eq} and occupancy (continued)

atom	x	y	z	B_{eq}	occ
C(8)	0.6337(4)	0.1336(4)	0.2597(4)	2.4(2)	
C(9)	0.6039(4)	0.0697(4)	0.1808(4)	2.6(2)	
C(10)	0.6425(4)	-0.0058(4)	0.1859(4)	2.6(2)	
C(11)	0.6396(5)	0.0167(5)	0.4688(4)	4.0(2)	
C(12)	0.4633(6)	-0.1323(5)	0.3677(4)	4.3(2)	
C(13)	0.2618(5)	-0.0503(5)	0.3020(4)	3.9(2)	
C(14)	0.3232(5)	0.1516(5)	0.3637(4)	4.0(2)	
C(15)	0.5512(5)	0.1968(4)	0.4658(4)	3.4(2)	
C(16)	0.7556(5)	-0.0524(5)	0.2979(4)	3.8(2)	
C(17)	0.7608(5)	0.1483(5)	0.3980(4)	3.5(2)	
C(18)	0.6125(6)	0.2263(5)	0.2828(5)	4.3(2)	
C(19)	0.5479(5)	0.0837(6)	0.1050(4)	4.6(2)	
C(20)	0.6355(5)	-0.0879(5)	0.1154(4)	4.4(2)	
C(21)	0.2821(7)	0.2007(5)	0.1422(6)	4.7(2)	
C(22)	0.3744(5)	-0.2365(5)	0.0472(4)	3.9(2)	
C(23)	-0.3270(4)	-0.3721(4)	0.2494(4)	2.5(2)	
C(24)	-0.3160(5)	-0.3741(4)	0.3256(4)	2.7(2)	
C(25)	-0.2845(5)	-0.4542(4)	0.3257(4)	3.0(2)	
C(26)	-0.2762(5)	-0.5018(4)	0.2499(4)	2.9(2)	
C(27)	-0.3027(4)	-0.4512(4)	0.2021(4)	2.5(2)	
C(28)	0.0080(5)	-0.2099(4)	0.4196(4)	3.3(2)	
C(29)	-0.0637(5)	-0.2152(4)	0.4567(4)	3.5(2)	
C(30)	-0.0475(5)	-0.2847(4)	0.4838(4)	3.2(2)	
C(31)	0.0334(5)	-0.3244(4)	0.4609(4)	3.5(2)	
C(32)	0.0678(5)	-0.2783(4)	0.4207(4)	3.2(2)	
C(33)	-0.3630(5)	-0.3009(4)	0.2201(5)	4.4(2)	
C(34)	-0.3498(5)	-0.3098(5)	0.3903(5)	4.9(2)	
C(35)	-0.2728(6)	-0.4904(6)	0.3899(5)	5.7(3)	
C(36)	-0.2542(6)	-0.5941(5)	0.2219(5)	5.1(2)	
C(37)	-0.3059(6)	-0.4788(5)	0.1161(4)	4.4(2)	
C(38)	0.0238(6)	-0.1407(5)	0.3896(5)	4.8(2)	
C(39)	-0.1349(6)	-0.1475(5)	0.4741(4)	4.5(2)	
C(40)	-0.0968(6)	-0.3048(5)	0.5372(4)	5.2(2)	
C(41)	0.0797(6)	-0.3982(5)	0.4816(5)	5.4(2)	
C(42)	0.1551(5)	-0.2966(5)	0.3884(5)	4.8(2)	
C(43)	-0.0017(5)	-0.5991(5)	0.1415(5)	4.3(2)	
C(44)	0.0124(8)	-0.2908(6)	0.1428(7)	5.6(3)	
C(45)	0.0329(5)	-0.1373(4)	-0.1293(4)	3.6(2)	
C(46)	0.1139(6)	-0.1408(5)	-0.0552(5)	5.8(3)	

Table 1. Atomic coordinates and B_{iso}/B_{eq} and occupancy (continued)

atom	x	y	z	B_{eq}	occ
C(47)	0.1044(5)	0.0066(5)	-0.1192(4)	4.2(2)	
C(48)	0.0293(7)	0.0569(5)	-0.0872(5)	5.5(2)	
C(49)	0.1571(5)	-0.1254(5)	-0.1984(6)	5.1(2)	
C(50)	0.1345(7)	-0.2191(6)	-0.2556(8)	9.0(4)	
C(51)	-0.0208(5)	-0.0965(4)	-0.2450(4)	3.4(2)	
C(52)	-0.0024(6)	-0.0507(5)	-0.2972(5)	4.6(2)	
C(53)	0.4236(5)	-0.5129(5)	0.1162(4)	3.5(2)	
C(54)	0.4133(6)	-0.6052(5)	0.0598(5)	4.7(2)	
C(55)	0.3621(5)	-0.5552(4)	0.2111(4)	3.3(2)	
C(56)	0.4661(6)	-0.5529(5)	0.2669(5)	4.5(2)	
C(57)	0.3859(5)	-0.4006(4)	0.2247(4)	3.0(2)	
C(58)	0.3251(6)	-0.3683(4)	0.2806(5)	4.5(2)	
C(59)	0.2442(5)	-0.5085(4)	0.1136(4)	3.0(2)	
C(60)	0.2161(5)	-0.4507(5)	0.0666(4)	4.0(2)	
C(61)	0.603(1)	0.441(1)	0.5262(9)	4.4(3)	1/2
C(62)	0.5129(9)	0.4294(7)	0.4854(7)	7.3(2)	
C(63)	0.432(2)	0.407(1)	0.446(1)	6.7(5)	1/2
C(64)	0.341(1)	0.4604(8)	0.4231(8)	10.3(3)	
C(65)	0.569(1)	0.519(1)	0.533(1)	6.0(4)	1/2
C(101)	0.4509	0.0349	0.3861	0.2000	0.001
C(102)	0.6543	0.0611	0.2412	0.2000	0.001
C(103)	-0.3012	-0.4307	0.2706	0.2000	0.001
C(104)	-0.0005	-0.2626	0.4484	0.2000	0.001
H(1)	0.6360	-0.0034	0.5094	4.6982	
H(2)	0.6715	-0.0250	0.4348	4.6982	
H(3)	0.6848	0.0702	0.4942	4.6982	
H(4)	0.4004	-0.1673	0.3349	5.3599	
H(5)	0.5148	-0.1554	0.3452	5.3599	
H(6)	0.4806	-0.1355	0.4203	5.3599	
H(7)	0.2188	-0.0295	0.3335	4.8554	
H(8)	0.2340	-0.0414	0.2521	4.8554	
H(9)	0.2613	-0.1113	0.2890	4.8554	
H(10)	0.3208	0.1899	0.4151	4.5976	
H(11)	0.3451	0.1867	0.3390	4.5976	
H(12)	0.2563	0.1241	0.3309	4.5976	
H(13)	0.6219	0.1960	0.4922	4.1160	
H(14)	0.5456	0.2287	0.4324	4.1160	
H(15)	0.5224	0.2261	0.5073	4.1160	
H(16)	0.7110	-0.1043	0.2856	4.5724	

Table 1. Atomic coordinates and B_{iso}/B_{eq} and occupancy (continued)

atom	x	y	z	B_{eq}	occ
H(17)	0.8069	-0.0712	0.2740	4.5724	
H(18)	0.7871	-0.0283	0.3553	4.5724	
H(19)	0.7950	0.1098	0.4233	4.3115	
H(20)	0.8112	0.1883	0.4005	4.3115	
H(21)	0.7216	0.1796	0.4309	4.3115	
H(22)	0.6392	0.2589	0.3379	5.4204	
H(23)	0.6402	0.2548	0.2544	5.4204	
H(24)	0.5398	0.2294	0.2649	5.4204	
H(25)	0.5279	0.1407	0.1169	5.5759	
H(26)	0.5876	0.0755	0.0708	5.5759	
H(27)	0.4858	0.0432	0.0750	5.5759	
H(28)	0.5653	-0.1111	0.0842	5.3898	
H(29)	0.6672	-0.0781	0.0808	5.3898	
H(30)	0.6666	-0.1318	0.1332	5.3898	
H(31)	-0.3740	-0.2527	0.2624	5.0009	
H(32)	-0.3129	-0.2793	0.2029	5.0009	
H(33)	-0.4243	-0.3203	0.1757	5.0009	
H(34)	-0.2977	-0.2920	0.4423	5.7498	
H(35)	-0.3683	-0.2602	0.3791	5.7498	
H(36)	-0.4083	-0.3365	0.3957	5.7498	
H(37)	-0.3221	-0.5386	0.3730	6.7681	
H(38)	-0.2068	-0.5066	0.4069	6.7681	
H(39)	-0.2817	-0.4464	0.4380	6.7681	
H(40)	-0.3048	-0.6335	0.2211	5.7898	
H(41)	-0.2519	-0.6133	0.1667	5.7898	
H(42)	-0.1895	-0.6018	0.2543	5.7898	
H(43)	-0.3736	-0.4810	0.0818	5.2510	
H(44)	-0.2621	-0.4396	0.1099	5.2510	
H(45)	-0.2856	-0.5354	0.0982	5.2510	
H(46)	0.0422	-0.0851	0.4323	5.5258	
H(47)	0.0777	-0.1515	0.3665	5.5258	
H(48)	-0.0360	-0.1391	0.3488	5.5258	
H(49)	-0.0989	-0.0918	0.5089	5.4341	
H(50)	-0.1777	-0.1426	0.4247	5.4341	
H(51)	-0.1797	-0.1628	0.4988	5.4341	
H(52)	-0.1511	-0.2718	0.5451	5.9796	
H(53)	-0.1271	-0.3664	0.5139	5.9796	
H(54)	-0.0498	-0.2968	0.5894	5.9796	
H(55)	0.0291	-0.4488	0.4596	6.3565	

Table 1. Atomic coordinates and B_{iso}/B_{eq} and occupancy (continued)

atom	x	y	z	B_{eq}	occ
H(56)	0.1323	-0.4158	0.4581	6.3565	
H(57)	0.1070	-0.3831	0.5378	6.3565	
H(58)	0.1832	-0.3467	0.3939	5.7782	
H(59)	0.1324	-0.3071	0.3306	5.7782	
H(60)	0.2071	-0.2485	0.4142	5.7782	
H(61)	-0.0227	-0.1143	-0.1126	4.3748	
H(62)	0.0092	-0.1978	-0.1652	4.3748	
H(63)	0.0891	-0.1722	-0.0300	6.4272	
H(64)	0.1701	-0.1655	-0.0694	6.4272	
H(65)	0.1380	-0.0821	-0.0167	6.4272	
H(66)	0.1600	0.0110	-0.0733	5.0090	
H(67)	0.1236	0.0359	-0.1484	5.0090	
H(68)	0.0550	0.1152	-0.0536	5.8294	
H(69)	-0.0308	0.0560	-0.1302	5.8294	
H(70)	0.0054	0.0308	-0.0552	5.8294	
H(71)	0.1806	-0.0921	-0.2228	6.1289	
H(72)	0.2124	-0.1220	-0.1505	6.1289	
H(73)	0.1115	-0.2549	-0.2316	10.3296	
H(74)	0.0796	-0.2250	-0.3038	10.3296	
H(75)	0.1908	-0.2405	-0.2698	10.3296	
H(76)	-0.0418	-0.1577	-0.2777	4.1580	
H(77)	-0.0770	-0.0747	-0.2273	4.1580	
H(78)	0.0506	-0.0730	-0.3184	5.5240	
H(79)	-0.0628	-0.0595	-0.3439	5.5240	
H(80)	0.0148	0.0098	-0.2683	5.5240	
H(81)	0.4115	-0.4767	0.0843	4.3504	
H(82)	0.4929	-0.4960	0.1513	4.3504	
H(83)	0.3440	-0.6235	0.0227	5.5759	
H(84)	0.4574	-0.6147	0.0292	5.5759	
H(85)	0.4252	-0.6429	0.0898	5.5759	
H(86)	0.3160	-0.5420	0.2423	4.0480	
H(87)	0.3398	-0.6139	0.1727	4.0480	
H(88)	0.4668	-0.5915	0.2942	5.2000	
H(89)	0.5127	-0.5671	0.2380	5.2000	
H(90)	0.4890	-0.4950	0.3074	5.2000	
H(91)	0.4558	-0.3952	0.2582	3.6394	
H(92)	0.3829	-0.3639	0.1956	3.6394	
H(93)	0.3478	-0.3094	0.3167	5.3360	
H(94)	0.2544	-0.3711	0.2497	5.3360	

Table 1. Atomic coordinates and B_{iso}/B_{eq} and occupancy (continued)

atom	x	y	z	B_{eq}	occ
H(95)	0.3269	-0.4030	0.3121	5.3360	
H(96)	0.2289	-0.5680	0.0757	3.7082	
H(97)	0.2019	-0.5018	0.1469	3.7082	
H(98)	0.2286	-0.3906	0.1033	4.6736	
H(99)	0.2559	-0.4566	0.0322	4.6736	
H(100)	0.1461	-0.4624	0.0346	4.6736	
H(150)	0.0000	0.0000	0.0000	0.2000	0.001

$B_{eq} = 8/3\ \pi^2(U_{11}(aa^*)^2 + U_{22}(bb^*)^2 + U_{33}(cc^*)^2 + 2U_{12}(aa^*bb^*)\cos\gamma + 2U_{13}(aa^*cc^*)\cos\beta + 2U_{23}(bb^*cc^*)\cos\alpha)$

Table 2. Anisotropic Displacement Parameters

atom	U_{11}	U_{22}	U_{33}	U_{12}	U_{13}	U_{23}
Ce(1)	0.0223(2)	0.0251(2)	0.0231(2)	0.0013(2)	0.0075(2)	0.0096(2)
Ce(2)	0.0260(2)	0.0323(2)	0.0281(3)	0.0031(2)	0.0051(2)	0.0071(2)
S(1)	0.0280(10)	0.0340(10)	0.042(1)	0.0047(7)	0.0057(8)	0.0176(8)
S(2)	0.037(1)	0.0272(9)	0.036(1)	0.0015(7)	0.0094(8)	0.0119(8)
S(3)	0.030(1)	0.036(1)	0.068(1)	0.0046(8)	0.0167(9)	0.0149(10)
S(4)	0.037(1)	0.052(1)	0.042(1)	0.0001(9)	0.0125(9)	0.0187(10)
F(1)	0.096(4)	0.053(3)	0.135(5)	0.017(3)	0.043(4)	0.061(3)
F(2)	0.129(5)	0.046(3)	0.088(4)	0.033(3)	0.032(3)	0.019(3)
F(3)	0.084(4)	0.082(4)	0.098(4)	0.035(3)	-0.005(3)	0.053(3)
F(4)	0.091(4)	0.119(4)	0.042(3)	-0.035(3)	0.019(3)	0.020(3)
F(5)	0.081(4)	0.087(4)	0.058(3)	0.044(3)	0.010(3)	-0.012(3)
F(6)	0.047(3)	0.066(3)	0.048(3)	-0.007(2)	-0.008(2)	0.006(2)
F(7)	0.067(3)	0.065(3)	0.102(4)	0.018(3)	0.042(3)	-0.002(3)
F(8)	0.045(3)	0.082(4)	0.086(4)	-0.022(3)	0.020(3)	-0.017(3)
F(9)	0.081(4)	0.087(4)	0.072(4)	0.002(3)	0.012(3)	0.033(3)
F(10)	0.224(9)	0.122(6)	0.33(1)	0.114(6)	0.216(9)	0.134(7)
F(11)	0.102(4)	0.113(5)	0.102(4)	0.022(3)	0.072(4)	0.050(4)
F(12)	0.048(4)	0.255(9)	0.118(6)	-0.008(5)	0.022(4)	0.076(6)
O(1)	0.028(2)	0.035(3)	0.035(3)	0.003(2)	0.002(2)	0.013(2)
O(2)	0.042(3)	0.052(3)	0.034(3)	0.004(2)	0.003(2)	0.013(2)
O(3)	0.028(3)	0.061(3)	0.077(4)	0.005(2)	0.020(3)	0.030(3)
O(4)	0.031(3)	0.035(3)	0.034(3)	0.006(2)	0.005(2)	0.010(2)
O(5)	0.033(3)	0.028(3)	0.050(3)	0.002(2)	0.004(2)	0.011(2)
O(6)	0.064(4)	0.033(3)	0.057(3)	-0.006(2)	0.022(3)	0.019(2)
O(7)	0.068(4)	0.059(4)	0.106(5)	0.015(3)	0.037(4)	0.049(4)
O(8)	0.029(3)	0.053(3)	0.073(4)	-0.003(2)	0.011(3)	0.011(3)
O(9)	0.028(3)	0.035(3)	0.066(4)	0.004(2)	0.010(2)	-0.000(2)
O(10)	0.044(3)	0.053(3)	0.047(3)	-0.005(2)	0.010(2)	0.021(3)
O(11)	0.082(5)	0.149(6)	0.044(4)	-0.062(4)	-0.011(3)	0.035(4)
O(12)	0.114(5)	0.055(4)	0.105(5)	0.041(4)	0.075(4)	0.044(3)
N(1)	0.026(3)	0.036(3)	0.055(4)	0.001(2)	0.011(3)	0.020(3)
N(2)	0.026(3)	0.033(3)	0.038(3)	0.003(2)	0.015(2)	0.012(3)
C(1)	0.038(4)	0.048(4)	0.017(4)	0.008(3)	0.013(3)	0.014(3)
C(2)	0.046(4)	0.035(4)	0.030(4)	0.008(3)	0.020(3)	0.015(3)
C(3)	0.034(4)	0.042(4)	0.026(4)	-0.001(3)	0.019(3)	0.007(3)
C(4)	0.037(4)	0.032(4)	0.026(4)	0.013(3)	0.018(3)	0.010(3)
C(5)	0.037(4)	0.028(4)	0.030(4)	0.003(3)	0.015(3)	0.009(3)
C(6)	0.025(4)	0.034(4)	0.037(4)	0.004(3)	0.016(3)	0.016(3)
C(7)	0.017(3)	0.035(4)	0.028(4)	-0.001(3)	0.007(3)	0.010(3)

Table 2. Anisotropic Displacement Parameters (continued)

atom	U_{11}	U_{22}	U_{33}	U_{12}	U_{13}	U_{23}
C(8)	0.021(3)	0.031(4)	0.043(4)	-0.002(3)	0.013(3)	0.016(3)
C(9)	0.019(3)	0.053(4)	0.032(4)	-0.003(3)	0.010(3)	0.022(4)
C(10)	0.025(4)	0.042(4)	0.025(4)	-0.004(3)	0.012(3)	0.003(3)
C(11)	0.039(4)	0.083(6)	0.043(5)	0.021(4)	0.017(4)	0.037(4)
C(12)	0.085(6)	0.047(5)	0.054(5)	0.018(4)	0.036(5)	0.032(4)
C(13)	0.040(4)	0.065(5)	0.041(5)	-0.006(4)	0.023(4)	0.011(4)
C(14)	0.048(5)	0.063(5)	0.046(5)	0.025(4)	0.024(4)	0.020(4)
C(15)	0.051(5)	0.044(4)	0.035(4)	0.002(4)	0.020(4)	0.008(3)
C(16)	0.034(4)	0.060(5)	0.066(5)	0.015(4)	0.021(4)	0.038(4)
C(17)	0.026(4)	0.059(5)	0.036(4)	-0.008(3)	0.005(3)	0.006(4)
C(18)	0.051(5)	0.049(5)	0.079(6)	0.008(4)	0.033(4)	0.032(4)
C(19)	0.036(4)	0.106(7)	0.043(5)	0.002(4)	0.014(4)	0.040(5)
C(20)	0.035(4)	0.062(5)	0.055(5)	-0.010(4)	0.027(4)	-0.007(4)
C(21)	0.058(6)	0.042(5)	0.078(7)	0.011(4)	0.014(5)	0.029(5)
C(22)	0.037(5)	0.047(5)	0.047(5)	-0.003(4)	0.003(4)	0.007(4)
C(23)	0.022(3)	0.026(4)	0.046(4)	-0.000(3)	0.008(3)	0.016(3)
C(24)	0.029(4)	0.038(4)	0.033(4)	0.006(3)	0.013(3)	0.005(3)
C(25)	0.027(4)	0.048(4)	0.043(5)	0.005(3)	0.010(3)	0.024(4)
C(26)	0.024(4)	0.029(4)	0.057(5)	0.005(3)	0.018(3)	0.014(3)
C(27)	0.027(4)	0.037(4)	0.028(4)	-0.007(3)	0.007(3)	0.008(3)
C(28)	0.043(4)	0.031(4)	0.031(4)	-0.006(3)	-0.000(3)	-0.002(3)
C(29)	0.047(5)	0.044(4)	0.026(4)	0.007(4)	0.001(3)	0.004(3)
C(30)	0.049(5)	0.046(4)	0.016(4)	0.002(4)	0.002(3)	0.006(3)
C(31)	0.038(4)	0.043(4)	0.030(4)	0.006(3)	-0.009(3)	0.006(3)
C(32)	0.027(4)	0.045(4)	0.032(4)	-0.004(3)	-0.002(3)	0.004(3)
C(33)	0.035(4)	0.039(4)	0.096(7)	0.007(3)	0.014(4)	0.035(4)
C(34)	0.037(5)	0.075(6)	0.053(5)	0.013(4)	0.013(4)	0.001(4)
C(35)	0.054(5)	0.107(7)	0.079(7)	0.003(5)	0.016(5)	0.067(6)
C(36)	0.051(5)	0.030(4)	0.117(8)	0.007(4)	0.040(5)	0.022(5)
C(37)	0.054(5)	0.059(5)	0.041(5)	-0.021(4)	0.013(4)	0.008(4)
C(38)	0.067(6)	0.037(5)	0.051(5)	-0.011(4)	0.004(4)	0.000(4)
C(39)	0.062(5)	0.054(5)	0.044(5)	0.022(4)	0.012(4)	0.008(4)
C(40)	0.079(6)	0.077(6)	0.030(5)	-0.002(5)	0.011(4)	0.013(4)
C(41)	0.070(6)	0.062(6)	0.061(6)	0.013(5)	-0.006(5)	0.030(5)
C(42)	0.032(4)	0.055(5)	0.065(6)	-0.006(4)	0.004(4)	-0.002(4)
C(43)	0.030(4)	0.043(5)	0.079(6)	0.003(4)	0.022(4)	0.007(4)
C(44)	0.078(7)	0.065(6)	0.091(8)	0.013(5)	0.047(6)	0.036(6)
C(45)	0.034(4)	0.040(4)	0.068(6)	0.005(3)	0.015(4)	0.027(4)
C(46)	0.071(6)	0.064(6)	0.092(7)	0.000(5)	0.006(5)	0.052(5)

Table 2. Anisotropic Displacement Parameters (continued)

atom	U_{11}	U_{22}	U_{33}	U_{12}	U_{13}	U_{23}
C(47)	0.048(5)	0.050(5)	0.048(5)	-0.018(4)	-0.015(4)	0.028(4)
C(48)	0.105(7)	0.041(5)	0.056(6)	-0.001(5)	0.031(5)	0.006(4)
C(49)	0.026(4)	0.063(6)	0.128(8)	0.011(4)	0.032(5)	0.058(6)
C(50)	0.085(7)	0.052(6)	0.25(1)	0.034(5)	0.120(9)	0.062(8)
C(51)	0.025(4)	0.056(5)	0.039(4)	-0.002(3)	0.005(3)	0.013(4)
C(52)	0.057(5)	0.073(6)	0.046(5)	0.010(4)	0.018(4)	0.021(4)
C(53)	0.031(4)	0.062(5)	0.048(5)	0.007(4)	0.020(3)	0.025(4)
C(54)	0.057(5)	0.062(5)	0.052(5)	0.016(4)	0.026(4)	0.006(4)
C(55)	0.043(4)	0.031(4)	0.055(5)	0.004(3)	0.016(4)	0.021(4)
C(56)	0.062(6)	0.061(5)	0.058(5)	0.014(4)	0.020(4)	0.033(4)
C(57)	0.036(4)	0.032(4)	0.042(4)	-0.002(3)	0.009(3)	0.014(3)
C(58)	0.071(6)	0.034(4)	0.065(6)	0.002(4)	0.035(5)	0.007(4)
C(59)	0.028(4)	0.042(4)	0.042(4)	0.001(3)	0.010(3)	0.013(3)
C(60)	0.042(5)	0.067(5)	0.043(5)	0.014(4)	0.011(4)	0.020(4)

The general temperature factor expression:
$\exp(-2\pi^2(a^{*2}U_{11}h^2 + b^{*2}U_{22}k^2 + c^{*2}U_{33}l^2 + 2a^*b^*U_{12}hk + 2a^*c^*U_{13}hl + 2b^*c^*U_{23}kl))$

$Cp^*_2Ce(2,2'\text{-bipyridine})(Cl)$

EXPERIMENTAL DETAILS

A. Crystal Data

Empirical Formula	$H_{38}C_{30}N_2ClCe$
Formula Weight	602.22
Crystal Color, Habit	brown, block
Crystal Dimensions	0.07 X 0.07 X 0.07 mm
Crystal System	monoclinic
Lattice Type	Primitive
Lattice Parameters	a = 10.6983(5)Å
	b = 14.1160(7) Å
	c = 18.1198(9) Å
	β = 89.318(1)^o
	V = 2736.2(2) Å^3
Space Group	$P2_1/c$ (#14)
Z value	4
D_{calc}	1.462 g/cm^3
F_{000}	1228.00
μ(MoKα)	17.81 cm^{-1}

B. Intensity Measurements

Diffractometer	Bruker SMART CCD
Radiation	MoKα (λ = 0.71069 Å) graphite monochromated
Detector Position	60.00 mm
Exposure Time	10.0 seconds per frame.
Scan Type	ω (0.3 degrees per frame)
$2\theta_{max}$	52.8^o
No. of Reflections Measured	Total: 15047
Unique:	4245 (R_{int} = 0.020)
Corrections	Lorentz-polarization

Absorption (Tmax = 1.00 Tmin = 0.57)

C. Structure Solution and Refinement

Structure Solution	Direct Methods (SIR97)
Refinement	Full-matrix least-squares
Function Minimized	Σ w (|Fo| - |Fc|)^2
Least Squares Weights	$1/\sigma^2(Fo) = 4Fo^2/\sigma^2(Fo^2)$
p-factor	0.0300
Anomalous Dispersion	All non-hydrogen atoms
No. Observations (I>3.00σ(I))	4342
No. Variables	307
Reflection/Parameter Ratio	14.14
Residuals: R; Rw; Rall	0.024 ; 0.031; 0.033
Goodness of Fit Indicator	1.48
Max Shift/Error in Final Cycle	0.00
Maximum peak in Final Diff. Map	1.40 $e^-/Å^3$
Minimum peak in Final Diff. Map	-0.46 $e^-/Å^3$

Table 1. Atomic coordinates and B_{iso}/B_{eq} and occupancy

atom	x	y	z	B_{eq}	occ
Ce(1)	0.21951(1)	0.27989(1)	0.635335(8)	1.369(4)	
Cl(1)	0.07581(7)	0.13016(5)	0.58646(4)	2.51(2)	
N(1)	0.2301(2)	0.3965(2)	0.7506(1)	1.66(5)	
N(2)	0.0282(2)	0.2833(2)	0.7373(1)	1.73(5)	
C(1)	0.3825(3)	0.1211(2)	0.6211(2)	1.90(6)	
C(2)	0.4563(3)	0.1962(2)	0.5932(2)	1.81(6)	
C(3)	0.4861(3)	0.2572(2)	0.6532(2)	1.70(6)	
C(4)	0.4299(3)	0.2186(2)	0.7182(2)	1.63(6)	
C(5)	0.3637(3)	0.1351(2)	0.6971(2)	1.66(6)	
C(6)	0.2531(3)	0.4034(2)	0.5162(2)	1.81(6)	
C(7)	0.2192(3)	0.4654(2)	0.5738(2)	2.01(6)	
C(8)	0.0920(3)	0.4471(2)	0.5921(2)	2.21(7)	
C(9)	0.0491(3)	0.3741(2)	0.5455(2)	2.28(7)	
C(10)	0.1490(3)	0.3465(2)	0.4985(2)	1.94(6)	
C(11)	0.3499(3)	0.0328(2)	0.5787(2)	2.81(7)	
C(12)	0.5121(3)	0.2002(2)	0.5165(2)	2.77(7)	
C(13)	0.5770(3)	0.3383(2)	0.6481(2)	2.36(7)	
C(14)	0.4519(3)	0.2493(2)	0.7962(2)	2.22(6)	
C(15)	0.2942(3)	0.0707(2)	0.7498(2)	2.81(7)	
C(16)	0.3718(3)	0.4109(2)	0.4710(2)	2.38(7)	
C(17)	0.2984(3)	0.5475(2)	0.5995(2)	2.91(7)	
C(18)	0.0126(4)	0.5052(3)	0.6441(2)	3.62(9)	
C(19)	-0.0837(3)	0.3401(3)	0.5426(2)	3.67(9)	
C(20)	0.1449(3)	0.2739(2)	0.4376(2)	2.70(7)	
C(21)	0.3322(3)	0.4510(2)	0.7576(2)	2.06(6)	
C(22)	0.3489(3)	0.5165(2)	0.8134(2)	2.33(7)	
C(23)	0.2567(3)	0.5239(2)	0.8665(2)	2.49(7)	
C(24)	0.1519(3)	0.4681(2)	0.8618(2)	2.31(7)	
C(25)	0.1386(3)	0.4058(2)	0.8029(1)	1.66(6)	
C(26)	0.0244(3)	0.3485(2)	0.7920(1)	1.64(6)	
C(27)	-0.0824(3)	0.3625(2)	0.8359(2)	2.23(7)	
C(28)	-0.1871(3)	0.3079(2)	0.8240(2)	2.53(7)	
C(29)	-0.1837(3)	0.2409(2)	0.7693(2)	2.43(7)	
C(30)	-0.0758(3)	0.2305(2)	0.7276(2)	2.16(7)	
C(101)	0.4237	0.1856	0.6566	0.2000	0.001
C(102)	0.1525	0.4073	0.5452	0.2000	0.001
H(1)	0.3334	0.0489	0.5288	3.3784	
H(2)	0.5038	0.2044	0.8200	2.6681	
H(3)	0.3478	0.0532	0.7889	3.3724	

Table 1. Atomic coordinates and B_{iso}/B_{eq} and occupancy (continued)

atom	x	y	z	B_{eq}	occ
H(4)	0.5565	0.2579	0.5102	3.3260	
H(5)	0.5890	0.3644	0.6959	2.8352	
H(6)	0.1164	0.3031	0.3936	3.2472	
H(7)	0.3642	0.4613	0.4366	2.8540	
H(8)	0.3838	0.5291	0.5995	3.4937	
H(9)	0.0643	0.5349	0.6794	4.3398	
H(10)	-0.0861	0.2798	0.5195	4.4018	
H(11)	0.2779	0.0042	0.6003	3.3784	
H(12)	0.4179	-0.0104	0.5802	3.3784	
H(13)	0.5677	0.1484	0.5096	3.3260	
H(14)	0.4472	0.1967	0.4813	3.3260	
H(15)	0.6547	0.3161	0.6290	2.8352	
H(16)	0.5447	0.3857	0.6164	2.8352	
H(17)	0.4915	0.3096	0.7962	2.6681	
H(18)	0.3741	0.2536	0.8219	2.6681	
H(19)	0.2232	0.1029	0.7692	3.3724	
H(20)	0.2682	0.0155	0.7243	3.3724	
H(21)	0.3857	0.3532	0.4452	2.8540	
H(22)	0.4400	0.4231	0.5027	2.8540	
H(23)	0.2877	0.5997	0.5671	3.4937	
H(24)	0.2732	0.5651	0.6480	3.4937	
H(25)	-0.0309	0.5522	0.6169	4.3398	
H(26)	-0.0460	0.4651	0.6685	4.3398	
H(27)	-0.1167	0.3351	0.5914	4.4018	
H(28)	-0.1322	0.3838	0.5153	4.4018	
H(29)	0.0891	0.2244	0.4513	3.2472	
H(30)	0.2260	0.2487	0.4295	3.2472	
H(31)	0.3974	0.4441	0.7218	2.4773	
H(32)	0.4216	0.5552	0.8148	2.8003	
H(33)	0.2654	0.5673	0.9062	2.9860	
H(34)	0.0884	0.4722	0.8988	2.7752	
H(35)	-0.0829	0.4094	0.8736	2.6724	
H(36)	-0.2604	0.3166	0.8533	3.0300	
H(37)	-0.2546	0.2022	0.7603	2.9216	
H(38)	-0.0745	0.1835	0.6900	2.5993	

$B_{eq} = 8/3\ \pi^2(U_{11}(aa^*)^2 + U_{22}(bb^*)^2 + U_{33}(cc^*)^2 + 2U_{12}(aa^*bb^*)\cos\gamma + 2U_{13}(aa^*cc^*)\cos\beta + 2U_{23}(bb^*cc^*)\cos\alpha)$

Table 2. Anisotropic Displacement Parameters

atom	U_{11}	U_{22}	U_{33}	U_{12}	U_{13}	U_{23}
Ce(1)	0.01608(10)	0.01661(9)	0.01933(10)	0.00031(6)	-0.00055(6)	0.00046(6)
Cl(1)	0.0286(4)	0.0271(4)	0.0398(4)	-0.0078(3)	-0.0003(3)	-0.0059(3)
N(1)	0.020(1)	0.020(1)	0.023(1)	0.0002(10)	-0.0021(10)	0.0015(10)
N(2)	0.019(1)	0.020(1)	0.027(1)	0.0000(10)	0.0009(10)	0.0005(10)
C(1)	0.022(2)	0.022(1)	0.029(2)	0.006(1)	-0.002(1)	-0.001(1)
C(2)	0.019(1)	0.025(2)	0.024(2)	0.006(1)	0.003(1)	-0.000(1)
C(3)	0.015(1)	0.024(1)	0.025(2)	0.003(1)	0.000(1)	0.001(1)
C(4)	0.018(1)	0.022(1)	0.022(1)	0.007(1)	-0.001(1)	0.002(1)
C(5)	0.018(1)	0.017(1)	0.028(2)	0.006(1)	-0.000(1)	0.006(1)
C(6)	0.029(2)	0.019(1)	0.021(1)	-0.001(1)	-0.004(1)	0.006(1)
C(7)	0.037(2)	0.018(1)	0.022(2)	0.001(1)	-0.003(1)	0.005(1)
C(8)	0.033(2)	0.028(2)	0.023(2)	0.017(1)	-0.000(1)	0.008(1)
C(9)	0.023(2)	0.035(2)	0.029(2)	0.003(1)	-0.007(1)	0.012(1)
C(10)	0.029(2)	0.024(2)	0.020(1)	-0.002(1)	-0.004(1)	0.002(1)
C(11)	0.040(2)	0.026(2)	0.041(2)	0.005(1)	-0.003(2)	-0.007(1)
C(12)	0.036(2)	0.037(2)	0.032(2)	0.008(1)	0.007(1)	0.001(1)
C(13)	0.020(2)	0.033(2)	0.037(2)	-0.003(1)	0.002(1)	0.005(1)
C(14)	0.024(2)	0.035(2)	0.025(2)	0.007(1)	-0.002(1)	0.003(1)
C(15)	0.038(2)	0.027(2)	0.042(2)	0.002(1)	0.005(2)	0.011(1)
C(16)	0.032(2)	0.031(2)	0.028(2)	-0.006(1)	0.001(1)	0.005(1)
C(17)	0.056(2)	0.024(2)	0.031(2)	-0.001(1)	-0.007(2)	0.001(1)
C(18)	0.056(2)	0.042(2)	0.039(2)	0.028(2)	0.011(2)	0.013(2)
C(19)	0.024(2)	0.064(3)	0.051(2)	0.002(2)	-0.007(2)	0.024(2)
C(20)	0.047(2)	0.034(2)	0.022(2)	-0.010(2)	-0.006(1)	0.000(1)
C(21)	0.019(2)	0.029(2)	0.030(2)	0.001(1)	-0.000(1)	0.002(1)
C(22)	0.027(2)	0.025(2)	0.037(2)	-0.003(1)	-0.010(1)	0.002(1)
C(23)	0.036(2)	0.027(2)	0.031(2)	0.001(1)	-0.007(1)	-0.008(1)
C(24)	0.028(2)	0.030(2)	0.029(2)	0.006(1)	0.002(1)	-0.004(1)
C(25)	0.020(1)	0.020(1)	0.023(1)	0.005(1)	-0.002(1)	0.003(1)
C(26)	0.020(1)	0.021(1)	0.021(1)	0.005(1)	-0.002(1)	0.004(1)
C(27)	0.025(2)	0.032(2)	0.027(2)	0.004(1)	0.001(1)	-0.001(1)
C(28)	0.022(2)	0.036(2)	0.038(2)	0.005(1)	0.006(1)	0.007(1)
C(29)	0.022(2)	0.031(2)	0.039(2)	-0.004(1)	0.000(1)	0.009(1)
C(30)	0.026(2)	0.022(2)	0.034(2)	-0.005(1)	0.001(1)	-0.001(1)

The general temperature factor expression:
$\exp(-2\pi^2(a^{*2}U_{11}h^2 + b^{*2}U_{22}k^2 + c^{*2}U_{33}l^2 + 2a^*b^*U_{12}hk + 2a^*c^*U_{13}hl + 2b^*c^*U_{23}kl))$

Table 3. Bond Lengths(Å)

atom	atom	distance	atom	atom	distance
Ce(1)	Cl(1)	2.7654(7)	Ce(1)	N(1)	2.662(2)
Ce(1)	N(2)	2.741(2)	Ce(1)	C(1)	2.850(3)
Ce(1)	C(2)	2.890(3)	Ce(1)	C(3)	2.892(3)
Ce(1)	C(4)	2.854(3)	Ce(1)	C(5)	2.802(3)
Ce(1)	C(6)	2.795(3)	Ce(1)	C(7)	2.846(3)
Ce(1)	C(8)	2.841(3)	Ce(1)	C(9)	2.795(3)
Ce(1)	C(10)	2.766(3)	Ce(1)	C(101)	2.5908(2)
Ce(1)	C(102)	2.5385(1)	N(1)	C(21)	1.344(4)
N(1)	C(25)	1.362(3)	N(2)	C(26)	1.353(4)
N(2)	C(30)	1.353(4)	C(1)	C(2)	1.411(4)
C(1)	C(5)	1.405(4)	C(1)	C(11)	1.507(4)
C(1)	C(101)	1.202(3)	C(2)	C(3)	1.426(4)
C(2)	C(12)	1.508(4)	C(2)	C(101)	1.206(3)
C(3)	C(4)	1.424(4)	C(3)	C(13)	1.504(4)
C(3)	C(101)	1.213(3)	C(4)	C(5)	1.428(4)
C(4)	C(14)	1.501(4)	C(4)	C(101)	1.211(3)
C(5)	C(15)	1.507(4)	C(5)	C(101)	1.203(3)
C(6)	C(7)	1.406(4)	C(6)	C(10)	1.413(4)
C(6)	C(16)	1.506(4)	C(6)	C(102)	1.193(3)
C(7)	C(8)	1.420(4)	C(7)	C(17)	1.512(4)
C(7)	C(102)	1.208(3)	C(8)	C(9)	1.413(4)
C(8)	C(18)	1.505(4)	C(8)	C(102)	1.201(3)
C(9)	C(10)	1.414(4)	C(9)	C(19)	1.501(4)
C(9)	C(102)	1.201(3)	C(10)	C(20)	1.506(4)
C(10)	C(102)	1.207(3)	C(21)	C(22)	1.384(4)
C(22)	C(23)	1.375(4)	C(23)	C(24)	1.373(4)
C(24)	C(25)	1.391(4)	C(25)	C(26)	1.481(4)
C(26)	C(27)	1.398(4)	C(27)	C(28)	1.378(4)
C(28)	C(29)	1.370(5)	C(29)	C(30	1.380(4)

$Cp^*_2Ce(bipy)(I)$ (I = 93%)

EXPERIMENTAL DETAILS

A. Crystal Data

Empirical Formula	$H_{38}C_{30}N_2I_{0.93}CeCl_{0.07}$
Formula Weight	687.27
Crystal Color, Habit	red, plate
Crystal Dimensions	0.10 X 0.10 X 0.10 mm
Crystal System	monoclinic
Lattice Type	Primitive
Lattice Parameters	a = 11.8276(8)Å
	b = 15.615(1) Å
	c = 15.109(1) Å
	β = 94.727(1)^o
	V = 2781.1(3) Å^3
Space Group	$P2_1/n$ (#14)
Z value	4
D_{calc}	1.641 g/cm^3
F_{000}	1361.92
μ(MoKα)	26.96 cm^{-1}

B. Intensity Measurements

Diffractometer	Bruker SMART CCD
Radiation	MoKα (λ = 0.71069 Å) graphite monochromated
Detector Position	60.00 mm
Exposure Time	10.0 seconds per frame.
Scan Type	ω (0.3 degrees per frame)
$2\theta_{max}$	51.3^o
No. of Reflections Measured	Total: 12349 Unique: 4000 (R_{int} = 0.033)
Corrections	Lorentz-polarization
	Absorption (Tmin/max =0.6)

C. Structure Solution and Refinement

Structure Solution	Direct Methods (SIR97)
Refinement	Full-matrix least-squares
Function Minimized	Σ w (|Fo| - |Fc|)^2
p-factor	0.0300
Anomalous Dispersion	All non-hydrogen atoms
No. Observations (I>3.00σ(I))	4043
No. Variables	312
Reflection/Parameter Ratio	12.96
Residuals: R; Rw; Rall	0.030 ; 0.041; 0.036
Goodness of Fit Indicator	1.57
Max Shift/Error in Final Cycle	0.00
Maximum peak in Final Diff. Map	0.77 e^-/Å^3
Minimum peak in Final Diff. Map	-1.23 e^-/Å^3

Table 1. Atomic coordinates and B_{iso}/B_{eq} and occupancy

atom	x	y	z	B_{eq}	occ
Ce1	0.25556(2)	0.24138(1)	-0.01106(2)	1.216(6)	
I1	0.36640(3)	0.30905(3)	0.17987(3)	2.038(10)	0.930(3)
Cl1	0.375(3)	0.288(2)	0.154(2)	3.9(9)	0.070
N1	0.4745(3)	0.2146(2)	-0.0434(2)	1.87(8)	
N2	0.3009(3)	0.1773(2)	-0.1654(2)	1.58(8)	
C1	0.2861(3)	0.3927(3)	-0.1139(3)	1.60(9)	
C2	0.2683(3)	0.4220(3)	-0.0278(3)	1.54(9)	
C3	0.1544(3)	0.4025(2)	-0.0116(3)	1.52(9)	
C4	0.1012(3)	0.3633(2)	-0.0898(3)	1.62(9)	
C5	0.1823(3)	0.3584(3)	-0.1524(3)	1.60(9)	
C6	0.1722(4)	0.1291(3)	0.1190(3)	1.93(9)	
C7	0.0810(3)	0.1402(3)	0.0538(3)	1.82(9)	
C8	0.1073(3)	0.0975(3)	-0.0248(3)	1.74(9)	
C9	0.2176(4)	0.0622(3)	-0.0085(3)	1.73(9)	
C10	0.2586(4)	0.0834(3)	0.0795(3)	1.75(9)	
C11	0.3931(4)	0.4016(3)	-0.1607(3)	2.2(1)	
C12	0.3483(4)	0.4781(3)	0.0286(3)	2.5(1)	
C13	0.0974(4)	0.4216(3)	0.0717(3)	2.15(10)	
C14	-0.0224(4)	0.3417(3)	-0.1061(3)	2.3(1)	
C15	0.1565(4)	0.3440(3)	-0.2510(3)	2.4(1)	
C16	0.1672(4)	0.1452(3)	0.2166(3)	2.9(1)	
C17	-0.0334(4)	0.1745(3)	0.0710(4)	2.9(1)	
C18	0.0212(4)	0.0766(3)	-0.1016(3)	2.5(1)	
C19	0.2770(4)	0.0020(3)	-0.0675(3)	2.6(1)	
C20	0.3692(4)	0.0553(3)	0.1268(4)	3.1(1)	
C21	0.5614(4)	0.2424(3)	0.0120(3)	2.4(1)	
C22	0.6734(4)	0.2429(3)	-0.0068(3)	2.7(1)	
C23	0.6995(4)	0.2104(3)	-0.0873(3)	2.6(1)	
C24	0.6126(4)	0.1789(3)	-0.1463(3)	2.04(10)	
C25	0.5023(3)	0.1817(3)	-0.1228(3)	1.55(9)	
C26	0.4056(3)	0.1521(3)	-0.1847(3)	1.62(9)	
C27	0.4224(4)	0.1021(3)	-0.2582(3)	2.08(10)	
C28	0.3302(4)	0.0799(3)	-0.3172(3)	2.4(1)	
C29	0.2243(4)	0.1081(3)	-0.2991(3)	2.16(10)	
C30	0.2126(3)	0.1552(3)	-0.2230(3)	1.73(9)	
C101	0.1984	0.3878	-0.0792	0.2000	0.001
C102	0.1673	0.1024	0.0438	0.2000	0.001
H1	0.2750	-0.0551	-0.0466	3.0350	
H2	0.1219	0.1011	0.2417	3.4798	

Table 1. Atomic coordinates and B_{iso}/B_{eq} and occupancy (continued)

atom	x	y	z	B_{eq}	occ
H3	-0.0173	0.1278	-0.1231	3.2582	
H4	0.3147	0.4964	0.0802	2.9587	
H5	0.2219	0.3220	-0.2760	2.9111	
H6	-0.0337	0.2864	-0.1320	2.8234	
H7	0.5456	0.2638	0.0689	3.1441	
H8	0.7315	0.2659	0.0352	3.1610	
H9	0.7759	0.2090	-0.1029	3.0462	
H10	0.6306	0.1537	-0.2022	2.5273	
H11	0.4990	0.0826	-0.2677	2.5916	
H12	0.3426	0.0459	-0.3696	2.8855	
H13	0.1576	0.0947	-0.3390	2.5448	
H14	0.1377	0.1734	-0.2096	2.1636	
H15	0.4187	0.3475	-0.1804	2.6446	
H16	0.3814	0.4387	-0.2112	2.6446	
H17	0.4523	0.4260	-0.1211	2.6446	
H18	0.4163	0.4466	0.0467	2.9587	
H19	0.3688	0.5267	-0.0045	2.9587	
H20	0.0999	0.4817	0.0826	2.5987	
H21	0.0226	0.4020	0.0664	2.5987	
H22	0.1388	0.3935	0.1213	2.5987	
H23	-0.0573	0.3408	-0.0496	2.8234	
H24	-0.0622	0.3830	-0.1428	2.8234	
H25	0.1365	0.3976	-0.2798	2.9111	
H26	0.0954	0.3053	-0.2618	2.9111	
H27	0.2409	0.1434	0.2471	3.4798	
H28	0.1331	0.1990	0.2273	3.4798	
H29	-0.0328	0.2014	0.1272	3.7054	
H30	-0.0592	0.2167	0.0262	3.7054	
H31	-0.0896	0.1297	0.0679	3.7054	
H32	0.0579	0.0522	-0.1499	3.2582	
H33	-0.0338	0.0373	-0.0838	3.2582	
H34	0.2403	0.0031	-0.1275	3.0350	
H35	0.3541	0.0189	-0.0713	3.0350	
H36	0.3565	0.0194	0.1766	3.7805	
H37	0.4143	0.0251	0.0883	3.7805	
H38	0.4116	0.1046	0.1496	3.7805	

$B_{eq} = 8/3\ \pi^2(U_{11}(aa^*)^2 + U_{22}(bb^*)^2 + U_{33}(cc^*)^2 + 2U_{12}(aa^*bb^*)\cos\gamma + 2U_{13}(aa^*cc^*)\cos\beta + 2U_{23}(bb^*cc^*)\cos\alpha)$

Table 2. Anisotropic Displacement Parameters

atom	U_{11}	U_{22}	U_{33}	U_{12}	U_{13}	U_{23}
Ce1	0.0149(2)	0.0160(2)	0.0149(2)	-0.00011(9)	-0.00068(10)	0.00037(9)
I1	0.0269(2)	0.0312(3)	0.0182(3)	0.0017(2)	-0.0052(2)	-0.0010(2)
N1	0.020(2)	0.028(2)	0.023(2)	0.001(2)	0.000(2)	-0.002(2)
N2	0.024(2)	0.015(2)	0.021(2)	-0.001(1)	0.003(2)	0.001(1)
C1	0.024(2)	0.016(2)	0.021(2)	-0.001(2)	0.003(2)	0.006(2)
C2	0.024(2)	0.015(2)	0.019(2)	-0.001(2)	-0.004(2)	0.001(2)
C3	0.021(2)	0.016(2)	0.020(2)	0.001(2)	0.001(2)	0.001(2)
C4	0.020(2)	0.013(2)	0.028(2)	0.002(2)	-0.002(2)	0.005(2)
C5	0.025(2)	0.017(2)	0.018(2)	-0.001(2)	-0.002(2)	0.001(2)
C6	0.029(2)	0.020(2)	0.024(2)	-0.006(2)	0.002(2)	0.003(2)
C7	0.020(2)	0.020(2)	0.029(3)	-0.004(2)	0.006(2)	0.004(2)
C8	0.022(2)	0.020(2)	0.023(2)	-0.006(2)	-0.004(2)	0.003(2)
C9	0.027(2)	0.014(2)	0.024(2)	0.000(2)	0.003(2)	0.003(2)
C10	0.028(2)	0.017(2)	0.021(2)	-0.004(2)	-0.002(2)	0.005(2)
C11	0.030(3)	0.028(3)	0.028(3)	-0.003(2)	0.006(2)	0.005(2)
C12	0.038(3)	0.025(3)	0.030(3)	-0.011(2)	-0.005(2)	-0.001(2)
C13	0.032(3)	0.023(2)	0.027(3)	0.006(2)	0.003(2)	-0.001(2)
C14	0.019(2)	0.034(3)	0.035(3)	0.002(2)	-0.005(2)	0.001(2)
C15	0.041(3)	0.027(3)	0.022(3)	0.001(2)	-0.004(2)	0.001(2)
C16	0.044(3)	0.043(3)	0.026(3)	-0.009(2)	0.007(2)	-0.002(2)
C17	0.027(3)	0.036(3)	0.049(3)	0.001(2)	0.011(2)	0.006(2)
C18	0.031(3)	0.033(3)	0.031(3)	-0.011(2)	-0.006(2)	0.009(2)
C19	0.045(3)	0.019(2)	0.035(3)	0.002(2)	0.009(2)	0.003(2)
C20	0.034(3)	0.033(3)	0.049(3)	0.007(2)	-0.008(2)	0.011(2)
C21	0.023(3)	0.046(3)	0.023(3)	0.003(2)	-0.002(2)	-0.009(2)
C22	0.023(3)	0.043(3)	0.035(3)	0.001(2)	-0.005(2)	-0.002(2)
C23	0.020(2)	0.040(3)	0.039(3)	0.004(2)	0.005(2)	0.007(3)
C24	0.025(2)	0.028(2)	0.024(2)	-0.000(2)	0.006(2)	0.003(2)
C25	0.022(2)	0.016(2)	0.021(2)	0.002(2)	0.001(2)	0.003(2)
C26	0.025(2)	0.016(2)	0.020(2)	-0.000(2)	0.002(2)	0.001(2)
C27	0.031(3)	0.024(2)	0.025(2)	-0.002(2)	0.009(2)	-0.001(2)
C28	0.047(3)	0.024(2)	0.022(3)	-0.006(2)	0.009(2)	-0.006(2)
C29	0.035(3)	0.025(2)	0.022(2)	-0.008(2)	-0.002(2)	-0.002(2)
C30	0.020(2)	0.022(2)	0.024(2)	-0.004(2)	-0.002(2)	0.005(2)

The general temperature factor expression:
$\exp(-2\pi^2(a^{*2}U_{11}h^2 + b^{*2}U_{22}k^2 + c^{*2}U_{33}l^2 + 2a^*b^*U_{12}hk + 2a^*c^*U_{13}hl + 2b^*c^*U_{23}kl))$

Table 3. Bond Lengths(Å)

atom	atom	distance	atom	atom	distance
CE1	I1	3.2457(6)	CE1	CL1	2.86(3)
CE1	N1	2.707(3)	CE1	N2	2.633(3)
CE1	C1	2.867(4)	CE1	C2	2.838(4)
CE1	C3	2.786(4)	CE1	C4	2.830(4)
CE1	C5	2.889(4)	CE1	C6	2.868(4)
CE1	C7	2.838(4)	CE1	C8	2.847(4)
CE1	C9	2.835(4)	CE1	C10	2.820(4)
CE1	C101	2.5749(2)	CE1	C102	2.5748(2)
I1	CL1	0.53(4)	N1	C21	1.343(6)
N1	C25	1.370(5)	N2	C26	1.354(5)
N2	C30	1.348(5)	C1	C2	1.411(6)
C1	C5	1.419(6)	C1	C11	1.506(6)
C1	C101	1.203(4)	C2	C3	1.422(6)
C2	C12	1.502(6)	C2	C101	1.211(4)
C3	C4	1.430(6)	C3	C13	1.505(6)
C3	C101	1.206(4)	C4	C5	1.404(6)
C4	C14	1.501(6)	C4	C101	1.209(4)
C5	C15	1.513(6)	C5	C101	1.197(4)
C6	C7	1.410(6)	C6	C10	1.419(6)
C6	C16	1.502(6)	C6	C102	1.207(4)
C7	C8	1.419(6)	C7	C17	1.498(6)
C7	C102	1.199(4)	C8	C9	1.420(6)
C8	C18	1.514(6)	C8	C102	1.210(4)
C9	C10	1.416(6)	C9	C19	1.507(6)
C9	C102	1.204(4)	C10	C20	1.503(6)
C10	C102	1.204(4)	C21	C22	1.378(7)
C22	C23	1.377(7)	C23	C24	1.393(6)
C24	C25	1.381(6)	C25	C26	1.490(6)
C26	C27	1.386(6)	C27	C28	1.394(6)
C28	C29	1.376(6)	C29	C30	1.381(6)

$Cp^*_2Ce(bipy)(I)$ (I = 73%)

EXPERIMENTAL DETAILS

A. Crystal Data

Empirical Formula	$C_{30}H_{58}N_2CeI_{0.73}Cl_{0.27}$
Formula Weight	689.13
Crystal Color, Habit	red, plates
Crystal Dimensions	0.15 X 0.15 X 0.15 mm
Crystal System	monoclinic
Lattice Type	Primitive
Lattice Parameters	a = 10.5878(9)Å
	b = 14.434(1) Å
	c = 18.253(2) Å
	β = 90.085(1)^o
	V = 2789.5(4) Å^3
Space Group	$P2_1/c$ (#14)
Z value	4
D_{calc}	1.641 g/cm^3
F_{000}	1413.12
μ(MoKα)	28.58 cm^{-1}

B. Intensity Measurements

Diffractometer	Bruker SMART CCD
Radiation	MoKα (λ = 0.71069 Å) graphite monochromated
Detector Position	60.00 mm
Exposure Time	10.0 seconds per frame.
Scan Type	ω (0.3 degrees per frame)
$2\theta_{max}$	52.8^o
No. of Reflections Measured (R_{int} = 0.028)	Total: 13534 Unique: 3492
Corrections	Lorentz-polarization
	Absorption (Tmin/max = 0.9)

C. Structure Solution and Refinement

Structure Solution	Direct Methods (SIR97)
Refinement	Full-matrix least-squares
Function Minimized	Σ w (|Fo| - |Fc|)^2
Least Squares Weights	$1/\sigma^2(Fo) = 4Fo^2/\sigma^2(Fo^2)$
p-factor	0.0300
Anomalous Dispersion	All non-hydrogen atoms
No. Observations (I>3.00σ(I))	3654
No. Variables	312
Reflection/Parameter Ratio	11.71
Residuals: R; Rw; Rall	0.033 ; 0.034; 0.067
Goodness of Fit Indicator	1.29
Max Shift/Error in Final Cycle	0.02
Maximum peak in Final Diff. Map	0.52 $e^-/Å^3$
Minimum peak in Final Diff. Map	-0.47 $e^-/Å^3$

Table 1. Atomic coordinates and B_{iso}/B_{eq} and occupancy

atom	x	y	z	B_{eq}	occ
Ce(1)	0.21817(3)	0.21918(2)	0.13262(2)	1.468(6)	
I(1)	0.04423(8)	0.37701(5)	0.06403(5)	2.55(2)	0.731(3)
Cl(1)	0.067(1)	0.3695(8)	0.0867(5)	3.6(3)	0.269
N(1)	0.2370(4)	0.1107(3)	0.2487(2)	1.61(10)	
N(2)	0.0294(4)	0.2189(3)	0.2372(2)	1.87(10)	
C(1)	0.4836(5)	0.2476(4)	0.1521(3)	1.8(1)	
C(2)	0.4525(5)	0.3050(4)	0.0924(3)	2.0(1)	
C(3)	0.3768(5)	0.3785(4)	0.1181(3)	2.1(1)	
C(4)	0.3593(5)	0.3653(4)	0.1942(3)	1.8(1)	
C(5)	0.4269(5)	0.2859(4)	0.2161(2)	1.6(1)	
C(6)	0.2273(6)	0.0346(4)	0.0773(3)	2.2(1)	
C(7)	0.2560(5)	0.0931(4)	0.0178(3)	1.9(1)	
C(8)	0.1480(5)	0.1449(4)	-0.0017(3)	2.0(1)	
C(9)	0.0497(5)	0.1173(4)	0.0467(3)	2.5(1)	
C(10)	0.1004(6)	0.0495(4)	0.0951(3)	2.3(1)	
C(11)	0.5773(5)	0.1692(4)	0.1491(3)	2.7(1)	
C(12)	0.5082(6)	0.2994(4)	0.0169(3)	2.8(1)	
C(13)	0.3470(6)	0.4646(4)	0.0749(3)	3.3(2)	
C(14)	0.2875(6)	0.4302(4)	0.2440(3)	2.8(1)	
C(15)	0.4487(5)	0.2582(4)	0.2945(3)	2.1(1)	
C(16)	0.3077(6)	-0.0439(4)	0.1031(3)	3.1(1)	
C(17)	0.3749(5)	0.0869(4)	-0.0269(3)	2.3(1)	
C(18)	0.1390(5)	0.2086(4)	-0.0660(3)	3.0(1)	
C(19)	-0.0864(6)	0.1441(5)	0.0426(3)	3.8(2)	
C(20)	0.0231(6)	-0.0047(4)	0.1496(3)	3.5(2)	
C(21)	0.3399(5)	0.0575(4)	0.2539(3)	2.2(1)	
C(22)	0.3631(5)	-0.0044(4)	0.3099(3)	2.5(1)	
C(23)	0.2754(7)	-0.0091(4)	0.3647(3)	3.2(1)	
C(24)	0.1696(6)	0.0461(4)	0.3618(3)	2.8(1)	
C(25)	0.1492(5)	0.1033(4)	0.3018(3)	1.8(1)	
C(26)	0.0317(5)	0.1579(4)	0.2922(3)	1.7(1)	
C(27)	-0.0715(5)	0.1433(4)	0.3377(3)	2.5(1)	
C(28)	-0.1786(5)	0.1953(4)	0.3273(3)	2.5(1)	
C(29)	-0.1814(5)	0.2589(4)	0.2718(3)	2.5(1)	
C(30)	-0.0763(6)	0.2685(4)	0.2287(3)	2.3(1)	
C(101)	0.4199	0.3166	0.1548	0.2000	0.001
C(102)	0.1565	0.0875	0.0468	0.2000	0.001
H(1)	0.4459	0.0793	0.0049	2.3439	
H(2)	0.5676	0.1298	0.1925	2.2663	

Table 1. Atomic coordinates and B_{iso}/B_{eq} and occupancy (continued)

atom	x	y	z	B_{eq}	occ
H(3)	0.6613	0.1912	0.1488	2.2663	
H(4)	0.5625	0.1313	0.1076	2.2663	
H(5)	0.5574	0.2469	0.0124	2.9735	
H(6)	0.4420	0.3006	-0.0184	2.9735	
H(7)	0.5605	0.3542	0.0084	2.9735	
H(8)	0.2961	0.4450	0.0349	3.1463	
H(9)	0.4224	0.4895	0.0598	3.1463	
H(10)	0.3013	0.5033	0.1063	3.1463	
H(11)	0.2238	0.3926	0.2686	2.8734	
H(12)	0.3439	0.4524	0.2803	2.8734	
H(13)	0.2504	0.4763	0.2176	2.8734	
H(14)	0.4997	0.2039	0.2947	1.8952	
H(15)	0.3691	0.2438	0.3166	1.8952	
H(16)	0.4885	0.3059	0.3206	1.8952	
H(17)	0.2582	-0.1021	0.1026	3.1069	
H(18)	0.3800	-0.0535	0.0753	3.1069	
H(19)	0.3320	-0.0360	0.1543	3.1069	
H(20)	0.3706	0.0363	-0.0596	2.3439	
H(21)	0.3874	0.1429	-0.0546	2.3439	
H(22)	0.1487	0.1726	-0.1103	2.9213	
H(23)	0.0625	0.2386	-0.0657	2.9213	
H(24)	0.2079	0.2514	-0.0638	2.9213	
H(25)	-0.0953	0.2059	0.0220	3.4237	
H(26)	-0.1299	0.1028	0.0088	3.4237	
H(27)	-0.1251	0.1417	0.0879	3.4237	
H(28)	-0.0379	-0.0411	0.1244	3.7233	
H(29)	0.0770	-0.0465	0.1770	3.7233	
H(30)	-0.0186	0.0345	0.1837	3.7233	
H(31)	0.4029	0.0658	0.2180	1.7688	
H(32)	0.4381	-0.0420	0.3088	2.5736	
H(33)	0.2867	-0.0505	0.4054	3.6724	
H(34)	0.1117	0.0492	0.4015	2.9294	
H(35)	-0.0671	0.0991	0.3765	2.3404	
H(36)	-0.2469	0.1826	0.3587	2.5008	
H(37)	-0.2549	0.2930	0.2633	2.8857	
H(38)	-0.0770	0.3153	0.1912	2.3203	

$B_{eq} = 8/3\ \pi^2(U_{11}(aa^*)^2 + U_{22}(bb^*)^2 + U_{33}(cc^*)^2 + 2U_{12}(aa^*bb^*)\cos\gamma + 2U_{13}(aa^*cc^*)\cos\beta + 2U_{23}(bb^*cc^*)\cos\alpha)$

Table 2. Anisotropic Displacement Parameters

atom	U_{11}	U_{22}	U_{33}	U_{12}	U_{13}	U_{23}
Ce(1)	0.0166(2)	0.0191(2)	0.0200(2)	-0.0003(1)	-0.0003(1)	-0.0013(2)
I(1)	0.0356(4)	0.0272(4)	0.0340(5)	0.0103(3)	0.0003(4)	0.0005(3)
N(1)	0.015(2)	0.024(2)	0.023(2)	-0.000(2)	0.001(2)	-0.003(2)
N(2)	0.020(2)	0.026(2)	0.025(2)	0.002(2)	0.003(2)	-0.005(2)
C(1)	0.016(3)	0.025(3)	0.027(3)	-0.005(2)	0.001(2)	-0.006(2)
C(2)	0.018(3)	0.031(3)	0.026(3)	-0.012(2)	0.003(2)	-0.002(2)
C(3)	0.027(3)	0.023(3)	0.031(3)	-0.010(3)	-0.005(3)	0.004(3)
C(4)	0.020(3)	0.020(3)	0.029(3)	-0.007(2)	-0.002(2)	-0.006(2)
C(5)	0.016(3)	0.026(3)	0.019(3)	-0.006(3)	-0.000(2)	-0.001(3)
C(6)	0.041(4)	0.019(3)	0.022(3)	-0.003(3)	-0.004(3)	-0.005(2)
C(7)	0.029(3)	0.020(3)	0.023(3)	-0.003(2)	0.001(2)	-0.001(2)
C(8)	0.028(3)	0.031(3)	0.017(3)	-0.001(3)	-0.006(2)	-0.006(2)
C(9)	0.019(3)	0.041(4)	0.034(3)	-0.002(3)	-0.003(3)	-0.019(3)
C(10)	0.040(4)	0.024(3)	0.023(3)	-0.014(3)	-0.005(3)	-0.006(3)
C(11)	0.025(4)	0.042(4)	0.037(3)	-0.002(3)	0.001(3)	-0.005(3)
C(12)	0.039(4)	0.038(4)	0.030(3)	-0.011(3)	0.010(3)	0.002(3)
C(13)	0.045(4)	0.031(4)	0.048(4)	-0.012(3)	-0.005(3)	0.006(3)
C(14)	0.034(4)	0.030(3)	0.043(4)	-0.000(3)	0.001(3)	-0.012(3)
C(15)	0.025(3)	0.032(3)	0.024(3)	-0.004(2)	-0.002(2)	-0.003(2)
C(16)	0.061(5)	0.022(3)	0.035(3)	0.006(3)	-0.003(3)	-0.003(3)
C(17)	0.034(4)	0.029(3)	0.026(3)	0.003(3)	-0.001(3)	-0.006(3)
C(18)	0.032(4)	0.047(4)	0.035(3)	0.013(3)	-0.003(3)	-0.002(3)
C(19)	0.029(4)	0.064(5)	0.049(4)	-0.007(3)	0.001(3)	-0.025(4)
C(20)	0.053(5)	0.041(4)	0.040(4)	-0.025(3)	0.007(3)	-0.013(3)
C(21)	0.024(3)	0.032(3)	0.028(3)	-0.004(3)	0.002(2)	0.001(3)
C(22)	0.027(3)	0.034(4)	0.035(3)	0.010(3)	-0.007(3)	0.000(3)
C(23)	0.054(4)	0.043(4)	0.026(3)	0.004(4)	-0.003(3)	0.008(3)
C(24)	0.032(4)	0.043(4)	0.030(3)	0.007(3)	0.007(3)	0.002(3)
C(25)	0.024(3)	0.026(3)	0.021(3)	-0.004(2)	-0.003(2)	-0.003(2)
C(26)	0.021(3)	0.025(3)	0.020(3)	-0.002(2)	-0.004(2)	-0.009(2)
C(27)	0.027(4)	0.038(4)	0.030(3)	-0.009(3)	-0.001(3)	0.001(3)
C(28)	0.021(3)	0.037(4)	0.037(3)	-0.006(3)	0.007(3)	-0.007(3)
C(29)	0.021(3)	0.035(4)	0.039(3)	0.003(3)	0.000(3)	-0.011(3)
C(30)	0.032(4)	0.022(3)	0.031(3)	0.001(3)	0.001(3)	-0.002(3)

The general temperature factor expression:
$\exp(-2\pi^2(a^{*2}U_{11}h^2 + b^{*2}U_{22}k^2 + c^{*2}U_{33}l^2 + 2a^*b^*U_{12}hk + 2a^*c^*U_{13}hl + 2b^*c^*U_{23}kl))$

Table 3. Bond Lengths(Å)

atom	atom	distance	atom	atom	distance
Ce(1)	I(1)	3.185(1)	Ce(1)	Cl(1)	2.82(1)
Ce(1)	N(1)	2.641(4)	Ce(1)	N(2)	2.766(4)
Ce(1)	C(1)	2.862(5)	Ce(1)	C(2)	2.869(5)
Ce(1)	C(3)	2.860(5)	Ce(1)	C(4)	2.818(5)
Ce(1)	C(5)	2.851(5)	Ce(1)	C(6)	2.851(5)
Ce(1)	C(7)	2.805(5)	Ce(1)	C(8)	2.776(5)
Ce(1)	C(9)	2.792(5)	Ce(1)	C(10)	2.831(5)
Ce(1)	C(101)	2.5885(3)	Ce(1)	C(102)	2.5475(3)
I(1)	Cl(1)	0.489(9)	N(1)	C(21)	1.336(7)
N(1)	C(25)	1.349(6)	N(2)	C(26)	1.336(6)
N(2)	C(30)	1.338(7)	C(1)	C(2)	1.406(7)
C(1)	C(5)	1.426(7)	C(1)	C(11)	1.506(8)
C(1)	C(101)	1.204(5)	C(2)	C(3)	1.410(7)
C(2)	C(12)	1.503(7)	C(2)	C(101)	1.202(5)
C(3)	C(4)	1.414(7)	C(3)	C(13)	1.506(8)
C(3)	C(101)	1.206(5)	C(4)	C(5)	1.409(7)
C(4)	C(14)	1.512(7)	C(4)	C(101)	1.193(5)
C(5)	C(15)	1.503(7)	C(5)	C(101)	1.206(5)
C(6)	C(7)	1.409(7)	C(6)	C(10)	1.400(8)
C(6)	C(16)	1.494(8)	C(6)	C(102)	1.205(6)
C(7)	C(8)	1.411(7)	C(7)	C(17)	1.503(7)
C(7)	C(102)	1.183(5)	C(8)	C(9)	1.422(7)
C(8)	C(18)	1.494(7)	C(8)	C(102)	1.215(5)
C(9)	C(10)	1.424(8)	C(9)	C(19)	1.494(8)
C(9)	C(102)	1.210(6)	C(10)	C(20)	1.508(8)
C(10)	C(102)	1.197(5)	C(21)	C(22)	1.379(7)
C(22)	C(23)	1.368(8)	C(23)	C(24)	1.375(8)
C(24)	C(25)	1.388(7)	C(25)	C(26)	1.483(7)
C(26)	C(27)	1.389(7)	C(27)	C(28)	1.373(8)
C(28)	C(29)	1.366(8)	C(29)	C(30)	1.371(8)

[Cp*$_2$Ce(2,2',6',2''-terpyridine)][OTf]

EXPERIMENTAL DETAILS

A. Crystal Data

Empirical Formula	C36 H41 Ce F3 N3 O3 S
Formula Weight	792.90
Crystal Color, Habit	red, block
Crystal Dimensions	0.09 x 0.08 x 0.08 mm
Crystal System	Monoclinic
Lattice Type	primitive
Lattice Parameters	a = 11.468(7) Å b = 15.827(10) Å c = 19.298(12) Å α= 90 ^{o} β= 94.212(10) ^{o} γ = 90^o V = 3493(4) Å^3
Space Group	P 21/c
Z value	4
D_{calc}	1.508 g/cm^3
F_{000}	1612
μ(MoK)	1.42 cm^{-1}

B. Intensity Measurements

Diffractometer	Bruker APEX
Radiation	MoK(λ = 0.71073 Å) graphite monochromated
Detector Position	60.00 mm
Exposure Time	20 seconds per frame.
Scan Type	ω (0.3 degrees per frame)
θ_{max}	21.96^o
No. of Reflections Measured	Total: 12277 Unique: 4260 (R_{int} = 0.0868)
Corrections	Lorentz-polarization Absorption (Tmax = 1.00, Tmin = 0.57)

C. Structure Solution and Refinement

Structure Solution	direct (SHELXS-97 (Sheldrick, 1990))
Refinement	Full-matrix least-squares
Function Minimized	$\Sigma w(\|F_o\|^2 - \|F_c\|^2)^2$
Least Squares Weighting scheme	$w = 1/[\sigma^2(F_o^2) + (qP)^2 + 0.000P]$ where $P = [F_o^2 + 2F_c^2]/3$
q-factor	0.063
Anomalous Dispersion	All non-hydrogen atoms
No. Observations (I>2.00σ(I))	2833
No. Variables	434
Reflection/Parameter Ratio	9.81
Residuals: R; wR_2; Rall	0.0499; 0.1081; 0.0928
Goodness of Fit Indicator	0.974
Max Shift/Error in Final Cycle	0.004
Maximum peak in Final Diff. Map	0.728 $e^-/Å^3$
Minimum peak in Final Diff. Map	-1.416 $e^-/Å^3$

Table 1. Atomic coordinates and U_{iso}/U_{eq} and occupancy

atom	x	y	z	U_{eq}	Occupancy
Ce1	0.2677(1)	0.8073(1)	0.8474(1)	0.023(1)	1
S1	0.2471(2)	1.3600(2)	0.9769(1)	0.037(1)	1
F1	0.1581(8)	1.2169(4)	1.0130(4)	0.106(3)	1
F2	0.2584(7)	1.2101(4)	0.9263(4)	0.099(3)	1
F3	0.0866(8)	1.2618(6)	0.9192(5)	0.132(4)	1
O1	0.2725(7)	1.3915(4)	0.9115(4)	0.075(3)	1
O2	0.1562(7)	1.4052(4)	1.0061(5)	0.093(3)	1
O3	0.3427(9)	1.3415(6)	1.0235(6)	0.137(5)	1
N1	0.0928(7)	0.8849(4)	0.7818(4)	0.039(2)	1
N2	0.3002(7)	0.8692(4)	0.7233(4)	0.030(2)	1
N3	0.4709(6)	0.7888(4)	0.8016(4)	0.024(2)	1
C1	0.2341(8)	0.9578(6)	0.9218(5)	0.038(3)	1
C2	0.3445(9)	0.9678(6)	0.8954(5)	0.040(3)	1
C3	0.4229(8)	0.9112(6)	0.9319(5)	0.035(2)	1
C4	0.3606(10)	0.8627(6)	0.9780(5)	0.044(3)	1
C5	0.2417(9)	0.8916(6)	0.9714(5)	0.039(3)	1
C6	0.1331(9)	1.0170(6)	0.9088(7)	0.075(4)	1
C7	0.3786(10)	1.0337(6)	0.8450(6)	0.063(3)	1
C8	0.5556(7)	0.9133(7)	0.9300(6)	0.057(3)	1
C9	0.4095(11)	0.7997(7)	1.0307(5)	0.074(4)	1
C10	0.1463(11)	0.8658(7)	1.0177(6)	0.079(4)	1
C11	0.2690(9)	0.6427(6)	0.7919(5)	0.038(3)	1
C12	0.1555(8)	0.6722(6)	0.7734(5)	0.037(3)	1
C13	0.0979(7)	0.6757(5)	0.8364(5)	0.032(2)	1
C14	0.1790(8)	0.6519(5)	0.8917(4)	0.029(2)	1
C15	0.2857(8)	0.6310(5)	0.8643(5)	0.030(2)	1
C16	0.3566(11)	0.6169(7)	0.7398(7)	0.086(5)	1
C17	0.0979(11)	0.6849(7)	0.7016(5)	0.078(4)	1
C18	-0.0319(8)	0.6882(6)	0.8398(7)	0.061(3)	1
C19	0.1478(9)	0.6367(6)	0.9652(5)	0.046(3)	1
C20	0.3866(8)	0.5916(6)	0.9060(6)	0.059(3)	1
C21	-0.0093(9)	0.8887(6)	0.8103(6)	0.053(3)	1
C22	-0.1102(9)	0.9235(7)	0.7774(7)	0.060(3)	1
C23	-0.1044(10)	0.9579(7)	0.7126(8)	0.063(4)	1
C24	0.0004(10)	0.9546(6)	0.6820(6)	0.060(3)	1
C25	0.0983(9)	0.9192(6)	0.7174(5)	0.039(3)	1
C26	0.2142(9)	0.9166(6)	0.6884(5)	0.036(2)	1
C27	0.2375(10)	0.9628(6)	0.6293(5)	0.045(3)	1
C28	0.3463(11)	0.9590(7)	0.6063(5)	0.056(3)	1
C29	0.4331(9)	0.9089(6)	0.6390(5)	0.040(3)	1

C30	0.4065(8)	0.8648(5)	0.6989(5)	0.031(2)	1
C31	0.4965(7)	0.8133(5)	0.7379(5)	0.031(2)	1
C32	0.6002(8)	0.7899(6)	0.7102(6)	0.045(3)	1
C33	0.6793(9)	0.7421(7)	0.7499(6)	0.049(3)	1
C34	0.6573(8)	0.7170(6)	0.8158(6)	0.041(3)	1
C35	0.5537(8)	0.7425(6)	0.8395(5)	0.037(2)	1
C40	0.1822(12)	1.2587(7)	0.9559(6)	0.056(3)	1

U_{eq} is defined as one third of the orthogonalized U_{ij} tensor

Table 2. Anisotropic Displacement Parameters

atom	U_{11}	U_{22}	U_{33}	U_{12}	U_{13}	U_{23}
Ce1	0.022(1)	0.028(1)	0.018(1)	-0.001(1)	0.001(1)	0.001(1)
S1	0.038(2)	0.045(2)	0.028(2)	-0.002(1)	0.001(1)	-0.010(1)
F1	0.158(8)	0.068(5)	0.103(7)	-0.002(4)	0.077(6)	-0.033(5)
F2	0.123(7)	0.056(5)	0.128(7)	-0.035(4)	0.073(6)	-0.012(4)
F3	0.098(7)	0.128(7)	0.158(9)	-0.033(6)	-0.068(7)	-0.044(6)
O1	0.124(7)	0.053(5)	0.054(5)	0.005(4)	0.044(5)	-0.017(5)
O2	0.101(7)	0.048(5)	0.140(8)	-0.048(5)	0.075(6)	-0.018(5)
O3	0.136(9)	0.093(7)	0.164(11)	0.031(7)	-0.118(8)	-0.017(6)
N1	0.028(5)	0.028(5)	0.058(6)	-0.006(4)	-0.005(5)	0.001(4)
N2	0.037(5)	0.033(5)	0.019(4)	0.006(4)	-0.010(4)	-0.005(4)
N3	0.024(4)	0.024(4)	0.024(4)	0.007(3)	0.002(3)	-0.002(3)
C1	0.040(6)	0.036(6)	0.039(7)	-0.008(5)	0.007(5)	-0.006(5)
C2	0.063(7)	0.024(6)	0.034(6)	-0.015(5)	0.016(6)	-0.019(5)
C3	0.030(6)	0.042(6)	0.032(6)	-0.017(5)	0.001(5)	-0.003(5)
C4	0.063(8)	0.049(7)	0.017(6)	-0.022(5)	-0.013(5)	-0.007(6)
C5	0.039(7)	0.052(7)	0.028(6)	-0.021(5)	0.016(5)	-0.014(5)
C6	0.047(7)	0.045(7)	0.131(12)	-0.031(7)	-0.002(8)	0.014(6)
C7	0.086(9)	0.035(6)	0.070(9)	0.002(6)	0.017(7)	-0.017(6)
C8	0.026(6)	0.066(7)	0.078(9)	-0.040(7)	-0.006(6)	-0.014(5)
C9	0.119(11)	0.074(8)	0.022(6)	0.008(6)	-0.040(7)	0.000(8)
C10	0.098(10)	0.084(9)	0.062(9)	-0.039(7)	0.054(8)	-0.032(8)
C11	0.048(7)	0.030(6)	0.037(7)	-0.020(5)	0.019(6)	-0.013(5)
C12	0.039(6)	0.045(7)	0.026(6)	-0.001(5)	-0.004(5)	-0.012(5)
C13	0.017(5)	0.032(6)	0.045(6)	0.003(5)	0.001(5)	-0.008(4)
C14	0.035(6)	0.032(5)	0.020(5)	0.004(4)	-0.004(5)	-0.004(5)
C15	0.027(6)	0.017(5)	0.044(7)	0.000(4)	-0.005(5)	0.000(4)
C16	0.096(10)	0.076(9)	0.096(11)	-0.052(8)	0.066(9)	-0.038(7)
C17	0.105(10)	0.091(9)	0.032(7)	0.015(6)	-0.023(7)	-0.062(8)
C18	0.029(6)	0.051(7)	0.102(10)	0.013(7)	-0.002(6)	0.001(6)
C19	0.057(7)	0.046(7)	0.037(7)	0.016(5)	0.012(6)	-0.012(5)
C20	0.041(7)	0.038(6)	0.097(10)	0.015(6)	-0.004(7)	0.005(5)
C21	0.040(7)	0.046(7)	0.073(9)	-0.009(6)	0.002(7)	-0.005(6)
C22	0.027(7)	0.047(7)	0.102(11)	-0.011(7)	-0.008(7)	0.012(6)
C23	0.030(7)	0.048(7)	0.106(12)	0.002(8)	-0.027(7)	0.012(6)
C24	0.069(9)	0.040(7)	0.065(8)	0.010(6)	-0.041(7)	0.011(6)
C25	0.051(7)	0.025(5)	0.039(7)	0.006(5)	-0.015(6)	0.002(5)
C26	0.053(7)	0.030(6)	0.024(6)	-0.001(5)	-0.012(5)	-0.002(5)
C27	0.067(8)	0.035(6)	0.030(7)	0.005(5)	-0.013(6)	0.002(6)
C28	0.090(10)	0.050(7)	0.028(7)	0.010(5)	-0.002(7)	-0.019(7)
C29	0.045(7)	0.044(6)	0.031(6)	-0.001(5)	0.009(5)	-0.006(5)

C30	0.036(6)	0.035(6)	0.024(6)	-0.006(5)	0.008(5)	-0.002(5)
C31	0.027(5)	0.036(6)	0.031(6)	-0.001(5)	0.003(5)	0.002(5)
C32	0.030(6)	0.058(7)	0.050(7)	-0.006(6)	0.021(6)	-0.005(5)
C33	0.020(6)	0.073(8)	0.055(8)	-0.012(6)	0.009(6)	-0.002(6)
C34	0.022(6)	0.047(7)	0.053(8)	0.003(5)	0.005(5)	0.000(5)
C35	0.036(6)	0.039(6)	0.036(6)	-0.006(5)	0.001(5)	0.001(5)
C40	0.084(10)	0.035(7)	0.053(8)	-0.021(6)	0.026(8)	-0.013(7)

The general temperature factor expression:

$\exp(-2\Pi^2(a^{*2}U_{11}h^2 + b^{*2}U_{22}k^2 + c^{*2}U_{33}l^2 + 2a^*b^*U_{12}hk + 2a^*c^*U_{13}\,hl + 2b^*c^*U_{23}kl))$

[Cp^*_2Ce(2,2'-bipyridine)][BPh_4]

EXPERIMENTAL DETAILS

A. Crystal Data

Empirical Formula	$GdC_{54}N_2H_{58}B$
Formula Weight	903.13
Crystal Color, Habit	yellow, plate
Crystal Dimensions	0.67 X 0.28 X 0.27 mm
Crystal System	monoclinic
Lattice Type	Primitive
Lattice Parameters	a = 12.331(2)Å
	b = 14.835(3) Å
	c = 24.337(5) Å
	β = 90.229(3)^o
	V = 4451(1) Å^3
Space Group	$P2_1/n$ (#14)
Z value	4
D_{calc}	1.347 g/cm^3
F_{000}	1860.00
μ(MoKα)	15.32 cm^{-1}

B. Intensity Measurements

Diffractometer	Bruker SMART CCD
Radiation	MoKα (λ = 0.71069 Å)
	graphite monochromated
Detector Position	60.00 mm
Exposure Time	20.0 seconds per frame.
Scan Type	ω (0.3 degrees per frame)
$2\theta_{max}$	52.8^o
No. of Reflections Measured	Total: 21600
	Unique: 6244 (R_{int} = 0.023)
Corrections	Lorentz-polarization
Absorption	(Tmax = 1.00 Tmin = 0.70)

C. Structure Solution and Refinement

Structure Solution	Direct Methods (SIR92)
Refinement	Full-matrix least-squares
Function Minimized	Σ w (|Fo| - |Fc|)^2
Least Squares Weights	$1/\sigma^2(Fo) = 4Fo^2/\sigma^2(Fo^2)$
p-factor	0.0300
Anomalous Dispersion	All non-hydrogen atoms
No. Observations (I>3.00σ(I))	6363
No. Variables	523
Reflection/Parameter Ratio	12.17
Residuals: R; Rw; Rall	0.025 ; 0.032; 0.039
Goodness of Fit Indicator	1.43
Max Shift/Error in Final Cycle	0.00
Maximum peak in Final Diff. Map	0.96 $e^-/Å^3$
Minimum peak in Final Diff. Map	-0.31 $e^-/Å^3$

Table 1. Atomic coordinates and B_{iso}/B_{eq} and occupancy

atom	x	y	z	B_{eq}	occ
Gd(1)	-0.24536(1)	0.375078(9)	0.120082(6)	1.565(3)	
N(1)	-0.2288(2)	0.2193(2)	0.0900(1)	1.94(5)	
N(2)	-0.0903(2)	0.2976(2)	0.1615(1)	1.77(5)	
C(1)	-0.0870(2)	0.4646(2)	0.0685(1)	2.54(7)	
C(2)	-0.1250(3)	0.4017(2)	0.0300(1)	2.57(7)	
C(3)	-0.2323(3)	0.4266(2)	0.0149(1)	2.38(7)	
C(4)	-0.2599(2)	0.5049(2)	0.0446(1)	2.15(7)	
C(5)	-0.1704(3)	0.5287(2)	0.0782(1)	2.36(7)	
C(6)	-0.4506(2)	0.3587(2)	0.1543(1)	2.20(7)	
C(7)	-0.4124(2)	0.4423(2)	0.1763(1)	2.23(7)	
C(8)	-0.3316(2)	0.4225(2)	0.2159(1)	2.05(7)	
C(9)	-0.3207(2)	0.3274(2)	0.2192(1)	1.78(6)	
C(10)	-0.3944(2)	0.2881(2)	0.1813(1)	1.89(6)	
C(11)	0.0277(3)	0.4694(3)	0.0901(2)	4.6(1)	
C(12)	-0.0595(3)	0.3264(3)	0.0053(2)	4.4(1)	
C(13)	-0.3018(3)	0.3849(3)	-0.0294(2)	3.87(9)	
C(14)	-0.3614(3)	0.5601(2)	0.0352(2)	3.42(9)	
C(15)	-0.1630(4)	0.6125(2)	0.1140(2)	3.95(10)	
C(16)	-0.5411(3)	0.3490(3)	0.1128(2)	3.46(9)	
C(17)	-0.4657(3)	0.5328(2)	0.1671(2)	3.35(8)	
C(18)	-0.2751(3)	0.4905(2)	0.2522(1)	2.92(8)	
C(19)	-0.2571(3)	0.2745(2)	0.2613(1)	2.36(7)	
C(20)	-0.4157(2)	0.1885(2)	0.1763(1)	2.52(7)	
C(21)	-0.2995(3)	0.1826(2)	0.0541(1)	2.44(7)	
C(22)	-0.2966(3)	0.0935(2)	0.0390(1)	2.63(7)	
C(23)	-0.2179(3)	0.0391(2)	0.0614(1)	2.76(8)	
C(24)	-0.1439(3)	0.0747(2)	0.0978(1)	2.42(7)	
C(25)	-0.1519(2)	0.1652(2)	0.1122(1)	1.74(6)	
C(26)	-0.0792(2)	0.2076(2)	0.1536(1)	1.65(6)	
C(27)	-0.0047(2)	0.1582(2)	0.1847(1)	2.22(7)	
C(28)	0.0572(2)	0.2005(2)	0.2244(1)	2.33(7)	
C(29)	0.0467(2)	0.2923(2)	0.2319(1)	2.31(7)	
C(30)	-0.0271(2)	0.3381(2)	0.1996(1)	2.08(7)	
C(31)	0.2920(2)	0.0661(2)	0.1943(1)	2.43(7)	
C(32)	0.2925(3)	0.0224(3)	0.2455(2)	3.48(9)	
C(33)	0.3054(3)	0.0682(4)	0.2950(2)	4.9(1)	
C(34)	0.3237(3)	0.1595(4)	0.2952(2)	5.2(1)	
C(35)	0.3262(3)	0.2047(3)	0.2456(2)	4.6(1)	
C(36)	0.3094(3)	0.1594(2)	0.1966(2)	3.23(8)	

Table 1. Atomic coordinates and B_{iso}/B_{eq} and occupancy (continued)

atom	x	y	z	B_{eq}	occ
C(37)	0.2948(2)	0.0763(2)	0.0836(1)	1.96(7)	
C(38)	0.3859(2)	0.0779(2)	0.0499(1)	2.06(7)	
C(39)	0.3967(3)	0.1358(2)	0.0050(1)	2.43(7)	
C(40)	0.3159(3)	0.1965(2)	-0.0072(1)	2.96(8)	
C(41)	0.2248(3)	0.1986(2)	0.0252(2)	3.44(9)	
C(42)	0.2146(3)	0.1401(2)	0.0693(2)	3.04(8)	
C(43)	0.1565(2)	-0.0401(2)	0.1308(1)	1.88(6)	
C(44)	0.0952(3)	-0.0711(2)	0.1750(1)	2.43(7)	
C(45)	0.0007(3)	-0.1220(2)	0.1677(2)	3.42(8)	
C(46)	-0.0370(3)	-0.1418(2)	0.1156(2)	3.36(9)	
C(47)	0.0198(3)	-0.1113(2)	0.0712(2)	3.10(8)	
C(48)	0.1138(2)	-0.0606(2)	0.0789(1)	2.44(7)	
C(49)	0.3694(2)	-0.0717(2)	0.1362(1)	1.86(6)	
C(50)	0.4791(2)	-0.0505(2)	0.1467(1)	2.11(7)	
C(51)	0.5604(2)	-0.1142(2)	0.1445(1)	2.14(7)	
C(52)	0.5367(3)	-0.2043(2)	0.1340(1)	2.27(7)	
C(53)	0.4295(3)	-0.2281(2)	0.1249(1)	2.38(7)	
C(54)	0.3495(2)	-0.1627(2)	0.1249(1)	2.18(7)	
C(101)	-0.1749	0.4653	0.0472	0.2000	0.001
C(102)	-0.3820	0.3678	0.1894	0.2000	0.001
B(1)	0.2771(3)	0.0090(2)	0.1365(2)	1.87(7)	
H(1)	0.0460	0.4141	0.1075	5.5384	
H(2)	0.0760	0.4798	0.0604	5.5384	
H(3)	0.0338	0.5173	0.1158	5.5384	
H(4)	-0.0353	0.2869	0.0334	5.2918	
H(5)	-0.1039	0.2934	-0.0200	5.2918	
H(6)	0.0009	0.3504	-0.0137	5.2918	
H(7)	-0.3700	0.3681	-0.0144	4.6450	
H(8)	-0.3128	0.4271	-0.0582	4.6450	
H(9)	-0.2666	0.3328	-0.0435	4.6450	
H(10)	-0.3619	0.6097	0.0600	4.0993	
H(11)	-0.3624	0.5818	-0.0015	4.0993	
H(12)	-0.4232	0.5235	0.0414	4.0993	
H(13)	-0.0948	0.6130	0.1324	4.7131	
H(14)	-0.1694	0.6645	0.0916	4.7131	
H(15)	-0.2195	0.6116	0.1403	4.7131	
H(16)	-0.6059	0.3737	0.1274	4.1291	
H(17)	-0.5223	0.3807	0.0802	4.1291	
H(18)	-0.5517	0.2872	0.1045	4.1291	

Table 1. Atomic coordinates and B_{iso}/B_{eq} and occupancy (continued)

atom	x	y	z	B_{eq}	occ
H(19)	-0.4121	0.5761	0.1578	3.9884	
H(20)	-0.5171	0.5282	0.1381	3.9884	
H(21)	-0.5015	0.5511	0.1998	3.9884	
H(22)	-0.2244	0.4606	0.2753	3.5327	
H(23)	-0.2383	0.5333	0.2300	3.5327	
H(24)	-0.3273	0.5207	0.2742	3.5327	
H(25)	-0.3056	0.2442	0.2851	2.8206	
H(26)	-0.2125	0.2318	0.2431	2.8206	
H(27)	-0.2129	0.3146	0.2820	2.8206	
H(28)	-0.4434	0.1665	0.2103	3.0257	
H(29)	-0.4674	0.1782	0.1480	3.0257	
H(30)	-0.3502	0.1580	0.1679	3.0257	
H(31)	-0.3539	0.2201	0.0384	2.9210	
H(32)	-0.3481	0.0697	0.0137	3.1667	
H(33)	-0.2142	-0.0229	0.0519	3.2969	
H(34)	-0.0881	0.0380	0.1128	2.8958	
H(35)	0.0033	0.0953	0.1785	2.6498	
H(36)	0.1066	0.1667	0.2464	2.8747	
H(37)	0.0892	0.3232	0.2587	2.7538	
H(38)	-0.0334	0.4016	0.2042	2.5164	
H(39)	0.2833	-0.0412	0.2464	4.1828	
H(40)	0.3016	0.0360	0.3287	5.8553	
H(41)	0.3347	0.1908	0.3287	6.3090	
H(42)	0.3395	0.2677	0.2452	5.5718	
H(43)	0.3095	0.1928	0.1633	3.8504	
H(44)	0.4436	0.0374	0.0579	2.4709	
H(45)	0.4601	0.1333	-0.0170	2.9252	
H(46)	0.3228	0.2364	-0.0375	3.5382	
H(47)	0.1685	0.2405	0.0173	4.0914	
H(48)	0.1506	0.1430	0.0908	3.6488	
H(49)	0.1184	-0.0572	0.2113	2.9189	
H(50)	-0.0377	-0.1432	0.1988	4.0812	
H(51)	-0.1015	-0.1760	0.1108	4.0622	
H(52)	-0.0050	-0.1244	0.0349	3.7096	
H(53)	0.1509	-0.0391	0.0474	2.9260	
H(54)	0.4976	0.0099	0.1556	2.5286	
H(55)	0.6335	-0.0966	0.1503	2.5889	
H(56)	0.5925	-0.2482	0.1332	2.6994	
H(57)	0.4108	-0.2894	0.1185	2.8608	

Table 1. Atomic coordinates and B_{iso}/B_{eq} and occupancy (continued)

atom	x	y	z	B_{eq}	occ
H(58)	0.2772	-0.1805	0.1167	2.6195	

$B_{eq} = 8/3\ \pi^2(U_{11}(aa^*)^2 + U_{22}(bb^*)^2 + U_{33}(cc^*)^2 + 2U_{12}(aa^*bb^*)\cos\gamma + 2U_{13}(aa^*cc^*)\cos\beta + 2U_{23}(bb^*cc^*)\cos\alpha)$

Table 2. Anisotropic Displacement Parameters

atom	U_{11}	U_{22}	U_{33}	U_{12}	U_{13}	U_{23}
Gd(1)	0.02272(8)	0.01520(8)	0.02153(9)	0.00221(6)	-0.00142(5)	0.00006(7)
N(1)	0.028(1)	0.021(1)	0.025(1)	0.001(1)	0.001(1)	-0.003(1)
N(2)	0.024(1)	0.020(1)	0.023(1)	0.0011(10)	-0.001(1)	0.001(1)
C(1)	0.025(2)	0.039(2)	0.032(2)	-0.008(1)	-0.003(1)	0.016(2)
C(2)	0.041(2)	0.029(2)	0.027(2)	0.003(1)	0.011(2)	0.008(1)
C(3)	0.042(2)	0.028(2)	0.020(2)	-0.004(1)	-0.003(1)	0.003(1)
C(4)	0.034(2)	0.021(2)	0.027(2)	0.001(1)	-0.005(1)	0.006(1)
C(5)	0.044(2)	0.020(2)	0.026(2)	-0.009(1)	-0.003(1)	0.003(1)
C(6)	0.021(2)	0.030(2)	0.033(2)	0.003(1)	0.000(1)	-0.000(1)
C(7)	0.031(2)	0.024(2)	0.029(2)	0.010(1)	0.006(1)	0.002(1)
C(8)	0.033(2)	0.022(2)	0.023(2)	0.003(1)	0.004(1)	-0.003(1)
C(9)	0.023(2)	0.021(2)	0.023(2)	0.004(1)	0.005(1)	0.004(1)
C(10)	0.021(1)	0.021(2)	0.030(2)	-0.001(1)	0.005(1)	0.001(1)
C(11)	0.037(2)	0.077(3)	0.060(3)	-0.014(2)	-0.010(2)	0.033(2)
C(12)	0.067(3)	0.047(2)	0.054(3)	0.017(2)	0.031(2)	0.013(2)
C(13)	0.071(3)	0.046(2)	0.030(2)	-0.010(2)	-0.012(2)	-0.003(2)
C(14)	0.050(2)	0.036(2)	0.045(2)	0.009(2)	-0.008(2)	0.014(2)
C(15)	0.076(3)	0.031(2)	0.043(2)	-0.019(2)	0.001(2)	-0.002(2)
C(16)	0.032(2)	0.049(2)	0.050(2)	-0.001(2)	-0.011(2)	0.008(2)
C(17)	0.050(2)	0.032(2)	0.045(2)	0.023(2)	0.008(2)	0.004(2)
C(18)	0.050(2)	0.029(2)	0.032(2)	-0.004(2)	-0.000(2)	-0.007(2)
C(19)	0.030(2)	0.034(2)	0.026(2)	0.003(1)	0.003(1)	0.005(2)
C(20)	0.028(2)	0.026(2)	0.041(2)	-0.005(1)	0.006(1)	0.000(2)
C(21)	0.033(2)	0.028(2)	0.031(2)	0.001(1)	-0.002(1)	-0.004(1)
C(22)	0.039(2)	0.030(2)	0.032(2)	-0.005(1)	0.001(2)	-0.011(1)
C(23)	0.047(2)	0.019(2)	0.038(2)	-0.001(1)	0.004(2)	-0.007(2)
C(24)	0.040(2)	0.020(2)	0.032(2)	0.005(1)	0.002(1)	-0.004(1)
C(25)	0.023(2)	0.021(1)	0.022(2)	0.003(1)	0.006(1)	0.001(1)
C(26)	0.020(1)	0.020(2)	0.022(2)	0.003(1)	0.004(1)	0.002(1)
C(27)	0.026(2)	0.025(2)	0.033(2)	0.006(1)	0.004(1)	0.006(1)
C(28)	0.019(2)	0.040(2)	0.030(2)	0.004(1)	0.002(1)	0.011(2)
C(29)	0.024(2)	0.038(2)	0.025(2)	-0.004(1)	-0.000(1)	0.005(1)
C(30)	0.029(2)	0.025(2)	0.025(2)	-0.003(1)	-0.002(1)	-0.001(1)
C(31)	0.022(2)	0.034(2)	0.036(2)	0.005(1)	-0.001(1)	-0.010(2)
C(32)	0.047(2)	0.053(2)	0.032(2)	0.021(2)	-0.011(2)	-0.010(2)
C(33)	0.056(3)	0.094(4)	0.036(2)	0.035(3)	-0.015(2)	-0.023(2)
C(34)	0.036(2)	0.101(4)	0.063(3)	0.019(2)	-0.018(2)	-0.054(3)
C(35)	0.027(2)	0.057(3)	0.092(4)	-0.002(2)	0.000(2)	-0.048(3)
C(36)	0.025(2)	0.038(2)	0.060(3)	-0.004(1)	0.006(2)	-0.022(2)

Table 2. Anisotropic Displacement Parameters (continued)

atom	U_{11}	U_{22}	U_{33}	U_{12}	U_{13}	U_{23}
C(37)	0.026(2)	0.017(2)	0.031(2)	-0.001(1)	-0.002(1)	-0.005(1)
C(38)	0.029(2)	0.022(2)	0.027(2)	-0.001(1)	-0.002(1)	-0.001(1)
C(39)	0.034(2)	0.028(2)	0.030(2)	-0.004(1)	0.001(1)	-0.002(1)
C(40)	0.047(2)	0.028(2)	0.037(2)	-0.002(2)	0.001(2)	0.009(2)
C(41)	0.039(2)	0.033(2)	0.058(3)	0.010(2)	0.003(2)	0.014(2)
C(42)	0.030(2)	0.035(2)	0.050(2)	0.005(1)	0.009(2)	0.009(2)
C(43)	0.025(2)	0.018(2)	0.028(2)	0.005(1)	0.004(1)	0.001(1)
C(44)	0.035(2)	0.023(2)	0.034(2)	0.007(1)	0.008(1)	0.005(1)
C(45)	0.034(2)	0.028(2)	0.068(3)	0.002(2)	0.019(2)	0.016(2)
C(46)	0.028(2)	0.023(2)	0.076(3)	-0.005(1)	0.002(2)	-0.002(2)
C(47)	0.029(2)	0.033(2)	0.055(2)	0.001(1)	-0.008(2)	-0.018(2)
C(48)	0.028(2)	0.033(2)	0.032(2)	-0.001(1)	0.007(1)	-0.005(2)
C(49)	0.030(2)	0.023(2)	0.018(2)	-0.000(1)	0.002(1)	0.000(1)
C(50)	0.033(2)	0.019(2)	0.028(2)	-0.001(1)	-0.003(1)	0.001(1)
C(51)	0.024(2)	0.033(2)	0.024(2)	-0.002(1)	-0.001(1)	0.002(1)
C(52)	0.035(2)	0.029(2)	0.022(2)	0.012(1)	-0.002(1)	-0.001(1)
C(53)	0.043(2)	0.022(2)	0.026(2)	0.004(1)	-0.006(1)	-0.005(1)
C(54)	0.030(2)	0.026(2)	0.027(2)	-0.002(1)	-0.005(1)	-0.003(1)
B(1)	0.024(2)	0.021(2)	0.026(2)	0.000(1)	0.000(1)	-0.003(2)

The general temperature factor expression:
$\exp(-2\pi^2(a^{*2}U_{11}h^2 + b^{*2}U_{22}k^2 + c^{*2}U_{33}l^2 + 2a^*b^*U_{12}hk + 2a^*c^*U_{13}hl + 2b^*c^*U_{23}kl))$

Cp^*_2Ce(2,2'-bipyridine)

EXPERIMENTAL DETAILS

A. Crystal Data

Empirical Formula	$H_{38}C_{30}N_2Ce$
Formula Weight	566.76
Crystal Color, Habit	dark red, block
Crystal Dimensions	0.02 X 0.01 X 0.01 mm
Crystal System	triclinic
Lattice Type	Primitive
Lattice Parameters	a = 9.4379(5)Å b = 9.5732(5) Å c = 15.6479(9) Å α = 81.125(1)^o β = 82.073(1)^o γ = 70.851(1)^o V = 1313.8(1) Å^3
Space Group	P-1(#2)
Z value	2
D_{calc}	1.433 g/cm^3
F_{000}	580.00
μ(MoKα)	17.51 cm^{-1}

B. Intensity Measurements

Diffractometer	Bruker APEX CCD
Radiation	MoKα (λ = 0.71069 Å) graphite monochromated
Detector Position	60.00 mm
Exposure Time	10.0 seconds per frame.
Scan Type	ω (0.3 degrees per frame)
$2\theta_{max}$	52.8^o
No. of Reflections Measured (R_{int} = 0.014)	Total: 8481 Unique: 5320
Corrections Absorption (Tmin/max =0.79)	Lorentz-polarization

C. Structure Solution and Refinement

Structure Solution	Direct Methods (SIR92)
Refinement	Full-matrix least-squares
Function Minimized	Σ w (|Fo| - |Fc|)^2
p-factor	0.0300
Anomalous Dispersion	All non-hydrogen atoms
No. Observations (I>3.00σ(I))	4540
No. Variables	298
Reflection/Parameter Ratio	15.23
Residuals: R; Rw; Rall	0.028 ; 0.035; 0.032
Goodness of Fit Indicator	1.56
Max Shift/Error in Final Cycle	0.00
Maximum peak in Final Diff. Map	0.82 e^-/Å^3
Minimum peak in Final Diff. Map	-0.32 e^-/Å^3

Table 1. Atomic coordinates and B_{iso}/B_{eq} and occupancy

atom	x	y	z	B_{eq}	occ
Ce(1)	0.37394(2)	0.25850(2)	0.25327(1)	2.560(4)	
N(1)	0.2454(3)	0.0682(3)	0.3098(2)	2.75(6)	
N(2)	0.2163(3)	0.2170(3)	0.1505(2)	2.87(6)	
C(1)	0.6585(4)	0.2471(4)	0.1712(2)	3.05(7)	
C(2)	0.6837(4)	0.1811(4)	0.2571(2)	3.21(7)	
C(3)	0.6524(4)	0.0453(4)	0.2678(2)	3.18(7)	
C(4)	0.6101(4)	0.0243(4)	0.1892(2)	2.90(7)	
C(5)	0.6137(4)	0.1511(4)	0.1289(2)	2.90(7)	
C(6)	0.3344(4)	0.5260(3)	0.3164(2)	2.85(7)	
C(7)	0.2793(4)	0.4416(3)	0.3873(2)	2.65(6)	
C(8)	0.1446(4)	0.4259(4)	0.3657(2)	2.85(7)	
C(9)	0.1171(4)	0.5012(4)	0.2813(2)	3.30(7)	
C(10)	0.2344(4)	0.5612(4)	0.2511(2)	3.21(7)	
C(11)	0.6860(4)	0.3900(4)	0.1275(3)	4.22(9)	
C(12)	0.7442(4)	0.2384(5)	0.3239(3)	4.57(10)	
C(13)	0.6698(5)	-0.0659(5)	0.3497(3)	4.57(9)	
C(14)	0.5729(4)	-0.1074(4)	0.1700(2)	3.91(8)	
C(15)	0.5892(5)	0.1678(5)	0.0345(2)	4.20(9)	
C(16)	0.4613(4)	0.5883(4)	0.3169(3)	4.27(9)	
C(17)	0.3469(4)	0.3857(5)	0.4723(2)	4.10(9)	
C(18)	0.0427(4)	0.3530(4)	0.4247(3)	4.15(9)	
C(19)	-0.0223(5)	0.5229(5)	0.2373(3)	5.2(1)	
C(20)	0.2518(6)	0.6515(4)	0.1642(3)	5.0(1)	
C(21)	0.2587(4)	-0.0040(4)	0.3921(2)	3.42(8)	
C(22)	0.1891(4)	-0.1065(4)	0.4271(2)	4.14(8)	
C(23)	0.0972(4)	-0.1411(4)	0.3750(3)	4.18(9)	
C(24)	0.0793(4)	-0.0702(4)	0.2938(2)	3.53(8)	
C(25)	0.1538(3)	0.0365(3)	0.2591(2)	2.53(6)	
C(26)	0.1388(3)	0.1148(3)	0.1739(2)	2.56(6)	
C(27)	0.0490(4)	0.0941(4)	0.1144(2)	3.64(8)	
C(28)	0.0391(4)	0.1734(5)	0.0344(3)	4.36(9)	
C(29)	0.1161(4)	0.2800(4)	0.0113(2)	4.03(8)	
C(30)	0.2002(4)	0.2961(4)	0.0702(2)	3.56(8)	
C(101)	0.6437	0.1298	0.2028	0.2000	0.001
C(102)	0.2228	0.4912	0.3204	0.2000	0.001
H(1)	0.7157	0.4370	0.1690	5.2030	
H(2)	0.7662	0.3685	0.0819	5.2030	
H(3)	0.5984	0.4573	0.1040	5.2030	
H(4)	0.8401	0.1725	0.3378	5.5154	

Table 1. Atomic coordinates and B_{iso}/B_{eq} and occupancy (continued)

atom	x	y	z	B_{eq}	occ
H(5)	0.7553	0.3344	0.3014	5.5154	
H(6)	0.6771	0.2505	0.3758	5.5154	
H(7)	0.6082	-0.0181	0.3979	5.4006	
H(8)	0.6420	-0.1482	0.3423	5.4006	
H(9)	0.7727	-0.0980	0.3631	5.4006	
H(10)	0.4732	-0.0782	0.1524	4.7514	
H(11)	0.6421	-0.1549	0.1248	4.7514	
H(12)	0.5783	-0.1790	0.2208	4.7514	
H(13)	0.5136	0.2614	0.0203	5.1306	
H(14)	0.6811	0.1697	-0.0001	5.1306	
H(15)	0.5594	0.0899	0.0221	5.1306	
H(16)	0.5523	0.5091	0.3293	5.1626	
H(17)	0.4798	0.6409	0.2615	5.1626	
H(18)	0.4385	0.6546	0.3600	5.1626	
H(19)	0.2893	0.3313	0.5092	4.9446	
H(20)	0.4477	0.3201	0.4620	4.9446	
H(21)	0.3495	0.4661	0.4994	4.9446	
H(22)	0.0067	0.3994	0.4760	5.0678	
H(23)	-0.0412	0.3552	0.3958	5.0678	
H(24)	0.0973	0.2491	0.4411	5.0678	
H(25)	-0.1095	0.5771	0.2710	6.3124	
H(26)	-0.0166	0.5749	0.1811	6.3124	
H(27)	-0.0318	0.4276	0.2325	6.3124	
H(28)	0.3430	0.6040	0.1319	5.9972	
H(29)	0.1692	0.6609	0.1306	5.9972	
H(30)	0.2489	0.7488	0.1718	5.9972	
H(31)	0.3242	0.0163	0.4274	4.1064	
H(32)	0.2014	-0.1527	0.4860	4.8774	
H(33)	0.0494	-0.2139	0.3970	5.1934	
H(34)	0.0169	-0.0936	0.2575	4.2403	
H(35)	-0.0049	0.0229	0.1315	4.3202	
H(36)	-0.0206	0.1574	-0.0059	5.0310	
H(37)	0.1092	0.3391	-0.0451	4.8888	
H(38)	0.2499	0.3726	0.0550	4.2980	

$B_{eq} = 8/3\ \pi^2(U_{11}(aa^*)^2 + U_{22}(bb^*)^2 + U_{33}(cc^*)^2 + 2U_{12}(aa^*bb^*)\cos\gamma + 2U_{13}(aa^*cc^*)\cos\beta + 2U_{23}(bb^*cc^*)\cos\alpha)$

Table 2. Anisotropic Displacement Parameters

atom	U_{11}	U_{22}	U_{33}	U_{12}	U_{13}	U_{23}
Ce(1)	0.0383(1)	0.0362(1)	0.0293(1)	-0.02001(8)	-0.00373(7)	-0.00416(7)
N(1)	0.042(2)	0.036(1)	0.030(1)	-0.018(1)	-0.000(1)	-0.004(1)
N(2)	0.043(2)	0.044(2)	0.027(1)	-0.020(1)	-0.006(1)	-0.001(1)
C(1)	0.037(2)	0.043(2)	0.038(2)	-0.020(2)	0.003(1)	-0.002(1)
C(2)	0.035(2)	0.049(2)	0.042(2)	-0.017(2)	-0.006(1)	-0.006(2)
C(3)	0.040(2)	0.044(2)	0.037(2)	-0.015(2)	-0.007(1)	0.004(1)
C(4)	0.039(2)	0.037(2)	0.035(2)	-0.014(1)	-0.001(1)	-0.004(1)
C(5)	0.040(2)	0.042(2)	0.029(2)	-0.017(2)	0.002(1)	-0.003(1)
C(6)	0.046(2)	0.029(2)	0.037(2)	-0.018(1)	-0.004(1)	-0.006(1)
C(7)	0.042(2)	0.035(2)	0.028(1)	-0.016(1)	-0.005(1)	-0.006(1)
C(8)	0.038(2)	0.037(2)	0.036(2)	-0.015(1)	0.000(1)	-0.008(1)
C(9)	0.042(2)	0.040(2)	0.044(2)	-0.008(2)	-0.014(1)	-0.008(2)
C(10)	0.060(2)	0.031(2)	0.032(2)	-0.017(2)	-0.007(2)	0.001(1)
C(11)	0.054(2)	0.045(2)	0.064(2)	-0.026(2)	0.008(2)	-0.002(2)
C(12)	0.042(2)	0.076(3)	0.064(2)	-0.019(2)	-0.014(2)	-0.025(2)
C(13)	0.055(2)	0.068(3)	0.045(2)	-0.019(2)	-0.013(2)	0.017(2)
C(14)	0.056(2)	0.043(2)	0.053(2)	-0.021(2)	-0.000(2)	-0.007(2)
C(15)	0.063(3)	0.066(3)	0.030(2)	-0.022(2)	-0.001(2)	-0.003(2)
C(16)	0.056(2)	0.046(2)	0.071(3)	-0.028(2)	0.006(2)	-0.021(2)
C(17)	0.059(2)	0.068(3)	0.031(2)	-0.019(2)	-0.014(2)	-0.005(2)
C(18)	0.053(2)	0.058(2)	0.056(2)	-0.032(2)	0.014(2)	-0.017(2)
C(19)	0.054(3)	0.074(3)	0.072(3)	-0.008(2)	-0.028(2)	-0.020(2)
C(20)	0.099(3)	0.044(2)	0.041(2)	-0.018(2)	-0.009(2)	0.009(2)
C(21)	0.050(2)	0.049(2)	0.030(2)	-0.016(2)	-0.005(1)	0.000(1)
C(22)	0.054(2)	0.051(2)	0.042(2)	-0.014(2)	0.005(2)	0.012(2)
C(23)	0.047(2)	0.044(2)	0.065(2)	-0.021(2)	0.005(2)	0.010(2)
C(24)	0.038(2)	0.043(2)	0.058(2)	-0.020(2)	-0.002(2)	-0.004(2)
C(25)	0.030(2)	0.029(2)	0.037(2)	-0.010(1)	0.001(1)	-0.008(1)
C(26)	0.030(2)	0.034(2)	0.036(2)	-0.010(1)	-0.004(1)	-0.011(1)
C(27)	0.045(2)	0.048(2)	0.052(2)	-0.016(2)	-0.018(2)	-0.010(2)
C(28)	0.056(2)	0.061(2)	0.052(2)	-0.012(2)	-0.027(2)	-0.012(2)
C(29)	0.053(2)	0.061(2)	0.031(2)	-0.005(2)	-0.010(2)	-0.002(2)
C(30)	0.054(2)	0.051(2)	0.031(2)	-0.020(2)	-0.004(2)	0.003(2)

The general temperature factor expression:
$\exp(-2\pi^2(a^{*2}U_{11}h^2 + b^{*2}U_{22}k^2 + c^{*2}U_{33}l^2 + 2a^*b^*U_{12}hk + 2a^*c^*U_{13}hl + 2b^*c^*U_{23}kl))$

$Cp^*_2Ce(^iPr\text{-}N\text{-}C{=}C\text{-}N{=}CMe_2)$

EXPERIMENTAL DETAILS

A. Crystal Data

Empirical Formula	$H_{45}C_{28}N_2Ce$
Formula Weight	549.80
Crystal Color, Habit	red, block
Crystal Dimensions	0.21 X 0.20 X 0.18 mm
Crystal System	monoclinic
Lattice Type	Primitive
Lattice Parameters	a = 9.3540(9)Å
	b = 19.295(2) Å
	c = 15.150(1) Å
	β = 97.918(2)^o
	V = 2708.3(4) Å^3
Space Group	$P2_1/c$ (#14)
Z value	4
D_{calc}	1.348 g/cm^3
F_{000}	1140.00
μ(MoKα)	16.97 cm^{-1}

B. Intensity Measurements

Diffractometer	Bruker APEX CCD
Radiation	MoKα (λ = 0.71069 Å) graphite monochromated
Detector Position	60.00 mm
Exposure Time	20.0 seconds per frame.
Scan Type	ω (0.3 degrees per frame)
$2\theta_{max}$	52.7^o
No. of Reflections Measured	Total: 17608 Unique: 3756
(R_{int} = 0.046)	
Corrections	Lorentz-polarization
	Absorption (Tmax = 1.00 Tmin = 0.71)

C. Structure Solution and Refinement

Structure Solution	Direct Methods (SIR97)
Refinement	Full-matrix least-squares
Function Minimized	Σ w (|Fo| - |Fc|)^2
Least Squares Weights	$1/\sigma^2(Fo) = 4Fo^2/\sigma^2(Fo^2)$
p-factor	0.0300
Anomalous Dispersion	All non-hydrogen atoms
No. Observations (I>3.00σ(I))	3881
No. Variables	280
Reflection/Parameter Ratio	13.86
Residuals: R; Rw; Rall	0.036 ; 0.043; 0.061
Goodness of Fit Indicator	1.23
Max Shift/Error in Final Cycle	0.00
Maximum peak in Final Diff. Map	0.86 $e^-/Å^3$
Minimum peak in Final Diff. Map	-0.39 $e^-/Å^3$

Table 1. Atomic coordinates and B_{iso}/B_{eq} and occupancy

atom	x	y	z	B_{eq}	occ
Ce(1)	0.68661(3)	0.10646(1)	0.75704(2)	1.431(6)	
N(1)	0.9263(4)	0.1190(2)	0.8622(3)	2.03(9)	
N(2)	0.8358(4)	0.0051(2)	0.7441(3)	2.13(9)	
C(1)	0.4575(5)	0.0386(2)	0.8163(3)	1.9(1)	
C(2)	0.4175(5)	0.1096(2)	0.8159(3)	2.1(1)	
C(3)	0.5075(5)	0.1430(2)	0.8857(3)	2.0(1)	
C(4)	0.6033(5)	0.0929(2)	0.9292(3)	1.8(1)	
C(5)	0.5715(5)	0.0284(2)	0.8858(3)	1.9(1)	
C(6)	0.5621(5)	0.1618(2)	0.5915(3)	1.9(1)	
C(7)	0.6116(6)	0.2205(2)	0.6435(3)	2.0(1)	
C(8)	0.7644(5)	0.2191(2)	0.6548(3)	2.1(1)	
C(9)	0.8093(5)	0.1603(3)	0.6101(3)	2.2(1)	
C(10)	0.6843(6)	0.1253(2)	0.5713(3)	2.1(1)	
C(11)	0.3864(6)	-0.0156(3)	0.7532(4)	3.0(1)	
C(12)	0.2863(6)	0.1413(3)	0.7627(4)	2.9(1)	
C(13)	0.4911(6)	0.2167(3)	0.9154(4)	3.1(1)	
C(14)	0.7070(6)	0.1017(3)	1.0142(3)	2.7(1)	
C(15)	0.6445(6)	-0.0383(3)	0.9191(3)	2.6(1)	
C(16)	0.4094(6)	0.1451(3)	0.5518(4)	2.6(1)	
C(17)	0.5193(7)	0.2778(3)	0.6711(4)	3.2(1)	
C(18)	0.8661(7)	0.2754(3)	0.6952(4)	3.6(1)	
C(19)	0.9641(6)	0.1407(3)	0.6051(4)	3.5(1)	
C(20)	0.6812(7)	0.0657(3)	0.5068(4)	3.4(1)	
C(21)	0.9998(5)	0.0554(3)	0.8662(3)	2.5(1)	
C(22)	0.9511(6)	0.0035(2)	0.8076(4)	2.4(1)	
C(23)	0.9707(6)	0.1699(3)	0.9144(3)	2.4(1)	
C(24)	0.8824(6)	0.2351(3)	0.9116(3)	2.8(1)	
C(25)	1.1026(6)	0.1659(3)	0.9832(4)	3.3(1)	
C(26)	0.8147(6)	-0.0554(3)	0.6841(4)	3.0(1)	
C(27)	0.9401(7)	-0.0662(3)	0.6316(4)	4.2(2)	
C(28)	0.7804(7)	-0.1223(3)	0.7284(4)	4.0(2)	
C(101)	0.5115	0.0825	0.8666	0.2000	0.001
C(102)	0.6863	0.1774	0.6142	0.2000	0.001
H(1)	0.4262	-0.0598	0.7696	3.6550	
H(2)	0.4024	-0.0049	0.6942	3.6550	
H(3)	0.2856	-0.0162	0.7562	3.6550	
H(4)	0.2890	0.1334	0.7011	3.5249	
H(5)	0.2853	0.1897	0.7738	3.5249	
H(6)	0.2020	0.1207	0.7797	3.5249	

Table 1. Atomic coordinates and B_{iso}/B_{eq} and occupancy (continued)

atom	x	y	z	B_{eq}	occ
H(7)	0.4502	0.2440	0.8661	3.7670	
H(8)	0.4296	0.2179	0.9604	3.7670	
H(9)	0.5831	0.2349	0.9386	3.7670	
H(10)	0.6849	0.0689	1.0571	3.2362	
H(11)	0.6982	0.1473	1.0367	3.2362	
H(12)	0.8029	0.0946	1.0022	3.2362	
H(13)	0.5967	-0.0763	0.8881	3.1657	
H(14)	0.6401	-0.0430	0.9811	3.1657	
H(15)	0.7425	-0.0374	0.9091	3.1657	
H(16)	0.3998	0.1498	0.4889	3.1724	
H(17)	0.3873	0.0988	0.5666	3.1724	
H(18)	0.3449	0.1760	0.5750	3.1724	
H(19)	0.4343	0.2588	0.6892	3.8066	
H(20)	0.4936	0.3082	0.6221	3.8066	
H(21)	0.5714	0.3028	0.7191	3.8066	
H(22)	0.9499	0.2548	0.7272	4.2967	
H(23)	0.8191	0.3028	0.7346	4.2967	
H(24)	0.8931	0.3039	0.6491	4.2967	
H(25)	1.0207	0.1814	0.6041	4.2390	
H(26)	0.9691	0.1146	0.5525	4.2390	
H(27)	1.0000	0.1135	0.6557	4.2390	
H(28)	0.7598	0.0355	0.5253	4.1178	
H(29)	0.6889	0.0829	0.4489	4.1178	
H(30)	0.5930	0.0411	0.5057	4.1178	
H(31)	1.0826	0.0483	0.9093	2.9521	
H(32)	1.0052	-0.0384	0.8125	2.8730	
H(33)	0.8143	0.2353	0.8590	3.2950	
H(34)	0.8332	0.2368	0.9623	3.2950	
H(35)	0.9443	0.2741	0.9117	3.2950	
H(36)	1.1827	0.1514	0.9555	3.9931	
H(37)	1.0864	0.1335	1.0279	3.9931	
H(38)	1.1217	0.2102	1.0093	3.9931	
H(39)	0.7330	-0.0451	0.6415	3.5323	
H(40)	1.0250	-0.0761	0.6716	5.0180	
H(41)	0.9191	-0.1040	0.5917	5.0180	
H(42)	0.9543	-0.0255	0.5988	5.0180	
H(43)	0.7673	-0.1582	0.6851	4.8251	
H(44)	0.8580	-0.1339	0.7732	4.8251	
H(45)	0.6946	-0.1167	0.7546	4.8251	

Table 1. Atomic coordinates and B_{iso}/B_{eq} and occupancy (continued)

atom	x	y	z	B_{eq}	occ

$B_{eq} = 8/3\ \pi^2(U_{11}(aa^*)^2 + U_{22}(bb^*)^2 + U_{33}(cc^*)^2 + 2U_{12}(aa^*bb^*)\cos\gamma + 2U_{13}(aa^*cc^*)\cos\beta + 2U_{23}(bb^*cc^*)\cos\alpha)$

Table 2. Anisotropic Displacement Parameters

atom	U_{11}	U_{22}	U_{33}	U_{12}	U_{13}	U_{23}
Ce(1)	0.0211(1)	0.0177(1)	0.0160(1)	0.0000(1)	0.00416(9)	0.0006(1)
N(1)	0.028(2)	0.031(2)	0.018(2)	-0.002(2)	0.005(2)	0.000(2)
N(2)	0.030(3)	0.020(2)	0.032(2)	0.002(2)	0.010(2)	-0.001(2)
C(1)	0.028(3)	0.028(3)	0.018(3)	-0.009(2)	0.005(2)	-0.003(2)
C(2)	0.025(3)	0.030(3)	0.024(3)	0.002(2)	0.005(2)	0.000(2)
C(3)	0.027(3)	0.028(3)	0.024(3)	-0.005(2)	0.010(2)	-0.004(2)
C(4)	0.024(3)	0.028(3)	0.017(2)	-0.006(2)	0.007(2)	0.001(2)
C(5)	0.030(3)	0.021(2)	0.022(3)	-0.004(2)	0.012(2)	0.001(2)
C(6)	0.025(3)	0.022(3)	0.024(3)	-0.003(2)	0.001(2)	0.006(2)
C(7)	0.041(3)	0.016(2)	0.021(3)	0.000(2)	0.006(2)	0.005(2)
C(8)	0.033(3)	0.025(3)	0.021(3)	-0.009(2)	0.002(2)	0.009(2)
C(9)	0.026(3)	0.037(3)	0.021(3)	-0.002(2)	0.003(2)	0.012(2)
C(10)	0.037(3)	0.024(3)	0.018(3)	-0.003(2)	0.004(2)	0.003(2)
C(11)	0.037(3)	0.044(3)	0.033(3)	-0.017(3)	-0.001(2)	-0.006(3)
C(12)	0.034(3)	0.047(3)	0.031(3)	0.001(3)	0.006(2)	0.006(3)
C(13)	0.048(4)	0.036(3)	0.037(3)	0.001(3)	0.014(3)	-0.008(3)
C(14)	0.038(3)	0.044(3)	0.021(3)	-0.007(3)	0.007(2)	-0.000(3)
C(15)	0.043(3)	0.030(3)	0.029(3)	-0.001(2)	0.013(2)	0.005(2)
C(16)	0.035(3)	0.031(3)	0.033(3)	-0.006(2)	0.003(2)	0.010(2)
C(17)	0.061(4)	0.025(3)	0.037(3)	0.005(3)	0.015(3)	0.004(3)
C(18)	0.055(4)	0.042(3)	0.036(3)	-0.022(3)	-0.006(3)	0.014(3)
C(19)	0.030(3)	0.062(4)	0.042(4)	0.005(3)	0.007(3)	0.018(3)
C(20)	0.061(4)	0.041(4)	0.028(3)	0.005(3)	0.001(3)	0.001(3)
C(21)	0.023(3)	0.038(3)	0.032(3)	0.005(2)	-0.000(2)	0.004(2)
C(22)	0.033(3)	0.027(3)	0.034(3)	0.011(2)	0.014(2)	0.007(2)
C(23)	0.032(3)	0.039(3)	0.021(3)	-0.007(2)	0.006(2)	0.002(2)
C(24)	0.042(3)	0.035(3)	0.027(3)	-0.009(3)	0.003(2)	-0.004(2)
C(25)	0.040(3)	0.051(4)	0.033(3)	-0.003(3)	-0.005(2)	-0.009(3)
C(26)	0.043(4)	0.029(3)	0.041(4)	0.001(2)	0.006(3)	-0.009(3)
C(27)	0.067(5)	0.044(4)	0.050(4)	0.007(3)	0.014(3)	-0.015(3)
C(28)	0.062(5)	0.029(3)	0.062(5)	-0.004(3)	0.009(3)	-0.008(3)

The general temperature factor expression:
$\exp(-2\pi^2(a^{*2}U_{11}h^2 + b^{*2}U_{22}k^2 + c^{*2}U_{33}l^2 + 2a^*b^*U_{12}hk + 2a^*c^*U_{13}hl + 2b^*c^*U_{23}kl))$

Cp_3Ce(pyridine-N-oxide)

EXPERIMENTAL DETAILS

A. Crystal Data

Empirical Formula	$H_{20}C_{20}NOCe$
Formula Weight	430.50
Crystal Color, Habit	red, block
Crystal Dimensions	0.21 X 0.13 X 0.11 mm
Crystal System	monoclinic
Lattice Type	I-centered
Lattice Parameters	a = 14.464(3)Å
	b = 9.482(2) Å
	c = 26.882(7) Å
	β = 90.557(4)^o
	V = 3686(1) Å^3
Space Group	I2/a (#15)
Z value	8
D_{calc}	1.551 g/cm^3
F_{000}	1704.00
μ(MoKα)	24.72 cm^{-1}

B. Intensity Measurements

Diffractometer	Bruker SMART CCD
Radiation	MoKα (λ = 0.71069 Å) graphite monochromated
Detector Position	60.00 mm
Exposure Time	30.0 seconds per frame.
Scan Type	ω (0.3 degrees per frame)
$2\theta_{max}$	52.9^o
No. of Reflections Measured	Total: 9749 Unique: 3824
(R_{int} = 0.022)	
Corrections	Lorentz-polarization
	Absorption (Tmax = 1.00 Tmin = 0.65)

C. Structure Solution and Refinement

Structure Solution	Direct Methods (SIR97)
Refinement	Full-matrix least-squares
Function Minimized	Σ w (|Fo| - |Fc|)^2
Least Squares Weights	$1/\sigma^2(Fo) = 4Fo^2/\sigma^2(Fo^2)$
p-factor	0.0300
Anomalous Dispersion	All non-hydrogen atoms
No. Observations (I>3.00σ(I))	7397
No. Variables	208
Reflection/Parameter Ratio	35.56
Residuals: R; Rw; Rall	0.024 ; 0.031; 0.036
Goodness of Fit Indicator	1.29
Max Shift/Error in Final Cycle	0.00
Maximum peak in Final Diff. Map	1.00 $e^-/Å^3$
Minimum peak in Final Diff. Map	-0.41 $e^-/Å^3$

Table 1. Atomic coordinates and B_{iso}/B_{eq} and occupancy

atom	x	y	z	B_{eq}	occ
Ce(1)	-0.116785(8)	0.48744(1)	0.141422(5)	3.400(3)	
O(1)	0.0273(1)	0.3654(2)	0.13441(6)	5.05(5)	
N(1)	0.0595(1)	0.2499(2)	0.11257(8)	4.09(5)	
C(1)	-0.1842(2)	0.6457(4)	0.0602(1)	6.95(10)	
C(2)	-0.1487(3)	0.7480(3)	0.0921(1)	7.2(1)	
C(3)	-0.0539(3)	0.7353(3)	0.0923(1)	6.89(10)	
C(4)	-0.0304(2)	0.6263(3)	0.0610(1)	5.81(8)	
C(5)	-0.1103(3)	0.5704(3)	0.04114(10)	6.08(9)	
C(6)	-0.0247(2)	0.5194(3)	0.2338(1)	5.90(8)	
C(7)	-0.1096(3)	0.4717(3)	0.2456(1)	6.00(8)	
C(8)	-0.1745(2)	0.5750(5)	0.2354(1)	6.89(9)	
C(9)	-0.1263(3)	0.6912(3)	0.2166(1)	7.17(10)	
C(10)	-0.0343(3)	0.6540(4)	0.2159(1)	6.82(10)	
C(11)	-0.1798(4)	0.2088(4)	0.1527(3)	12.1(2)	
C(12)	-0.2482(4)	0.2869(5)	0.1702(1)	9.0(1)	
C(13)	-0.2888(2)	0.3545(3)	0.1321(2)	7.3(1)	
C(14)	-0.2461(4)	0.3146(5)	0.0898(2)	9.0(1)	
C(15)	-0.1762(4)	0.2219(6)	0.1032(3)	11.4(2)	
C(16)	0.0927(2)	0.1454(3)	0.14143(9)	5.04(7)	
C(17)	0.1278(2)	0.0269(3)	0.1190(1)	6.06(8)	
C(18)	0.1286(2)	0.0146(3)	0.0688(1)	6.10(9)	
C(19)	0.0938(2)	0.1224(3)	0.0403(1)	6.05(8)	
C(20)	0.0594(2)	0.2385(3)	0.0633(1)	4.97(7)	
C(101)	-0.1053	0.6651	0.0693	0.2000	0.000
C(102)	-0.0939	0.5823	0.2295	0.2000	0.000
C(103)	-0.2278	0.2774	0.1296	0.2000	0.000
H(1)	-0.2477	0.6301	0.0527	8.3450	
H(2)	-0.1836	0.8148	0.1104	8.6920	
H(3)	-0.0118	0.7920	0.1109	8.2655	
H(4)	0.0307	0.5951	0.0542	6.9690	
H(5)	-0.1142	0.4938	0.0184	7.2942	
H(6)	0.0317	0.4688	0.2372	7.0752	
H(7)	-0.1227	0.3811	0.2590	7.1976	
H(8)	-0.2394	0.5685	0.2402	8.2621	
H(9)	-0.1520	0.7788	0.2063	8.6081	
H(10)	0.0148	0.7123	0.2048	8.1806	
H(11)	-0.1394	0.1521	0.1723	14.5339	
H(12)	-0.2655	0.2938	0.2041	10.8001	
H(13)	-0.3388	0.4190	0.1344	8.7778	

Table 1. Atomic coordinates and B_{iso}/B_{eq} and occupancy (continued)

atom	x	y	z	B_{eq}	occ
H(14)	-0.2612	0.3447	0.0570	10.7534	
H(15)	-0.1340	0.1766	0.0815	13.6742	
H(16)	0.0920	0.1533	0.1767	6.0452	
H(17)	0.1518	-0.0475	0.1389	7.2767	
H(18)	0.1529	-0.0676	0.0536	7.3153	
H(19)	0.0936	0.1161	0.0051	7.2631	
H(20)	0.0349	0.3133	0.0437	5.9630	

$B_{eq} = 8/3\ \pi^2(U_{11}(aa^*)^2 + U_{22}(bb^*)^2 + U_{33}(cc^*)^2 + 2U_{12}(aa^*bb^*)\cos\gamma + 2U_{13}(aa^*cc^*)\cos\beta + 2U_{23}(bb^*cc^*)\cos\alpha)$

Table 2. Anisotropic Displacement Parameters

atom	U_{11}	U_{22}	U_{33}	U_{12}	U_{13}	U_{23}
Ce(1)	0.03978(8)	0.04643(8)	0.04296(8)	-0.00139(6)	0.00006(5)	-0.00304(6)
O(1)	0.057(1)	0.0583(10)	0.077(1)	0.0143(8)	0.0043(9)	-0.0051(8)
N(1)	0.044(1)	0.051(1)	0.061(1)	0.0055(9)	0.005(1)	0.0083(9)
C(1)	0.064(2)	0.130(3)	0.070(2)	0.021(2)	-0.012(2)	0.037(2)
C(2)	0.129(3)	0.074(2)	0.073(2)	0.040(2)	0.015(2)	0.018(2)
C(3)	0.115(3)	0.068(2)	0.079(2)	-0.023(2)	-0.016(2)	0.025(2)
C(4)	0.064(2)	0.085(2)	0.072(2)	0.012(2)	0.014(2)	0.034(2)
C(5)	0.097(3)	0.089(2)	0.045(2)	0.002(2)	-0.000(2)	0.010(1)
C(6)	0.082(2)	0.089(2)	0.052(2)	0.015(2)	-0.017(2)	-0.017(1)
C(7)	0.103(3)	0.078(2)	0.048(2)	-0.007(2)	0.001(2)	0.002(1)
C(8)	0.069(2)	0.138(3)	0.055(2)	0.011(2)	0.013(2)	-0.030(2)
C(9)	0.146(4)	0.066(2)	0.060(2)	0.032(2)	-0.008(2)	-0.022(1)
C(10)	0.107(3)	0.088(2)	0.065(2)	-0.034(2)	0.003(2)	-0.025(2)
C(11)	0.080(4)	0.051(2)	0.328(9)	-0.022(2)	-0.056(5)	0.014(4)
C(12)	0.134(4)	0.133(4)	0.075(3)	-0.088(3)	-0.006(3)	0.018(2)
C(13)	0.049(2)	0.090(2)	0.139(4)	-0.018(2)	0.006(2)	-0.024(2)
C(14)	0.107(4)	0.139(4)	0.094(3)	-0.075(3)	-0.029(3)	-0.004(3)
C(15)	0.096(4)	0.126(4)	0.211(6)	-0.061(3)	0.055(4)	-0.111(5)
C(16)	0.072(2)	0.065(2)	0.055(2)	0.011(1)	-0.002(1)	0.018(1)
C(17)	0.085(2)	0.059(2)	0.087(2)	0.023(1)	-0.002(2)	0.022(1)
C(18)	0.080(2)	0.059(2)	0.092(3)	0.013(1)	0.011(2)	-0.008(1)
C(19)	0.092(2)	0.076(2)	0.062(2)	0.008(2)	0.009(2)	-0.004(1)
C(20)	0.072(2)	0.064(2)	0.053(2)	0.012(1)	0.002(1)	0.014(1)

The general temperature factor expression:
$\exp(-2\pi^2(a^{*2}U_{11}h^2 + b^{*2}U_{22}k^2 + c^{*2}U_{33}l^2 + 2a^*b^*U_{12}hk + 2a^*c^*U_{13}hl + 2b^*c^*U_{23}kl))$

$(Cp^*_2CeOTf)_2(\mu\text{-}4,4'\text{-bipyridine})$

EXPERIMENTAL DETAILS

A. Crystal Data

Empirical Formula	$Ce_2C_{52}H_{68}N_2S_2F_6O_6$
Formula Weight	1275.47
Crystal Color, Habit	red, block
Crystal Dimensions	0.16 X 0.20 X 0.13 mm
Crystal System	triclinic
Lattice Type	Primitive
Lattice Parameters	a = 9.019(3)Å b = 10.523(4) Å c = 15.393(5) Å α = 94.171(5)^o β = 91.747(5)^o γ = 106.016(4)^o V = 1398.5(8) Å^3
P-1	
Z value	1
D_{calc}	1.514 g/cm^3
F_{000}	644.00
μ(MoKα)	17.48 cm^{-1}

B. Intensity Measurements

Diffractometer	Bruker SMART CCD
Radiation	MoKα (λ = 0.71069 Å) graphite monochromated
Detector Position	60.00 mm
Exposure Time	20.0 seconds per frame.
Scan Type	ω (0.3 degrees per frame)
$2\theta_{max}$	52.5^o
No. of Reflections Measured	Total: 6942 Unique: 3205 (R_{int} = 0.024)
Corrections	Lorentz-polarization
Absorption	(Tmax = 1.00 Tmin = 0.86)

C. Structure Solution and Refinement

Structure Solution	Direct Methods (SIR92)
Refinement	Full-matrix least-squares
Function Minimized	Σ w (|Fo| - |Fc|)^2
Least Squares Weights	$1/\sigma^2(Fo) = 4Fo^2/\sigma^2(Fo^2)$
p-factor	0.0300
Anomalous Dispersion	All non-hydrogen atoms
No. Observations (I>3.00σ(I))	3234
No. Variables	316
Reflection/Parameter Ratio	10.23
Residuals: R; Rw; Rall	0.052 ; 0.049; 0.092
Goodness of Fit Indicator	1.58
Max Shift/Error in Final Cycle	0.00
Maximum peak in Final Diff. Map	1.74 $e^-/Å^3$
Minimum peak in Final Diff. Map	-0.97 $e^-/Å^3$

Table 1. Atomic coordinates and B_{iso}/B_{eq} and occupancy

atom	x	y	z	B_{eq}	occ
Ce(1)	0.69226(6)	0.30172(5)	0.75046(3)	1.84(1)	
S(1)	0.9298(2)	0.5995(2)	0.7689(1)	2.33(5)	
F(1)	1.1467(6)	0.5978(5)	0.6556(4)	4.5(1)	
F(2)	1.2239(6)	0.7264(5)	0.7739(4)	4.3(1)	
F(3)	1.0853(6)	0.7825(5)	0.6736(4)	4.6(2)	
O(1)	0.9627(6)	0.4858(5)	0.8069(3)	2.6(1)	
O(2)	0.8056(6)	0.5504(5)	0.7001(3)	2.5(1)	
O(3)	0.9144(7)	0.7053(5)	0.8295(4)	3.9(2)	
N(1)	0.8442(8)	0.1771(6)	0.8458(4)	2.2(2)	
C(1)	0.6074(10)	0.4043(8)	0.9124(6)	2.7(2)	
C(2)	0.5236(10)	0.4484(8)	0.8467(6)	2.8(2)	
C(3)	0.4129(10)	0.3353(9)	0.8053(6)	2.9(2)	
C(4)	0.4257(10)	0.2212(8)	0.8461(7)	3.3(2)	
C(5)	0.5436(10)	0.2627(8)	0.9121(6)	2.6(2)	
C(6)	0.7889(9)	0.2427(8)	0.5858(5)	2.1(2)	
C(7)	0.643(1)	0.2628(8)	0.5707(5)	2.7(2)	
C(8)	0.5279(10)	0.1508(9)	0.5994(5)	2.7(2)	
C(9)	0.6063(10)	0.0640(8)	0.6321(5)	2.4(2)	
C(10)	0.7681(9)	0.1193(8)	0.6237(5)	2.1(2)	
C(11)	0.727(1)	0.4892(8)	0.9808(6)	3.4(2)	
C(12)	0.534(1)	0.5914(9)	0.8313(7)	3.7(3)	
C(13)	0.288(1)	0.347(1)	0.7370(7)	4.9(3)	
C(14)	0.317(1)	0.0816(9)	0.8300(7)	4.7(3)	
C(15)	0.578(1)	0.1779(9)	0.9806(7)	4.6(3)	
C(16)	0.945(1)	0.3272(9)	0.5589(6)	3.8(2)	
C(17)	0.608(1)	0.3781(10)	0.5277(7)	4.2(3)	
C(18)	0.355(1)	0.1169(10)	0.5800(6)	4.2(3)	
C(19)	0.525(1)	-0.0770(9)	0.6540(6)	3.8(2)	
C(20)	0.8929(10)	0.0504(8)	0.6381(6)	3.0(2)	
C(21)	0.7889(9)	0.0441(8)	0.8501(5)	2.3(2)	
C(22)	0.8448(10)	-0.0284(7)	0.9072(6)	2.5(2)	
C(23)	0.9657(9)	0.0369(8)	0.9666(5)	2.0(2)	
C(24)	1.025(1)	0.1721(9)	0.9640(6)	4.1(3)	
C(25)	0.964(1)	0.2378(8)	0.9049(6)	3.6(2)	
C(26)	1.106(1)	0.6806(9)	0.7137(6)	2.8(2)	
C(101)	0.5026	0.3344	0.8645	0.2000	0.001
C(102)	0.6668	0.1679	0.6023	0.2000	0.001
H(1)	0.7843	0.4360	1.0053	4.0574	
H(2)	0.7950	0.5596	0.9541	4.0574	

Table 1. Atomic coordinates and B_{iso}/B_{eq} and occupancy (continued)

atom	x	y	z	B_{eq}	occ
H(3)	0.6759	0.5248	1.0254	4.0574	
H(4)	0.5522	0.6051	0.7719	4.4324	
H(5)	0.6157	0.6492	0.8674	4.4324	
H(6)	0.4391	0.6095	0.8452	4.4324	
H(7)	0.2103	0.3766	0.7659	5.8968	
H(8)	0.3342	0.4089	0.6969	5.8968	
H(9)	0.2425	0.2628	0.7064	5.8968	
H(10)	0.2980	0.0592	0.7690	5.6466	
H(11)	0.2227	0.0780	0.8565	5.6466	
H(12)	0.3636	0.0205	0.8544	5.6466	
H(13)	0.6819	0.1739	0.9770	5.5657	
H(14)	0.5099	0.0910	0.9710	5.5657	
H(15)	0.5649	0.2156	1.0368	5.5657	
H(16)	0.9765	0.2835	0.5096	4.5359	
H(17)	1.0198	0.3396	0.6059	4.5359	
H(18)	0.9357	0.4111	0.5445	4.5359	
H(19)	0.5273	0.4029	0.5565	5.0206	
H(20)	0.6981	0.4513	0.5318	5.0206	
H(21)	0.5770	0.3518	0.4681	5.0206	
H(22)	0.3247	0.1964	0.5773	5.0342	
H(23)	0.3282	0.0652	0.5256	5.0342	
H(24)	0.3022	0.0679	0.6248	5.0342	
H(25)	0.5857	-0.1029	0.6972	4.5347	
H(26)	0.4267	-0.0793	0.6756	4.5347	
H(27)	0.5120	-0.1362	0.6029	4.5347	
H(28)	0.8487	-0.0430	0.6309	3.5898	
H(29)	0.9698	0.0758	0.5969	3.5898	
H(30)	0.9386	0.0752	0.6955	3.5898	
H(31)	0.7052	-0.0024	0.8107	2.7566	
H(32)	0.8015	-0.1217	0.9060	2.9849	
H(33)	1.0000	0.0000	1.0000	2.4583	1/2
H(34)	1.1074	0.2199	1.0035	4.8631	
H(35)	1.0078	0.3310	0.9049	4.3103	

$B_{eq} = 8/3\ \pi^2(U_{11}(aa^*)^2 + U_{22}(bb^*)^2 + U_{33}(cc^*)^2 + 2U_{12}(aa^*bb^*)\cos\gamma + 2U_{13}(aa^*cc^*)\cos\beta + 2U_{23}(bb^*cc^*)\cos\alpha)$

Table 2. Anisotropic Displacement Parameters

atom	U_{11}	U_{22}	U_{33}	U_{12}	U_{13}	U_{23}
Ce(1)	0.0261(3)	0.0176(3)	0.0235(3)	0.0040(2)	-0.0003(2)	-0.0058(2)
S(1)	0.034(1)	0.023(1)	0.029(1)	0.004(1)	0.004(1)	-0.003(1)
F(1)	0.055(4)	0.044(3)	0.065(4)	0.004(3)	0.031(3)	-0.002(3)
F(2)	0.037(3)	0.052(4)	0.063(4)	-0.006(3)	-0.002(3)	-0.003(3)
F(3)	0.068(4)	0.038(3)	0.066(4)	0.003(3)	0.006(3)	0.020(3)
O(1)	0.042(4)	0.025(3)	0.028(4)	0.001(3)	-0.000(3)	0.007(3)
O(2)	0.030(3)	0.029(3)	0.033(4)	0.005(3)	-0.009(3)	-0.002(3)
O(3)	0.057(4)	0.028(4)	0.057(5)	0.003(3)	0.017(3)	-0.023(3)
N(1)	0.042(5)	0.017(4)	0.024(4)	0.009(3)	-0.002(3)	-0.007(3)
C(1)	0.036(6)	0.025(5)	0.041(6)	0.009(4)	0.016(5)	-0.005(4)
C(2)	0.037(6)	0.020(5)	0.049(6)	0.009(4)	0.017(5)	-0.000(4)
C(3)	0.028(5)	0.036(6)	0.049(6)	0.016(4)	0.005(5)	-0.011(5)
C(4)	0.032(6)	0.022(5)	0.068(7)	0.005(4)	0.026(5)	-0.009(5)
C(5)	0.038(6)	0.027(5)	0.029(6)	0.003(4)	0.011(4)	0.004(4)
C(6)	0.030(5)	0.034(6)	0.011(5)	0.005(4)	-0.004(4)	-0.008(4)
C(7)	0.048(6)	0.031(5)	0.022(5)	0.014(5)	-0.011(4)	-0.012(4)
C(8)	0.032(6)	0.040(6)	0.024(5)	0.007(5)	-0.005(4)	-0.017(4)
C(9)	0.037(6)	0.025(5)	0.025(5)	0.005(4)	-0.004(4)	-0.013(4)
C(10)	0.025(5)	0.029(5)	0.022(5)	0.009(4)	-0.003(4)	-0.010(4)
C(11)	0.049(6)	0.037(6)	0.034(6)	0.002(5)	0.008(5)	-0.014(5)
C(12)	0.044(6)	0.031(6)	0.069(8)	0.017(5)	0.017(5)	-0.003(5)
C(13)	0.037(6)	0.068(8)	0.082(9)	0.021(6)	0.002(6)	-0.023(6)
C(14)	0.042(6)	0.035(6)	0.093(9)	0.001(5)	0.029(6)	-0.019(6)
C(15)	0.079(8)	0.044(6)	0.059(7)	0.018(6)	0.043(6)	0.016(6)
C(16)	0.051(6)	0.046(6)	0.038(6)	0.000(5)	0.007(5)	-0.002(5)
C(17)	0.071(8)	0.046(6)	0.043(7)	0.024(6)	-0.020(5)	-0.012(5)
C(18)	0.034(6)	0.067(7)	0.055(7)	0.016(5)	-0.011(5)	-0.028(6)
C(19)	0.056(7)	0.033(6)	0.042(6)	-0.002(5)	-0.005(5)	-0.015(5)
C(20)	0.035(6)	0.040(6)	0.035(6)	0.011(5)	-0.006(4)	-0.016(5)
C(21)	0.030(5)	0.031(5)	0.026(5)	0.010(4)	-0.005(4)	-0.002(4)
C(22)	0.038(6)	0.015(5)	0.038(6)	0.005(4)	-0.008(4)	-0.007(4)
C(23)	0.037(5)	0.030(5)	0.015(5)	0.015(4)	0.005(4)	0.004(4)
C(24)	0.080(8)	0.024(5)	0.037(6)	-0.005(5)	-0.034(6)	0.008(5)
C(25)	0.063(7)	0.017(5)	0.045(7)	-0.004(5)	-0.013(5)	-0.005(5)
C(26)	0.039(6)	0.029(5)	0.035(6)	0.006(5)	0.002(5)	0.000(5)

The general temperature factor expression:
$\exp(-2\pi^2(a^{*2}U_{11}h^2 + b^{*2}U_{22}k^2 + c^{*2}U_{33}l^2 + 2a^*b^*U_{12}hk + 2a^*c^*U_{13}hl + 2b^*c^*U_{23}kl))$

$[(C_5H_4Me)_3Ce]_2(\mu$-4,4'-bipyridine)

A yellow plate 0.04 x 0.04 x 0.02 mm in size was mounted on a Cryoloop with Paratone oil. Data were collected in a nitrogen gas stream at 150(2) K using omega scans. Crystal-to-detector distance was 60 mm and exposure time was 1 seconds per frame using a scan width of 0.3°. Data collection was 99.3% complete to 29.00° in θ. A total of 8575 reflections were collected covering the indices, -11<=*h*<=11, -12<=*k*<=12, -18<=*l*<=18. 8575 reflections were found to be symmetry independent, with an R_{int} of 0.0581. Indexing and unit cell refinement indicated a primitive, triclinic lattice. The space group was found to be P-1 (No. 2). The data were integrated using the Bruker SAINT software program and scaled using the TWINABS software program. Solution by Patterson methods (DIRDIF-99) produced a complete heavy-atom phasing model consistent with the proposed structure. All non-hydrogen atoms were refined anisotropically by full-matrix least-squares (SHELXL-97). All hydrogen atoms were placed using a riding model. Their positions were constrained relative to their parent atom using the appropriate HFIX command in SHELXL-97.

Table 1. Crystal data and structure refinement for dk01.

X-ray ID	dk01	
Sample/notebook ID	MeCp346	
Empirical formula	C46 H50 Ce2 N2	
Formula weight	911.12	
Temperature	150(2) K	
Wavelength	0.77490 Å	
Crystal system	Triclinic	
Space group	P-1	
Unit cell dimensions	a = 8.3740(10) Å	α= 74.170(2)°.
	b = 9.0311(11) Å	β= 84.904(2)°.
	c = 13.9920(16) Å	γ = 70.714(2)°.
Volume	960.9(2) $Å^3$	
Z	1	
Density (calculated)	1.575 Mg/m^3	
Absorption coefficient	2.373 mm^{-1}	
F(000)	456	
Crystal size	0.04 x 0.04 x 0.02 mm^3	
Crystal color/habit	yellow plate	
Theta range for data collection	2.77 to 31.17°.	
Index ranges	-11<=h<=11, -12<=k<=12, -18<=l<=18	
Reflections collected	8575	
Independent reflections	8575 [R(int) = 0.0581]	
Completeness to theta = 29.00°	99.3 %	
Absorption correction	Semi-empirical from equivalents	
Max. and min. transmission	0.9541 and 0.9111	
Refinement method	Full-matrix least-squares on F^2	
Data / restraints / parameters	8575 / 0 / 230	
Goodness-of-fit on F^2	1.021	
Final R indices [I>2sigma(I)]	R1 = 0.0584, wR2 = 0.1572	
R indices (all data)	R1 = 0.0631, wR2 = 0.1601	
Largest diff. peak and hole	1.937 and -2.054 e.$Å^{-3}$	

Table 2. Atomic coordinates (x 10^4) and equivalent isotropic displacement parameters ($Å^2$x 10^3) for dk01. U(eq) is defined as one third of the trace of the orthogonalized U^{ij} tensor.

	x	y	z	U(eq)
C(1)	3067(9)	172(9)	1111(5)	29(1)
C(2)	3148(9)	1762(10)	948(5)	32(2)
C(3)	1612(10)	2881(9)	516(5)	32(2)
C(4)	563(9)	1970(10)	433(5)	34(2)
C(5)	1459(9)	329(9)	801(5)	31(1)
C(6)	4531(13)	-1369(12)	1433(6)	60(3)
C(7)	293(8)	4772(8)	2848(5)	25(1)
C(8)	1951(8)	4221(7)	2469(5)	22(1)
C(9)	2915(8)	2830(8)	3150(5)	22(1)
C(10)	1900(8)	2492(8)	3970(4)	23(1)
C(11)	287(9)	3670(8)	3806(5)	26(1)
C(12)	-1142(9)	6244(8)	2383(6)	36(2)
C(13)	-2885(8)	2644(9)	2039(5)	29(1)
C(14)	-2324(8)	949(8)	2151(5)	24(1)
C(15)	-1862(9)	162(9)	3150(5)	32(2)
C(16)	-2138(8)	1381(9)	3668(5)	27(1)
C(17)	-2771(7)	2906(8)	2979(5)	28(1)
C(18)	-3638(9)	3949(11)	1122(6)	41(2)
C(19)	2190(8)	-2500(8)	3574(5)	25(1)
C(20)	3078(8)	-4017(8)	4147(5)	26(1)
C(21)	4514(7)	-4210(7)	4672(4)	19(1)
C(22)	5034(8)	-2847(7)	4516(4)	22(1)
C(23)	4060(8)	-1380(8)	3925(4)	24(1)
Ce(1)	640(1)	1737(1)	2431(1)	15(1)
N(1)	2619(7)	-1142(6)	3472(4)	22(1)

$[(C_5H_4Me)_3Ce]_2$(1,4-benzoquinone)

EXPERIMENTAL DETAILS

A. Crystal Data

Empirical Formula	$CeOC_{24.50}H_{27}$
Formula Weight	477.60
Crystal Color, Habit	dark red, block
Crystal Dimensions	0.20 X 0.18 X 0.11 mm
Crystal System	triclinic
Lattice Type	Primitive
Lattice Parameters	a = 8.193(2)Å
	b = 8.216(2) Å
	c = 18.038(4) Å
	α = 84.730(3)^o
	β = 76.940(3)^o
	γ = 61.588(2)^o
V = 1040.1(4) Å^3	
Z value	2
D_{calc}	1.525 g/cm^3
F_{000}	480.00
μ(MoKα)	21.98 cm^{-1}

B. Intensity Measurements

Diffractometer	Bruker SMART CCD
Radiation	MoKα (λ = 0.71069 Å) graphite monochromated
Detector Position	60.00 mm
Exposure Time	10.0 seconds per frame.
Scan Type	ω (0.3 degrees per frame)
$2\theta_{max}$	53.7^o
No. of Reflections Measured	
Total: 5858	Unique: 2999 (R_{int} = 0.021)
Corrections	Lorentz-polarization
Absorption	(Tmax = 1.00 Tmin = 0.84)

C. Structure Solution and Refinement

Structure Solution	Direct Methods
Refinement	Full-matrix least-squares
Function Minimized	Σ w (|Fo| - |Fc|)^2
Least Squares Weights	$1/\sigma^2(Fo) = 4Fo^2/\sigma^2(Fo^2)$
p-factor	0.0300
Anomalous Dispersion	All non-hydrogen atoms
No. Observations (I>3.00σ(I))	4612
No. Variables	236
Reflection/Parameter Ratio	19.54
Residuals: R; Rw; Rall	0.039 ; 0.042; 0.059
Goodness of Fit Indicator	1.42
Max Shift/Error in Final Cycle	0.00
Maximum peak in Final Diff. Map	1.65 $e^-/Å^3$
Minimum peak in Final Diff. Map	-0.78 $e^-/Å^3$

Table 1. Atomic coordinates and B_{iso}/B_{eq} and occupancy

atom	x	y	z	B_{eq}	occ
Ce(1)	-0.02968(4)	0.26816(4)	-0.23395(2)	1.444(6)	
O(1)	-0.2086(5)	0.3388(5)	-0.1251(2)	2.51(9)	
C(1)	-0.0938(8)	0.5246(8)	-0.3515(3)	2.8(1)	
C(2)	-0.1956(8)	0.6285(7)	-0.2841(4)	2.6(1)	
C(3)	-0.3421(7)	0.5874(8)	-0.2556(4)	4.0(2)	
C(4)	-0.3335(10)	0.457(1)	-0.3017(6)	5.3(2)	
C(5)	-0.180(1)	0.4205(9)	-0.3609(4)	4.3(2)	
C(6)	0.0638(10)	0.5412(9)	-0.4075(4)	4.5(2)	
C(7)	-0.0925(7)	-0.0371(7)	-0.1967(3)	2.3(1)	
C(8)	0.1041(8)	-0.1078(7)	-0.2104(3)	2.4(1)	
C(9)	0.1678(8)	-0.0911(7)	-0.2878(3)	2.6(1)	
C(10)	0.0150(9)	-0.0110(8)	-0.3231(3)	2.8(2)	
C(11)	-0.1491(8)	0.0245(8)	-0.2656(4)	2.6(1)	
C(12)	-0.2175(9)	-0.0404(9)	-0.1226(4)	4.5(2)	
C(13)	0.2460(8)	0.1969(9)	-0.1509(3)	2.6(1)	
C(14)	0.3466(7)	0.1162(8)	-0.2231(4)	2.5(1)	
C(15)	0.3197(7)	0.2553(8)	-0.2775(3)	2.1(1)	
C(16)	0.2048(8)	0.4241(8)	-0.2389(3)	2.3(1)	
C(17)	0.1574(7)	0.3898(8)	-0.1617(3)	2.6(1)	
C(18)	0.2384(9)	0.102(1)	-0.0769(4)	4.7(2)	
C(19)	-0.3529(8)	0.4180(8)	-0.0633(3)	2.3(1)	
C(20)	-0.3195(8)	0.4648(8)	0.0021(3)	2.6(1)	
C(21)	-0.5341(7)	0.4558(8)	-0.0661(3)	2.5(1)	
C(22)	-0.387(3)	0.217(3)	-0.498(1)	7.3(6)	1/2
C(23)	-0.495(2)	0.185(2)	-0.5352(10)	5.5(4)	1/2
C(24)	-0.593(2)	0.078(2)	-0.5443(8)	3.2(3)	1/2
C(25)	-0.551(2)	-0.084(2)	-0.5036(9)	4.3(3)	1/2
C(26)	-0.433(2)	-0.137(2)	-0.4506(6)	1.5(2)	1/2
C(27)	-0.342(2)	-0.018(2)	-0.4468(7)	3.1(3)	1/2
C(28)	-0.645(2)	-0.135(3)	-0.5190(9)	4.3(4)	1/2
C(101)	-0.2290	0.5236	-0.3108	0.2000	0.001
C(102)	0.0091	-0.0445	-0.2567	0.2000	0.001
C(103)	0.2549	0.2765	-0.2104	0.2000	0.001
H(1)	-0.1687	0.7115	-0.2621	3.0708	
H(2)	-0.4357	0.6409	-0.2107	4.8083	
H(3)	-0.4163	0.4038	-0.2942	6.3329	
H(4)	-0.1394	0.3363	-0.4020	5.1358	
H(5)	0.1809	-0.1584	-0.1735	2.8660	
H(6)	0.2962	-0.1289	-0.3123	3.0971	

Table 1. Atomic coordinates and B_{iso}/B_{eq} and occupancy (continued)

atom	x	y	z	B_{eq}	occ
H(7)	0.0188	0.0153	-0.3757	3.4159	
H(8)	-0.2758	0.0807	-0.2729	3.0678	
H(9)	0.4215	-0.0129	-0.2336	3.0022	
H(10)	0.3704	0.2375	-0.3307	2.5031	
H(11)	0.1652	0.5427	-0.2611	2.7484	
H(12)	0.0785	0.4814	-0.1230	3.1601	
H(13)	0.0132	0.6553	-0.4331	5.3555	
H(14)	0.1539	0.5370	-0.3812	5.3555	
H(15)	0.1239	0.4417	-0.4435	5.3555	
H(16)	-0.2091	0.4730	0.0045	2.1571	
H(17)	-0.5967	0.4035	-0.1018	2.1571	
H(18)	0.3100	0.1218	-0.0474	5.6086	
H(19)	0.1103	0.1496	-0.0501	5.6086	
H(20)	0.2902	-0.0274	-0.0859	5.6086	
H(21)	-0.1634	-0.0368	-0.0818	5.4160	
H(22)	-0.3395	0.0640	-0.1188	5.4160	
H(23)	-0.2292	-0.1506	-0.1201	5.4160	

$B_{eq} = 8/3\ \pi^2(U_{11}(aa^*)^2 + U_{22}(bb^*)^2 + U_{33}(cc^*)^2 + 2U_{12}(aa^*bb^*)\cos\gamma + 2U_{13}(aa^*cc^*)\cos\beta + 2U_{23}(bb^*cc^*)\cos\alpha)$

Table 2. Anisotropic Displacement Parameters

atom	U_{11}	U_{22}	U_{33}	U_{12}	U_{13}	U_{23}
Ce(1)	0.0136(2)	0.0139(2)	0.0259(2)	-0.0051(1)	-0.0029(1)	-0.0035(1)
O(1)	0.022(2)	0.038(2)	0.031(2)	-0.014(2)	0.008(2)	-0.020(2)
C(1)	0.042(4)	0.025(4)	0.035(4)	-0.011(3)	-0.013(3)	0.008(3)
C(2)	0.024(3)	0.013(3)	0.052(4)	-0.004(3)	-0.006(3)	0.002(3)
C(3)	0.012(3)	0.023(4)	0.091(6)	0.007(3)	0.001(3)	0.012(4)
C(4)	0.040(4)	0.044(5)	0.143(8)	-0.029(4)	-0.068(5)	0.058(5)
C(5)	0.073(5)	0.034(4)	0.069(5)	-0.020(4)	-0.056(5)	0.011(4)
C(6)	0.062(5)	0.046(5)	0.038(4)	-0.010(4)	-0.003(4)	0.005(3)
C(7)	0.028(3)	0.018(3)	0.039(4)	-0.015(3)	0.005(3)	-0.001(3)
C(8)	0.039(4)	0.022(3)	0.033(4)	-0.014(3)	-0.016(3)	0.007(3)
C(9)	0.027(3)	0.016(3)	0.046(4)	-0.006(3)	0.005(3)	-0.012(3)
C(10)	0.058(4)	0.024(3)	0.030(4)	-0.020(3)	-0.011(3)	-0.007(3)
C(11)	0.027(3)	0.019(3)	0.054(4)	-0.011(3)	-0.014(3)	-0.001(3)
C(12)	0.061(5)	0.038(4)	0.064(5)	-0.027(4)	0.009(4)	0.010(4)
C(13)	0.026(3)	0.045(4)	0.036(4)	-0.022(3)	-0.011(3)	0.005(3)
C(14)	0.016(3)	0.025(3)	0.051(4)	-0.005(3)	-0.011(3)	-0.003(3)
C(15)	0.014(3)	0.039(4)	0.030(4)	-0.016(3)	-0.003(3)	0.000(3)
C(16)	0.029(3)	0.029(4)	0.043(4)	-0.022(3)	-0.014(3)	0.002(3)
C(17)	0.024(3)	0.033(4)	0.044(4)	-0.008(3)	-0.015(3)	-0.016(3)
C(18)	0.051(4)	0.090(6)	0.047(5)	-0.039(4)	-0.020(4)	0.018(4)
C(19)	0.031(3)	0.029(4)	0.030(4)	-0.015(3)	-0.003(3)	-0.007(3)
C(20)	0.027(3)	0.047(4)	0.032(4)	-0.023(3)	-0.005(3)	-0.009(3)
C(21)	0.021(3)	0.047(4)	0.030(4)	-0.019(3)	0.006(3)	-0.020(3)

The general temperature factor expression:

$\exp(-2\pi^2(a^{*2}U_{11}h^2 + b^{*2}U_{22}k^2 + c^{*2}U_{33}l^2 + 2a^*b^*U_{12}hk + 2a^*c^*U_{13}hl + 2b^*c^*U_{23}kl))$

Table 3. Bond Lengths(Å)

atom	atom	distance	atom	atom	distance
Ce(1)	O(1)	2.107(4)	Ce(1)	C(1)	2.800(5)
Ce(1)	C(2)	2.768(5)	Ce(1)	C(3)	2.731(5)
Ce(1)	C(4)	2.729(6)	Ce(1)	C(5)	2.758(6)
Ce(1)	C(7)	2.787(5)	Ce(1)	C(8)	2.770(5)
Ce(1)	C(9)	2.747(5)	Ce(1)	C(10)	2.756(5)
Ce(1)	C(11)	2.760(5)	Ce(1)	C(13)	2.792(5)
Ce(1)	C(14)	2.769(5)	Ce(1)	C(15)	2.744(4)
Ce(1)	C(16)	2.754(5)	Ce(1)	C(17)	2.765(5)
O(1)	C(19)	1.367(6)	C(1)	C(2)	1.399(8)
C(1)	C(5)	1.383(8)	C(1)	C(6)	1.503(8)
C(2)	C(3)	1.376(7)	C(3)	C(4)	1.38(1)
C(4)	C(5)	1.380(9)	C(7)	C(8)	1.396(7)
C(7)	C(11)	1.391(7)	C(7)	C(12)	1.497(7)
C(8)	C(9)	1.393(7)	C(9)	C(10)	1.381(8)
C(10)	C(11)	1.421(7)	C(13)	C(14)	1.403(7)
C(13)	C(17)	1.411(8)	C(13)	C(18)	1.488(8)
C(14)	C(15)	1.403(7)	C(15)	C(16)	1.390(7)
C(16)	C(17)	1.397(7)	C(19)	C(20)	1.395(7)
C(19)	C(21)	1.377(7)	C(20)	C(21)	1.401(7)
C(22)	C(23)	1.36(3)	C(22)	C(25)	1.40(3)
C(22)	C(28)	0.66(2)	C(23)	C(24)	1.48(2)
C(23)	C(25)	1.02(2)	C(23)	C(26)	0.94(2)
C(23)	C(28)	1.56(3)	C(24)	C(25)	1.39(2)
C(24)	C(25)	1.63(2)	C(24)	C(26)	0.61(2)
C(24)	C(27)	0.92(2)	C(25)	C(26)	1.41(2)
C(25)	C(27)	1.34(2)	C(25)	C(28)	1.13(2)
C(26)	C(27)	1.50(2)	C(27)	C(28)	1.32(2)

$Cp^*_2Sm(2,2'\text{-bipyridine})(OTf)$

EXPERIMENTAL DETAILS

A. Crystal Data

Empirical Formula	$SmH_{38}C_{31}N_2O_3F_3S$
Formula Weight	726.11
Crystal Color, Habit	red, block
Crystal Dimensions	0.16 X 0.16 X 0.14 mm
Crystal System	monoclinic
Lattice Type	Primitive
Lattice Parameters	a = 12.1726(7)Å
	b = 15.3264(9) Å
	c = 16.0752(9) Å
	β = 91.045(1)^o
	V = 2998.5(3) Å^3
Space Group	$P2_1/n$ (#14)
Z value	4
D_{calc}	1.608 g/cm^3
F_{000}	1468.00
μ(MoKα)	20.86 cm^{-1}

B. Intensity Measurements

Diffractometer	Bruker SMART CCD
Radiation	MoKα (λ = 0.71069 Å) graphite monochromated
Detector Position	60.00 mm
Exposure Time	10.0 seconds per frame.
Scan Type	ω (0.3 degrees per frame)
$2\theta_{max}$	52.7^o
No. of Reflections Measured	
Total: 14568	Unique: 3640 (R_{int} = 0.019)
Corrections	Lorentz-polarization
Absorption	(Tmax = 1.00 Tmin = 0.85)

C. Structure Solution and Refinement

Structure Solution	Direct Methods (SIR97)
Refinement	Full-matrix least-squares
Function Minimized	Σ w (|Fo| - |Fc|)^2
Least Squares Weights	$1/\sigma^2(Fo) = 4Fo^2/\sigma^2(Fo^2)$
p-factor	0.0300
Anomalous Dispersion	All non-hydrogen atoms
No. Observations (I>3.00σ(I))	3749
No. Variables	370
Reflection/Parameter Ratio	10.13
Residuals: R; Rw; Rall	0.026 ; 0.032; 0.051
Goodness of Fit Indicator	1.47
Max Shift/Error in Final Cycle	0.00
Maximum peak in Final Diff. Map	1.08 $e^-/Å^3$
Minimum peak in Final Diff. Map	-0.35 $e^-/Å^3$

Table 1. Atomic coordinates and B_{iso}/B_{eq} and occupancy

atom	x	y	z	B_{eq}	occ
Sm(1)	0.76234(1)	0.25118(2)	0.46951(1)	1.329(4)	
S(1)	0.89291(8)	0.35719(7)	0.68365(7)	1.80(2)	
F(1)	0.8510(2)	0.5253(2)	0.6585(2)	3.07(6)	
F(2)	0.8767(2)	0.4880(2)	0.7857(2)	3.48(7)	
F(3)	0.7250(2)	0.4563(2)	0.7226(2)	3.12(6)	
O(1)	0.8338(2)	0.3311(2)	0.6077(2)	1.76(6)	
O(2)	1.0062(2)	0.3783(2)	0.6712(2)	2.58(7)	
O(3)	0.8707(2)	0.3044(2)	0.7551(2)	2.65(7)	
N(1)	0.9727(3)	0.2329(2)	0.4502(2)	1.98(8)	
N(2)	0.8242(3)	0.1720(2)	0.3396(2)	1.69(8)	
C(1)	0.7660(3)	0.1154(3)	0.5771(3)	1.93(9)	
C(2)	0.6747(3)	0.1655(3)	0.6016(3)	1.75(9)	
C(3)	0.5928(3)	0.1580(3)	0.5387(3)	2.04(10)	
C(4)	0.6323(4)	0.1021(3)	0.4761(3)	2.3(1)	
C(5)	0.7393(4)	0.0758(3)	0.5004(3)	2.23(10)	
C(6)	0.7744(3)	0.4211(3)	0.4294(3)	1.70(9)	
C(7)	0.6665(3)	0.4071(3)	0.4590(3)	1.76(9)	
C(8)	0.6070(3)	0.3599(3)	0.3955(3)	1.77(9)	
C(9)	0.6796(3)	0.3461(3)	0.3293(2)	1.73(9)	
C(10)	0.7826(3)	0.3827(3)	0.3511(3)	1.91(9)	
C(11)	0.8717(4)	0.1003(3)	0.6271(3)	3.0(1)	
C(12)	0.6560(4)	0.2072(3)	0.6850(3)	2.7(1)	
C(13)	0.4756(4)	0.1881(4)	0.5482(3)	3.5(1)	
C(14)	0.5601(4)	0.0650(3)	0.4068(3)	3.6(1)	
C(15)	0.8091(5)	0.0077(3)	0.4578(3)	3.6(1)	
C(16)	0.8642(4)	0.4757(3)	0.4698(3)	2.8(1)	
C(17)	0.6205(4)	0.4371(3)	0.5400(3)	2.7(1)	
C(18)	0.4856(3)	0.3434(3)	0.3916(3)	2.6(1)	
C(19)	0.6434(4)	0.3205(3)	0.2424(3)	2.6(1)	
C(20)	0.8796(4)	0.3863(3)	0.2949(3)	2.8(1)	
C(21)	1.0469(4)	0.2687(3)	0.5029(3)	2.8(1)	
C(22)	1.1587(4)	0.2660(3)	0.4915(3)	2.8(1)	
C(23)	1.1985(3)	0.2243(3)	0.4231(3)	2.6(1)	
C(24)	1.1242(3)	0.1851(3)	0.3687(3)	2.26(10)	
C(25)	1.0125(3)	0.1907(3)	0.3829(2)	1.71(9)	
C(26)	0.9297(3)	0.1522(3)	0.3243(2)	1.81(9)	
C(27)	0.9585(3)	0.0996(3)	0.2574(3)	2.25(10)	
C(28)	0.8769(4)	0.0692(3)	0.2033(3)	2.6(1)	
C(29)	0.7701(3)	0.0908(3)	0.2173(3)	2.17(10)	

Table 1. Atomic coordinates and B_{iso}/B_{eq} and occupancy (continued)

atom	x	y	z	B_{eq}	occ
C(30)	0.7465(3)	0.1415(3)	0.2849(3)	1.82(9)	
C(31)	0.8335(3)	0.4621(3)	0.7134(3)	2.09(10)	
C(101)	0.6810	0.1233	0.5388	0.2000	0.000
C(102)	0.7020	0.3834	0.3929	0.2000	0.000
H(1)	0.8773	0.1422	0.6720	3.5653	
H(2)	0.8732	0.0436	0.6505	3.5653	
H(3)	0.9342	0.1079	0.5928	3.5653	
H(4)	0.7213	0.2073	0.7179	3.4723	
H(5)	0.6317	0.2667	0.6778	3.4723	
H(6)	0.5999	0.1765	0.7140	3.4723	
H(7)	0.4723	0.2437	0.5752	4.1113	
H(8)	0.4387	0.1928	0.4953	4.1113	
H(9)	0.4351	0.1471	0.5814	4.1113	
H(10)	0.6031	0.0421	0.3622	4.4128	
H(11)	0.5116	0.1083	0.3840	4.4128	
H(12)	0.5156	0.0179	0.4273	4.4128	
H(13)	0.8832	0.0287	0.4544	4.4759	
H(14)	0.8087	-0.0448	0.4883	4.4759	
H(15)	0.7819	-0.0025	0.4026	4.4759	
H(16)	0.8340	0.5192	0.5051	3.5519	
H(17)	0.9126	0.4396	0.5031	3.5519	
H(18)	0.9075	0.5039	0.4286	3.5519	
H(19)	0.5429	0.4362	0.5380	3.1901	
H(20)	0.6455	0.4947	0.5522	3.1901	
H(21)	0.6458	0.3993	0.5844	3.1901	
H(22)	0.4482	0.3834	0.3550	3.3383	
H(23)	0.4535	0.3524	0.4469	3.3383	
H(24)	0.4679	0.2856	0.3753	3.3383	
H(25)	0.7026	0.2979	0.2115	3.2690	
H(26)	0.6122	0.3692	0.2129	3.2690	
H(27)	0.5869	0.2757	0.2444	3.2690	
H(28)	0.9273	0.3364	0.3036	3.3776	
H(29)	0.8562	0.3846	0.2370	3.3776	
H(30)	0.9216	0.4376	0.3035	3.3776	
H(31)	1.0205	0.2974	0.5515	3.2244	
H(32)	1.2081	0.2935	0.5306	3.2316	
H(33)	1.2762	0.2222	0.4137	2.9622	
H(34)	1.1497	0.1539	0.3209	2.7378	
H(35)	1.0354	0.0832	0.2489	2.7359	

Table 1. Atomic coordinates and B_{iso}/B_{eq} and occupancy (continued)

atom	x	y	z	B_{eq}	occ
H(36)	0.8952	0.0339	0.1541	3.0533	
H(37)	0.7110	0.0706	0.1811	2.5409	
H(38)	0.6720	0.1578	0.2936	2.1720	

$B_{eq} = 8/3\ \pi^2(U_{11}(aa^*)^2 + U_{22}(bb^*)^2 + U_{33}(cc^*)^2 + 2U_{12}(aa^*bb^*)\cos\gamma + 2U_{13}(aa^*cc^*)\cos\beta + 2U_{23}(bb^*cc^*)\cos\alpha)$

Table 2. Anisotropic Displacement Parameters

atom	U_{11}	U_{22}	U_{33}	U_{12}	U_{13}	U_{23}
Sm(1)	0.0165(1)	0.0162(1)	0.0178(1)	-0.0003(1)	-0.00003(7)	0.0011(1)
S(1)	0.0225(5)	0.0236(6)	0.0221(6)	0.0009(5)	-0.0024(4)	0.0002(5)
F(1)	0.050(2)	0.026(1)	0.040(2)	0.001(1)	0.004(1)	0.003(1)
F(2)	0.054(2)	0.046(2)	0.032(2)	0.014(1)	-0.018(1)	-0.016(1)
F(3)	0.025(1)	0.049(2)	0.046(2)	0.005(1)	0.007(1)	-0.004(1)
O(1)	0.022(1)	0.022(2)	0.023(2)	0.000(1)	-0.003(1)	-0.000(1)
O(2)	0.023(2)	0.041(2)	0.033(2)	-0.000(1)	-0.003(1)	-0.006(1)
O(3)	0.041(2)	0.031(2)	0.029(2)	-0.004(2)	-0.004(1)	0.007(1)
N(1)	0.020(2)	0.034(3)	0.021(2)	0.001(2)	-0.003(1)	-0.003(2)
N(2)	0.023(2)	0.020(2)	0.021(2)	0.002(2)	0.001(1)	-0.001(2)
C(1)	0.029(2)	0.021(2)	0.023(2)	-0.003(2)	0.000(2)	0.007(2)
C(2)	0.027(2)	0.017(2)	0.022(2)	-0.006(2)	0.002(2)	0.006(2)
C(3)	0.023(2)	0.029(3)	0.025(2)	-0.006(2)	0.001(2)	0.011(2)
C(4)	0.039(3)	0.021(2)	0.027(3)	-0.015(2)	-0.005(2)	0.006(2)
C(5)	0.042(3)	0.021(2)	0.022(2)	0.000(2)	0.004(2)	0.005(2)
C(6)	0.026(2)	0.013(2)	0.026(3)	-0.004(2)	-0.003(2)	0.004(2)
C(7)	0.029(2)	0.013(2)	0.024(2)	0.004(2)	-0.006(2)	-0.001(2)
C(8)	0.028(2)	0.015(2)	0.024(2)	0.004(2)	-0.003(2)	0.006(2)
C(9)	0.027(2)	0.020(2)	0.019(2)	-0.003(2)	-0.003(2)	0.002(2)
C(10)	0.027(2)	0.020(2)	0.026(3)	0.000(2)	-0.002(2)	0.008(2)
C(11)	0.035(3)	0.041(3)	0.039(3)	0.003(2)	-0.003(2)	0.018(2)
C(12)	0.041(3)	0.036(3)	0.026(3)	-0.004(2)	0.008(2)	0.000(2)
C(13)	0.033(3)	0.049(3)	0.051(3)	-0.005(3)	0.003(2)	0.016(3)
C(14)	0.056(3)	0.045(3)	0.036(3)	-0.026(3)	-0.009(3)	0.005(2)
C(15)	0.078(4)	0.022(3)	0.039(3)	0.012(3)	0.017(3)	0.005(2)
C(16)	0.047(3)	0.031(3)	0.030(3)	-0.015(2)	-0.010(2)	0.009(2)
C(17)	0.039(3)	0.034(3)	0.029(3)	0.013(2)	-0.003(2)	-0.005(2)
C(18)	0.023(2)	0.036(3)	0.040(3)	0.001(2)	-0.004(2)	0.004(2)
C(19)	0.040(3)	0.038(3)	0.021(3)	0.001(2)	-0.006(2)	0.002(2)
C(20)	0.035(3)	0.038(3)	0.035(3)	-0.006(2)	0.003(2)	0.013(2)
C(21)	0.029(2)	0.049(4)	0.027(3)	-0.000(2)	-0.002(2)	-0.010(2)
C(22)	0.026(2)	0.051(4)	0.030(3)	-0.007(2)	-0.005(2)	-0.008(2)
C(23)	0.019(2)	0.046(3)	0.033(3)	-0.002(2)	0.002(2)	0.001(2)
C(24)	0.027(2)	0.033(3)	0.026(3)	0.004(2)	0.002(2)	0.002(2)
C(25)	0.027(2)	0.020(2)	0.017(2)	0.000(2)	0.001(2)	0.003(2)
C(26)	0.027(2)	0.022(2)	0.020(2)	-0.001(2)	-0.001(2)	0.004(2)
C(27)	0.024(2)	0.032(3)	0.030(3)	-0.000(2)	0.006(2)	-0.007(2)
C(28)	0.039(3)	0.031(3)	0.028(3)	-0.002(2)	0.003(2)	-0.010(2)
C(29)	0.028(2)	0.028(2)	0.027(3)	-0.004(2)	-0.001(2)	-0.005(2)

Table 2. Anisotropic Displacement Parameters (continued)

atom	U_{11}	U_{22}	U_{33}	U_{12}	U_{13}	U_{23}
C(30)	0.023(2)	0.022(2)	0.024(2)	0.001(2)	-0.003(2)	0.004(2)
C(31)	0.025(2)	0.032(3)	0.022(2)	0.002(2)	-0.003(2)	0.000(2)

The general temperature factor expression:
$\exp(-2\pi^2(a^{*2}U_{11}h^2 + b^{*2}U_{22}k^2 + c^{*2}U_{33}l^2 + 2a^*b^*U_{12}hk + 2a^*c^*U_{13}hl + 2b^*c^*U_{23}kl))$

$Cp^*_2Gd(2,2'\text{-bipyridine})(Cl)$

EXPERIMENTAL DETAILS

A. Crystal Data

Empirical Formula	$GdC_{30}N_2ClH_{38}$
Formula Weight	619.35
Crystal Color, Habit	red, block
Crystal Dimensions	0.07 X 0.08 X 0.07 mm
Crystal System	monoclinic
Lattice Type	Primitive
Lattice Parameters	a = 10.6307(8)Å
	b = 13.950(1) Å
	c = 18.153(1) Å
	β = 90.065(1)^o
	V = 2691.9(3) Å^3
Space Group	$P2_1/c$ (#14)
Z value	4
D_{calc}	1.528 g/cm^3
F_{000}	1252.00
μ(MoKα)	25.90 cm^{-1}

B. Intensity Measurements

Diffractometer	Bruker SMART CCD
Radiation	MoKα (λ = 0.71069 Å) graphite monochromated
Detector Position	60.00 mm
Exposure Time	10.0 seconds per frame.
Scan Type	ω (0.3 degrees per frame)
$2\theta_{max}$	52.7^o
No. of Reflections Measured	Total: 13053
Unique:	3633 (R_{int} = 0.029)
Corrections	Lorentz-polarization

Absorption (Tmax = 1.00 Tmin = 0.76)

C. Structure Solution and Refinement

Structure Solution	Direct Methods (SIR92)
Refinement	Full-matrix least-squares
Function Minimized	Σ w (|Fo| - |Fc|)^2
Least Squares Weights	$1/\sigma^2(Fo) = 4Fo^2/\sigma^2(Fo^2)$
p-factor	0.0300
Anomalous Dispersion	All non-hydrogen atoms
No. Observations (I>3.00σ(I))	3765
No. Variables	307
Reflection/Parameter Ratio	12.26
Residuals: R; Rw; Rall	0.027 ; 0.031; 0.045
Goodness of Fit Indicator	1.21
Max Shift/Error in Final Cycle	0.00
Maximum peak in Final Diff. Map	1.09 $e^-/Å^3$
Minimum peak in Final Diff. Map	-0.52 $e^-/Å^3$

Table 1. Atomic coordinates and B_{iso}/B_{eq} and occupancy

atom	x	y	z	B_{eq}	occ
Gd(1)	0.28180(2)	0.28152(1)	0.13592(1)	1.319(4)	
Cl(1)	0.4244(1)	0.13404(8)	0.08946(6)	2.32(2)	
N(1)	0.4664(3)	0.2835(2)	0.2340(2)	1.70(7)	
N(2)	0.2639(3)	0.3978(2)	0.2458(2)	1.52(7)	
C(1)	0.0772(4)	0.2210(3)	0.2183(2)	1.58(8)	
C(2)	0.0218(4)	0.2590(3)	0.1535(2)	1.76(9)	
C(3)	0.0541(4)	0.1962(3)	0.0948(2)	1.78(9)	
C(4)	0.1281(4)	0.1219(3)	0.1228(2)	1.90(9)	
C(5)	0.1463(4)	0.1385(3)	0.1989(2)	1.44(8)	
C(6)	0.4051(4)	0.4453(3)	0.0927(2)	1.95(9)	
C(7)	0.2777(4)	0.4634(3)	0.0748(2)	1.79(9)	
C(8)	0.2439(4)	0.3990(3)	0.0182(2)	1.69(9)	
C(9)	0.3495(4)	0.3408(3)	0.0013(2)	1.88(9)	
C(10)	0.4500(4)	0.3708(3)	0.0472(2)	2.3(1)	
C(11)	0.0512(4)	0.2526(3)	0.2964(2)	2.11(9)	
C(12)	-0.0750(4)	0.3378(3)	0.1480(2)	2.4(1)	
C(13)	-0.0038(5)	0.1960(3)	0.0190(2)	2.7(1)	
C(14)	0.1606(5)	0.0314(3)	0.0822(3)	2.7(1)	
C(15)	0.2162(4)	0.0732(3)	0.2517(3)	2.6(1)	
C(16)	0.4854(5)	0.5066(4)	0.1426(3)	3.2(1)	
C(17)	0.1994(5)	0.5477(3)	0.0980(2)	2.6(1)	
C(18)	0.1256(4)	0.4076(3)	-0.0271(2)	2.3(1)	
C(19)	0.3559(5)	0.2687(3)	-0.0598(2)	2.6(1)	
C(20)	0.5835(4)	0.3388(4)	0.0434(3)	3.3(1)	
C(21)	0.5705(4)	0.2291(3)	0.2257(2)	2.3(1)	
C(22)	0.6785(4)	0.2404(3)	0.2682(3)	2.4(1)	
C(23)	0.6802(4)	0.3088(3)	0.3222(3)	2.5(1)	
C(24)	0.5751(4)	0.3639(3)	0.3325(2)	2.18(10)	
C(25)	0.4692(4)	0.3494(3)	0.2883(2)	1.56(8)	
C(26)	0.3546(4)	0.4081(3)	0.2982(2)	1.72(9)	
C(27)	0.3395(4)	0.4712(3)	0.3563(2)	2.13(10)	
C(28)	0.2337(4)	0.5271(3)	0.3609(2)	2.5(1)	
C(29)	0.1424(4)	0.5190(3)	0.3070(2)	2.19(10)	
C(30)	0.1611(4)	0.4522(3)	0.2519(2)	1.80(9)	
C(101)	0.0853	0.1873	0.1577	0.2000	0.001
C(102)	0.3452	0.4039	0.0468	0.2000	0.001
H(1)	0.0062	0.2037	0.3215	2.5309	
H(2)	0.1286	0.2643	0.3211	2.5309	
H(3)	0.0025	0.3097	0.2958	2.5309	

Table 1. Atomic coordinates and B_{iso}/B_{eq} and occupancy (continued)

atom	x	y	z	B_{eq}	occ
H(4)	-0.0894	0.3642	0.1955	2.9068	
H(5)	-0.0553	0.1408	0.0134	3.2330	
H(6)	0.0859	-0.0035	0.0721	3.2323	
H(7)	0.1781	0.0116	0.2515	3.1205	
H(8)	-0.0451	0.3865	0.1159	2.9068	
H(9)	-0.1513	0.3122	0.1292	2.9068	
H(10)	-0.0535	0.2520	0.0128	3.2330	
H(11)	0.0610	0.1951	-0.0171	3.2330	
H(12)	0.2013	0.0472	0.0372	3.2323	
H(13)	0.2153	-0.0065	0.1116	3.2323	
H(14)	0.3014	0.0678	0.2367	3.1205	
H(15)	0.2127	0.0993	0.3000	3.1205	
H(16)	0.4329	0.5410	0.1757	3.7951	
H(17)	0.2310	0.5726	0.1431	3.1706	
H(18)	0.5883	0.2800	0.0172	3.9946	
H(19)	0.4156	0.2205	-0.0476	3.1606	
H(20)	0.1240	0.3583	-0.0632	2.7506	
H(21)	0.6153	0.3300	0.0919	3.9946	
H(22)	0.6321	0.3860	0.0187	3.9946	
H(23)	0.5412	0.4669	0.1698	3.7951	
H(24)	0.5326	0.5506	0.1138	3.7951	
H(25)	0.2031	0.5959	0.0611	3.1706	
H(26)	0.1147	0.5279	0.1045	3.1706	
H(27)	0.1238	0.4683	-0.0508	2.7506	
H(28)	0.0543	0.4016	0.0041	2.7506	
H(29)	0.2756	0.2401	-0.0664	3.1606	
H(30)	0.3807	0.2996	-0.1041	3.1606	
H(31)	0.5701	0.1807	0.1889	2.7056	
H(32)	0.7501	0.2011	0.2599	2.8355	
H(33)	0.7528	0.3180	0.3519	2.9434	
H(34)	0.5742	0.4119	0.3696	2.6100	
H(35)	0.4027	0.4759	0.3931	2.5583	
H(36)	0.2233	0.5708	0.4005	3.0108	
H(37)	0.0692	0.5581	0.3078	2.6261	
H(38)	0.0966	0.4445	0.2161	2.1618	

$B_{eq} = 8/3\ \pi^2(U_{11}(aa^*)^2 + U_{22}(bb^*)^2 + U_{33}(cc^*)^2 + 2U_{12}(aa^*bb^*)\cos\gamma + 2U_{13}(aa^*cc^*)\cos\beta + 2U_{23}(bb^*cc^*)\cos\alpha)$

Table 2. Anisotropic Displacement Parameters

atom	U_{11}	U_{22}	U_{33}	U_{12}	U_{13}	U_{23}
Gd(1)	0.0160(1)	0.0161(1)	0.0180(1)	0.00005(10)	-0.00016(7)	0.00052(10)
Cl(1)	0.0269(6)	0.0259(6)	0.0355(6)	0.0065(5)	-0.0011(5)	-0.0052(5)
N(1)	0.025(2)	0.017(2)	0.023(2)	-0.001(2)	-0.001(1)	0.001(2)
N(2)	0.018(2)	0.019(2)	0.020(2)	-0.004(1)	0.002(1)	0.004(1)
C(1)	0.018(2)	0.021(2)	0.022(2)	-0.008(2)	-0.001(2)	0.000(2)
C(2)	0.018(2)	0.024(2)	0.024(2)	-0.004(2)	0.000(2)	0.001(2)
C(3)	0.017(2)	0.026(3)	0.025(2)	-0.009(2)	-0.002(2)	0.001(2)
C(4)	0.029(3)	0.019(2)	0.024(2)	-0.005(2)	0.002(2)	-0.004(2)
C(5)	0.017(2)	0.013(2)	0.025(2)	-0.006(2)	0.001(2)	0.005(2)
C(6)	0.034(3)	0.021(2)	0.019(2)	-0.014(2)	-0.001(2)	0.006(2)
C(7)	0.031(3)	0.015(2)	0.022(2)	-0.002(2)	0.002(2)	0.002(2)
C(8)	0.024(2)	0.020(2)	0.020(2)	0.002(2)	0.001(2)	0.008(2)
C(9)	0.027(2)	0.027(3)	0.017(2)	-0.003(2)	0.004(2)	0.004(2)
C(10)	0.022(2)	0.035(3)	0.031(2)	-0.002(2)	0.006(2)	0.014(2)
C(11)	0.027(3)	0.031(2)	0.022(2)	-0.008(2)	0.004(2)	0.001(2)
C(12)	0.022(2)	0.035(3)	0.035(3)	-0.000(2)	-0.003(2)	0.004(2)
C(13)	0.035(3)	0.037(3)	0.030(3)	-0.010(2)	-0.007(2)	-0.001(2)
C(14)	0.036(3)	0.021(2)	0.045(3)	-0.004(2)	0.003(2)	-0.009(2)
C(15)	0.033(3)	0.028(3)	0.037(3)	-0.001(2)	-0.007(2)	0.010(2)
C(16)	0.048(3)	0.038(3)	0.034(3)	-0.023(2)	-0.009(2)	0.013(2)
C(17)	0.052(3)	0.018(2)	0.031(3)	-0.002(2)	0.005(2)	0.002(2)
C(18)	0.037(3)	0.024(2)	0.026(2)	0.005(2)	-0.004(2)	0.001(2)
C(19)	0.043(3)	0.032(3)	0.025(2)	0.009(2)	0.005(2)	0.003(2)
C(20)	0.024(3)	0.053(3)	0.049(3)	0.000(2)	0.006(2)	0.021(3)
C(21)	0.029(3)	0.022(3)	0.034(2)	0.004(2)	-0.001(2)	-0.000(2)
C(22)	0.025(3)	0.027(3)	0.038(3)	0.004(2)	-0.003(2)	0.007(2)
C(23)	0.019(2)	0.038(3)	0.037(3)	-0.003(2)	-0.006(2)	0.006(2)
C(24)	0.024(2)	0.028(3)	0.031(2)	-0.003(2)	-0.004(2)	-0.001(2)
C(25)	0.020(2)	0.020(2)	0.019(2)	-0.005(2)	0.001(2)	0.006(2)
C(26)	0.024(2)	0.019(2)	0.022(2)	-0.007(2)	0.004(2)	0.005(2)
C(27)	0.028(3)	0.026(2)	0.026(2)	-0.006(2)	-0.005(2)	-0.003(2)
C(28)	0.034(3)	0.030(3)	0.031(2)	-0.002(2)	0.005(2)	-0.008(2)
C(29)	0.023(3)	0.023(2)	0.036(3)	0.002(2)	0.005(2)	-0.000(2)
C(30)	0.020(2)	0.022(2)	0.026(2)	0.002(2)	0.001(2)	0.005(2)

The general temperature factor expression:
$\exp(-2\pi^2(a^{*2}U_{11}h^2 + b^{*2}U_{22}k^2 + c^{*2}U_{33}l^2 + 2a^*b^*U_{12}hk + 2a^*c^*U_{13}hl + 2b^*c^*U_{23}kl))$

Table 3. Bond Lengths(Å)

atom	atom	distance	atom	atom	distance
GD1	CL1	2.692(1)	GD1	N1	2.648(3)
GD1	N2	2.578(3)	GD1	C1	2.773(4)
GD1	C2	2.800(4)	GD1	C3	2.797(4)
GD1	C4	2.773(4)	GD1	C5	2.714(4)
GD1	C6	2.748(4)	GD1	C7	2.769(4)
GD1	C8	2.723(4)	GD1	C9	2.680(4)
GD1	C10	2.710(4)	GD1	C101	2.4999(2)
GD1	C102	2.4471(2)	N1	C21	1.350(5)
N1	C25	1.349(5)	N2	C26	1.362(5)
N2	C30	1.335(5)	C1	C2	1.417(6)
C1	C5	1.412(6)	C1	C11	1.510(6)
C1	C101	1.200(4)	C2	C3	1.422(6)
C2	C12	1.509(6)	C2	C101	1.209(4)
C3	C4	1.396(6)	C3	C13	1.508(6)
C3	C101	1.194(4)	C4	C5	1.414(5)
C4	C14	1.502(6)	C4	C101	1.201(4)
C5	C15	1.515(6)	C5	C101	1.202(4)
C6	C7	1.414(6)	C6	C10	1.411(6)
C6	C16	1.510(6)	C6	C102	1.196(4)
C7	C8	1.411(6)	C7	C17	1.501(6)
C7	C102	1.209(4)	C8	C9	1.419(6)
C8	C18	1.507(6)	C8	C102	1.197(4)
C9	C10	1.418(6)	C9	C19	1.499(6)
C9	C102	1.208(4)	C10	C20	1.489(6)
C10	C102	1.206(4)	C21	C22	1.391(6)
C22	C23	1.368(7)	C23	C24	1.369(6)
C24	C25	1.396(5)	C25	C26	1.479(6)
C26	C27	1.383(6)	C27	C28	1.371(6)
C28	C29	1.382(6)	C29	C30	1.381(6)

[Cp^*_2Gd(2,2'-bipyridine)][BPh_4]

EXPERIMENTAL DETAILS

A. Crystal Data

Empirical Formula	$GdC_{54}N_2H_{58}B$
Formula Weight	903.13
Crystal Color, Habit	yellow, plate
Crystal Dimensions	0.67 X 0.28 X 0.27 mm
Crystal System	monoclinic
Lattice Type	Primitive
Lattice Parameters	a = 12.331(2)Å
	b = 14.835(3) Å
	c = 24.337(5) Å
	β = 90.229(3)^o
V = 4451(1) Å^3	
Space Group	$P2_1/n$ (#14)
Z value	4
D_{calc}	1.347 g/cm^3
F_{000}	1860.00
μ(MoKα)	15.32 cm^{-1}

B. Intensity Measurements

Diffractometer	Bruker SMART CCD
Radiation	MoKα (λ = 0.71069 Å) graphite monochromated
Detector Position	60.00 mm
Exposure Time	20.0 seconds per frame.
Scan Type	ω (0.3 degrees per frame)
$2\theta_{max}$	52.8^o
No. of Reflections Measured (R_{int} = 0.023)	Total: 21600 Unique: 6244
Corrections	Lorentz-polarization
Absorption	(Tmax = 1.00 Tmin = 0.70)

C. Structure Solution and Refinement

Structure Solution	Direct Methods (SIR92)
Refinement	Full-matrix least-squares
Function Minimized	Σ w (|Fo| - |Fc|)^2
Least Squares Weights	$1/\sigma^2(Fo) = 4Fo^2/\sigma^2(Fo^2)$
p-factor	0.0300
Anomalous Dispersion	All non-hydrogen atoms
No. Observations (I>3.00σ(I))	6363
No. Variables	523
Reflection/Parameter Ratio	12.17
Residuals: R; Rw; Rall	0.025 ; 0.032; 0.039
Goodness of Fit Indicator	1.43
Max Shift/Error in Final Cycle	0.00
Maximum peak in Final Diff. Map	0.96 $e^-/Å^3$
Minimum peak in Final Diff. Map	-0.31 $e^-/Å^3$

Table 1. Atomic coordinates and B_{iso}/B_{eq} and occupancy

atom	x	y	z	B_{eq}	occ
Gd(1)	-0.24536(1)	0.375078(9)	0.120082(6)	1.565(3)	
N(1)	-0.2288(2)	0.2193(2)	0.0900(1)	1.94(5)	
N(2)	-0.0903(2)	0.2976(2)	0.1615(1)	1.77(5)	
C(1)	-0.0870(2)	0.4646(2)	0.0685(1)	2.54(7)	
C(2)	-0.1250(3)	0.4017(2)	0.0300(1)	2.57(7)	
C(3)	-0.2323(3)	0.4266(2)	0.0149(1)	2.38(7)	
C(4)	-0.2599(2)	0.5049(2)	0.0446(1)	2.15(7)	
C(5)	-0.1704(3)	0.5287(2)	0.0782(1)	2.36(7)	
C(6)	-0.4506(2)	0.3587(2)	0.1543(1)	2.20(7)	
C(7)	-0.4124(2)	0.4423(2)	0.1763(1)	2.23(7)	
C(8)	-0.3316(2)	0.4225(2)	0.2159(1)	2.05(7)	
C(9)	-0.3207(2)	0.3274(2)	0.2192(1)	1.78(6)	
C(10)	-0.3944(2)	0.2881(2)	0.1813(1)	1.89(6)	
C(11)	0.0277(3)	0.4694(3)	0.0901(2)	4.6(1)	
C(12)	-0.0595(3)	0.3264(3)	0.0053(2)	4.4(1)	
C(13)	-0.3018(3)	0.3849(3)	-0.0294(2)	3.87(9)	
C(14)	-0.3614(3)	0.5601(2)	0.0352(2)	3.42(9)	
C(15)	-0.1630(4)	0.6125(2)	0.1140(2)	3.95(10)	
C(16)	-0.5411(3)	0.3490(3)	0.1128(2)	3.46(9)	
C(17)	-0.4657(3)	0.5328(2)	0.1671(2)	3.35(8)	
C(18)	-0.2751(3)	0.4905(2)	0.2522(1)	2.92(8)	
C(19)	-0.2571(3)	0.2745(2)	0.2613(1)	2.36(7)	
C(20)	-0.4157(2)	0.1885(2)	0.1763(1)	2.52(7)	
C(21)	-0.2995(3)	0.1826(2)	0.0541(1)	2.44(7)	
C(22)	-0.2966(3)	0.0935(2)	0.0390(1)	2.63(7)	
C(23)	-0.2179(3)	0.0391(2)	0.0614(1)	2.76(8)	
C(24)	-0.1439(3)	0.0747(2)	0.0978(1)	2.42(7)	
C(25)	-0.1519(2)	0.1652(2)	0.1122(1)	1.74(6)	
C(26)	-0.0792(2)	0.2076(2)	0.1536(1)	1.65(6)	
C(27)	-0.0047(2)	0.1582(2)	0.1847(1)	2.22(7)	
C(28)	0.0572(2)	0.2005(2)	0.2244(1)	2.33(7)	
C(29)	0.0467(2)	0.2923(2)	0.2319(1)	2.31(7)	
C(30)	-0.0271(2)	0.3381(2)	0.1996(1)	2.08(7)	
C(31)	0.2920(2)	0.0661(2)	0.1943(1)	2.43(7)	
C(32)	0.2925(3)	0.0224(3)	0.2455(2)	3.48(9)	
C(33)	0.3054(3)	0.0682(4)	0.2950(2)	4.9(1)	
C(34)	0.3237(3)	0.1595(4)	0.2952(2)	5.2(1)	
C(35)	0.3262(3)	0.2047(3)	0.2456(2)	4.6(1)	
C(36)	0.3094(3)	0.1594(2)	0.1966(2)	3.23(8)	

Table 1. Atomic coordinates and B_{iso}/B_{eq} and occupancy (continued)

atom	x	y	z	B_{eq}	occ
C(37)	0.2948(2)	0.0763(2)	0.0836(1)	1.96(7)	
C(38)	0.3859(2)	0.0779(2)	0.0499(1)	2.06(7)	
C(39)	0.3967(3)	0.1358(2)	0.0050(1)	2.43(7)	
C(40)	0.3159(3)	0.1965(2)	-0.0072(1)	2.96(8)	
C(41)	0.2248(3)	0.1986(2)	0.0252(2)	3.44(9)	
C(42)	0.2146(3)	0.1401(2)	0.0693(2)	3.04(8)	
C(43)	0.1565(2)	-0.0401(2)	0.1308(1)	1.88(6)	
C(44)	0.0952(3)	-0.0711(2)	0.1750(1)	2.43(7)	
C(45)	0.0007(3)	-0.1220(2)	0.1677(2)	3.42(8)	
C(46)	-0.0370(3)	-0.1418(2)	0.1156(2)	3.36(9)	
C(47)	0.0198(3)	-0.1113(2)	0.0712(2)	3.10(8)	
C(48)	0.1138(2)	-0.0606(2)	0.0789(1)	2.44(7)	
C(49)	0.3694(2)	-0.0717(2)	0.1362(1)	1.86(6)	
C(50)	0.4791(2)	-0.0505(2)	0.1467(1)	2.11(7)	
C(51)	0.5604(2)	-0.1142(2)	0.1445(1)	2.14(7)	
C(52)	0.5367(3)	-0.2043(2)	0.1340(1)	2.27(7)	
C(53)	0.4295(3)	-0.2281(2)	0.1249(1)	2.38(7)	
C(54)	0.3495(2)	-0.1627(2)	0.1249(1)	2.18(7)	
C(101)	-0.1749	0.4653	0.0472	0.2000	0.001
C(102)	-0.3820	0.3678	0.1894	0.2000	0.001
B(1)	0.2771(3)	0.0090(2)	0.1365(2)	1.87(7)	
H(1)	0.0460	0.4141	0.1075	5.5384	
H(2)	0.0760	0.4798	0.0604	5.5384	
H(3)	0.0338	0.5173	0.1158	5.5384	
H(4)	-0.0353	0.2869	0.0334	5.2918	
H(5)	-0.1039	0.2934	-0.0200	5.2918	
H(6)	0.0009	0.3504	-0.0137	5.2918	
H(7)	-0.3700	0.3681	-0.0144	4.6450	
H(8)	-0.3128	0.4271	-0.0582	4.6450	
H(9)	-0.2666	0.3328	-0.0435	4.6450	
H(10)	-0.3619	0.6097	0.0600	4.0993	
H(11)	-0.3624	0.5818	-0.0015	4.0993	
H(12)	-0.4232	0.5235	0.0414	4.0993	
H(13)	-0.0948	0.6130	0.1324	4.7131	
H(14)	-0.1694	0.6645	0.0916	4.7131	
H(15)	-0.2195	0.6116	0.1403	4.7131	
H(16)	-0.6059	0.3737	0.1274	4.1291	
H(17)	-0.5223	0.3807	0.0802	4.1291	
H(18)	-0.5517	0.2872	0.1045	4.1291	

Table 1. Atomic coordinates and B_{iso}/B_{eq} and occupancy (continued)

atom	x	y	z	B_{eq}	occ
H(19)	-0.4121	0.5761	0.1578	3.9884	
H(20)	-0.5171	0.5282	0.1381	3.9884	
H(21)	-0.5015	0.5511	0.1998	3.9884	
H(22)	-0.2244	0.4606	0.2753	3.5327	
H(23)	-0.2383	0.5333	0.2300	3.5327	
H(24)	-0.3273	0.5207	0.2742	3.5327	
H(25)	-0.3056	0.2442	0.2851	2.8206	
H(26)	-0.2125	0.2318	0.2431	2.8206	
H(27)	-0.2129	0.3146	0.2820	2.8206	
H(28)	-0.4434	0.1665	0.2103	3.0257	
H(29)	-0.4674	0.1782	0.1480	3.0257	
H(30)	-0.3502	0.1580	0.1679	3.0257	
H(31)	-0.3539	0.2201	0.0384	2.9210	
H(32)	-0.3481	0.0697	0.0137	3.1667	
H(33)	-0.2142	-0.0229	0.0519	3.2969	
H(34)	-0.0881	0.0380	0.1128	2.8958	
H(35)	0.0033	0.0953	0.1785	2.6498	
H(36)	0.1066	0.1667	0.2464	2.8747	
H(37)	0.0892	0.3232	0.2587	2.7538	
H(38)	-0.0334	0.4016	0.2042	2.5164	
H(39)	0.2833	-0.0412	0.2464	4.1828	
H(40)	0.3016	0.0360	0.3287	5.8553	
H(41)	0.3347	0.1908	0.3287	6.3090	
H(42)	0.3395	0.2677	0.2452	5.5718	
H(43)	0.3095	0.1928	0.1633	3.8504	
H(44)	0.4436	0.0374	0.0579	2.4709	
H(45)	0.4601	0.1333	-0.0170	2.9252	
H(46)	0.3228	0.2364	-0.0375	3.5382	
H(47)	0.1685	0.2405	0.0173	4.0914	
H(48)	0.1506	0.1430	0.0908	3.6488	
H(49)	0.1184	-0.0572	0.2113	2.9189	
H(50)	-0.0377	-0.1432	0.1988	4.0812	
H(51)	-0.1015	-0.1760	0.1108	4.0622	
H(52)	-0.0050	-0.1244	0.0349	3.7096	
H(53)	0.1509	-0.0391	0.0474	2.9260	
H(54)	0.4976	0.0099	0.1556	2.5286	
H(55)	0.6335	-0.0966	0.1503	2.5889	
H(56)	0.5925	-0.2482	0.1332	2.6994	
H(57)	0.4108	-0.2894	0.1185	2.8608	

Table 1. Atomic coordinates and B_{iso}/B_{eq} and occupancy (continued)

atom	x	y	z	B_{eq}	occ
H(58)	0.2772	-0.1805	0.1167	2.6195	

$B_{eq} = 8/3\ \pi^2(U_{11}(aa^*)^2 + U_{22}(bb^*)^2 + U_{33}(cc^*)^2 + 2U_{12}(aa^*bb^*)\cos\gamma + 2U_{13}(aa^*cc^*)\cos\beta + 2U_{23}(bb^*cc^*)\cos\alpha)$

Table 2. Anisotropic Displacement Parameters

atom	U_{11}	U_{22}	U_{33}	U_{12}	U_{13}	U_{23}
Gd(1)	0.02272(8)	0.01520(8)	0.02153(9)	0.00221(6)	-0.00142(5)	0.00006(7)
N(1)	0.028(1)	0.021(1)	0.025(1)	0.001(1)	0.001(1)	-0.003(1)
N(2)	0.024(1)	0.020(1)	0.023(1)	0.0011(10)	-0.001(1)	0.001(1)
C(1)	0.025(2)	0.039(2)	0.032(2)	-0.008(1)	-0.003(1)	0.016(2)
C(2)	0.041(2)	0.029(2)	0.027(2)	0.003(1)	0.011(2)	0.008(1)
C(3)	0.042(2)	0.028(2)	0.020(2)	-0.004(1)	-0.003(1)	0.003(1)
C(4)	0.034(2)	0.021(2)	0.027(2)	0.001(1)	-0.005(1)	0.006(1)
C(5)	0.044(2)	0.020(2)	0.026(2)	-0.009(1)	-0.003(1)	0.003(1)
C(6)	0.021(2)	0.030(2)	0.033(2)	0.003(1)	0.000(1)	-0.000(1)
C(7)	0.031(2)	0.024(2)	0.029(2)	0.010(1)	0.006(1)	0.002(1)
C(8)	0.033(2)	0.022(2)	0.023(2)	0.003(1)	0.004(1)	-0.003(1)
C(9)	0.023(2)	0.021(2)	0.023(2)	0.004(1)	0.005(1)	0.004(1)
C(10)	0.021(1)	0.021(2)	0.030(2)	-0.001(1)	0.005(1)	0.001(1)
C(11)	0.037(2)	0.077(3)	0.060(3)	-0.014(2)	-0.010(2)	0.033(2)
C(12)	0.067(3)	0.047(2)	0.054(3)	0.017(2)	0.031(2)	0.013(2)
C(13)	0.071(3)	0.046(2)	0.030(2)	-0.010(2)	-0.012(2)	-0.003(2)
C(14)	0.050(2)	0.036(2)	0.045(2)	0.009(2)	-0.008(2)	0.014(2)
C(15)	0.076(3)	0.031(2)	0.043(2)	-0.019(2)	0.001(2)	-0.002(2)
C(16)	0.032(2)	0.049(2)	0.050(2)	-0.001(2)	-0.011(2)	0.008(2)
C(17)	0.050(2)	0.032(2)	0.045(2)	0.023(2)	0.008(2)	0.004(2)
C(18)	0.050(2)	0.029(2)	0.032(2)	-0.004(2)	-0.000(2)	-0.007(2)
C(19)	0.030(2)	0.034(2)	0.026(2)	0.003(1)	0.003(1)	0.005(2)
C(20)	0.028(2)	0.026(2)	0.041(2)	-0.005(1)	0.006(1)	0.000(2)
C(21)	0.033(2)	0.028(2)	0.031(2)	0.001(1)	-0.002(1)	-0.004(1)
C(22)	0.039(2)	0.030(2)	0.032(2)	-0.005(1)	0.001(2)	-0.011(1)
C(23)	0.047(2)	0.019(2)	0.038(2)	-0.001(1)	0.004(2)	-0.007(2)
C(24)	0.040(2)	0.020(2)	0.032(2)	0.005(1)	0.002(1)	-0.004(1)
C(25)	0.023(2)	0.021(1)	0.022(2)	0.003(1)	0.006(1)	0.001(1)
C(26)	0.020(1)	0.020(2)	0.022(2)	0.003(1)	0.004(1)	0.002(1)
C(27)	0.026(2)	0.025(2)	0.033(2)	0.006(1)	0.004(1)	0.006(1)
C(28)	0.019(2)	0.040(2)	0.030(2)	0.004(1)	0.002(1)	0.011(2)
C(29)	0.024(2)	0.038(2)	0.025(2)	-0.004(1)	-0.000(1)	0.005(1)
C(30)	0.029(2)	0.025(2)	0.025(2)	-0.003(1)	-0.002(1)	-0.001(1)
C(31)	0.022(2)	0.034(2)	0.036(2)	0.005(1)	-0.001(1)	-0.010(2)
C(32)	0.047(2)	0.053(2)	0.032(2)	0.021(2)	-0.011(2)	-0.010(2)
C(33)	0.056(3)	0.094(4)	0.036(2)	0.035(3)	-0.015(2)	-0.023(2)
C(34)	0.036(2)	0.101(4)	0.063(3)	0.019(2)	-0.018(2)	-0.054(3)
C(35)	0.027(2)	0.057(3)	0.092(4)	-0.002(2)	0.000(2)	-0.048(3)
C(36)	0.025(2)	0.038(2)	0.060(3)	-0.004(1)	0.006(2)	-0.022(2)

Table 2. Anisotropic Displacement Parameters (continued)

atom	U_{11}	U_{22}	U_{33}	U_{12}	U_{13}	U_{23}
C(37)	0.026(2)	0.017(2)	0.031(2)	-0.001(1)	-0.002(1)	-0.005(1)
C(38)	0.029(2)	0.022(2)	0.027(2)	-0.001(1)	-0.002(1)	-0.001(1)
C(39)	0.034(2)	0.028(2)	0.030(2)	-0.004(1)	0.001(1)	-0.002(1)
C(40)	0.047(2)	0.028(2)	0.037(2)	-0.002(2)	0.001(2)	0.009(2)
C(41)	0.039(2)	0.033(2)	0.058(3)	0.010(2)	0.003(2)	0.014(2)
C(42)	0.030(2)	0.035(2)	0.050(2)	0.005(1)	0.009(2)	0.009(2)
C(43)	0.025(2)	0.018(2)	0.028(2)	0.005(1)	0.004(1)	0.001(1)
C(44)	0.035(2)	0.023(2)	0.034(2)	0.007(1)	0.008(1)	0.005(1)
C(45)	0.034(2)	0.028(2)	0.068(3)	0.002(2)	0.019(2)	0.016(2)
C(46)	0.028(2)	0.023(2)	0.076(3)	-0.005(1)	0.002(2)	-0.002(2)
C(47)	0.029(2)	0.033(2)	0.055(2)	0.001(1)	-0.008(2)	-0.018(2)
C(48)	0.028(2)	0.033(2)	0.032(2)	-0.001(1)	0.007(1)	-0.005(2)
C(49)	0.030(2)	0.023(2)	0.018(2)	-0.000(1)	0.002(1)	0.000(1)
C(50)	0.033(2)	0.019(2)	0.028(2)	-0.001(1)	-0.003(1)	0.001(1)
C(51)	0.024(2)	0.033(2)	0.024(2)	-0.002(1)	-0.001(1)	0.002(1)
C(52)	0.035(2)	0.029(2)	0.022(2)	0.012(1)	-0.002(1)	-0.001(1)
C(53)	0.043(2)	0.022(2)	0.026(2)	0.004(1)	-0.006(1)	-0.005(1)
C(54)	0.030(2)	0.026(2)	0.027(2)	-0.002(1)	-0.005(1)	-0.003(1)
B(1)	0.024(2)	0.021(2)	0.026(2)	0.000(1)	0.000(1)	-0.003(2)

The general temperature factor expression:
$\exp(-2\pi^2(a^{*2}U_{11}h^2 + b^{*2}U_{22}k^2 + c^{*2}U_{33}l^2 + 2a^*b^*U_{12}hk + 2a^*c^*U_{13}hl + 2b^*c^*U_{23}kl))$

Cp^*_2Gd(2,2'-bipyridine)

EXPERIMENTAL DETAILS

A. Crystal Data

Empirical Formula	$C_{30}H_{38}N_2Gd$
Formula Weight	583.89
Crystal Color, Habit	red, block
Crystal Dimensions	0.08 X 0.08 X 0.07 mm
Crystal System	triclinic
Lattice Type	Primitive
Lattice Parameters	a = 9.419(1)Å b = 9.450(1) Å c = 15.505(2) Å α = 82.314(1)^o β = 81.757(1)^o γ = 71.051(1)^o V = 1286.2(2) Å^3
Space Group	P-1(#2)
Z value	2
D_{calc}	1.508 g/cm^3
F_{000}	592.00
μ(MoKα)	26.05 cm^{-1}

B. Intensity Measurements

Diffractometer	Bruker SMART CCD
Radiation	MoKα (λ = 0.71069 Å) graphite monochromated
Detector Position	60.00 mm
Exposure Time	10.0 seconds per frame.
Scan Type	ω (0.3 degrees per frame)
$2\theta_{max}$	52.8^o
No. of Reflections Measured	
Total: 10123	Unique: 4811 (R_{int} = 0.039)
Corrections	
Lorentz-polarization	

Absorption (Tmax = 1.00 Tmin = 0.81)

C. Structure Solution and Refinement

Structure Solution	Direct Methods (SIR97)
Refinement	Full-matrix least-squares
Function Minimized	Σ w (|Fo| - |Fc|)^2
Least Squares Weights	$1/\sigma^2(Fo) = 4Fo^2/\sigma^2(Fo^2)$
p-factor	0.0300
Anomalous Dispersion	All non-hydrogen atoms
No. Observations (I>3.00σ(I))	3544
No. Variables	298
Reflection/Parameter Ratio	11.89
Residuals: R; Rw; Rall	0.036 ; 0.035; 0.062
Goodness of Fit Indicator	1.24
Max Shift/Error in Final Cycle	0.01
Maximum peak in Final Diff. Map	1.03 $e^-/Å^3$
Minimum peak in Final Diff. Map	-0.45 $e^-/Å^3$

Table 1. Atomic coordinates and B_{iso}/B_{eq} and occupancy

atom	x	y	z	B_{eq}	occ
Gd(1)	0.37204(4)	0.26312(3)	0.25209(2)	1.973(6)	
N(1)	0.2545(5)	0.0760(5)	0.3118(3)	2.0(1)	
N(2)	0.2227(5)	0.2234(5)	0.1504(3)	2.1(1)	
C(1)	0.6004(6)	0.0313(6)	0.1903(4)	2.1(1)	
C(2)	0.6410(6)	0.0563(6)	0.2698(4)	2.4(1)	
C(3)	0.6704(6)	0.1960(6)	0.2577(4)	2.2(1)	
C(4)	0.6459(6)	0.2577(6)	0.1708(4)	2.2(1)	
C(5)	0.6029(6)	0.1561(6)	0.1293(4)	2.1(1)	
C(6)	0.2807(6)	0.4390(6)	0.3857(3)	2.0(1)	
C(7)	0.3365(6)	0.5249(6)	0.3157(4)	2.4(1)	
C(8)	0.2392(6)	0.5595(6)	0.2498(4)	2.3(1)	
C(9)	0.1209(6)	0.4978(6)	0.2798(4)	2.3(1)	
C(10)	0.1461(6)	0.4241(6)	0.3631(4)	2.2(1)	
C(11)	0.5662(7)	-0.1058(6)	0.1723(4)	3.0(1)	
C(12)	0.6625(7)	-0.0525(7)	0.3512(4)	3.4(2)	
C(13)	0.7388(6)	0.2512(7)	0.3233(4)	3.2(2)	
C(14)	0.6785(6)	0.3966(7)	0.1259(4)	3.0(1)	
C(15)	0.5828(7)	0.1688(7)	0.0342(4)	3.2(2)	
C(16)	0.3453(7)	0.3850(7)	0.4722(4)	3.4(2)	
C(17)	0.4605(7)	0.5919(7)	0.3181(4)	3.3(2)	
C(18)	0.2570(7)	0.6533(7)	0.1646(4)	3.5(2)	
C(19)	-0.0179(7)	0.5217(8)	0.2349(4)	4.0(2)	
C(20)	0.0405(7)	0.3528(7)	0.4220(4)	3.1(1)	
C(21)	0.2667(6)	0.0074(7)	0.3936(4)	2.6(1)	
C(22)	0.1950(7)	-0.0934(7)	0.4300(4)	3.3(2)	
C(23)	0.1000(7)	-0.1283(7)	0.3797(4)	3.4(2)	
C(24)	0.0826(6)	-0.0620(7)	0.2977(4)	2.7(1)	
C(25)	0.1597(6)	0.0433(6)	0.2618(4)	2.1(1)	
C(26)	0.1435(6)	0.1205(6)	0.1769(4)	2.0(1)	
C(27)	0.0528(7)	0.0988(7)	0.1177(4)	2.8(1)	
C(28)	0.0417(7)	0.1762(7)	0.0372(4)	3.4(2)	
C(29)	0.1182(7)	0.2807(7)	0.0131(4)	3.4(2)	
C(30)	0.2057(7)	0.3002(7)	0.0708(4)	2.9(1)	
C(101)	0.6321	0.1395	0.2036	0.2000	0.000
C(102)	0.2247	0.4891	0.3189	0.2000	0.000
H(1)	0.4668	-0.0773	0.1550	3.6703	
H(2)	0.6367	-0.1539	0.1268	3.6703	
H(3)	0.5719	-0.1737	0.2239	3.6703	
H(4)	0.5710	-0.0738	0.3709	3.9373	

Table 1. Atomic coordinates and B_{iso}/B_{eq} and occupancy (continued)

atom	x	y	z	B_{eq}	occ
H(5)	0.7401	-0.1427	0.3376	3.9373	
H(6)	0.6903	-0.0090	0.3951	3.9373	
H(7)	0.8361	0.1830	0.3320	3.7936	
H(8)	0.7474	0.3475	0.3019	3.7936	
H(9)	0.6761	0.2585	0.3774	3.7936	
H(10)	0.7057	0.4457	0.1674	3.5340	
H(11)	0.7595	0.3688	0.0809	3.5340	
H(12)	0.5912	0.4616	0.1012	3.5340	
H(13)	0.5065	0.2598	0.0200	3.9432	
H(14)	0.6754	0.1686	0.0002	3.9432	
H(15)	0.5549	0.0861	0.0227	3.9432	
H(16)	0.2873	0.3292	0.5078	4.1406	
H(17)	0.4468	0.3228	0.4623	4.1406	
H(18)	0.3418	0.4691	0.5007	4.1406	
H(19)	0.5106	0.5509	0.3692	4.0220	
H(20)	0.5317	0.5702	0.2677	4.0220	
H(21)	0.4187	0.6981	0.3191	4.0220	
H(22)	0.3509	0.6073	0.1329	4.1112	
H(23)	0.1772	0.6612	0.1307	4.1112	
H(24)	0.2519	0.7510	0.1763	4.1112	
H(25)	-0.1045	0.5785	0.2689	4.8020	
H(26)	-0.0085	0.5739	0.1786	4.8020	
H(27)	-0.0282	0.4267	0.2285	4.8020	
H(28)	-0.0537	0.4272	0.4343	3.7186	
H(29)	0.0265	0.2763	0.3937	3.7186	
H(30)	0.0833	0.3106	0.4752	3.7186	
H(31)	0.3312	0.0297	0.4277	3.1352	
H(32)	0.2072	-0.1384	0.4883	3.9709	
H(33)	0.0499	-0.1986	0.4036	4.0282	
H(34)	0.0188	-0.0857	0.2639	3.2950	
H(35)	-0.0015	0.0286	0.1344	3.3098	
H(36)	-0.0182	0.1592	-0.0022	4.1154	
H(37)	0.1109	0.3381	-0.0424	4.0613	
H(38)	0.2579	0.3714	0.0536	3.4321	

$B_{eq} = 8/3\ \pi^2(U_{11}(aa^*)^2 + U_{22}(bb^*)^2 + U_{33}(cc^*)^2 + 2U_{12}(aa^*bb^*)\cos\gamma + 2U_{13}(aa^*cc^*)\cos\beta + 2U_{23}(bb^*cc^*)\cos\alpha)$

Table 2. Anisotropic Displacement Parameters

atom	U_{11}	U_{22}	U_{33}	U_{12}	U_{13}	U_{23}
Gd(1)	0.0292(2)	0.0270(2)	0.0220(2)	-0.0132(1)	-0.0048(1)	0.0001(1)
N(1)	0.029(3)	0.030(3)	0.019(3)	-0.012(2)	-0.003(2)	0.004(2)
N(2)	0.030(3)	0.030(3)	0.021(3)	-0.009(2)	-0.005(2)	-0.000(2)
C(1)	0.027(3)	0.023(3)	0.028(3)	-0.006(3)	-0.001(3)	-0.002(3)
C(2)	0.028(3)	0.033(4)	0.027(3)	-0.010(3)	-0.004(3)	0.009(3)
C(3)	0.021(3)	0.028(3)	0.035(4)	-0.006(3)	-0.006(3)	-0.001(3)
C(4)	0.023(3)	0.028(3)	0.031(4)	-0.007(3)	0.003(3)	0.001(3)
C(5)	0.026(3)	0.027(3)	0.025(3)	-0.007(3)	-0.004(3)	0.002(3)
C(6)	0.035(3)	0.025(3)	0.017(3)	-0.008(3)	-0.007(3)	-0.000(2)
C(7)	0.033(3)	0.027(3)	0.035(4)	-0.012(3)	0.001(3)	-0.011(3)
C(8)	0.039(3)	0.018(3)	0.030(3)	-0.006(3)	-0.007(3)	-0.002(3)
C(9)	0.027(3)	0.027(3)	0.032(4)	-0.001(3)	-0.007(3)	-0.004(3)
C(10)	0.026(3)	0.026(3)	0.028(4)	-0.005(3)	-0.000(3)	-0.006(3)
C(11)	0.045(4)	0.031(4)	0.040(4)	-0.012(3)	-0.004(3)	-0.004(3)
C(12)	0.031(4)	0.053(4)	0.037(4)	-0.008(3)	-0.012(3)	0.016(3)
C(13)	0.025(3)	0.042(4)	0.055(4)	-0.009(3)	-0.007(3)	-0.011(3)
C(14)	0.032(3)	0.035(4)	0.048(4)	-0.015(3)	0.003(3)	-0.001(3)
C(15)	0.037(4)	0.049(4)	0.033(4)	-0.010(3)	-0.002(3)	-0.002(3)
C(16)	0.049(4)	0.056(4)	0.031(4)	-0.020(3)	-0.004(3)	-0.009(3)
C(17)	0.042(4)	0.032(4)	0.060(4)	-0.020(3)	0.002(3)	-0.015(3)
C(18)	0.062(4)	0.028(4)	0.034(4)	-0.006(3)	-0.005(3)	0.004(3)
C(19)	0.042(4)	0.058(5)	0.047(4)	-0.001(4)	-0.019(3)	-0.013(4)
C(20)	0.035(4)	0.046(4)	0.039(4)	-0.019(3)	0.008(3)	-0.013(3)
C(21)	0.037(4)	0.038(4)	0.024(3)	-0.012(3)	-0.002(3)	0.001(3)
C(22)	0.043(4)	0.042(4)	0.031(4)	-0.008(3)	0.003(3)	0.012(3)
C(23)	0.038(4)	0.034(4)	0.055(5)	-0.020(3)	0.008(3)	0.006(3)
C(24)	0.031(3)	0.035(4)	0.042(4)	-0.017(3)	-0.001(3)	-0.003(3)
C(25)	0.023(3)	0.025(3)	0.028(3)	-0.005(3)	-0.000(3)	-0.002(3)
C(26)	0.025(3)	0.021(3)	0.029(3)	-0.007(3)	-0.001(3)	-0.007(3)
C(27)	0.036(4)	0.033(4)	0.042(4)	-0.014(3)	-0.009(3)	-0.010(3)
C(28)	0.042(4)	0.047(4)	0.046(4)	-0.008(3)	-0.022(3)	-0.014(3)
C(29)	0.045(4)	0.053(4)	0.025(4)	-0.003(3)	-0.008(3)	-0.008(3)
C(30)	0.041(4)	0.041(4)	0.025(4)	-0.011(3)	-0.001(3)	0.000(3)

The general temperature factor expression:
$\exp(-2\pi^2(a^{*2}U_{11}h^2 + b^{*2}U_{22}k^2 + c^{*2}U_{33}l^2 + 2a^*b^*U_{12}hk + 2a^*c^*U_{13}hl + 2b^*c^*U_{23}kl))$

[Cp^*_2Yb(p-tolyl-diazadiene)][BPh_4]

EXPERIMENTAL DETAILS

A. Crystal Data

Empirical Formula	$YbBN_2C_{60}H_{66}$
Formula Weight	999.04
Crystal Color, Habit	brown, block
Crystal Dimensions	0.08 X 0.08 X 0.07 mm
Crystal System	monoclinic
Lattice Type	C-centered
Lattice Parameters	a = 18.037(2)Å
	b = 15.732(1) Å
	c = 19.141(2) Å
	$\beta = 115.677(1)^o$
	V = 4894.9(7) $Å^3$
Space Group	C2/c (#15)
Z value	4
D_{calc}	1.356 g/cm^3
F_{000}	2060.00
μ(MoKα)	19.51 cm^{-1}

B. Intensity Measurements

Diffractometer	Bruker SMART CCD
Radiation	MoKα (λ = 0.71069 Å) graphite monochromated
Detector Position	60.00 mm
Exposure Time	20.0 seconds per frame.
Scan Type	ω (0.3 degrees per frame)
$2\theta_{max}$	53.1^o
No. of Reflections Measured	
Total:	11714
Unique:	3503 (R_{int} = 0.033)
Corrections	Lorentz-polarization
Absorption (Tmax = 1.00 Tmin = 0.62)	

C. Structure Solution and Refinement

Structure Solution	Direct Methods (SIR97)
Refinement	Full-matrix least-squares
Function Minimized	Σ w (|Fo| - |Fc|)^2
Least Squares Weights	$1/\sigma^2(Fo) = 4Fo^2/\sigma^2(Fo^2)$
p-factor	0.0300
Anomalous Dispersion	All non-hydrogen atoms
No. Observations (I>3.00σ(I))	3576
No. Variables	290
Reflection/Parameter Ratio	12.33
Residuals: R; Rw; Rall	0.036 ; 0.039; 0.054
Goodness of Fit Indicator	1.40
Max Shift/Error in Final Cycle	0.00
Maximum peak in Final Diff. Map	2.26 $e^-/Å^3$
Minimum peak in Final Diff. Map	-1.93 $e^-/Å^3$

Table 1. Atomic coordinates and B_{iso}/B_{eq} and occupancy

atom	x	y	z	B_{eq}	occ
Yb(1)	0.0000	0.00666(2)	-0.2500	1.494(6)	1/2
N(1)	0.0513(2)	0.1347(2)	-0.2873(2)	1.61(8)	
C(1)	-0.0988(3)	0.0182(3)	-0.3968(2)	1.69(9)	
C(2)	-0.1519(2)	0.0057(3)	-0.3595(2)	1.68(8)	
C(3)	-0.1379(3)	-0.0778(3)	-0.3275(3)	1.63(10)	
C(4)	-0.0770(3)	-0.1172(3)	-0.3454(3)	1.60(10)	
C(5)	-0.0528(3)	-0.0575(3)	-0.3877(3)	1.60(10)	
C(6)	-0.1042(3)	0.0936(3)	-0.4468(3)	2.0(1)	
C(7)	-0.2201(3)	0.0659(3)	-0.3665(3)	2.2(1)	
C(8)	-0.1872(3)	-0.1229(3)	-0.2918(3)	2.4(1)	
C(9)	-0.0592(3)	-0.2107(3)	-0.3412(3)	2.1(1)	
C(10)	0.0019(3)	-0.0802(3)	-0.4258(3)	1.9(1)	
C(11)	0.0275(3)	0.2048(3)	-0.2695(3)	1.8(1)	
C(12)	0.1009(3)	0.1379(3)	-0.3290(3)	1.70(10)	
C(13)	0.1063(3)	0.2088(3)	-0.3706(3)	2.2(1)	
C(14)	0.1534(3)	0.2053(3)	-0.4115(3)	2.2(1)	
C(15)	0.1962(3)	0.1320(3)	-0.4134(3)	2.1(1)	
C(16)	0.1900(3)	0.0615(3)	-0.3723(3)	2.0(1)	
C(17)	0.1427(3)	0.0643(3)	-0.3313(3)	1.9(1)	
C(18)	0.2464(3)	0.1281(4)	-0.4593(3)	2.8(1)	
C(19)	0.0737(3)	0.4300(3)	-0.1949(3)	1.82(10)	
C(20)	0.1386(3)	0.4046(3)	-0.2131(3)	2.0(1)	
C(21)	0.1974(3)	0.3439(3)	-0.1690(3)	2.3(1)	
C(22)	0.1934(3)	0.3062(3)	-0.1055(3)	2.5(1)	
C(23)	0.1301(3)	0.3289(3)	-0.0862(3)	2.5(1)	
C(24)	0.0718(3)	0.3890(3)	-0.1306(3)	2.1(1)	
C(25)	0.0318(3)	0.5584(3)	-0.3010(3)	1.8(1)	
C(26)	-0.0100(3)	0.5742(3)	-0.3807(3)	2.2(1)	
C(27)	0.0207(4)	0.6285(3)	-0.4196(3)	2.8(1)	
C(28)	0.0956(3)	0.6694(3)	-0.3794(3)	2.7(1)	
C(29)	0.1379(3)	0.6564(3)	-0.3005(3)	2.2(1)	
C(30)	0.1062(3)	0.6028(3)	-0.2624(3)	2.2(1)	
C(101)	-0.1037	-0.0457	-0.3634	0.2000	0.001
B(1)	0.0000	0.4962(5)	-0.2500	1.8(1)	1/2
H(1)	-0.1488	0.0863	-0.4962	2.4496	
H(2)	-0.2440	0.0473	-0.3337	2.5969	
H(3)	-0.2180	-0.1677	-0.3251	2.8936	
H(4)	-0.0018	-0.2193	-0.3228	2.4933	
H(5)	0.0446	-0.1166	-0.3929	2.2994	

Table 1. Atomic coordinates and B_{iso}/B_{eq} and occupancy (continued)

atom	x	y	z	B_{eq}	occ
H(6)	-0.0543	0.0986	-0.4520	2.4496	
H(7)	-0.1124	0.1437	-0.4231	2.4496	
H(8)	-0.1982	0.1214	-0.3518	2.5969	
H(9)	-0.2608	0.0666	-0.4188	2.5969	
H(10)	-0.2234	-0.0840	-0.2847	2.8936	
H(11)	-0.1506	-0.1461	-0.2430	2.8936	
H(12)	-0.0781	-0.2370	-0.3075	2.4933	
H(13)	-0.0870	-0.2347	-0.3918	2.4933	
H(14)	-0.0296	-0.1081	-0.4736	2.2994	
H(15)	0.0251	-0.0297	-0.4353	2.2994	
H(16)	0.0418	0.2603	-0.2855	2.1180	
H(17)	0.0776	0.2594	-0.3704	2.6496	
H(18)	0.1567	0.2541	-0.4393	2.7169	
H(19)	0.2186	0.0109	-0.3721	2.4990	
H(20)	0.1387	0.0152	-0.3043	2.2953	
H(21)	0.2132	0.1466	-0.5109	3.4600	
H(22)	0.2642	0.0718	-0.4597	3.4600	
H(23)	0.2926	0.1648	-0.4360	3.4600	
H(24)	0.1422	0.4294	-0.2568	2.4034	
H(25)	0.2408	0.3289	-0.1824	2.8025	
H(26)	0.2334	0.2653	-0.0754	2.9858	
H(27)	0.1265	0.3034	-0.0429	2.9697	
H(28)	0.0287	0.4025	-0.1170	2.5385	
H(29)	-0.0617	0.5473	-0.4095	2.6284	
H(30)	-0.0091	0.6377	-0.4737	3.3641	
H(31)	0.1173	0.7053	-0.4058	3.2975	
H(32)	0.1888	0.6847	-0.2723	2.6578	
H(33)	0.1361	0.5960	-0.2078	2.6368	

$B_{eq} = 8/3\ \pi^2(U_{11}(aa^*)^2 + U_{22}(bb^*)^2 + U_{33}(cc^*)^2 + 2U_{12}(aa^*bb^*)\cos\gamma + 2U_{13}(aa^*cc^*)\cos\beta + 2U_{23}(bb^*cc^*)\cos\alpha)$

Table 2. Anisotropic Displacement Parameters

atom	U_{11}	U_{22}	U_{33}	U_{12}	U_{13}	U_{23}
Yb(1)	0.0178(1)	0.0169(2)	0.0231(1)	0.0104	0.0098(1)	0.0008
N(1)	0.019(2)	0.019(2)	0.023(2)	0.001(2)	0.009(2)	0.002(2)
C(1)	0.018(2)	0.023(3)	0.021(2)	-0.002(2)	0.006(2)	-0.004(2)
C(2)	0.017(2)	0.023(2)	0.023(2)	-0.000(2)	0.008(2)	-0.001(2)
C(3)	0.017(2)	0.020(2)	0.024(2)	-0.003(2)	0.008(2)	-0.002(2)
C(4)	0.021(3)	0.014(2)	0.025(2)	-0.000(2)	0.009(2)	-0.005(2)
C(5)	0.020(3)	0.020(3)	0.021(2)	-0.004(2)	0.009(2)	-0.001(2)
C(6)	0.028(3)	0.022(3)	0.026(3)	0.003(2)	0.011(2)	0.003(2)
C(7)	0.022(3)	0.031(3)	0.028(3)	0.004(2)	0.010(2)	0.000(2)
C(8)	0.029(3)	0.026(3)	0.040(3)	-0.011(2)	0.019(3)	-0.007(2)
C(9)	0.026(3)	0.020(3)	0.034(3)	-0.002(2)	0.011(2)	-0.004(2)
C(10)	0.025(3)	0.022(3)	0.026(2)	-0.000(2)	0.013(2)	-0.002(2)
C(11)	0.019(3)	0.019(3)	0.029(3)	-0.001(2)	0.009(2)	0.003(2)
C(12)	0.016(2)	0.023(3)	0.025(2)	-0.007(2)	0.008(2)	-0.001(2)
C(13)	0.025(3)	0.022(3)	0.034(3)	-0.001(2)	0.012(2)	0.003(2)
C(14)	0.032(3)	0.025(3)	0.028(3)	-0.009(2)	0.013(2)	0.003(2)
C(15)	0.018(3)	0.036(3)	0.022(2)	-0.007(2)	0.005(2)	-0.005(2)
C(16)	0.022(3)	0.029(3)	0.026(3)	0.001(2)	0.010(2)	-0.002(2)
C(17)	0.020(3)	0.022(3)	0.027(3)	-0.004(2)	0.007(2)	0.003(2)
C(18)	0.027(3)	0.049(4)	0.032(3)	-0.007(3)	0.015(3)	-0.004(3)
C(19)	0.021(3)	0.015(2)	0.029(3)	-0.005(2)	0.007(2)	-0.004(2)
C(20)	0.025(3)	0.019(3)	0.032(3)	-0.003(2)	0.012(2)	-0.002(2)
C(21)	0.021(3)	0.024(3)	0.041(3)	-0.001(2)	0.012(2)	-0.001(2)
C(22)	0.026(3)	0.021(3)	0.038(3)	0.001(2)	0.005(3)	0.004(2)
C(23)	0.040(3)	0.022(3)	0.029(3)	-0.002(2)	0.012(3)	0.005(2)
C(24)	0.026(3)	0.023(3)	0.032(3)	-0.001(2)	0.014(2)	-0.000(2)
C(25)	0.023(3)	0.017(2)	0.030(3)	0.005(2)	0.014(2)	0.001(2)
C(26)	0.024(3)	0.024(3)	0.036(3)	0.004(2)	0.013(2)	0.002(2)
C(27)	0.047(4)	0.034(3)	0.033(3)	0.013(3)	0.023(3)	0.010(2)
C(28)	0.042(3)	0.022(3)	0.054(4)	0.006(2)	0.035(3)	0.006(3)
C(29)	0.025(3)	0.018(3)	0.052(3)	-0.001(2)	0.025(3)	-0.001(2)
C(30)	0.028(3)	0.021(3)	0.036(3)	0.005(2)	0.014(3)	-0.000(2)
B(1)	0.022(3)	0.023(4)	0.026(3)	0.0000	0.012(3)	0.0000

The general temperature factor expression:
$\exp(-2\pi^2(a^{*2}U_{11}h^2 + b^{*2}U_{22}k^2 + c^{*2}U_{33}l^2 + 2a^*b^*U_{12}hk + 2a^*c^*U_{13}hl + 2b^*c^*U_{23}kl))$

Cp^*_2Yb(5,5'-dimethyl-2,2'bipyridine)

EXPERIMENTAL DETAILS

A. Crystal Data

Empirical Formula	$YbN_2C_{32}H_{42}$
Formula Weight	627.74
Crystal Color, Habit	black, block
Crystal Dimensions	0.13 X 0.06 X 0.06 mm
Crystal System	orthorhombic
Lattice Type	Primitive
Lattice Parameters	a = 18.0957(9)Å
	b = 15.9925(8) Å
	c = 19.674(1) Å
	V = 5693.7(5) $Å^3$
Space Group	Pbca (#61)
Z value	8
D_{calc}	1.465 g/cm^3
F_{000}	2544.00
μ(MoKα)	33.07 cm^{-1}

B. Intensity Measurements

Diffractometer	Bruker APEX CCD
Radiation	MoKα (λ = 0.71069 Å) graphite monochromated
Detector Position	60.00 mm
Exposure Time	10.0 seconds per frame.
Scan Type	ω (0.3 degrees per frame)
$2\theta_{max}$	52.8^o
No. of Reflections Measured	
Total: 32626	Unique: 3784 (R_{int} = 0.037)
Corrections	Lorentz-polarization
Absorption	(Tmax = 1.00 Tmin = 0.86)

C. Structure Solution and Refinement

Structure Solution	Direct Methods (SIR97)
Refinement	Full-matrix least-squares
Function Minimized	Σ w (|Fo| - |Fc|)^2
Least Squares Weights	$1/\sigma^2(Fo) = 4Fo^2/\sigma^2(Fo^2)$
p-factor	0.0300
Anomalous Dispersion	All non-hydrogen atoms
No. Observations (I>3.00σ(I))	3998
No. Variables	316
Reflection/Parameter Ratio	12.65
Residuals: R; Rw; Rall	0.028 ; 0.035; 0.051
Goodness of Fit Indicator	1.37
Max Shift/Error in Final Cycle	0.00
Maximum peak in Final Diff. Map	0.82 $e^-/Å^3$
Minimum peak in Final Diff. Map	-0.40 $e^-/Å^3$

Table 1. Atomic coordinates and B_{iso}/B_{eq} and occupancy

atom	x	y	z	B_{eq}	occ
Yb(1)	0.88867(1)	0.30353(1)	0.151474(9)	1.680(4)	
N(1)	0.9586(2)	0.1861(2)	0.1235(2)	2.14(9)	
N(2)	0.8549(2)	0.1890(2)	0.2194(2)	1.92(8)	
C(1)	0.7611(3)	0.3553(3)	0.1040(2)	2.2(1)	
C(2)	0.8144(3)	0.3875(3)	0.0576(2)	2.1(1)	
C(3)	0.8461(3)	0.3190(3)	0.0229(2)	2.2(1)	
C(4)	0.8127(3)	0.2452(3)	0.0460(2)	2.1(1)	
C(5)	0.7593(3)	0.2678(3)	0.0964(2)	2.3(1)	
C(6)	1.0179(3)	0.3544(3)	0.1997(2)	2.5(1)	
C(7)	0.9758(3)	0.3315(3)	0.2573(3)	2.6(1)	
C(8)	0.9178(3)	0.3883(3)	0.2633(2)	2.7(1)	
C(9)	0.9231(3)	0.4476(3)	0.2101(3)	2.5(1)	
C(10)	0.9849(3)	0.4257(3)	0.1700(2)	2.4(1)	
C(11)	0.7114(3)	0.4055(4)	0.1500(3)	3.4(1)	
C(12)	0.8245(3)	0.4773(3)	0.0378(3)	3.4(1)	
C(13)	0.9029(3)	0.3259(4)	-0.0332(3)	3.4(1)	
C(14)	0.8249(3)	0.1584(3)	0.0187(3)	3.0(1)	
C(15)	0.7051(3)	0.2088(3)	0.1284(3)	3.2(1)	
C(16)	1.0893(3)	0.3145(4)	0.1796(3)	4.1(1)	
C(17)	0.9945(3)	0.2606(4)	0.3057(3)	3.9(1)	
C(18)	0.8609(3)	0.3924(4)	0.3189(3)	4.0(1)	
C(19)	0.8807(3)	0.5281(4)	0.2067(3)	4.4(2)	
C(20)	1.0149(3)	0.4746(4)	0.1106(3)	4.4(2)	
C(21)	1.0081(3)	0.1860(3)	0.0711(2)	2.4(1)	
C(22)	1.0453(3)	0.1171(3)	0.0489(2)	2.8(1)	
C(23)	1.0319(3)	0.0419(3)	0.0831(3)	2.9(1)	
C(24)	0.9847(3)	0.0398(3)	0.1368(2)	2.8(1)	
C(25)	0.9469(3)	0.1125(3)	0.1569(2)	2.04(10)	
C(26)	0.8917(2)	0.1156(3)	0.2109(2)	1.80(9)	
C(27)	0.8757(3)	0.0465(3)	0.2532(3)	2.5(1)	
C(28)	0.8229(3)	0.0537(3)	0.3027(2)	2.7(1)	
C(29)	0.7849(3)	0.1292(3)	0.3120(2)	2.3(1)	
C(30)	0.8025(3)	0.1926(3)	0.2692(2)	2.2(1)	
C(31)	1.0974(3)	0.1227(4)	-0.0112(3)	4.1(1)	
C(32)	0.7272(3)	0.1381(4)	0.3668(3)	3.6(1)	
C(101)	0.7987	0.3149	0.0654	0.2000	0.000
C(102)	0.9639	0.3895	0.2201	0.2000	0.000
H(1)	0.7232	0.4644	0.1467	4.1639	
H(2)	0.6612	0.3984	0.1379	4.1639	

Table 1. Atomic coordinates and B_{iso}/B_{eq} and occupancy (continued)

atom	x	y	z	B_{eq}	occ
H(3)	0.7181	0.3894	0.1964	4.1639	
H(4)	0.8757	0.4920	0.0386	4.1599	
H(5)	0.8060	0.4863	-0.0071	4.1599	
H(6)	0.7985	0.5132	0.0683	4.1599	
H(7)	0.9457	0.2931	-0.0221	4.0740	
H(8)	0.8829	0.3050	-0.0749	4.0740	
H(9)	0.9177	0.3822	-0.0396	4.0740	
H(10)	0.7963	0.1181	0.0429	3.7416	
H(11)	0.8119	0.1555	-0.0285	3.7416	
H(12)	0.8762	0.1428	0.0226	3.7416	
H(13)	0.6745	0.2369	0.1601	3.7171	
H(14)	0.6742	0.1839	0.0941	3.7171	
H(15)	0.7305	0.1643	0.1514	3.7171	
H(16)	1.0819	0.2563	0.1720	4.7684	
H(17)	1.1072	0.3402	0.1399	4.7684	
H(18)	1.1245	0.3213	0.2156	4.7684	
H(19)	0.9567	0.2576	0.3406	4.5996	
H(20)	0.9952	0.2086	0.2824	4.5996	
H(21)	1.0404	0.2703	0.3269	4.5996	
H(22)	0.8659	0.4427	0.3435	4.7497	
H(23)	0.8123	0.3895	0.2997	4.7497	
H(24)	0.8668	0.3459	0.3492	4.7497	
H(25)	0.8900	0.5627	0.2450	5.0982	
H(26)	0.8924	0.5584	0.1662	5.0982	
H(27)	0.8277	0.5171	0.2056	5.0982	
H(28)	1.0568	0.4478	0.0907	5.1288	
H(29)	0.9774	0.4788	0.0748	5.1288	
H(30)	1.0281	0.5304	0.1226	5.1288	
H(31)	1.0169	0.2400	0.0480	2.9720	
H(32)	1.0558	-0.0096	0.0680	3.6380	
H(33)	0.9766	-0.0119	0.1623	3.2784	
H(34)	0.9026	-0.0053	0.2472	3.0084	
H(35)	0.8105	0.0063	0.3305	3.2711	
H(36)	0.7761	0.2444	0.2747	2.7838	
H(37)	1.1194	0.0685	-0.0195	5.0388	
H(38)	1.0719	0.1396	-0.0507	5.0388	
H(39)	1.1363	0.1611	-0.0017	5.0388	
H(40)	0.7410	0.1839	0.3974	4.3856	
H(41)	0.6804	0.1540	0.3473	4.3856	

Table 1. Atomic coordinates and B_{iso}/B_{eq} and occupancy (continued)

atom	x	y	z	B_{eq}	occ
H(42)	0.7214	0.0896	0.3926	4.3856	

$B_{eq} = 8/3\ \pi^2(U_{11}(aa^*)^2 + U_{22}(bb^*)^2 + U_{33}(cc^*)^2 + 2U_{12}(aa^*bb^*)\cos\gamma + 2U_{13}(aa^*cc^*)\cos\beta + 2U_{23}(bb^*cc^*)\cos\alpha)$

Table 2. Anisotropic Displacement Parameters

atom	U_{11}	U_{22}	U_{33}	U_{12}	U_{13}	U_{23}
Yb(1)	0.0237(1)	0.0200(1)	0.0201(1)	-0.00094(9)	-0.00152(8)	0.00126(9)
N(1)	0.026(2)	0.030(2)	0.025(2)	-0.001(2)	-0.002(2)	-0.001(2)
N(2)	0.024(2)	0.023(2)	0.026(2)	-0.001(2)	-0.001(2)	0.001(2)
C(1)	0.024(3)	0.034(3)	0.026(3)	0.005(2)	-0.007(2)	-0.004(2)
C(2)	0.029(3)	0.023(3)	0.028(3)	0.002(2)	-0.009(2)	0.001(2)
C(3)	0.030(3)	0.036(3)	0.018(2)	0.001(2)	-0.006(2)	-0.000(2)
C(4)	0.032(3)	0.028(3)	0.021(2)	0.000(2)	-0.008(2)	0.001(2)
C(5)	0.030(3)	0.033(3)	0.024(3)	-0.005(2)	-0.006(2)	0.001(2)
C(6)	0.024(3)	0.037(3)	0.034(3)	-0.008(2)	-0.005(2)	-0.007(2)
C(7)	0.040(3)	0.027(3)	0.031(3)	-0.005(2)	-0.015(2)	0.000(2)
C(8)	0.048(3)	0.031(3)	0.023(3)	-0.006(2)	-0.007(2)	-0.008(2)
C(9)	0.035(3)	0.022(3)	0.038(3)	-0.003(2)	-0.013(2)	-0.002(2)
C(10)	0.034(3)	0.027(3)	0.031(3)	-0.012(2)	-0.006(2)	0.003(2)
C(11)	0.034(3)	0.055(4)	0.040(3)	0.012(3)	-0.005(3)	-0.011(3)
C(12)	0.058(4)	0.033(3)	0.039(3)	0.000(3)	-0.017(3)	0.009(3)
C(13)	0.053(4)	0.052(4)	0.023(3)	0.002(3)	0.000(2)	0.005(2)
C(14)	0.047(3)	0.033(3)	0.035(3)	-0.006(3)	-0.005(3)	-0.008(2)
C(15)	0.028(3)	0.049(4)	0.043(3)	-0.010(3)	-0.003(2)	0.006(3)
C(16)	0.035(3)	0.061(4)	0.059(4)	-0.007(3)	-0.009(3)	-0.009(3)
C(17)	0.057(4)	0.053(4)	0.039(3)	-0.007(3)	-0.025(3)	0.015(3)
C(18)	0.054(4)	0.061(4)	0.038(3)	-0.013(3)	0.005(3)	-0.019(3)
C(19)	0.063(4)	0.034(3)	0.068(4)	0.010(3)	-0.024(3)	-0.012(3)
C(20)	0.053(4)	0.065(4)	0.049(4)	-0.031(3)	-0.013(3)	0.019(3)
C(21)	0.027(3)	0.040(3)	0.024(2)	-0.002(2)	0.001(2)	0.000(2)
C(22)	0.029(3)	0.052(3)	0.027(3)	0.006(2)	-0.004(2)	-0.009(3)
C(23)	0.032(3)	0.043(3)	0.037(3)	0.012(3)	-0.006(2)	-0.014(3)
C(24)	0.040(3)	0.028(3)	0.037(3)	0.007(2)	-0.011(2)	-0.004(2)
C(25)	0.030(3)	0.027(3)	0.021(2)	-0.000(2)	-0.007(2)	-0.002(2)
C(26)	0.024(2)	0.018(2)	0.026(2)	-0.002(2)	-0.006(2)	-0.002(2)
C(27)	0.037(3)	0.027(3)	0.032(3)	-0.001(2)	-0.008(2)	0.003(2)
C(28)	0.042(3)	0.034(3)	0.027(3)	-0.013(3)	-0.007(2)	0.014(2)
C(29)	0.026(3)	0.041(3)	0.021(3)	-0.003(2)	-0.005(2)	0.005(2)
C(30)	0.028(3)	0.027(3)	0.028(3)	0.003(2)	-0.000(2)	0.001(2)
C(31)	0.043(3)	0.078(5)	0.034(3)	0.010(3)	0.009(3)	-0.018(3)
C(32)	0.037(3)	0.068(4)	0.033(3)	-0.005(3)	0.004(2)	0.012(3)

The general temperature factor expression:
$\exp(-2\pi^2(a^{*2}U_{11}h^2 + b^{*2}U_{22}k^2 + c^{*2}U_{33}l^2 + 2a^*b^*U_{12}hk + 2a^*c^*U_{13}hl + 2b^*c^*U_{23}kl))$

Cp^*_2Yb(6,6'-dimethyl-2,2'-bipyridine)

EXPERIMENTAL DETAILS

A. Crystal Data

Empirical Formula	C32 H42 N2 Yb
Formula Weight	627.72
Crystal Color, Habit	brown, block
Crystal Dimensions	0.10 x 0.06 x 0.06 mm
Crystal System	Orthorhombic
Lattice Type	primitive
Lattice Parameters	a = 23.847(2) Å b = 15.177(2) Å c = 31.291(3) Å α= 90 ^{o} β= 90 ^{o} γ = 90^o V = 11325(2) Å^3
Space Group	P b c a
Z value	16
D_{calc}	1.473 g/cm^3
F_{000}	5088
μ(MoK)	3.33 cm^{-1}

B. Intensity Measurements

Diffractometer	Bruker APEX
Radiation	MoK(λ = 0.71073 Å) graphite monochromated
Detector Position	60.00 mm
Exposure Time	10 seconds per frame.
Scan Type	ω (0.3 degrees per frame)
θ_{max}	23.22^o
No. of Reflections Measured	Total: 54138 Unique: 8087 (R_{int} = 0.1172)
Corrections	Lorentz-polarization
Absorption	(Tmax = 1.0, Tmin = 0.8)

C. Structure Solution and Refinement

Structure Solution	direct (SHELXS-97 (Sheldrick, 1990))
Refinement	Full-matrix least-squares
Function Minimized	$\Sigma w(\|F_o\|^2 - \|F_c\|^2)^2$
Least Squares Weighting scheme	$w = 1/[\sigma^2(F_o^2) + (qP)^2 + 0.000P]$ where $P = [F_o^2 + 2F_c^2]/3$
q-factor	0.045
Anomalous Dispersion	All non-hydrogen atoms
No. Observations (I>2.00σ(I))	4310
No. Variables	655
Reflection/Parameter Ratio	6.6
Residuals: R; wR_2; Rall	0.0507; 0.1002; 0.1180
Goodness of Fit Indicator	0.980
Max Shift/Error in Final Cycle	0.003
Maximum peak in Final Diff. Map	1.129 $e^-/Å^3$
Minimum peak in Final Diff. Map	-0.564 $e^-/Å^3$

Table 1. Atomic coordinates and U_{iso}/U_{eq} and occupancy

atom	x	y	z	U_{eq}	Occupancy
Yb1	0.1186(1)	0.2530(1)	-0.0146(1)	0.031(1)	1
N1	0.0923(3)	0.2852(6)	0.0611(3)	0.041(2)	1
N2	0.1455(4)	0.4037(5)	0.0086(3)	0.036(2)	1
C1	0.2202(6)	0.2100(10)	0.0218(4)	0.066(4)	1
C2	0.2316(5)	0.2276(8)	-0.0193(5)	0.062(4)	1
C3	0.2057(6)	0.1594(10)	-0.0434(4)	0.060(4)	1
C4	0.1803(5)	0.1011(6)	-0.0154(4)	0.051(3)	1
C5	0.1884(6)	0.1343(9)	0.0258(4)	0.061(4)	1
C6	0.0073(5)	0.2803(7)	-0.0302(3)	0.042(3)	1
C7	0.0354(4)	0.3420(7)	-0.0575(3)	0.036(3)	1
C8	0.0621(4)	0.2940(7)	-0.0904(3)	0.034(3)	1
C9	0.0520(6)	0.2042(7)	-0.0825(4)	0.056(4)	1
C10	0.0176(5)	0.1931(7)	-0.0463(4)	0.052(4)	1
C11	0.2430(6)	0.2680(11)	0.0578(5)	0.146(9)	1
C12	0.2730(6)	0.2935(11)	-0.0377(8)	0.174(11)	1
C13	0.2129(7)	0.1418(13)	-0.0919(4)	0.155(10)	1
C14	0.1514(6)	0.0138(9)	-0.0244(7)	0.154(10)	1
C15	0.1763(6)	0.0872(13)	0.0682(5)	0.164(11)	1
C16	-0.0315(5)	0.3065(9)	0.0057(4)	0.067(4)	1
C17	0.0281(5)	0.4409(7)	-0.0551(4)	0.053(3)	1
C18	0.0907(5)	0.3305(8)	-0.1297(3)	0.065(4)	1
C19	0.0640(6)	0.1304(8)	-0.1148(4)	0.089(5)	1
C20	-0.0088(6)	0.1093(7)	-0.0337(4)	0.095(5)	1
C21	0.0701(5)	0.2257(9)	0.0866(4)	0.058(4)	1
C22	0.0683(5)	0.2315(12)	0.1311(4)	0.081(5)	1
C23	0.0902(6)	0.3024(12)	0.1490(4)	0.087(5)	1
C24	0.1137(5)	0.3682(10)	0.1241(4)	0.077(4)	1
C25	0.1123(5)	0.3577(8)	0.0789(3)	0.046(3)	1
C26	0.1351(4)	0.4255(8)	0.0512(4)	0.047(3)	1
C27	0.1449(5)	0.5110(10)	0.0655(5)	0.082(5)	1
C28	0.1677(6)	0.5729(9)	0.0368(6)	0.096(6)	1
C29	0.1793(5)	0.5528(8)	-0.0043(4)	0.063(4)	1
C30	0.1671(4)	0.4665(7)	-0.0162(4)	0.040(3)	1
C31	0.0458(5)	0.1432(9)	0.0662(4)	0.073(4)	1
C32	0.1789(5)	0.4407(7)	-0.0626(4)	0.063(4)	1
Yb51	0.1249(1)	0.7409(1)	0.2604(1)	0.031(1)	1
N51	0.1491(4)	0.8963(6)	0.2389(3)	0.048(2)	1
N52	0.0988(4)	0.7735(8)	0.1842(3)	0.056(3)	1
C51	0.2317(4)	0.7128(8)	0.2271(4)	0.042(3)	1
C52	0.2370(5)	0.7178(8)	0.2714(4)	0.049(3)	1

C53	0.2119(5)	0.6428(8)	0.2900(3)	0.044(3)	1
C54	0.1875(5)	0.5917(7)	0.2561(4)	0.053(3)	1
C55	0.2017(5)	0.6345(8)	0.2174(4)	0.051(3)	1
C56	0.0135(4)	0.7618(9)	0.2765(3)	0.049(3)	1
C57	0.0389(4)	0.8178(7)	0.3061(3)	0.034(3)	1
C58	0.0670(4)	0.7655(7)	0.3361(3)	0.036(3)	1
C59	0.0577(5)	0.6767(7)	0.3254(4)	0.046(3)	1
C60	0.0251(6)	0.6760(9)	0.2886(4)	0.058(4)	1
C61	0.2579(5)	0.7764(9)	0.1951(4)	0.084(5)	1
C62	0.2754(6)	0.7821(10)	0.2933(4)	0.105(6)	1
C63	0.2154(6)	0.6187(11)	0.3363(4)	0.103(6)	1
C64	0.1613(6)	0.5039(8)	0.2603(5)	0.110(6)	1
C65	0.1938(5)	0.5968(10)	0.1734(4)	0.092(5)	1
C66	-0.0259(5)	0.7928(10)	0.2418(4)	0.088(4)	1
C67	0.0307(5)	0.9161(7)	0.3071(4)	0.062(4)	1
C68	0.0933(5)	0.7977(9)	0.3775(3)	0.083(5)	1
C69	0.0732(6)	0.5993(9)	0.3545(5)	0.126(8)	1
C70	-0.0021(6)	0.5915(10)	0.2732(5)	0.135(8)	1
C71	0.1639(5)	0.9578(7)	0.2665(5)	0.061(4)	1
C72	0.1699(5)	1.0463(9)	0.2544(6)	0.087(5)	1
C73	0.1590(6)	1.0692(11)	0.2121(6)	0.107(7)	1
C74	0.1420(6)	1.0068(11)	0.1831(5)	0.089(5)	1
C75	0.1381(5)	0.9174(8)	0.1966(4)	0.052(3)	1
C76	0.1196(5)	0.8486(10)	0.1680(3)	0.060(4)	1
C77	0.1242(6)	0.8590(12)	0.1223(4)	0.097(6)	1
C78	0.1040(7)	0.7946(16)	0.0960(5)	0.113(8)	1
C79	0.0820(6)	0.7185(13)	0.1138(4)	0.091(5)	1
C80	0.0798(5)	0.7120(10)	0.1574(4)	0.065(4)	1
C81	0.1767(5)	0.9311(8)	0.3107(4)	0.072(4)	1
C82	0.0541(5)	0.6301(9)	0.1766(4)	0.081(4)	1
H11A	0.2839	0.2616	0.0594	0.220	1
H11B	0.2263	0.2498	0.0850	0.220	1
H11C	0.2335	0.3297	0.0521	0.220	1
H12A	0.2709	0.3486	-0.0214	0.261	1
H12B	0.2637	0.3050	-0.0677	0.261	1
H12C	0.3110	0.2694	-0.0357	0.261	1
H13A	0.1962	0.0848	-0.0992	0.233	1
H13B	0.2529	0.1411	-0.0990	0.233	1
H13C	0.1942	0.1885	-0.1082	0.233	1
H14A	0.1117	0.0182	-0.0167	0.231	1
H14B	0.1691	-0.0328	-0.0075	0.231	1
H14C	0.1548	-0.0003	-0.0549	0.231	1
H15A	0.2112	0.0619	0.0794	0.246	1
H15B	0.1489	0.0401	0.0634	0.246	1
H15C	0.1612	0.1296	0.0888	0.246	1
H16A	-0.0117	0.3459	0.0254	0.100	1

H16B	-0.0436	0.2536	0.0212	0.100	1
H16C	-0.0643	0.3368	-0.0060	0.100	1
H17A	0.0417	0.4623	-0.0274	0.080	1
H17B	-0.0117	0.4557	-0.0582	0.080	1
H17C	0.0495	0.4689	-0.0781	0.080	1
H18A	0.1285	0.3058	-0.1319	0.097	1
H18B	0.0930	0.3948	-0.1275	0.097	1
H18C	0.0690	0.3145	-0.1552	0.097	1
H19A	0.0315	0.1229	-0.1336	0.134	1
H19B	0.0711	0.0752	-0.0994	0.134	1
H19C	0.0969	0.1459	-0.1319	0.134	1
H20A	-0.0308	0.0861	-0.0576	0.142	1
H20B	-0.0335	0.1193	-0.0091	0.142	1
H20C	0.0204	0.0668	-0.0258	0.142	1
H22	0.0520	0.1861	0.1479	0.098	1
H23	0.0898	0.3083	0.1793	0.105	1
H24	0.1303	0.4187	0.1368	0.092	1
H27	0.1365	0.5274	0.0941	0.098	1
H28	0.1751	0.6309	0.0467	0.116	1
H31A	0.0081	0.1559	0.0554	0.110	1
H31B	0.0438	0.0960	0.0875	0.110	1
H31C	0.0698	0.1245	0.0424	0.110	1
H32A	0.2192	0.4301	-0.0663	0.094	1
H32B	0.1671	0.4886	-0.0816	0.094	1
H32C	0.1581	0.3870	-0.0697	0.094	1
H61A	0.2372	0.7736	0.1681	0.126	1
H61B	0.2971	0.7599	0.1901	0.126	1
H61C	0.2562	0.8365	0.2065	0.126	1
H62A	0.3143	0.7696	0.2853	0.157	1
H62B	0.2712	0.7765	0.3243	0.157	1
H62C	0.2657	0.8423	0.2846	0.157	1
H63A	0.1988	0.6658	0.3536	0.155	1
H63B	0.2548	0.6108	0.3443	0.155	1
H63C	0.1949	0.5636	0.3412	0.155	1
H64A	0.1833	0.4605	0.2443	0.165	1
H64B	0.1230	0.5059	0.2488	0.165	1
H64C	0.1600	0.4871	0.2905	0.165	1
H65A	0.1700	0.6364	0.1565	0.139	1
H65B	0.1759	0.5389	0.1755	0.139	1
H65C	0.2304	0.5907	0.1594	0.139	1
H66A	-0.0467	0.7423	0.2304	0.132	1
H66B	-0.0043	0.8203	0.2188	0.132	1
H66C	-0.0523	0.8357	0.2537	0.132	1
H67A	0.0485	0.9404	0.3328	0.092	1
H67B	-0.0095	0.9295	0.3075	0.092	1
H67C	0.0479	0.9423	0.2816	0.092	1

H68A	0.1341	0.8010	0.3741	0.125	1
H68B	0.0842	0.7567	0.4007	0.125	1
H68C	0.0786	0.8563	0.3845	0.125	1
H69A	0.0420	0.5574	0.3555	0.189	1
H69B	0.0810	0.6213	0.3834	0.189	1
H69C	0.1067	0.5699	0.3432	0.189	1
H70A	-0.0232	0.6032	0.2469	0.202	1
H70B	-0.0276	0.5693	0.2952	0.202	1
H70C	0.0270	0.5474	0.2674	0.202	1
H72	0.1811	1.0895	0.2746	0.105	1
H73	0.1634	1.1287	0.2032	0.129	1
H74	0.1331	1.0229	0.1545	0.107	1
H77	0.1411	0.9102	0.1106	0.117	1
H78	0.1051	0.8019	0.0658	0.136	1
H79	0.0688	0.6720	0.0962	0.109	1
H81A	0.1489	0.9569	0.3302	0.107	1
H81B	0.2142	0.9520	0.3186	0.107	1
H81C	0.1754	0.8667	0.3130	0.107	1
H82A	0.0815	0.6014	0.1953	0.122	1
H82B	0.0432	0.5896	0.1537	0.122	1
H82C	0.0209	0.6464	0.1933	0.122	1

U_{eq} is defined as one third of the orthogonalized U_{ij} tensor

Table 2. Anisotropic Displacement Parameters

atom	U_{11}	U_{22}	U_{33}	U_{12}	U_{13}	U_{23}
Yb1	0.036(1)	0.030(1)	0.028(1)	0.001(1)	-0.002(1)	-0.003(1)
N1	0.039(6)	0.058(6)	0.027(5)	0.004(5)	0.000(4)	0.004(5)
N2	0.029(5)	0.041(6)	0.038(6)	0.002(4)	-0.007(4)	-0.002(5)
C1	0.061(10)	0.097(12)	0.040(8)	-0.026(8)	-0.029(7)	0.025(8)
C2	0.041(8)	0.037(9)	0.108(13)	0.018(8)	0.000(8)	0.009(6)
C3	0.072(10)	0.084(11)	0.025(7)	0.017(7)	0.010(6)	0.043(8)
C4	0.044(8)	0.021(7)	0.090(11)	-0.005(6)	-0.001(7)	-0.005(6)
C5	0.057(10)	0.076(10)	0.050(9)	0.030(8)	0.018(7)	0.021(8)
C6	0.038(8)	0.057(8)	0.032(7)	0.011(6)	-0.007(5)	-0.006(6)
C7	0.040(8)	0.036(7)	0.031(7)	-0.008(5)	-0.016(5)	-0.003(5)
C8	0.040(8)	0.037(6)	0.026(6)	-0.004(5)	-0.008(5)	0.011(5)
C9	0.095(12)	0.026(7)	0.047(9)	-0.013(6)	-0.027(8)	0.018(7)
C10	0.049(9)	0.043(8)	0.065(10)	0.017(7)	-0.033(7)	-0.015(6)
C11	0.092(12)	0.19(2)	0.160(16)	-0.133(15)	-0.080(11)	0.074(13)
C12	0.054(12)	0.111(16)	0.36(3)	0.111(19)	0.041(15)	0.012(10)
C13	0.167(18)	0.28(3)	0.022(8)	-0.018(12)	-0.007(10)	0.145(17)
C14	0.067(13)	0.044(10)	0.35(3)	-0.034(13)	-0.050(15)	0.016(9)
C15	0.086(14)	0.27(2)	0.135(16)	0.161(17)	0.065(12)	0.091(15)
C16	0.035(8)	0.107(12)	0.058(9)	0.021(8)	-0.012(6)	-0.003(7)
C17	0.057(9)	0.045(7)	0.057(8)	-0.009(5)	0.008(6)	-0.009(6)
C18	0.065(10)	0.087(10)	0.043(8)	-0.004(7)	-0.009(7)	0.014(7)
C19	0.109(13)	0.061(10)	0.099(12)	-0.049(8)	-0.042(10)	0.015(8)
C20	0.112(13)	0.066(9)	0.106(12)	0.047(9)	-0.069(10)	-0.045(9)
C21	0.040(8)	0.093(11)	0.041(8)	0.022(7)	0.008(5)	-0.008(7)
C22	0.033(8)	0.166(17)	0.046(9)	0.027(10)	0.009(6)	0.020(10)
C23	0.048(11)	0.177(19)	0.036(9)	0.004(10)	0.010(8)	0.022(10)
C24	0.054(10)	0.131(13)	0.045(8)	-0.036(8)	-0.011(7)	0.016(9)
C25	0.036(7)	0.078(9)	0.025(6)	-0.003(6)	0.002(5)	0.013(7)
C26	0.020(7)	0.065(8)	0.057(7)	-0.036(6)	-0.012(6)	0.006(6)
C27	0.048(10)	0.089(12)	0.109(13)	-0.046(10)	-0.006(8)	-0.003(8)
C28	0.062(11)	0.048(10)	0.179(19)	-0.049(11)	0.005(11)	-0.014(7)
C29	0.055(9)	0.041(8)	0.093(11)	-0.026(7)	0.018(8)	0.000(7)
C30	0.023(7)	0.040(8)	0.058(9)	-0.010(6)	-0.009(6)	-0.002(5)
C31	0.077(11)	0.088(11)	0.055(9)	0.043(8)	0.008(8)	0.002(9)
C32	0.064(10)	0.065(9)	0.059(9)	0.023(7)	0.012(7)	-0.012(7)
Yb51	0.034(1)	0.031(1)	0.028(1)	-0.002(1)	0.002(1)	0.000(1)
N51	0.044(6)	0.044(6)	0.055(7)	0.001(5)	0.009(5)	-0.010(4)
N52	0.038(6)	0.102(9)	0.029(5)	-0.017(6)	0.005(4)	0.011(5)
C51	0.026(7)	0.049(7)	0.051(8)	0.002(6)	0.007(5)	-0.003(5)
C52	0.045(7)	0.053(8)	0.050(8)	-0.020(6)	-0.017(6)	0.011(6)

C53	0.056(8)	0.050(8)	0.028(7)	0.020(5)	0.012(6)	0.025(6)
C54	0.045(8)	0.031(7)	0.083(10)	-0.004(6)	0.009(7)	0.000(5)
C55	0.042(8)	0.072(9)	0.039(8)	-0.015(7)	0.004(6)	0.013(7)
C56	0.041(7)	0.068(10)	0.038(7)	-0.015(7)	0.007(5)	0.017(7)
C57	0.039(8)	0.034(7)	0.030(6)	0.005(5)	0.005(6)	0.008(5)
C58	0.036(6)	0.049(8)	0.022(5)	-0.002(5)	0.010(4)	0.014(6)
C59	0.038(8)	0.043(8)	0.058(9)	0.002(6)	0.031(7)	0.020(5)
C60	0.062(10)	0.053(9)	0.060(10)	-0.016(7)	0.028(8)	-0.001(7)
C61	0.054(9)	0.086(10)	0.112(12)	0.051(9)	0.038(6)	0.037(8)
C62	0.070(11)	0.120(13)	0.125(14)	-0.064(11)	-0.016(9)	-0.010(9)
C63	0.098(12)	0.179(17)	0.033(8)	0.031(9)	0.015(8)	0.086(11)
C64	0.082(12)	0.039(9)	0.21(2)	-0.020(10)	0.048(12)	-0.003(7)
C65	0.066(11)	0.142(14)	0.069(11)	-0.061(10)	-0.012(8)	0.041(9)
C66	0.056(9)	0.164(15)	0.044(8)	-0.005(9)	0.004(7)	0.024(9)
C67	0.071(10)	0.061(9)	0.053(8)	0.007(6)	0.020(7)	-0.001(7)
C68	0.102(12)	0.121(12)	0.027(7)	-0.007(7)	-0.003(7)	0.022(9)
C69	0.151(16)	0.102(13)	0.125(14)	0.081(11)	0.096(12)	0.075(11)
C70	0.127(15)	0.119(14)	0.157(17)	-0.094(12)	0.082(13)	-0.078(11)
C71	0.028(8)	0.033(8)	0.120(13)	0.004(8)	-0.008(8)	-0.001(5)
C72	0.041(9)	0.052(10)	0.169(17)	0.017(10)	-0.040(10)	-0.013(7)
C73	0.051(11)	0.064(12)	0.21(2)	0.045(13)	-0.026(12)	-0.015(8)
C74	0.046(10)	0.105(14)	0.116(14)	0.072(11)	0.023(9)	0.008(9)
C75	0.029(8)	0.062(9)	0.065(9)	0.019(6)	0.018(6)	0.001(6)
C76	0.052(9)	0.097(11)	0.030(7)	0.018(7)	0.004(7)	0.019(8)
C77	0.080(12)	0.164(16)	0.047(9)	0.050(10)	0.015(9)	0.067(12)
C78	0.075(14)	0.25(3)	0.017(9)	0.005(11)	-0.008(8)	0.072(14)
C79	0.056(11)	0.183(19)	0.033(10)	-0.040(10)	-0.007(7)	0.036(11)
C80	0.030(8)	0.123(13)	0.043(8)	-0.032(8)	-0.016(6)	0.042(7)
C81	0.067(11)	0.062(9)	0.086(11)	-0.018(8)	-0.020(8)	-0.001(7)
C82	0.055(10)	0.097(12)	0.092(12)	-0.059(10)	-0.012(8)	-0.017(9)

The general temperature factor expression:

$\exp(-2\Pi^2(a^{*2}U_{11}h^2 + b^{*2}U_{22}k^2 + c^{*2}U_{33}l^2 + 2a^*b^*U_{12}hk + 2a^*c^*U_{13}\,hl + 2b^*c^*U_{23}kl))$

Cp^*_2Yb(6,6'-dimethyl-2,2'-bipyridine)·(benzene)

EXPERIMENTAL DETAILS

A. Crystal Data

Empirical Formula	$H_{48}C_{38}YbN_2$
Formula Weight	705.85
Crystal Color, Habit	black, thin plate
Crystal Dimensions	0.08 X 0.07 X 0.02 mm
Crystal System	monoclinic
Lattice Type	Primitive
Lattice Parameters	a = 14.127(1)Å
	b = 15.283(1) Å
	c = 15.312(1) Å
	β = 92.180(2)^o
V = 3303.5(5) Å^3	
Space Group	$P2_1/c$ (#14)
Z value	4
D_{calc}	1.419 g/cm^3
F_{000}	1440.00
μ(MoKα)	28.58 cm^{-1}

B. Intensity Measurements

Diffractometer	Bruker APEX CCD
Radiation	MoKα (λ = 0.71069 Å) graphite monochromated
Detector Position	600.00 mm
Exposure Time	10.0 seconds per frame.
Scan Type	ω (0.3 degrees per frame)
$2\theta_{max}$	48.8^o
No. of Reflections Measured	Total: 16177 Unique: 3600
(R_{int} = 0.048)	
Corrections	Lorentz-polarization
	Absorption (Tmax = 1.00 Tmin = 0.84)

C. Structure Solution and Refinement

Structure Solution	Direct Methods (SIR97)
Refinement	Full-matrix least-squares
Function Minimized	Σ w (|Fo| - |Fc|)^2
Least Squares Weights	$1/\sigma^2(Fo) = 4Fo^2/\sigma^2(Fo^2)$
p-factor	0.0300
Anomalous Dispersion	All non-hydrogen atoms
No. Observations (I>3.00σ(I))	3739
No. Variables	370
Reflection/Parameter Ratio	10.11
Residuals: R; Rw; Rall	0.037 ; 0.043; 0.064
Goodness of Fit Indicator	1.23
Max Shift/Error in Final Cycle	0.00
Maximum peak in Final Diff. Map	0.67 $e^-/Å^3$
Minimum peak in Final Diff. Map	-0.54 $e^-/Å^3$

Table 1. Atomic coordinates and B_{iso}/B_{eq} and occupancy

atom	x	y	z	B_{eq}	occ
Yb(1)	-0.25122(2)	0.03607(2)	0.79045(2)	1.791(7)	
N(1)	-0.1344(4)	0.0843(4)	0.6808(4)	2.3(1)	
N(2)	-0.3272(4)	0.0768(4)	0.6453(4)	1.9(1)	
C(1)	-0.3156(5)	0.2020(4)	0.8238(5)	2.3(2)	
C(2)	-0.2177(5)	0.2049(5)	0.8431(5)	2.7(2)	
C(3)	-0.2041(6)	0.1503(6)	0.9217(5)	3.7(2)	
C(4)	-0.2932(7)	0.1187(5)	0.9425(5)	3.8(2)	
C(5)	-0.3604(6)	0.1482(5)	0.8842(5)	3.3(2)	
C(6)	-0.1640(6)	-0.1244(5)	0.8207(5)	3.0(2)	
C(7)	-0.2003(5)	-0.1271(4)	0.7342(5)	2.4(2)	
C(8)	-0.3003(5)	-0.1282(4)	0.7364(5)	2.0(2)	
C(9)	-0.3259(5)	-0.1234(5)	0.8238(5)	2.8(2)	
C(10)	-0.2409(7)	-0.1213(5)	0.8771(5)	3.3(2)	
C(11)	-0.3666(6)	0.2563(5)	0.7541(5)	3.6(2)	
C(12)	-0.1482(6)	0.2605(6)	0.7997(6)	4.5(2)	
C(13)	-0.1146(8)	0.1429(7)	0.9763(7)	7.6(3)	
C(14)	-0.313(1)	0.0720(7)	1.0291(7)	7.7(3)	
C(15)	-0.4664(7)	0.1351(6)	0.8932(7)	5.6(3)	
C(16)	-0.0628(7)	-0.1418(6)	0.8510(8)	6.4(3)	
C(17)	-0.1444(6)	-0.1398(6)	0.6539(6)	4.2(2)	
C(18)	-0.3662(6)	-0.1469(5)	0.6576(5)	3.3(2)	
C(19)	-0.4242(6)	-0.1332(5)	0.8586(6)	3.8(2)	
C(20)	-0.2332(8)	-0.1301(5)	0.9750(5)	5.4(3)	
C(21)	-0.0394(5)	0.0779(5)	0.6950(6)	3.2(2)	
C(22)	0.0237(5)	0.0908(6)	0.6290(6)	3.8(2)	
C(23)	-0.0117(6)	0.1125(7)	0.5466(6)	4.5(2)	
C(24)	-0.1080(5)	0.1221(6)	0.5323(5)	3.3(2)	
C(25)	-0.1669(5)	0.1082(5)	0.5997(4)	2.2(2)	
C(26)	-0.2713(5)	0.1174(4)	0.5863(5)	2.3(2)	
C(27)	-0.3086(5)	0.1647(5)	0.5157(5)	2.8(2)	
C(28)	-0.4059(6)	0.1638(5)	0.5000(5)	3.4(2)	
C(29)	-0.4631(5)	0.1205(5)	0.5563(5)	3.2(2)	
C(30)	-0.4222(5)	0.0797(5)	0.6296(5)	2.4(2)	
C(31)	-0.0037(6)	0.0594(6)	0.7866(6)	4.7(2)	
C(32)	-0.4838(5)	0.0376(6)	0.6942(5)	3.5(2)	
C(33)	-0.2757(5)	-0.0462(5)	0.4102(5)	2.8(2)	
C(34)	-0.2751(5)	-0.1326(5)	0.3881(5)	3.0(2)	
C(35)	-0.2694(5)	-0.1569(5)	0.3007(6)	3.3(2)	
C(36)	-0.2629(6)	-0.0947(6)	0.2374(5)	3.6(2)	

Table 1. Atomic coordinates and B_{iso}/B_{eq} and occupancy (continued)

atom	x	y	z	B_{eq}	occ
C(37)	-0.2636(6)	-0.0079(5)	0.2599(5)	2.9(2)	
C(38)	-0.2702(5)	0.0163(4)	0.3454(5)	2.7(2)	
C(101)	-0.2782	0.1648	0.8831	0.2000	0.001
C(102)	-0.2463	-0.1249	0.7984	0.2000	0.001
H(1)	-0.3240	0.2869	0.7195	4.4474	
H(2)	-0.4047	0.2181	0.7153	4.4474	
H(3)	-0.4094	0.2964	0.7794	4.4474	
H(4)	-0.0851	0.2503	0.8242	4.8845	
H(5)	-0.1474	0.2485	0.7386	4.8845	
H(6)	-0.1624	0.3211	0.8075	4.8845	
H(7)	-0.0967	0.0834	0.9875	8.4065	
H(8)	-0.0608	0.1697	0.9470	8.4065	
H(9)	-0.1186	0.1724	1.0311	8.4065	
H(10)	-0.3509	0.1083	1.0654	9.1184	
H(11)	-0.3502	0.0189	1.0174	9.1184	
H(12)	-0.2572	0.0560	1.0598	9.1184	
H(13)	-0.4894	0.1617	0.9447	7.0565	
H(14)	-0.5025	0.1619	0.8437	7.0565	
H(15)	-0.4837	0.0746	0.8931	7.0565	
H(16)	-0.0549	-0.1977	0.8771	7.4959	
H(17)	-0.0205	-0.1399	0.8013	7.4959	
H(18)	-0.0395	-0.0981	0.8912	7.4959	
H(19)	-0.1590	-0.1950	0.6258	4.6192	
H(20)	-0.1605	-0.0948	0.6100	4.6192	
H(21)	-0.0783	-0.1368	0.6655	4.6192	
H(22)	-0.4311	-0.1443	0.6712	4.1099	
H(23)	-0.3561	-0.1055	0.6107	4.1099	
H(24)	-0.3539	-0.2043	0.6337	4.1099	
H(25)	-0.4373	-0.0854	0.8976	4.5992	
H(26)	-0.4709	-0.1317	0.8117	4.5992	
H(27)	-0.4298	-0.1864	0.8897	4.5992	
H(28)	-0.2937	-0.1265	1.0000	6.3892	
H(29)	-0.2049	-0.1852	0.9919	6.3892	
H(30)	-0.1936	-0.0846	1.0001	6.3892	
H(31)	0.0917	0.0835	0.6410	4.5694	
H(32)	0.0308	0.1191	0.4994	5.5686	
H(33)	-0.1340	0.1383	0.4740	4.0536	
H(34)	-0.2661	0.1976	0.4781	3.2701	
H(35)	-0.4338	0.1935	0.4488	3.9666	

Table 1. Atomic coordinates and B_{iso}/B_{eq} and occupancy (continued)

atom	x	y	z	B_{eq}	occ
H(36)	-0.5308	0.1178	0.5450	3.8915	
H(37)	-0.0289	0.0061	0.8081	5.7248	
H(38)	0.0637	0.0565	0.7904	5.7248	
H(39)	-0.0228	0.1059	0.8258	5.7248	
H(40)	-0.4739	0.0625	0.7505	4.1702	
H(41)	-0.5488	0.0427	0.6764	4.1702	
H(42)	-0.4689	-0.0243	0.6984	4.1702	
H(43)	-0.2805	-0.0274	0.4698	3.4927	
H(44)	-0.2798	-0.1771	0.4334	3.7717	
H(45)	-0.2707	-0.2181	0.2841	3.9430	
H(46)	-0.2578	-0.1102	0.1767	4.3607	
H(47)	-0.2606	0.0364	0.2158	3.5236	
H(48)	-0.2713	0.0776	0.3594	3.4018	

$B_{eq} = 8/3\ \pi^2(U_{11}(aa^*)^2 + U_{22}(bb^*)^2 + U_{33}(cc^*)^2 + 2U_{12}(aa^*bb^*)\cos\gamma + 2U_{13}(aa^*cc^*)\cos\beta + 2U_{23}(bb^*cc^*)\cos\alpha)$

Table 2. Anisotropic Displacement Parameters

atom	U_{11}	U_{22}	U_{33}	U_{12}	U_{13}	U_{23}
Yb(1)	0.0226(2)	0.0261(2)	0.0194(2)	0.0006(2)	0.0012(1)	0.0013(2)
N(1)	0.027(3)	0.026(3)	0.034(4)	-0.003(3)	0.009(3)	-0.001(3)
N(2)	0.026(3)	0.023(3)	0.023(3)	-0.002(3)	-0.001(3)	0.003(3)
C(1)	0.038(4)	0.019(4)	0.030(4)	0.004(3)	-0.000(4)	-0.002(3)
C(2)	0.031(4)	0.033(4)	0.040(5)	-0.000(4)	0.007(4)	-0.010(4)
C(3)	0.062(6)	0.045(5)	0.033(5)	0.018(5)	-0.024(5)	-0.017(4)
C(4)	0.082(7)	0.034(5)	0.028(5)	0.004(5)	0.007(5)	-0.009(4)
C(5)	0.054(5)	0.033(5)	0.040(5)	0.006(4)	0.016(5)	-0.007(4)
C(6)	0.040(5)	0.027(5)	0.046(5)	0.001(4)	-0.008(4)	0.003(4)
C(7)	0.038(5)	0.022(4)	0.031(5)	0.003(3)	0.004(4)	0.000(3)
C(8)	0.027(4)	0.027(4)	0.023(4)	-0.003(3)	0.002(3)	0.002(3)
C(9)	0.044(5)	0.036(5)	0.026(5)	0.004(4)	0.009(4)	0.008(4)
C(10)	0.072(6)	0.021(4)	0.031(5)	0.002(4)	-0.013(5)	0.010(4)
C(11)	0.048(5)	0.029(5)	0.060(6)	0.007(4)	-0.007(5)	-0.004(4)
C(12)	0.040(5)	0.046(6)	0.085(7)	-0.004(4)	0.012(5)	-0.012(5)
C(13)	0.102(9)	0.092(9)	0.090(9)	0.048(7)	-0.064(7)	-0.057(7)
C(14)	0.20(1)	0.054(6)	0.042(6)	0.034(8)	0.037(8)	0.001(5)
C(15)	0.061(6)	0.069(7)	0.087(8)	-0.019(5)	0.043(6)	-0.021(6)
C(16)	0.063(6)	0.052(6)	0.124(10)	0.018(5)	-0.054(7)	0.006(6)
C(17)	0.055(6)	0.051(6)	0.056(6)	-0.002(4)	0.025(5)	-0.016(5)
C(18)	0.045(5)	0.040(5)	0.040(5)	-0.013(4)	-0.007(4)	-0.002(4)
C(19)	0.048(5)	0.043(5)	0.055(6)	-0.013(4)	0.017(5)	0.001(4)
C(20)	0.144(10)	0.030(5)	0.030(5)	-0.000(6)	-0.014(6)	0.003(4)
C(21)	0.030(4)	0.037(5)	0.054(6)	0.002(4)	-0.007(4)	-0.002(4)
C(22)	0.024(4)	0.054(6)	0.069(7)	-0.001(4)	0.018(4)	-0.007(5)
C(23)	0.047(5)	0.085(7)	0.043(6)	-0.021(5)	0.023(5)	-0.005(5)
C(24)	0.038(5)	0.060(6)	0.029(5)	-0.008(4)	0.009(4)	0.002(4)
C(25)	0.035(4)	0.026(4)	0.021(4)	-0.012(3)	0.004(3)	-0.004(3)
C(26)	0.036(4)	0.021(4)	0.028(4)	-0.010(3)	0.001(4)	-0.005(3)
C(27)	0.047(5)	0.029(4)	0.029(5)	-0.000(4)	0.004(4)	0.002(3)
C(28)	0.054(5)	0.037(5)	0.037(5)	0.007(4)	-0.012(4)	0.010(4)
C(29)	0.035(4)	0.047(5)	0.038(5)	0.004(4)	-0.001(4)	0.007(4)
C(30)	0.028(4)	0.027(4)	0.037(5)	0.005(3)	-0.002(4)	0.002(3)
C(31)	0.030(5)	0.079(7)	0.068(7)	0.004(4)	0.004(5)	0.022(5)
C(32)	0.018(4)	0.068(6)	0.045(5)	0.007(4)	-0.004(4)	0.019(5)
C(33)	0.031(4)	0.042(5)	0.032(4)	0.002(4)	0.004(3)	-0.002(4)
C(34)	0.028(4)	0.042(5)	0.043(5)	-0.006(4)	0.001(4)	0.014(4)
C(35)	0.037(5)	0.022(4)	0.065(7)	-0.005(4)	0.001(5)	-0.005(4)
C(36)	0.050(5)	0.059(6)	0.028(5)	0.005(5)	0.003(4)	-0.012(4)

Table 2. Anisotropic Displacement Parameters (continued)

atom	U_{11}	U_{22}	U_{33}	U_{12}	U_{13}	U_{23}
C(37)	0.045(5)	0.036(5)	0.032(5)	-0.007(4)	0.008(4)	0.006(4)
C(38)	0.040(5)	0.024(5)	0.039(5)	0.004(3)	0.009(4)	0.003(3)

The general temperature factor expression:
$\exp(-2\pi^2(a^{*2}U_{11}h^2 + b^{*2}U_{22}k^2 + c^{*2}U_{33}l^2 + 2a^*b^*U_{12}hk + 2a^*c^*U_{13}hl + 2b^*c^*U_{23}kl))$

Cp^*_2Yb(6-methyl-2,2'-bipyridine)

EXPERIMENTAL DETAILS

A. Crystal Data

Empirical Formula	$YbN_2C_{31}H_{40}$
Formula Weight	613.71
Crystal Color, Habit	green, plate
Crystal Dimensions	0.10 X 0.03 X 0.04 mm
Crystal System	orthorhombic
Lattice Type	Primitive
Lattice Parameters	a = 15.924(2)Å
	b = 16.524(3) Å
	c = 20.318(3) Å
	V = 5346(1) $Å^3$
Space Group	Pbca (#61)
Z value	8
D_{calc}	1.525 g/cm^3
F_{000}	2480.00
μ(MoKα)	35.20 cm^{-1}

B. Intensity Measurements

Diffractometer	Bruker SMART CCD
Radiation	MoKα (λ = 0.71069 Å) graphite monochromated
Detector Position	60.00 mm
Exposure Time	10.0 seconds per frame.
Scan Type	ω (0.3 degrees per frame)
$2\theta_{max}$	38.4^o
No. of Reflections Measured	
Total: 13041	Unique: 2511 (R_{int} = 0.097)
Corrections	
Lorentz-polarization	
Absorption	(Tmax = 1.00 Tmin = 0.83)

C. Structure Solution and Refinement

Structure Solution	Direct Methods
Refinement	Full-matrix least-squares
Function Minimized	Σ w (|Fo| - |Fc|)^2
Least Squares Weights	$1/\sigma^2(Fo) = 4Fo^2/\sigma^2(Fo^2)$
p-factor	0.0300
Anomalous Dispersion	All non-hydrogen atoms
No. Observations (I>3.00σ(I))	1276
No. Variables	142
Reflection/Parameter Ratio	8.99
Residuals: R; Rw; Rall	0.037 ; 0.039; 0.088
Goodness of Fit Indicator	1.46
Max Shift/Error in Final Cycle	0.00
Maximum peak in Final Diff. Map	1.08 $e^-/Å^3$
Minimum peak in Final Diff. Map	-0.47 $e^-/Å^3$

Table 1. Atomic coordinates and B_{iso}/B_{eq} and occupancy

atom	x	y	z	B_{eq}	occ
Yb(1)	0.89627(4)	0.21996(4)	0.12477(4)	2.25(2)	
N(1)	0.9826(8)	0.3410(7)	0.1031(6)	3.2(3)	
N(2)	0.8594(7)	0.3373(7)	0.1935(6)	2.8(3)	
C(1)	0.7480(10)	0.2590(8)	0.0717(8)	2.0(4)	
C(2)	0.8045(10)	0.2705(10)	0.0204(7)	2.3(3)	
C(3)	0.834(1)	0.1927(9)	0.0026(8)	3.0(4)	
C(4)	0.7962(9)	0.1360(8)	0.0421(8)	2.3(3)	
C(5)	0.7417(9)	0.1763(9)	0.0873(7)	2.0(3)	
C(6)	1.0059(10)	0.1023(9)	0.1505(7)	2.6(4)	
C(7)	1.0421(10)	0.1726(9)	0.1808(8)	3.0(4)	
C(8)	0.9904(9)	0.1944(8)	0.2321(8)	2.9(4)	
C(9)	0.9261(9)	0.1379(9)	0.2373(8)	2.8(4)	
C(10)	0.9369(9)	0.0802(9)	0.1869(8)	2.4(4)	
C(11)	0.6934(9)	0.3242(9)	0.0997(7)	2.8(3)	
C(12)	0.823(1)	0.3490(10)	-0.0129(8)	3.7(4)	
C(13)	0.886(1)	0.1715(9)	-0.0575(7)	2.9(3)	
C(14)	0.801(1)	0.0448(9)	0.0304(8)	3.7(4)	
C(15)	0.6851(9)	0.1361(8)	0.1344(9)	3.2(3)	
C(16)	1.045(1)	0.0561(10)	0.0942(9)	4.3(4)	
C(17)	1.127(1)	0.209(1)	0.1639(10)	5.7(5)	
C(18)	1.011(1)	0.263(1)	0.281(1)	5.7(5)	
C(19)	0.859(1)	0.137(1)	0.288(1)	4.9(5)	
C(20)	0.888(1)	0.0039(9)	0.1796(9)	4.4(4)	
C(21)	1.043(1)	0.344(1)	0.0579(10)	5.0(5)	
C(22)	1.098(1)	0.408(1)	0.0482(9)	4.5(4)	
C(23)	1.084(1)	0.472(1)	0.090(1)	6.0(5)	
C(24)	1.023(1)	0.473(1)	0.136(1)	5.1(5)	
C(25)	0.9694(10)	0.4074(9)	0.1405(8)	3.3(4)	
C(26)	0.905(1)	0.4049(9)	0.1896(8)	3.3(4)	
C(27)	0.890(1)	0.4707(9)	0.2359(8)	3.2(3)	
C(28)	0.826(1)	0.4587(9)	0.2775(8)	3.0(4)	
C(29)	0.776(1)	0.392(1)	0.2821(9)	5.1(5)	
C(30)	0.7954(10)	0.3303(9)	0.2379(9)	3.4(4)	
C(31)	1.050(1)	0.273(1)	0.014(1)	5.5(5)	
C(101)	0.7848	0.2069	0.0448	0.2000	0.000
C(102)	0.9803	0.1375	0.1975	0.2000	0.000
H(1)	0.7254	0.3682	0.1177	3.3856	
H(2)	0.6567	0.3462	0.0666	3.3856	
H(3)	0.6579	0.3040	0.1348	3.3856	

Table 1. Atomic coordinates and B_{iso}/B_{eq} and occupancy (continued)

atom	x	y	z	B_{eq}	occ
H(4)	0.8439	0.3910	0.0174	4.1060	
H(5)	0.8659	0.3444	-0.0466	4.1060	
H(6)	0.7743	0.3721	-0.0337	4.1060	
H(7)	0.9342	0.1371	-0.0470	3.9521	
H(8)	0.8540	0.1419	-0.0902	3.9521	
H(9)	0.9092	0.2183	-0.0801	3.9521	
H(10)	0.7686	0.0159	0.0643	4.3720	
H(11)	0.7766	0.0294	-0.0110	4.3720	
H(12)	0.8566	0.0242	0.0323	4.3720	
H(13)	0.6524	0.1739	0.1611	3.5632	
H(14)	0.6420	0.1010	0.1138	3.5632	
H(15)	0.7129	0.1006	0.1662	3.5632	
H(16)	1.0634	0.0030	0.1060	5.3617	
H(17)	1.0064	0.0500	0.0572	5.3617	
H(18)	1.0942	0.0839	0.0757	5.3617	
H(19)	1.1657	0.2009	0.2005	7.0211	
H(20)	1.1512	0.1842	0.1263	7.0211	
H(21)	1.1234	0.2660	0.1567	7.0211	
H(22)	1.0587	0.2503	0.3074	6.6209	
H(23)	1.0154	0.3136	0.2624	6.6209	
H(24)	0.9632	0.2665	0.3143	6.6209	
H(25)	0.8239	0.1860	0.2877	4.9550	
H(26)	0.8186	0.0924	0.2839	4.9550	
H(27)	0.8801	0.1332	0.3328	4.9550	
H(28)	0.8282	0.0147	0.1745	5.3578	
H(29)	0.9043	-0.0287	0.1424	5.3578	
H(30)	0.8930	-0.0304	0.2182	5.3578	
H(31)	1.1399	0.4095	0.0135	5.6227	
H(32)	1.1290	0.5163	0.0879	8.7664	
H(33)	1.0177	0.5216	0.1640	5.8360	
H(34)	0.9259	0.5188	0.2351	4.2707	
H(35)	0.8134	0.5065	0.3084	4.6351	
H(36)	0.7289	0.3872	0.3139	5.9944	
H(37)	0.7581	0.2823	0.2398	4.0717	
H(38)	0.9980	0.2617	-0.0108	6.4963	
H(39)	1.0935	0.2773	-0.0182	6.4963	
H(40)	1.0607	0.2224	0.0381	6.4963	

$B_{eq} = 8/3\ \pi^2(U_{11}(aa^*)^2 + U_{22}(bb^*)^2 + U_{33}(cc^*)^2 + 2U_{12}(aa^*bb^*)\cos\gamma + 2U_{13}(aa^*cc^*)\cos\beta + 2U_{23}(bb^*cc^*)\cos\alpha)$

Table 2. Anisotropic Displacement Parameters

atom	U_{11}	U_{22}	U_{33}	U_{12}	U_{13}	U_{23}
Yb(1)	0.0306(4)	0.0250(4)	0.0300(4)	0.0002(4)	0.0005(5)	-0.0023(5)

The general temperature factor expression:
$\exp(-2\pi^2(a^{*2}U_{11}h^2 + b^{*2}U_{22}k^2 + c^{*2}U_{33}l^2 + 2a^*b^*U_{12}hk + 2a^*c^*U_{13}hl + 2b^*c^*U_{23}kl))$

[$Cp^*_2Lu(2,2'\text{-bipyridine})][(Cp^*Lu)_4Cl_7O$]

EXPERIMENTAL DETAILS

A. Crystal Data

Empirical Formula	$C_{71}H_{100}Lu_5OCl_9N_2$
Formula Weight	2191.50
Crystal Color, Habit	orange, block
Crystal Dimensions	0.21 X 0.20 X 0.18 mm
Crystal System	monoclinic
Lattice Type	Primitive
Lattice Parameters	a = 12.739(1)Å
	b = 33.248(4) Å
	c = 18.583(2) Å
	$\beta = 103.563(2)^o$
	$V = 7650(1)$ Å^3
Space Group	$P2_1/c$ (#14)
Z value	4
D_{calc}	1.902 g/cm^3
F_{000}	4224.00
μ(MoKα)	67.47 cm^{-1}

B. Intensity Measurements

Diffractometer	Bruker APEX CCD
Radiation	MoKα (λ = 0.71069 Å) graphite monochromated
Detector Position	60.00 mm
Exposure Time	20.0 seconds per frame.
Scan Type	ω (0.3 degrees per frame)
$2\theta_{max}$	46.6^o
No. of Reflections Measured (R_{int} = 0.069)	Total: 38743 Unique: 5951
Corrections	Lorentz-polarization
	Absorption (Tmax = 1.00 Tmin = 0.67)

C. Structure Solution and Refinement

Structure Solution	Direct Methods (SIR97)
Refinement	Full-matrix least-squares
Function Minimized	Σ w (|Fo| - |Fc|)^2
Least Squares Weights	$1/\sigma^2(Fo) = 4Fo^2/\sigma^2(Fo^2)$
p-factor	0.0300
Anomalous Dispersion	All non-hydrogen atoms
No. Observations (I>3.00σ(I))	6319
No. Variables	790
Reflection/Parameter Ratio	8.00
Residuals: R; Rw; Rall	0.049 ; 0.056; 0.108
Goodness of Fit Indicator	1.28
Max Shift/Error in Final Cycle	0.00
Maximum peak in Final Diff. Map	1.42 $e^-/Å^3$
Minimum peak in Final Diff. Map	-1.05 $e^-/Å^3$

Table 1. Atomic coordinates and B_{iso}/B_{eq} and occupancy

atom	x	y	z	B_{eq}	occ
Lu(1)	-0.02201(6)	0.06054(2)	0.27253(4)	2.04(2)	
Lu(2)	0.22370(6)	0.10776(2)	0.38267(4)	2.47(2)	
Lu(3)	-0.42701(6)	0.14174(2)	-0.16046(4)	2.23(2)	
Lu(4)	0.18884(6)	0.11000(2)	0.19111(4)	1.98(2)	
Lu(5)	0.00990(6)	0.16643(2)	0.27264(5)	2.83(2)	
Cl(1)	0.0622(3)	0.0446(1)	0.1575(2)	2.06(10)	
Cl(2)	0.3144(7)	0.0742(3)	0.2946(4)	10.8(3)	
Cl(3)	0.0260(7)	0.1572(3)	0.1370(4)	2.8(2)	0.634(8)
Cl(4)	0.1226(6)	0.0391(2)	0.3912(5)	2.6(2)	0.634
Cl(5)	0.2376(5)	0.1743(2)	0.2976(4)	1.6(2)	0.634
Cl(6)	0.0561(6)	0.1434(2)	0.4139(4)	3.2(2)	0.634
Cl(7)	-0.145(1)	0.1190(4)	0.2127(8)	8.6(4)	0.634
Cl(8)	-0.0343(7)	0.3442(3)	0.1153(5)	10.7(3)	
Cl(9)	-0.2460(9)	0.3639(6)	0.0321(7)	19.4(7)	0.90(3)
Cl(10)	0.066(2)	0.1711(9)	0.146(2)	7.1(7)	0.282
Cl(11)	0.149(1)	0.0362(5)	0.368(1)	2.5(4)	0.282
Cl(12)	0.219(2)	0.1826(6)	0.326(1)	4.2(5)	0.282
Cl(13)	0.008(2)	0.1245(6)	0.397(1)	4.0(4)	0.282
Cl(14)	-0.116(2)	0.1176(7)	0.261(1)	5.7(5)	0.282
O(1)	0.0948(8)	0.1075(3)	0.2772(5)	1.9(3)	
N(1)	-0.282(1)	0.1032(4)	-0.0968(8)	1.9(3)	
N(2)	-0.376(1)	0.0951(4)	-0.2388(8)	2.7(4)	
C(1)	-0.519(2)	0.0865(5)	-0.099(1)	3.4(5)	
C(2)	-0.531(2)	0.1235(6)	-0.064(1)	3.0(5)	
C(3)	-0.597(1)	0.1481(5)	-0.111(1)	3.0(5)	
C(4)	-0.630(1)	0.1290(6)	-0.181(1)	2.8(5)	
C(5)	-0.581(1)	0.0908(6)	-0.175(1)	2.8(5)	
C(6)	-0.271(2)	0.1936(6)	-0.136(1)	4.7(6)	
C(7)	-0.365(2)	0.2127(6)	-0.1246(10)	2.9(5)	
C(8)	-0.441(1)	0.2161(5)	-0.193(1)	3.8(6)	
C(9)	-0.394(2)	0.1977(6)	-0.2473(10)	3.5(5)	
C(10)	-0.289(2)	0.1835(6)	-0.214(2)	5.3(7)	
C(11)	-0.468(2)	0.0478(6)	-0.066(1)	4.2(6)	
C(12)	-0.489(2)	0.1302(7)	0.018(1)	4.4(6)	
C(13)	-0.651(2)	0.1866(7)	-0.090(1)	5.4(6)	
C(14)	-0.711(2)	0.1438(6)	-0.250(1)	4.0(5)	
C(15)	-0.604(2)	0.0578(7)	-0.230(1)	4.9(6)	
C(16)	-0.168(2)	0.1906(7)	-0.080(2)	7.3(8)	
C(17)	-0.376(2)	0.2331(6)	-0.054(1)	5.2(7)	

Table 1. Atomic coordinates and B_{iso}/B_{eq} and occupancy (continued)

atom	x	y	z	B_{eq}	occ
C(18)	-0.540(2)	0.2425(6)	-0.212(2)	7.3(8)	
C(19)	-0.446(3)	0.1973(8)	-0.330(1)	8.6(9)	
C(20)	-0.207(3)	0.1666(8)	-0.248(2)	10(1)	
C(21)	-0.237(1)	0.1083(6)	-0.027(1)	2.4(4)	
C(22)	-0.151(2)	0.0875(6)	0.014(1)	3.1(5)	
C(23)	-0.113(2)	0.0566(6)	-0.023(1)	3.3(5)	
C(24)	-0.158(1)	0.0501(5)	-0.097(1)	2.7(5)	
C(25)	-0.242(1)	0.0745(6)	-0.1324(9)	2.4(5)	
C(26)	-0.293(1)	0.0685(5)	-0.210(1)	2.9(5)	
C(27)	-0.265(2)	0.0393(7)	-0.254(1)	4.5(6)	
C(28)	-0.315(2)	0.0370(8)	-0.332(1)	6.0(8)	
C(29)	-0.396(2)	0.0642(7)	-0.360(1)	3.7(5)	
C(30)	-0.423(1)	0.0921(6)	-0.311(1)	3.0(5)	
C(31)	-0.085(2)	-0.0107(6)	0.306(1)	4.1(6)	
C(32)	-0.125(2)	-0.0057(6)	0.230(1)	3.4(5)	
C(33)	-0.204(2)	0.0242(7)	0.216(1)	3.8(6)	
C(34)	-0.213(2)	0.0381(7)	0.287(1)	4.0(6)	
C(35)	-0.140(2)	0.0190(6)	0.343(1)	3.7(6)	
C(36)	0.350(1)	0.0879(6)	0.135(1)	2.6(5)	
C(37)	0.262(2)	0.0858(5)	0.076(1)	3.0(5)	
C(38)	0.221(2)	0.1251(7)	0.059(1)	4.2(6)	
C(39)	0.290(2)	0.1525(6)	0.110(1)	3.7(6)	
C(40)	0.367(1)	0.1297(5)	0.1572(10)	2.3(5)	
C(41)	-0.001(2)	0.2425(5)	0.257(1)	3.7(6)	
C(42)	-0.002(2)	0.2360(7)	0.333(2)	5.1(7)	
C(43)	-0.106(2)	0.2176(7)	0.326(2)	6.4(9)	
C(44)	-0.160(3)	0.211(1)	0.255(3)	9(1)	
C(45)	-0.102(3)	0.2279(9)	0.212(2)	7.3(9)	
C(46)	0.398(2)	0.1372(7)	0.472(1)	4.8(6)	
C(47)	0.314(2)	0.1387(6)	0.512(1)	4.2(6)	
C(48)	0.289(2)	0.0994(6)	0.526(1)	3.8(6)	
C(49)	0.354(2)	0.0738(6)	0.496(1)	3.1(5)	
C(50)	0.421(2)	0.0956(7)	0.465(1)	3.6(5)	
C(51)	-0.011(2)	-0.0426(6)	0.346(1)	4.3(6)	
C(52)	-0.095(2)	-0.0347(8)	0.174(1)	6.9(8)	
C(53)	-0.273(2)	0.0354(8)	0.143(1)	5.2(6)	
C(54)	-0.291(2)	0.0683(7)	0.298(1)	5.5(7)	
C(55)	-0.123(2)	0.0250(6)	0.425(1)	5.0(7)	
C(56)	0.421(2)	0.0530(6)	0.164(1)	5.0(6)	

Table 1. Atomic coordinates and B_{iso}/B_{eq} and occupancy (continued)

atom	x	y	z	B_{eq}	occ
C(57)	0.221(2)	0.0499(7)	0.029(1)	4.6(6)	
C(58)	0.130(2)	0.1383(7)	-0.005(1)	5.7(7)	
C(59)	0.282(1)	0.1972(6)	0.109(1)	3.5(5)	
C(60)	0.461(1)	0.1456(5)	0.215(1)	3.3(5)	
C(61)	0.089(3)	0.2659(7)	0.237(2)	8.5(10)	
C(62)	0.076(2)	0.2500(7)	0.399(1)	7.5(8)	
C(63)	-0.147(4)	0.2041(10)	0.388(4)	20(2)	
C(64)	-0.271(2)	0.1982(9)	0.232(4)	26(2)	
C(65)	-0.134(5)	0.2325(10)	0.134(2)	22(1)	
C(66)	0.450(2)	0.173(1)	0.451(1)	10(1)	
C(67)	0.268(2)	0.1770(9)	0.535(1)	7.9(9)	
C(68)	0.200(2)	0.0867(7)	0.566(1)	5.7(7)	
C(69)	0.361(2)	0.0295(7)	0.509(1)	4.4(6)	
C(70)	0.507(2)	0.0808(9)	0.429(1)	6.3(7)	
C(71)	-0.119(3)	0.3748(10)	0.045(2)	9(1)	
C(101)	-0.5719	0.1155	-0.1262	0.2000	0.001
C(102)	-0.3522	0.2008	-0.1831	0.2000	0.200
C(103)	-0.1535	0.0130	0.2765	0.2000	0.001
C(104)	0.2981	0.1162	0.1077	0.2000	0.001
C(105)	-0.0743	0.2271	0.2768	0.2000	0.001
C(106)	0.3550	0.1091	0.4944	0.2000	0.001
H(1)	-0.3981	0.0453	-0.0760	5.0874	
H(2)	-0.4609	0.0481	-0.0141	5.0874	
H(3)	-0.5113	0.0257	-0.0873	5.0874	
H(4)	-0.4365	0.1510	0.0254	5.3428	
H(5)	-0.4580	0.1062	0.0403	5.3428	
H(6)	-0.5475	0.1380	0.0386	5.3428	
H(7)	-0.5961	0.2050	-0.0665	6.4193	
H(8)	-0.6947	0.1799	-0.0570	6.4193	
H(9)	-0.6937	0.1986	-0.1333	6.4193	
H(10)	-0.7722	0.1264	-0.2602	4.7303	
H(11)	-0.7339	0.1702	-0.2413	4.7303	
H(12)	-0.6786	0.1440	-0.2908	4.7303	
H(13)	-0.6373	0.0684	-0.2774	5.9328	
H(14)	-0.5385	0.0447	-0.2324	5.9328	
H(15)	-0.6512	0.0389	-0.2156	5.9328	
H(16)	-0.1454	0.2165	-0.0612	8.7623	
H(17)	-0.1773	0.1737	-0.0404	8.7623	
H(18)	-0.1141	0.1791	-0.1017	8.7623	

Table 1. Atomic coordinates and B_{iso}/B_{eq} and occupancy (continued)

atom	x	y	z	B_{eq}	occ
H(19)	-0.3743	0.2134	-0.0171	6.1972	
H(20)	-0.3176	0.2513	-0.0386	6.1972	
H(21)	-0.4422	0.2473	-0.0633	6.1972	
H(22)	-0.5193	0.2699	-0.2060	8.8555	
H(23)	-0.5855	0.2364	-0.1788	8.8555	
H(24)	-0.5783	0.2375	-0.2610	8.8555	
H(25)	-0.4377	0.2229	-0.3500	10.2655	
H(26)	-0.5198	0.1908	-0.3371	10.2655	
H(27)	-0.4107	0.1775	-0.3530	10.2655	
H(28)	-0.1540	0.1866	-0.2495	12.2052	
H(29)	-0.1730	0.1444	-0.2192	12.2052	
H(30)	-0.2389	0.1578	-0.2966	12.2052	
H(31)	-0.2662	0.1286	-0.0015	2.9039	
H(32)	-0.1198	0.0938	0.0641	3.7172	
H(33)	-0.0551	0.0400	0.0027	3.9764	
H(34)	-0.1313	0.0293	-0.1227	3.3022	
H(35)	-0.2111	0.0200	-0.2330	5.3071	
H(36)	-0.2935	0.0176	-0.3630	7.2980	
H(37)	-0.4318	0.0640	-0.4105	4.4260	
H(38)	-0.4797	0.1105	-0.3310	3.5750	
H(39)	-0.0433	-0.0683	0.3344	5.1791	
H(40)	0.0021	-0.0383	0.3981	5.1791	
H(41)	0.0555	-0.0416	0.3314	5.1791	
H(42)	-0.1562	-0.0509	0.1532	8.2242	
H(43)	-0.0743	-0.0198	0.1365	8.2242	
H(44)	-0.0374	-0.0513	0.1988	8.2242	
H(45)	-0.3141	0.0128	0.1211	6.3632	
H(46)	-0.2284	0.0441	0.1112	6.3632	
H(47)	-0.3206	0.0566	0.1484	6.3632	
H(48)	-0.3519	0.0549	0.3097	6.6443	
H(49)	-0.3151	0.0838	0.2549	6.6443	
H(50)	-0.2589	0.0852	0.3385	6.6443	
H(51)	-0.1748	0.0440	0.4341	5.9632	
H(52)	-0.1331	0.0002	0.4477	5.9632	
H(53)	-0.0526	0.0349	0.4450	5.9632	
H(54)	0.4606	0.0454	0.1292	5.9492	
H(55)	0.3771	0.0309	0.1723	5.9492	
H(56)	0.4690	0.0600	0.2096	5.9492	
H(57)	0.2254	0.0268	0.0597	5.4718	

Table 1. Atomic coordinates and B_{iso}/B_{eq} and occupancy (continued)

atom	x	y	z	B_{eq}	occ
H(58)	0.2638	0.0460	-0.0058	5.4718	
H(59)	0.1480	0.0543	0.0038	5.4718	
H(60)	0.1273	0.1208	-0.0463	6.8272	
H(61)	0.1428	0.1650	-0.0189	6.8272	
H(62)	0.0634	0.1371	0.0092	6.8272	
H(63)	0.3168	0.2079	0.0741	4.1710	
H(64)	0.3147	0.2074	0.1572	4.1710	
H(65)	0.2076	0.2048	0.0970	4.1710	
H(66)	0.5122	0.1572	0.1914	3.9995	
H(67)	0.4362	0.1653	0.2440	3.9995	
H(68)	0.4938	0.1241	0.2458	3.9995	
H(69)	0.0927	0.2924	0.2564	4.0000	
H(70)	0.0786	0.2676	0.1841	4.0000	
H(71)	0.1570	0.2528	0.2562	4.0000	
H(72)	0.1470	0.2410	0.3987	4.0000	
H(73)	0.0575	0.2393	0.4427	4.0000	
H(74)	0.0759	0.2785	0.4020	4.0000	
H(75)	-0.1386	0.1757	0.3984	4.0000	
H(76)	-0.1033	0.2166	0.4365	4.0000	
H(77)	-0.2191	0.2115	0.3874	4.0000	
H(78)	-0.2823	0.1837	0.1856	4.0000	
H(79)	-0.3203	0.2198	0.2260	4.0000	
H(80)	-0.2888	0.1795	0.2675	4.0000	
H(81)	-0.1334	0.2082	0.1066	4.0000	
H(82)	-0.0832	0.2510	0.1159	4.0000	
H(83)	-0.2037	0.2450	0.1166	4.0000	
H(84)	0.4011	0.1881	0.4139	4.0000	
H(85)	0.5104	0.1654	0.4302	4.0000	
H(86)	0.4772	0.1898	0.4924	4.0000	
H(87)	0.2417	0.1939	0.4936	4.0000	
H(88)	0.2093	0.1708	0.5577	4.0000	
H(89)	0.3219	0.1911	0.5704	4.0000	
H(90)	0.1503	0.0689	0.5352	4.0000	
H(91)	0.1608	0.1102	0.5753	4.0000	
H(92)	0.2307	0.0740	0.6115	6.9108	
H(93)	0.2990	0.0168	0.4789	5.2958	
H(94)	0.4241	0.0192	0.4975	5.2958	
H(95)	0.3626	0.0242	0.5598	5.2958	
H(96)	0.4878	0.0868	0.3779	7.4267	

Table 1. Atomic coordinates and B_{iso}/B_{eq} and occupancy (continued)

atom	x	y	z	B_{eq}	occ
H(97)	0.5734	0.0938	0.4513	7.4267	
H(98)	0.5150	0.0526	0.4362	7.4267	
H(99)	-0.0972	0.3710	0.0000	11.8542	
H(100)	-0.1085	0.4022	0.0599	11.8542	

$B_{eq} = 8/3\ \pi^2(U_{11}(aa^*)^2 + U_{22}(bb^*)^2 + U_{33}(cc^*)^2 + 2U_{12}(aa^*bb^*)\cos\gamma + 2U_{13}(aa^*cc^*)\cos\beta + 2U_{23}(bb^*cc^*)\cos\alpha)$

Table 2. Anisotropic Displacement Parameters

atom	U_{11}	U_{22}	U_{33}	U_{12}	U_{13}	U_{23}
Lu(1)	0.0242(4)	0.0255(5)	0.0281(5)	-0.0006(4)	0.0067(4)	-0.0005(4)
Lu(2)	0.0308(5)	0.0322(5)	0.0289(5)	-0.0059(4)	0.0034(4)	-0.0015(4)
Lu(3)	0.0277(5)	0.0206(4)	0.0380(5)	0.0033(4)	0.0108(4)	0.0065(4)
Lu(4)	0.0220(4)	0.0241(4)	0.0293(5)	-0.0014(4)	0.0064(4)	-0.0025(4)
Lu(5)	0.0235(4)	0.0261(5)	0.0566(6)	-0.0006(4)	0.0068(4)	-0.0080(5)
Cl(1)	0.029(3)	0.022(2)	0.028(3)	-0.002(2)	0.007(2)	-0.004(2)
Cl(2)	0.104(7)	0.22(1)	0.089(6)	-0.024(7)	0.019(5)	0.002(7)
Cl(8)	0.123(8)	0.116(7)	0.168(9)	0.010(6)	0.037(6)	0.049(6)
Cl(9)	0.088(9)	0.52(3)	0.15(1)	0.11(1)	0.059(8)	0.12(1)
O(1)	0.028(7)	0.027(7)	0.020(6)	0.005(6)	0.009(5)	-0.003(6)
N(1)	0.029(9)	0.019(8)	0.025(9)	-0.011(7)	0.013(8)	-0.009(7)
N(2)	0.038(10)	0.039(10)	0.020(9)	-0.004(8)	-0.001(8)	-0.000(8)
C(1)	0.04(1)	0.01(1)	0.08(2)	0.017(9)	0.03(1)	0.02(1)
C(2)	0.03(1)	0.04(1)	0.04(1)	-0.01(1)	0.01(1)	0.01(1)
C(3)	0.03(1)	0.03(1)	0.06(1)	-0.008(10)	0.02(1)	-0.02(1)
C(4)	0.02(1)	0.04(1)	0.04(1)	0.012(10)	0.009(10)	0.01(1)
C(5)	0.03(1)	0.03(1)	0.04(1)	-0.001(10)	0.007(10)	-0.01(1)
C(6)	0.05(2)	0.02(1)	0.10(2)	-0.01(1)	-0.01(1)	0.01(1)
C(7)	0.04(1)	0.04(1)	0.03(1)	-0.00(1)	0.00(1)	-0.02(1)
C(8)	0.03(1)	0.02(1)	0.09(2)	0.011(10)	0.03(1)	0.03(1)
C(9)	0.07(2)	0.04(1)	0.02(1)	-0.02(1)	-0.00(1)	0.02(1)
C(10)	0.08(2)	0.03(1)	0.11(2)	0.01(1)	0.07(2)	-0.01(2)
C(11)	0.04(1)	0.07(2)	0.06(1)	-0.01(1)	0.00(1)	0.00(1)
C(12)	0.05(1)	0.08(2)	0.05(1)	0.01(1)	0.02(1)	-0.00(1)
C(13)	0.03(1)	0.07(2)	0.11(2)	0.01(1)	0.03(1)	-0.03(2)
C(14)	0.04(1)	0.04(1)	0.06(1)	0.00(1)	-0.00(1)	0.02(1)
C(15)	0.04(1)	0.07(2)	0.08(2)	-0.03(1)	0.02(1)	0.03(1)
C(16)	0.03(1)	0.05(2)	0.18(3)	-0.01(1)	-0.01(2)	0.05(2)
C(17)	0.09(2)	0.05(1)	0.07(2)	-0.01(1)	0.02(1)	-0.02(1)
C(18)	0.06(2)	0.04(1)	0.17(3)	0.01(1)	0.01(2)	0.06(2)
C(19)	0.18(3)	0.08(2)	0.06(2)	-0.07(2)	-0.00(2)	0.00(2)
C(20)	0.15(3)	0.06(2)	0.24(4)	-0.02(2)	0.16(3)	-0.04(2)
C(21)	0.013(10)	0.05(1)	0.03(1)	-0.006(9)	0.010(9)	0.01(1)
C(22)	0.03(1)	0.05(1)	0.04(1)	-0.02(1)	0.02(1)	0.00(1)
C(23)	0.04(1)	0.04(1)	0.04(1)	-0.02(1)	-0.01(1)	0.01(1)
C(24)	0.03(1)	0.03(1)	0.04(1)	-0.002(9)	0.003(10)	0.00(1)
C(25)	0.02(1)	0.05(1)	0.02(1)	-0.004(10)	0.003(9)	0.01(1)
C(26)	0.02(1)	0.03(1)	0.06(1)	0.019(9)	0.02(1)	-0.00(1)
C(27)	0.05(1)	0.06(2)	0.05(2)	0.03(1)	-0.01(1)	-0.01(1)

Table 2. Anisotropic Displacement Parameters (continued)

atom	U_{11}	U_{22}	U_{33}	U_{12}	U_{13}	U_{23}
C(28)	0.09(2)	0.09(2)	0.05(2)	0.01(2)	0.02(1)	-0.04(2)
C(29)	0.04(1)	0.05(1)	0.05(1)	0.01(1)	0.00(1)	-0.00(1)
C(30)	0.03(1)	0.03(1)	0.05(1)	-0.003(9)	-0.00(1)	0.01(1)
C(31)	0.06(2)	0.02(1)	0.07(2)	0.00(1)	0.01(1)	-0.01(1)
C(32)	0.04(1)	0.05(1)	0.04(1)	-0.03(1)	0.02(1)	-0.01(1)
C(33)	0.04(1)	0.07(2)	0.03(1)	-0.03(1)	0.00(1)	0.00(1)
C(34)	0.05(1)	0.06(2)	0.04(1)	-0.02(1)	0.00(1)	0.02(1)
C(35)	0.05(1)	0.04(1)	0.07(2)	-0.00(1)	0.04(1)	0.01(1)
C(36)	0.03(1)	0.04(1)	0.03(1)	0.000(10)	0.000(10)	-0.01(1)
C(37)	0.08(2)	0.01(1)	0.03(1)	-0.01(1)	0.05(1)	-0.007(10)
C(38)	0.06(1)	0.09(2)	0.02(1)	-0.03(1)	0.01(1)	0.01(1)
C(39)	0.07(2)	0.04(1)	0.03(1)	-0.02(1)	0.02(1)	-0.02(1)
C(40)	0.04(1)	0.03(1)	0.02(1)	-0.009(9)	0.016(10)	0.001(9)
C(41)	0.04(1)	0.004(10)	0.10(2)	-0.002(9)	0.02(1)	0.01(1)
C(42)	0.05(2)	0.04(1)	0.09(2)	0.01(1)	0.02(2)	0.02(2)
C(43)	0.08(2)	0.03(1)	0.17(3)	0.00(1)	0.10(2)	0.03(2)
C(44)	0.04(2)	0.07(2)	0.23(5)	-0.00(2)	0.01(3)	-0.03(3)
C(45)	0.08(2)	0.06(2)	0.11(3)	0.04(2)	-0.04(2)	-0.02(2)
C(46)	0.04(1)	0.07(2)	0.05(2)	-0.05(1)	-0.01(1)	0.04(1)
C(47)	0.08(2)	0.04(1)	0.03(1)	-0.02(1)	-0.02(1)	-0.00(1)
C(48)	0.07(2)	0.04(1)	0.04(1)	-0.02(1)	0.00(1)	-0.00(1)
C(49)	0.04(1)	0.03(1)	0.05(1)	-0.00(1)	0.01(1)	0.01(1)
C(50)	0.05(1)	0.06(2)	0.03(1)	-0.00(1)	-0.00(1)	0.02(1)
C(51)	0.06(2)	0.05(1)	0.05(1)	0.00(1)	0.02(1)	0.01(1)
C(52)	0.10(2)	0.10(2)	0.07(2)	-0.06(2)	0.03(2)	-0.05(2)
C(53)	0.02(1)	0.11(2)	0.06(2)	-0.02(1)	0.02(1)	-0.00(2)
C(54)	0.07(2)	0.09(2)	0.06(2)	0.01(2)	0.05(1)	0.01(1)
C(55)	0.11(2)	0.05(1)	0.05(1)	-0.02(1)	0.04(1)	-0.01(1)
C(56)	0.07(2)	0.03(1)	0.10(2)	-0.00(1)	0.06(2)	-0.01(1)
C(57)	0.05(1)	0.08(2)	0.05(1)	-0.02(1)	0.03(1)	-0.05(1)
C(58)	0.07(2)	0.09(2)	0.06(2)	-0.05(2)	0.02(1)	-0.00(1)
C(59)	0.05(1)	0.04(1)	0.04(1)	0.00(1)	0.01(1)	0.00(1)
C(60)	0.04(1)	0.04(1)	0.05(1)	-0.00(1)	0.02(1)	-0.00(1)
C(61)	0.18(3)	0.03(1)	0.14(3)	0.02(2)	0.08(2)	0.00(2)
C(62)	0.10(2)	0.06(2)	0.10(2)	0.04(2)	-0.03(2)	-0.04(2)
C(63)	0.29(6)	0.06(2)	0.56(9)	0.07(3)	0.33(7)	0.06(4)
C(64)	0.02(2)	0.06(2)	0.8(1)	0.01(2)	-0.05(4)	-0.13(4)
C(65)	0.41(8)	0.08(3)	0.21(4)	0.10(4)	-0.21(5)	-0.05(3)
C(66)	0.12(3)	0.18(3)	0.07(2)	-0.08(2)	-0.05(2)	0.06(2)

Table 2. Anisotropic Displacement Parameters (continued)

atom	U_{11}	U_{22}	U_{33}	U_{12}	U_{13}	U_{23}
C(67)	0.10(2)	0.10(2)	0.07(2)	-0.02(2)	-0.04(2)	0.01(2)
C(68)	0.09(2)	0.09(2)	0.05(1)	-0.02(2)	0.04(1)	-0.02(1)
C(69)	0.05(1)	0.07(2)	0.04(1)	-0.01(1)	-0.00(1)	0.01(1)
C(70)	0.01(1)	0.16(3)	0.05(2)	0.01(1)	-0.01(1)	-0.01(2)
C(71)	0.14(3)	0.14(3)	0.09(2)	0.02(2)	0.01(2)	0.05(2)

The general temperature factor expression:
$\exp(-2\pi^2(a^{*2}U_{11}h^2 + b^{*2}U_{22}k^2 + c^{*2}U_{33}l^2 + 2a^*b^*U_{12}hk + 2a^*c^*U_{13}hl + 2b^*c^*U_{23}kl))$

References:

1. SMART: Area-Detector Software Package, Bruker Analytical X-ray Systems, Inc.: Madison, WI, (2001-03)
2. SAINT: SAX Area-Dectector Integration Program, V7.06; Bruker Analytical X-ray Systems Inc.: Madison, WI, (2005)
3. XPREP:(v 6.12) Part of the SHELXTL Crystal Structure Determination Package, Bruker Analytical X-ray Systems, Inc.: Madison, WI, (2001)
4. SADABS: Bruker-Nonius Area Detector Scaling and Absorption v. 2.10 Bruker Analytical X-ray Systems, Inc.: Madison, WI (2005).
5. SIR97: Altomare, A., Burla, M. C., Camalli, M., Cascarano, G., Giacovazzo, C., Guagliardi, A., Moliterni, A. G. G., Polidori, G., & Spagna, R. SIR97: A new tool for crystal structure determination and refinement. J. App. Cryst. (1998)
6. DIRDIF94: Beurskens, P.T., Admiraal, G., Beurskens, G., Bosman, W.P., de Gelder, R., Israel, R. and Smits, J.M.M.(1994). The DIRDIF-94 program system, Technical Report of the Crystallography Laboratory, University of Nijmegen, The Netherlands.
7. Cromer, D. T. & Waber, J. T.; "International Tables for X-ray Crystallography", Vol. IV, The Kynoch Press, Birmingham, England, Table 2.2 A (1974).
8. Ibers, J. A. & Hamilton, W. C.; Acta Crystallogr., 17, 781 (1964).
9. Creagh, D. C. & McAuley, W.J .; "International Tables for Crystallography", Vol C, (A.J.C. Wilson, ed.), Kluwer Academic Publishers, Boston, Table 4.2.6.8, pages 219-222 (1992).
10. Creagh, D. C. & Hubbell, J.H..; "International Tables for Crystallography", Vol C, (A.J.C. Wilson, ed.), Kluwer Academic Publishers, Boston, Table 4.2.4.3, pages 200-206 (1992).
11. teXsan: Crystal Structure Analysis Package, Molecular Structure Corporation (1985 & 1992).
12. Sheldrick, G. *SHELXS-97, Program for solution of crystal structures*, University of Göttingen: Göttingen, Germany, 1997.
13. Sheldrick, G. *SHELXL-97, Program for refinement of crystal structures*, University of Göttingen: Göttingen, Germany, 1997.